

5-2017

TARGETING AUTOPHAGY TO IMPROVE EFFICACY OF CDK4/6 INHIBITION IN BREAST CANCER

Smruthi Vijayaraghavan

Follow this and additional works at: https://digitalcommons.library.tmc.edu/utgsbs_dissertations



Part of the [Cancer Biology Commons](#), and the [Translational Medical Research Commons](#)

Recommended Citation

Vijayaraghavan, Smruthi, "TARGETING AUTOPHAGY TO IMPROVE EFFICACY OF CDK4/6 INHIBITION IN BREAST CANCER" (2017). *The University of Texas MD Anderson Cancer Center UTHealth Graduate School of Biomedical Sciences Dissertations and Theses (Open Access)*. 772.
https://digitalcommons.library.tmc.edu/utgsbs_dissertations/772

This Dissertation (PhD) is brought to you for free and open access by the The University of Texas MD Anderson Cancer Center UTHealth Graduate School of Biomedical Sciences at DigitalCommons@TMC. It has been accepted for inclusion in The University of Texas MD Anderson Cancer Center UTHealth Graduate School of Biomedical Sciences Dissertations and Theses (Open Access) by an authorized administrator of DigitalCommons@TMC. For more information, please contact digitalcommons@library.tmc.edu.

**TARGETING AUTOPHAGY TO IMPROVE EFFICACY OF CDK4/6 INHIBITION IN
BREAST CANCER**

by

Smruthi Vijayaraghavan, B.S.

APPROVED:

Khandan Keyomarsi, Ph.D.
Advisory Professor

Jeffrey N. Myers, MD.

Robert C. Bast Jr., MD.

Sendurai Mani, Ph.D.

Raghu Kalluri, MD, Ph.D.

Stephanie S. Watowich, Ph.D.

APPROVED:

Dean, The University of Texas
MD Anderson Cancer Center UTHealth Graduate School of Biomedical Sciences

**TARGETING AUTOPHAGY TO IMPROVE EFFICACY OF CDK4/6
INHIBITION IN BREAST CANCER**

A

DISSERTATION

Presented to the Faculty of

The University of Texas

MD Anderson Cancer Center UTHealth

Graduate School of Biomedical Sciences

in Partial Fulfillment

of the Requirements

for the Degree of

DOCTOR OF PHILOSOPHY

by

Smruthi Vijayaraghavan, B.S.

Houston, Texas

May, 2017

DEDICATION

This dissertation is dedicated to my parents and grandparents.

To my grandmother, Rajalakshmi N and my parents, Vijayaraghavan SV and Geetha A for their unconditional love, support and encouragement, which made it all possible.

To my grandfather, whose fight against cancer 10 years ago inspired and motivated me to pursue my graduate school research in the field of Cancer biology.

ACKNOWLEDGEMENTS

First, I would like to thank my mentor, Dr. Khandan Keyomarsi, for giving me the opportunity to pursue such a wonderful and impactful project in her laboratory; for her time, effort and guidance through this journey; and for letting me drive the project and for her support throughout this pursuit, for my development as a scientist. I would like to thank all my current and past advisory committee members Dr. Jeffrey Myers, Dr. Sendurai Mani, Dr. Jill Schumacher, Dr. Robert Bast, Dr. Raghu Kalluri and Dr. Stephanie Watowich for their valuable suggestions and feedback during the committee meetings which helped move the project forward in the right direction. I would also like to thank Dr. Kelly Hunt for her support and valuable suggestions at lab meetings.

I would like to extend thanks to all the present and past members of the Keyomarsi lab, for being great colleagues and friends, and for making my 5 years in grad school fun and memorable, Dr. Cansu Karakas, Dr. Kavitha Balaji, Dr. Dong Yang, Dr. Jason Carey, Dr. Natalie Jabbour, Dr. Kwang Low, Dr. Xian Chen, Dr. Said Akli, Dr. Angela Alexander, Tuyen Bui, Dr. Iman Doostan, Dr. Kimberly S. Lucenay, Amanda Hanks, Dr. Amanda Say and Dana Richardson. In particular, I would like to thank Natalie Jabbour and Jason Carey for their valuable inputs and insights for the project, Tuyen Bui for his technical help, Xian Chen and Iman Doostan for their help with the mouse experiments and Cansu Karakas for help with the IHC experiments.

I would also like to thank Nalini Patel and Wendy Schober from the MD Anderson Flow cytometry core facility for their assistance and technical guidance for numerous experiments performed in this project. I would also like to thank our clinical collaborators from Breast Medical Oncology, Dr. Debu Tripathy and team for obtained the samples for the clinical biomarker studies. I would also like to acknowledge the constant support and guidance form

the GSBS staff including Brenda Gaughan and Joy Lademora, the deans, Dr. Michelle Barton and Dr. Michael Blackburn and associate dean, Dr. Willam Mattox.

I would like to acknowledge and thank the great friends I have had over the years, who have helped me have fun and stay sane amidst the long and hectic hours of science and research, Kavitha Balaji, Mrinal Srivastava, Vaishnavi Sambandam, Preeti Priya, Apurva Hegde and several others from GSBS. I would also like to thank my mentors from undergrad and internships, who motivated and encouraged me to pursue a PhD in biomedical sciences, Dr. Norman Drinkwater, Dr. Srinivasan Narayanaswamy, Dr. Anuradha Dhanasekaran, Dr. Gautam Pennathur, Dr. Tamilselvan Jayavelu and Dr. Radha Sriram.

Finally, I would not be who I am today if not for my family, my parents, Vijayaraghavan S. Venkatadri and Geetha Anantharaman, and my grandparents, Anantharaman A. Subramanian and Rajalakshmi Narayanawamy. From their support and encouragement to let me pursue my dream, to their constant love and motivation, even if it has to be from 10,000 miles away, they have been instrumental for my success till date. A special mention to my grandmother, Rajalakshmi Narayanawamy, who has supported and encouraged me in my education from KG till date and for her unconditional love and sacrifice for me.

TARGETING AUTOPHAGY TO IMPROVE EFFICACY OF CDK4/6 INHIBITION IN BREAST CANCER

Smruthi Vijayaraghavan, B.S

Advisory Professor: Khandan Keyomarsi, Ph.D.

Deregulation of the cell cycle machinery is a hallmark of cancer, leading to aberrant proliferation and tumorigenesis. The crucial role of the CDK4/6-Cyclin D pathway has led to the development and FDA approval (palbociclib, ribociclib) of CDK4/6 inhibitors for the treatment of advanced estrogen receptor positive breast cancer. However, three major clinical challenges remain: i) adverse events leading to discontinuation of therapy and ii) lack of reliable biomarkers to identify responsive patients and iii) acquired resistance to CDK4/6 inhibitors. Previous *in vitro* studies have shown that palbociclib mediated CDK4/6 inhibition induces G1 arrest and senescence in ER+ breast cancer cells, and a recent study in fibroblasts implicated a role for palbociclib in inducing autophagy, a catabolic process that facilitates survival of the cells under stress. Thus, we hypothesize that **in the presence of an intact G1/S checkpoint, autophagy protects ER positive breast cancer cells from palbociclib induced senescence**. Further, based on our preliminary results, we hypothesize that cancer stem cells and EMT mediates acquired resistance to palbociclib. Results from this study show that breast cancer cells activate autophagy in response to palbociclib, and that the combination of autophagy and CDK4/6 inhibitors induces irreversible growth inhibition and senescence *in vitro*, and diminishes growth of cell line and patient-derived xenograft tumors *in vivo*. Furthermore, intact G1/S transition is necessary and predictive of preclinical sensitivity to this drug combination, and Rb positive and low-molecular-weight isoform of cyclin E negative status are reliable prognostic biomarkers in advanced estrogen receptor positive breast cancer patients. Inhibition of CDK4/6 and autophagy was also synergistic in other solid cancers with an intact

G1/S checkpoint, providing a novel and promising biomarker-driven combination therapeutic strategy to treat breast and other solid tumors. Lastly, combined targeting with STAT-3 and PARP inhibitors can effectively target acquired resistance to palbociclib. Collectively, results from this study can help improve the efficacy, selectivity and treat acquired resistance to CDK4/6 inhibition in breast and other solid tumors.

TABLE OF CONTENTS

Approval Page	i
Title Page	ii
Dedication	iii
Acknowledgements	iv
Abstract	vi
Table of Contents	viii
List of Illustrations	xvi
List of Tables	xx
CHAPTER 1: INTRODUCTION	1
1.1. Breast cancer	1
1.1.1. Epidemiology of breast cancer.....	1
1.1.2. Breast cancer subtyping.....	1
1.1.3. Hormone receptor positive breast cancer – current treatments	4
1.1.4. HER2 positive breast cancer – current treatments	5
1.1.5. Triple negative breast cancer – current treatments.....	7
1.2. ER positive breast cancer	11
1.2.1 role of estrogen and ER in breast cancer.....	11
1.2.2. Current treatments for ER positive breast cancer	12
1.2.3. SERM – tamoxifen	13
1.2.4. SERD – fulvestrant.....	16
1.2.5. Aromatase inhibitors	17
1.3. Cell cycle	20
1.3.1. Cell cycle regulation	20

1.3.2. Cell cycle in cancer	24
1.3.3. CDK inhibitors in breast cancer.....	25
1.4. CDK4/6 inhibitors in breast cancer.....	27
1.4.1. Discovery and development of CDK4/6 inhibitors.....	27
1.4.2. Palbociclib	28
1.4.3. Ribociclib.....	32
1.4.4. Abemaciclib.....	33
1.4.5. Biomarker studies with CDK4/6 inhibitors	34
1.4.6. Mechanisms of resistance to CDK4/6 inhibitors.....	35
1.5. Limitations with CDK4/6 treatment and gaps in knowledge	36
1.6. Goal of the project	37
CHAPTER 2: MATERIALS AND METHODS	38
2.1. Cell lines.....	38
2.2. Antibodies and drugs	39
2.3. siRNA knockdown	39
2.4. shRNA knockdown and cyclin e overexpression	40
2.5. Dose-response studies	41
2.6. Cellular proliferation assay.....	41
2.7. Cell cycle and BrdU analyses	42
2.8. Measurement of senescence	43
2.9. Annexin V and caspase-3 apoptosis assays.....	44
2.10. Cellular ROS measurement	44
2.11. Monodansylcadavarine measurement	45
2.12. Immunofluorescence.....	45
2.13. Transmission electron microscopy.....	46
2.14. <i>In vivo</i> xenograft studies	46

2.15. Patient-derived xenograft studies.....	48
2.16. Immunohistochemistry analysis of mouse tumor tissues	49
2.17. Western blot analysis	50
2.18. RPPA and data analysis	51
2.19. Bioinformatics and TCGA analysis.....	52
2.20. Breast cancer patient samples and statistical analysis	52
2.21. Immunohistochemical staining of patient samples.....	54
2.22. Immunohistochemical scoring of Rb and cyclin E.....	54
2.23. Mammosphere formation assay.....	55
2.24. CD44/ CD24 flow cytometry analysis.....	56
2.25. Aldefluor assay.....	56
2.26. Migration assay	57
2.27. Statistical analysis.....	57

CHAPTER 3: CHARACTERIZING THE EFFECT OF CDK4/6 INHIBITION IN ER+ BREAST CANCER	58
3.1. Introduction.....	58
3.1.1. Role of CDK4/6-cyclin d on growth of breast cancer	58
3.1.2. Mechanistic studies of palbociclib in breast and other cancer	60
3.1.3. Interplay between ROS and senescence.....	62
3.1.4. Gap in knowledge	63
3.2. Results	64
3.2.1. Deregulation of CDK4/6-cyclin D pathway in breast cancer	64
3.2.2. Impact of siRNA or shRNA knockdown of CDK4/6	66
3.2.3. Dose dependent effect of palbociclib on growth, cell cycle arrest and senescence	68
3.2.4. Time dependent effect of palbociclib on growth, cell cycle arrest and senescence	74
3.2.5. Effect of palbociclib on inducing apoptosis in ER+ve breast cancer.....	76

3.2.6. On-target vs off-target effects of palbociclib.....	78
3.2.7. Induction of reactive oxygen species (ROS) by CDK4/6 inhibition	80
3.2.8. Impact of ROS ablation on palbociclib induced growth inhibition and senescence .	82
3.2.9. Palbociclib mediated tumor growth inhibition and senescence <i>in vivo</i>	84
3.2.10. Palbociclib mediated induction of ROS <i>in vivo</i>	89
3.3. Discussion	91

CHAPTER 4: INDUCTION OF AUTOPHAGY IN RESPONSE TO CDK4/6 INHIBITION IN ER+ BREAST CANCER 94

4.1. Introduction.....	94
4.1.1. Autophagy – definition and regulation.....	94
4.1.2. Role of autophagy in cancer	96
4.1.3. CDK4/6 inhibition and autophagy.....	98
4.1.4. Gap in knowledge	98
4.2. Results	100
4.2.1. Induction of autophagy with CDK4/6 knockdown and low doses of palbociclib	100
4.2.2. Induction of intact autophagic flux with low doses of palbociclib	104
4.2.3. Deregulated autophagic flux at high doses of palbociclib	107
4.2.4. Dependence of palbociclib-induced autophagy on the induction of ROS	109
4.2.5. Palbociclib mediated induction of dose-dependent autophagy <i>in vivo</i>	111
4.3. Discussion	114

CHAPTER 5: *IN VITRO* AND *IN VIVO* SYNERGY BETWEEN CDK4/6 AND AUTOPHAGY INHIBITION IN ER+ BREAST CANCER 118

5.1. Introduction.....	118
5.1.1. Autophagy as a stress response process in cancer.....	118
5.1.2. Pharmacological inhibitors of autophagy	120

5.1.3. Clinical development of autophagy inhibitors.....	122
5.1.4. Gap in knowledge	124
5.2. Results	126
5.2.1. Impact of Beclin1 or Atg5 downregulation on palbociclib action	126
5.2.2. Synergy between siRNA or shRNA mediated knockdown of CDK4/6 and autophagy inhibition	129
5.2.3. Impact of autophagy inhibition on palbociclib mediated growth inhibition, cell cycle arrest, ROS and senescence	131
5.2.4. Synergy between autophagy inhibition (HCQ) and other CDK4/6 inhibitors – ribociclib and abemaciclib	135
5.2.5. Synergism between palbociclib and other autophagy inhibitors	137
5.2.6. Synergy between CDK4/6 and autophagy inhibitor in aromatase inhibitor resistant cells.....	140
5.2.7. Synergy between palbociclib and autophagy inhibition by HCQ <i>in vivo</i>	142
5.2.8. Synergy between palbociclib and autophagy inhibition (Lys-05) <i>in vivo</i>	149
5.3. Discussion	153
 CHAPTER 6: BIOMARKER IDENTIFICATION FOR PALBOCICLIB AND ITS COMBINATION WITH AUTOPHAGY INHIBITOR IN ER+ BREAST CANCER	 156
6.1. Introduction.....	156
6.1.1. Rb protein in breast cancer	156
6.1.2. Cyclin E and LMWE in breast cancer.....	157
6.1.3. Pre-clinical biomarker studies for palbociclib in breast cancer.....	159
6.1.4. Gap in knowledge	160
6.2. Results	162
6.2.1. Gene set enrichment analysis to identify biomarkers for palbociclib in breast cancer	162
6.2.2. Role of p53 in determining response to palbociclib in ER+ breast cancer.....	164

6.2.3. Role of Rb in mediating palbociclib induced ROS and senescence	166
6.2.4. Role of Rb in mediating palbociclib induced autophagy	170
6.2.5. Role of LMWE in mediating palbociclib action	172
6.2.6. LMWE as a mediator of resistance to the combination of CDK4/6 and autophagy inhibitor.....	177
6.2.7. LMWE as a mediator of resistance to the triple combination of CDK4/6, letrozole and autophagy inhibitor.....	179
6.3. Discussion	181

CHAPTER 7: RB AND CYCLIN E AS PROGNOSTIC BIOMARKERS OF PALBOCICLIB ACTION IN ADVANCED ER+ BREAST CANCER PATIENTS..... 183

7.1. Introduction.....	183
7.1.1. Clinical studies and biomarker analysis	183
7.1.2. Gap in knowledge	185
7.2. Results	186
7.2.1. TCGA analysis showing deregulation of Rb and cyclin E in breast and other solid cancer patients.....	186
7.2.2. Alterations in Rb and LMWE protein in breast cancer patients.....	188
7.2.3. Correlation between expression of Rb and LMWE and response to palbociclib in advanced ER positive breast cancer patients	190
7.3. Discussion	199

CHAPTER 8: SYNERGISM BETWEEN CDK4/6 AND AUTOPHAGY INHIBITION IN TNBC AND OTHER SOLID TUMORS..... 201

8.1. Introduction.....	201
8.1.1. Pre-clinical studies with CDK4/6 inhibitors in TNBC	201
8.1.2. Pre-clinical studies with CDK4/6 inhibitors in solid tumors.....	202
8.1.3. Clinical studies with CDK4/6 inhibitors in solid tumors.....	204

8.1.4. Gap in knowledge	206
8.2. Results	207
8.2.1. Palbociclib mediated growth inhibition in TNBC cell lines.....	207
8.2.2. Synergism between palbociclib and autophagy inhibition in TNBC cell lines	211
8.2.3. Synergism between palbociclib and autophagy inhibition in TNBC PDX model....	215
8.2.4. Palbociclib treatment in other solid tumor cell lines	217
8.2.5. Synergism between palbociclib and autophagy inhibition in other solid tumor cell lines.....	220
8.3. Discussion	222
CHAPTER 9: MECHANISM OF ACQUIRED RESISTANCE TO PALBOCICLIB.....	225
9.1. Introduction.....	225
9.1.1. Mechanisms of acquired resistance to CDK4/6 inhibition	225
9.1.2. Cancer stem cells, EMT and drug resistance	226
9.1.3. IL-6/STAT-3 pathway – role in CSC and breast cancer	227
9.1.4. Targeting DNA repair pathway in breast cancer	228
9.1.5. Gap in knowledge	229
9.2. Results	230
9.2.1. Development and characterization of palbociclib resistant cells.....	230
9.2.2. Gene expression profile of palbociclib resistant cells.....	233
9.2.3. EMT and cancer stem cell properties in palbociclib resistant cells	236
9.2.4. Targeting IL-6/STAT-3 pathway in palbociclib resistant cells.....	240
9.2.5. Targeting DNA repair deficiency in palbociclib resistant cells.....	242
9.2.6. Combined treatment with STAT-3 and PARP inhibitors in palbociclib resistant cells	244
9.3. Discussion	246

CHAPTER 10: CONCLUSIONS AND FUTURE DIRECTIONS.....	248
10.1. Major findings	248
10.2. Significance	251
10.3. Future directions.....	252
 Appendix	 255
Clinical trial protocol for combination of palbociclib and HCQ in Rb+ LMWE- ER positive breast cancer patients.....	 255
 Bibliography	 269
Vita	325

LIST OF ILLUSTRATIONS

Figure 1: Breast cancer subtypes.....	2
Figure 2: Mammalian cell cycle	21
Figure 3: Cell cycle in normal and cancer cells	25
Figure 4: CDK4/6 inhibitors in cancer cells	28
Figure 5: Regulation of the G1/S checkpoint.....	59
Figure 6: Deregulation of CDK4/6-Cyclin D pathway in Breast Cancer	65
Figure 7: Impact of siRNA or shRNA knockdown of CDK4/6	67
Figure 8: Dose-dependent effect of palbociclib on growth of ER+ breast cancer cells	71
Figure 9: Dose-dependent effect of palbociclib on cell cycle of ER+ breast cancer cells	72
Figure 10: Effect of palbociclib on senescence in ER+ breast cancer cells	73
Figure 11: Time-dependent effect of palbociclib on cell cycle of ER+ breast cancer cells	75
Figure 12: Effect of palbociclib on inducing apoptosis in ER+ breast cancer cells.....	77
Figure 13: On-target vs Off-target effects of palbociclib	79
Figure 14: Induction of ROS by CDK4/6 inhibition	81
Figure 15: Impact of ROS ablation on palbociclib induced growth inhibition and senescence .	83
Figure 16: Characterization of MCF7-T cell in-vitro.....	86
Figure 17: Palbociclib mediated tumor growth inhibition <i>in vivo</i>	87
Figure 18: Palbociclib mediated cell cycle arrest and senescence <i>in vivo</i>	88
Figure 19: Palbociclib mediated induction of ROS <i>in vivo</i>	90
Figure 20: Regulation of autophagy	95
Figure 21: Palbociclib mediated induction of autophagy	102
Figure 22: Palbociclib mediated induction of autophagy	103
Figure 23: Induction of intact autophagy with low doses of palbociclib	106
Figure 24: Deregulated autophagy flux at high doses of palbociclib	108

Figure 25: Dependence of palbociclib induced autophagy on the induction of ROS	110
Figure 26: Induction of dose-dependent autophagy <i>in vivo</i> by palbociclib	113
Figure 27: Working model	115
Figure 28: Impact of Beclin-1 or Atg-5 downregulation on palbociclib mediated growth inhibition	127
Figure 29: Impact of Beclin-1 or Atg-5 downregulation on palbociclib mediated G1 arrest and senescence	128
Figure 30: Synergy between siRNA or shRNA mediated knockdown of CDK4/6 and autophagy inhibition	130
Figure 31: Impact of autophagy inhibition on palbociclib mediated growth inhibition and G1 arrest	133
Figure 32: Impact of autophagy inhibition on palbociclib induced ROS and senescence	134
Figure 33: Synergy between autophagy inhibition (HCQ) and other CDK4/6 inhibitors – ribociclib and abemaciclib	136
Figure 34: Synergism between palbociclib and other autophagy inhibitors (CQ, BafA1)	138
Figure 35: Synergism between palbociclib and other autophagy inhibitors (Spautin-1, Lys-05)	139
Figure 36: Synergy between CDK4/6 and autophagy inhibitors in aromatase inhibitor resistant cells	141
Figure 37: Synergy between palbociclib and autophagy inhibition by HCQ <i>in vivo</i>	145
Figure 38: Impact of palbociclib and autophagy inhibition on cell cycle, senescence and autophagy <i>in vivo</i>	146
Figure 39: Impact of palbociclib and autophagy inhibition on growth, senescence and ROS <i>in vivo</i>	147
Figure 40: Toxicity profile of palbociclib and autophagy inhibitor treatment <i>in vivo</i>	148
Figure 41: Toxicity profile of Lys-05 <i>in vivo</i>	151
Figure 42: Synergism between palbociclib and Lys-05 mediated autophagy inhibition <i>in vivo</i>	152
Figure 43: Working Model	154
Figure 44: Low molecular weight isoforms of cyclin E (LMWE)	158

Figure 45: Gene set enrichment analysis to identify biomarkers for palbociclib in breast cancer	163
Figure 46: Role of p53 in determining response to palbociclib in ER+ve breast cancer	165
Figure 47: Role of Rb in mediating palbociclib induced growth inhibition	168
Figure 48: Role of Rb in mediating palbociclib induced ROS and senescence	169
Figure 49: Role of Rb in mediating palbociclib induced autophagy.....	171
Figure 50: Role of LMWE in mediating palbociclib action	174
Figure 51: Role of LMWE in mediating palbociclib induced ROS and G1 arrest	175
Figure 52: Role of LMWE in mediating palbociclib induced senescence	176
Figure 53: LMWE as a mediator of resistance to the combination of CDK4/6 and autophagy inhibitors	178
Figure 54: LMWE as a mediator of resistance to the triple combination of CDK4/6, letrozole and autophagy inhibitor	180
Figure 55: Working model – Rb and LMWE as identifiers of sensitivity to CDK4/6 inhibition .	182
Figure 56: TCGA analysis showing deregulation of Rb and cyclin E in breast and other solid cancer patients	187
Figure 57: Alterations in Rb and LMWE protein in breast cancer patients.....	189
Figure 58: Expression of Rb and LMWE in advanced ER positive breast cancer patients treated with palbociclib	195
Figure 59: Correlation between expression of Rb and LMWE and response to palbociclib in advanced ER positive breast cancer patients	196
Figure 60: Palbociclib mediated induction of growth inhibition and cell cycle arrest in TNBC cell lines	209
Figure 61: Palbociclib mediated induction of growth inhibition and senescence in TNBC cell lines	210
Figure 62: Palbociclib mediated induction of autophagy in TNBC cell lines.....	213
Figure 63: Synergism between palbociclib and autophagy inhibition in TNBC cell lines	214
Figure 64: Synergism between palbociclib and autophagy inhibition in TNBC PDX model	216
Figure 65: Palbociclib treatment in other solid tumor cell lines	219

Figure 66: Synergism between palbociclib and autophagy inhibition in other solid tumor cell lines	221
Figure 67: Synergism between CDK4/6 and autophagy inhibition in cancers with an intact G1/S checkpoint	223
Figure 68: Development and characterization of palbociclib resistant cells	232
Figure 69: Gene expression profile of palbociclib resistant cells	235
Figure 70: EMT properties in palbociclib resistant cells	238
Figure 71: Cancer stem cell properties of palbociclib resistant cells	239
Figure 72: Targeting IL-6/STAT-3 in palbociclib resistant cells	241
Figure 73: Targeting DNA repair deficiency in palbociclib resistant cells	243
Figure 74: Combined treatment with STAT-3 and PARP inhibitors in palbociclib resistant cells	245
Figure 75. Overall working model.....	249

LIST OF TABLES

Table 1: Breast cancer subtypes	2
Table 2: Anti-estrogens	13
Table 3: Defects in CDK and cyclin knockout mice	23
Table 4: CDK4/6 inhibitors in breast cancer	29
Table 5: CDK4/6 inhibitor clinical trials in ER+ breast cancer	32
Table 6: Drug-induced autophagy in cancer	119
Table 7: Autophagy targeting drugs	121
Table 8: Phase-II clinical trials with HCQ	123
Table 9: Clinical studies and biomarker analysis	184
Table 10: Clinical, pathologic, and treatment characteristics of patients treated with palbociclib + letrozole	193
Table 11: Clinical, pathologic, and treatment characteristics of patients treated with palbociclib + fulvestrant	194
Table 12: Cox model for univariate analyses for the factors associated with PFS	197
Table 13: Cox model for multivariable analyses for the factors associated with PFS	198
Table 14: Pre-clinical studies with CDK4/6 inhibitors in other cancers	203
Table 15: Clinical studies with CDK4/6 inhibitors in other cancers	205

CHAPTER 1: INTRODUCTION

1.1. BREAST CANCER

1.1.1. EPIDEMIOLOGY OF BREAST CANCER

Breast cancer is the most commonly diagnosed cancer in women worldwide, with an estimated 252,710 new patients expected to be diagnosed with the disease in 2017 (Siegel, Miller et al. 2016). It is also the second most common cause of cancer death in women, accounting for about 15% of all cancer related deaths and an estimated 40,610 deaths in 2017 (Siegel, Miller et al. 2016). While there has been a decrease in breast cancer deaths over the years, the continued increase in cancer incidence emphasizes the need for more reliable and efficacious treatment strategies to combat the disease.

1.1.2. BREAST CANCER SUBTYPING

Like most cancers, breast cancer is highly heterogeneous. Breast cancers can be classified based on numerous features such as histopathology, grade, stage, receptor status and genomic / DNA based classification (Sotiriou, Neo et al. 2003, Onitilo, Engel et al. 2009). Historically, breast cancer was classified based on staining for the hormone receptors such as estrogen receptor (ER), progesterone receptor (PR), and Her-2 (Onitilo, Engel et al. 2009). Based on the presence or absence of these receptors, breast cancer can be divided into four subtypes: i) hormone receptor positive (ER+/PR+/HER2-), ii) hormone receptor and Her-2 positive (ER+/PR+/HER2+), iii) Her-2 amplified (ER-/PR-/HER2+) and iv) triple negative (ER-/PR-/HER2-) (**Figure 1**) (Sorlie, Perou et al. 2001, Sorlie, Tibshirani et al. 2003). The hormone receptor positive is the most prevalent subtype, comprising about 66% of all breast tumors (**Figure 1**) (Sorlie, Perou et al. 2001, Sorlie, Tibshirani et al. 2003). They can also be classified based on histopathological features of the tumor biopsy specimens such as ducts and lobules

Breast Cancer

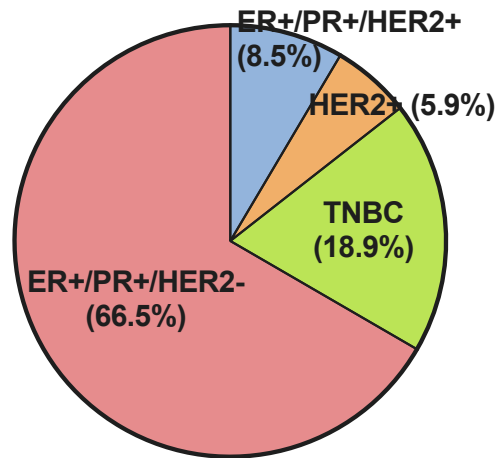


Figure 1: Breast cancer subtypes: Pie chart showing the subtypes of breast cancer based on the receptor status

Subtype	ER PR HER2 expression	Frequency	Characteristics	Prognosis	Current treatments
Luminal A	ER+, PR+, HER2-	50-60%	low Ki67	Good	Endocrine therapy
Luminal B	ER+, PR+, HER2	10-18%	high Ki67	Intermediate / Poor	Endocrine therapy plus chemotherapy
HER2 positive	ER-, PR-, HER2+	10-15%	Her2 amplification	Poor	Trastuzumab, lapatinib (plus chemotherapy)
Basal-like	ER-,PR-, HER2-	10-20%	CK 5/6, EGFR	Very poor	Chemotherapy, surgery
Normal- like	ER-/+, HER2-	3-10%	Low PARP1, Chk1, high ALDH	Good	Undetermined
Claudin- low	ER-,PR-, HER2-	12-14%	Low claudin 3,4,7, E- cadherin, high CSC	Poor	Chemotherapy (dependent upon HR/HER2 status)

Table 1: Breast cancer subtypes: Table showing the subtypes of breast cancer and their characteristics when classified based on gene expression profiles

into i) Invasive ductal carcinoma, ii) Invasive lobular carcinoma and iii) Ductal carcinoma in situ (DCIS) (Eheman, Shaw et al. 2009)

A more recent classification of breast tumors was carried out based on gene expression profile of normal and tumor tissues using cDNA microarray (Perou, Sorlie et al. 2000).

Classification of 42 patient tumors identified four distinct molecular subtypes within breast cancer namely, ER positive / luminal, Her2 / ErbB2 positive, basal-like and normal subtypes (Perou, Sorlie et al. 2000). Further classification was performed using microarray based gene

expression profiles from 99 breast tumors to yield six intrinsic subtypes namely Luminal A, Luminal B, Her2 positive, basal-like, normal breast and claudin-like subtypes (**Table 1**)

(Sotiriou, Neo et al. 2003, Eroles, Bosch et al. 2012). Luminal A breast cancer, which is the most common type is characterized by the expression of ER, PR, absence of expression of Her2 and low expression of Ki67. This subtype is currently being treated using aromatase inhibitors, selective ER modifiers or selective regulators of ER, depending on the menopausal status of the patient and the source of estrogen (Baum, Budzar et al. 2002). In pre-menopausal women, ovaries are the primary source of estrogen, making anti-estrogens such as tamoxifen or fulvestrant as the mainstay treatment (Baum, Budzar et al. 2002). In post-menopausal women, however, since estrogen is produced by the conversion of androgens (from the adipose tissue) by the aromatase enzyme, the aromatase inhibitors such as letrozole and anastrozole are more commonly used (Baum, Budzar et al. 2002). Luminal B tumors have a more aggressive phenotype and exhibit expression of ER, presence or absence of Her2 and high levels of Ki67 (Sotiriou, Neo et al. 2003). Her2 positive breast cancers are characterized by high levels of expression of Her2 and have poor prognosis. Basal-like or triple negative breast cancers have the absence of the key receptors of ER, PR and Her2. They have very poor prognosis and high relapse rates and frequently harbor mutations in critical tumor suppressor genes like p53 and BRCA1 (Liedtke, Mazouni et al. 2008, Hernandez-Aya, Chavez-Macgregor et al. 2011). The normal breast subtype is very poorly classified and comprise of

fibroadenomas and some normal breast samples. They have characteristics intermediate between the luminal and basal subtypes, and they do not respond to neoadjuvant chemotherapy (Sotiriou, Neo et al. 2003). Finally, the claudin-like, subtype which was a newly identified subtype has low expression of cell adhesion and tight junction genes. These tumors also have a high expression of genes involved in EMT and exhibit a cancer stem cell phenotype, which makes them resistant to standard chemotherapy (Sotiriou, Neo et al. 2003). Hence, genomic analysis of these tumors might help to understand their mutation profile, and in turn utilize targeted therapy options such as PARP, EGFR inhibitors to treat this subtype (Sotiriou, Neo et al. 2003).

1.1.3. HORMONE RECEPTOR POSITIVE BREAST CANCER – CURRENT TREATMENTS

The hormone receptor (HR) positive subtype is the most common subtype of breast cancer comprising of over 65% of all breast cancer patients (**Figure 1**) (Eroles, Bosch et al. 2012). Due the presence of the hormone receptors, the mainstay treatment for these tumors are hormonal therapy (Goldhirsch, Wood et al. 2011). Typically, early stage HR positive cancers are treated with anti-estrogens, which includes tamoxifen in the case of premenopausal women and aromatase inhibitors in the case of post-menopausal women (Baum, Budzar et al. 2002). The biology of these treatments and the modes of resistance will be discussed in detail later in this chapter. While anti-estrogens are currently administered for a period of 5 years, studies propose longer treatment regimens, which have been shown to improve the disease free survival by 48% when patients were treated with letrozole following 5 year tamoxifen (Jin, Tu et al. 2012). However, this prolonged treatment with tamoxifen or aromatase inhibitors might give rise to side-effects including enhanced risk of endometrial cancer and joint pain or fracture respectively (Jin, Tu et al. 2012, Davies, Pan et al. 2013).

Unlike early HR positive breast cancer, patients presented with metastatic disease are often inherently resistance to the anti-hormonal therapy or acquire resistance within few

months (Piccart, Hortobagyi et al. 2014). Hence, fulvestrant, a drug that directly inhibits and downregulates ER protein is used in the metastatic setting to treat these patients (Agrawal, Robertson et al. 2016). The last few years has seen the advent of targeted therapies, specifically the CDK4/6 inhibitors, which showed great results in clinical trials, by prolonging progression free survival by 12 months, and are currently approved for the treatment of advanced ER positive breast cancers (Clark, Karasic et al. 2016, Sherr, Beach et al. 2016). Finally, several pre-clinical and clinical studies have shown promising results for the use of PI3K and mTOR inhibitors as single or combination treatments in HR positive breast cancer (Paplomata and O'Regan 2014). These targeted therapies and their application has been explained in detail later in this chapter.

1.1.4. HER2 POSITIVE BREAST CANCER – CURRENT TREATMENTS

About 15 to 20% of all breast cancers express Her-2 receptor (**Figure 1**) (Yaziji, Goldstein et al. 2004). Her-2 belongs to the EGFR family and is a trans-membrane receptor that is amplified or overexpressed in breast cancer patients (Owens, Horten et al. 2004). Thus, targeted therapy directly blocking the pathway, such as herceptin, lapatinib, pertuzumab and T-DM1 are currently used to treat early and advanced Her-2 positive breast cancer patients (Romond, Perez et al. 2005, Lewis Phillips, Li et al. 2008, Piccart-Gebhart, Holmes et al. 2016).

Trastuzumab (herceptin) is a monoclonal antibody that binds to and inhibits the extracellular domain of Her-2 receptor. Results from a phase II study conducted on 235 metastatic Her-2 positive breast cancer patients who received chemotherapy vs herceptin + chemotherapy, revealed that herceptin significantly prolonged time to progression and improved objective response rate (~50%) compared to chemotherapy alone (32%) (Slamon, Leyland-Jones et al. 2001). However, over time patients develop resistance to herceptin treatment as well (Oliveras-Ferraros, Vazquez-Martin et al. 2010). This resistance occurs either by loss of the receptor's extracellular domain (which prevents recognition by herceptin) or

formation of a heterodimer complex between the Her-2 and Her-3 receptors (which mediates tyrosine kinase activity despite herceptin treatment) (Hellyer, Kim et al. 2001, Scaltriti, Rojo et al. 2007, Junttila, Akita et al. 2009).

Lapatinib is a tyrosine kinase inhibitor, which binds to the intracellular domain of Her-2 and inhibits its kinase activity. Since lapatinib functions by targeting the receptor's intracellular domain, it can be effective even in tumors that have acquired resistance to herceptin by acquiring modifications in the extracellular domain (Scaltriti, Chandarlapaty et al. 2010). Hence, studies have shown that the combination of lapatinib and trastuzumab in Her-2 positive xenograft model results in enhanced tumor growth inhibition (Scaltriti, Verma et al. 2009).

Pertuzumab, is a monoclonal antibody, similar to herceptin and to bind to the extracellular domain of Her-2 at a site different from that of herceptin, which prevents the hetero-dimerization between Her-2 and Her-3, one of the resistance mechanisms to herceptin (Agus, Akita et al. 2002). Thus, preclinical studies have shown enhanced antitumor activity upon combination treatment with pertuzumab and herceptin (Scheuer, Friess et al. 2009), which was further confirmed in phase III clinical trial show, where the addition of pertuzumab to herceptin in Her-2 positive breast cancer patients proved to be an effective combination strategy (Baselga, Cortes et al. 2012)

TDM-1 is a conjugate of an antibody (herceptin) with a microtubule inhibitor emtasine (T-DM1). Upon binding of the antibody to Her-2 receptor, the chemotherapy agent is internalized and released resulting in cytotoxicity exclusively in the cancer cells. Phillips et al examined the combination of T-DM1 with pertuzumab in a xenograft model of breast cancer using Her-2 expressing cell lines. The results revealed that the combination synergistically inhibited cell proliferation and induced cell death *in vitro* and induced tumor regression *in vivo* (Phillips, Fields et al. 2014).

1.1.5. TRIPLE NEGATIVE BREAST CANCER – CURRENT TREATMENTS

About 15% of all cancers is characterized by the absence of ER, PR and Her2 and termed as Triple Negative or basal tumors (**Figure 1**). They show increased expression of cytokeratin, c-kit and epidermal growth factor receptor and frequently harbor mutations in tumor suppressors like p53 and BRCA (Foulkes, Stefansson et al. 2003). Several critical signaling pathways including MAPK, PI3K-Akt, NF-Kb, Wnt are seen to be deregulated in these cancers (Miki, Swensen et al. 1994). Genetic aberrations like copy number variation, gene amplification is also common in this cancer subtype (Foulkes, Stefansson et al. 2003). Further, epigenetic modifications, mainly DNA methylation has a distinct signature of basal or TNBC tumors (Wooster, Bignell et al. 1995). Given this diversity within the TNBC tumors, a recent study classified them further based on gene expression profile from 386 triple negative tumors (Lehmann, Bauer et al. 2011). This clustering resulted into 6 new TNBC subtypes namely basal, mesenchymal, mesenchymal stem-like (MSL), immunomodulatory (IM), luminal androgen receptor (LAR), basal like 1 (BL1), and basal like 2 (BL2), each having their own characteristic enrichment of genes and pathways (Lehmann, Bauer et al. 2011). For example, the LAR subtype showed enrichment in the androgen receptor signaling and metabolism pathways, while the BL1 subtype showed enrichment of the cell cycle and DNA replication pathways (Lehmann, Bauer et al. 2011). Further, the currently used TNBC cell lines can also be classified into these subtypes based on the gene expression profiles, and will facilitate better pre-clinical investigation (Lehmann, Bauer et al. 2011). Another recent study, which analyzed the RNA and DNA profiles of 198 TNBC tumors, classified them into four distinct molecular subtypes, each having their own characteristic gene amplification or target molecule:

- i) Luminal androgen receptor (LAR) subtype which overexpresses the cell surface mucin MUC1, ii) Mesenchymal (MES) subtype overexpressing the growth factor receptors, PDGF receptor A and c-kit, iii) Basal-like immune suppressed (BLIS) which expresses the immune

suppressing molecule VTCN1 and iv) Basal-like immune activated (BLIS) expresses STAT3 molecules and cytokines (Hartkopf, Taran et al. 2016).

By definition, the triple negative breast cancer (TNBC) tumors are negative for ER, PR and HER-2, and hence these patients will not benefit from hormonal therapy or Her-2 targeting therapies, leaving cytotoxic chemotherapy as the current standard of care for these patients (Rocca, Bravaccini et al. 2014). Overall, among all the breast cancer subtypes, patients with TNBC tumors have the worst prognosis (Carey, Perou et al. 2006, Liedtke, Mazouni et al. 2008). While there is no standard of care drug for TNBC, patients are usually treated with a variety of chemotherapy drugs including anthracyclines, flutoprimidines, taxanes and platinum-based drugs (Levine, Pritchard et al. 2005, Zeichner, Terawaki et al. 2016). Anthracyclines, such as doxorubicin, epirubicin and etoposide, which are one of the most commonly used class of chemo drugs in TNBC, work by intercalating the DNA or inhibiting the topoisomerase II activity (Zeichner, Terawaki et al. 2016). In many cases, the chemotherapy drugs are also given in combination to increase therapeutic benefit (Zeichner, Terawaki et al. 2016). TNBC patients are often given anthracyclines as adjuvant chemotherapy combination with taxanes, such as docetaxel and paclitaxel, which work by binding to β -tubulin and stabilizing the microtubules (Zeichner, Terawaki et al. 2016). Further, TNBC patients can also receive platinum-based chemotherapy, such as cisplatin or carboplatin both as a single agent and in combination therapy, with TNBC patients responding better to the platinum based drugs compared to other subtypes of breast cancer (Levine, Pritchard et al. 2005).

While TNBC tumors are highly prone to genetic mutations compared to the other subtypes, the lack of complete knowledge about the deregulated genes has made it difficult to develop targeted therapies for TNBC (Zeichner, Terawaki et al. 2016). Basal like or TNBC breast tumors frequently have mutations (commonly germline mutations) in the BRCA family of DNA repair genes, which are involved in repairing double strand DNA breaks via the efficient and homologues recombination (HR) pathway (Moynahan, Chiu et al. 1999). About 10-15% of

TNBC patients harbor BRCA-1 mutation and is associated with high-grade tumor (Foulkes, Stefansson et al. 2003). Interestingly, over 75% of the breast cancers that develop BRCA1 mutation belong to the TNBC subtype (Bayraktar, Gutierrez-Barrera et al. 2011). Cells deficient in BRCA1 are unable to repair the double strand breaks efficiently, forcing them to activate the alternate repair pathway, base excision repair (BER), which is regulated by the PARP (poly ADP ribose polymerase) family of proteins and are typically used to repair single strand DNA breaks (Ashworth 2008). PARP is a family of DNA binding proteins that are recruited to the site of single strand DNA breaks and repair them via the BER mechanism (Eustermann, Videler et al. 2011, Langelier, Planck et al. 2011). This results in synthetic lethality and increased genomic instability and apoptosis observed with PARP inhibitor treatment in BRCA1/2 deficient cell lines and $Brca1^{-/-}$, $p53^{-/-}$ mouse model (Farmer, McCabe et al. 2005, Ashworth 2008). Tumors developed in the $BRCA1^{-/-}$ $p53^{-/-}$ mouse model were treated with the PARP inhibitor (olaparib - AZD2281) and cisplatin as single agents or in combination and results revealed that PARP inhibitor treated tumors had improved survival compared to vehicle treatment, and the combination treatment further improved mouse survival, demonstrating synthetic lethality of PARP inhibition with BRCA mutation (Rottenberg, Jaspers et al. 2008).

The PARP inhibitors, olaparib, rucaparib and more recently niraparib have been FDA approved for the treatment of advanced ovarian cancers harboring BRCA1/2 mutation (2017, Lin and Kraus 2017). These drugs are under phase II/III clinical trials in TNBC tumors and are the one of the most promising results targeted therapies currently under investigation for TNBC (2017, Lin and Kraus 2017). A phase II clinical trial in which 54 breast cancer patients harboring BRCA1 or BRCA2 mutation, received two different doses of olaparib, 400 mg twice daily or 100 mg twice daily showed that 41% of the patients who received the higher dose displayed objective response while 22% of those who received the lower dose responded (Tutt, Robson et al. 2010). Olaparib treatment was largely well tolerated with the fatigue, nausea, and anemia being the most common side effects (Tutt, Robson et al. 2010). Another study showed

that the combination of PARP inhibitor (velaparib) with platinum based chemotherapy (carboplatin) in TNBC patients doubled the rate of pathologic complete response 52% compared to 26% with carboplatin alone (2014).

Apart from PARP inhibitors, other targeted treatment strategies that are currently under investigation in TNBC patients include angiogenesis inhibitors, EGFR inhibitors and immunotherapy (Baselga, Gomez et al. 2013, Stagg and Allard 2013, Makhoul, Klimberg et al. 2015). TNBC patients exhibit higher expression of EGFR compared to non-TNBC tumors, which led to a phase II study with the addition of the EGFR inhibitor, cetuximab to cisplatin in metastatic TNBC patients, which showed an increase in the response rate from 10% to 20% and prolonged progression free survival time (Baselga, Gomez et al. 2013). Similarly, TNBC tumor specimens also express higher levels of the angiogenesis factor VEGF, leading to a phase III clinical study combining bevacizumab, the monoclonal antibody against VEGF, along with docetaxel in metastatic Her2 negative breast cancer patients, and showed that addition of bevacizumab delayed tumor progression with no additional toxicity (Senger, Galli et al. 1983, Presta, Chen et al. 1997). (Miles, Chan et al. 2010). Finally, while breast cancer is considered non-immunogenic, they can induce an adaptive immune response and this has led to recent studies aimed at making the breast cancer tumors sensitive to immunotherapy and checkpoint blockade (Stagg and Allard 2013). Studies have shown that the TNBC subtype of breast tumors are particularly attractive for cancer immunotherapy since they have the presence of PD-1+ve TILs (tumor infiltrating lymphocytes) and higher rates of PD-L1 expression by the tumor and the immune cells (Cimino-Mathews, Thompson et al. 2016). This led to a phase I clinical study with the PD-1 inhibitor atezolizumab as a monotherapy in 112 heavily pretreated metastatic TNBC, which showed pathological complete response in 11 patients and partial response in 15 patients (2017). While only 10% of the patients responded to the anti-PD-L1 therapy, those who did had a median duration of response of 21 months (2017), Further, a combination treatment of atezolizumab with paclitaxel in metastatic TNBC patients exhibited an

overall response rate of 41.7% (Sylvia Adams 2016). These studies provide evidence to develop immunotherapy as a promising treatment strategy for TNBC in the future.

1.2. ER POSITIVE BREAST CANCER

1.2.1 ROLE OF ESTROGEN AND ER IN BREAST CANCER

Estrogen, which is the primary female sex hormone is primarily secreted by the ovaries in premenopausal women (Ryan 1959). In post-menopausal women, estrogen is obtained by the enzyme aromatase via the conversion of androgens (testosterone) produced from the adipose tissues (Ryan 1959, Thompson and Siiteri 1974). Estrogen mediated its function and biologic activity by binding to and activating its hormone receptor, estrogen receptor (ER) (Deroo and Korach 2006). There are two estrogen receptors, ER α and ER β , encoded by ESR1 and ESR2, respectively (Deroo and Korach 2006). The binding of estrogen to the receptor facilitates dimerization of ER and translocation into the nucleus, where it binds to ER responsive elements (ERE element) on the promoter region of the target genes (Yi, Driscoll et al. 2002). This is the classical and canonical pathway by which ER functions as a transcription factor in response to estrogen (Deroo and Korach 2006). The transcriptional function of the estrogen receptor is regulated by several coactivator and corepressor proteins, which interact with ER at the DNA and regulate gene transcription (Deroo and Korach 2006). Some of the crucial co-activators and co-repressors in breast cancer include, TRAP-220 (a link between ER alpha and RNA polymerase II), CARM1 (which is overexpressed in breast cancer), nuclear receptor co-repressor NCoR (represses ER gene transcription), RTA (repressor of tamoxifen activity, interacts with and represses ER) (Deroo and Korach 2006). Additionally, ER signaling can be directly activated in a ligand (estrogen) independent manner through MAPK and cAMP induced protein kinase A (PKA) (Arnold, Obourn et al. 1995, Chen, Washbrook et al. 2002, Carascossa, Dudek et al. 2010).

Data from clinical and animal studies show that estrogen and ER play a crucial role in mammary development and breast cancer (Deroo and Korach 2006). Two current hypothesis have been proposed to functionally explain this relationship: i) Increased estrogen activates ER and ER signaling, which increases cell division and DNA synthesis and the risk for replication errors, resulting in the acquisition of detrimental mutations, which lead to mammary tumor formation (Henderson and Feigelson 2000); ii) estrogen metabolism produces genotoxic products which directly induce DNA damage leading to mutations and cancer formation. Further, epidemiologic studies also show a strong link between estrogen and breast cancer formation (Trichopoulos, MacMahon et al. 1972), with greater duration of exposure to estrogen increasing the risk for breast cancer (Clavel-Chapelon and Group 2002, Press and Pharoah 2010).

1.2.2. CURRENT TREATMENTS FOR ER POSITIVE BREAST CANCER

Due to significant role of estrogen pathway in breast cancer and given that 65% of breast cancers being estrogen receptor (ER) positive, drugs targeting the hormone receptor have been developed and are currently used (**Table 2**). The estrogen pathway can be targeted by three different strategies: i) selective estrogen receptor modulator (SERM), such as tamoxifen, which inhibits binding of estrogen to ER (Sini, Cinieri et al. 2016); ii) selective estrogen receptor down regulator (SERD) such as fulvestrant, which competitively inhibits ER, by binding to it and degrading it (Dauvois, White et al. 1993, Nicholson, Gee et al. 1995); and iii) aromatase inhibitors (AI), which are primarily used in post-menopausal women and target aromatase, the enzyme required for the conversion of androgens to estrogen (Furet, Batzl et al. 1993). Recent years have witnessed the development of more specific and targeted agents such as CDK4/6 inhibitors, PI3K and mTOR inhibitors (Paplomata and O'Regan 2014, Sherr, Beach et al. 2016). The development and current clinical use of these drugs have been discussed in detail in sections below.

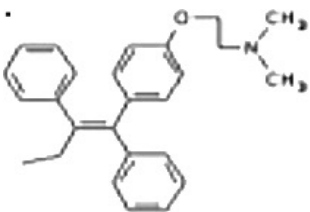
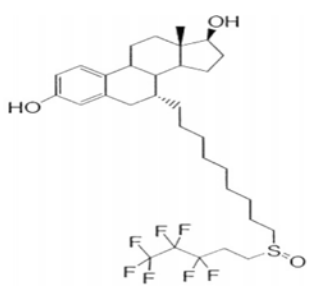
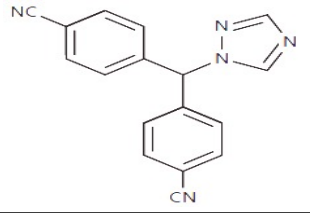
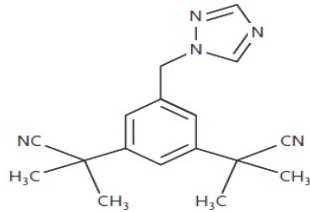
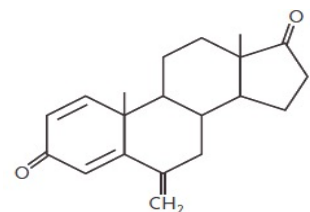
Class of drug	Drug	Structure
Selective estrogen receptor modulator (SERM)	Tamoxifen	
Selective estrogen receptor downregulator (SERD)	Fulvestrant	
Aromatase inhibitors	Letrozole	
	Anastrozole	
	Exemestane	

Table 2: Anti-estrogens: Table listing the anti-estrogens used for the treatment of ER positive breast cancer and their chemical structures.

1.2.3. SERM - TAMOXIFEN

The rationale for developing an anti-estrogen to treat breast cancer arises to from the principle block hormone production, which was achieved in the 1970s by irradiate ovaries of newly diagnosed ER positive breast cancer patients (Lees, Giuffre et al. 1980). The first trial

with tamoxifen (originally known as IC146474) in 1971 reported response in 10 out of 46 breast cancer patients (Cole, Jones et al. 1971), and the drug has revolutionized the field of breast cancer treatment since then. The primary mechanism of action of tamoxifen as a selective estrogen receptor modulator (SERM) involves binding of the drug to the estrogen receptor (ER) and preventing the binding of estrogen to ER, thus turning off the ER signaling pathways. The ability of tamoxifen to block the binding of estrogen to ER and prevent the induction and growth of ER dependent tumors was first tested in ER positive carcinogen-induced rat mammary carcinomas (Jordan 1976, Jordan and Dowse 1976). The anti-tumor effects of tamoxifen were further confirmed in a nude mouse model with subcutaneously implanted (in the presence of estrogen pellets) ER positive breast tumor (generated by injecting ER positive breast cancer cells lines, MCF7 or T47D) treated with daily dose of tamoxifen, exhibiting significant anti-tumor activity (Long, Jelowac et al. 2004). This led to about 28 clinical studies conducted in over 16,000 breast cancer patients, the consensus of which demonstrated that tamoxifen treatment provides significant advantage with reduction in mortality, leading to the recommendation that tamoxifen should be also be used as an adjuvant therapy for postmenopausal ER positive breast cancer patients with breast cancer (1985, Early Breast Cancer Trialists' Collaborative 1988).

Further, animal studies in mice with low burden or early mammary tumors showed that long term tamoxifen treatment in animals is better than shorter term adjuvant therapy in providing better efficacy and a longer tumor free state (Jordan and Brodie 2007). These studies combined with results from pilot clinical studies showed that long term tamoxifen treatment would prove to be more effective in treating women with ER positive breast cancer, and led to the current treatment regimen of 5-year anti-estrogen treatment. (Jordan and Brodie 2007). However, one of the concerns with long terms anti-estrogens is the non ER associated and side effects with this treatment (Love, Mazess et al. 1992, Zidan, Keidar et al. 2004). For example, tamoxifen has been shown to have oncogenic effect on uterus, results in higher

incidence (rate of 1.2% annually) of endometrial cancer in patients receiving long-term tamoxifen (Fisher, Costantino et al. 1994). Patients receiving long term estrogen treatment also suffered from higher rate of hot flashes, vaginal discharge and menstrual irregularities (Powles, Jones et al. 1994). On the other hand, tamoxifen treatment has beneficial effects such as reduction in cholesterol levels and decreased death from myocardial infarction (Bagdade, Wolter et al. 1990, Love, Newcomb et al. 1990, Love, Wiebe et al. 1991).

While tamoxifen has proven to be highly effective over the years in treating ER positive breast cancer, one concern is the development of resistance over time (Toy, Shen et al. 2013). Hence, several studies over the years have focused on understanding the molecular mechanism of resistance to tamoxifen, which include mutation of the estrogen receptor, loss of ER expression and non-canonical ER signaling pathways (Encarnacion, Ciocca et al. 1993, Fuqua, Wiltchke et al. 2000). Mutations in ER are more commonly detected in the resistant tumors compared to treatment naïve tumors (Toy, Shen et al. 2013). These mutations in the receptor allow ER to dimerize even in the absence of the ligand (estrogen) (Toy, Shen et al. 2013). This would result in activation of the downstream ER signaling pathway, even in the presence of anti-estrogens such as tamoxifen (Toy, Shen et al. 2013). Specifically, a study in 59 tissues with hyperplasia observed a Lys to Arg mutation (K303R) in the estrogen receptor in 20 tissues (Fuqua, Wiltchke et al. 2000). While mutations in ER are not common, they are frequently found in metastatic patients who have progressed on anti-estrogen therapy (Toy, Shen et al. 2013). These mutations are frequently located in the ligand-binding domain of the receptor and facilitates estrogen independent activity of the mutants (Toy, Shen et al. 2013). Further, loss of expression of the hormone receptor ER α is another established mechanism of resistance to tamoxifen (Encarnacion, Ciocca et al. 1993, Ellis, Tao et al. 2008). Given that tamoxifen functions by binding direct ER, loss of the receptor makes the cells / tumors become unresponsive to the drug (Ellis, Tao et al. 2008). Finally, another known mechanism of resistance to tamoxifen is the non-canonical crosstalk between ER and other major growth

factor signaling pathways such as Her-2, PI3K and MAPK pathways (Campbell, Bhat-Nakshatri et al. 2001, Riggio, Polo et al. 2012). ER can activate growth factor receptors such as Her-2 and EGFR (Lee, Cui et al. 2001), while PI3K and MAPK pathways can phosphorylate and activate ER in a ligand independent manner (Campbell, Bhat-Nakshatri et al. 2001, Riggio, Polo et al. 2012), ultimately resulting in cellular proliferation even in the absence of estrogen and resistant to tamoxifen treatment (Shou, Massarweh et al. 2004, Britton, Hutcheson et al. 2006). This suggests combination treatment strategies with the inhibitors targeting these signaling pathways to combat tamoxifen resistance. This has led to pre-clinical studies with the combination of tamoxifen and trastuzumab or lapatinib or the EGFR inhibitor, gefitinib, which significantly prolonged response to tamoxifen and delayed the acquired resistance (Benz, Scott et al. 1992, Massarweh, Osborne et al. 2008). Further, results from a phase II clinical study showed the efficacy of trastuzumab in breast cancer patients who have become resistant to tamoxifen (Kaufman, Mackey et al. 2009).

1.2.4. SERD - FULVESTRANT

Fulvestrant, an analogue of 17β -estradiol, acts as an anti-estrogen by selectively binding to the estrogen receptor (ER) preventing its dimerization and nuclear localization (Fawell, White et al. 1990, Dauvois, White et al. 1993). The drug also mediates degradation of ER, resulting in complete shutdown of the ER signaling pathway (Nicholson, Gee et al. 1995). Given that its mechanism of action is different from that of tamoxifen, early clinical studies focused on utilizing fulvestrant to treat patients who have acquired resistance to prior tamoxifen or aromatase inhibitor therapy (Freedman, Amir et al. 2009). A study in 19 patients who progressed on tamoxifen treatment showed that fulvestrant can successfully extend the duration of response of breast tumors to anti-estrogens (Howell, DeFriend et al. 1995). More recently, clinical studies have also been conducted to test the efficacy of fulvestrant in treatment naïve patients (Robertson, Llombart-Cussac et al. 2009). For example, on

comparison with the aromatase inhibitor, anastrozole in a phase II study in advanced post-menopausal breast cancer patients, patients on the fulvestrant arm had a longer time to progression compared to the anastrozole arm (Robertson, Llombart-Cussac et al. 2009). Further, a recently published phase III study confirmed that fulvestrant treatment improved progression free survival by 2.8 months compared to anastrozole treatment arm (Robertson, Bondarenko et al. 2016). Moreover, unlike tamoxifen, fulvestrant does not have an oncogenic effect and hence does not increase the risk of endometrial cancer (Bergman, Beelen et al. 2000). Thus, these studies show that fulvestrant can serve as an effective anti-estrogen treatment in early and advanced (resistant to other anti-estrogen treatment) stage ER+ breast cancer patients.

1.2.5. AROMATASE INHIBITORS

Aromatase inhibitors (AI) are a class of antiestrogens, primarily used to treat post-menopausal women with ER positive breast cancer, and functions by inhibiting the activity of aromatase, the enzyme required for the generation of estrogen in post-menopausal women (Yue, Wang et al. 2005). They are typically divided into two classes based on their structure: i) non-steroidal AIs such as letrozole and anastrozole and ii) steroidal AI such as exemestane (Yue, Wang et al. 2005). The non-steroidal AIs, letrozole and anastrozole, competitively inhibit aromatase in a reversible manner by binding to the enzyme non-covalently (Soudon 2000). They are FDA approved and are currently the standard of care drugs for post-menopausal ER positive breast cancer patients (Howell, Cuzick et al. 2005). The steroidal class of AI, exemestane, resembles in structure to androstenedione and inhibits aromatase in an irreversible manner by binding to the enzyme covalently (Oliveras-Ferraros, Vazquez-Martin et al. 2010). Exemestane has also been FDA approved for use in postmenopausal ER positive breast cancer patients (Coombes, Goss et al. 1984).

Numerous clinical studies have been performed to compare the efficacy of aromatase inhibitors against tamoxifen in post-menopausal breast cancer patients (Mouridsen, Gershanovich et al. 2001, Breast International Group 1-98 Collaborative, Thurlimann et al. 2005, Howell, Cuzick et al. 2005). Treatment of anastrozole in combination with tamoxifen a phase III randomized clinical trial in the adjuvant setting showed that anastrozole treated patients had significantly higher disease-free survival, time to recurrence and time to distant metastasis compared to treatment with tamoxifen alone (Howell, Cuzick et al. 2005). Further, to test the effectiveness of AI in the adjuvant setting, a phase III clinical trial was performed in 8010 postmenopausal ER+ non-metastatic patients by comparing long term letrozole treatment to tamoxifen (Breast International Group 1-98 Collaborative, Thurlimann et al. 2005). Results showed that the letrozole arm had greater disease-free survival with lower rates of distant metastasis compared to tamoxifen treatment arm (Breast International Group 1-98 Collaborative, Thurlimann et al. 2005). A similar phase III clinical study in advanced (stage IIIb with recurrent tumors) postmenopausal ER positive breast cancer where patients received letrozole or tamoxifen as first line therapy revealed that a significantly higher (increased by 15 weeks) time to progression and higher rate of objective response in the letrozole treated patients compared to tamoxifen treatment arm, indicating that AI treatment with letrozole is also beneficial in the advanced disease stage (Mouridsen, Gershanovich et al. 2001).

While aromatase inhibitors have been successful in the treating advanced and treatment naïve ER positive post-menopausal breast cancer patients, these tumors tend to eventually acquire resistance via numerous mechanisms (Jordan and Brodie 2007, Ma, Reinert et al. 2015). Research in the recent years have hence focused on elucidating these mechanisms, including androgen receptor (AR) expression, signaling through growth receptor pathways such as Her-2, PI3K and MAPK pathways, epithelial mesenchymal transition (EMT) and cancer stem cells (Ma, Reinert et al. 2015). Androgen receptor (AR) is a nuclear hormone receptor, similar to AR that gets activated when bound to androgen regulates downstream

effector genes (Schoenmakers, Alen et al. 1999), Since AR can activate the ER pathway independent of estrogen, it has been shown to mediate de novo resistance of AIs (Rechoum, Rovito et al. 2014). Hence, treatment with an AR antagonist (abiraterone) or an ER degrading drug (fulvestrant) can restore sensitivity to the aromatase inhibitors even in the AR overexpressing resistant cell (Rechoum, Rovito et al. 2014). Similar to tamoxifen resistance, the activation of the parallel growth signaling pathways is a common mechanism by which tumors acquire resistance to AIs (Ma, Reinert et al. 2015). This involves upregulation and activation of the growth factor receptors such as PI3K, MAPK, Her-2 and their downstream pathway proteins, thus enabling the AI resistant cells to adapt to and survive in low estrogen conditions (Sabnis, Schayowitz et al. 2009, Ma, Reinert et al. 2015). Hence, the AI resistant cells are significantly sensitive to the MAPK inhibitor (PD98059) or a MEK inhibitor (UO126) resulting in decreased proliferation (Jelovac, Sabnis et al. 2005). Moreover, drugs targeting the PI3K downstream protein, mTOR (everolimus) have been tested clinically (phase III study) in combination with exemestane in ER+ patients who have progressed on aromatase inhibitors (anastrozole or letrozole) and showed that addition of everolimus significantly improved progression-free survival in these patients (Baselga, Campone et al. 2012). Thus, these studies show that combined targeting of these growth signaling pathways might help re-sensitize the cells to AI treatment. Further, studies have shown a link between mutations in ER and other genes, and resistance (intrinsic and acquired resistance) to aromatase inhibitors (Ma, Reinert et al. 2015). A study using whole genome sequencing of 77 ER positive tumor biopsies before and after treatment with aromatase inhibitors, showed a correlation between ESR1 mutations and response to treatment (Ellis, Ding et al. 2012). This study also examined mutations in other genes such as PI3K, p53, Rb and p27, and showed that mutations in PI3K (41.3%) and p53 (16.1%) correlated with resistance (measured by change in Ki67) to aromatase inhibitor therapy (Ellis, Ding et al. 2012). A more recent study examined the ESR1 mutations in the plasma and correlated it with response to aromatase inhibitors (exemestane) or fulvestrant

(Fribbens, O'Leary et al. 2016). Results showed that while ESR1 mutations did not affect response to fulvestrant, a correlate between mutations and resistance to exemestane was observed (Fribbens, O'Leary et al. 2016). Finally, a link between EMT, cancer stem cells and resistance to AIs has also been shown by *in vitro* studies (Creighton, Li et al. 2009).

Further, ER alpha has been shown to promote progression through the cell cycle by binding to p27, which is one of the mechanisms by which ER alpha regulates cell proliferation (Moghadam, Hanks et al. 2011). A recent study shows a novel mechanism by which anti-estrogens control the cell cycle, where the stabilization of ER alpha delays cell cycle progression leading cell cycle arrest (Moghadam, Hanks et al. 2011). Results from this study also showed that ER alpha is cell cycle regulated, and the presence or absence of the estrogen ligand on the receptor (ER alpha) determines the duration of the cell cycle in both ER positive (MCF7) and TNBC cell lines (MDA-MB-231) (JavanMoghadam, Weihua et al. 2016). Thus, deregulation of the cell cycle is a mechanism of resistance to anti-estrogens, making it an attractive drug target in ER positive breast cancer.

1.3. CELL CYCLE

1.3.1. CELL CYCLE REGULATION

Cell cycle is the complex and highly regulated process by which a cell divides to form two daughter cells (Vermeulen, Van Bockstaele et al. 2003). The normal mammalian cell cycle typically lasts for 24 hours and comprises of two major phases, the interphase, which is the period during which the cells grow, undergo DNA replication and prepare for cell division and the mitotic phase, when the DNA, nuclear material and cytoplasm is separated into two daughter cells (Harper and Brooks 2005). The interphase in turn comprises of 3 phases, i) G1 phase, which is the longest phase of the cell cycle and the phase when the cells prepare for DNA synthesis, ii) S phase, the phase when the replication of the DNA content occurs, and iii)

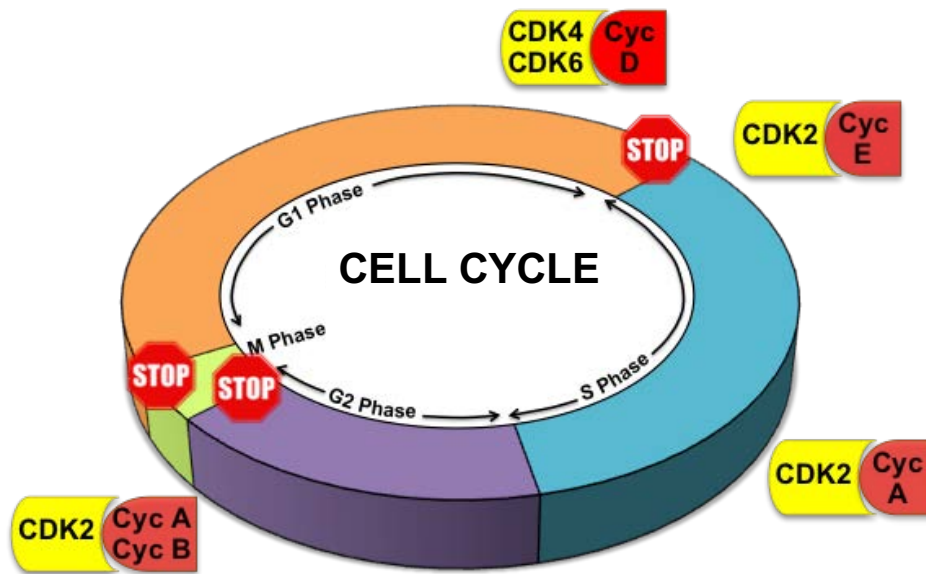


Figure 2: Mammalian cell cycle: Model depicting the mammalian cell cycle with its different phases, checkpoints and regulatory proteins, CDKs and cyclins

G2 phase, the phase when the cells increase their protein and other content to prepare for mitosis or cellular division (**Figure 2**) (Harper and Brooks 2005, Malumbres and Barbacid 2009). The mitotic phase or the M phase in turn comprises of four phases called prophase, metaphase, anaphase and telophase (Harper and Brooks 2005). The M phase is characterized by the condensation of the chromosomes, formation of the spindle fibers which enables separation of the sister chromatid and finally leading to cytokinesis, which gives rise to two identical daughter cells (Harper and Brooks 2005).

Tight regulation of the cell cycle is necessary for controlled cell division in a normal cell (Vermeulen, Van Bockstaele et al. 2003). This is achieved by regulatory checkpoints at different points in the cell cycle and through regulatory proteins – the CDKs and cyclins (Harper and Brooks 2005). There are three cell cycle checkpoints, namely i) G1/S, which ensures that there is no DNA damage and that the cell has accumulated sufficient materials for DNA synthesis, ii) G2/M, which ensures that the replicated DNA is intact and the proteins required for cell division are present and iii) M phase checkpoint, which is present at the end of the metaphase to ensure the proper attachment of the spindle fibers to the sister chromatids

(Figure 2) (Harper and Brooks 2005, Malumbres and Barbacid 2009). These checkpoints help regulate which cells can move forward and complete the cell division process (Malumbres and Barbacid 2009). The presence of any defect in the normal cell cycle process will halt the cells at checkpoint until the defect is repaired (Vermeulen, Van Bockstaele et al. 2003). The G1/S checkpoint is the most crucial transition checkpoint, since cells that have passed this checkpoint no longer rely on external stimuli are committed to divide (Bertoli, Skotheim et al. 2013).

Progression through the cell cycle is further regulated by the cyclin dependent kinases (CDKs) and their activating subunit, the cyclins **(Figure 2)** (Satyanarayana and Kaldis 2009). While CDKs are expressed at constant levels throughout the cell cycle, the expression levels of the cyclins oscillate through the different phases and regulate the kinase activity of the cyclin-CDK complex (Malumbres and Barbacid 2009). The activity of CDKs are inhibited by the cyclin dependent kinase inhibitors (CKIs), which belong to two families of CKIs, INK family proteins that inhibit CDK4/6 such as p15, p16, p18 and p19 and the Cip/Kip family proteins that inhibit CDK1 and CDK2 such as p21 and p27 (Hirai, Roussel et al. 1995) (Ball, Lain et al. 1997). Rb protein, a well-known tumor suppressor regulates the G1/S checkpoint (Malumbres and Barbacid 2009). While the hypophosphorylated state of Rb keeps the transcription factor E2F in its inactive state, the sequential phosphorylation of Rb by cyclin D-CDK4/6 and cyclin E-CDK2 complexes inactivates the protein, releasing E2F, which in turn transcriptionally activates genes needed for DNA synthesis (Ikeda, Jakoi et al. 1996, Connell-Crowley, Harper et al. 1997). Since the expression of cyclin E and cyclin A are also regulated by E2F, cyclin E protein levels increase through the G1 phase, reaching its peak at the of G1/S transition, where its activity is required for entry into the S phase (Duronio, Brook et al. 1996). Further, the expression of cyclin A increases through G2 phase and is replaced by cyclin B during mitosis to form a complex with CDK1 and enable cells to cross the G2/M checkpoint and enter mitosis (Lindqvist, van Zon et al. 2007). Finally, the degradation of cyclin B is required for the cells to exit mitosis

Gene deleted	Phenotypes	Lethality	Fertility
Cdk1	None	E2.5	
Cdk2	Reduced body size, impaired neural progenitor cell proliferation	Viable	Both males and females are sterile
Cdk4	Reduced body size, insulin deficient diabetes	Viable	Male and female infertility
Cdk6	Hypoplasia of thymus and spleen and defects in hematopoiesis	Viable	Fertile
Cdk2/4	Heart defects	E15.5	
Cdk2/6	Reduced body size, hematopoietic defects	Viable	Both male and female are sterile
Cdk4/6	Severe anemia	E14.5-E18.5	
Cdk2/4/6	Heart defects, hematopoietic defects	E13.5	
Cdk5	Severe neurological defects	Died immediately after birth	Not known
Cdk11	Mitotic defects	E3.5	Not known
Cyclin A1	No abnormalities	Viable	Only males are sterile
Cyclin A2	Not-known	E5.5	Not-known
Cyclin B1	Not-known	E10.5	Not-known
Cyclin B2	No abnormalities	Viable	Fertile
Cyclin D1	Reduced body size, neurological abnormalities, mammary gland defects	Viable	Fertile
Cyclin D2	Defects in B-lymphocyte and pancreatic-cell proliferation, adult neurogenesis and hypoplastic thymus	Viable	Females sterile; males fertile with hypoplastic testes
Cyclin D3	Defects in T-lymphocyte development	Viable	Fertile
Cyclin D1/D2	Reduced body size, hypoplastic cerebella	Viable but die within 3 weeks	
Cyclin D1/D3	Neurological abnormalities	Die soon after birth	
Cyclin D1/D2/D3	Proliferative defects in hematopoietic cells and cardiac myocytes	E16.5	
Cyclin E1	No abnormalities	Viable	Fertile
Cyclin E2	No abnormalities	Viable	Reduced male fertility
Cyclin E1/E2	Severe defects in extraembryonic tissues	E11.5	Not known

Table 3: Defects in CDK and cyclin knockout mice: Table summarizing the defects and survival of mice without knockout in the different cyclins and CDKs

(Malumbres and Barbacid 2009). The expression of the different cyclins and the activity of the CDKs tightly regulate the cell cycle and progression through the cell cycle checkpoints. To understand in detail the function of the different cyclins and the CDKs, knockout mice have been made over the years for the cyclin or the CDK proteins alone or multiple cyclins and CDKs in combination (**Table 3**).

1.3.2. CELL CYCLE IN CANCER

Deregulation of cell cycle is a common hallmark in cancers, causing uncontrolled proliferation and cell division (**Figure 3**), resulting in tumorigenesis (Malumbres and Barbacid 2009). This occurs due to the numerous alterations present in the components of cell cycle (CDKs, cyclins and CKIs) seen in cancers (Vermeulen, Van Bockstaele et al. 2003). For example, cyclin D1 is amplified in about 15% and overexpressed in about 50% of all breast cancers (Bartkova, Lukas et al. 1995). While cyclin E is rarely amplified, it is overexpressed in about 40% of all breast cancer, contributing to poor prognosis in breast cancer and hyper activation of CDK2 (Keyomarsi, Conte et al. 1995, Hunt, Karakas et al. 2016). Further, high cyclin B1 expression correlated with poor overall survival in breast cancer (Vermeulen, Van Bockstaele et al. 2003). Apart from aberrant expression of the cyclins, CKIs are also deregulated in cancer. p27 has lower expression and is seen to be mislocalized (localized in the cytoplasm instead of the nucleus) in breast cancer, thus correlating with high tumor grade, absence of ER and decreased disease free survival (Wu, Shen et al. 1999). Further, hypermethylation is seen about 20 to 30% of breast cancer, which can inactivate the CKIs by methylation at the promoter region, as seen with silencing of p16 (Merlo, Herman et al. 1995). p21, while is rarely mutated in breast cancer, p53, which is transcription factor of p21 is mutated in 54-82% of TNBC tumors (Vermeulen, Van Bockstaele et al. 2003). Thus, these alterations and the deregulated cell cycle make it an attractive target for drug development.

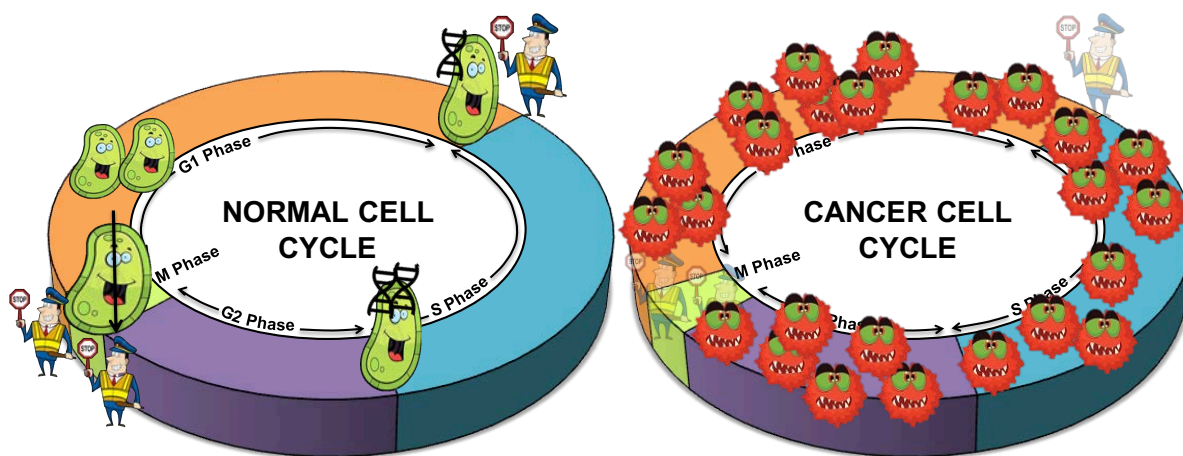


Figure 3: Cell cycle in normal and cancer cells: Models showing the regulation of the cell cycle in normal vs cancer cells. Normal cell cycle depicts the growth and division of the cells (green cartoon) along the difference phases. The cancer cell cycle depicts the uncontrolled division of the cancer cells (red cartoon).

1.3.3. CDK INHIBITORS IN BREAST CANCER

Given the importance of the cell cycle and CDKs in cancer, several drugs have been developed over the years. Typically, CDK inhibitors are small molecule inhibitors that inhibit the CDK kinase activity by competitively binding to the ATP pocket of the CDK proteins (De Azevedo, Leclerc et al. 1997). The first generation CDK inhibitors that were developed lacked specificity to a particular CDK and underwent clinical trials without a biomarker, resulting in increased toxicity and early termination of the clinical trials (Asghar, Witkiewicz et al. 2015). Hence these drugs cannot be used effectively as monotherapy (Asghar, Witkiewicz et al. 2015). Recent studies have given rise to a new class of more specific and potent CDK4/6 inhibitors, namely palbociclib, ribociclib and abemaciclib (Fry, Harvey et al. 2004). Given their promising results in clinical studies, they were FDA approved and are currently used to treat advanced ER positive breast cancer (O'Leary, Finn et al. 2016).

Flavopiridol (alvociclib) is one of the first generation of CDK inhibitors that was tested clinically. While flavopiridol can target CDK2, it is a pan-CDK inhibitor as it inhibits multiple other CDKs such as CDK1, CDK4, CDK6, CDK7 and CDK9 (Carlson, Dubay et al. 1996). Treatment with flavopiridol results in cell cycle arrest and apoptosis as measured by Annexin V

(Wirger, Perabo et al. 2005). A phase I study examined flavopiridol in two breast cancer patient among a cohort of 34 patients with advanced solid tumors, and showed no response in both the two breast cancer patients (Ramaswamy, Phelps et al. 2012). Another phase I trial which tested the combination of flavopiridol with docetaxel in breast cancer did not yield satisfactory results and had high toxicity (neutropenia) in most patients (Tan, Yang et al. 2004). Given their high levels of toxicity and lack of efficacy, flavopiridol was not pursued clinically beyond phase II in advanced colorectal cancer patients and malignant melanoma (Aklilu, Kindler et al. 2003, Burdette-Radoux, Tozer et al. 2004).

Roscovotine (seliciclib), is another first generation CDK2 inhibitor that can inhibit CDK1, CDK5, CDK7, and CDK9 in addition to CDK2 (IC₅₀ 0.7 μ M) (Meijer, Borgne et al. 1997). Pre-clinical analysis of roscovotine *in vitro* using ER positive breast cancer cell lines showed that degu treatment resulted in cell cycle arrest (G2 arrest) and cell death via apoptosis and enhanced anti-proliferative activity when combined with tamoxifen (Gritsch, Maurer et al. 2011). The effect of roscovotine of breast tumorigenesis was interrogated in an MCF7 xenograft mouse model, where treatment of tumors with roscovotine or doxorubicin resulted in decreased tumor volume in almost 50% of mice, with combination of roscovotine and doxorubicin resulting in a 70% tumor shrinkage. (Appleyard, O'Neill et al. 2009). Clinically, in a phase I study of 21 patients bearing solid tumors, treatment with roscovotine at a range of doses resulted in stable disease in about 8 out of the 21 patients (Benson, White et al. 2007).

Dinaciclib (SCH 727965), is another small pan-CDK inhibitor that targets multiple CDKs including CDK2 (IC₅₀=1nM), CDK5 (IC₅₀=1nM), CDK1 (IC₅₀=3nM) and CDK9 (IC₅₀=4nM) (Parry, Guzi et al. 2010). Pre-clinical studies have primarily tested the use of dinaciclib in triple negative cell lines, where it showed significant anti-proliferative effects *in vitro* and tumor regression in xenograft tumors *in vivo* (Horiuchi, Kusdra et al. 2012). Further, studies in ovarian cancer cell line A2780 showed that dinaciclib treatment decreased Rb phosphorylation and induced apoptosis (measured by PARP cleavage) (Chen, Xie et al. 2015). This led to clinical

studies in breast cancer patients, with a randomized phase II trial in patients with advanced breast cancer (patients who failed previous chemotherapy), who received either dinaciclib (50mg/m² once every three weeks) or capecitabine (Mita, Joy et al. 2014). While the study had to be stopped due to increased toxicity (neutropenia in 47% of patients and leukopenia in 21% of patients) and lower progression free survival in the dinaciclib arm, significant antitumor activity was seen in 2 out of 7 breast cancer (Mita, Joy et al. 2014). Further, a phase I clinical trial conducted at MD Anderson Cancer Center, which tested the combination of dinaciclib and epirubicin in advanced metastatic triple negative breast cancer patients also showed severe side effects (febrile neutropenia), resulting in early termination of the study (Mitri, Karakas et al. 2015). This suggests that while dinaciclib has shown promise in pre-clinical studies in breast cancer, the dosage and treatment regimen has to be optimized for efficacious clinical studies.

1.4. CDK4/6 INHIBITORS IN BREAST CANCER

1.4.1. DISCOVERY AND DEVELOPMENT OF CDK4/6 INHIBITORS

While pan-CDK inhibitors have been available since the early 1990's, they were mostly non-specific and toxic, limiting their clinical applicability (Asghar, Witkiewicz et al. 2015). The emerging significance of the G1/S checkpoint and the deregulation of the CDK4/6-cyclin D pathway in cancers fueled efforts for the discovery a selective and potent drug targeting CDK4/6 (Sherr, Beach et al. 2016). These drugs target the kinase activity of CDK4 and CDK6, resulting in decreased phosphorylation of Rb, which keeps the Rb protein bound to the E2F transcription factor (**Figure 4**) (Bertoli, Skotheim et al. 2013). This prevents E2F mediated transcription of the cell cycle proteins, resulting in the arrest of the cells at the G1 phase of the cell cycle (Bertoli, Skotheim et al. 2013). Thus, chemists at Parke-Davis developed the specific CDK4/6 inhibitor, PD0332991, which eventually became Pfizer's Palbociclib (Ibrance™) (Sherr, Beach et al. 2016). Palbociclib is now FDA approved for clinical use in advanced ER positive breast cancer (O'Leary, Finn et al. 2016). The other two CDK4/6 inhibitors, ribociclib and

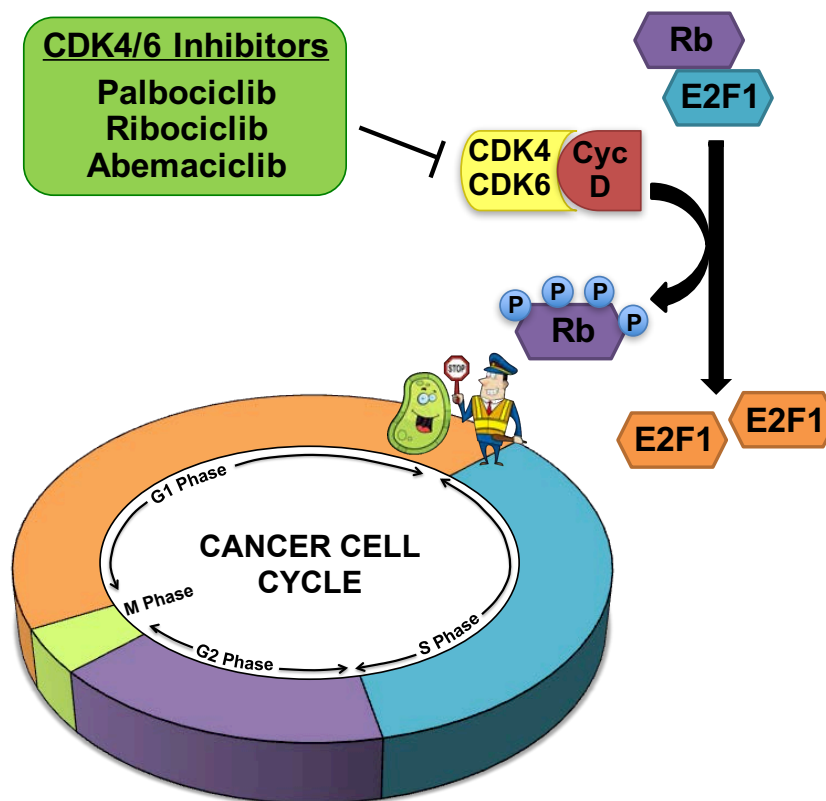


Figure 4: CDK4/6 inhibitors in cancer cells: Models how treatment with the CDK4/6 inhibitors molecular affects the G1/S transition and the cell cycle

abemaciclib were subsequently developed by Novartis and Eli Lilly respectively (O'Leary, Finn et al. 2016). Of these, ribociclib was recently approved for clinical use in advanced ER positive breast cancer and abemaciclib has obtained breakthrough FDA approval in the same group of cancers (Sherr, Beach et al. 2016). **Table 4** summarizes the basic characteristics of the three CDK4/6 inhibitors, with the stage of approval and clinical characteristics. The pre-clinical and clinical development of the individual CDK4/6 inhibitors along with their future utility has been described in detail in the sections below.

1.4.2. PALBOCICLIB

Palbociclib (PD-0332991) is an oral specific and potent inhibitor of the CDK4/6 developed by Pfizer (O'Leary, Finn et al. 2016). A study in 2009 examined the sensitivity (IC50

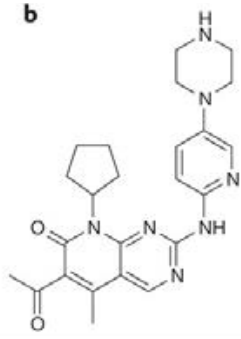
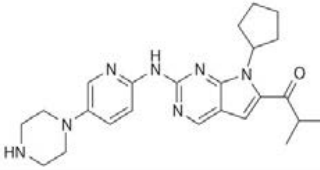
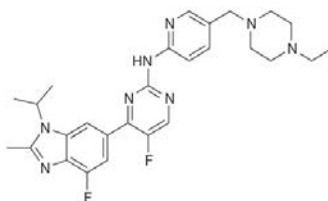
Drug	Palbociclib (Pfizer) (PD0332991, Ibrance)	Ribociclib (Novartis) (LEE011, Kisqali)	Abemaciclib (Eli Lilly) (LY2835219)
Structure			
Approval status	FDA approved - 1 st and 2 nd line ER+ HER2- metastatic breast cancer (2015)	FDA approved – 1 st line ER+ HER2- metastatic breast cancer (2017)	FDA breakthrough designation (2016)
IC ₅₀ (in vitro kinase assay)	CDK4 (D1): 11 nM CDK4 (D3): 9 nM CDK6 (D2): 15 nM CDK1: >10 µM CDK2: >10 µM	CDK4: 10 nM CDK6: 39 nM CDK1: >100 µM CDK2: >50 µM	CDK4 (D1): 0.6-2 nM CDK6 (D1): 2.4-5 nM CDK 9: 57 nM CDK1: > 1 µM CDK2: > 500 nM
PK	Tmax 4.2-5.5 hr t _{1/2} 25.9-26.7 hr	Tmax 4 hr t _{1/2} 24-36 h	Tmax 4-6 hr, t _{1/2} 17-38 hr (crosses blood brain barrier)
PD	Reduced RB phosphorylation in paired tumor biopsies, and reduced fluoro-thymidine-PET uptake	Reduced RB phosphorylation and Ki67 expression in paired tumor biopsies	Reduced RB phosphorylation and topoisomerase IIα expression in paired tumor and skin biopsies
Dosing	125 mg daily (3 weeks on 1 week off)	600 mg daily (3 weeks on 1 week off)	200 mg twice daily (continuous dosing)
Dose-limiting toxicities	Neutropenia, Thrombocytopenia	Neutropenia, Thrombocytopenia	Fatigue

Table 4: CDK4/6 inhibitors in breast cancer: Table showing the CDK4/6 inhibitors that are currently used in breast cancer and their characteristics.

value) of a panel of breast cancer cell lines to palbociclib treatment, which showed that most of the sensitive cell lines belonged to the ER positive subtype of breast cancer (Finn, Dering et al. 2009). Further, analysis of the gene expression profile between sensitive and resistant lines revealed that sensitive lines have a higher expression of cyclin D1, Rb1 and reduced

expression or loss of p16 (Finn, Dering et al. 2009). Mechanistically, palbociclib decreased Rb phosphorylation and induced G1 arrest exclusively in the sensitive cell lines (Finn, Dering et al. 2009). A more recent study that examined the changes in gene expression in the MCF7 cell line following palbociclib treatment showed that unlike long term estrogen deprivation or anti-estrogen treatment, palbociclib did not directly affect the ER target genes, but only reduced expression of the cell cycle regulatory genes (Knudsen and Witkiewicz 2016). The induction of palbociclib mediated G1 arrest and senescence has been verified further by numerous pre-clinical studies including a study which showed that expression of FOXM1, a CDK4/6 target decreases with palbociclib treatment and is required for the induction of senescence by the drug (Anders, Ke et al. 2011). Moreover, palbociclib has been shown be synergistic in combination with tamoxifen in a tumor explant model of breast cancer, which showed a significant decrease in Ki67 and Rb protein in 11 out of the 13 explants (Dean, McClendon et al. 2012). A more recent study even evaluated the use of palbociclib in tamoxifen resistant tumors, expressing ESR1 mutations, and showed that the combination of palbociclib with SERDs such as fulvestrant was effective in decreasing growth of the patient derived xenograft (PDX) tumors (Wardell, Ellis et al. 2015). More detailed mechanistic studies have been discussed in Chapter 3 (in breast cancer) and Chapter 8 (in other solid tumors). These studies provided the pre-clinical basis for testing the use of palbociclib clinically in ER advanced positive breast cancer cell lines in combination with anti-estrogens (O'Leary, Finn et al. 2016).

A phase I single arm dose finding and toxicity study in Rb positive advanced solid tumors, where patients received escalating doses of palbociclib (3 weeks on and 1 week off schedule) showed that neutropenia was the only significant toxicity suggested a dose of 125 mg of palbociclib for future clinical studies (Flaherty, Lorusso et al. 2012). Further, a single-arm phase II clinical trial was conducted in 37 advanced breast cancer patients (acquired resistance to prior hormonal therapy), where patients were treated with a dose of 125 mg for three week on and on week off regiment (DeMichele, Clark et al. 2015). Results showed partial response in

2 patients and stable disease in 5 patients, with non-febrile (not accompanied by fever), neutropenia detected 50 to 60% of the patients, with no bone marrow damage (DeMichele, Clark et al. 2015). These studies showed that palbociclib is well-tolerated. Further clinical studies were conducted to interrogate the efficacy of palbociclib in advanced ER positive breast cancer in comparison with the current standard of care treatments, such as aromatase inhibitors and fulvestrant (studies summarized in **Table 5**).

PALOMA-1, a randomized multicenter phase II study tested letrozole alone or letrozole in combination with palbociclib in postmenopausal advanced ER positive /HER2-ve breast cancer patients (Finn, Crown et al. 2015). Results showed that combining palbociclib with letrozole increased the median progression-free-survival from 10.2 months (letrozole alone arm) to 20.2 months, with neutropenia reported in 54% and leucopenia reported in 19% of patients who received the combination drug treatment (Finn, Crown et al. 2015). However, the overall survival of patients did not significantly change upon addition of the CDK4/6 inhibitor palbociclib to letrozole (37.5 months in combination arm vs 33.3 months in the letrozole arm) (Finn, Crown et al. 2015). The improved progression free survival in patients receiving palbociclib plus letrozole was further confirmed in phase III randomized clinical trial (PALOMA-2) conducted in 666 ER+/HER2- breast cancer patients (Finn, Martin et al. 2016). Results showed that the combination of palbociclib with letrozole increased the progression-free survival from 14.5 months to 24.8 months, compared to letrozole alone, with neutropenia (non-febrile), however, detected in a majority (79%) of combination treated patients (Finn, Martin et al. 2016). Finally, the benefit of adding palbociclib to fulvestrant was tested in PALOMA-3, a phase III randomized study in 521 advanced ER+/Her-2- patients, who have relapsed on prior on endocrine therapy (Turner, Ro et al. 2015). Results revealed that addition of palbociclib to fulvestrant regimen prolonged the median progression-free survival to 11.2 months compared to 3.6 months with fulvestrant alone, with grade 3 and 4 neutropenia seen in 62% of the combination treated patients (similar to PALOMA-2) (Turner, Ro et al. 2015). Further, the pre-

Trial	Drugs	Phase	Results	Identifier
PALOMA-1	Palbociclib Letrozole	II	Median PFS: 20.2 months for the combination vs 10.2 months with letrozole alone	NCT00721409 NCT01740427
PALOMA-2	Palbociclib Letrozole	III	Median PFS: 24.8 months for the combination vs 14.5 months with letrozole alone	NCT00721409 NCT01740427
PALOMA-3	Palbociclib Fulvestrant	III	Median PFS: 11.2 months for the combination vs 4.6 months with fulvestrant alone	NCT01942135
MONARCH-1	Abemaciclib	II	Median PFS: 5.95 months for abemaciclib monotherapy	NCT02102490
MONARCH-2	Abemaciclib Fulvestrant	III	Not reported	NCT02107703
MONARCH-3	Abemaciclib Aromatase Inhibitors	III	Not reported	NCT02246621
MONALEESA-2	Ribociclib Letrozole	III	Median PFS: 25.3 months for the combination vs 16 months with letrozole alone	NCT01958021
MONALEESA-3	Ribociclib Fulvestrant	III	Not reported	NCT02422615

Table 5: CDK4/6 inhibitor clinical trials in ER+ breast cancer: Table showing the seminal clinical trials that have been completed and are underway with CDK4/6 inhibitors in advanced ER+ve breast cancer

clinical and the clinical studies examining the use of palbociclib in cancers other than breast have been discussed in detail in Chapter 8.

1.4.3. RIBOCICLIB

Ribociclib is another selective CDK4/6 inhibitor that inhibits phosphorylation of Rb in a dose dependent manner, inducing G1 arrest *in vitro* cell cycle arrest and delayed tumor growth in glioblastoma xenograft tumors *in vivo* (Rader, Russell et al. 2013). Ribociclib was first tested in patient in a phase I study with 132 advanced cancer patients including 18 breast cancer

patients, which showed neutropenia as being the only significant side-effect similar to palbociclib (Infante, Cassier et al. 2016). Further, MONALEESA-2, a multi-center randomized phase III study examined the efficacy of combining ribociclib with letrozole in 669 postmenopausal advanced or metastatic ER positive breast cancer patients, with ribociclib given in a 3 week on 2 week off treatment regimen (**Table 5**) (Hortobagyi, Stemmer et al. 2016). Study results showed that addition of ribociclib significantly delayed the progression to 25.3 months compared to 16 months with letrozole alone (Hortobagyi, Stemmer et al. 2016). The study showed that toxicity with ribociclib treatment is similar to that seen with palbociclib, with 59% of the patients experience neutropenia and 21% of patients experience leukopenia (Hortobagyi, Stemmer et al. 2016). Further, a randomized phase III trial (MONALEESA-3) is currently underway examine the effect of the combination of ribociclib and fulvestrant in advanced ER positive breast cancer (**Table 5**).

1.4.4. ABEMACICLIB

Abemaciclib is the third CDK4/6 inhibitor currently under clinical investigation for breast and other solid tumors (O'Leary, Finn et al. 2016). It inhibits CDK4/6 at low nanomolar concentrations and reduced Rb1 phosphorylation in colorectal cancer and melanoma xenografts (Patnaik, Rosen et al. 2016).

A phase I study examined the safety and efficacy of abemaciclib in solid tumors including 47 breast cancer patients, who received abemaciclib as a monotherapy (Patnaik, Rosen et al. 2016). Results showed that overall response was seen in almost 35% of the breast cancer patients, accompanied by a marked decrease in Ki67 expression in the tumor tissues (Patnaik, Rosen et al. 2016, 2017). In an expansion cohort, where abemaciclib was administered as a monotherapy in 25 patients with advanced HR+/HER2- disease, clinical benefit rate was seen in 72% of the patients, with only one of the partial responders receiving concomitant hormonal therapy (O'Leary, Finn et al. 2016, Patnaik, Rosen et al. 2016). Thus,

the ER positive subtype of breast cancer patients exhibited a median duration of response of 13.4 months and median PFS of 8.8 months (Patnaik, Rosen et al. 2016), suggesting the clinical utility of abemaciclib as a single agent than palbociclib. Moreover, results from MONARCH-1, a phase II study of abemaciclib as monotherapy in 132 HR+/HER2- advanced breast cancer was recently reported (Maura N. Dickler 2017). Results showed a clinical benefit rate of 42.4%, with patients exhibited a median progression-free survival of 5.95 months and median overall survival of 22.3 months (Maura N. Dickler 2017).

Unlike palbociclib and ribociclib, abemaciclib is administered to patients on a continuous daily or twice a day regimen, which has been shown to be highly tolerated (Patnaik, Rosen et al. 2016, Maura N. Dickler 2017). Further, the common dose limiting side-effects associated with abemaciclib fatigue and diarrhea, and not high-grade neutropenia and leukopenia as seen with palbociclib and abemaciclib (Patnaik, Rosen et al. 2016, Sherr, Beach et al. 2016, Maura N. Dickler 2017). While reason for this remains uncertain, it may be due to the preferential selectivity of abemaciclib for CDK4 over CDK6 and its reported potential activity against CDK9, although, preliminary studied show that this may not translate into inhibition of the cellular activity of CDK9 (Patnaik, Rosen et al. 2016, Sherr, Beach et al. 2016). Moreover, another characteristic of abemaciclib is its ability to cross the blood brain barrier and its appearance in the cerebrospinal fluid in animal models, which suggests that the drug might possess additional activity in treating brain metastasis in patients with breast cancer (Raub, Wishart et al. 2015, Tate, Burke et al. 2016).

1.4.5. BIOMARKER STUDIES WITH CDK4/6 INHIBITORS

Since biomarkers are essentially for the selectivity of drug treatment, numerous pre-clinical and clinical studies have been conducted to identify biomarkers for this treatment (O'Leary, Finn et al. 2016). While pre-clinical studies identified Rb, cyclin D and p16 among other proteins as biomarkers for the CDK4/6 inhibitors, clinical studies showed that none of

these proteins can efficiently predict response to therapy (Sherr, Beach et al. 2016). The summary and results of the pre-clinical and the clinical studies conducted with the CDK4/6 inhibitors have been described in detail in Chapters 6 and 7.

1.4.6. MECHANISMS OF RESISTANCE TO CDK4/6 INHIBITORS

While CDK4/6 inhibitors have shown promising results in the clinic in ER positive breast cancer, about 16% of the ER positive cancer patients exhibit progression within 24 weeks, resulting in no overall survival benefit with the treatment (Finn, Martin et al. 2016). More than half the patients acquire clinical resistance with progression on therapy within 25 months (Finn, Martin et al. 2016), and it is expected that most will eventually become resistant to the drugs. Hence, numerous studies are currently underway in trying to understand the mechanism of resistance to CDK4/6 inhibitors, both intrinsic and acquired resistance (Sherr, Beach et al. 2016). Early pre-clinical studies aimed at identifying biomarkers showed that loss of Rb mediates resistance to CDK4/6 inhibition in breast cancer cells lines and xenograft tumors (Finn, Dering et al. 2009). A study in breast cancer showed the activation of the PI3K mediated growth signaling pathways as a mode of resistance to CDK4/6 inhibitor (ribociclib) mediated growth inhibition and senescence, particularly in PIK3CA mutant cell lines (Vora, Juric et al. 2014). Hence, combination treatment with PI3K inhibitor was synergistic with ribociclib in the ER positive breast cancer cell lines, MCF7 and T47D, and also prevented acquired resistance to ribociclib (Vora, Juric et al. 2014)

Moreover, an ovarian cancer pre-clinical study showed that expression of cyclin E mediates resistance to palbociclib mediated growth inhibition and senescence (Taylor-Harding, Aspuria et al. 2015). Further, a more recent study showed that high levels of CDK2 and cyclin E can mediate early adaptation (intrinsic drug resistance) and acquired resistance in breast cancer (Herrera-Abreu, Palafox et al. 2016). This study showed that high CDK2 levels maintain Rb phosphorylation despite palbociclib treatment and showed that high expression of cyclin E

post mitotic exit determines early adaptation and resistance to CDK4/6 inhibitors (Herrera-Abreu, Palafox et al. 2016). Another recently reported study confirmed this observation, by showing that cell lines that have a greater CDK high population are more resistant to palbociclib treatment since the CDK2 activity mediates mitotic exit and resistance to palbociclib mediated cell cycle arrest (Uzma Asghar 2016). Thus, knockdown of CDK2 or combined treatment with the CDK2 inhibitor, dinaciclib, was synergistic with the CDK4/6 inhibitor, ribociclib and helped reverse drug resistance (Herrera-Abreu, Palafox et al. 2016, Jansen, Bhola et al. 2017). Finally, activation of the AKT1 signaling pathway via PI3K-PDK1 has been shown to mediate resistance to ribociclib treatment, which was effectively reversed upon treatment with a PDK1 inhibitor (GSK2334470) or PI3K inhibitor (alisertib) *in vitro* and *in vivo* (Jansen, Bhola et al. 2017).

Thus, while these studies have suggested potential mechanism of intrinsic and acquired resistance to palbociclib and other CDK4/6 inhibitors, more detailed study is essential to devise efficient treatment regimens to combat drug resistance.

1.5. LIMITATIONS WITH CDK4/6 TREATMENT AND GAPS IN KNOWLEDGE

Despite these promising clinical advances with CDK4/6 inhibitors in ER positive breast and other cancers, there are three major clinical limitations with this treatment strategy: (i) adverse events leading to treatment interruption/ discontinuation, (ii) lack of overall survival benefit and (iii) lack of predictive biomarkers.

Both palbociclib and ribociclib treatment is associated with increased toxicity and adverse events in patients, with over 55% of the patients having grade 3&4 neutropenia and about 25% of patients having leukopenia (Finn, Crown et al. 2015) (Hortobagyi, Stemmer et al. 2016). This often requires delay in treatment delays or even discontinuation of treatment, which might attenuating therapy benefit , thus highlighting the need to improve efficacy of CDK4/6 inhibitor treatment (Finn, Crown et al. 2015, Turner, Ro et al. 2015). Further, about 16% of the

ER positive breast cancer patients do not respond (intrinsic resistance) exhibit progression within 24 weeks (early adaptive resistance) to palbociclib treatment (Finn, Martin et al. 2016). Additionally, more than half the patients develop clinical resistance accompanied disease progression within 25 months, resulting in no overall survival benefit (Finn, Martin et al. 2016). Finally, while previous *in vitro* studies showed that Rb, Cyclin D and p16 could predict response to palbociclib (Wiedemeyer, Dunn et al. 2010, Konecny, Winterhoff et al. 2011, Cen, Carlson et al. 2012), results from Phase II/III trials showed no significant correlation between progression-free survival or clinical response and the expression of p16, *CCND1* amplification (Finn, Crown et al. 2015), Ki67, *PIK3CA* or ESR1 mutational status (Turner, Jiang et al. 2016). Similarly, biomarker analysis with ribociclib also showed no correlation between response and the expression of Rb, p16, CDKN2A amplification, cyclin D and PIK3CA mutation (Hortobagyi, Stemmer et al. 2016). This leaves us with no established predictive biomarkers for CDK4/6 inhibitors.

1.6. GOAL OF THE PROJECT

Thus, the goal of this thesis and project is to address the aforementioned limitations of CDK4/6 inhibitor therapy and to ***improve the selectivity and efficacy of CDK4/6 inhibition***. This has been achieved in this project through a biomarker-driven combination treatment approach that targets CDK4/6 and autophagy in breast and other solid tumors. Further, the project also aims at understanding the ***mechanisms of acquired resistance to CDK4/6 inhibition*** via palbociclib.

CHAPTER 2: MATERIALS AND METHODS

2.1. CELL LINES

All cell lines used in this study were obtained from ATCC. MCF7, T47D, ZR75-1, MCF7-T, MDA-MB-231, HCC38, HCC1806, MDA-MB-157, HeyA8, 59M, and FUOV1 were maintained in minimum essential medium Eagle alpha modification (alpha MEM) supplemented with 10% fetal bovine serum (FBS), 10mM HEPES, nonessential amino acids, 2mM L-glutamine, sodium pyruvate, and hydrocortisone. 293T and MDA-MB-468 cells were cultured in Dulbecco modified Eagle medium (DMEM) supplemented with 10% FBS. SUM-159 and BT-549 cells were cultured in a 1:1 mixture of alpha MEM and nutrient F-12 Ham medium supplemented with 10% FBS and 5% insulin. Calu-1, H358, A549, PC3, and Du145 cells were cultured in RPMI-1640 medium supplemented with 10% FBS. The pancreatic cancer cell lines (Panc-1 and BxPC-3) were a gift from the laboratory of Dr. Anirban Maitra (MD Anderson Cancer Center) and were cultured in DMEM and RPMI 1640, respectively, supplemented with 10% FBS. The colon cancer cell lines (Colo-205, SW-620, and HCT-116) were obtained from the laboratory of Dr. Jae-II Park (MD Anderson Cancer Center) and cultured in DMEM supplemented with 10% FBS.

The MCF7 aromatase expressing cells were maintained in DMEM supplemented with 10% tet-free FBS + 4µg/ml blasticidin, 1 µg/ml puromycin (InvivoGen, San Diego, CA) and 400 µg/ml G418. Prior to experimental setup, they were estrogen deprived for 4 days using phenol red free IMEM supplemented with 10% charcoal dextran treated tet-free FBS. During the experiment, the cells were maintained in estrogen deprivation condition in the presence of 25nM 4-Androstene-3,17-dione. To induce the expression of empty vector and LMW-E, the cells were treated with 5 ng/ml Doxycyclin (Sigma) for 24 hours before the start of the experiment. The aromatase resistant cell lines were maintained in phenol red DMEM supplemented with 10% charcoal dextran treated FBS + 25nM 4-Androstene-3,17-dione + 400

µg/ml G418. All cell lines were maintained free of mycoplasma contamination and authenticated on a regular basis by karyotype and short tandem repeat analysis at MD Anderson's Characterized Cell Line core facility.

2.2. ANTIBODIES AND DRUGS

Antibodies against p-Rb (Ser807/811), FOXM1, total Rb (4H1), PARP, caspase-7, LC3B, p62 (SQSTM1), Beclin-1, Atg-5, and p53 were purchased from Cell Signaling Technology (Danvers, MA). Antibodies against CDK4 (C-22), CDK6 (C-29), cyclin E (HE-12), and Mdm2 were purchased from Santa Cruz Biotechnology (Dallas, TX); antibodies against actin (C-4) and vinculin were purchased from Millipore and Sigma-Aldrich (St. Louis, MO).

Palbociclib was obtained from Pfizer, Inc (San Diego, CA). It was diluted in dimethyl sulfoxide (DMSO) for *in vitro* use and in 0.5% methylcellulose (Sigma-Aldrich, St. Louis, MO) for *in vivo* use and administered to mice via oral gavage. Hydroxychloroquine sulfate (HCQ) was purchased from Sigma-Aldrich and Selleckem. Lys-05 was provided by Dr. Ravi Amaravadi (University of Pennsylvania). HCQ and Lys-05 were diluted in sterile water for *in vitro* use and in sterile phosphate-buffered saline solution (PBS) for *in vivo* use and administered to mice via intraperitoneal injection. N-acetyl-L-cysteine (NAC), trolox [(±)-6-hydroxy-2,5,7,8-tetramethylchromane-2-carboxylic acid], bafilomycin A1, spautin-1, and chloroquine diphosphate (CQ) were all purchased from Sigma-Aldrich. Ribociclib was purchased from Selleckem and abemaciclib from MedChem Express; NAC and CQ were diluted in sterile water. Trolox, bafilomycin A1, spautin-1, ribociclib, and abemaciclib were diluted in DMSO.

2.3. siRNA KNOCKDOWN

siRNA knockdown of CDK4 and CDK6 were generated as described previously (Jabbour-Leung, Chen et al. 2016). ON-TARGETplus SMARTpool siRNA for CDK4

(L-003238-00-0005) and CDK6 (L-003240-00-0005) were purchased from Dharmacon. Briefly, cells were plated on 6-well or 12 well plates and transfected with siRNA targeting CDK4 and/or CDK6 using JetPRIME transfection reagent (Polyplus transfection, New York, NY), as per manufacturer's protocol. Non-coding siRNA pool (siNT) was used as a negative control for comparison. Cells were harvested 72 hours post transfection for western blot analysis, MDC analysis, CellROX assay and on days 3 and 6 for cell counting.

2.4. shRNA KNOCKDOWN AND CYCLIN E OVEREXPRESSION

Stable shRNA knockdown cells were generated as described previously (Jabbour-Leung, Chen et al. 2016, Nanos-Webb, Bui et al. 2016). All shRNA constructs were purchased from Thermo Scientific (Open Biosystems, Waltham, MA). For single knockdown of CDK4, CDK6, Beclin-1, Atg-5, or Rb, GIPZ lentiviral shRNA was used [CDK4: V3LHS_641689, V3LHS_641690; CDK6: V2LHS_112906, V3LHS_404083; Beclin-1: V3LHS_349514, V3LHS_349513; Atg-5: V2LHS_67978, V3LHS_301131; Rb: V2LHS_130611, V2LHS_130606, V3LHS_340829]. For dual knockdown of CDK4 and CDK6, TRIPZ inducible shRNA for CDK6 was utilized for better selection of knockdowns. To generate lentivirus expressing shRNA, HEK 293T cells were transfected with pCMVdeltaR8.2, pMD2.G (produced by the Didier Trono laboratory and made available through the Addgene repository) and pGIPZ vector (scrambled shRNA or shRNA against gene of interest) using LipoD293 (SignaGen) or polyethylenimine transfection reagent according to manufacturer's protocol. After 48 hours of transfection, the virus-containing medium was collected, filtered through a 0.45- μ m filter, and added to the cells of interest in the presence of 8 μ g/mL of polybrene (Millipore). GFP or RFP expression was confirmed and the lentivirus-infected cells were selected with 1 μ g/mL puromycin (InvivoGen, San Diego, CA). MCF7 and T47D cells overexpressing different isoforms of cyclin E (vector, full-length cyclin E [EL], or low-molecular-weight cyclin E [LMW-E]) were generated previously (Akli, Zheng et al. 2004) and verified in this study by western blot.

2.5. DOSE-RESPONSE STUDIES

For dose-response studies, 1000 to 3000 cells (depending on plating efficiency of each cell line; data not shown) were plated in each well of a 96-well plate and treated with increasing concentrations (0.01 to 12 μ M) of palbociclib, ribociclib, or abemaciclib for 1, 2, 4, 6, or 8 days. The medium was replaced with drug-containing medium every other day. At completion of drug treatment, cultures were continued in drug-free medium (also replaced every other day) until day 12, after which they were stained with 0.5% crystal violet solution. The plates were then solubilized with a solution of 0.1% sodium citrate in 50% ethanol, and absorbance was measured at 570 nm using the Epoch Microplate Spectrophotometer (BioTek Instruments, Inc, Winooski, VT). Values were normalized to those of their no treatment controls and analyzed in GraphPad Prism by non-linear regression to obtain the half-maximal inhibitory concentrations (IC_{50} values) as used in Figure 1a.

2.6. CELLULAR PROLIFERATION ASSAY

For cell proliferation studies, 7,500 to 15,000 cells (depending on plating efficiency of each cell line; data not shown) were plated in each well of 6-well plates and treated with the indicated agents for 6 days and cells were allowed to recover for 4 days in the absence of drug to examine reversibility. The medium was replaced every other day during the course of the experiment, either with drug-containing medium (days 2 and 4) or drug-free medium (days 6 and 8). Cells were then harvested and counted using the BioRad TC20 Automated Cell Counter on days 0, 3, 6, and 10.

For clonogenic/colony-formation assay, 5,000 to 10,000 cells (depending on the plating efficiency of each cell line; data not shown) were plated in each well of 6-well plates, treated for 6 days, and allowed to recover for 6 days in the absence of drug. Cells were then washed with

PBS and stained with a 0.5% crystal violet solution in 25% methanol for 10 minutes. Plates were then scanned to obtain pictures.

2.7. CELL CYCLE AND BRDU ANALYSES

Cells were plated (1×10^5 cells/plate) on 10-cm plates and treated with the indicated agents for 6 days; they were allowed to recover without drug(s) for 4 days to examine reversibility. Medium was replaced every other day during the course of the experiment, either with drug-containing medium (days 2 and 4) or drug-free medium (days 6 and 8). For cell cycle analysis, following treatment or treatment (6 days) and recovery (6 days + 4 days of recovery), cells were subjected to trypsinization, washed with PBS, and fixed with 3.5 mL ice-cold PBS and 1.5 mL of 95% ethanol. Cells were prepared as described previously (Jabbour-Leung, Chen et al. 2016) and incubated in a solution of propidium iodide (PI; 1 mg/mL) and RNAase (1 mg/mL) at 4°C overnight. Samples were then analyzed on the Beckman Coulter Gallios Flow Cytometer, and data were analyzed with the Kaluza software (Beckman Coulter) after excluding doublet cells.

For BrdU analysis, following treatment or recovery, cells were incubated with 10 μ M 5-bromo-2'-deoxyuridine (BrdU; Sigma-Aldrich) for 1 hour, after which they were subjected to trypsinization, washed with PBS, and fixed with 70% ethanol. Cells were then washed with PBS containing 0.5% bovine serum albumin (BSA) and denatured with a solution of 2M HCl + 0.5% Triton X-100 at room temperature for 20 minutes. Cells were washed again and incubated in 200 μ L 0.1 M sodium borate, pH 8.5, to neutralize any residual acid for 2 minutes at room temperature. Cells were then stained with fluorescein isothiocyanate–conjugated anti-BrdU (BD Biosciences) for 20 minutes at room temperature, protected from light. Cells were finally washed and incubated in a solution of 0.5 mL PI (10 μ g/mL in PBS) for 30 minutes at room temperature, protected from light. Samples were analyzed on the Beckman Coulter Gallios

Flow Cytometer and data were analyzed with Kaluza software to obtain the percentages of BrdU-positive cells.

2.8. MEASUREMENT OF SENESENCE

For *in vitro* studies, senescence was measured by the senescence-associated galactosidase (SA- β gal) staining kit (Millipore, Billerica, MA) according to the manufacturer's standard protocol. Briefly, cells were plated at a low density of 2,000 to 4,000 cells (depending on the plating efficiency of the cell line; data not shown) in each well of 12-well plates and treated with the indicated agents for 72 hours or 6 days. The medium was replaced every other day during the course of the experiment with drug-containing medium (days 2 and 4). Cells were then washed with PBS, fixed, and stained with SA- β gal solution overnight. The cells were then photographed using the Evos XL Core cell imaging system (ThermoFischer, Waltham, MA) and senescent cells were quantified by counting 100 cells in three different fields for each replicate. A minimum of three technical and three biological replicates were performed for each condition.

For *in vivo* studies, mouse tumors tissues were snap-frozen in liquid nitrogen, embedded in OCT, and cut into thin sections (5 μ m). Senescence was measured by the SA- β gal detection kit (Biovision, Milpitas, CA) by following the manufacturer's protocol. Briefly, slides were washed with PBS and incubated in staining solution (prepared according to protocol) overnight. Slides were then washed with PBS and fixed in 70% glycerol. Images of the tissue sections were obtained by a Leica DM light microscope using the 20 \times and 40 \times optical lenses. Images were acquired with a SPOT Imaging Solutions camera and SPOT Advanced software.

For quantitation of cellular granularity, cells were plated (1×10^5 cells/plate) on 10-cm plates and treated for 6 days; some of the cells were allowed to recover for 4 without drug. Following treatment, cells were harvested, stained with PI (1 mg/mL), and analyzed on the

Beckman Coulter Gallios Flow Cytometer. The data were then analyzed with the FlowJo software to obtain a distribution curve of side-scatter vs normalized cell counts.

2.9. ANNEXIN V AND CASPASE-3 APOPTOSIS ASSAYS

Apoptotic cells were measured by using the Alexa Fluor 488 Annexin V Dead Cell Apoptosis kit (Invitrogen, Waltham, MA) according to the manufacturer's protocol. Briefly, cells were plated (1×10^5 cells/plate) on 10-cm plates and treated with the indicated agents for 6 days and allowed to recover for 4 days. Cells were harvested at the end of treatment (6 days) or after treatment + recovery, washed with $1 \times$ Annexin binding buffer and stained with a solution of Alexa Fluor 488 Annexin V and PI (100 $\mu\text{g/mL}$) as directed by the protocol. Samples were then analyzed on the Beckman Coulter Gallios Flow Cytometer, and data were analyzed with Kaluza software to obtain the percentages of Annexin V-positive/PI-negative (early apoptosis) and Annexin V-positive/PI-positive (late apoptosis) cells.

For the caspase-3 activity assay, following drug treatment, cells were harvested, washed with a solution of PBS with 2% FBS and fixed with 100 μL of the fixation solution from the Cytofix/CytoPerm kit (BD Biosciences). Cells were then washed with Perm/Wash buffer and stained with phycoerythrin-conjugated rabbit active caspase-3 antibody (BD Biosciences) for 30 minutes on ice. Cells were finally washed, resuspended in the PBS with 2% FBS solution, and analyzed on the Becton Dickinson FACS Calibur Flow Cytometer to obtain the percentage of caspase-3-positive cells.

2.10. CELLULAR ROS MEASUREMENT

Cellular ROS levels were measured by using the CellROX Deep Red Flow Cytometry assay kit (ThermoFischer Scientific, Waltham, MA) according to the manufacturer's protocol. Briefly, cells were plated (1×10^5 cells/dish) on 10-cm dishes and treated for 6 days. Cells were then harvested and stained with 500 nM CellROX reagent for 1 hour at 37°C . Samples were

analyzed on the Beckman Coulter Gallios Flow Cytometer using the 635-nm laser; data were analyzed with the FlowJo software, and mean fluorescence intensity (MFI) was obtained.

2.11. MONODANSYLCADAVARINE MEASUREMENT

Cells were seeded at a density of 1×10^5 cells on 10-cm plates and treated for 6 days with various concentrations of palbociclib. At the end of drug treatment, cells were incubated with 50 μ M monodansylcadavarine (MDC; Sigma-Aldrich) at 37°C for 45 minutes. Cells were then harvested, washed with PBS, and suspended in a solution of PBS with 1% FBS. Samples were analyzed on the Becton Dickinson FACS LSR II Flow Cytometer using the 355-nm ultraviolet laser. Data were analyzed with the FlowJo software, and percentages of MDC-positive cells and Mean Fluorescence Intensity (MFI) were obtained.

2.12. IMMUNOFLUORESCENCE

For the GFP-LC3 puncta assay, MCF7, MDA-MB-231 and MDA-MB-468 cells stably expressing GFP-LC3 were plated in 6-well plates and treated with drug for 48 hours. Following treatment, cells were washed with 1X PBS, fixed with 4% paraformaldehyde for 10 mins and mounted with Vectashield mounting media with DAPI. Cells were then visualized with Zeiss Confocal microscope LSM880 using the 488nm laser (GFP) for the presence of GFP-LC3 puncta. The puncta was quantified using ImageJ.

For RFP-GFP-LC3 dual reporter assay, cells were transfected with ptf-LC3 vector and analyzed as described previously (Kimura, Noda et al. 2007). Briefly, ptfLC3 vector was transfected using Lipofectamine 2000 as per manufacturer's instructions. Cells were then treated with the drug for 48 hours, washed with 1X PBS, fixed briefly (for 10 mins) with 4% paraformaldehyde and mounted with Vectashield mounting media. They were then visualized using with Zeiss Confocal microscope LSM880 using the 488nm and 643nm channels to image the GFP+ve and RFP+ve LC3 puncta respectively. The puncta was quantified using ImageJ to

obtained the number of autophagosomes (yellow – RFP+ GFP+) and autophagolysosomes (red – RFP+).

2.13. TRANSMISSION ELECTRON MICROSCOPY

For cell lines, ~5000 cells were plated in each well of 12-well plates and treated with the drug for 6 days. For xenografts, tumors were harvested and samples were cut into 1-mm³ pieces. The cell lines and tumor samples were processed similarly and Electron microscopy was performed at the High Resolution electron microscopy facility at MD Anderson Cancer Center as described previously (Chauhan, Goodwin et al. 2013). Briefly, they were fixed with a solution containing 3% glutaraldehyde plus 2% paraformaldehyde in 0.1M cacodylate buffer, pH 7.3. Samples were then washed in 0.1M sodium cacodylate buffer and treated with 0.1% Millipore-filtered cacodylate-buffered tannic acid. They were fixed with 1% buffered osmium tetroxide for 30 minutes and stained *en bloc* with 1% Millipore-filtered uranyl acetate. The samples were dehydrated in increasing concentrations of ethanol, filtrated, and embedded in LX-112 medium. They were then polymerized in a 60°C oven for approximately 3 days. Ultrathin sections were cut in a Leica Ultracut microtome (Leica, Deerfield, IL), stained with uranyl acetate and lead citrate in a Leica EM Stainer, and examined in a JEM 1010 transmission electron microscope (JEOL, USA, Inc., Peabody, MA) at an accelerating voltage of 80 kV. Digital images were obtained at magnifications of 5000×, 25000×, and 50000× using the AMT Imaging System (Advanced Microscopy Techniques Corp, Danvers, MA).

2.14. *IN VIVO* XENOGRAFT STUDIES

For all xenograft experiments, estrogen pellets (0.72 mg 17-beta estradiol pellet, 90-day release, Innovative Research of America, Sarasota, FL) were implanted subcutaneously into 4- to 6-week-old female nude mice. MCF7-T cells (5×10^6 in a 1:1 ratio with matrigel [BD Biosciences]) were injected into the 5th and 10th inguinal mammary fat pads bilaterally. For the

dose-determining experiment, once the tumors reached an average volume of 200 mm³, the tumor-bearing mice were randomized into five groups (n=3/group) and treated with vehicle (0.5% methylcellulose) or 25 mg/kg, 50 mg/kg, 75 mg/kg, or 150 mg/kg palbociclib. Palbociclib was administered daily via oral gavage for 7 consecutive days. For the combination treatment experiment, once the tumors reached an average volume of 250 mm³, the tumor-bearing mice were randomized into four groups (n=9/group) and treated with vehicle (0.5% methylcellulose and PBS), hydroxychloroquine (60mg/kg), palbociclib (25 mg/kg), or a combination of palbociclib (25 mg/kg) and hydroxychloroquine (60mg/kg). Drugs were administered daily via oral gavage (palbociclib) or intraperitoneally (HCQ) for 21 days.

For Lys-05 toxicity experiment, non-tumor bearing female nude mice were treated with varying concentrations of Lys-05 (1 mg/kg, 5 mg/kg, 10 mg/kg and 20 mg/kg) daily for 21 days via I.P. For the Lys-05 combination treatment experiment, once the orthotopic xenograft tumors reached an average volume of 250 mm³, the tumor-bearing mice were randomized into four groups (n=5/group) and treated with vehicle (0.5% methylcellulose and PBS), Lys-05 (10mg/kg), palbociclib (25 mg/kg), or a combination of palbociclib (25 mg/kg) and Lys-05 (10mg/kg). Drugs were administered daily via oral gavage (palbociclib) or intraperitoneally (Lys-05) for 21 days.

For all xenograft studies, tumor volumes $[(L \times W^2) / 2]$ were measured twice per week with calipers and mouse weight was measured every day. At the end of the treatment and recovery periods, mice were euthanized and the tumors were collected for further analysis. At the time the mice were euthanized, blood (0.2 mL) was collected by cardiac puncture through the left ventricle. Blood samples were subjected to complete blood count analysis (white blood cells, platelets, and red blood cells) by the Siemens Adiva 120 Hematology System (Erlangen, Germany). Nude mice for all experiments were obtained from the Department of Experimental Radiation Oncology at The University of Texas MD Anderson Cancer Center, and mice received care in accordance with the Animal Welfare Act and the institutional guidelines of MD

Anderson Cancer Center. The protocol for this study was approved by the Institutional Animal Care and Use Committee (IACUC) at The University of Texas MD Anderson Cancer Center (Houston, TX).

2.15. PATIENT-DERIVED XENOGRAFT STUDIES

Breast tumor samples were obtained during routine surgery after informed consent was obtained under protocols approved by the MD Anderson Institutional Review Board. Patient-derived xenograft (PDX) models were developed as previously described (McAuliffe, Evans et al. 2015). Briefly, fresh primary tumors were collected using sterile technique, and approximately 3-mm³ fragments of the tissue were transplanted to the fat pad of the 4th pair of mammary glands (both sides) in immunodeficient (SCID) mice within 1 hour of surgical resection. When the primary tumor outgrowths reached 10 mm in diameter, 3-mm³ fragments of the outgrowths were explanted to new hosts (n=3/tumor) as secondary passage. Since the tumor tissues can stably grow after two passages with our protocol, we considered the PDX line to have been successfully established at that point. The histology of the patient tumors of origin and the corresponding PDX lines were compared by hematoxylin and eosin (H&E) staining and had very similar histology (data not shown). For the drug treatment experiment, 3-mm³ fragments of the PDX line were transplanted into the fat pad of the 4th mammary gland of female nude mice. Once the tumors reached an average volume of 200 mm³, mice were randomized into four groups (n=4/group) and treated with vehicle (0.5% methylcellulose and PBS), hydroxychloroquine (60mg/kg), palbociclib (25 mg/kg), or combination of palbociclib (25mg/kg) and hydroxychloroquine (60mg/kg). Drugs were administered daily via oral gavage (palbociclib) or intraperitoneally (HCQ) for 21 days. Tumor volumes $[(L \times W^2) / 2]$ were measured twice per week with calipers, and mouse weight was measured every day.

At the end of the treatment period, mice were euthanized and their tumors were collected for further analysis. All mice were obtained from the Department of Experimental

Radiation Oncology at The University of Texas MD Anderson Cancer Center and received care in accordance with the Animal Welfare Act and the institutional guidelines of MD Anderson Cancer Center. The protocol for this study was approved by the IUCUC at MD Anderson Cancer Center.

2.16. IMMUNOHISTOCHEMISTRY ANALYSIS OF MOUSE TUMOR TISSUES

For BrdU assessment, mice were administered BrdU solution (5 mg/kg intraperitoneally) 2 hours before euthanasia. After death, the tumor was resected and snap-frozen in liquid nitrogen, embedded in OCT, cut, and utilized for measurement of senescence by SA- β gal staining. The remaining tissue was fixed in formalin and used for assessment of histology and of proliferation by BrdU as described previously (Nanos-Webb, Bui et al. 2016). Briefly, 5- μ m sections from the formalin-fixed, paraffin-embedded tumor tissues were stained with standard hematoxylin and eosin. Other sections of the tumor blocks were subjected to immunohistochemical (IHC) staining. After paraffin removal, tumor sections were heated in a water bath for 20 minutes in 10 mM sodium citrate buffer (pH 6.0) at 90°C to retrieve nuclear antigens. Endogenous peroxidase activity was quenched with a 3% hydrogen peroxide solution. Sections were blocked with 1.5% normal goat serum and incubated overnight at 4°C with rat monoclonal antibody to BrdU (clone BU1/75 [ICR1]; GeneTex Inc, San Antonio, TX) diluted at 1:500. Slides were developed using the VECTASTAIN Elite ABC kit (PK4004; Vector Laboratories, Burlingame, CA), followed by staining with DAB substrate (Vector Laboratories) and counterstaining with hematoxylin (DAKO), and then were mounted. Staining was evaluated with a Leica DM light microscope using the 40 \times optical lenses. Images were acquired on a SPOT Imaging Solutions camera with SPOT Advanced software. BrdU was quantified as percentage of BrdU-positive cells, which was calculated as percentage of BrdU-positive nuclei from a total of 300 tumor cells from three fields of view.

For 4HNE and Anti-8OHdG immunostaining; after paraffin removal, heat induced antigen retrieval was performed for 10 minutes in 10 mM sodium citrate buffer (pH 6.0) at 98°C. Endogenous peroxidase activity was blocked with 3% hydrogen peroxidase for 15 minutes. Slides were then incubated for 1 hour with diluted rabbit blocking serum. The sections were incubated for overnight at 4 °C with Anti-8-OHdG mouse monoclonal antibody (clone N45.1, Genox, Baltimore, MD, 1:100 dilution) and Anti-4-HNE mouse monoclonal antibody (clone HNEJ-2, Genox, Baltimore, MD, 1:50 dilution). The slides were incubated for 30 minutes with diluted biotinylated secondary antibody and 30 minutes with Vectastain Elite ABC kit (Vector Laboratories, United States). For the evaluation of 4HNE and Anti-8OHdG antibody expression, slides were scored separately for percentage and intensity of the cells. Percentage positivity was graded using 0 to 4 scale, where 0 represented no stained cells, 1 was 1 to 5% stained cells, 2 was 6 to 30% stained cells, 3 was 31 to 70% stained cells, and 4 was 71 to 100% stained cells. Staining intensity was scored as follows: 0, no staining; 1, weak positive; 2, intermediate positive; and 3, strong positive. H score calculated by multiplying the percentage of positive cells and intensity of staining.

2.17. WESTERN BLOT ANALYSIS

Western blot analysis was performed as described previously (Jabbour-Leung, Chen et al. 2016). Briefly, cells were seeded at a density of 1×10^5 cells on 10-cm plates and treated for 6 days with the indicated drugs. Following treatment, cells were harvested and subjected to lysis with RIPA buffer (150 mM NaCl, 10 mM Tris, pH 7.3, 0.1% sodium dodecyl sulfate [SDS], 1% Triton X-100, 1% deoxycholate, and 5 mM ethylene-diaminetetraacetic acid) containing protease inhibitors. For mouse tissues, the tumors were minced into small pieces on dry ice and immersed in RIPA buffer for lysis. Lysates were then subjected to centrifugation at 45,000rpm for 45 minutes at 4°C to obtain the protein lysates in the supernatant. Protein concentration was determined by Bradford Protein Assay dye (Bio-Rad), and 50 µg of protein

per sample was resolved by SDS–polyacrylamide gel electrophoresis as described previously(Akli, Zheng et al. 2004). Blots were blocked with Blotto milk for 1 hour at room temperature and incubated with primary antibody overnight at 4°C. They were then incubated with goat anti-rabbit or goat anti-mouse immunoglobulin–horseradish peroxidase conjugates (Pierce, Rockford, IL) at a dilution of 1:5000 in Blotto for 1 hour. Blots were then washed and developed using a Renaissance chemiluminescence system (Perkin Elmer Life Sciences, Inc.) by following the manufacturer's instructions. The developed and scanned blots were then analyzed by the ImageJ software to obtain densitometry values.

2.18. RPPA AND DATA ANALYSIS

The mouse tumor tissues were dissected on dry ice and subjected to lysis in RIPA buffer (1% Triton X-100, 50 mM HEPES, pH 7.4, 150 mM NaCl, 1.5 mM MgCl₂, 1 mM EGTA, 100 mM NaF, 10 mM Na pyrophosphate, 1 mM Na₃VO₄, 10% glycerol, and freshly added protease and phosphatase inhibitors; Roche Applied Science, Indianapolis, IN). Tumor lysates were then subjected to centrifugation and protein concentration was determined by using the Bradford reagent. Protein concentration was adjusted to 1.5 µg/µL and mixed with 4× SDS Sample Buffer containing 40% glycerol, 8% SDS, 0.25M Tris-HCL, and 2-mercapto-ethanol at pH 6.8. Samples were boiled for 5 minutes, and the reverse-phase protein array (RPPA) analysis was performed by the Functional Proteomics core facility at MD Anderson Cancer Center. The slide images were quantified using MicroVigene 4.0 (Vigene-Tech, Carlisle, MA). The spot level raw data was processed with the R package SuperCurve (<https://r-forge.r-project.org/projects/supercurve>), which returns the estimated protein concentration (raw concentration) and a quality control (QC) score for each slide. The raw concentration data was then normalized by median-centering for each sample across all the proteins, to correct for loading bias.

For RPPA data analysis, one-way ANOVA was used to identify proteins that are differentially expressed between treatment groups. To adjust for multiple comparisons, Benjamini-Hochberg procedure was used to estimate false discovery rate (FDR). Tukey HSD tests were used for *post hoc* pairwise comparisons. To compare the different Palbociclib doses treatments *in vivo* (Vehicle, 25 mg/kg, 75 mg/kg and 150 mg/kg), proteins with 20% FDR in ANOVA, Tukey $p < 0.05$ and fold change $> \pm 1.2$ was identified as significantly differentially expressed between groups. A heat map was then drawn using significant proteins from the ANOVA analysis, and ordered based on KEGG cell cycle, senescence and autophagy/catabolism pathways. Pearson distance metric and Ward's minimum variance was used to cluster the samples in the heat map. For comparing the combination treatments (Vehicle, HCQ, Palbociclib, and Palbociclib + HCQ) *in vivo*, proteins with 15% FDR in ANOVA, Tukey $p < 0.05$ and fold change $> \pm 1.2$ were identified as significantly differentially expressed in pairwise analysis. Pathway score for cell cycle and senescence pathways was calculated using mean expression level (in \log_2 scale) of the selected proteins from ANOVA analysis.

2.19. BIOINFORMATICS AND TCGA ANALYSIS

Alterations in CDK4, CDK6, CCND1, Rb1 and CCNE1 were obtained using cBio Portal (Cerami, Gao et al. 2012) from the TCGA RNA seq data for breast, ovarian, lung, pancreatic, colon and prostate cancer. For biomarker analysis, gene expression data for the 23 cell lines under study was obtained from Kao et. al.(Kao, Salari et al. 2009), and Gene Set Enrichment Analysis (GSEA) was performed against the BioCarta gene sets(Subramanian, Tamayo et al. 2005) to obtain a heat map of the cell cycle genes.

2.20. BREAST CANCER PATIENT SAMPLES AND STATISTICAL ANALYSIS

The Department of Medical Oncology at MD Anderson maintains a prospective curated database of patients from 1997 onward. This database was searched for all patients with

breast cancer who had received palbociclib, and this search was supplemented with a manual search. Key demographic, clinical, and pathologic data, cancer treatment details, and response to therapy were abstracted into a working database for analysis under an IRB-approved protocol. Outcomes of interest that were recorded included response, stable disease, and progression (based on the physician's determination, but not always based on RECIST criteria) and associated durations of disease response and stability. To demonstrate the applicability of our staining procedure, blocks with the largest available tumor specimen was chosen for each patient and retrieved from the archives of the Department of Pathology at MD Anderson under an IRB-approved protocol; this included specimens from the primary tumor and/or local and/or metastatic recurrences. Our working database includes results of pathology reports, including tumor histology and grade and standard IHC analyses for ER and progesterone receptors for primary breast cancer biopsies and surgical specimens as well as local and distant recurrences that were subject to biopsy or surgical excision.

Patient, tumor, and treatment characteristics were evaluated and compared between patients who were or were not free from progression; 6-month and 12-month progression rates were calculated for each of factor using the Kaplan-Meier method, and differences were examined using the log-rank test (Supplementary Tables 1 and 2). Univariable and multivariable Cox model analyses were used to determine the influence of patient, tumor, and treatment factors of known or potential prognostic value on progression-free survival (Supplementary Tables 3 and 4). All factors with $P \leq 0.1$ in the univariable analyses were entered into a full model, and the final model was selected by using a backwards elimination procedure. Model performance was quantified using Harrell's concordance index.(Gonen and Heller 2005) The discriminative ability of the model was assessed using the concordance index (C-index) for comparative purposes with the literature, as well as the concordance probability estimate (CPE) due to the high degree of censoring in the data.(Gonen and Heller 2005) The C-index can range from perfect concordance (1.0) to random predictions (0.5). Similar to the

area under the receiver operating characteristic curve, CPE can range from perfect concordance (1.0) to perfect discordance (0.0). In addition, Akaike's information criterion (AIC) was calculated.(Akaike 1974) The AIC takes into account how well the model fits the data as well as the complexity of a model, thereby reducing the risk of overfitting. After comparisons, the final model with the lowest AIC value and the highest C-index was reported. All statistical analyses were performed using R 3.3.2 (<http://www.r-project.org/>). All P values were two-tailed, and $P \leq 0.05$ was considered significant, and adjustments for multiple factors were not made.

2.21. IMMUNOHISTOCHEMICAL STAINING OF PATIENT SAMPLES

For the 109 breast cancer samples recovered, two serial 5- μ m sections were cut and mounted on Superfrost Plus glass slides. The antigen retrieval and washing steps were performed as described for BrdU immunohistochemistry analysis. For cyclin E and Rb IHC, two commercially available primary antibodies were used: rabbit polyclonal antibody to cyclin E (clone C19; Santa Cruz Biotechnology, Santa Cruz, CA) diluted 1:1000 and Rb mouse monoclonal antibody (Clone 4H1; Cell Signaling Technology, Denvers, MA) diluted 1:100. Slides were developed using the VECTASTAIN Elite ABC kit (PK6101 and PK6102; Vector Laboratories, Burlingame, CA) followed by staining with DAB substrate (Vector) and counterstaining with hematoxylin (DAKO), and then were mounted. Tumor cell blocks known to express high levels of LMWE and Rb were included in each batch as positive controls, and negative controls were prepared by replacing the primary antibody with PBS buffer. Staining was evaluated with a Leica DM light microscope using the 20 \times and 40 \times optical lenses. Images were acquired by a SPOT Imaging Solutions camera and SPOT Advanced software.

2.22. IMMUNOHISTOCHEMICAL SCORING OF RB AND CYCLIN E

Cyclin E staining was scored by two pathologists blinded to patient outcomes (data not shown). Scores (0=negative, 1=weak staining, 2=moderate staining, and 3=strong staining)

were assigned for nuclear and cytoplasmic staining according to percentage of cells stained and intensity of staining, as described previously (Karakas, Biernacka et al. 2016). Each tumor sample was scored separately for nuclear and cytoplasmic cyclin E expression, and LMWE status was assigned as follows: LMWE negative was defined as no staining or nuclear staining only; LMWE positive was defined as nuclear + cytoplasmic staining or cytoplasmic staining only.

For Rb staining, the intensity of staining and percentage of positive cells were evaluated separately. Staining intensity was scored as follows: 0, no staining; 1, weak positive (faint yellow staining); 2, intermediate positive; and 3, strong positive (brown staining). The number of positive cells was visually evaluated and stratified as follows: <1%, 0 (negative); 1 to <5% positive cells, 1 (weak); 5-50% positive cells, 2 (moderate); >50% positive cells, 3 (strong). The sum of the staining intensity and percentage of positive cell scores was used to determine the staining index for each section, with a minimum score of 0 and maximum score of 6; scores >1 were defined as Rb positivity. Using this cutoff, we compared Rb-positive to Rb-negative tumors.

IHC analysis for Rb and cyclin E for the NCI TMA tumor samples were performed and scored as described above for the Palbociclib treated patient samples.

2.23. MAMMOSPHERE FORMATION ASSAY

To generate primary mammospheres, the cells were grown in serum-free, media in low attachment plates as previously described (Duong, Akli et al. 2013). Briefly, cells were trypsinized, and single cells seeded in 6-well ultra-low attachment plates (10,000 cells/ml) in serum-free MEM supplemented with 20 ng/ml bFGF, 20 ng/ml EGF and B27 (Invitrogen) and incubated for 5- 7 days. For secondary mammosphere assay, cells from primary mammospheres were dispersed with 0.05% trypsin, seeded in 6-well ultra-low attachment plates (7,500 cells/ml) in mammosphere media and incubated for 5-7 days. Mammospheres

with at least a size of 100µm were counted with an automated colony counter (Oxford Optronix, Oxford, UK) following MTT staining (Sigma Aldrich, St. Louis, MO).

2.24. CD44/ CD24 FLOW CYTOMETRY ANALYSIS

Cells were plated (1×10^5 cells/dish) on 10-cm dishes then harvested by trypsinization. Half a million cells were washed 3 times with PBS containing 1% horse serum and resuspended in 10 µl PE anti-mouse CD24, 10 µl APC anti-mouse CD44 (BD Pharmingen) and 30 µl of the 1% serum PBS buffer. The samples were incubated for 20 minutes on ice, washed with 1% serum PBS buffer and analyzed with the Beckman Coulter Gallios Flow Cytometer. The data was analyzed by the Kaluza software to identify the CD44 high and CD24 low population of cells. Cells with only a single antibody staining were used to set up the gates for analysis.

2.25. ALDEFLUOR ASSAY

Measurement of cancer stem cells based on ALDH positivity was performed using the Aldefluor kit (StemCell technologies, Cambridge, MA) according to the manufacturer's protocol. Briefly, cells were plated (1×10^5 cells/dish) on 10-cm dishes then harvested by trypsinization and resuspended in the Aldefluor buffer. Each sample was divided into two tubes, Control and Test, where the Aldefluor reagent was added to both tubes, while the Aldefluor DEAB reagent (specific inhibitor of Aldefluor) was also added to the control tube alone. The samples were incubated in 37C water bath for 30 minutes and then analyzed on the Beckman Coulter Gallios Flow Cytometer to obtain the percentage of Aldefluor (ALDH) positive cells. Measurement for each sample was done from the Test tube and using the control tube for gating the ALDH negative population.

2.26. MIGRATION ASSAY

The *in vitro* migration assay was performed as described previously (Justus, Leffler et al. 2014). Briefly, cells were plated at a concentration of 0.5 million per well in a 6-well dish and grown until they reach 90% confluence. A scratch was made in the wells with a pipette tip, and cells were allowed to grow under normal culture conditions for 48 hours. Pictures were taken at 0hr, 24hr and 48hr to measure the migration capacity of the cells. The distance moved by the cells divided by time was used to obtain the percentage of wound closure.

2.27. STATISTICAL ANALYSIS

All experiments were performed with a minimum of three technical and three biological replicates, and values reported are the mean of the three biological replicates, unless otherwise indicated. Error bars represent the standard deviation from the mean, unless otherwise indicated. Pairwise comparisons were analyzed using multiple *t*-tests (one unpaired *t*-test per row), with corrections applied (Holm-Sidak method) for multiple comparisons. When comparing data from experiments with multiple groups, a regular one-way ANOVA (no matching) was used with the Benjamini-Hochberg procedure to adjust for multiple comparisons. Tukey HSD tests were used for *post hoc* analysis. Kaplan-Meier survival analysis was performed by using the log rank (Mantel-Cox) test. For all tests, differences were considered statistically significant at a *p*-value of 0.05 or less. For all figures, ns: $p > 0.05$; * $p < 0.05$; ** $p < 0.01$; *** $p < 0.001$; **** $p < 0.0001$. All statistical analyses were performed using the GraphPad Prism software and R.

CHAPTER 3: CHARACTERIZING THE EFFECT OF CDK4/6 INHIBITION IN ER+

BREAST CANCER

3.1. INTRODUCTION

3.1.1. ROLE OF CDK4/6-CYCLIN D ON GROWTH OF BREAST CANCER

Deregulation of the cell cycle is a prevalent hallmark of cancers including breast cancer (Malumbres and Carnero 2003). The G1/S checkpoint is one of the key checkpoints that maintain cellular integrity and regulate passage through the cell cycle (Bertoli, Skotheim et al. 2013). Typically, cells that have successfully crossed the G1/S checkpoint and entered the S or the DNA synthesis phase are committed to complete the cell cycle and undergo cellular division (Bertoli, Skotheim et al. 2013). The G1/S checkpoint is regulated by the 2 families of CDKs and cyclins: CDK/CDK6 - cyclin D and CDK2 – cyclin E (**Figure 5**) (Resnitzky, Gossen et al. 1994).

The D-type cyclins, comprising of cyclin D1, cyclin D2 and cyclin D3 are the key drivers of the G1/S checkpoint are often deregulated in several cancer such as breast, lung, bladder and head and neck cancer (Berenson, Koga et al. 1990, Proctor, Coombs et al. 1991, Wang, Pavelic et al. 1995). About 15% of all breast cancer patients exhibit amplification of the 11q13 locus, which contains CCND1, the gene encoding for cyclin D1 (Schuuring, Verhoeven et al. 1992). Further, about 50% of all breast cancers exhibit upregulation of cyclin D1 at both the mRNA and protein levels (Arnold and Papanikolaou 2005). This suggests a crucial regulatory role for cyclin D1 in the process of cell cycle and tumorigenesis. Moreover, cyclin D1 overexpression in transgenic mouse models resulted in the formation of mammary tumors, suggesting a breast cancer specific oncogenic role for the protein (Wang, Cardiff et al. 1994). Cyclin D1 in turn can be regulated by numerous pathways, including the estrogen receptor (ER) signaling pathway, Her-2 pathways and other major growth signaling pathways such as

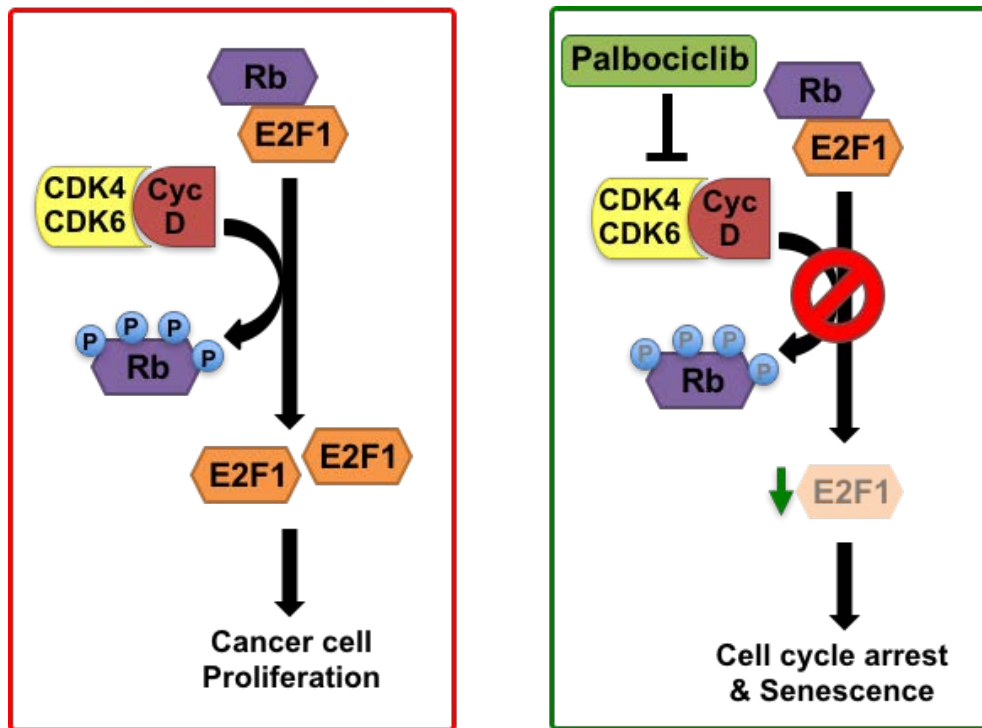


Figure 5: Regulation of the G1/S checkpoint: Schematic showing how the cell cycle proteins CDK4, CDK6 and cyclin D regulate progression through the cell cycle, and how palbociclib treatment cause G1 arrest and senescence

PI3K and MAPK pathways, all of which have been shown to positive regulate cyclin D1 expression (Zwijsen, Wientjens et al. 1997, Paternot and Roger 2009). Thus, cyclin D1 acts as a key point of convergence for growth signaling pathways and cell cycle progression, and an ideal drug target in cancer.

The canonical interacting partners of cyclin D1 involved in the regulation of the G1/S checkpoint are CDK4 and CDK6 (Otto and Sicinski 2017). These proteins work together with cyclin D to phosphorylate the tumor suppressor Rb, which gets further phosphorylated by the CDK2-cyclin E complex, inactivating the Rb protein and facilitates the release of E2F (Bertoli, Skotheim et al. 2013, Otto and Sicinski 2017). The transcription factor, E2F, in turn regulates expression of genes required for growth and progression through the cell cycle (Bertoli, Skotheim et al. 2013). Thus, the crucial role of CDK4/6 – cyclin D in tumorigenesis and cell

cycle progression, specifically in ER positive breast cancer, has led to the development of drugs targeting this pathway in the recent years, the CDK4/6 inhibitors (Finn, Crown et al. 2015, Finn, Martin et al. 2016). The CDK4/6 inhibitors, palbociclib, ribociclib and abemaciclib have shown great results in pre-clinical research and clinical trials, which has led to the FDA approval of these drugs (palbociclib, ribociclib) for the treatment of advanced ER positive breast cancer in combination with aromatase inhibitors (O'Leary, Finn et al. 2016, Sherr, Beach et al. 2016).

3.1.2. MECHANISTIC STUDIES OF PALBOCICLIB IN BREAST AND OTHER CANCER

Palbociclib (PD-0332991) the potent and specific CDK4/6 inhibitor has been tested in numerous pre-clinical cancer models including breast cancer (Toogood, Harvey et al. 2005). Treatment of cancer cell lines with palbociclib, specifically breast cancer cell lines, has been shown to decrease phosphorylation of Rb and induce a cell cycle arrest (G1 arrest) and senescence (Fry, Harvey et al. 2004, Finn, Dering et al. 2009). Palbociclib treatment also cause a reduction in Rb phosphorylation and Ki67 (marker of proliferation) in breast tumors *in vivo* and a dose-dependent decrease in the growth of mouse tumor xenografts (Fry, Harvey et al. 2004). One of the early studies in breast cancer with this drug examined the growth inhibitory effect of the drug and its half maximal inhibitory concentrations (IC50 values) across a panel of 44 breast cancer cell lines belonging ER positive, HER2 positive and TNBC subtypes (Finn, Dering et al. 2009). Results from this study showed that a majority of the cell lines that were sensitive to palbociclib belonged to the ER positive subtype of breast cancer (Finn, Dering et al. 2009). While, majority of the ER negative or TNBC cell lines were resistant to palbociclib, a small proportion of the sensitive cells belonged to this subtype (Finn, Dering et al. 2009). The study also showed that the sensitive cell lines exhibited high expression of Rb, cyclin D1 and loss of p16 (Finn, Dering et al. 2009). Another study which examined the changes in gene expression following treatment with palbociclib in ER positive breast cancer

cell line showed a significant downregulation in the proliferative and cell cycle regulatory genes at the mRNA level (Knudsen and Witkiewicz 2016). These studies provided the rationale for further pre-clinical and clinical investigation of CDK4/6 inhibition in ER positive breast cancer.

Additionally, numerous pre-clinical studies have been conducted with palbociclib in other cancers such as mantle cell lymphoma, myeloma, acute myeloid leukemia, glioblastoma, ovarian cancer, esophageal adenocarcinoma, mantle cell lymphoma and prostate cancer (Baughn, Di Liberto et al. 2006, Marzec, Kasprzycka et al. 2006, Wang, Wang et al. 2007, Michaud, Solomon et al. 2010, Ismail, Bandla et al. 2011, Konecny, Winterhoff et al. 2011, Leonard, LaCasce et al. 2012, Comstock, Augello et al. 2013). All of these studies showed significant and potent anti-proliferative activity accompanied by the induction of G1 arrest in tumor cell lines *in vitro* and anti-tumor activity in tumors *in vivo* with palbociclib treatment, and also showed an association between sensitivity to the drug and expression of Rb.

A study conducted primarily in U2OS cells and verified in other cancers identified FOXM1 as a direct substrate of CDK4/6, which protects cells from the induction of senescence (Anders, Ke et al. 2011). Results from this study showed that palbociclib mediated downregulation of FOXM1 coupled with pRb and G1 arrest results in the induction of ROS-mediated senescence (Anders, Ke et al. 2011). Another study in melanoma cells *in vitro* showed that prolonged treatment with the CDK4/6 inhibitor along with mTOR expression is required for the induction of an irreversible growth inhibition and senescence (Leontieva and Blagosklonny 2013). Recent studies also suggest a role for palbociclib in regulating EMT and cancer stem cells (Qin, Xu et al. 2015, Bonuccelli, Peiris-Pages et al. 2017). Finally, palbociclib mediated CDK4/6 inhibition has been shown to regulate increase mitochondrial mass and cause metabolic reprogramming in pancreatic cancer cell lines models, and regulate autophagy in fibroblasts and promyelocytic leukemia (Capparelli, Chiavarina et al. 2012, Acevedo, Vernier et al. 2016, Franco, Balaji et al. 2016).

3.1.3. INTERPLAY BETWEEN ROS AND SENESENCE

The concept of senescence first originated from studies that showed that primary cells obtained from human tissues were mortal and had limited replicative potential (Hayflick and Moorhead 1961). This is associated with shortening of the telomere length, which in turn has been shown to trigger a DNA damage response leading to senescence (Harley, Futcher et al. 1990, d'Adda di Fagagna, Reaper et al. 2003). However, in cancers, senescence can be induced even in the absence of telomere shortening, which may be stress induced, oncogene induced or tumor suppressor loss induced senescence (Kuilman, Michaloglou et al. 2010). The induction of senescence is typically characterized by the presence of prolonged cell cycle arrest, morphological transformation (cells acquire a large and flat morphology), activation of tumor suppressor networks such as p16 and p21, induction of SA- β gal activity, presence of senescence associated heterochromatin foci (SAHF) and senescence associated secretory phenotype (SASP) (pro-inflammatory cytokine factors that are secreted by senescent cells) (Dimri, Lee et al. 1995, Serrano, Lin et al. 1997, Campisi 2005, Kuilman, Michaloglou et al. 2010).

The well-established triggers of stress-induced senescence in cancer model systems include DNA damage and oxidative stress mediated by reactive oxygen species (ROS) (d'Adda di Fagagna 2008, Lu and Finkel 2008, Kuilman, Michaloglou et al. 2010). Reactive oxygen species (ROS) are highly reactive free radicals, ions or molecules that are generated as a result of response to stress due to increased metabolic activity, mitochondrial dysfunction, oncogene activity, etc. (Liou and Storz 2010, Jajic, Sarna et al. 2015). The levels of the reactive oxygen species in cancer cells can determine its pro-tumorigenic vs anti-tumorigenic role (Liou and Storz 2010). Low levels of ROS can promote tumor growth and cell cycle progression by directly regulating the expression of cell cycle proteins including G1/S cyclins such as cyclin B2, cyclin D3 and cyclin E (Felty, Singh et al. 2005, Liou and Storz 2010). However, significantly higher levels of ROS can induce cell cycle arrest, senescence, and even turn on

cell death signaling and apoptosis (Liou and Storz 2010). Moreover, numerous studies have shown that ROS is indispensable for the induction of senescence in cancers. For example, ROS has been shown to be required for anticancer drug induced DNA damage and senescence in lung cancer, p21 mediated senescence in lung fibroblasts and radiation induced senescence in human endothelial cells (Luo, Zou et al. 2011, Luo, Yang et al. 2013, Park, Kim et al. 2016). Finally, treatment with the CDK4/6 inhibitor palbociclib and abemaciclib induces ROS dependent senescence in cancers (Anders, Ke et al. 2011, Franco, Balaji et al. 2016, Patnaik, Rosen et al. 2016).

3.1.4. GAP IN KNOWLEDGE

While current pre-clinical mechanistic studies provide insight into the mechanism of CDK4/6 inhibition mediated by palbociclib and other drugs, several questions remain:

1. Is there a time dependent difference in the growth inhibition mediated by palbociclib?
(i.e.) Is long term drug treatment required for the induction of senescence?
2. Is there a dose dependent variation in palbociclib action? Is there an off-target effect of the drug observed at higher doses?
3. Does palbociclib induce cytotoxic effects or apoptosis?
4. Is ROS required for palbociclib mediated irreversible growth inhibition and senescence?
5. Is ROS induced in ER+ve breast tumors *in vivo*?

Thus, studies in this chapter are aimed at addressing these gaps in knowledge, which will provide valuable information in understanding the mechanism by which CDK4/6 inhibition impacts the growth ER positive breast cancer cells.

3.2. RESULTS

3.2.1. DEREGLATION OF CDK4/6-CYCLIN D PATHWAY IN BREAST CANCER

To interrogate the importance of the G1/S checkpoint in breast tumors, The Cancer Genome Atlas's (TCGA) breast cancer dataset was examined to mine for mutations, amplifications, mRNA upregulation and protein upregulation of genes within the CDK4/6-Cyclin D pathway. TCGA's breast tumor cohort comprises of 971 completely annotated tumors, with 594 tumors belonging to the ER positive subtype, 58 tumors belonging to the Her2 positive subtype and 82 tumors belonging to Triple Negative Breast Cancer (TNBC) subtype. Detailed analysis revealed alterations in the CDK4/CDK6/Cyclin-D pathway in about 37% of all breast cancer patients (CDK4 - 7%, CDK6 – 8%, cyclin D – 22%) (**Figure 6A**). Further, 35% of ER positive breast cancer patients (CDK4 - 4%, CDK6 – 3%, cyclin D – 28%) (**Figure 6A**), 29% of the Her2+ breast cancer patients (CDK4 - 10%, CDK6 – 0%, cyclin D – 19%) (**Figure 6D**), and 64% of TNBC patients (CDK4 - 22%, CDK6 – 37%, cyclin D – 5%) (**Figure 6A**) exhibited alterations in the CDK4/6-cyclin D pathway. Moreover, gene amplification and mRNA upregulation of cyclin D contributed the most to the pathway deregulation seen in the ER+ve and Her2 +ve subtypes of breast cancer (**Figure 6B,D**), while mRNA upregulation of CDK4 and CDK6 were the most prevalent alterations in the TNBC tumors (**Figure 6C**).

Thus, these results reveal the importance of the CDK4/6 pathway in all subtypes of breast cancer and help identify ER positive breast cancer as an ideal population for targeting CDK4 and CDK6, since 70% of all breast cancers are of the ER positive subtype.

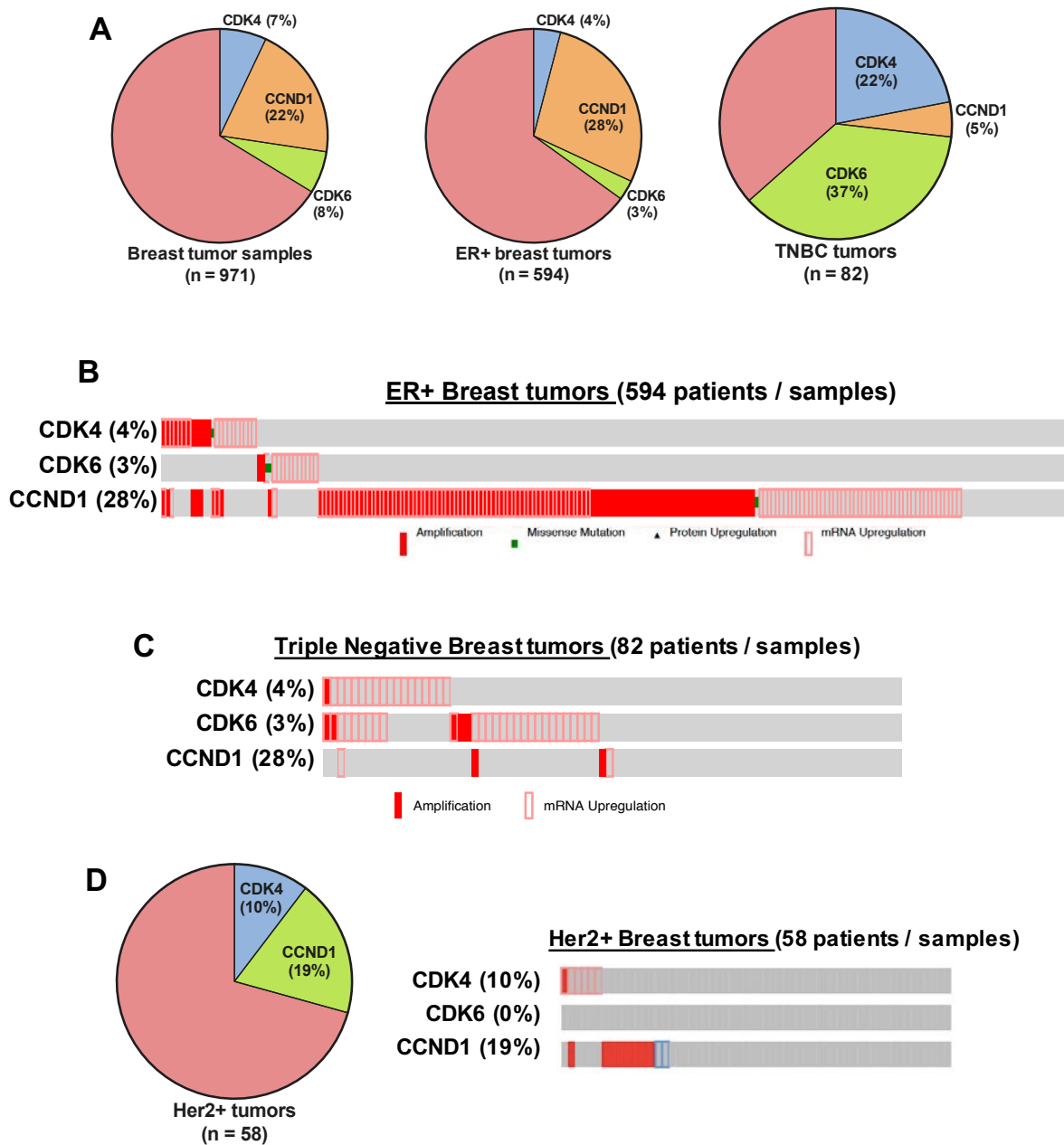


Figure 6: Deregulation of CDK4/6-Cyclin D pathway in Breast Cancer: A) Pie chart showing alterations in CDK4, CDK6 and cyclin D at the gene and protein levels based on The Cancer genome Atlas (TCGA) analysis of breast tumors. B,C) Detailed analysis of gene amplifications, mutations and proteins upregulations in CDK4, CDK6 and cyclin D genes in ER positive (B) and Triple negative (C) breast cancer as obtained from TCGA. D) Pie chart showing alterations in CDK4, CDK6 and cyclin D at the gene and protein levels and detailed analysis from TCGA database of Her2+ tumors.

3.2.2. IMPACT OF siRNA OR shRNA KNOCKDOWN OF CDK4/6

To interrogate the biological effect of downregulating CDK4 and CDK6, we utilized two independent methods knockdown the two proteins namely, i) short hairpin RNA (shRNA) and ii) small interfering RNA (siRNA). shRNA knockdown typically provides a stable downregulation of the mRNA and protein, while siRNA provides a transient or temporary (usually lasting 72 hours) but effective knockdown (Aagaard and Rossi 2007).

First, we performed shRNA mediated knockdown of CDK4 and/ or CDK6 in two established ER positive breast cancer cell lines - MCF7 and T47D (Mackay, Tamber et al. 2009) using at least 2 different shRNA constructs (**Figure 7A and 7B**). Results revealed that downregulation of the individual kinases had little to no growth inhibitory potential as measured by doubling time and cell counting over a 10-day period (**Figure 7C and 7D**). In comparison, a significant growth inhibition was observed upon combined shRNA knockdown of CDK4 and CDK6 (**Figure 7D**), concomitant with an increase in their doubling time when compared to Control (Scrambled) cells (**Figure 7C**).

Since the short term transient knockdown effect obtained with siRNA is considered more similar to the effect observed in the presence of a pharmacological inhibitor, we next performed siRNA mediated downregulation of CDK4 or CDK6 using pooled siRNA constructs (used for better knockdown efficiency) (**Figure 7E**). Results from cell counting assay performed over 6-day period showed little to no growth inhibition upon knockdown of the individual proteins (**Figure 7F**). However, similar to the results from the shRNA experiments, siRNA-mediated combined CDK4 and CDK6 knockdown (**Figure 7E**) elicited a significant growth inhibitory effect on the ER positive breast cancer cells (**Figure 7F**).

Thus, these results provide a strong rational for combined targeting of CDK4 and CDK6 in ER positive breast cancer.

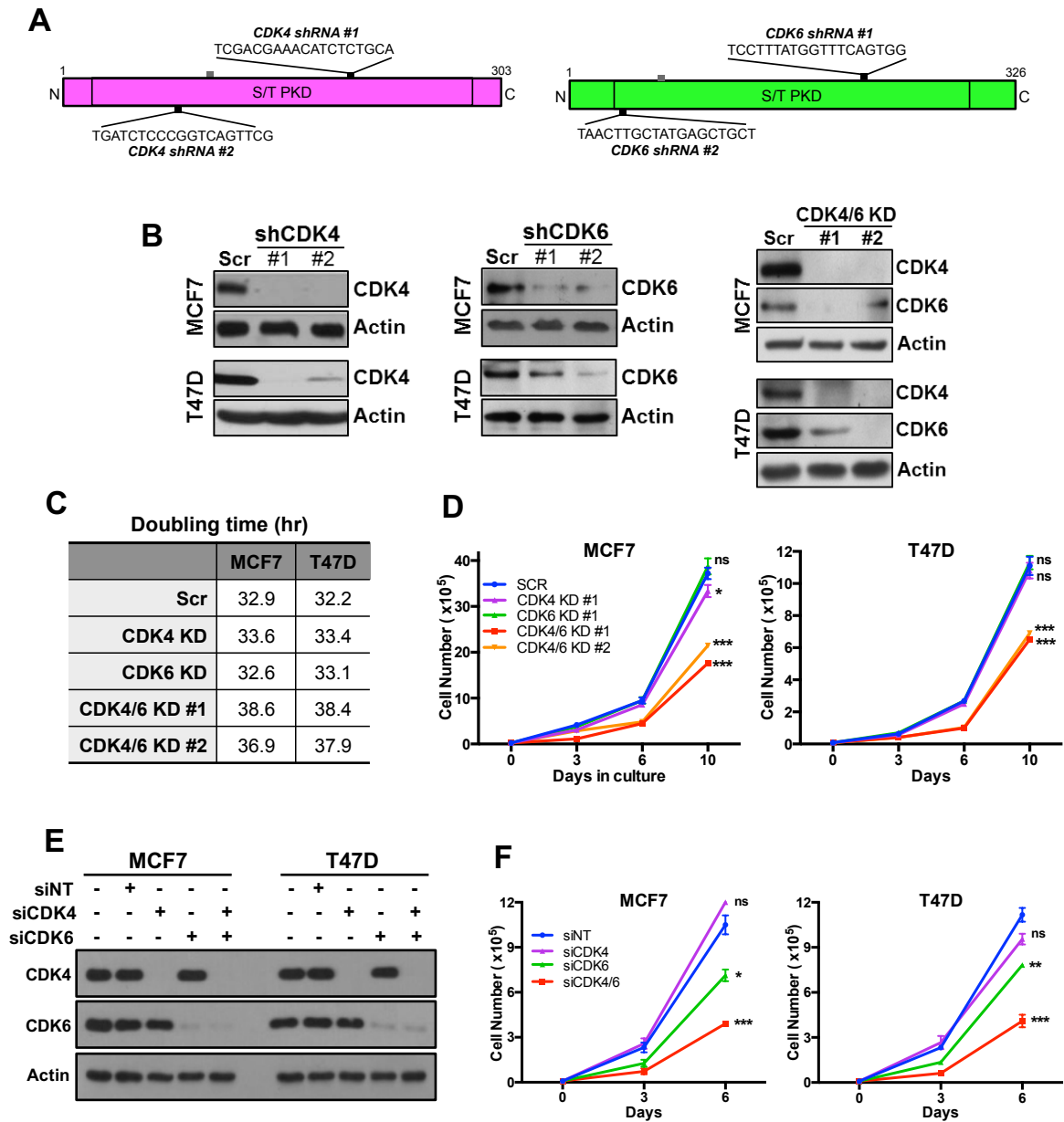


Figure 7: Impact of siRNA or shRNA knockdown of CDK4/6: A) Schematic showing location of shRNAs on the CDK4 and CDK6 genes. B) Western blot analysis showing protein levels of CDK4 and CDK6 upon transfection with shRNA for CDK4 and CDK6 alone or in combination. C) Doubling time of MCF7 and T47D upon knockdown of CDK4 and/or CDK6 via shRNA when compared to Scrambled (Scr) cells. D) Cell counting to examine impact of shRNA knockdown of CDK4 and/or CDK6 on proliferations of MCF7 and T47D cells. E) Western blot showing levels of CDK4 and CDK6 proteins in MCF7 and T47D cells after transfection with ON-TARGETplus SMARTpool siRNA non-targeting (siNT) or CDK4 and CDK6, separately or combined. F) Impact of siRNA knocking down of CDK4 and/or CDK6 on the proliferation of MCF7 and T47D cells compared to NT siRNA transfected cells. All data represent mean \pm SD from three independent experiments; p-values were calculated in comparison to cells treated with SCR or siNT. ns: $p > 0.05$; * $p < 0.05$; ** $p < 0.01$; *** $p < 0.001$; **** $p < 0.0001$.

3.2.3. DOSE DEPENDENT EFFECT OF PALBOCICLIB ON GROWTH, CELL CYCLE ARREST AND SENESENCE

Having shown the impact of downregulating CDK4 and CDK6 in ER positive breast cancer, we next compared the growth inhibitory potential of the FDA approved CDK4/6 inhibitor, palbociclib, in three ER positive breast cancer cell lines, MCF7, T47D and ZR75-1, in comparison with an immortalized human mammary epithelial cell line (HMEC - MCF10A). In order to examine the time and dose-dependent effect of the drug, we performed dose response studies where the cells were treated with varying concentrations of the drug for different time periods (1,2,4,6, or 8 days), and provided with a recovery time to interrogate the reversibility of drug action (**Figure 8A**). Results demonstrate that palbociclib inhibited the growth of ER positive breast cancer cell lines in a time and dose-dependent manner, resulting in a significant irreversible growth inhibition (**Figure 8B**), with half-maximal inhibitory concentrations (IC₅₀) of 0.73μM to 0.93μM following 8 days of continuous treatment and 4 days of recovery (**Figures 8C,D**). In contrast, the HMEC cell line MCF-10A was more resistant to palbociclib, displaying a >5-fold (5.98μM) higher IC₅₀ value than the ER positive cell lines (**Figures 8B-3D**). These results suggest that palbociclib induces a time and dose dependent growth inhibition that is specific to the ER positive breast cancer cells, but not in HMECs.

To further investigate palbociclib mediated growth inhibition, we performed colony formation assay with 6 days of drug treatment and 6-day recovery, which revealed that palbociclib treatment of ER positive, but not HMEC cells, resulted in a dose-dependent reduction in colony counts (**Figure 8E**). Next, to examine the ability of ER positive breast cancer cells to recover from palbociclib-mediated growth inhibition, cells were treated continuously for 6 days (which was the least duration of treatment having the lowest IC₅₀ value from Figure 3C) with increasing concentrations of the drug, and cultured in the absence of palbociclib for another 4 days (**Figure 8F**). Cell counting and S-phase progression (BrDU incorporation measured via flow cytometry) assays revealed that treatment with palbociclib at

doses of 1 μ M or less resulted in a reversible growth inhibition (**Figures 8G** - compare solid lines to dashed lines and **Figure 9A** –compare black vs white shaded bars). On the other hand, higher doses of palbociclib (>2.5 μ M) resulted in an irreversible inhibition of growth and S-phase progression (measured by BrdU incorporation) in the ER positive breast cancer cells (**Figures 8G** - compare solid lines to dashed lines and **Figure 9A** –compare black vs white shaded bars). Strikingly, this effect of palbociclib on growth and proliferation was not observed in the HMEC cell lines MCF10A, where the growth inhibition induced was reversible at all doses (**Figures 8G** - compare solid lines to dashed lines and **Figure 9A** –compare black vs white shaded bars), thus demonstrating a dose-dependent growth inhibition mediated by palbociclib, specifically in ER positive cancer cells.

Next, to interrogate the impact of palbociclib treatment on the cell cycle, we treated the cells for 6 days and allowed the cells to recover for 4 days to examine reversibility of the drug effect (**Figure 8F**). Results show that palbociclib treatment induces a dose-dependent cell cycle arrest (G1 arrest), which was readily reversible at the lower doses (<1 μ M), while higher doses of palbociclib induced an irreversible G1 arrest (**Figure 9B and 9C** - compare black vs white shaded bars). Additionally, this dose-dependent induction of G1 arrest was observed only in MCF7 and T47D cells and not in MCF10A (**Figure 9B and 9C**), further demonstrating specificity of palbociclib to ER positive cancer cells, and not HMECs. Further, western blot analysis showed a dose-dependent decrease in known palbociclib effectors such as Rb, pRb and FOXM1 (Anders, Ke et al. 2011), but no alteration in the protein levels of CDK4 and CDK6 (**Figure 9D**).

Finally, we examined if palbociclib induces senescence in the ER positive breast cancer cells, and if this occurs in a dose-dependent manner. Measurement of senescence activity by senescence associated- β galactosidase (SA- β gal) assay indicates that palbociclib induces moderate senescence at the lower doses (<1 μ M) and significant levels of senescence only at higher doses (>2.5 μ M) in MCF7 and T47D cells (**Figure 10A**). Moreover, no induction of

senescence was observed in the HMEC cell line, MCF10A at all doses of palbociclib (**Figure 10A**). Further, cells undergoing senescence display a change in morphology as well as an increase in cellular complexity and granularity, which can be measured by changes in the side scatter (Anders, Ke et al. 2011, Bielak-Zmijewska, Wnuk et al. 2014). Flow cytometry analysis showed a significant increase in side-scatter of ER+ve breast cancer cells in a dose-dependent manner, which the increase being reversible at the lower doses and irreversible at higher doses of 5uM (**Figure 10B**).

The summary of these results is shown in **Figure 10C**, which depicts the effects of palbociclib as a variant of dose: i) BrdU incorporation / cell proliferation – red solid line on the right Y-axis, ii) sustained G1 arrest (post recovery) – blue solid line on the right Y-axis, iii) protein levels of pRb (measured by densitometry) – orange solid line on the left Y-axis and iv) measurement of senescence – green solid line on the left Y-axis. Collectively, these results show that palbociclib treatment induces dose-dependent growth inhibition, G1 arrest, decrease in Rb phosphorylation and increase in senescence, specifically in the ER positive breast cancer cells.

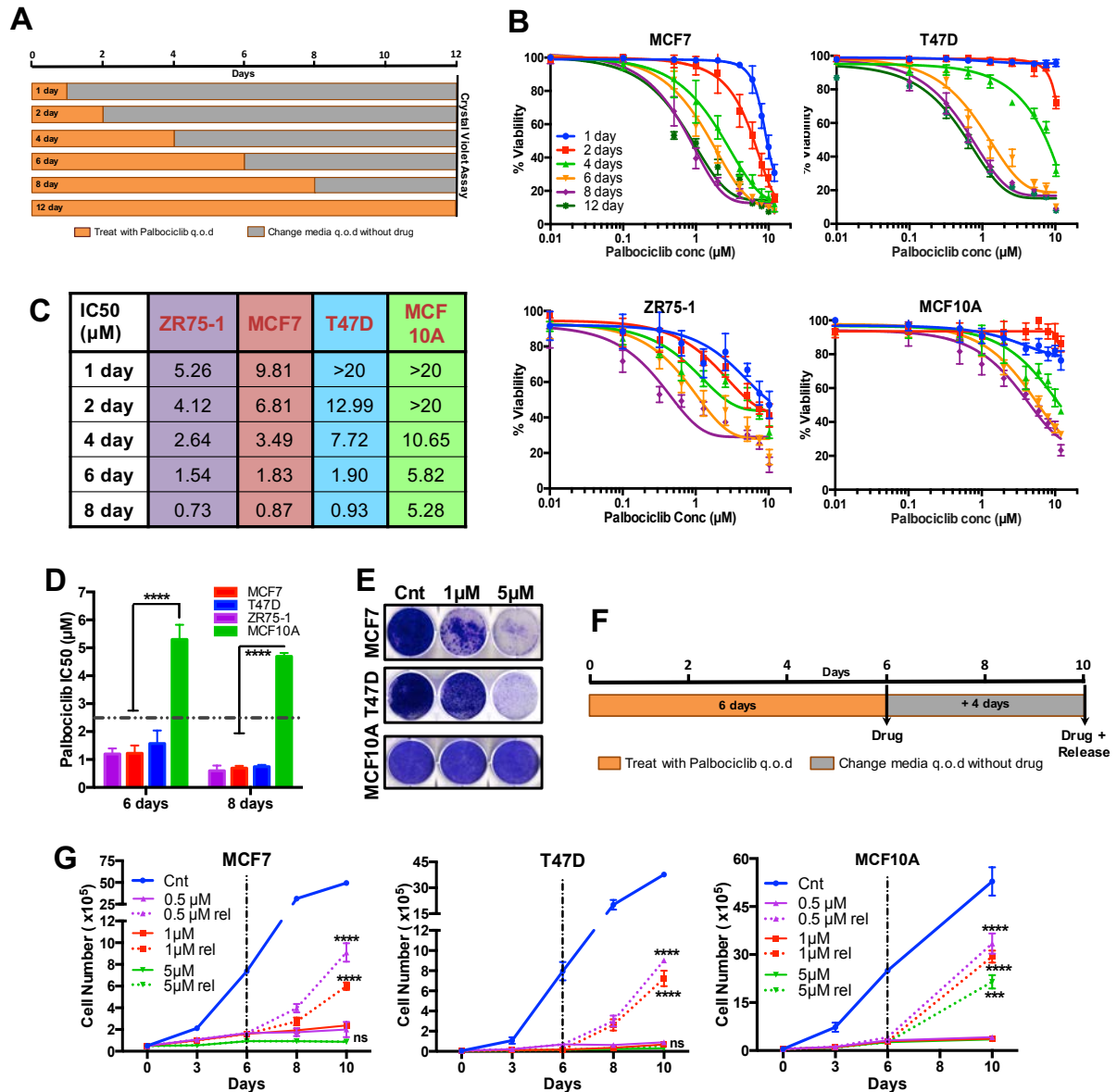


Figure 8: Dose-dependent effect of palbociclib on growth of ER+ breast cancer cells: A) Schematic depicting the palbociclib treatment schedule for the dose-response experiments shown in Fig 3B. Drug-containing medium or drug-free medium was replaced every other day (q.o.d). B) Dose-response curves for MCF7, T47D, MCF10A, and ZR75-1 cells treated with DMSO or increasing concentrations (conc) of CDK4/6 inhibitor palbociclib (0.01 to 12 μM) for 1, 2, 4, 6, 8 or 12 days. C, D) Half-maximal inhibitory concentration (IC₅₀) values of MCF7, T47D, ZR75-1, and MCF10A cells as calculated from dose-response experiments in Figs 1a and Supplementary Fig. 2b. E) Clonogenic assay examining the effect of palbociclib on breast cancer cells post 6 days of treatment. F) Schematic depicting the palbociclib treatment schedule where cells were treated for 6 days and cultured in drug-free medium for 4 days to examine reversibility. Medium was replaced every other day (q.o.d). G) MCF7, T47D, and MCF10A cells were treated with DMSO (Cnt) or varying concentrations of palbociclib for 6 days cells were then subjected to cell counting to assess growth inhibition. All data represent mean±SD from three independent experiments; p-values were calculated by comparing values at the end of 6 day drug treatment with those at the end of drug + release. ns: p>0.05; *p<0.05; **p<0.01; ***p<0.001; ****p<0.0001.

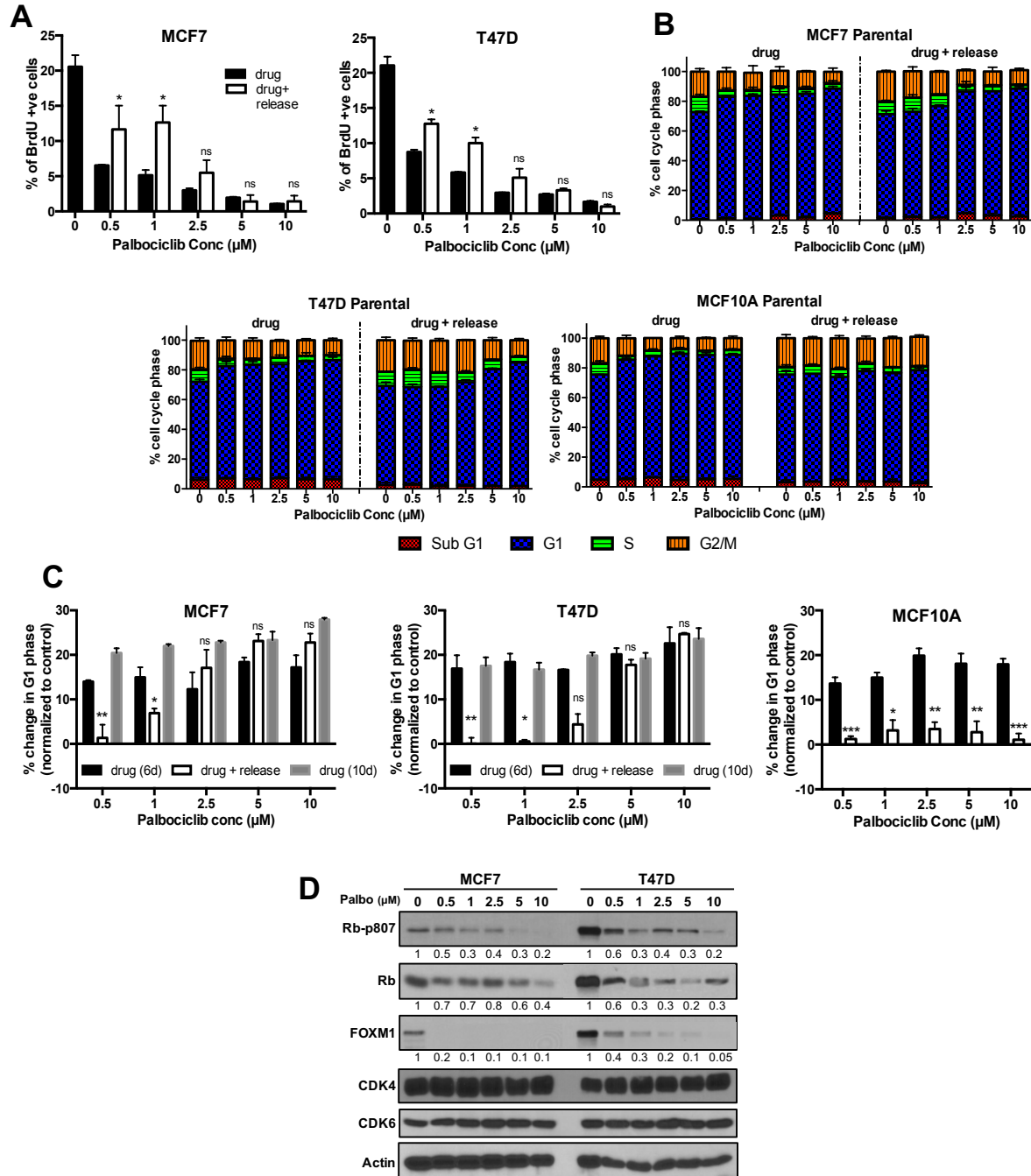


Figure 9: Dose-dependent effect of palbociclib on cell cycle of ER+ breast cancer cells: MCF7, T47D, and MCF10A cells were treated with DMSO (Cnt) or varying concentrations of palbociclib for 6 days and subjected to A) flow cytometry analysis for BrdU-positive cells, a measure of S phase progression; B) cell cycle analysis via flow cytometry; and C) cell cycle analysis to determine percentage change in the G1 phase. D) Western blot analysis of MCF7 and T47D cells treated with DMSO or palbociclib for levels of cell cycle proteins: Rb, p-Rb (S807), FOXM1, CDK4, and CDK6. Values show densitometry of the western blots as normalized to the loading control actin. All data represent mean \pm SD from three independent experiments; p-values were calculated by comparing values at the end of 6 day drug treatment with those at the end of drug + release. ns: $p > 0.05$; * $p < 0.05$; ** $p < 0.01$; *** $p < 0.001$; **** $p < 0.0001$.

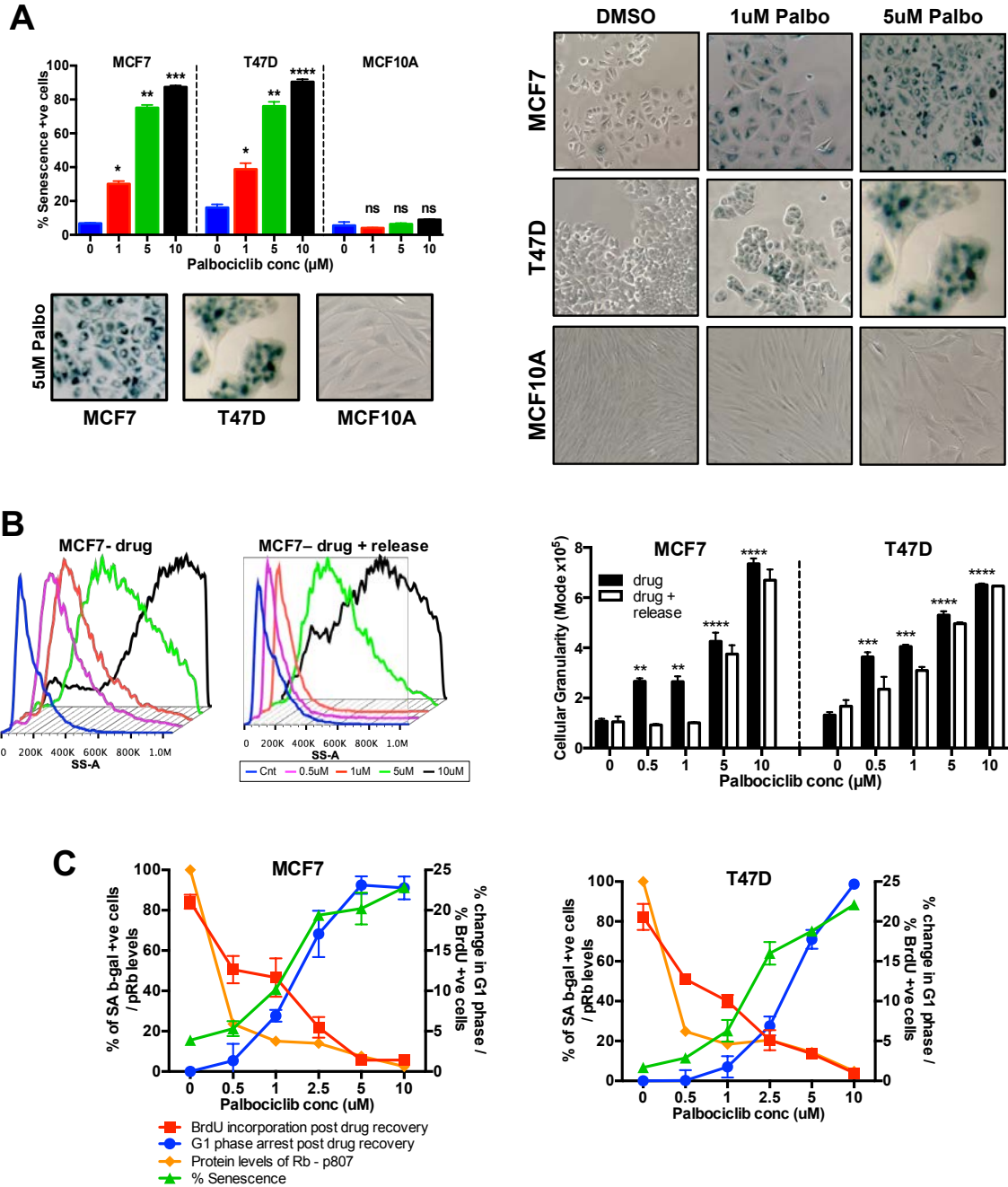


Figure 10: Effect of palbociclib on senescence in ER+ breast cancer cells: A) Senescence-associated SA- β gal staining (left) as a measure of senescence with representative images (right) in MCF7, T47D and MCF10A cells upon treatment with DMSO or palbociclib for 6 days. B) Side scatter analysis (left) and quantification (right) to assess granularity of MCF7 and T47D cells treated for 6 days with palbociclib with release for 4 days. C) Graph showing changes in pRb levels, G1 phase, BrdU postivity and SA- β gal cells with varying concentrations of palbociclib. All data represent mean \pm SD from three independent experiments; p-values were calculated by comparing values at the end of 6 day drug treatment with those at the end of drug + release. ns: $p > 0.05$; * $p < 0.05$; ** $p < 0.01$; *** $p < 0.001$; **** $p < 0.0001$.

3.2.4. TIME DEPENDENT EFFECT OF PALBOCICLIB ON GROWTH, CELL CYCLE ARREST AND SENESENCE

Having shown that the dose of palbociclib treatment has a significant impact of the drug effect, we next wanted to examine if the time of treatment plays a role, (i.e.) if long-term treatment is necessary to achieve a sustained effect on ER positive breast cancer cells. Since our previous results showing the induction of dose-dependent growth inhibition and senescence (Figures 2-5) were performed long-term (6 day) treatments with palbociclib, we wanted to examine the effect with shorter treatment times. Hence, we treated the ER positive breast cancer cells for 72 hours with 2 doses, low (1 μ M) and high (5 μ M) doses of palbociclib and then cultured the cells in the absence of the drug for another 3 days, to examine reversibility of drug effect. Cell counting assay showed that the growth inhibition induced by palbociclib was readily reversible at all concentrations once the drug was removed (**Figure 11A**). Further, BrdU analysis (a measure of cellular proliferation and S phase progression), where cells were treated with varying concentrations of palbociclib, showed that 72 hour was only able to induce a reversible growth inhibition in ER+ve and HMEC cell lines (**Figures 11B – compare black and white shaded bars**). Finally, measurement of senescence activity by senescence associated- β galactosidase (SA- β gal) assay revealed that short-term palbociclib treatment (72 hours) does not induce significant levels of senescence in MCF7, T47D and MCF10A cells (**Figure 11C**).

Thus, this data indicate that long term is required for palbociclib mediated CDK4/6 inhibition to have a sustained and irreversible growth inhibitory effect in ER positive breast cancer.

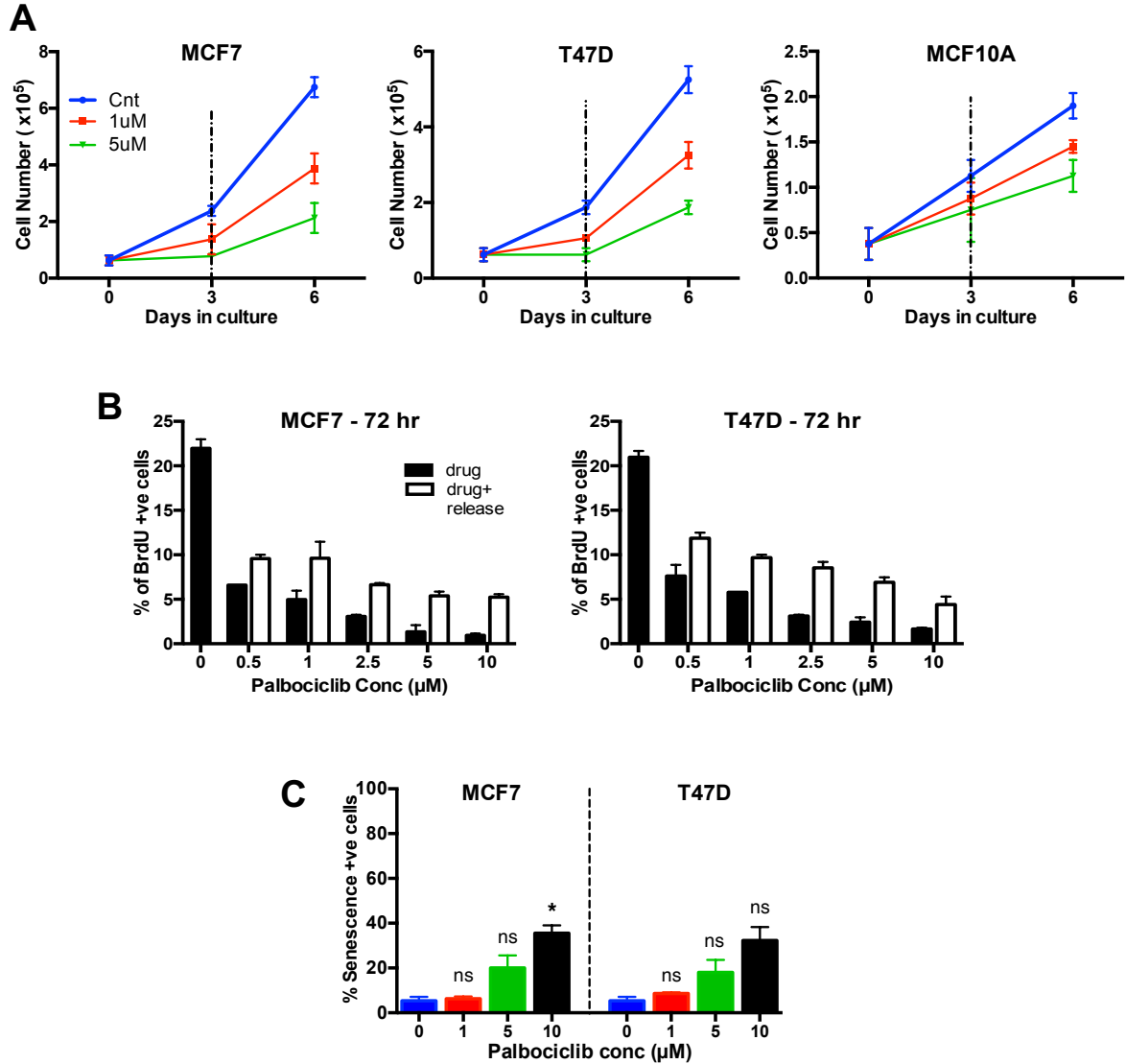


Figure 11: Time-dependent effect of palbociclib on cell cycle of ER+ breast cancer cells: MCF7, T47D, and MCF10A cells were treated with DMSO (Cnt) or varying concentrations of palbociclib for 3 days with release for 3 days, and subjected to A) Cell counting to examine effect on proliferation; B) flow cytometry analysis for BrdU-positive cells, a measure of S phase progression and C) Quantification of Senescence-associated SA- β gal staining. All data represent mean \pm SD from three independent experiments; p-values were calculated by comparing values at the end of 6 day drug treatment with those at the end of drug + release. ns: $p > 0.05$; * $p < 0.05$; ** $p < 0.01$; *** $p < 0.001$; **** $p < 0.0001$.

3.2.5. EFFECT OF PALBOCICLIB ON INDUCING APOPTOSIS IN ER+ve BREAST CANCER

Having shown that the CDK4/6 inhibitor palbociclib mediates a time and dose dependent growth inhibition, cell cycle arrest and senescence, we next wanted to investigate if palbociclib might have a cytotoxic effect in ER positive breast cancer. Flow cytometry analysis of Annexin V and PI stained MCF7 and T47D cells revealed no significant increase in early (Annexin V +ve /PI –ve) or late (Annexin V +ve /PI +ve) apoptotic cells upon treatment with the CDK4/6 inhibitor (**Figure 12A**). Further, cell cycle analysis to examine sub G1 population and Caspase 3 activity assay revealed no increase in sub G1 population (**Figure 12B**) and Caspase 3 activity (**Figure 12C**) with drug treatment. Finally, western blot analysis of known apoptotic genes, cleaved PARP, cleaved Caspase 7 showed no increase in apoptosis upon treated with palbociclib (**Figure 12D**).

Thus, these results show that treatment with the CDK4/6 inhibitor palbociclib does not induce a cytotoxic effect via apoptosis in ER+ve breast cancer cell lines.

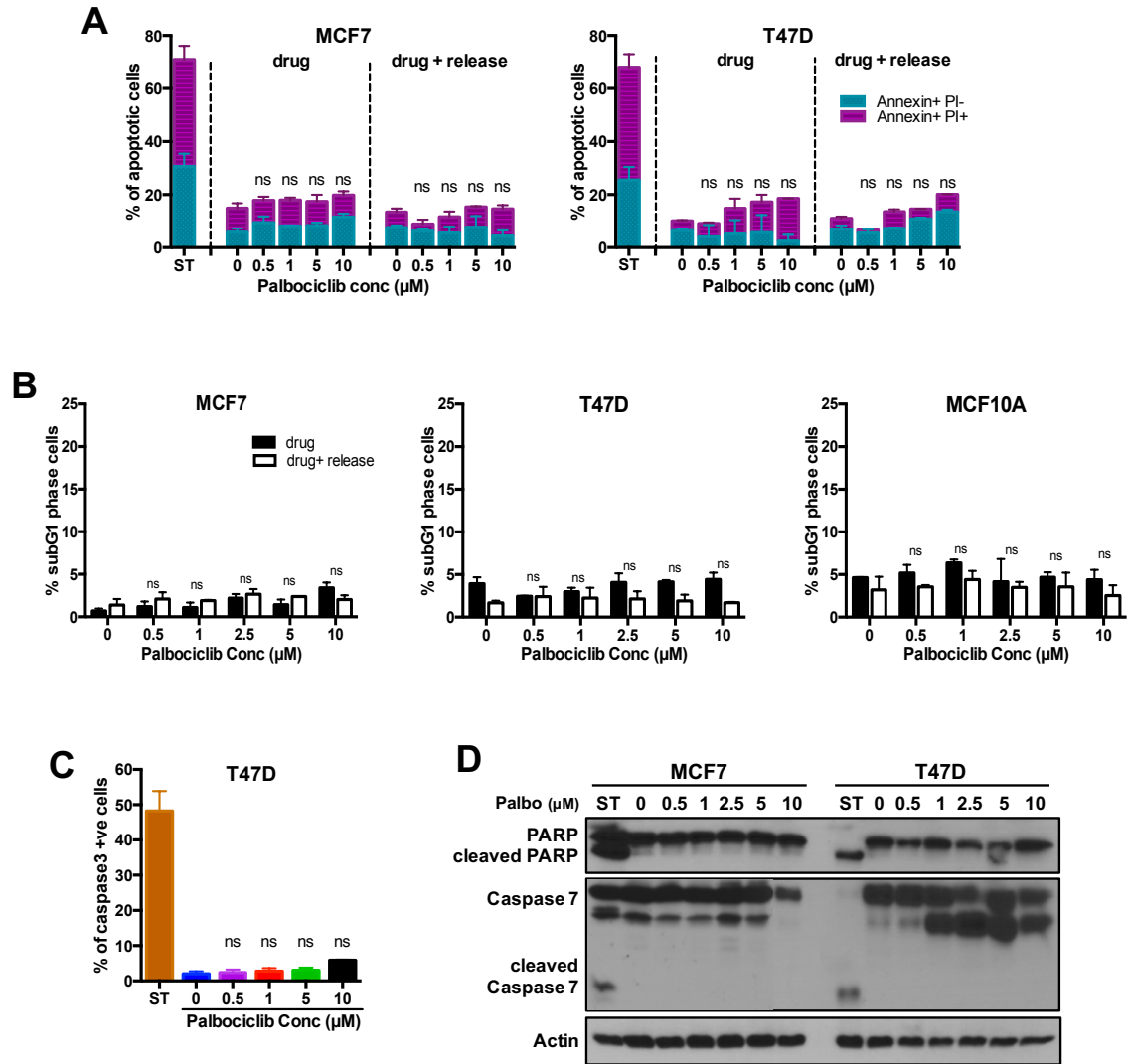


Figure 12: Effect of palbociclib on inducing apoptosis in ER+ breast cancer cells: A) Flow cytometry measurement of apoptotic cells (early apoptosis: Annexin V+/ PI-; late apoptosis: Annexin V+/PI+) in cells treated as in (a). B) Cell cycle analysis to determine percentage of cell in sub G1 phase, as a measure of apoptosis. C) Percentage of caspase-3 positive cells determined by flow cytometry in T47D cells treated with DMSO, 3 μM staurosporine (positive control), or varying concentrations of palbociclib for 6 days. D) Western blot analysis of apoptotic proteins in MCF7 and T47D treated with DMSO or palbociclib (Palbo) for 6 days: PARP, cleaved PARP, caspase-7, and cleaved caspase-7, with actin as loading control. All data represent mean±SD from three independent experiments; p-values were calculated by comparing values at the end of 6 day drug treatment with those at the end of drug + release. ns: p>0.05; *p<0.05; **p<0.01; ***p<0.001; ****p<0.0001.

3.2.6. ON-TARGET vs OFF-TARGET EFFECTS OF PALBOCICLIB

Given that all kinase inhibitors can have potential off-target effects, we next wanted to examine if the different doses of palbociclib that induce growth inhibition and / or senescence in ER positive breast cancer cell lines are due to on-target (due to inhibition of CDK4 and CDK6) or off-target (due to inhibition of other kinases). A recent chemical proteomic study revealed that the CDK4/6 inhibitor palbociclib interacts with targets other than CDK4 and CDK6, such as CDK9, Caesin kinase 2, PIK3R4 and other Class III PI3 kinases (Sumi, Kuenzi et al. 2015).

To examine the specificity of palbociclib to CDK4 and CDK6, the two genes were downregulated using either shRNA or siRNA technologies (Figure 7) in MCF7 and T47D cells. Treatment of cells with knockdown of CDK4 and/ or CDK6 with increasing concentrations of palbociclib showed that knockdown of either protein alone was not sufficient to recapitulate the effect of the drug, as downregulation of just one kinase did not result in “rescue” from palbociclib mediated growth inhibition (**Figure 13A**). However, combined knockdown of both CDK4 and CDK6, recapitulated palbociclib treatment and mediates resistance (i.e. rescue) to palbociclib-induced growth inhibition only at the lower concentrations ($\leq 1\mu\text{M}$) (**Figure 13A**). Intriguingly, higher concentrations of palbociclib ($>1\mu\text{M}$) had a growth inhibitory effect of the CDK4/6 double knockdown cells, indicating potential off-target effects of palbociclib at these higher concentrations (**Figure 13A**). To further understand the on-target vs off-target effects of palbociclib in ER+ve breast cancer cell lines, we treated siRNA mediated CDK4/6 knockdown cells with low (1uM) and high (5uM) dose palbociclib. Results show that that while low-dose (1uM) palbociclib had no additional growth inhibitory effect on the CDK4/6 knockdown cells, higher doses (5uM) of palbociclib induced additional growth inhibition (**Figure 13B**).

Thus, these results indicate that indicating that the irreversible grown inhibition and high levels of senescence observed at $5\mu\text{M}$ could be due to off-target effects at higher palbociclib concentrations.

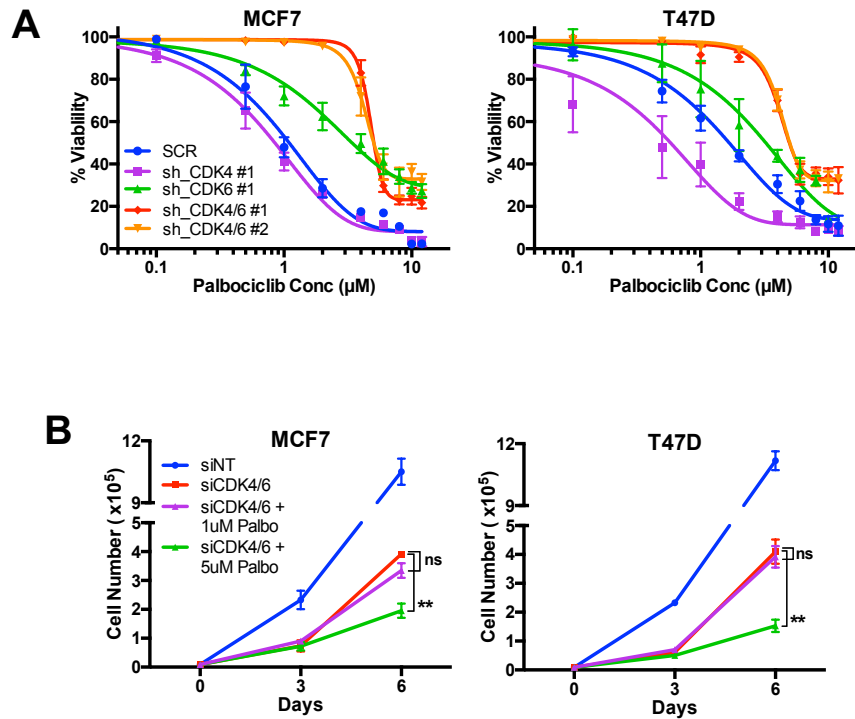


Figure 13: On-target vs Off-target effects of palbociclib: A) Proliferation of MCF7 and T47D cells upon knockdown of CDK4 and/or CDK6 and treatment with DMSO or increasing concentrations of palbociclib (0.01 to 12 μM) for 6 days. B) Cell counting to examine proliferation of MCF7 and T47D cells upon dual siRNA against CDK4 and CDK6, and treated with 1uM or 5uM palbociclib. All data represent mean \pm SD from three independent experiments; p-values were calculated by comparing values at the end of 6 day drug treatment with those at the end of drug + release. ns: $p>0.05$; * $p<0.05$; ** $p<0.01$; *** $p<0.001$; **** $p<0.0001$.

3.2.7. INDUCTION OF REACTIVE OXYGEN SPECIES (ROS) BY CDK4/6 INHIBITION

Recent studies have shown that CDK4/6 inhibition via palbociclib and ribociclib can trigger and activate the reactive oxygen species (ROS) machinery (Anders, Ke et al. 2011, Franco, Balaji et al. 2016). This led us to hypothesize that palbociclib may induce ROS in a dose-dependent manner in ER positive breast cancer, and that levels of ROS may dictate the induction of senescence. Consistent with this, siRNA knockdown of CDK4/6 in MCF7 and T47D cell lines increased cellular ROS levels as measured by CellROX assay (**Figure 14A**). Similarly, treatment of ER positive cells with low concentration (1uM) of Palbociclib for 6 days also increased ROS levels, albeit moderately (measured by CellROX), while treatment with high concentration (5uM) resulted in a significant increase in ROS levels, and this corresponds to the palbociclib concentrations at which senescence is induced (**Figure 14B**). In contrast, treatment of HMEC cells did not result in any significant changes in ROS levels at both low (1µM) and high (5 µM) palbociclib concentrations (**Figure 14B**), indicating specificity of drug action. Further, short-term (72hr) treatment with low or high doses of palbociclib did not increase ROS levels or induce a senescence phenotype in ER positive breast cancer cells (**Figure 14C and 14D**).

These results indicate that CDK4/6 inhibition via palbociclib induced reactive oxygen species, which may be required for the induction of senescence by palbociclib.

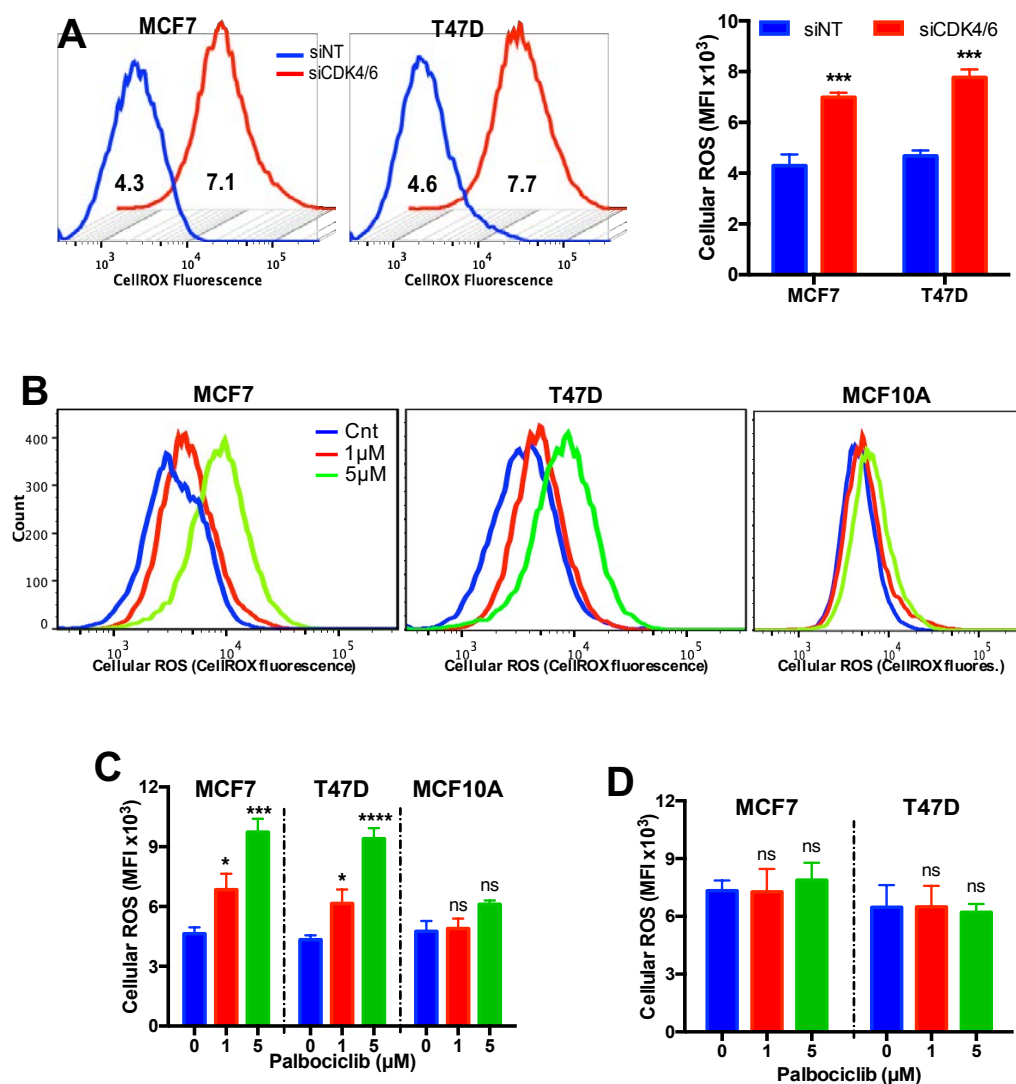


Figure 14: Induction of ROS by CDK4/6 inhibition: A) Cellular reactive oxygen species (ROS) measurement and quantification (mean fluorescence intensity [MFI]) of ROS levels in MCF7 and T47D cells upon transfection with NT siRNA or siRNA against CDK4 and CDK6. B, C) Cellular reactive oxygen species (ROS) measurement (B) and quantification (mean fluorescence intensity [MFI]) of reactive oxygen species (ROS) levels (C) in MCF7, T47D and MCF10A cells upon treatment with DMSO or palbociclib for 6 days. D) Quantification (mean fluorescence intensity [MFI]) of ROS levels in MCF7 and T47D cells upon treatment with DMSO or palbociclib for 72 hours. All data represent mean \pm SD from three independent experiments; p-values were calculated in comparison to cells treated with DMSO (Control) or siNT unless indicated. ns: $p > 0.05$; * $p < 0.05$; ** $p < 0.01$; *** $p < 0.001$; **** $p < 0.0001$.

3.2.8. IMPACT OF ROS ABLATION ON PALBOCICLIB INDUCED GROWTH INHIBITION AND SENESENCE

Given the well-established link between Reactive oxygen species (ROS) and cell cycle arrest and senescence and the known requirement of high ROS levels for the induction of senescence (Boonstra and Post 2004, Kuilman, Michaloglou et al. 2010), we wanted to examine if palbociclib induced ROS is required for the induction of sustained growth inhibition and senescence in ER positive breast cancer cells. To interrogate this, we ablated ROS using the ROS scavengers N-acetyl cysteine (NAC) or trolox (Hamad, Arda et al. 2010, Sun 2010), by treating the cells with NAC or trolox in combination with palbociclib for the 6 day period (**Figure 15A**). ROS ablation mediates significant resistance to the ability of palbociclib to induce a sustained growth inhibition even at higher doses of 5uM, as measured by clonogenic assay (**Figure 15B**). Further, measurement of cellular proliferation by cell counting after drug treatment for 6 days and recovery for 4 days (to measure reversibility) also showed ROS ablation by NAC or trolox prevented the induction of irreversible or sustained growth inhibition in MCF7 and T47D cells even with high doses of palbociclib (**Figure 15C**). Moreover, ablation of ROS by NAC or trolox also significantly decreased the induction of senescence by high doses (5uM) of palbociclib in MCF7 and T47D cell lines, as measured by SA- β gal, wherein a significant decrease in SA- β gal positive cells (blue staining) was observed with NAC or trolox treatment in combination with 5uM palbociclib, compared to palbociclib alone (**Figure 15D**).

Thus, these results demonstrate the dependence of the palbociclib action (its ability to induce sustained growth inhibition and senescence) on elevated ROS levels.

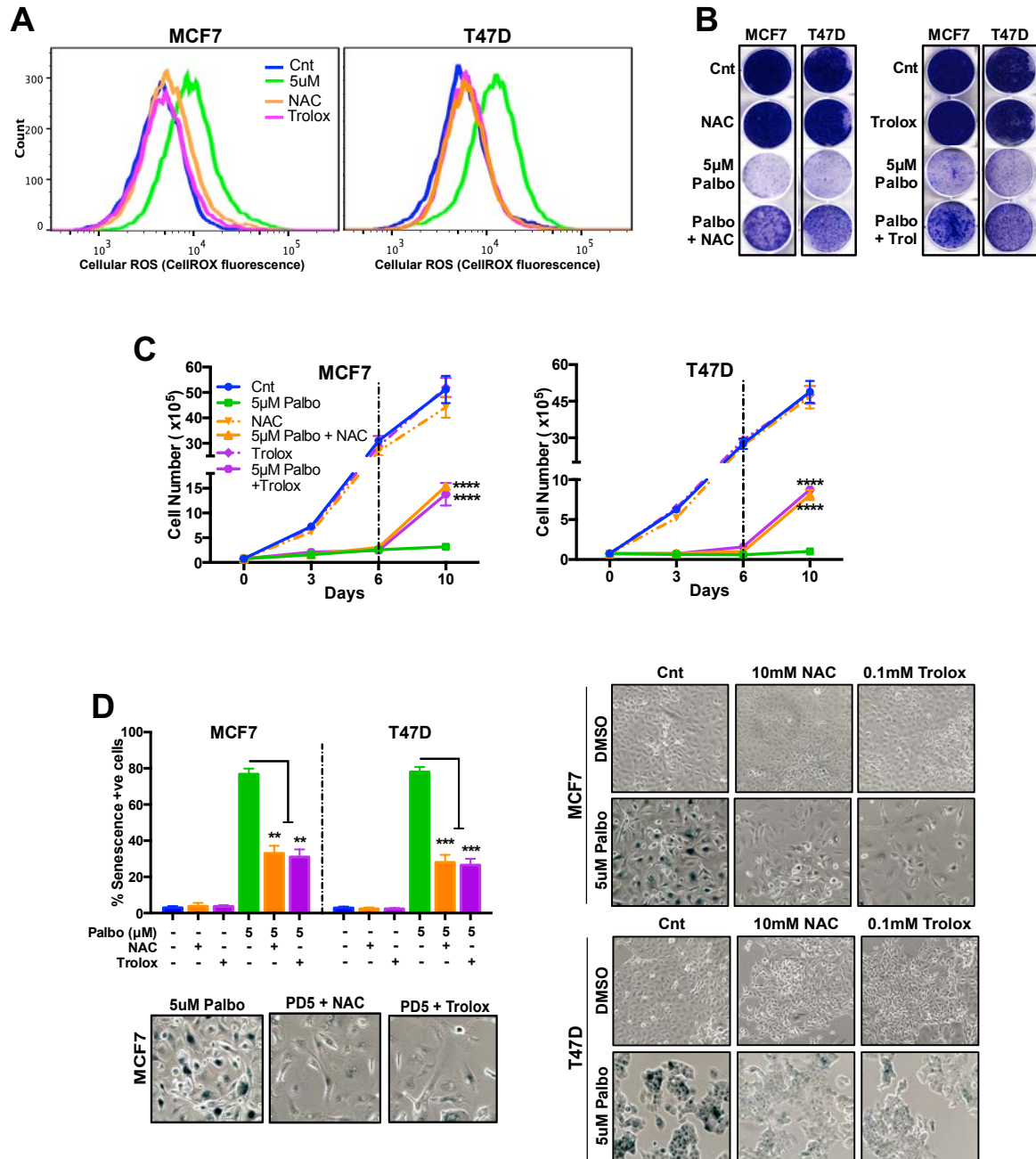


Figure 15: Impact of ROS ablation on palbociclib induced growth inhibition and senescence: MCF7 and T47D cells were treated with DMSO (Cnt), 5 μ M palbociclib (Palbo), or a combination of ROS scavenger (10 mM NAC or 0.1 mM trolox) with 5 μ M palbociclib for 6 days and subjected to A) measurement of cellular ROS levels with CellROX deep red; B) clonogenic assay; C) cell counting to assess proliferation (p-values were calculated in comparison with cells treated with 5 μ M palbociclib) and D) Quantification and representative images of Senescence associated β galactosidase (SA- β gal) activity as a measurement of senescence. All data represent mean \pm SD from three independent experiments; p-values were calculated in comparison to cells treated with DMSO (Control) or siNT unless indicated. ns: $p > 0.05$; * $p < 0.05$; ** $p < 0.01$; *** $p < 0.001$; **** $p < 0.0001$.

3.2.9. PALBOCICLIB MEDIATED TUMOR GROWTH INHIBITION AND SENESCENCE *IN VIVO*

We next set out to translate our findings from cultured cells *in vitro* to tumor xenografts *in vivo*. For the *in vivo* studies, since MCF7 cells are not very tumorigenic (ability to form tumors in mice), we established MCF7T cells by passaging MCF7 cells through mice and verified that they behave similar to MCF7 cells in response to CDK4/6 inhibition via palbociclib *in vitro*. Results show that treatment of MCF7-T cells with increasing concentrations of palbociclib resulted in a time and dose-dependent growth inhibition (**Figure 16A and 16B**) and cell cycle arrest (G1 arrest) (**Figure 16C**), that were very similar to what observed in the MCF-7 cells (Figure 2-5). Further, palbociclib induced senescence in a dose-dependent manner in MCF7-T cells (**Figure 16D**). Palbociclib treatment in MCF7-T cells also induced autophagy (**Figure 16E**) and responded to autophagy inhibition (**Figure 16F**), similar to MCF7 cells (described in Chapter 4 and 5). Thus, these results show that MCF7-T cells behave similar to MCF7 and can be utilized for the *in vivo* mouse studies.

Next, to assess the therapeutic effect of CDK4/6 inhibition *in vivo*, we established a mouse orthotropic xenograft model by injecting MCF7T cells into the mammary fat pad of immunocompromised nude mice. Once the tumors reached an average volume of 200mm³, the mice were treated with Vehicle (0.5% Methylcellulose) or varying concentrations of Palbociclib (25, 50, 75 or 150 mg/kg/day) via oral gavage for 7 days (**Figure 17A**). Treatment with palbociclib significantly decreased tumor volume in a dose-dependent manner, when compared to the vehicle treated mice (**Figures 17B and 17C**). This resulted in significantly smaller tumors and decreased tumor weight upon 7-day treatment with palbociclib in a dose-dependent manner (**Figure 17D**). To examine palbociclib-mediated toxicity in mice, we measured mouse weight every day during the 7-day treatment period. While treatment with Vehicle, 25 mg/kg and 50 mg/kg Palbociclib was well tolerated by the mice, a moderate decrease in mouse weight was observed with 75mg/kg and 150 mg/kg palbociclib (**Figures 17E and 17F**) This

suggests potential toxicity by palbociclib at the higher concentrations, and emphasizes the need to optimize the use of lower drug concentrations.

Treatment of *in vivo* xenograft tumors with palbociclib also resulted in decrease in protein levels of G1/S checkpoint proteins and known palbociclib targets – Rb, pRb and FOXM1 as measured by western blot analysis (**Figure 17G**). Next, the tumor tissues were harvested, sectioned and stained with hematoxylin and eosin (H&E), to examine the morphology of the tumor cells post treatment (Fischer, Jacobson et al. 2008).

The remaining tumors were sectioned for further immunohistochemistry (IHC) analysis, which revealed that palbociclib treatment increased SA- β gal activity (measure of induction of senescence) and decreased expression of BrdU (indicator of decreased proliferation), indicating the induction of a dose-dependent tumor growth inhibition and senescence (**Figure 18A**). Consistently, RPPA analysis of tumors (**Figure 18B**) treated with palbociclib showed a dose-dependent downregulation of cell cycle and proliferation proteins, such as pRb, FOXM1, cyclin B, CDK1, cdc25c, cdc2, PLK1, ARID1, BRD4, ATM and Wee1 (**Figure 18C**). A concomitant up-regulation of proteins within the senescence pathway, such as Chk1, YAP, TAZ, EIF4E, IGFFBP2, PEA15, 14-3-3-beta, 14-3-3-zeta and c-IAP (**Figure 18D**), when compared to vehicle treated tumors.

Collectively, these results show that CDK4/6 inhibition via palbociclib induces a dose-dependent reduction in tumor growth and induction of senescence in ER positive tumor xenografts.

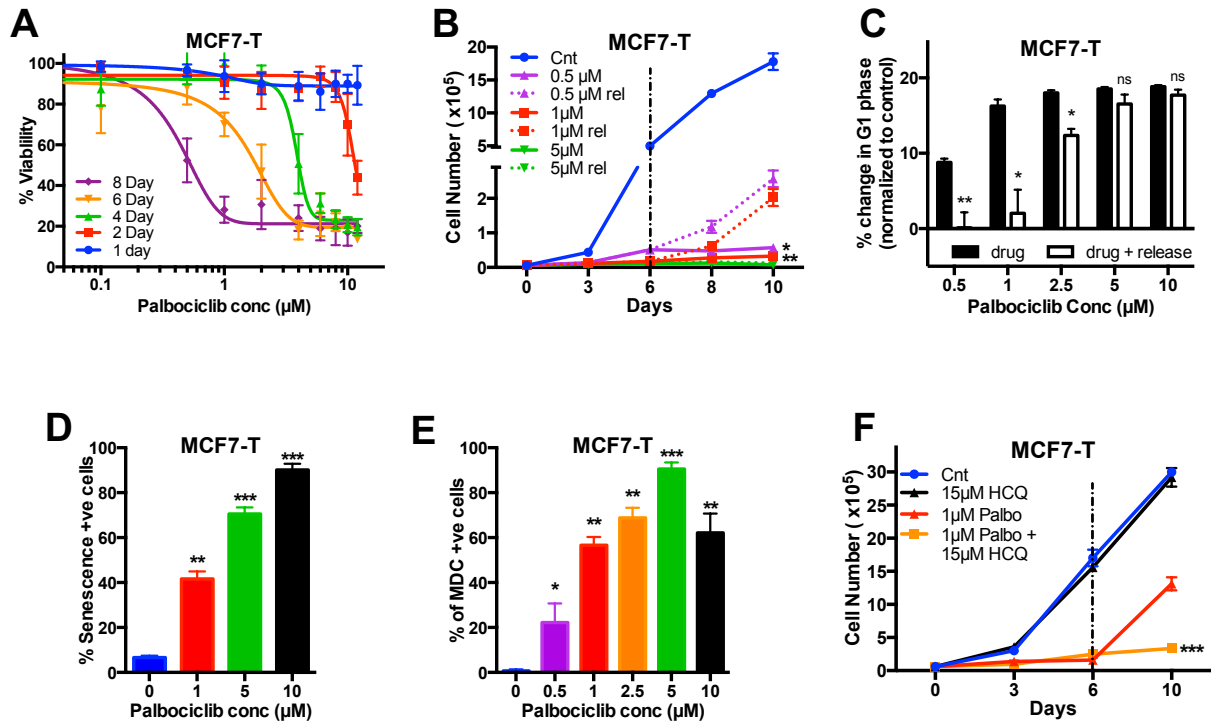


Figure 16: Characterization of MCF7-T cell in-vitro: A) Proliferation of MCF7-T cells treated with DMSO or increasing concentrations (conc) of palbociclib (0.01 to 12 μM) for 1, 2, 4, 6, or 8 days. MCF7-T cells were treated with DMSO (Cnt) or varying concentrations (0.5, 1, or 5 μM) of palbociclib for 6 days and allowed to recover for 4 days (release, or rel) to examine reversibility. Cells were then subjected to B) cell counting to assess the effect on growth; C) cell cycle analysis to determine percentage change in G1 phase (p-values were calculated by comparing values at the end of drug treatment with those at the end of drug + release); and D) quantification of senescence-associated SA-β gal positive cells. E) Monodansylcadavarine (MDC) positive MCF7-T cells were quantified with flow cytometry after treatment with DMSO or varying concentrations of palbociclib for 6 days. F) Cell counting was used to assess effect on growth of MCF7-T cells treated with a combination of DMSO or palbociclib (Palbo; 0.5 or 1 μM) and autophagy inhibitor hydroxychloroquine (HCQ; 15 μM) for 6 days. Cells were allowed to recover for 4 days to examine reversibility. All data represent mean ± SD from three independent experiments; p-values were calculated in comparison to cells treated with DMSO (Control) unless indicated. ns: p > 0.05; *p < 0.05; **p < 0.01; ***p < 0.001; ****p < 0.0001

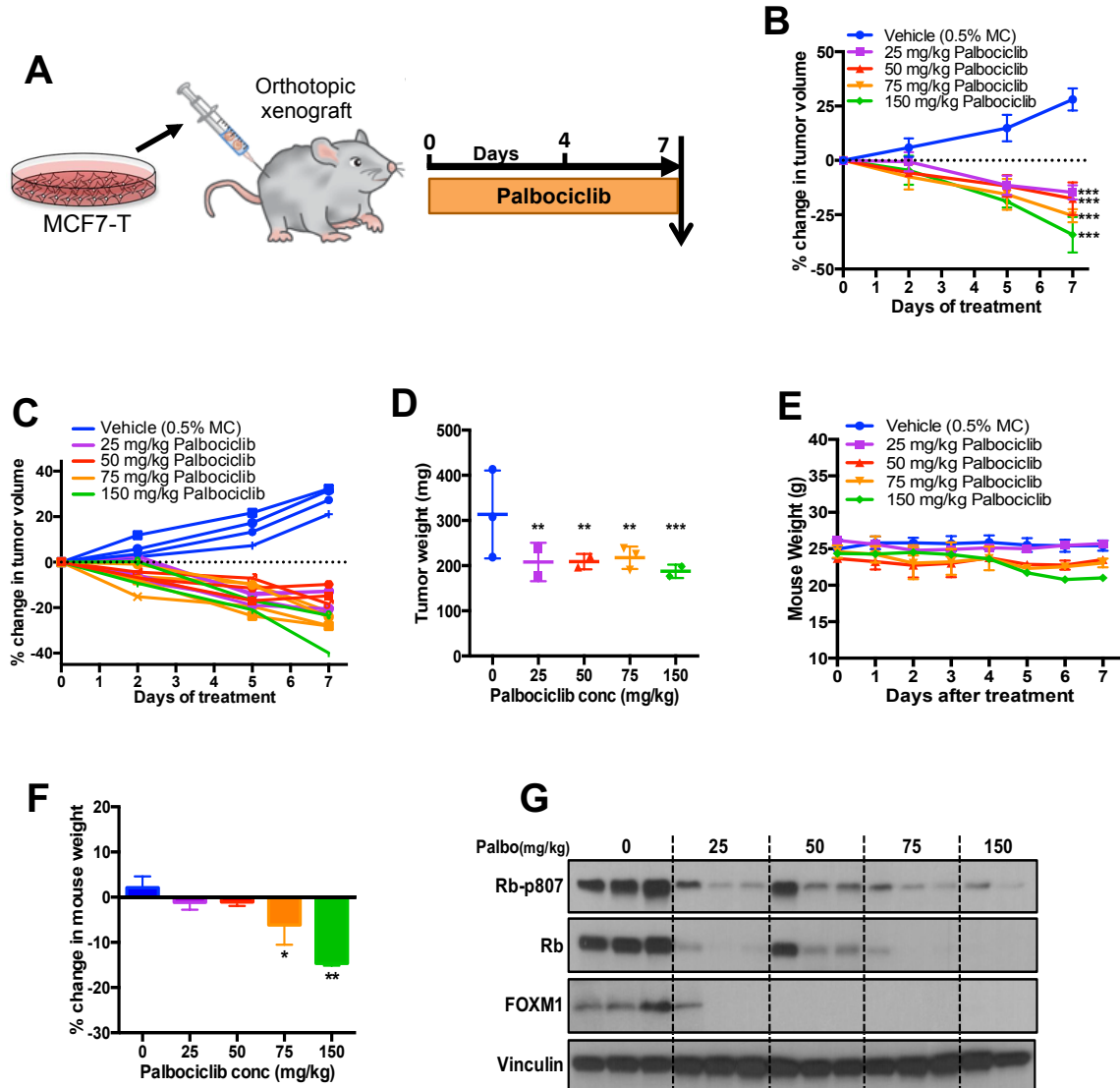


Figure 17: Palbociclib mediated tumor growth inhibition in vivo: A) Schematic showing treatment schedule of orthotopic MCF7-T xenograft mice with vehicle (0.5% methylcellulose [MC]) or varying concentrations of palbociclib for 7 days. B) Percentage change in tumor volume (normalized to Day 0) upon treatment with vehicle or palbociclib ($n \geq 4$ tumors per group) daily for 7 days. C) Percentage change in tumor volume of orthotopic xenograft mice (normalized to volume on Day 0) of individual tumors treated with vehicle (0.5% methylcellulose) or varying concentrations of palbociclib daily for 7 days via oral gavage ($n \geq 4$ mice tumors/treatment group). D) Tumors were harvested at the treatment for tumor weight measurement. E) Mean mouse weights for each treatment group after 7 days of treatment as described in A. F) Percentage change in mouse weights after 7 days treatment as described in A. G) Western blot of harvested tumors upon treatment with palbociclib analyzed for cell cycle proteins (phospho-Rb, Rb, FOXM1). All data represent mean \pm SD; p-values were calculated in comparison to mice treated with vehicle (Control) unless indicated. ns: $p > 0.05$; * $p < 0.05$; ** $p < 0.01$; *** $p < 0.001$; **** $p < 0.0001$.

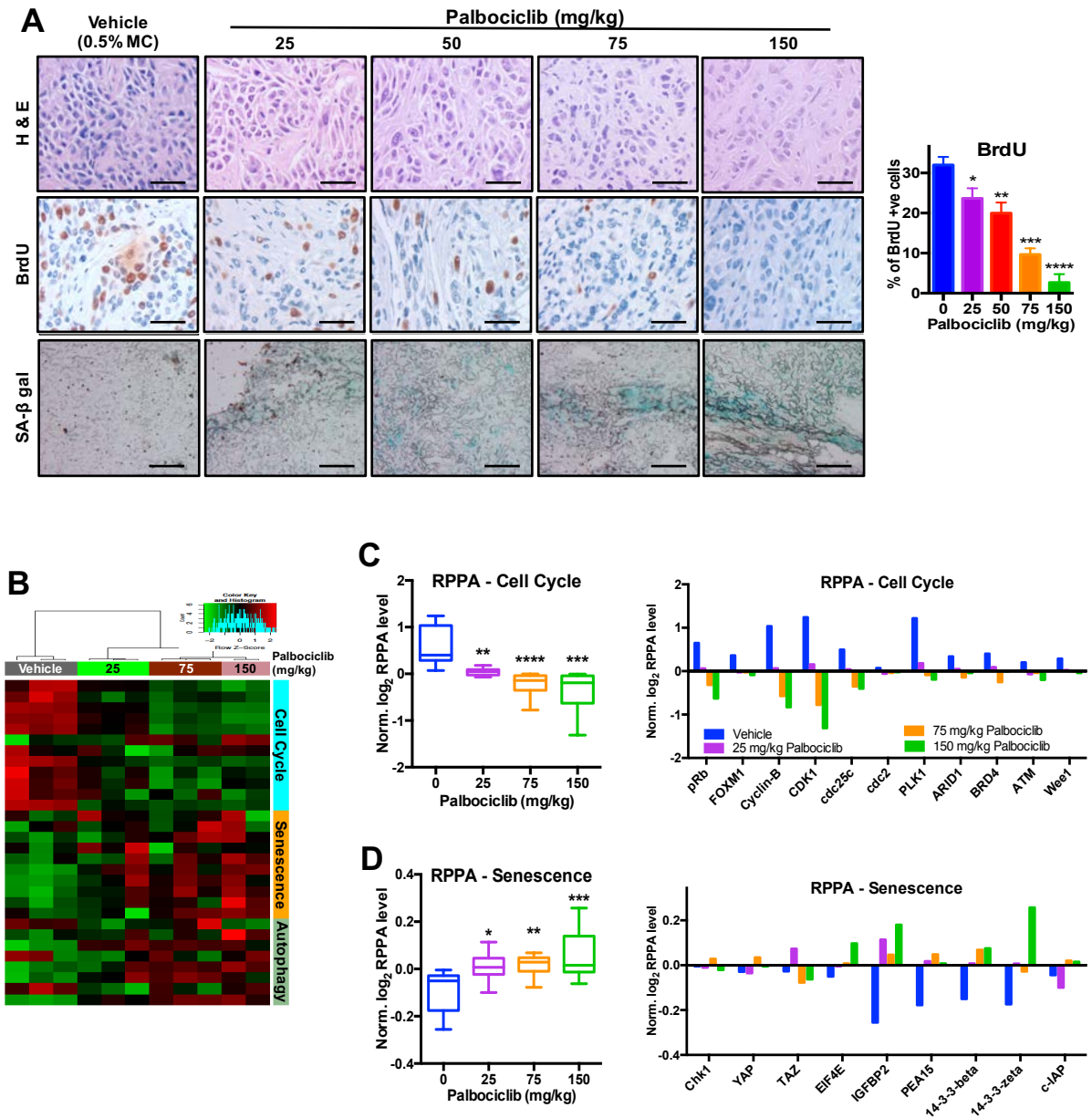


Figure 18: Palbociclib mediated cell cycle arrest and senescence in vivo: A) Quantification (BrdU) and representative images of hematoxylin and eosin (H&E), BrdU and SA-β gal immunohistochemical staining of tumor tissues harvested after treatment with vehicle (0.5% methylcellulose [MC]) or varying concentrations of palbociclib for 7 days. Scale bars equal 50μm. B) Heat map obtained from RPPA analysis of tumors harvested after treatment as described in A and ordered based on Cell cycle, senescence and autophagy pathways. Pathway scores and expression (normalized log₂ level) of individual proteins within the C) cell cycle (n=10 proteins) and D) senescence pathways (n=13 proteins) determined from RPPA analysis of tumors harvested after 7 days treatment as described in A. All data represent mean±SD; p-values were calculated in comparison to mice treated with vehicle (Control) unless indicated. ns:p>0.05; *p<0.05; **p<0.01; ***p<0.001; ****p<0.0001.

3.2.10. PALBOCICLIB MEDIATED INDUCTION OF ROS *IN VIVO*

Since our results showed that palbociclib mediated CDK4/6 inhibition has been shown to induce ROS in ER positive breast cancer cell line model systems (Figure 14), which is required for the induction of senescence (Figure 15), we wanted to examine if palbociclib would induce ROS *in vivo* as well. For this purpose, we utilized tumors harvested post treatment with vehicle or varying concentrations of palbociclib (25mg/kg, 50mg/kg, 75mg/kg and 150mg/kg) (Figure 12A), and performed immunohistochemistry (IHC) analysis for known markers of Reactive oxygen species (ROS): i) 8-hydroxydeoxy-guanosine (8-OHdG), a marker of oxidative stress induced DNA damage (Valavanidis, Vlachogianni et al. 2009) and ii) 4-hydroxynonenal 4-HNE, a marker of oxidative stress induced lipid peroxidation (Liou and Storz 2015). Results showed a significant dose dependent up-regulation of 8-OHdG and 4-HNE staining, with highest staining with 150 mg/kg palbociclib, which has been shown to induce senescence (**Figures 19A and 19B**). Further, RPPA analysis of the palbociclib treated tumors exhibited downregulation a ROS sequestering gene Caveolin (CAV-1) (Chen, Barman et al. 2014) and upregulation of SOD-2, which is known to be induced by higher ROS levels (**Figure 19C**).

Thus, palbociclib mediated CDK4/6 inhibition *in vivo* induces ROS levels, which is required for the sustained tumor growth inhibition and senescence *in vivo*.

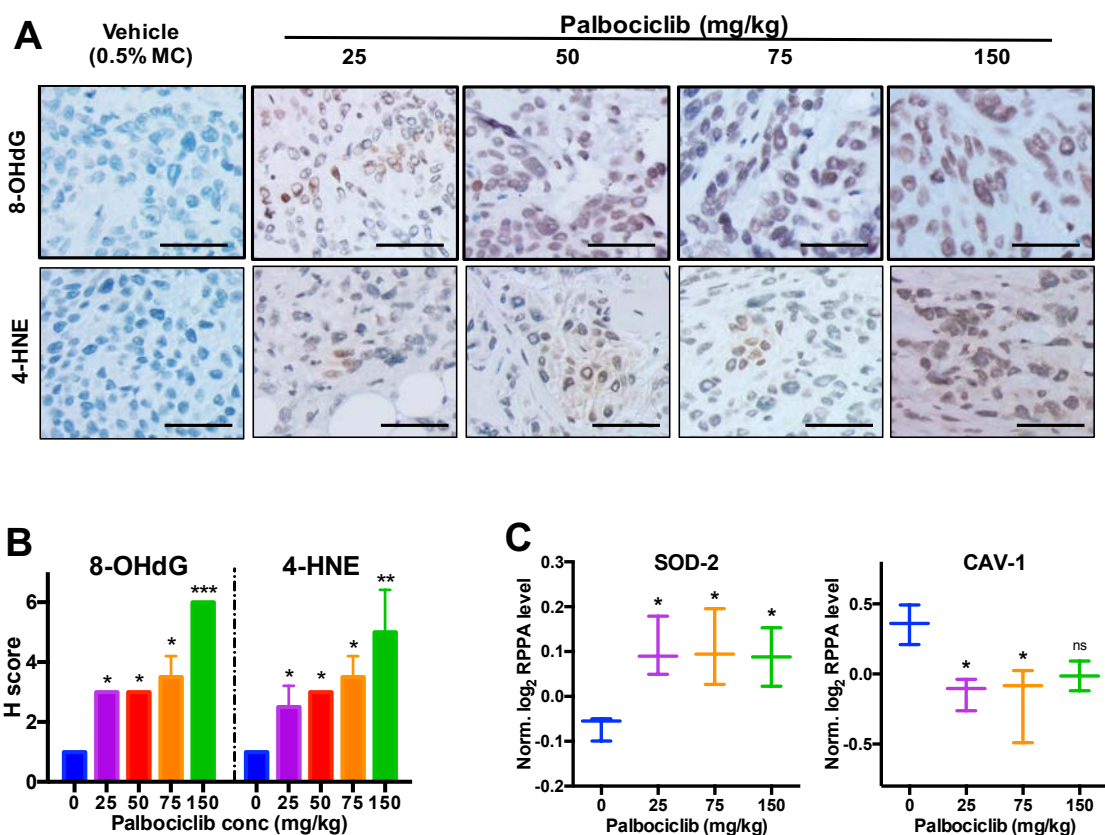


Figure 19: Palbociclib mediated induction of ROS in vivo: A) Representative images of ROS markers, 8-hydroxydeoxy-guanosine (8-OHdG) and 4-hydroxynonenal (4-HNE) immunohistochemical staining of tumor tissues harvested after 7 days of treatment with vehicle (0.5% methylcellulose [MC]) or varying concentrations of palbociclib. Scale bars equal 50µm. B) Quantification (H-score) of 8-OHdG and 4-HNE staining in tumors after 7 days of treatment with vehicle or increasing concentrations of palbociclib. C) Expression (normalized log₂ level) of ROS associated proteins, SOD-2 and Caveolin (CAV-1) as determined from RPPA analysis of tumors harvested after treatment as described in A. All data represent mean±SD; p-values were calculated in comparison to mice treated with vehicle (Control) unless indicated. ns:p>0.05; *p<0.05; **p<0.01; ***p<0.001; ****p<0.0001.

3.3. DISCUSSION

Most preclinical studies conducted thus far with palbociclib have used the drug at low conc. (<1uM) and for short exposure times (<72 hrs.). Under these treatment conditions, the drug only induces a reversible cell cycle arrest at these conditions, leading to a poor recapitulation of the effect seen in clinic, where patients are treated continuously for 3 weeks (DeMichele, Clark et al. 2015). Hence in this study, we examined the action of the CDK4/6 inhibitors as a function of both time and dose, and also interrogated the reversibility of the drug effect; making it the first clinically relevant model to investigate the mechanism of Palbociclib action. Our results demonstrated that a biphasic effect was seen with palbociclib treatment in ER positive breast cancer cells *in vitro*, where lower doses of the drug (~1uM) were more specific to CDK4/6 and was able to induce only a reversible inhibition of growth and cell cycle (G1 arrest), while the higher doses of the drug (>2.5uM) resulted in an irreversible inhibition of cellular proliferation, an irreversible G1 arrest and senescence. Further, results show that long-term treatment with palbociclib is necessary for the induction of sustained drug effect and senescence. While a previous study suggested that long-term treatment may be required to prevent reversibility in the growth inhibition induced by palbociclib (Leontieva and Blagosklonny 2013), this has not been elucidated in detail. Further, the higher doses which resulted in the induction of senescence (5uM) is significantly higher than higher than the clinically achievable dose and the plasma concentration, which 3.4uM (Pfizer-Inc-and-Affiliates 2011). Hence, understanding the dose-dependent mechanism of action of palbociclib is crucial to improve the efficacy of CDK4/6 inhibition and potentially lower the dose of the drug administered in patients.

Further, treatment with palbociclib failed to induce any apoptosis or cytotoxic effects, indicting that the mechanism of drug mediated growth inhibition is likely due to the induction of senescence. This was observed both in cultured cells *in vitro* and tumors *in vivo*, and corroborates with previous studies (Anders, Ke et al. 2011). This effect might be specific to

palbociclib since studies with the other CDK4/6 inhibitors such as abemaciclib have been showed to induce apoptosis in breast cancer cells *in vitro* (Patnaik, Rosen et al. 2016).

Intriguingly, the induction of senescence observed at the higher doses of palbociclib was coupled with drug effects not necessarily specific to CDK4/6 inhibition, indicating the presence of potential off-target effects for palbociclib at the higher doses. A mass spectrometry based chemoproteomics study in lung cancer aimed at identifying all possible direct and indirect kinase targets of the CDK4/6 inhibitors, palbociclib and ribociclib, showed that apart from CDK4 and CDK6, palbociclib has targets other kinases such as CDK9, casein kinase 2, PIK3R4 (regulator of autophagy) and lipid kinases such as PIK3CD and PIP4K2A/B/C (Sumi, Kuenzi et al. 2015). By pathway analysis, this study also showed that palbociclib treatment affect PI3K signaling and autophagy apart from cell cycle regulation (Sumi, Kuenzi et al. 2015). Hence, it is highly likely that palbociclib hits secondary targets at the higher concentrations (5uM or 150mg/kg) and this accounts for the biphasic effect observed with palbociclib treatment.

The results presented in this chapter also show that CDK4/6 inhibition and palbociclib treatment induces oxidative stress, measured by reactive oxygen species (ROS) in a dose-dependent manner, and that the high levels of ROS is required for the induction of senescence. However, the molecular mechanism by which CDK4/6 inhibition induces ROS remains unclear. Cyclin-D1 has been shown to bind to and phosphorylates Nrf1, which is a regulator of mitochondrial biogenesis and ROS, and this occurs in a CDK dependent manner (Wang, Li et al. 2006). Hence, it is possible that CDK4/6-cyclin D1 inhibition via palbociclib increases Nrf1 levels, thus increasing ROS activity. The levels of ROS and the subsequent induction of senescence, in turn, might also be controlled by c-jun through a previously elucidated mechanism involving the ROS genes, MnSOD and catalase(Katiyar, Casimiro et al. 2010). This provides a direct molecular mechanism by which CDK4/6-cyclin D regulates ROS through Nrf2 and c-jun. Alternatively, the induction of ROS might be mediated directly by the

Rb targets FOXM1 and BIRC5 (survivin), which have been shown to negatively regulate oxidative stress (Kwee, Luque et al. 2008, Park, Carr et al. 2009, Lim, Heo et al. 2015), providing a novel link between Rb and the ROS machinery. Concordantly, we and others have reported a significant decrease in FOXM1 levels (Figures 1G and 4C) (Anders, Ke et al. 2011), and observed a decrease in Survivin mRNA levels. This suggests that downregulation of FOXM1 and BIRC5, among other ROS regulating proteins might be the potential mechanism by which Rb regulates oxidative stress, under palbociclib treatment conditions, and this warrants further investigation.

These results suggest that there are potential mechanisms that are induced at the lower doses of palbociclib, which prevent the high ROS levels and the induction of senescence. Understanding this / these process(es) would help improve the efficacy of the drug at the lower doses as we have addressed in Chapters 4 and 5.

CHAPTER 4: INDUCTION OF AUTOPHAGY IN RESPONSE TO CDK4/6 INHIBITION

IN ER+ BREAST CANCER

4.1. INTRODUCTION

4.1.1. AUTOPHAGY – DEFINITION AND REGULATION

Autophagy, which is derived from the Greek word “eating of self” is a catabolic process in cells that recycles cellular constituents as an efficient way of generating energy (Deter and De Duve 1967). There are three types of autophagy: i) Macroautophagy, the most common form of autophagy mediated by cellular structures such as autophagosomes and lysosomes, ii) Micro autophagy, where the cellular components are directly transported to the lysosomes for degradation and iii) Chaperone mediated autophagy (CMA), where the chaperone protein Hsp70 mediates transport of the cargo to the lysosome by association with the lysosomal protein, LAMP2A (Saftig, Beertsen et al. 2008, Glick, Barth et al. 2010).

Macroautophagy, the most well-characterized and common form of autophagy (illustrated in **Figure 20**) begins with the formation of an isolation membrane, which surrounds the cargo or the cellular components to be degraded and then develops into a double-membraned vesicle called “autophagosomes” (Mizushima 2007). This is the structure that can be visualized as double-membrane electron dense vesicles by Transmission Electron Microscopy (TEM), which is the gold standard experiment to examine the induction of autophagy (Yla-Anttila, Vihinen et al. 2009). The autophagosomes, containing the cargo, fuse with the lysosomes, forming structures called autophagolysosomes, where the lysosomal acids facilitate degradation of the cargo, thus generating energy (Glick, Barth et al. 2010). Autophagy can be specific (degrades a single organelle) or non-specific (degrades multiple components), and can target several types of cellular components for degradation including individual proteins, protein aggregates, or entire organelles such as mitochondria (mitophagy), nucleus (nucleophagy), peroxisomes (pexophagy) and ribosomes (ribophagy) (Glick, Barth et al. 2010).

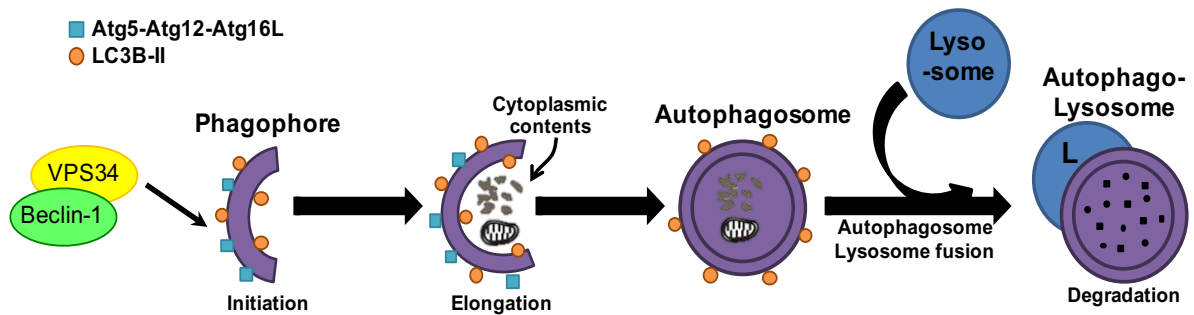


Figure 20: Regulation of autophagy: Schematic showing the steps and processes involved in autophagy and its molecular regulation.

While the molecular regulation of the autophagy pathway has not been fully characterized, numerous studies have identified key points of regulation within the pathway and characterized genes involved in this process. This primarily comprises of the core autophagy related genes or Atg genes, which were originally identified in yeast, but have mammalian homologs (Lamb, Yoshimori et al. 2013). About 32 genes belonging to the Atg family have been identified and characterized to play key roles at different steps of the autophagic process (Lamb, Yoshimori et al. 2013). Some of the crucial autophagy steps regulated by the Atg proteins are detailed here (**Figure 20**). The process of nucleation or phagophore formation is controlled by Atg6 or Beclin-1 which dissociates from the Bcl2/Beclin-1 complex to form a complex with the class III PI3K protein Vps34, at the stage of autophagy initiation (Glick, Barth et al. 2010). The next crucial step is the formation of the Atg5-Atg12-Atg16L complex, which is facilitated by Atg7 and Atg10 and is required for the elongation of the phagophore and the formation of the autophagosomes (Lamb, Yoshimori et al. 2013). Finally, the conjugation of the microtubule-associated protein light chain 3 (LC3B) protein with phosphatidylethanolamine (PE) to form the active LC3B-II is regulated by Atg3, Atg4 and Atg7 (Satoo, Noda et al. 2009). Apart from these core autophagy proteins, there are several other molecular pathways that regulate the process such as AMPK, PI3K/AKT and mTOR pathways (Mizushima 2007).

Deregulation of the autophagic process resulting from gains and losses of the autophagy genes has been linked to numerous diseases including cancer, cardiovascular

disease and neurodegenerative disorders (Mizushima 2007, Glick, Barth et al. 2010).

Deregulation of autophagy plays an integral role in neurodegenerative diseases such as Alzheimer's, ALS and Parkinson's disease. For example, the ubiquitin ligase, Parkin and its upstream kinase PINK1, which play key role in mitophagy are frequently mutated in Parkinson's disease (Lynch-Day, Mao et al. 2012). Further, in Alzheimer's disease, autophagy facilitates the removal of protein aggregates formed due to mutations in the tau gene (Zare-Shahabadi, Masliah et al. 2015). This has led to research aimed at developing drugs that upregulate autophagy in a tissue specific manner in these disease settings.

4.1.2. ROLE OF AUTOPHAGY IN CANCER

The precise role of autophagy in oncogenesis has been a widely-debated topic for numerous years, since studies have shown opposing roles for autophagy in cancer – as a pro-survival process (oncogenic role) and as a pro-death mechanism (tumor suppressor role) (White, Mehnert et al. 2015). In normal cells, autophagy primarily plays a housekeeping role wherein it removes the defective and damaged proteins and organelles, to maintain the integrity of cells, survive stress and provide energy when needed (Mizushima 2007). Research has shown that the role of autophagy in cancer is highly context-dependent – dependent on the type of tumor, stage of development of the tumor, whether it is basal or induced autophagy, etc. (White, Mehnert et al. 2015). Autophagy has been primarily shown to play a tumor suppressing role early on in the tumorigenesis, but later utilized by tumors as a mechanism to maintain proliferation capacity even in the presence stresses such as hypoxia, metabolic stress, hypoxia or drug induced stress (Mathew, Karantza-Wadsworth et al. 2007, White, Mehnert et al. 2015).

One of the crucial autophagy proteins, Beclin-1, a Bcl-2 interacting protein, is monoallelically deleted in about 40- 75% of all human cancers, including breast, ovarian and prostate cancers (Aita, Liang et al. 1999). Reintroduction of Beclin-1 into established cancer

cells such as MCF7, which exhibits a heterozygous loss of Beclin-1 resulted in a significant reduction in cellular proliferation, clonogenicity and tumorigenic potential *in vivo* (Aita, Liang et al. 1999). Further, allelic loss of Beclin-1 makes mice more susceptible to spontaneous tumor formation such as lymphoma, breast, lung liver cancers, and also makes them prone to Wnt1 mediated mammary tumorigenesis (Cicchini, Chakrabarti et al. 2014, White, Mehnert et al. 2015). Similar observations have been seen with other autophagy genes such as Atg5, whose loss has been shown to promote extensive liver damage and carcinoma, and the formation of benign tumors in the case of pancreatic cancer (Takamura, Komatsu et al. 2011, Rosenfeldt, O'Prey et al. 2013). These studies elucidate the tumor suppressive role of autophagy mainly at the early stages of tumor development.

However, at the later stages of tumor development, autophagy is believed to play a pro-survival function, since the cells can now use autophagy as a recycling facility to backup energy to survive under stress and maintain viability (Mathew, Karantza-Wadsworth et al. 2007, White 2015). Atg7 deletion in a K-ras G12D driven lung cancer mouse model resulted in tumor cells accumulating defective mitochondria, activating autophagy and the p53 tumor suppressor protein resulting in lower cell proliferation and increased apoptosis (Guo, Karsli-Uzunbas et al. 2013). Further the tumors developed upon knockdown of Atg7 in mouse models at early stages remained benign (Takamura, Komatsu et al. 2011). Also, deficiency of p62 causes suppression of autophagy induced tumorigenesis in cell lines and mouse models (Jiang, Overholtzer et al. 2015, White, Mehnert et al. 2015). Moreover, recent studies in pancreatic cancer and other Ras-driven tumors have shown that these cancers are addicted to autophagy to survive metabolic stress and maintain oxidative metabolism and survive (White, Mehnert et al. 2015). Finally, studies have shown an association between higher expression of autophagy proteins like LC3B and aggressiveness of the tumor or the presence of residual disease post chemotherapy (Karantza-Wadsworth and White 2007, Chen, Jiang et al. 2013).

Thus, these studies provide evidence for the dual role played by autophagy in cancers,

and highlights the oncogenic or pro-survival role of autophagy in developed tumors, which be required for the maintenance of the tumor phenotype and drug resistance.

4.1.3. CDK4/6 INHIBITION AND AUTOPHAGY

While the role of the G1 checkpoint proteins CDK4/6-cyclin D in cell cycle and cellular proliferation is well established, its role in autophagy is very poorly understood. A study in a breast cancer model showed that cyclin D1 can suppresses autophagy in mammary tumorigenesis, since mice deficient in cyclin D1 upregulate autophagy and failed to induce ErbB2 induced senescence (Brown, Jeselsohn et al. 2012). Further, genetic or pharmacological downregulation of cyclin D1 in human mammary epithelial cells (HMEC) showed significant upregulation of autophagy, the inhibition of which resulted in an increase in senescence (Brown, Jeselsohn et al. 2012).

Lastly, two recent studies suggest a role for CDK4/6 inhibition in inducing autophagy. A study in cancer-associated fibroblasts showed that CDK inhibitors such as p16, p21 and pharmacological CDK inhibitors such as palbociclib can upregulate proteins involved in both senescence and autophagy (Capparelli, Chiavarina et al. 2012). In addition, a recent study in promyelocytic leukemia reported that palbociclib induces autophagy-dependent degradation of the DNA methyl transferase DNMT1, which facilitates the induction of senescence in these cancers (Acevedo, Vernier et al. 2016).

4.1.4. GAP IN KNOWLEDGE

While these previous studies highlight the importance of autophagy in cancers and its role as a stress response process, the following questions remain to be addressed:

1. Does knockdown of CDK4/6 induce autophagy in breast cancer?
2. Does palbociclib induce autophagy in ER positive breast cancer?

3. Is the autophagy induced by palbociclib functional (ie) does it have an intact autophagic flux?
4. Is there a dose dependence in the induction of autophagy by palbociclib – effects of on-target vs off-target doses?
5. Does ROS play a role in mediating the induction of autophagy by palbociclib?

Thus, the experiments conducted in this chapter aimed at addressing these questions, since the ability of CDK4/6 inhibition to induce autophagy and its potential implications has not been well understood.

4.2. RESULTS

4.2.1. INDUCTION OF AUTOPHAGY WITH CDK4/6 KNOCKDOWN AND LOW DOSES OF PALBOCICLIB

Autophagy is an adaptive cellular stress response that recycles dysfunctional cellular organelles for energy and facilitates cancer cell survival (Glick, Barth et al. 2010). Hence, we hypothesized that CDK4/6 inhibition-mediated cell cycle arrest (on-target effect at 1 μ M palbociclib) triggers autophagy as a stress response, which mediates the reversal of sustained growth inhibition and prevents the induction of senescence at these doses. To interrogate the induction of autophagy upon knockdown of CDK4 and CDK6, we used Monodansylcadavarine (MDC) staining, a marker of acidic vesicles including autophagosomes (Biederbick, Kern et al. 1995). Results showed a significant increase in MDC positive cells in MCF7 and T47D cells upon double siRNA knockdown of CDK4 and CDK6, when compared to NT (**Figure 21A**).

Further, to examine the induction of autophagy upon palbociclib treatment, we used several different assays in MCF7 and T47D cells: i) Monodansylcadavarine (MDC) staining, a marker of acidic vesicles including autophagosomes, ii) Transmission Electron Microscopy (TEM), which helps visualize the presence of double-membrane electron dense autophagosomes (Yla-Anttila, Vihinen et al. 2009), iii) GFP-LC3 puncta, iv) qRT-PCR and Reverse Phase Protein Array (RPPA) analysis to measure levels of key autophagy related proteins and v) Western blot analysis of LC3B II, the active and phosphatidylethanolamine (PE) conjugated form of microtubule-associated protein light chain 3 (LC3B) located on the surface of autophagosomes (Satoo, Noda et al. 2009) and SQSTM1/ p62, an autophagy receptor whose degradation can be indicative of an intact autophagic flux (Mathew, Karp et al. 2009). Results showed that treatment of MCF7 and T47D cells with increasing concentrations of palbociclib significantly increased levels of MDC staining (**Figure 21B**) and expression of key autophagy proteins, such as BNIP3 (**Figure 21C**), Atg-7, Beclin-1 (**Figure 21D**), while decreasing levels of BCL2 (a known inhibitor of autophagy (Pattingre, Tassa et al. 2005))

(Figure 21D). Further, western blot analysis showed increase in LC3B II protein levels, while decreasing SQSTM1 levels, indicating the induction of autophagy with palbociclib treatment **(Figure 21E)** in ER positive breast cancer cell lines. Additionally, Transmission Electron Microscopy (TEM) performed by comparing the Control (DMSO treated) vs the palbociclib treated cells, showed significant accumulation of double-membrane electron-dense vesicles, which are indicative of autophagosomes upon treatment with low dose (1uM) of palbociclib **(Figure 22A – red arrows)**. Further, examination of GFP positive puncta in MCF7 cells stably expressing GFP-LC3 showed accumulation of LC3 puncta (indicative of autophagosomes) upon treatment with 1uM palbociclib **(Figure 22B)**.

Collectively, these results indicate that CDK4/6 inhibition and palbociclib treatment at low concentrations induces autophagy in ER positive breast cancer cell lines.

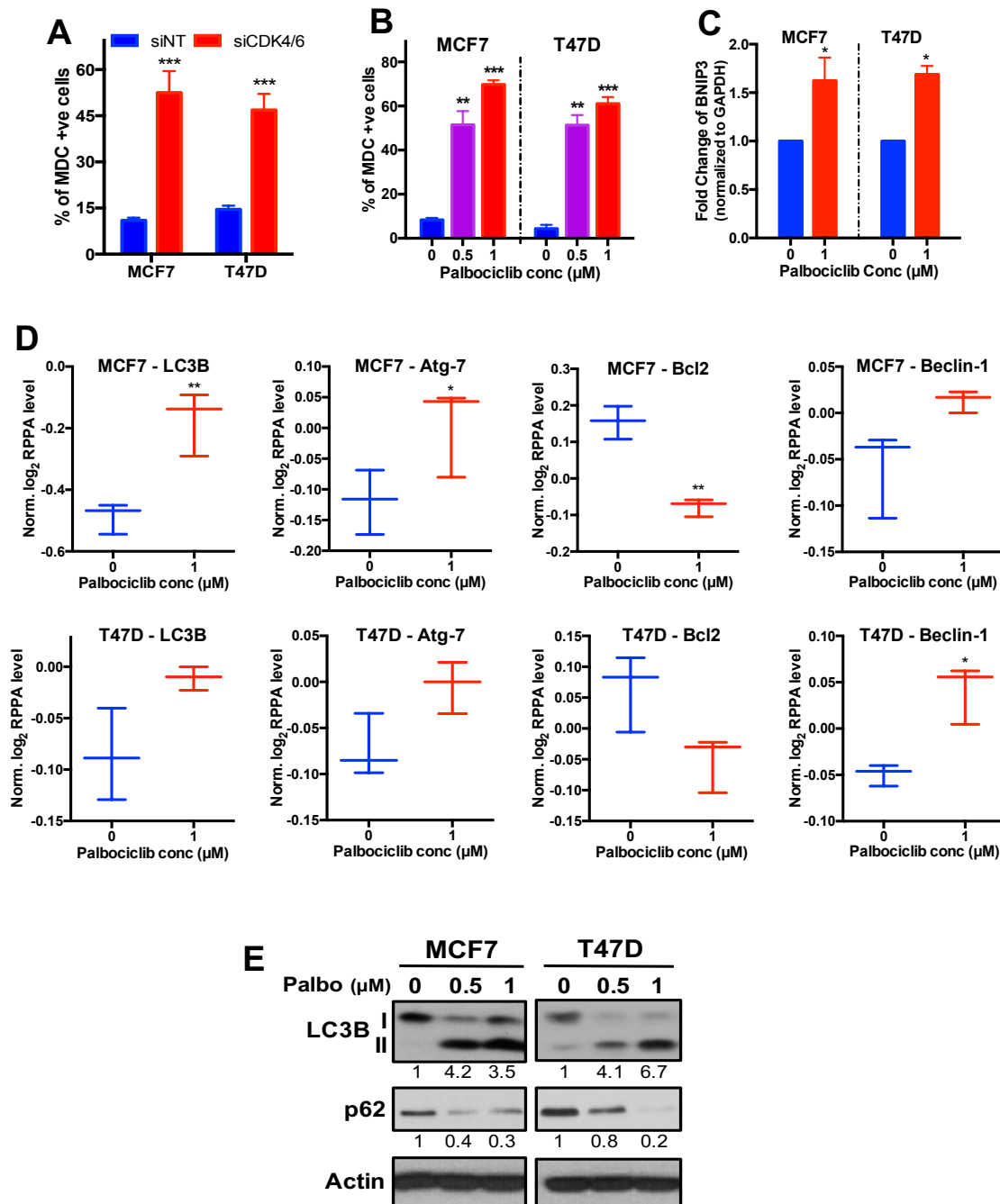


Figure 21: Palbociclib mediated induction of autophagy: A) Measurement of monodansylcadavarine (MDC)-positive acidic vesicles, including autophagosomes, by flow cytometry in MCF7 and T47D cells treated with siNT and dual siRNA against CDK4 and CDK6. B) Measurement of MDC positive MCF7 and T47D cells treated with varying concentrations of palbociclib for 6 days. C) mRNA level of BNIP3 (normalized to GAPDH) in MCF7 and T47D cells treated with 1 μ M palbociclib. D) Expression (normalized \log_2 level) of LC3B, Atg-7, Bcl2 and Beclin-1 determined by RPPA analysis of MCF7 and T47D cell lines treated with palbociclib for 6 days. E) Western blot analysis of autophagy proteins, LC3B I, II and p62 in MCF7 and T47D cells upon treatment with palbociclib for 6 days. All data represent mean \pm SD from three independent experiments; p-values were calculated in comparison to cells treated with DMSO (Control) or siNT unless indicated. ns: $p > 0.05$; * $p < 0.05$; ** $p < 0.01$; *** $p < 0.001$; **** $p < 0.0001$.

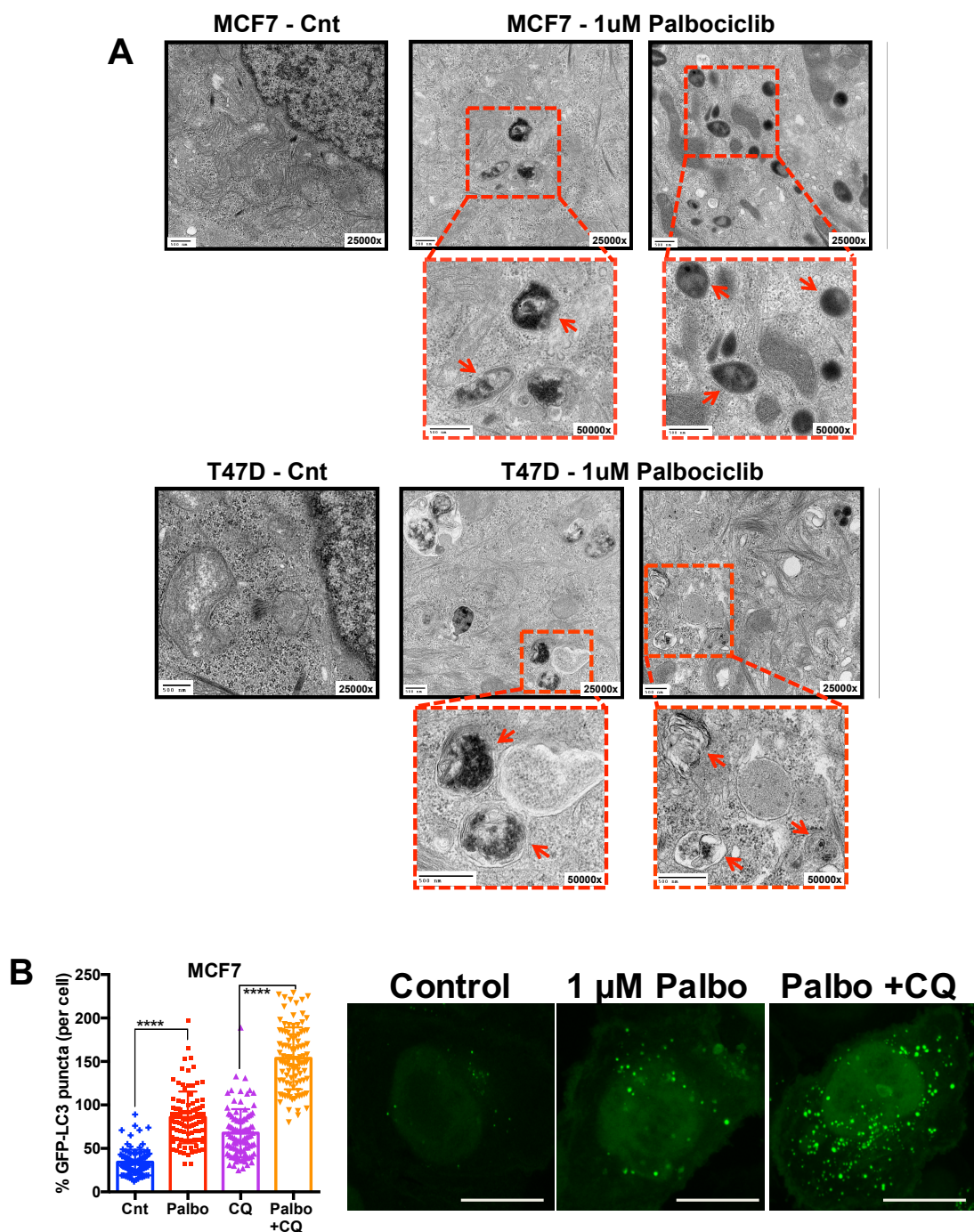


Figure 22: Palbociclib mediated induction of autophagy: A) Representative Transmission Electron microscopy (TEM) microphotographs of MCF7 and T47D cells treated with DMSO (Cnt) or 1 μ M palbociclib (Palbo) for 6 days. Red arrows indicate double-membraned autophagosomes. Scale bars equal 500 nm. B) Quantification and representative confocal images of GFP-LC3 expressing MCF7 cells treated with 25 μ M CQ (for 1 hour), 1 μ M palbociclib or combination of palbociclib and CQ for 48 hours. Scale bars are 50 μ m. All data represent mean \pm SD from three independent experiments; p-values were calculated in comparison to cells treated with DMSO (Control) unless indicated. ns: $p > 0.05$; * $p < 0.05$; ** $p < 0.01$; *** $p < 0.001$; **** $p < 0.0001$.

4.2.2. INDUCTION OF INTACT AUTOPHAGIC FLUX WITH LOW DOSES OF PALBOCICLIB

While our results show the induction of autophagy with CDK4/6 inhibition, examination of the presence of an intact autophagic flux, which indicates completion of the autophagy pathway and efficient recycling of the cellular cargo, is more critical than the induction of autophagy. Hence, we examined the presence of an intact autophagic flux following palbociclib treatment by: i) flux ratio (LC3B-II to LC3B-I and LC3B-II to p62), ii) treatment with lysosomal block chloroquine (CQ), which elevates lysosomal pH and impairs autophagic flux (Chittaranjan, Bortnik et al. 2015), iii) GFP-LC3 puncta with CQ treatment and iv) RFP-GFP-LC3 dual-reporter assay (Kimura, Noda et al. 2007).

Treatment with low dose (concentrations lower than 2.5 μ M) palbociclib, exhibited higher flux ratios, as indicated by the ratio of LC3BII protein levels to LC3BI (**Figure 23A**) and the ratio of the protein levels of LC3BII to SQSTM1 (**Figure 23B**). Further, short term (1 hour) with treatment with the lysosomal block, 25 μ M chloroquine significantly increases the protein levels of LC3B-II, compared to treatment with palbociclib alone, as measured by western blotting analysis (**Figure 23C**) and as quantified by densitometry analysis (**Figure 23D**). Additionally, CQ treatment significantly increased GFP positive LC3 puncta compared to palbociclib treatment alone at the on-target low doses of 1 μ M (**Figure 22B**). Finally, to confirm the induction of an intact autophagy, we performed the RFP-GFP-LC3 dual-reporter assay (Kimura, Noda et al. 2007), where pH-dependent degradation of GFP in the lysosomes enables the differential visualization of autophagosomes (as RFP+ve GFP+ve puncta – yellow puncta) and autophagolysosomes (as RFP+ve puncta). Our results reveal that the presence of an intact autophagic flux, which is indicated here by the increase in both RFP+ve GFP+ve puncta (autophagosomes) and RFP+ve puncta (autophagolysosomes) as observed in cells treated with 1 μ M palbociclib treatment (**Figure 23E**), while an impaired autophagic flux would be indicated by the accumulation of only autophagosomes (yellow puncta).

Thus, results demonstrate the presence of an intact autophagy flux at the low and on-target concentrations of palbociclib.

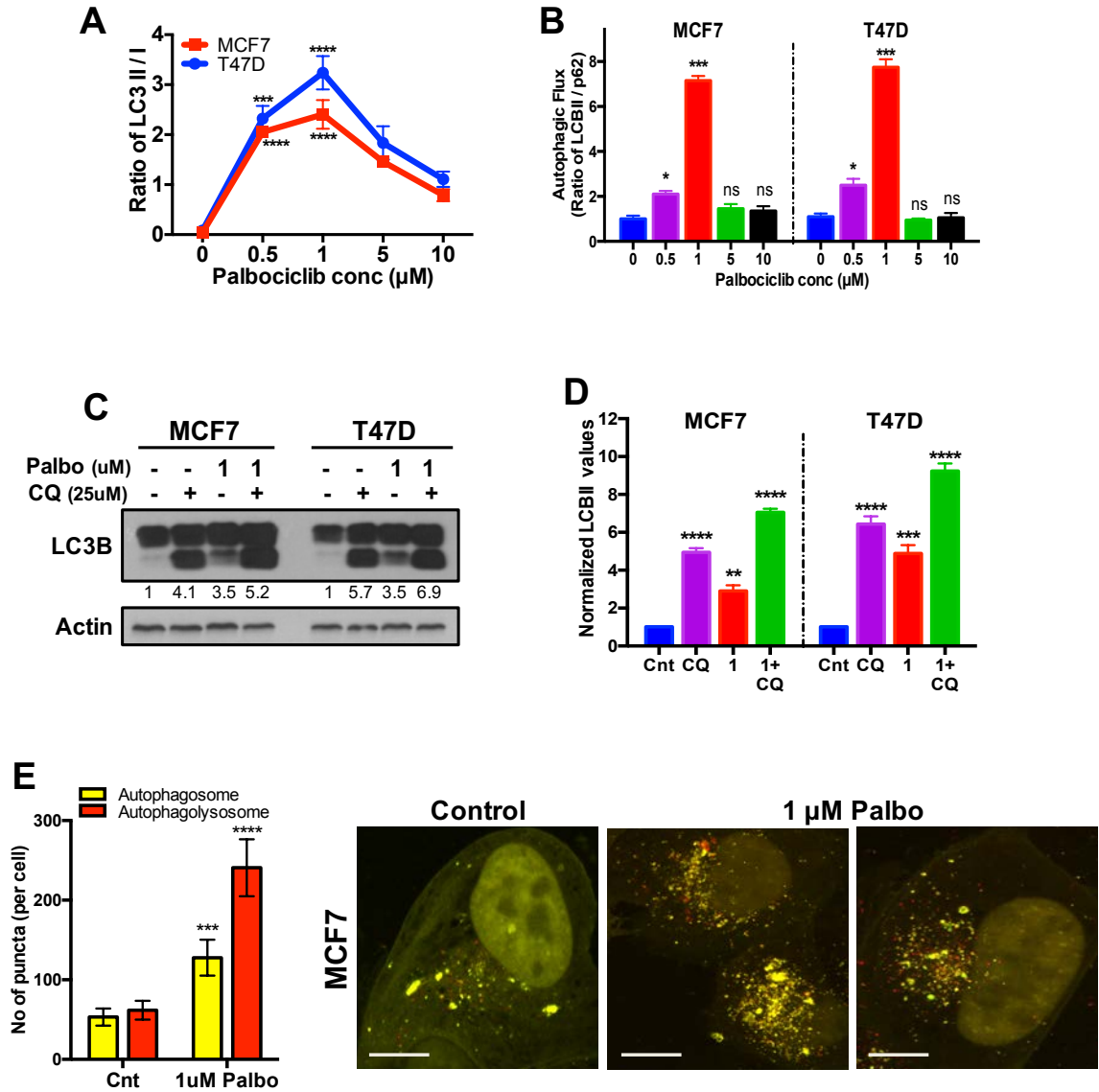


Figure 23: Induction of intact autophagy with low doses of palbociclib: A) Autophagic flux, calculated as ratio of LC3B-II to LC3B-I from densitometry values (normalized to corresponding levels of actin) of western blots from Figure 15E. B) Autophagic flux, calculated as ratio of LC3B-II to p62 from densitometry values (normalized to corresponding levels of actin) of western blots from Figure 15E. C) Western blot of LC3B and p62 in MCF7 and T47D cells treated with a combination of 25μM Chloroquine (CQ) for 1 hour and palbociclib for 6 days. D) Densitometry values for western blots in Figure 17C to obtain LC3B-II protein levels (normalized to corresponding levels of actin). E) Quantification of RFP-GFP-LC3 puncta representative confocal images of RFP-GFP-LC3 expressing MCF7 cells treated with 1 μM palbociclib for 48 hours. Scale bars are 50 μm. All data represent mean±SD from three independent experiments; p-values were calculated in comparison to cells treated with DMSO (Control) unless indicated. ns: p>0.05; *p<0.05; **p<0.01; ***p<0.001; ****p<0.0001.

4.2.3. DEREGULATED AUTOPHAGIC FLUX AT HIGH DOSES OF PALBOCICLIB

While our results show that autophagy induced by palbociclib at low (1 μ M) and on-target doses have an intact flux (Figure 16 and 17), the induction of autophagy at the higher palbociclib doses remain unexplored. Understanding this would help shed light on the processes regulating the dose-dependent effect of palbociclib in ER positive breast cancer cells. To interrogate this, we performed the autophagy assays as described in Figures 16 and 17 upon treatment with higher doses (>2.5 μ M) of palbociclib in the ER positive breast cancer cell lines, MCF7 and T47D.

Measurement of autophagy by MDC analysis showed significant increase in the percentage of MDC positive cells (**Figure 24A**), and western blotting analysis showed increase in the protein levels of LC3B-II, but no decrease in p62 (**Figure 24B**) in MCF7 and T47D cell lines. This indicated that high doses of palbociclib also induce autophagy, but the autophagy induced at these doses has a deregulated flux, defined by the presence of an incomplete autophagic process and no recycling of the cellular cargo occurs. This was confirmed by high flux ratios as calculated by the ratio of LC3B-II to LC3B-I (**Figure 23A**) and the ratio of LC3B-II to p62 (**Figure 23B**). Further, to examine the autophagic flux induced at the higher dose, MCF7 and T47D cells treated with palbociclib, were subjected to short term (24 hour) treatment with the lysosomal block, chloroquine (CQ) and examined for the presence of MDC positivity. Results show no significant change in the MDC levels, indicating that the flux was already impaired (**Figure 24C**). Finally, deregulated autophagy at the higher off-target doses of palbociclib was also corroborated by the presence of either dysfunctional lysosomes (multi-lamellar structures indicated by blue colored arrows) or early autophagosomes (non-electron dense structures indicated by black colored arrows) in Transmission Electron Microscopy (TEM) images (**Figure 24D**).

These results indicate that while higher doses of palbociclib induces autophagy at the higher doses as well, the autophagic flux appears to be deregulated.

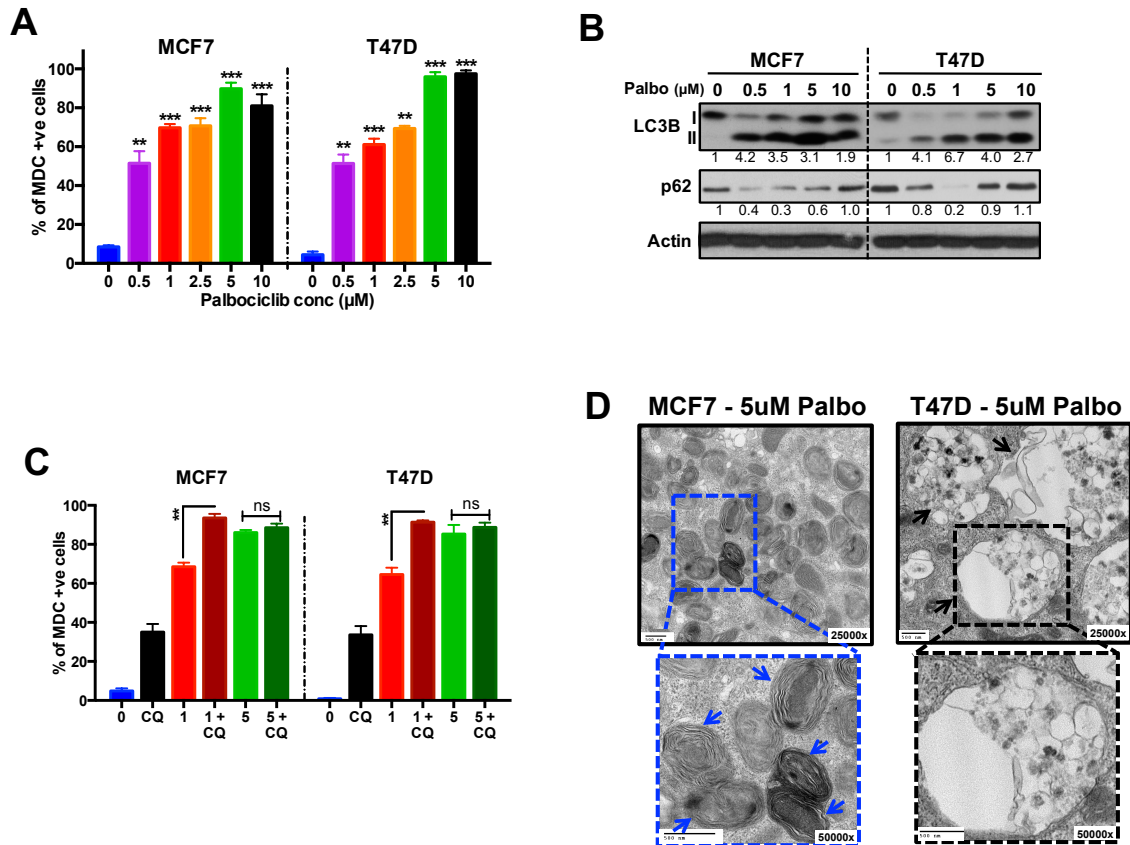


Figure 24: Deregulated autophagy flux at high doses of palbociclib: A) Measurement of MDC positive MCF7 and T47D cells treated with varying concentrations of palbociclib for 6 days. B) Western blot analysis of autophagy proteins, LC3B I, II and p62 in MCF7 and T47D cells upon treatment with varying concentrations of palbociclib for 6 days. C) Measurement of MDC positive MCF7 and T47D cells treated with a combination of 25μM Chloroquine (CQ) for 1 hour and palbociclib for 6 days. D) Representative Transmission Electron microscopy (TEM) microphotographs of MCF7 and T47D cells treated with DMSO (Cnt) or 5 μM palbociclib (Palbo) for 6 days. Blue arrows indicate multi-lamellate structures indicative of dysfunctional lysosomes. Black arrows indicate early stage autophagosomes. Scale bars equal 500 nm. All data represent mean±SD from three independent experiments; p-values were calculated in comparison to cells treated with DMSO (Control) unless indicated. ns: p>0.05; *p<0.05; **p<0.01; ***p<0.001; ****p<0.0001.

4.2.4. DEPENDENCE OF PALBOCICLIB-INDUCED AUTOPHAGY ON THE INDUCTION OF ROS

Results from Figure 9 show that treatment of ER positive breast cancer cell lines with palbociclib results in the induction of ROS at both on- and off-target doses. Given that palbociclib treatment at low on-target doses induces autophagy, and that ROS is known to induce autophagy (Kongara and Karantza 2012), we hypothesized that CDK4/6 inhibition mediated by on-target effects of palbociclib (1 μ M) may induce ROS, which in turn triggers autophagy.

Initially, we confirmed the induction of ROS at the on-target doses of palbociclib by Reverse phase protein array (RPPA) analysis for ROS-related proteins, SOD-1, CAV-1 and SOD-2, which showed a significant decrease in ROS ablating proteins SOD-1 (Papa, Manfredi et al. 2014) and CAV-1 (Chen, Barman et al. 2014), while an increase SOD-2, which is known to positively regulate ROS was observed (**Figure 25A**). This in combination with the results showed in Figure 9B confirm the induction of ROS at the low (on-target) doses of palbociclib in ER positive breast cancer cell lines.

Next, to directly interrogate the dependence of palbociclib-induced autophagy on ROS induction, ROS was ablated using the ROS scavengers, NAC and Trolox (Hamad, Arda et al. 2010, Sun 2010) in palbociclib treated ER positive cancer cells, which resulted in a significant decrease in MDC staining (**Figure 25B**). A concomitant decrease in LC3B-II protein expression levels was also observed with ROS ablation in cells treated with low doses of palbociclib (**Figure 25C, 25D**).

Thus, these results suggest that palbociclib-induced autophagy is dependent on ROS induction and the levels of ROS levels.

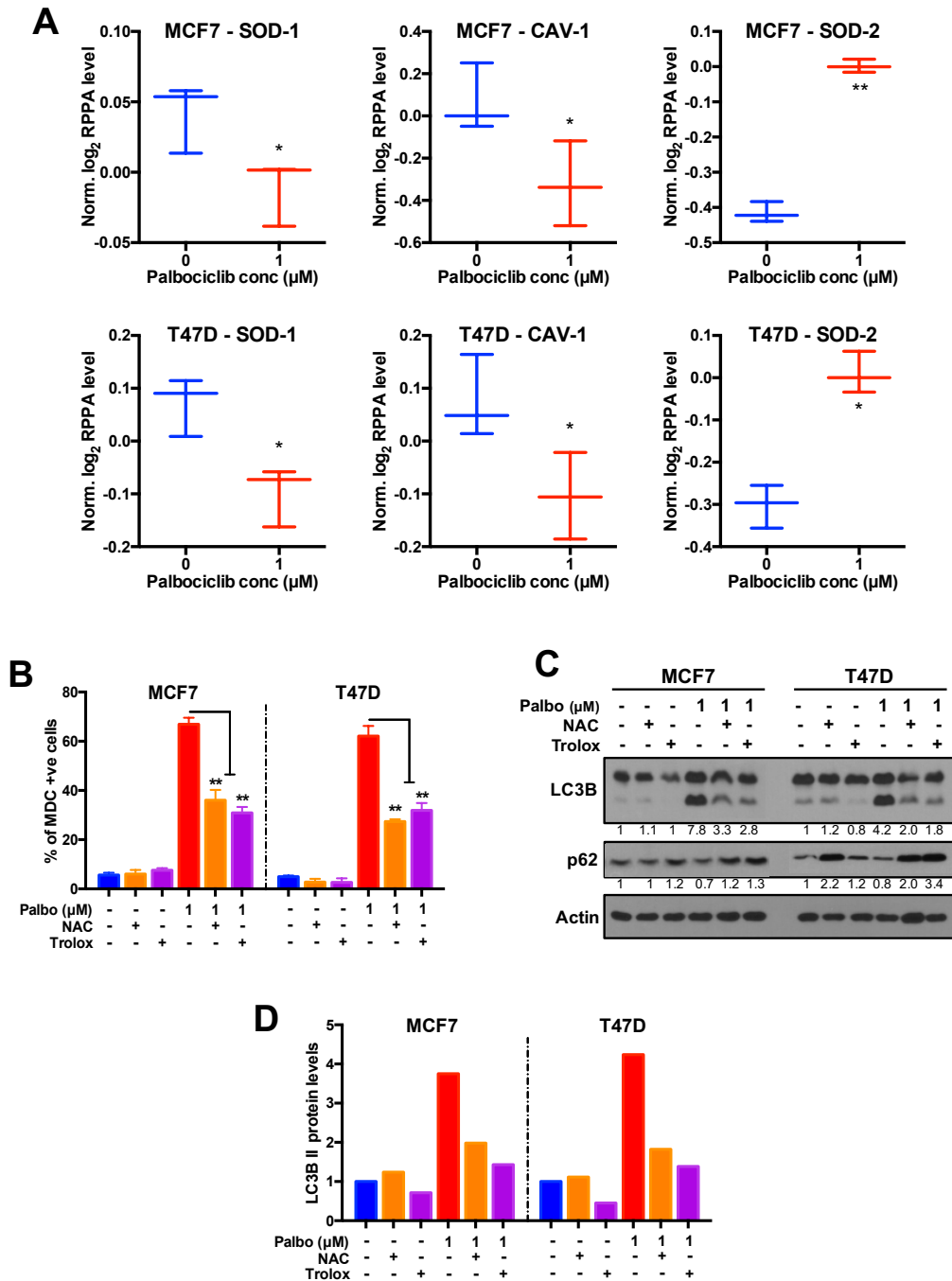


Figure 25: Dependence of palbociclib induced autophagy on the induction of ROS: A) Expression (normalized log₂ level) of SOD-1, CAV-1 and SOD-2 determined by RPPA analysis of MCF7 and T47D cell lines treated with palbociclib for 6 days. B) Quantification (MFI) of MDC staining in MCF7 and T47D cells treated with a combination of ROS scavenger (10 mM NAC or 0.1 mM trolox) and DMSO or 1 μM palbociclib for 6 days. C,D) Western blot analysis showing levels of LC3B and p62 proteins (C) and densitometry values of LC3B-II (D) in MCF7 and T47D cells treated as in B. All data represent mean±SD from three independent experiments; p-values were calculated in comparison to cells treated with DMSO (Control) or siNT unless indicated. ns: p>0.05; *p<0.05; **p<0.01; ***p<0.001; ****p<0.0001.

4.2.5. PALBOCICLIB MEDIATED INDUCTION OF DOSE-DEPENDENT AUTOPHAGY *IN VIVO*

To assess the ability of the CDK4/6 inhibitor palbociclib to induce autophagy *in vivo*, ER+ve mouse orthotopic xenograft tumors were treated with varying concentrations of Palbociclib (25 mg/kg, 50mg/kg, 75 mg/kg or 150 mg/kg/day) daily via oral gavage for 7 days and subject to autophagy assays: i) RPPA analysis, ii) Western blot analysis and flux quantification and iii) Transmission electron microscopy (TEM).

Analysis of the altered pathways from RPPA analysis showed up-regulation of autophagy related proteins (**Figure 18B**). Specifically, a significant increase in the protein levels of LC3B and Atg-7 was observed in the palbociclib treated tumors in a dose-dependent manner (**Figure 26A**). Further, western blot analysis of the tumors treated with palbociclib exhibited an increase in the levels of LC3B-II, indicating the induction of autophagy *in vivo* in a dose-dependent manner (**Figure 26B**). Specifically, tumor tissues treated with 25mg/kg palbociclib showed increased protein levels of LC3BII and decreased levels of SQSTM1/p62 via western blot analysis, thus demonstrating an induction of autophagy with an intact flux at this concentration (**Figure 26B**). This was confirmed by high autophagic flux ratio (calculated by LC3B-II to LC3B-I) upon treatment with 25mg/kg palbociclib (**Figure 26C**). Additionally, TEM showed the presence of double-membrane electron dense autophagosomes on the residual tumors treated with 25mg/kg palbociclib (**Figure 26D**), demonstrating the induction of autophagy.

However, in comparison, while treatment with 150mg/kg Palbociclib increased protein levels of LC3B-II and Atg-7 (**Figure 26A**), this concentration failed to decrease SQSTM1 levels (**Figure 26B**), exhibited low autophagic flux ratio (**figure 26C**), and displayed presence of dysfunctional lysosomes (**Figure 26D** - multi-lamellar structures indicated by blue colored arrows). These results are indicative of autophagy with impaired flux induced with high dose of

palbociclib (150mg/kg), and are similar to results observed *in vitro* with the higher off-target doses ($>2.5\mu\text{M}$) of palbociclib.

Collectively, these results show the induction of autophagy *in vivo* with palbociclib treatment in a dose-dependent manner.

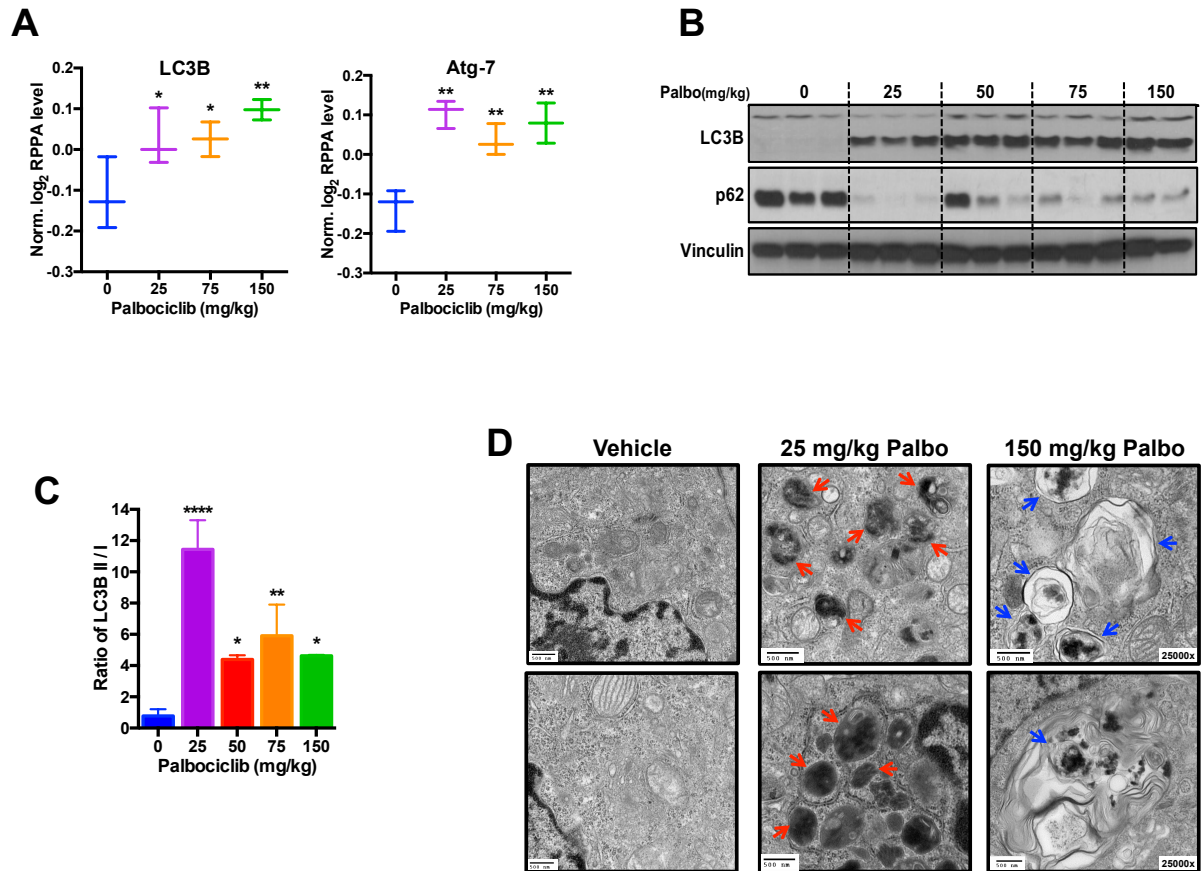


Figure 26: Induction of dose-dependent autophagy in vivo by palbociclib: A) Expression (normalized log₂ level) of LC3B and Atg-7 protein levels as determined from RPPA analysis of tumors harvested after treatment with Vehicle (0.5% Methylcellulose) or varying doses of palbociclib via oral gavage for 7 days. B) Western blot for autophagy proteins, LC3B and p62 in mice tumors upon 7 days of drug treatment as described in A. C) Autophagic flux, calculated as ratio of LC3B-II to LC3B-I from densitometry values (normalized to the corresponding levels of actin) of western blots from B. D) Representative TEM microphotographs of tumors harvested from mice treated with vehicle (0.5% MC), 25 mg/kg or 150 mg/kg of palbociclib for 7 days. Red arrows indicate double-membraned autophagosomes. Blue arrows indicate multi-lamellate structures indicative of dysfunctional lysosomes. Scale bars equal 500 nm. All data represent mean \pm SD from three independent experiments; p-values were calculated in comparison to mice treated with vehicle (Control) unless indicated. ns: $p > 0.05$; * $p < 0.05$; ** $p < 0.01$; *** $p < 0.001$; **** $p < 0.0001$.

4.3. DISCUSSION

Collectively, results from this chapter demonstrate that genetic downregulation of CDK4/6 and pharmacological inhibition via palbociclib induces autophagy in a dose-dependent manner. Palbociclib treatment of ER positive breast cancer induces ROS, which at low doses triggers autophagy, while elevated levels lead to the induction of sustained growth inhibition and induction of senescence (**Figure 27B**).

While the relationship between CDK4/6-cyclin D and autophagy is very poorly understood, recent studies have suggested that CDK4/6 inhibitors such as palbociclib can induce autophagy in fibroblast and promyelocytic leukemia as described in detail in the introduction of this chapter (Brown, Jeselsohn et al. 2012, Capparelli, Chiavarina et al. 2012, Acevedo, Vernier et al. 2016). Studies conducted in this chapter provided detailed evidence corroborating this hypothesis and establishing that palbociclib treatment of the ER positive cell lines in fact does trigger autophagy. Further, a biphasic effect on autophagy was observed with palbociclib treatment, both *in vitro* and *in vivo*, wherein at lower or on-target doses, the autophagy induced had an intact flux, while higher and possibly off-target doses of palbociclib induced a defective autophagy (**Figure 27A**).

However, the molecular mechanism by which autophagy is induced by palbociclib has not been understood yet. A possible mechanism could be that the drug directly regulates autophagy by altering expression of the autophagic proteins required for this process such as Beclin-1 or other class III PI3K proteins that are present in complex with Beclin-1, such as Vps34 (Hammond, Brunet et al. 1998). Phosphorylation of Beclin-1 and / or Vps34 has been shown to regulate the induction of autophagy in cancer, CDKs have been known to directly phosphorylate these proteins (Abrahamsen, Stenmark et al. 2012). This suggests a potential mechanism by which palbociclib induces autophagy that needs to be explored further.

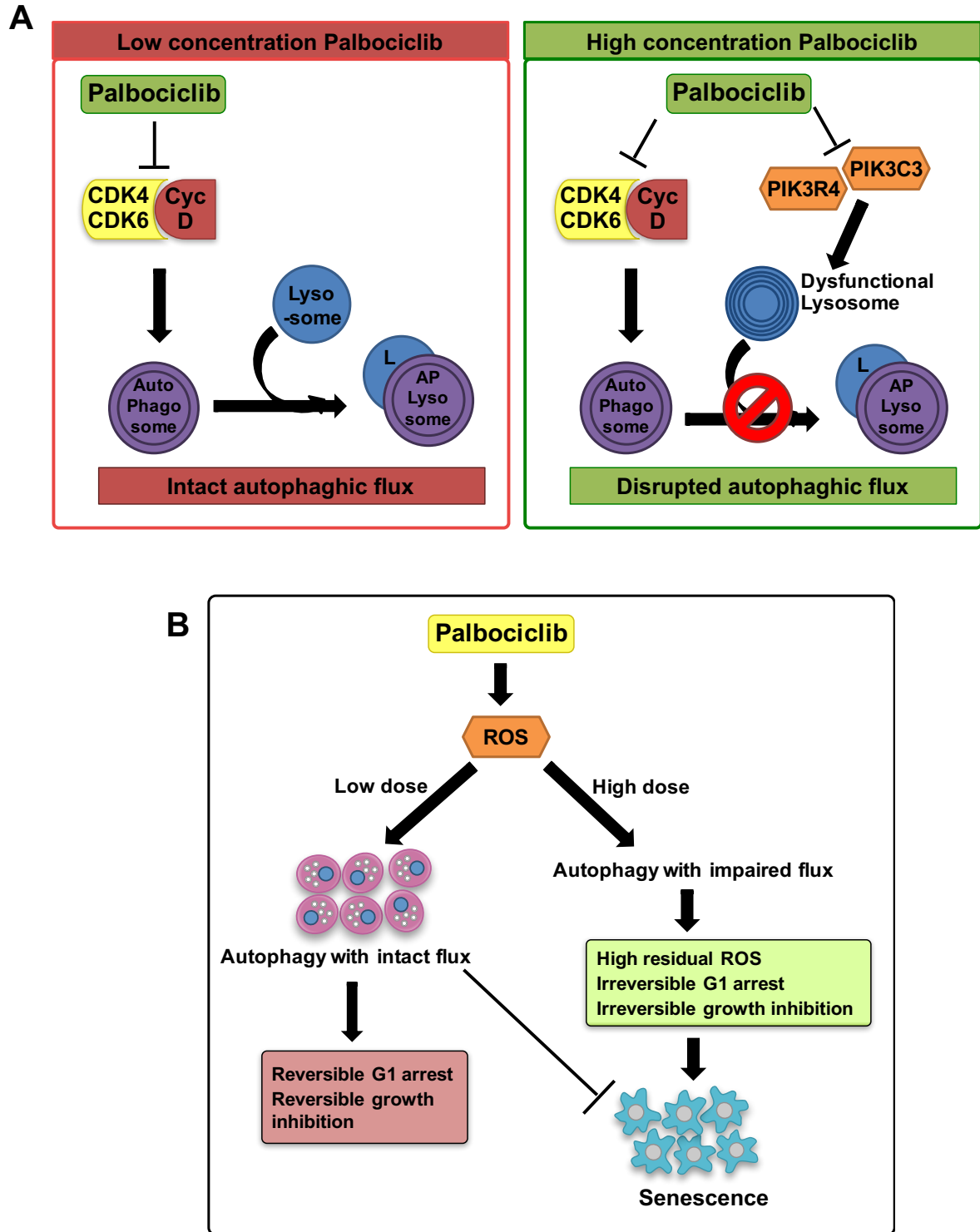


Figure 27: Working model: A) Schematic showing the biphasic (on-target vs off-target effect of palbociclib on ER+ breast cancer cells, with respect to the induction of autophagy. B) Schematic showing the mechanism by which palbociclib regulates ROS, autophagy and senescence in ER+ve breast cancer.

A recent study in lung cancer revealed that palbociclib has unique kinase targets, apart from CDK4 and CDK6, such as PIK3CD and PIK3R4 (Sumi, Kuenzi et al. 2015). Intriguingly, PIK3R4 / Vps15 is a class III Phosphatidylinositol 3-Kinase (PI3K) that has been shown to be required for autophagic clearance of proteins, and defects in Vps15 in the skeletal muscles leads to autophagic vascular myopathy and dysfunctional lysosomes (Lindmo, Brech et al. 2008, Nemazanyy, Blaauw et al. 2013). This closely resembles the multi-lamellar electron dense structures which represent defective lysosomes when treated with the higher doses (5uM *in vitro* and 150 mg/kg *in vivo*) of palbociclib. Hence, it is highly likely that Palbociclib hits secondary targets at the higher concentrations (5uM or 150mg/kg), and this accounts for the inhibition of autophagic flux at these doses and the observed off-target effects with siRNA against CDK4/6. This might also explain why treatment with the other CDK4/6 inhibitors (ribociclib and abemaciclib) failed to elicit a biphasic response, given that these secondary kinase targets were shown to be specific to palbociclib and not hit by ribociclib (Sumi, Kuenzi et al. 2015).

Autophagy is regulated by several stress signals including oxidative stress (Poillet-Perez, Despouy et al. 2015). Accumulation of oxidative stress induces ROS, which has been shown to have both a tumor promoting role and tumor suppressing role and this is most often controlled by the levels of ROS molecules (Azad, Chen et al. 2009, Liou and Storz 2010). Lower or moderate induction of ROS typically promotes cell cycle progress and stress response and survival processes such as autophagy (Boonstra and Post 2004). Results from this chapter show that the low / moderate levels of ROS induced with low doses of palbociclib, induces ROS-dependent autophagy in the ER positive breast cancer cells. Since autophagy has been shown to eliminate ROS (Scherz-Shouval and Elazar 2011), it is possible that autophagy induction also plays a role in maintaining the ROS levels low enough, such that it prevents the induction of irreversible cell cycle arrest and senescence. This will be examined in Chapter 5.

Collectively, the studies presented in this Chapter results show that palbociclib treatment intact autophagy in ER positive breast cancer *in vitro* and *in vivo*. Further, these studies suggest that the autophagy induced is a stress response to treatment with palbociclib and it may mediate resistance to palbociclib mediated sustained growth inhibition and senescence at the on-target doses. The implications of this hypothesis is that inhibition of autophagy could improve the efficacy of CDK4/6 inhibitor treatment, a topic that has been explored in detail in Chapter 5.

CHAPTER 5: IN VITRO AND IN VIVO SYNERGY BETWEEN CDK4/6 AND AUTOPHAGY INHIBITION IN ER+ BREAST CANCER

5.1. INTRODUCTION

5.1.1. AUTOPHAGY AS A STRESS RESPONSE PROCESS IN CANCER

Autophagy, the cell's recycling machinery, can be considered as a quality control mechanism within cells, which recycles damaged cellular components and organelles to maintain optimal cellular function and generate energy (White 2015). In established cancers, the physiological role of autophagy is that it is a stress response process, enabling cancer cells to combat various types of stresses, including nutrient deprivation, ER (endoplasmic reticulum) stress, DNA damage, oxidative stress and drug-induced stress (White, Mehnert et al. 2015). Many of these stresses are intrinsic to drug resistance suggesting that autophagy may mediate resistance to numerous cancer targeting therapies

For example, studies in the past few years have demonstrated the induction of pro-survival (oncogenic) autophagy in response to drugs such as chemotherapy and targeted therapy (Sui, Chen et al. 2013) Several of these agents are listed in **Table 6**, which lists the agents that have been shown to induce autophagy along with the type of stress they induce and the pathway the drugs activate leading to autophagy. These studies have shown that autophagy is induced in response to chemotherapy such as platinum agents (i.e. cisplatin and oxalating) in breast, ovarian and other solid cancers allowing the tumor cells to be rescued from the toxic effects of these therapies (Li, Hou et al. 2010, Liu, Yang et al. 2011, Sun, Chen et al. 2011, Sasaki, Tsuno et al. 2012, Wang and Wu 2014). Similar induction of autophagy has been reported in response to other targeted agents such as the angiogenesis inhibitor bevacizumab, sarafenib in hepatocellular carcinoma (Shi, Ding et al. 2011, Guo, Li et al. 2013) and tyrosine kinase inhibitors such as erlotinib, NVP-BEZ235 and imatinib in glioma, lung and renal cancer (Shingu, Fujiwara et al. 2009, Han, Pan et al. 2011, Zhao, Yang et al. 2011, Li, Jin et al. 2013).

Drug	Target / Stress	Cancer type	Reference
Aurora kinase A	mTOR	Breast	(Zou, Yuan et al. 2012)
Suberoylanilide hydroxamic acid (SAHA)	HDAC inhibitor	CML	(Carew, Nawrocki et al. 2007)
Tamoxifen	Antiestrogen	Breast	(Sun, Chen et al. 2011)
Epirubicin (EPI)	Anthracyclines	Breast	(Schoenlein, Periyasamy-Thandavan et al. 2009)
5-Fluorouracil	Thymidylate synthase inhibitor	Colorectal	(Li, Hou et al. 2010, Sasaki, Tsuno et al. 2012)
Irinotecan	MAPK14/p38 α	Colorectal	(Paillas, Causse et al. 2012)
Cisplatin	Genotoxic stress	Esophageal	(Liu, Yang et al. 2011)
		Ovarian	(Wang and Wu 2014)
Oxaliplatin	Genotoxic stress	Hepatocellular carcinoma	(Guo, Li et al. 2013)
Bevacizumab	Angiogenesis inhibitor	Hepatocellular carcinoma	(Guo, Li et al. 2013)
Sorafenib	ER stress	Hepatocellular carcinoma	(Shi, Ding et al. 2011)
High-mobility group box 1 protein (HMGB1)	DAMP molecule	CML	(Zhao, Yang et al. 2011)
Gefitinib or Erlotinib	EGFR tyrosine kinase inhibitor	Lung	(Han, Pan et al. 2011)
Topotecan	Genotoxic stress	Lung	(Kang, Tang et al. 2010)
NVP-BEZ235	PI3K/AKT/mTOR inhibitor	Renal	(Li, Jin et al. 2013)
Ursolic acid	Genotoxic stress	Prostate	(Shin, Kim et al. 2012)
Imatinib	Tyrosine kinase inhibitor	Glioma	(Shingu, Fujiwara et al. 2009)

Table 6: Drug-induced autophagy in cancer: Summary of studies showing the induction of pro-survival autophagy in response to chemotherapy and targeted therapy in cancers.

In breast cancer, autophagy has been shown to be induced and mediate resistance to epirubicin, aurora kinase inhibitor and antiestrogen treatment with tamoxifen (Schoenlein, Periyasamy-Thandavan et al. 2009, Sun, Chen et al. 2011, Zou, Yuan et al. 2012). Thus, these

studies indicate that autophagy may be a promising target in cancer, and has led to further research aimed at understanding the role of autophagy in response to drug induced stress.

5.1.2. PHARMACOLOGICAL INHIBITORS OF AUTOPHAGY

For autophagy process to be successful in recycling components, the autophagic flux has to be intact and the process needs to undergo completion, which involves the formation of the autophagosomes and its subsequent fusion with the lysosomes leading to cargo degradation (Mizushima 2007). Hence, autophagy can be inhibited at multiple steps and the most common points of inhibition are i) initiation, where inhibitors prevent the formation of the autophagosomes and ii) lysosomal fusion, where inhibitors prevent the fusion of the autophagosomes to the lysosome, thus inhibiting the autophagic flux and resulting in accumulation of autophagic vesicles (Yang, Hu et al. 2013, Wang, Hu et al. 2016). Thus, research over the years has led to the development of drugs targeting autophagy at these two points of intervention (**Table 7**) (Sui, Chen et al. 2013, Yang, Hu et al. 2013, Wang, Hu et al. 2016).

Given the key role of the class III PI3K proteins in the formation of the phagophore and autophagosomes (initiation and elongation steps of autophagy), several drugs targeting these proteins have been developed including 3-Methyladenine, Wortmannin, LY294002, etc, which have the ability to effectively suppress autophagy (**Table 7**) (Yang, Hu et al. 2013). Recently, Spautin-1, a drug that indirectly targets the class III PI3K complexes was developed, which inhibits the activity of USP10 and USP13, causing proteosomal degradation of Class III PI3K complexes and blocking autophagy induction (Shao, Li et al. 2014). Additionally, drugs (MRT68921 and MRT67307) that specifically inhibit the kinase activity of Ulk1 and Ulk2 (crucial for phagosome formation) have also been recently developed (Sui, Chen et al. 2013).

Drugs that inhibit the fusion of autophagosomes and lysosomes function either by altering the pH of the lysosomes or by targeting the vacuolar-type H (+)-ATPases (V-ATPases)

Drug	Target	Stage of autophagy inhibited
Chloroquine	Lysosomal pH	Fusion with lysosomes
Hydroxychloroquine	Lysosomal pH	Fusion with lysosomes
Bafilomycin A 1	Vacuolar-type H(+)-ATPase inhibitor	Initiation / Expansion
3-Methyladenine	Class III PI3K inhibitor	Initiation / Expansion
Wortmannin	Class III PI3K inhibitor	Initiation / Expansion
LY294002	Class III PI3K inhibitor	Initiation / Expansion
Pyruvinium	Class III PI3K inhibitor	Initiation / Expansion
Lys-05	Lysosomal pH	Fusion with lysosomes
Spautin-1	USP10/13 inhibitor	Initiation / Expansion
MRT68921, MRT67307	Ulk1/2 inhibitor	Initiation / Expansion

Table 7: Autophagy targeting drugs: Table summarizing the list of that target autophagy and the stage in the pathway they inhibit

that are found on the lysosomal membrane (Yang, Hu et al. 2013). BafilomycinA1, a specific inhibitor of the V-ATPase, blocks the acidification of the lysosome and prevents maturation of the autophagosomes, thus inhibiting autophagic flux (Yamamoto, Tagawa et al. 1998). The other class of late stage autophagy inhibitors are lysosomal lumen alkalizers, which includes the most commonly used autophagy drugs, chloroquine (CQ) and its analog hydroxychloroquine (HCQ) (Homewood, Warhurst et al. 1972, Wang, Hu et al. 2016). They prevent the fusion of the lysosomes with the autophagic vesicles, thus inhibiting flux and resulting in accumulation of autophagosomes in cells (Wang, Hu et al. 2016). These drugs are widely used as anti-malarial and anti-rheumatoid agents and are currently the only clinically relevant autophagy inhibitors (Homewood, Warhurst et al. 1972). A more recently developed modified analog of HCQ is Lys-05, which has been shown to be 10-fold more potent as an autophagy inhibitor

than HCQ *in vitro* and *in vivo* (McAfee, Zhang et al. 2012). It inhibits autophagy similar to CQ and HCQ, by accumulating within and deacidifying the lysosome, resulting in impaired autophagy (Amaravadi and Winkler 2012, McAfee, Zhang et al. 2012).

While there are several drugs available for targeting autophagy, the specificity of these drug to the autophagy process has been under question, highlighting the need to develop more specific and potent autophagy inhibitors.

5.1.3. CLINICAL DEVELOPMENT OF AUTOPHAGY INHIBITORS

While there are several autophagy inhibitors that are currently used for pre-clinical studies (**Table 7**), their lack of specificity in inhibiting the autophagy pathways and high toxicity *in vivo* has limited their translation into the clinic (Sui, Chen et al. 2013). Chloroquine (CQ) and hydroxychloroquine (HCQ) are the only autophagy inhibiting drugs that are currently FDA approved for human use (Sui, Chen et al. 2013, Wang, Hu et al. 2016). Clinical studies have shown with CQ and HCQ have shown that compared to CQ, HCQ can be safely dose escalated in cancer patients (Gunja, Roberts et al. 2009). This, coupled with the strong rationale of targeted autophagy in cancer has led to about 175 clinical trials currently open around the world with HCQ, more than 90% of which are in cancers (<http://clinicaltrials.gov/>). **Table 8** provides a list of the phase II clinical trials that are currently in progress with HCQ in combination with chemo or targeted therapy in various cancers. A recent phase I study in 22 patients with relapsed myeloma showed that the addition of HCQ to the proteasome inhibitor resulted in partial response in 28% of the patients and a stable disease in 45% of the patients (Vogl, Stadtmauer et al. 2014). Similar phase I studies in melanoma and solid tumors showed that the addition of HCQ to the current therapy of mTOR or HDAC inhibitors resulted in improved survival and improved response (Mahalingam, Mita et al. 2014, Rangwala, Chang et al. 2014).

Cancer type	Drugs	Phase	Identifier
Recurrent Breast cancer	HCQ+everolimus	II	NCT3132406
Breast cancer	HCQ+ixabepilone	I/II	NCT00765765
Platinum resistant Ovarian cancer	HCQ+itraconazole	I/II	NCT03081702
NSCLC	HCQ+gefitinib	I/II	NCT00765765
Advanced NSCLC	HCQ+carboplatin, paclitaxel, bevacizumab	II	NCT01649947
NSCLC	HCQ+carboplatin /gemcitabine	II	NCT02722369
Advanced NSCLC and (EGFR) mutations	HCQ+erlotinib	II	NCT00977470
Pancreatic cancer	HCQ+gemcitabine/abraxane	I/II	NCT01506973
Pancreatic cancer	HCQ+gemcitabine	I/II	NCT01128296
Pancreatic cancer	HCQ+gemcitabine/abraxane	II	NCT01978184
Pancreatic cancer	HCQ+capecitabine+radiation	II	NCT01494155
Hepatocellular carcinoma	HCQ+sorafenib	II	NCT03037437
Prostate cancer	HCQ+docetaxal	II	NCT00786682
Prostate cancer	HCQ+abiraterone+ABT-263	II	NCT01828476
Colorectal cancer	HCQ+vorinostat+regorafenib	II	NCT02316340
Colorectal cancer	HCQ+XELOX+bevacizumab	II	NCT01006369
Colorectal cancer	HCQ+FOLFOX/bevacizumab	I/II	NCT01206530
Melanoma	HCQ+trematinib	I/II	NCT02257424
Renal cell carcinoma	HCQ and IL-2	I/II	NCT01550367
Renal cell carcinoma	HCQ and RAD001	I/II	NCT01510119
Soft tissue sarcoma	HCQ+sirolimus	II	NCT01842594
Glioblastoma	HCQ+temozolomide	I/II	NCT00486603
Multiple myeloma	HCQ+bortezomib	I/II	NCT00568880
CML	HCQ+imatinib	II	NCT01227135

Table 8: Phase-II clinical trials with HCQ: Table summarizing the phase II clinical trials that are currently ongoing in cancers in combination with the autophagy inhibitor hydroxychloroquine

While hydroxychloroquine is currently used as a bonafide autophagy inhibitor, a concern with the use HCQ is the high doses required in humans to achieve successful blockade of autophagy. This emphasizes the need to identify more specific, potent and clinically relevant inhibitors. The recently developed inhibitor Lys-05, has been shown to be 10-fold more potent than HCQ and has a better therapeutic index (Amaravadi and Winkler 2012). Hence numerous phase I and II clinical trials are currently underway utilizing Lys-05 in combination with chemotherapy or targeted therapy in cancers (Rebecca and Amaravadi 2016).

5.1.4. GAP IN KNOWLEDGE

While results from Chapter 4 show that CDK4/6 inhibition via palbociclib results in the induction of autophagy, the following questions remain:

1. What is the role of the autophagy induced by palbociclib? Is it tumor suppressing or pro-survival and tumor promoting?
2. What is the impact of genetically ablating autophagy in breast cancer cells?
3. Would pharmacological inhibition of autophagy be synergistic with palbociclib in breast cancer cells?
4. Would pharmacological inhibition of autophagy be synergistic with other CDK4/6 inhibitors (ribociclib, abemaciclib) in breast cancer cells?
5. Would pharmacological inhibition of autophagy be synergistic with palbociclib in breast cancer cells?
6. Would HCQ treatment be synergistic with palbociclib in breast cancer cells resistant to the aromatase inhibitors?
7. What is the effect of combinatorial inhibition of the CDK4/6 and autophagy pathways *in vivo*?

Given the minimal work carried out in investigating the relationship between CDK4/6 and autophagy, studies conducted in this chapter are aimed at addressing the above gaps in knowledge.

5.2. RESULTS

5.2.1. IMPACT OF BECLIN1 OR ATG5 DOWNREGULATION ON PALBOCICLIB ACTION

To interrogate the hypothesis that autophagy protects ER positive breast cancer cells from palbociclib-induced senescence molecularly, we downregulated two crucial autophagy genes, Beclin-1 and Atg-5, which play key roles in the initiation and elongation of the autophagosomes respectively (Hammond, Brunet et al. 1998, Liang, Yu et al. 2001, Kang, Zeh et al. 2011) (**Figures 28A, B**). While shRNA mediated knockdown of Beclin-1 and Atg-5 had no significant impact on the growth of ER positive breast cancer cell lines (**Figure 28C**), downregulation of Beclin-1 or Atg-5 significantly increased the sensitivity of MCF7 and T47D cells to palbociclib, resulting in a 5-fold decrease in IC₅₀ values (as measured by dose response assay, where cells were treated for 6 days with a 6-day recovery), when compared to cells with Scrambled shRNA (SCR) (**Figure 28D, E**). Further, cell counting assay and cell cycle analysis showed that Beclin-1 or Atg-5 knockdown resulted in an irreversible growth inhibition and irreversible G1 arrest respectively, when treated with low (on-target) doses of palbociclib (0.5 μ M and 1 μ M), compared to Scr cells which exhibited a reversible growth inhibition at these concentrations (**Figure 28F, 29A**). Additionally, Beclin-1 or Atg-5 knockdown significantly elevated SA- β gal activity with 6 day treatment, even at low on-target palbociclib concentrations (1 μ M), indicating the induction of senescence when autophagy is ablated (**Figure 29B**).

Thus, these results suggest that ablation of autophagy significantly augments the drug's ability to induce a sustained growth inhibition and senescence, suggesting a pro-survival and drug resistance mediating role for the autophagy induced by CDK4/6 inhibition.

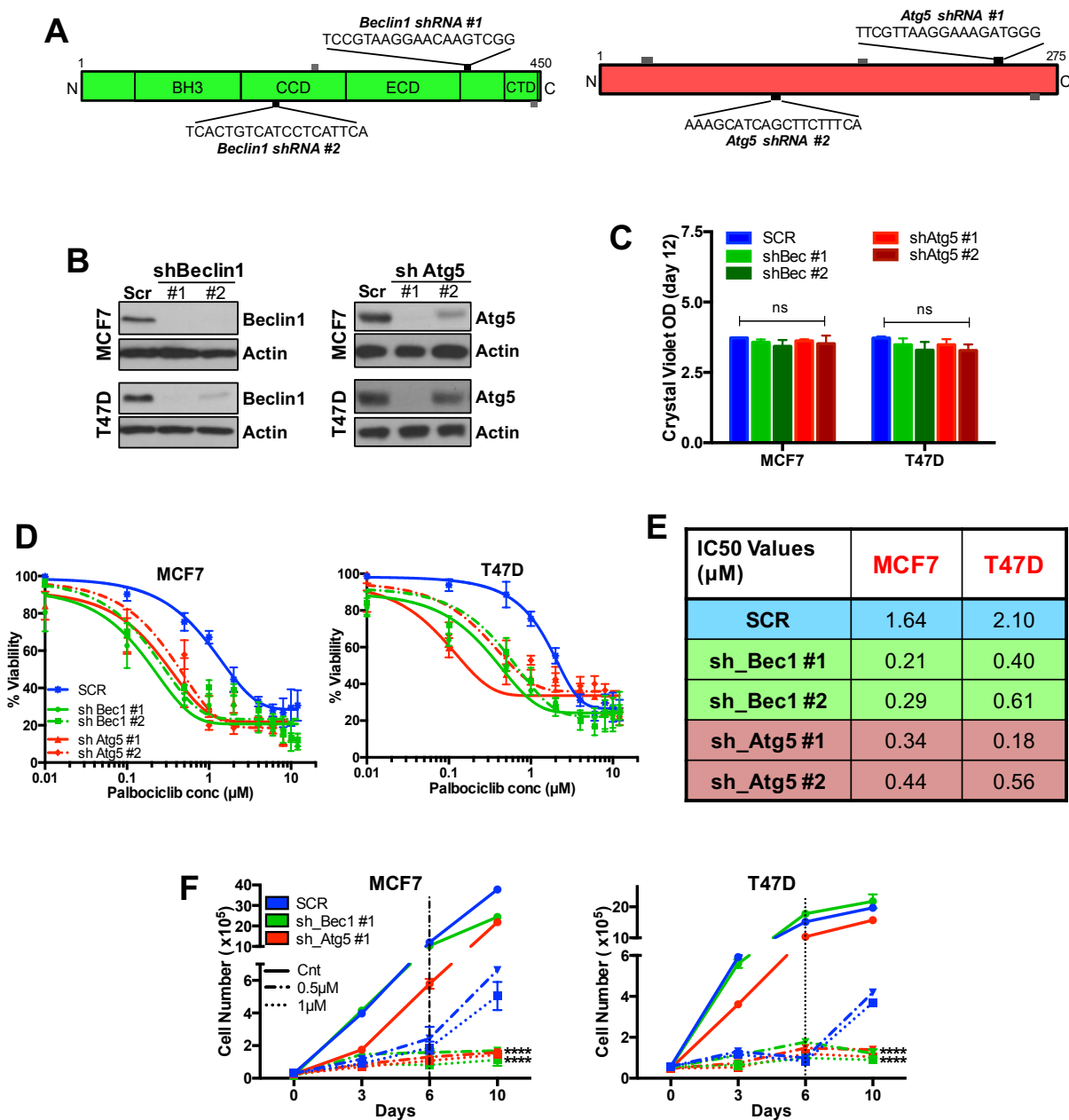


Figure 28: Impact of Beclin-1 or Atg-5 downregulation on palbociclib mediated growth inhibition: A) Schematic depicting locations of the shRNA sequences on the autophagy-associated *Beclin-1* and *Atg5* genes. B) Western blot for Beclin-1 and Atg-5 in MCF7 and T47D cells after transfection with Scrambled (Scr), Beclin1 or Atg5 shRNA. C) Crystal violet OD measured on day 12 from drug response studies performed in MCF7 Scr and Beclin1 or Atg5 knockdown cells. D, E) MCF7 and T47D cells with Beclin1 or Atg5 knocked down were treated with varying concentrations of palbociclib for 6 days and subjected to dose response assay after 6 days of recovery (D) and their corresponding half-maximal inhibitory concentrations (IC_{50}) values (E). F) Beclin-1 or Atg5-knockdown MCF7 and T47D cells were treated with 0.5 or 1 μ M of palbociclib (Palbo) for 6 days and recovery for 4 days (release) to examine reversibility and subjected to cell counting to assess proliferation. p-values were calculated in comparison to cells treated with Scramble shRNA [SCR] and 1 μ M palbociclib. All data represent mean \pm SD from three independent experiments; ns: $p > 0.05$; * $p < 0.05$; ** $p < 0.01$; *** $p < 0.001$; **** $p < 0.0001$.

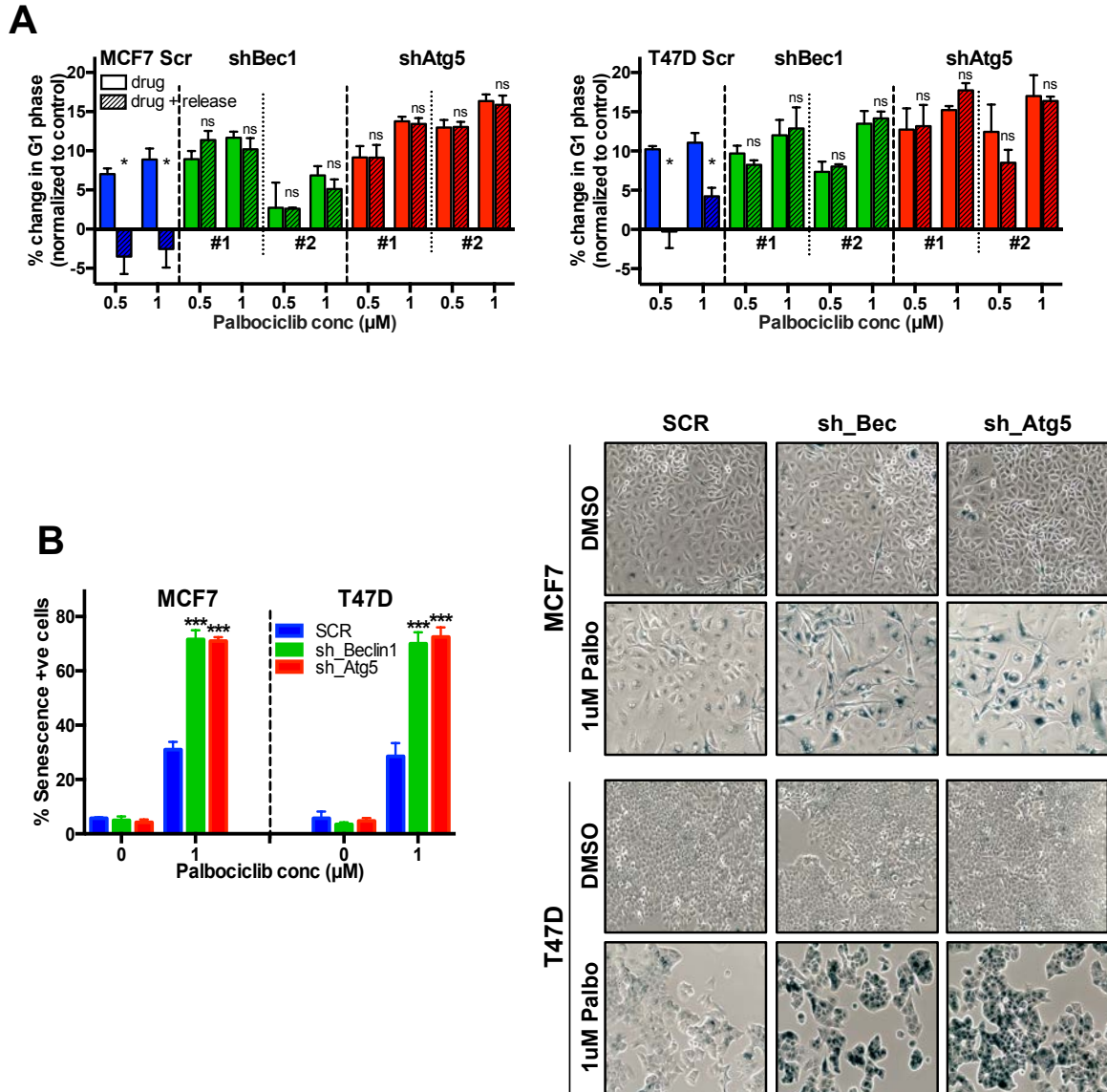


Figure 29: Impact of Beclin-1 or Atg-5 downregulation on palbociclib mediated G1 arrest and senescence: A) Cell cycle analysis to determine the percentage change in G1 phase in Beclin-1 or Atg5-knockdown MCF7 and T47D cells treated with 0.5 or 1 μ M of palbociclib (Palbo) for 6 days and recovery for 4 days (release) to examine reversibility. p-values were calculated by comparing values at the end of drug treatment with those at the end of drug + release. B) SA- β galactosidase assay as a measurement of senescence with representative images in Scr, Beclin 1 or Atg5 knockdown cells treated with palbociclib for 6 days. p-values calculated in comparison with SCR – 1 μ M palbociclib. All data represent mean \pm SD from three independent experiments; ns: $p > 0.05$; * $p < 0.05$; ** $p < 0.01$; *** $p < 0.001$; **** $p < 0.0001$.

5.2.2. SYNERGY BETWEEN siRNA OR shRNA MEDIATED KNOCKDOWN OF CDK4/6 AND AUTOPHAGY INHIBITION

Having shown that molecular ablation of autophagy sensitizes ER positive breast cancer cells to CDK4/6 inhibition via palbociclib, we next investigated if combined molecular downregulation of CDK4 and CDK6 would synergize with pharmacological autophagy inhibition. To interrogate this, we first downregulated CDK4 and CDK6 via siRNA mediated knockdown. Cell counting and clonogenic assays were performed to measure proliferation showed while that dual siRNA against CDK4 and CDK6 had moderate effect on cell proliferation, that its combination with autophagy inhibition (treatment with hydroxychloroquine) resulted in enhanced and synergistic growth inhibitory effect (**Figure 30A** - compare red to orange solid lines and **30B**). Similarly, shRNA mediated knockdown of CDK4 and CDK6 was also synergistic in combination with autophagy inhibition via HCQ, resulting in significantly enhanced growth inhibition of the ER+ve cell lines, MCF7 and T47D (**Figure 30C** – compare red to orange lines)

These results show that genetic ablation of CDK4 and CDK6 is synergistic with pharmacological inhibition of autophagy.

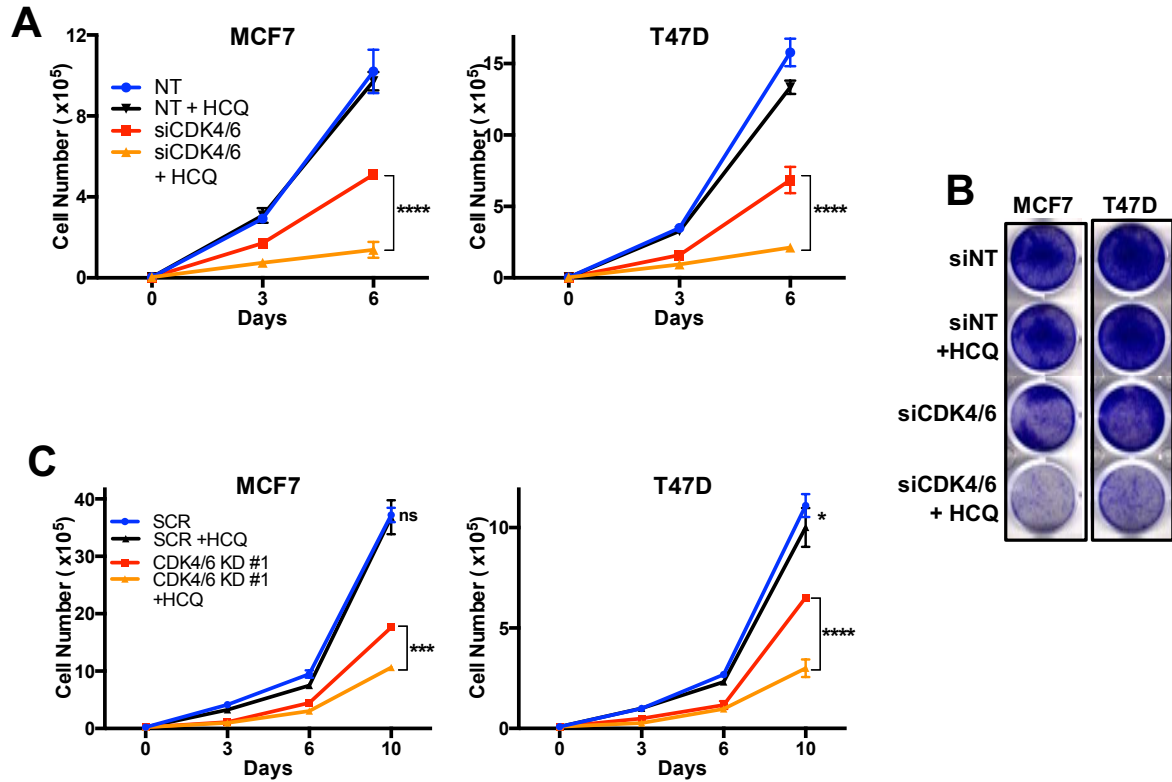


Figure 30: Synergy between siRNA or shRNA mediated knockdown of CDK4/6 and autophagy inhibition: A,B) MCF7 and T47D cell lines were transfected with siNT or siRNA against CDK4 and CDK6 for dual knockdown and cells were treated with DMSO or 15uM HCQ for 6 days and subjected to A) Cell counting and B) Clonogenic assay to assess proliferation. C) Cell counting to assess proliferation of MCF7 and T47D cells with shRNA mediated dual knockdown of CDK4 and CDK6 and treatment with DMSO or 15 μ M HCQ for 6 days and recovery for 4 days. All data represent mean \pm SD from three independent experiments; ns: $p > 0.05$; * $p < 0.05$; ** $p < 0.01$; *** $p < 0.001$; **** $p < 0.0001$.

5.2.3. IMPACT OF AUTOPHAGY INHIBITION ON PALBOCICLIB MEDIATED GROWTH INHIBITION, CELL CYCLE ARREST, ROS AND SENESENCE

We next interrogated if pharmacological inhibition of autophagy would synergize with pharmacological CDK4/6 inhibition via low dose (on-target) palbociclib ($< 2.5 \mu\text{M}$) to induce senescence. To this end, MCF7 and T47D cells were treated with the autophagy inhibitor, Hydroxychloroquine (HCQ), in combination with low dose palbociclib ($0.5\mu\text{M}$ or $1\mu\text{M}$) for 6 days and recovery for 4 days, and results revealed that this combination induced a sustained and irreversible inhibition of growth (measured via cell counting – **Figure 31A** – compare purple to light blue lines and red to orange lines) and colony formation (**Figure 31B**), when compared to the reversible inhibition induced by palbociclib alone. Next, to examine if combined treatment of palbociclib (low and on-target dose) and HCQ could result in sustained and long-term growth inhibition, MCF7 and T47D cells were treated for 6 days and allowed to recover in the absence of the drug for 12 days. Results revealed that combination of palbociclib and HCQ was able to achieve a sustained long lasting growth inhibition, compared to low-dose palbociclib alone (**Figure 31C** – compared red to orange line).

Furthermore, treatment of ER positive cells (MCF7 and T47D) with low dose Palbociclib in combination with HCQ resulted in an irreversible G1 arrest even after 4 days of recovery in the absence of the drug (white bars) and was even comparable to continuous drug treatment for 10 days (grey bars) (**Figure 31D**). However, combination treatment with on-target doses of palbociclib (0.5 and $1\mu\text{M}$) and HCQ did not trigger apoptosis, measured by Annexin V positivity (**Figure 31E**).

Given our previous findings that elevated ROS levels is required for palbociclib-induced senescence, and the known role of autophagy in protecting cells from oxidative stress by eliminating ROS (Kongara and Karantza 2012), we interrogated if inhibition of autophagy can also modulate ROS levels. Consistently, exposure of palbociclib treated ER positive breast cancer to the autophagy inhibitor, hydroxychloroquine (HCQ), resulted in a significant increase

in ROS levels (**Figure 32A**). This suggests that the autophagy induced by low (on-target) doses of palbociclib degrades ROS, accounting for the lower ROS levels and the resistance to the induction senescence at these concentrations. Additionally, a significant increase in SA- β gal activity (**Figure 32B**) and a shift in side-scatter (**Figure 32C**), upon treatment with the combination of palbociclib and HCQ, when compared to treatment with palbociclib alone, demonstrating the synergistic effect of the two drugs in inducing senescence.

Taken together, these results suggest that autophagy induced in response to palbociclib eliminates ROS and has a pro-survival role in ER positive breast cancer. Hence, pharmacological inhibition of autophagy via HCQ induces a synergistic response when combined with palbociclib treatment, resulting in a sustained growth inhibition and significantly elevated senescence.

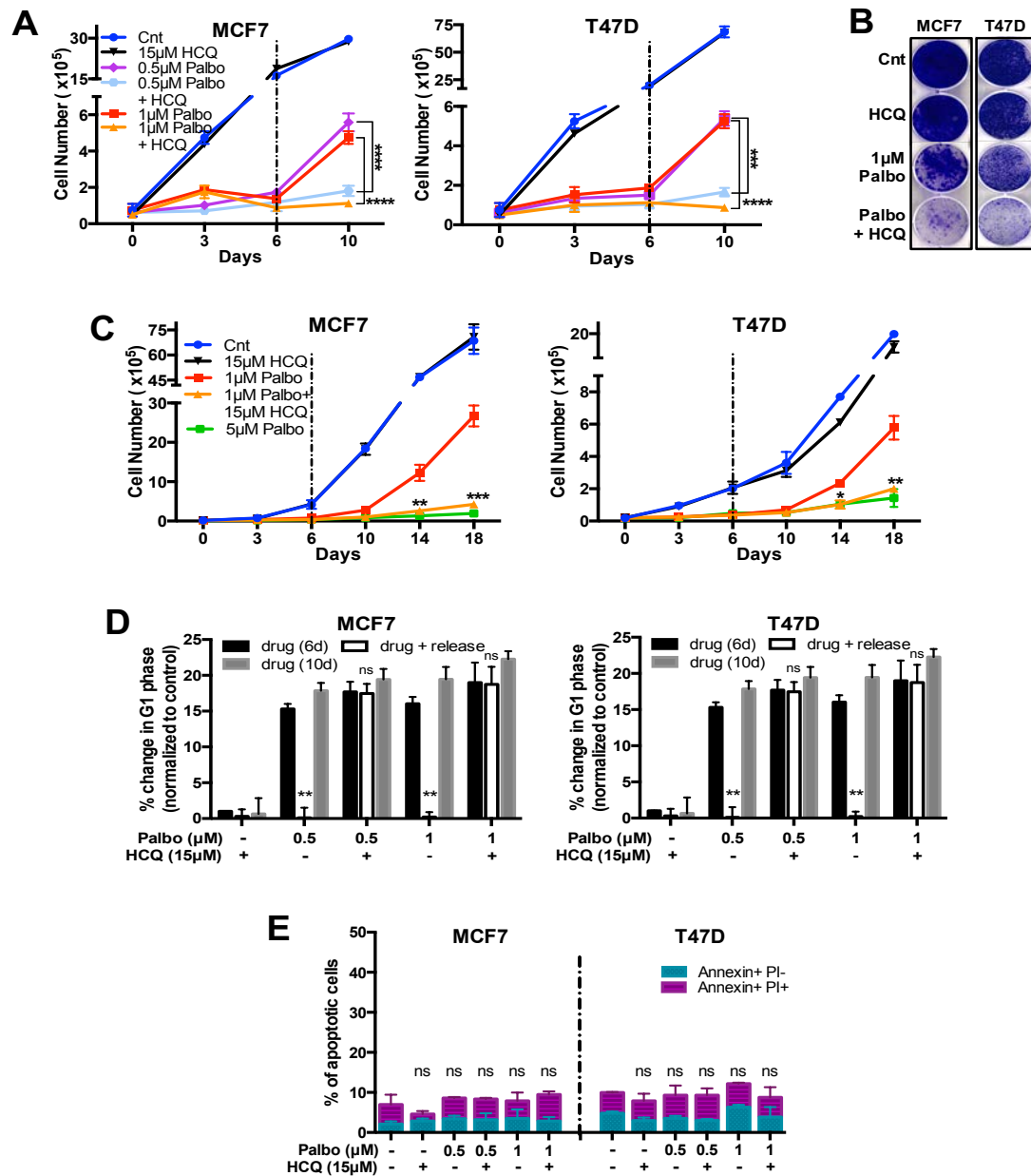


Figure 31: Impact of autophagy inhibition on palbociclib mediated growth inhibition and G1 arrest: A,B) MCF7 and T47D cells were treated with combination of palbociclib and 15μM hydroxychloroquine (HCQ) for 6 days. Cells were allowed to recover for 4 or 6 days in drug-free media and subjected to A) Cell counting and B) Clonogenic assay. C) Effect on cell viability when treated with a combination of DMSO or palbociclib (Palbo - 0.5 or 1 μM) and autophagy inhibitor hydroxychloroquine (HCQ; 15 μM) for a) 6 days and allowed to recover for 12 days to examine long-term reversibility. p-values were calculated in comparison to cells treated with 1 μM palbociclib. D,E) MCF7 and T47D cells were treated with 15 μM HCQ and/or palbociclib (0.5 or 1 μM) for 6 days and subjected to D) cell cycle analysis to determine the percentage change in G1 phase (p-values were calculated by comparing values at the end of 6 days drug treatment with those at the end of drug + release) and E) flow cytometry measurement of apoptotic cells (early apoptosis: Annexin V+/PI-; late apoptosis: Annexin V+/PI+). All data represent mean ± SD from three independent experiments; ns: p>0.05; *p<0.05; **p<0.01; ***p<0.001; ****p<0.0001.

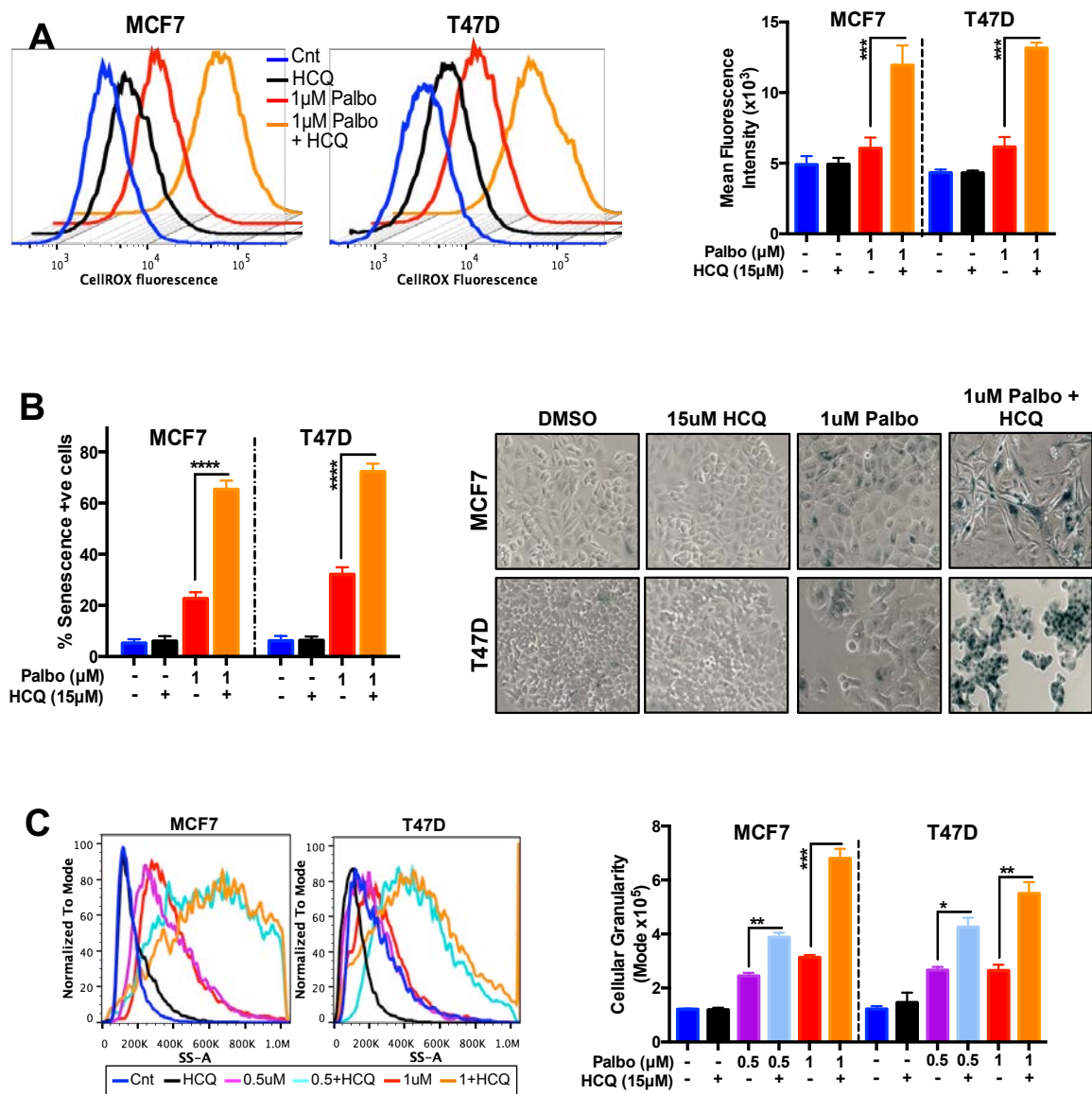


Figure 32: Impact of autophagy inhibition on palbociclib induced ROS and senescence: MCF7 and T47D cells were treated with 15 µM HCQ and/or palbociclib (0.5 or 1 µM) for 6 days and subjected to A) CellROX assay to measure cellular reactive oxygen species (ROS) levels and its quantification (Mean fluorescence intensity), B) Quantification of SA-β gal assay to measure senescence and representative images and C) measurement and quantification of side scatter analysis to assess cellular granularity. All data represent mean ± SD from three independent experiments; ns: $p > 0.05$; * $p < 0.05$; ** $p < 0.01$; *** $p < 0.001$; **** $p < 0.0001$.

5.2.4. SYNERGY BETWEEN AUTOPHAGY INHIBITION (HCQ) AND OTHER CDK4/6 INHIBITORS – RIBOCICLIB AND ABEMACICLIB

Given that autophagy inhibition synergizes with palbociclib to induce a sustained growth inhibition, we next wanted to examine the effect of other clinically available CDK4/6 inhibitors, abemaciclib and ribociclib. We first performed dose response studies by treating the ER positive breast cancer cells, MCF7 and T47D, with ribociclib and abemaciclib (range of concentrations from 0.01 to 12uM) for 6 days (**Figure 33A**), which revealed the IC₅₀ values of the two drugs to be ~4uM and 1.4uM respectively (**Figure 33B**). Next, the effect of the combination treatment of ribociclib or abemaciclib along with the autophagy inhibitor, HCQ in MCF7 and T47D cells was examined cell counting and colony formation / clonogenic assay with treatment for 6 days and recovery for 4 or 6 days to examine reversibility of the drug mediated effect. Results revealed the combined treated of CDK4/6 and autophagy inhibitors induced a sustained inhibition of growth and colony formation when compared to control (no treatment) or treatment with single drugs alone (**Figures 33C-F**). Additionally, co-treatment of abemaciclib with autophagy inhibition (HCQ) resulted in significant apoptosis in a dose-dependent manner, when compared to treatment with abemaciclib alone (**Figure 33G**).

These results show that CDK4/6 inhibitors other than palbociclib also synergize with autophagy inhibition to induce an irreversible growth arrest or apoptosis, in the case of abemaciclib.

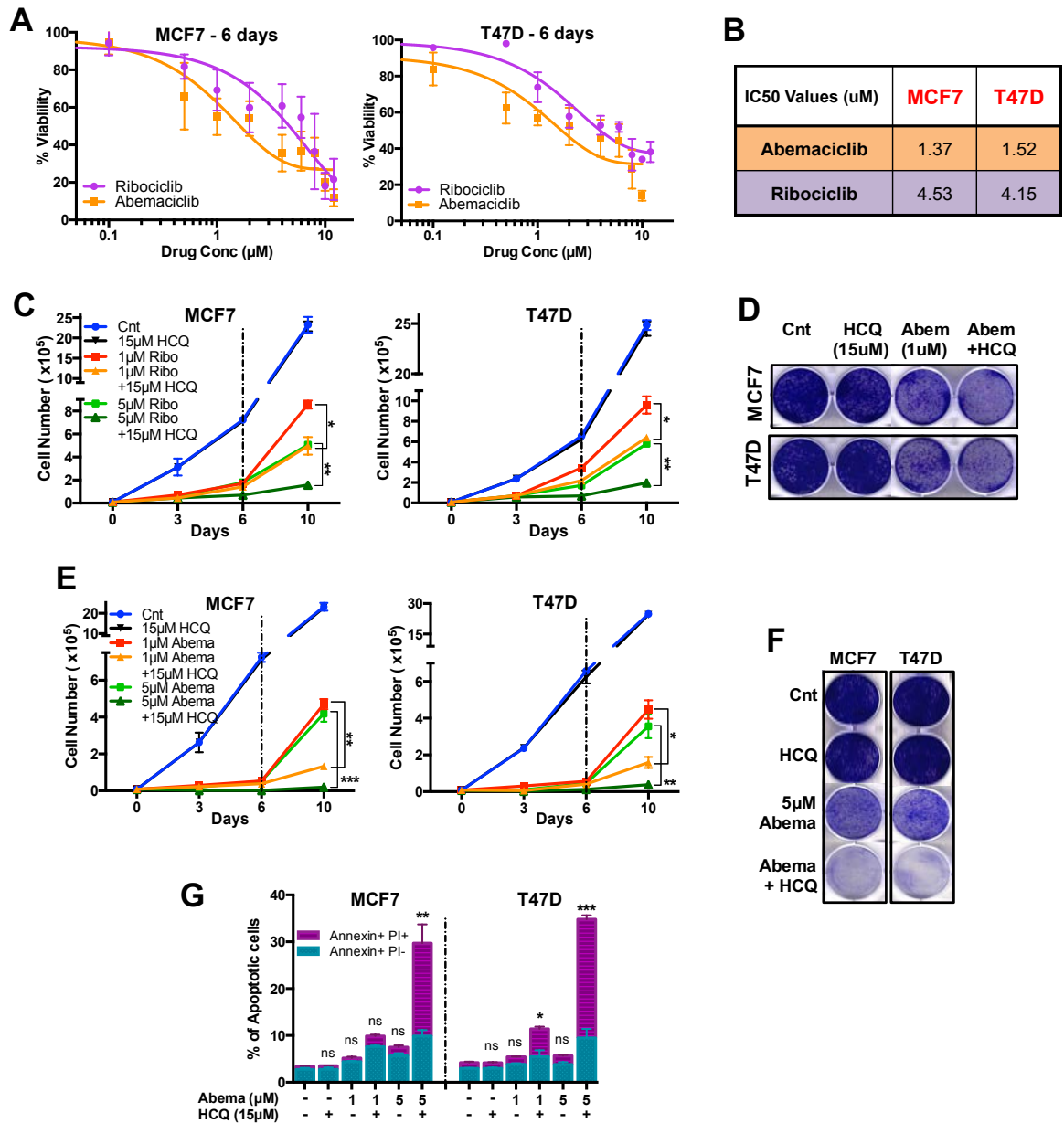


Figure 33: Synergy between autophagy inhibition (HCQ) and other CDK4/6 inhibitors – ribociclib and abemaciclib: A,B)Proliferation of MCF7 and T47D cells treated with DMSO or increasing concentrations (conc) of ribociclib or abemaciclib (0.01 to 12 μ M) for 6 days (A) and their corresponding half-maximal inhibitory concentration (IC_{50}) values (B). C,D) Cell counting (C) Clonogenic assay (D) to assess proliferation of MCF7 and T47D cells treated with a combination of DMSO (Cnt) or ribociclib (1 or 5 μ M) and 15 μ M hydroxychloroquine (HCQ) for 6 days and recovery for 4 or 6 days. E,F) Cell counting (E) and Clonogenic assay (F) to evaluate proliferation upon combined treatment with 5 μ M abemaciclib and HCQ for 6 days and recovery for 4 or 6 days. G) Flow cytometry measurement of apoptosis (early apoptosis: Annexin V+/PI-; late apoptosis: Annexin V+/PI+) in cells treated with 5 μ M abemaciclib combined with 15 μ M HCQ for 6 days. p-values were calculated in comparison to cells treated with DMSO (Control). All data represent mean \pm SD from three independent experiments; ns: $p > 0.05$; * $p < 0.05$; ** $p < 0.01$; *** $p < 0.001$; **** $p < 0.0001$.

5.2.5. SYNERGISM BETWEEN PALBOCICLIB AND OTHER AUTOPHAGY INHIBITORS

Finally, we interrogated if autophagy inhibitors other than hydroxychloroquine also synergize with low dose palbociclib to mediate sustained growth inhibition. To this end, we utilized four additional autophagy-inhibiting drugs, which target the autophagy pathway at different stages (**Table 7**): i) Chloroquine (a lysosomal blocker that acts similar to hydroxychloroquine), ii) Lys05, a potent and selective autophagy inhibitor that blocks the lysosomal fusion with the autophagosomes (McAfee, Zhang et al. 2012), iii) BaflomycinA1, a drug that inhibits the fusion of autophagosomes and lysosomes (Yamamoto, Tagawa et al. 1998) and iv) Spautin-1, which inhibits activity of USP10 and USP13, causing proteosomal degradation of Class III PI3K complexes and blocking autophagy induction (Shao, Li et al. 2014) (**Figure 34A**).

Results revealed that treatment of ER positive breast cancer cells (MCF7 and T47D) with the combination of low-dose or on-target dose of palbociclib and the autophagy inhibitors that target the lysosomal fusion, CQ or BaflomycinA1 results in an irreversible arrest of growth (measured by cell counting assay where cells are treated for 6 days with a 4 day recovery in the absence of the drug) and colony formation (with 6 day treated and 6 day recovery), when compared to the single drug or no treatment (Cnt) controls (**Figures 34B-D**). Combination treatment of palbociclib with the upstream autophagy inhibitor, Spautin-1 also resulted in a similar synergistic effect with low-dose palbociclib resulting in an irreversible and sustained inhibition of growth and colony formation (**Figures 35A,B**). Finally, treatment of on-target doses of palbociclib with the more potent autophagy inhibitor, Lys-05 also results in an irreversible growth inhibition (measured by cell counting assay) when compared to treatment with palbociclib alone (**Figure 35C** – compare red to orange lines).

Collectively, these results confirm the synergy between CDK4/6 and autophagy inhibitors in ER positive breast cancer cell lines, irrespective of the drug used to achieve the pharmacological inhibition.

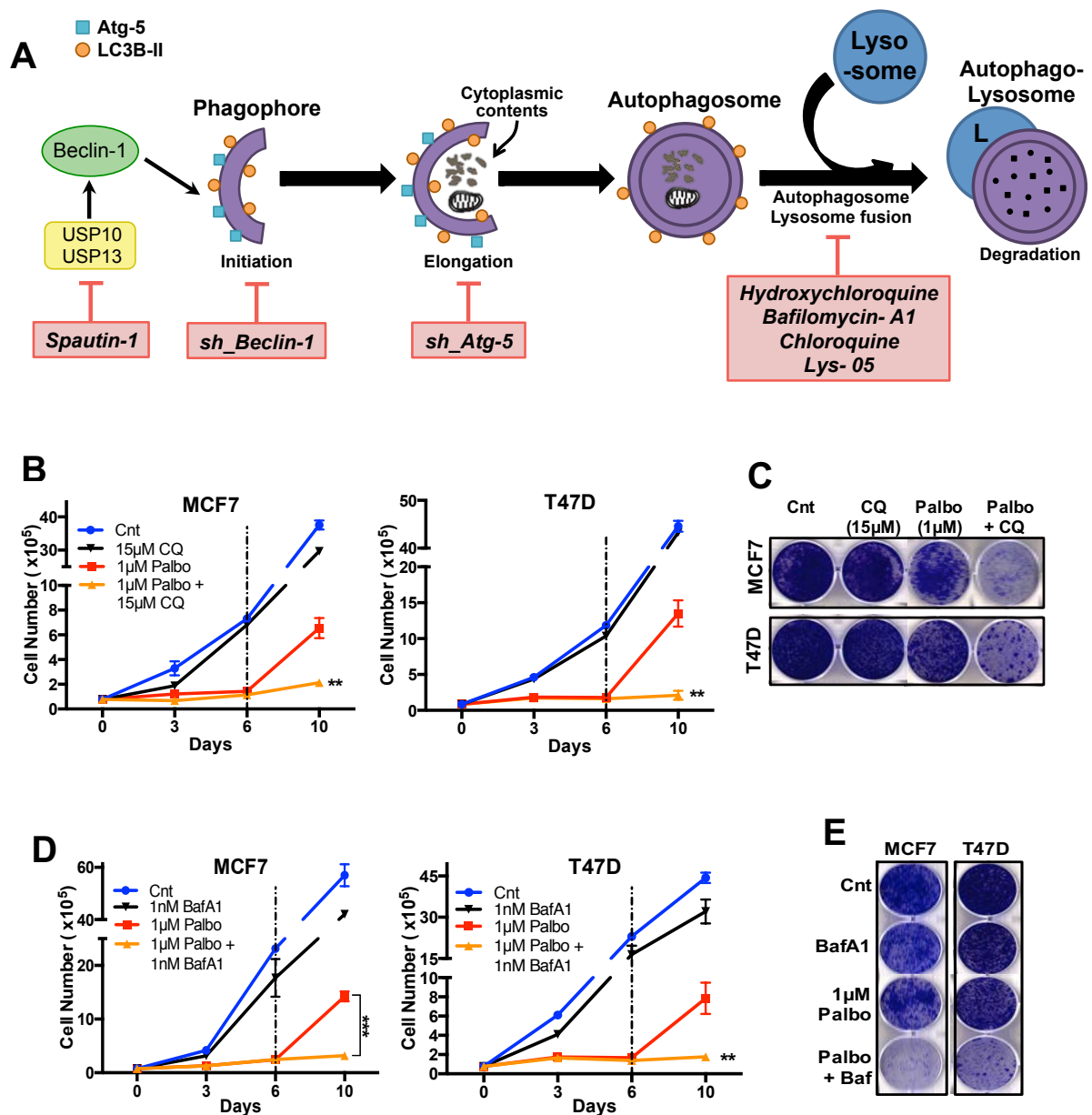


Figure 34: Synergism between palbociclib and other autophagy inhibitors (CQ, BafA1): A) Schematic of the autophagy pathway indicating the points of genetic and pharmacological interventions described in Fig. 2. B,C) MCF7 and T47D cells were treated with 1μM palbociclib and 15μM chloroquine (CQ) for 6 days and allowed to recover for 4 or 6 days. The effects on growth were examined by cell counting (B) and clonogenic assay (C). D,E) Cell counting (B) and Clonogenic assay (C) was used to assess proliferation of MCF7 and T47D cells treated with a combination of 1μM palbociclib and 1nM Bafilomycin (BafA1) for 6 days and allowed to recover for 4 or 6 days. All data represent mean \pm SD from three independent experiments; ns: $p > 0.05$; * $p < 0.05$; ** $p < 0.01$; *** $p < 0.001$; **** $p < 0.0001$.

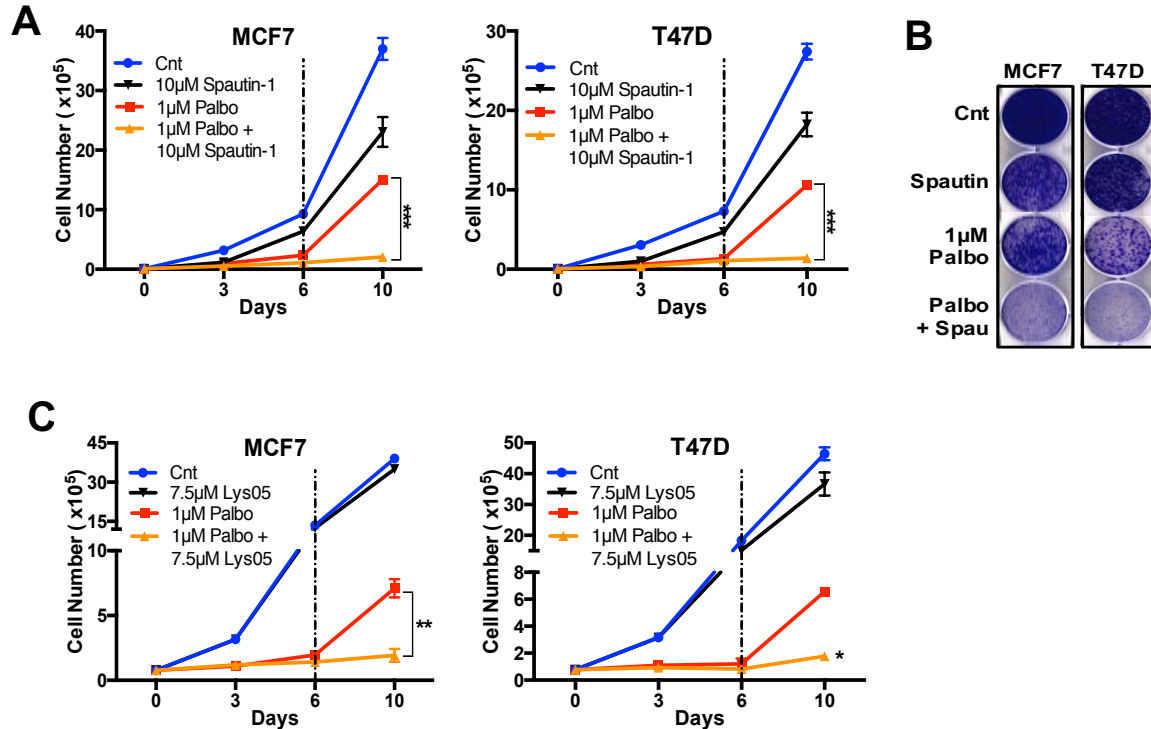


Figure 35: Synergism between palbociclib and other autophagy inhibitors (Spautin-1, Lys-05): A, B) cell counting (A) and Clonogenic assay (B) in MCF7 and T47D cells treated with 10µM spautin-1 or 1nM bafilomycin-A1 (Baf-A1) combined with 1µM palbociclib for 6 days and recovery for 4 or 6 days. C) Cell counting to assess proliferation of MCF7 and T47D cells treated with the combination of 1 µM palbociclib and 7.5 µM Lys-05 for 6 days. Cells were allowed to recover for 4 days to examine reversibility. All data represent mean \pm SD from three independent experiments; ns: $p > 0.05$; * $p < 0.05$; ** $p < 0.01$; *** $p < 0.001$; **** $p < 0.0001$.

5.2.6. SYNERGY BETWEEN CDK4/6 AND AUTOPHAGY INHIBITOR IN AROMATASE INHIBITOR RESISTANT CELLS

Advanced ER positive breast cancer patients who are currently being treated with the CDK4/6 inhibitor, palbociclib have in most cases received prior therapy including aromatase inhibitors such as letrozole and anastrozole. Hence, we wanted to examine the sensitivity of aromatase resistant cells to CDK4/6 inhibition as a single agent and in combination with autophagy inhibitors. To do so, we made MCF7 aromatase expressing cells resistant to letrozole or anastrozole by long term treatment with the respective drugs. Dose-response studies showed that the letrozole resistant cells were 10-fold resistant to letrozole and anastrozole resistant cells were 6-fold resistant to anastrozole (**Figure 36A**).

Interestingly the aromatase inhibitor resistant MCF7 and T47D cells remained sensitive to palbociclib as a single agent (**Figure 36B**), exhibiting IC50 values for palbociclib comparable to that of the parental cells (**Figure 36C**). Further, palbociclib treatment of the letrozole and anastrozole resistant cells resulted in a dose-dependent growth inhibition similar to that observed in the MCF7 aromatase expressing parental cells (**Figure 36D**). Further, monodansylcadavarine (MDC) staining revealed induction of autophagy in response to palbociclib treatment in the letrozole and anastrozole resistant MCF7 cells (**Figure 36E**). Therefore, similar to the MCF7 parental cells, the aromatase resistant (letrozole or anastrozole) were highly responsive to the combination of palbociclib and autophagy inhibition, resulting in an irreversible and sustained growth inhibition even with low and on-target doses of palbociclib (**Figure 36F**).

Thus, these results show that the aromatase inhibitor resistant cells remain sensitive to CDK4/6 inhibition and highlights the clinical utility of the drug combination in the aromatase inhibitor resistance setting.

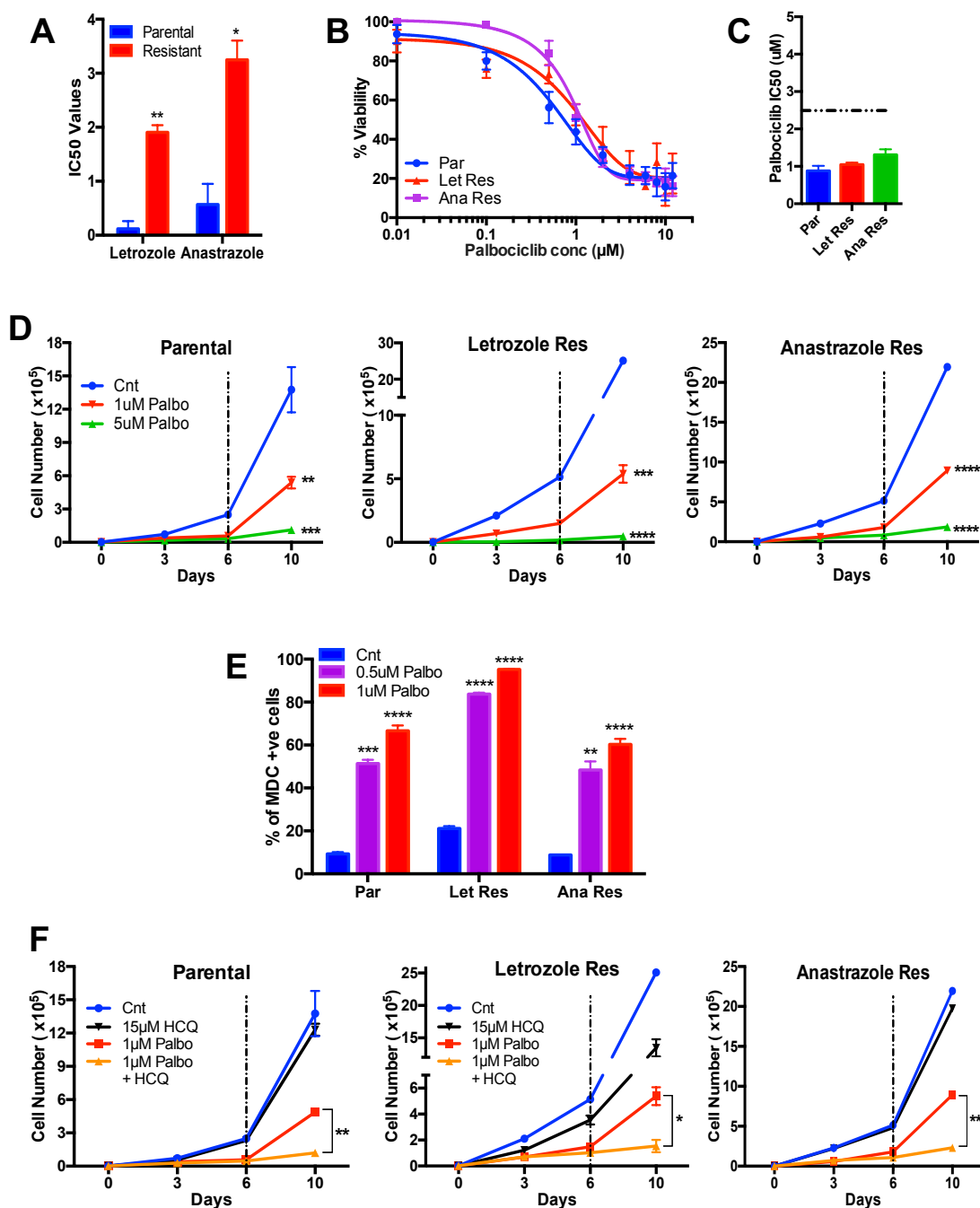


Figure 36: Synergy between CDK4/6 and autophagy inhibitors in aromatase inhibitor resistant cells: A) Half-maximal inhibitory concentration (IC₅₀) values of letrozole and anastrozole in parental vs letrozole or anastrozole resistant cells respectively. B, C) Dose-response studies (B) in MCF7 parental, letrozole and anastrozole resistant cells by treating with varying concentrations of palbociclib for 6 days and recovery for 6 days, and their corresponding IC₅₀ values (C). MCF7 parental and letrozole or anastrozole resistant cells were treated with varying concentrations of palbociclib (Palbo) for 6 days with recovery for 4 days and subjected to D) cell counting to assess cell proliferation, E) flow cytometry to quantify monodansylcadavarine (MDC) staining, a marker of autophagic vesicles and F) cell counting to measure growth inhibition combination with 15μM hydroxychloroquine (HCQ) for 6 days. All data represent mean ± SD from three independent experiments; ns: p>0.05; *p<0.05; **p<0.01; ***p<0.001; ****p<0.0001.

5.2.7. SYNERGY BETWEEN PALBOCICLIB AND AUTOPHAGY INHIBITION BY HCQ *IN VIVO*

Having shown the synergy between CDK4/6 and autophagy inhibitor *in vitro*, we interrogated if concomitant treatment of mice with an autophagy inhibitor and low dose palbociclib can mediate a synergistic response. Previously, we showed that palbociclib induces autophagy with an intact flux at 25mg/kg (Figure 20), which provided the optimal dose of palbociclib for the combination study. To this end, MCF-7T cells were injected into the mammary fat pad of nude mice, once the tumors grew to an average size of 250mm³, we randomized them into 4 treatment arms: (i) vehicle, (ii) hydroxychloroquine (60mg/kg), (iii) low dose palbociclib (25mg/kg/day) and (iv) HCQ + palbociclib (25mg/kg/day). Mice were treated for 21 days (treatment phase) and maintained for an additional 21 days without treatment (recovery phase) to examine the ability of the drug treatment to induce a sustained tumor growth inhibition (**Figure 37A**).

Results revealed that mice treated with combination of low dose palbociclib and HCQ had significantly decreased tumor volume at the end of treatment, compared to single drug or vehicle arms (**Figure 37B-D** – at the end of 21-day treatment phase). More strikingly, the tumor volumes in the HCQ + palbociclib combination arm did not increase even after the treatment was stopped, while the tumor volumes in the palbociclib alone arm readily increased during the end of the treatment phase and during the recovery phases of the experiment (**Figure 37B-D** – at the end of the treatment + recovery phase). A concomitant decrease in tumor weight was observed with the palbociclib + HCQ combination arm both at the end of the treatment and the treatment + recovery phases compared to the vehicle or the single treatment controls. These results suggest that co-treatment with HCQ enabled the induction of a sustained tumor growth inhibition even at a low dose (25mg/kg) of palbociclib, which is one-fifth the dose of palbociclib (150mg/kg) used in most preclinical studies (Fry, Harvey et al. 2004, Michaud, Solomon et al. 2010, Wardell, Ellis et al. 2015).

To illustrate the induction of a cell cycle arrest and senescence at the end of the 21 day treatment phase, we examined the protein levels of cell cycle proteins Rb and pRb via western blot analysis, which showed that combination treated led to a more significant decrease in both Rb and pRb compared to treatment with palbociclib alone (**Figure 38A**). Additionally, RPPA analysis of tumors post 3 weeks of treatment demonstrated a significant enrichment for the senescence and growth inhibition related proteins and a significant decrease in cell cycle related proteins in the combination treatment arm, when compared to no treatment arms and palbociclib alone arm (**Figure 38B,C**). As a proof of autophagy inhibition with the palbociclib + HCQ combination arm, western blot analysis showed impaired autophagic flux as indicated by increased LC3B-II levels and no decrease in p62, when compared to palbociclib alone arm, which confirmed the induction of autophagy with 21 days treatment with palbociclib (**Figure 38A**).

Further, immunohistochemistry (IHC) analysis showed that combination treatment with palbociclib and HCQ significantly increased SA- β gal activity (marker of senescence) and decreased expression of BrdU (a proliferation marker) at the end of the 21 day treatment period and following the 21 day recovery phase, while the vehicle and HCQ arms showed no change in BrdU or SA- β gal staining (**Figures 39A,B**). The palbociclib alone arm, on the other hand, showed an increase in SA- β gal and decrease in BrdU staining only at the end of the 21 treatment period, while these levels increased at the end of the recovery phase, demonstrating that palbociclib only induces a reversible tumor growth inhibition as a single agent (**Figures 39A,B**). Moreover, palbociclib + HCQ *in vivo* treatment resulted in significantly higher ROS levels (measured by IHC by 8-OHdG and 4-HNE staining) at the end of both treatment and recovery phases compared to the vehicle and HCQ treatment, while palbociclib alone treatment arm exhibited a moderate increase in ROS levels only at the end of the treatment phase (**Figures 39A,C,D**).

Lastly, we examined the tolerability and the toxicity of the drug treatments in mice by examining the changes in body weight and complete blood counts (given the induction of neutropenia and leukopenia in patients) at the end of the treatment and treatment + recovery phases. Measurement of mice weight every day during the 21-day treatment phase showed no significant changes in body weight in any of the treatment arms including the combination arm (**Figure 40A**). Additionally, analysis of the complete blood count profile revealed no significant changes in WBC, RBC, platelet, Neutrophils. RBC and WBC differential count in any of the treatment arms (including combination treatment), at the end of the treatment and treatment + recovery phases (**Figures 40B-D**). These results suggest that the administered drug treatments, including the combination of HCQ and low dose palbociclib, were well tolerated by the mice at both time intervals assessed (treatment and treatment + recovery).

Collectively, these results suggest that autophagy inhibition (via HCQ) synergizes with low doses of palbociclib to induce an irreversible tumor growth inhibition in mice xenograft tumors *in vivo*.

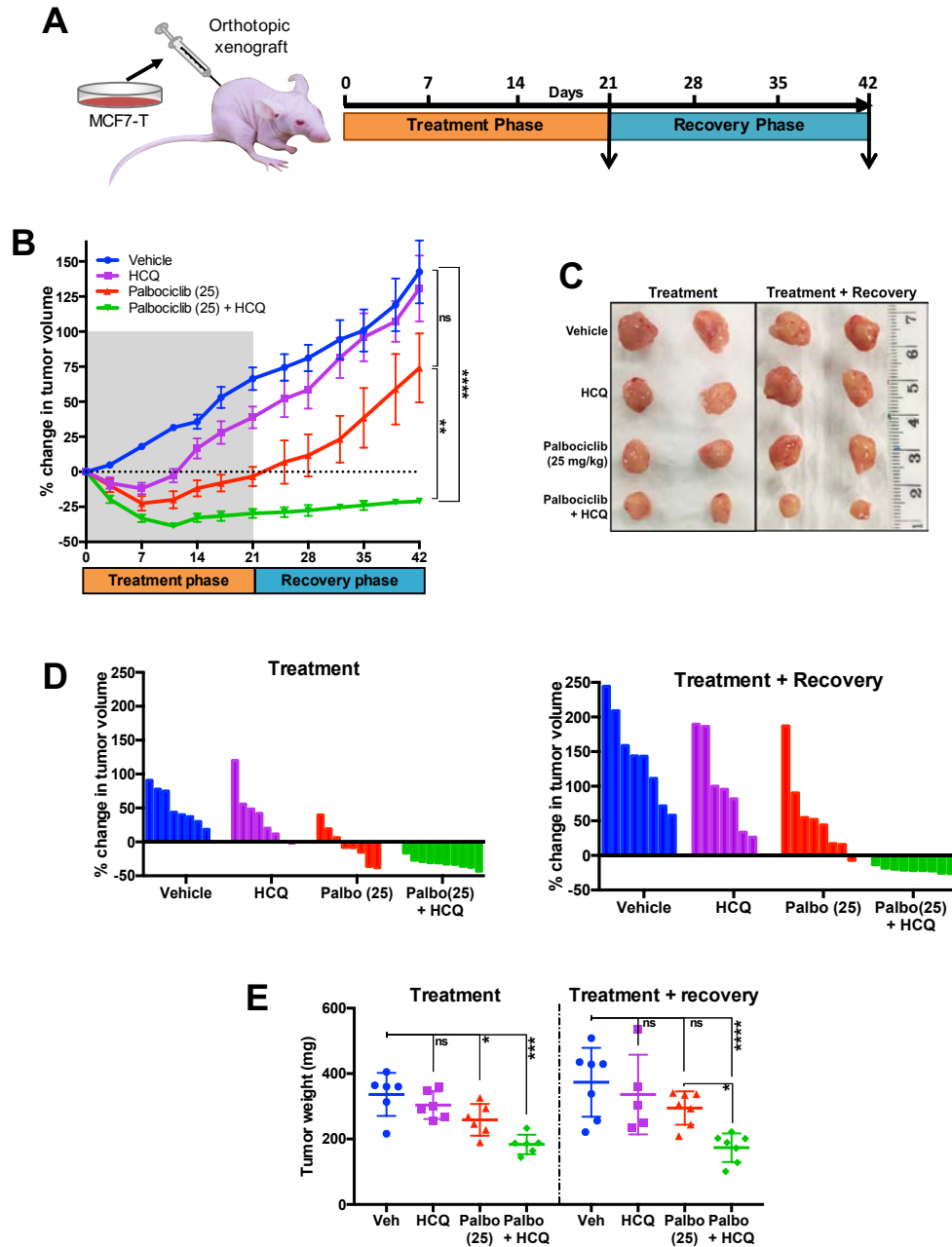


Figure 37: Synergy between palbociclib and autophagy inhibition by HCQ in vivo: A) Schematic showing treatment schedule of orthotopic MCF7-T xenograft mice with vehicle (veh; 0.5% methylcellulose and PBS), 60 mg/kg hydroxychloroquine (HCQ), 25 mg/kg palbociclib (Palbo); or combination of palbociclib (25mg/kg) and hydroxychloroquine (60mg/kg) for 21 days (treatment phase), followed by a recovery phase of 21 days without treatment. B,D) Percentage change in mean (B) or individual (D) tumor volumes (normalized to Day 0) upon treatment as described in A at the end of treatment and treatment + recovery phases. C) Representative images of tumors harvested at the end of the treatment phase and at the end of the recovery phase. E) Tumor weights measured at the end of treatment phase and treatment + recovery phase (n=6 mice/treatment group). All data represent mean \pm SD; p-values were calculated in comparison to mice treated with vehicle (Control) unless indicated. ns:p>0.05; *p<0.05; **p<0.01; ***p<0.001; ****p<0.0001.

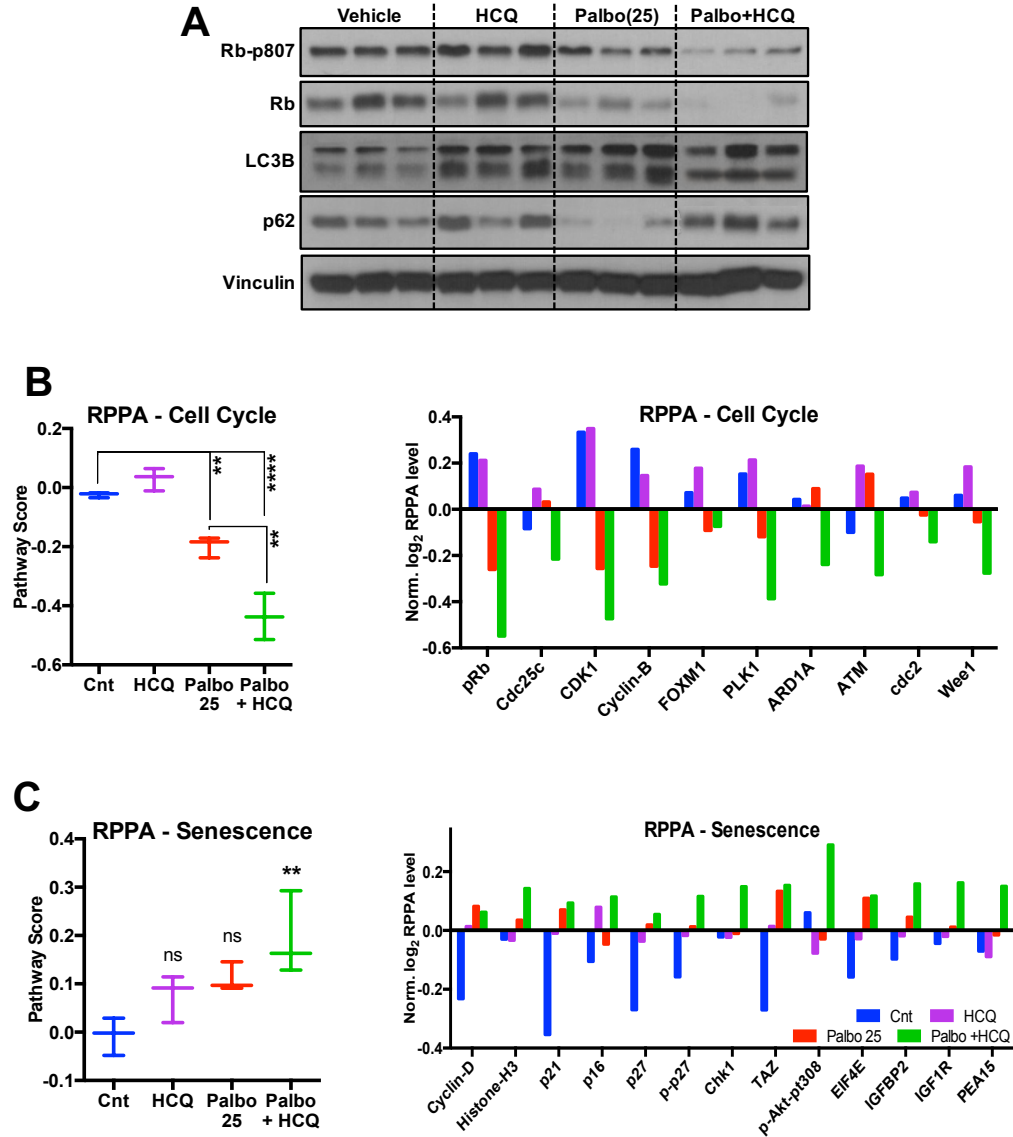


Figure 38: Impact of palbociclib and autophagy inhibition on cell cycle, senescence and autophagy in vivo: A) Western blot analysis of tumors harvested post treatment with vehicle (Cnt), 60 mg/kg hydroxychloroquine (HCQ), 25 mg/kg palbociclib (Palbo) or combination of palbociclib (25mg/kg) and hydroxychloroquine (60mg/kg) for 21 days to measure expression of cell cycle (phospho-Rb, Rb) and autophagy (LC3B, p62) proteins. B,C) Pathway score and expression (normalized log₂ expression level) of individual proteins belonging to the cell cycle (n=10 proteins) and senescence pathways (n=13 proteins) determined from RPPA analysis of tumors harvested after treatment as described in A. All data represent mean \pm SD; p-values were calculated in comparison to mice treated with vehicle (Control) unless indicated. ns:p>0.05; *p<0.05; **p<0.01; ***p<0.001; ****p<0.0001.

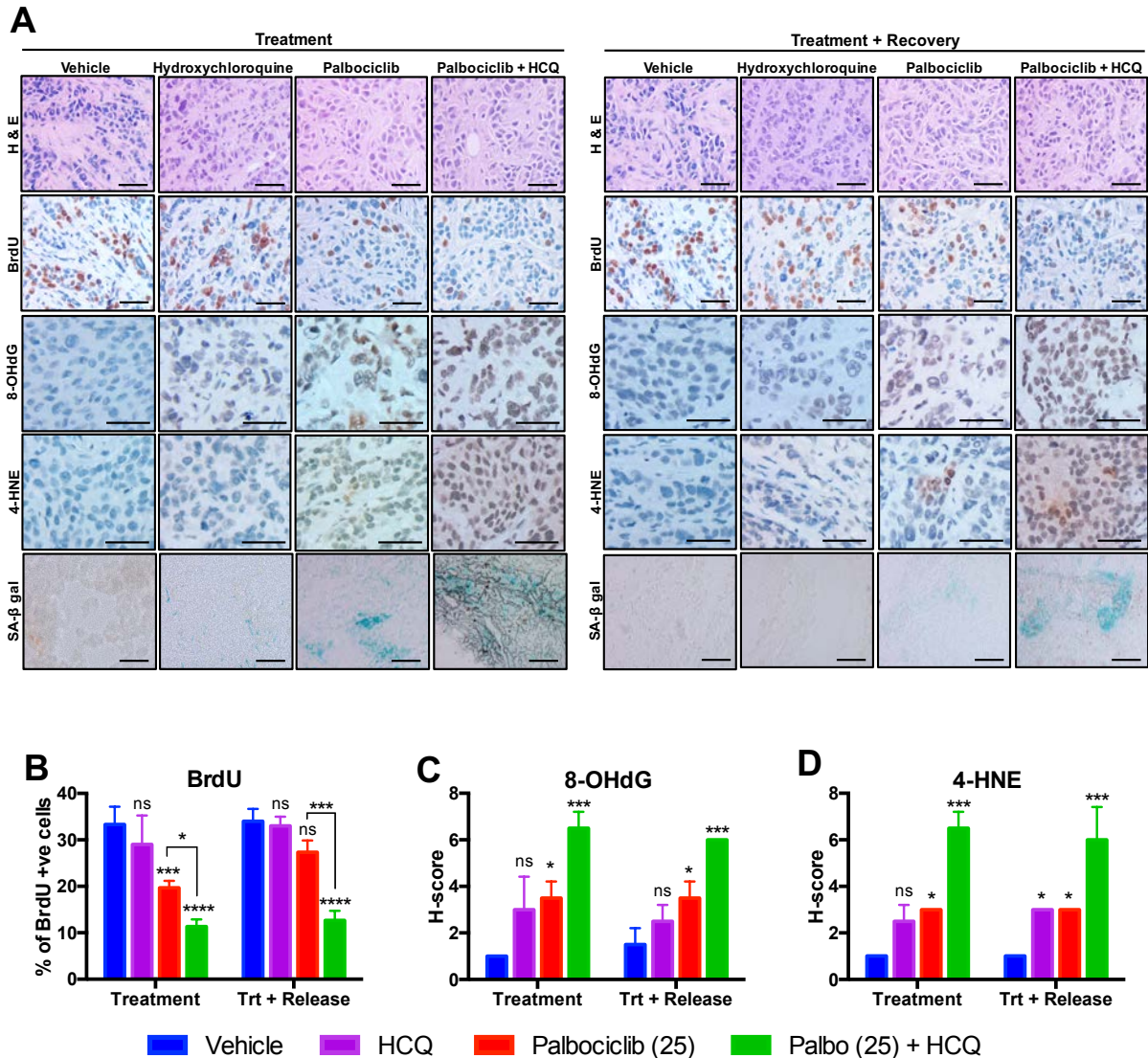


Figure 39: Impact of palbociclib and autophagy inhibition on growth, senescence and ROS in vivo: A) Representative images of hematoxylin and eosin (H&E), BrdU, 8-hydroxydeoxy-guanosine (8-OHdG), 4-hydroxynonenal (4-HNE) and senescence-associated SA-β gal immunohistochemical staining on tumor tissues harvested at the end of the 21 days treatment with vehicle, 60 mg/kg hydroxychloroquine (HCQ), 25 mg/kg palbociclib (Palbo) or combination of palbociclib and HCQ, or post 21 days of recovery in the absence of drug. Scale bars equal 50 μm. B) Quantification of BrdU positive cells or H-score of 8-OHdG and 4-HNE staining on tumors harvested at the end of treatment phase and treatment + recovery phase. All data represent mean±SD; p-values were calculated in comparison to mice treated with vehicle (Control) unless indicated. ns:p>0.05; *p<0.05; **p<0.01; ***p<0.001; ****p<0.0001.

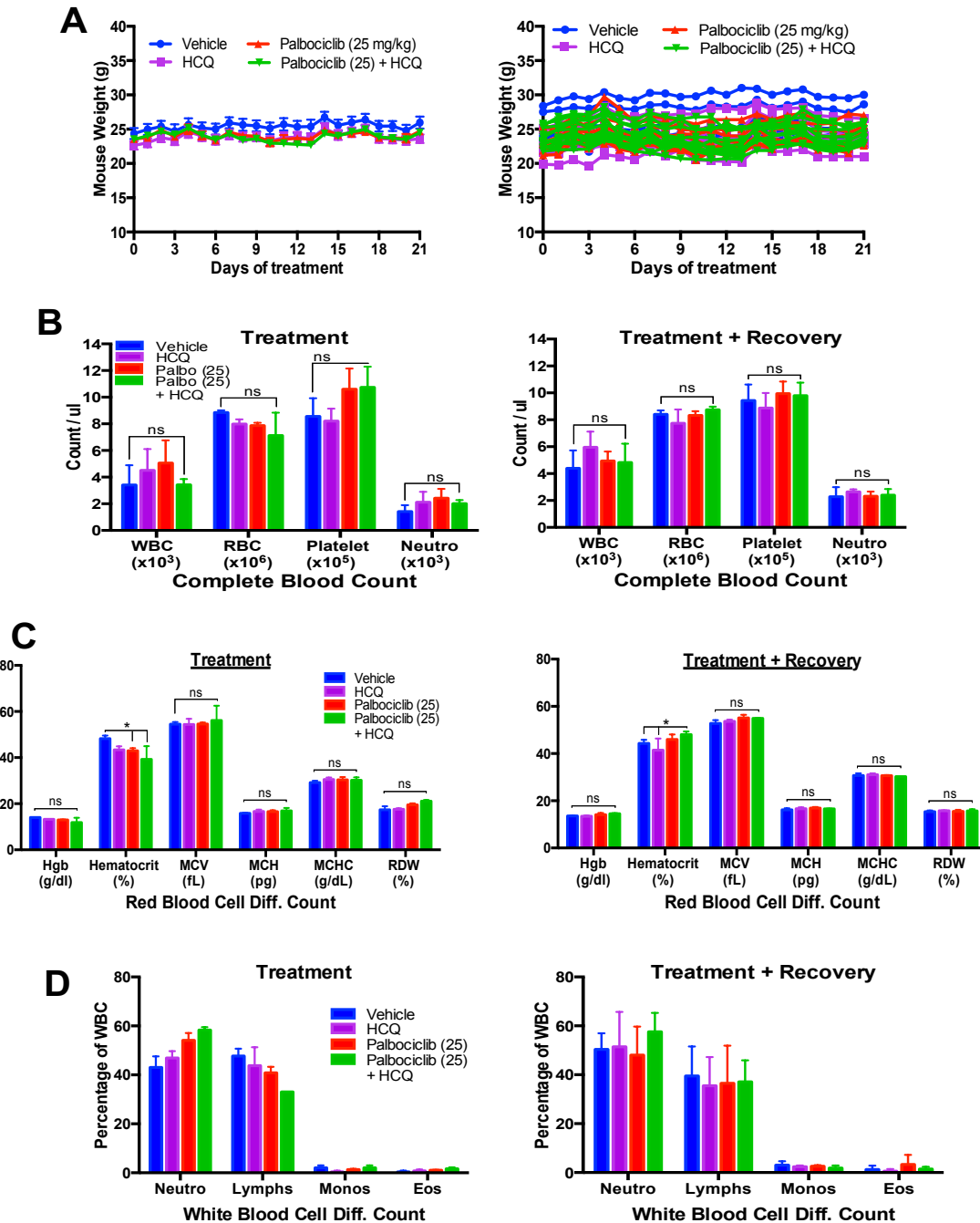


Figure 40: Toxicity profile of palbociclib and autophagy inhibitor treatment in vivo:

A) Mean mouse weight and Weight of individual mice upon 21 days treatment with vehicle, 60 mg/kg hydroxychloroquine (HCQ), 25 mg/kg palbociclib (Palbo) or combination of palbociclib and HCQ. Mice were treated for 21 days as described in A and blood samples collected at the end of treatment phase and at the end of the treatment + recovery phase (21 days post treatment) and subjected to B) complete blood counts (red blood cells [RBC], white blood cells [WBC], platelets, and neutrophils [Neutro]), C) RBC differential counts and D) WBC differential count. All data represent mean \pm SD; p-values were calculated in comparison to mice treated with vehicle (Control) unless indicated. ns: $p > 0.05$; * $p < 0.05$; ** $p < 0.01$; *** $p < 0.001$; **** $p < 0.0001$.

5.2.8. SYNERGY BETWEEN PALBOCICLIB AND AUTOPHAGY INHIBITION (LYS-05) *IN VIVO*

Having showing the *in vivo* synergy between CDK4/6 and autophagy inhibition via HCQ, we wanted to further confirm the synergy of the combination *in vivo* using another autophagy inhibitor, Lys05, a more potent inhibitor of autophagy compared to HCQ (McAfee, Zhang et al. 2012). To first examine the toxicity profile of Lys-05 as a single agent, non-tumor bearing mice were treated with varying concentrations of Lys-05 (1mg/kg, 5mg/kg, 10mg/kg or 20mg/kg) every day for 21 days and the mouse weight and their blood count were analyzed to examine toxicity. Results show that treatment with different doses of Lys-05 had no deleterious effect on mouse weight over the 21-day treatment period (**Figure 41A**). Similarly, there was no difference in the complete blood counts, RBC and WBC differential counts upon treatment with the varying concentrations of Lys-05 (**Figures 41B-D**).

Next, xenograft tumor-bearing mice (established by mammary fat pad injection of MCF7T cells and tumors were allowed to reach an average of 200mm³) were treated with vehicle, 10mg/kg/day Lys05 (chosen based on previous studies showing autophagy inhibition at this dose), 25mg/kg/day palbociclib or the combination of palbociclib and Lys05 for 21 days (treatment phase) with a recovery phase of 14 days. Treatment with the combination of palbociclib + Lys05 significantly decreased tumor volume during both the treatment and recovery phases, compared to no treatment (vehicle) or treatment with Lys-05 or palbociclib as a single agent (**Figures 42A,B**). Further, combination treatment with palbociclib + Lys-05 resulted in significantly smaller tumors (**Figure 42D**) with lesser tumor weight (**Figure 42C**), compared vehicle or single treatment controls. Treatment with the combination of palbociclib and Lys-05 also resulted in prolonged mouse survival, with none of the mouse tumors reaching 1000mm³, compared to the other treatment arms, whose tumors grew to above 1000mm³ and had to be sacrificed prior to the end of the experiment at 35 days (**Figure 42E**).

Collectively, these results demonstrate that autophagy inhibition mediated by an alternative inhibitor, Lys-05 also synergizes with low doses of palbociclib to induce irreversible tumor growth inhibition *in vivo*.

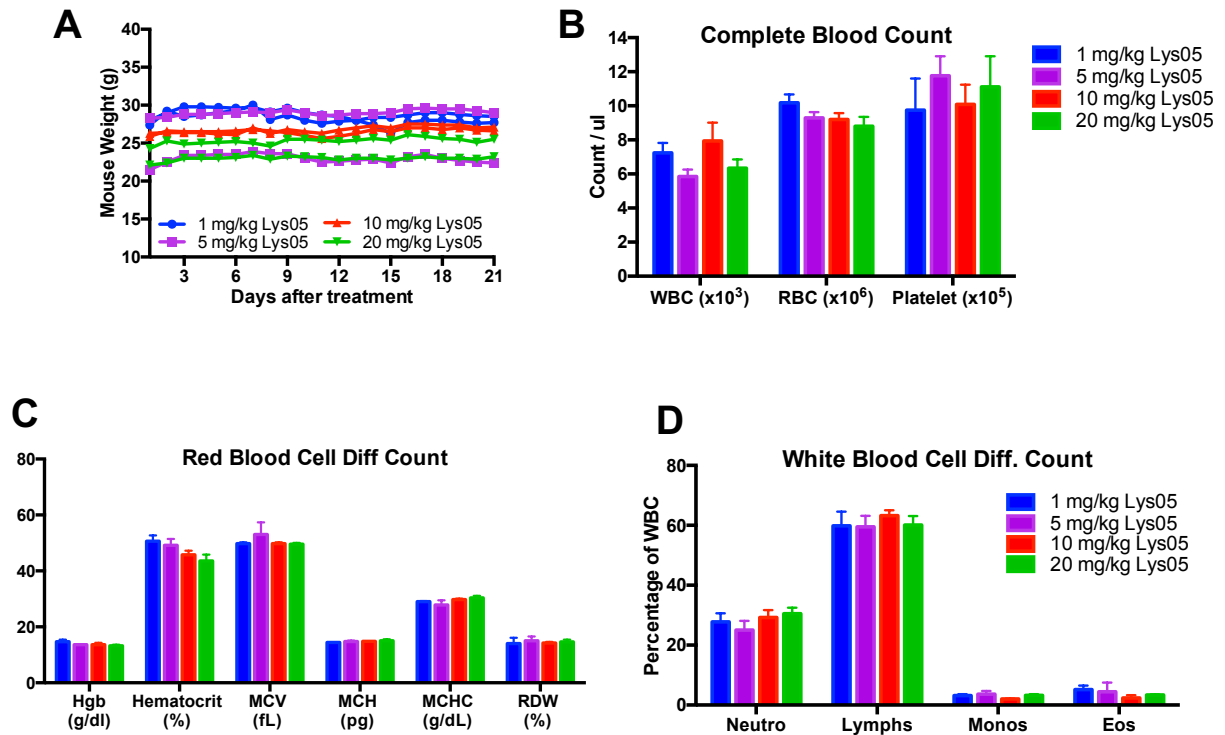


Figure 41: Toxicity profile of Lys-05 in vivo: A) Weight of individual non-tumor bearing mice treated with varying concentrations of Lys-05 daily for 21 days via I.P (n=2 mice/treatment group). Mice were treated for 21 days as described in A and blood samples were collected at the end of treatment and subjected to B) complete blood counts (red blood cells [RBC], white blood cells [WBC], platelets, C) RBC differential counts and D) WBC differential count. All data represent mean \pm SD; p-values were calculated in comparison to mice treated with vehicle (Control) unless indicated. ns:p>0.05; *p<0.05; **p<0.01; ***p<0.001; ****p<0.0001.

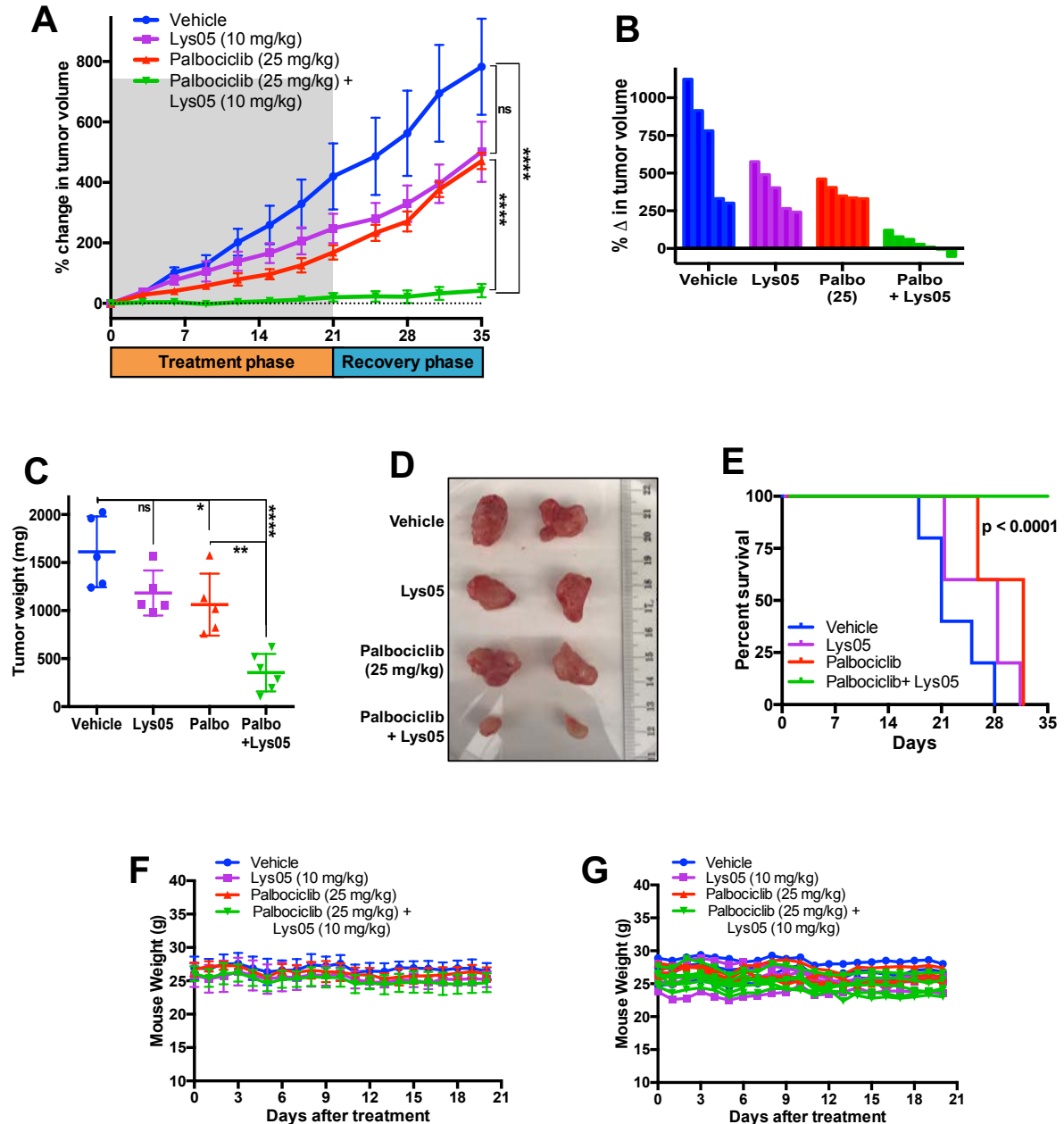


Figure 42: Synergism between palbociclib and Lys-05 mediated autophagy inhibition in vivo: A,B) Percentage change in mean (A) or individual (B) tumor volumes (normalized to Day 0) upon treatment with Vehicle, 5mg/kg palbociclib, 10mg/kg Lys-05 or combination of palbociclib and Lys-05 daily for 21 days (treatment phase) and recovery phase of 14 days. Data represented as Mean \pm SEM. $n \geq 5$ for each group. C) Weights of tumors harvested after treatment and recovery as described in A. D) Representative pictures of tumors harvested after 21 days treatment and 14 days recovery. E) Kaplan Meier survival curve with death and tumors exceeding 1000mm³ as endpoint upon treatment as in A. $n \geq 5$ for each group. F,G) Mean mouse weight (F) and weight of individual mice (G) during 21 days treatment phase. All data represent mean \pm SD; p-values were calculated in comparison to mice treated with vehicle (Control) unless indicated. ns: $p > 0.05$; * $p < 0.05$; ** $p < 0.01$; *** $p < 0.001$; **** $p < 0.0001$.

5.3. DISCUSSION

Collectively, studies in this chapter demonstrate that inhibition of autophagy significantly improves the efficacy of CDK4/6 inhibition and effectively induces a sustained growth inhibition and senescence *in vitro* and *in vivo*, even at low doses of palbociclib (**Figure 43**).

While research has shown opposing roles for autophagy – as a pro-survival and a pro-death mechanism, numerous recent studies have highlighted the importance of autophagy as a mediator of drug resistance, specifically in breast cancer (Chen, Jiang et al. 2013, Chittaranjan, Bortnik et al. 2014, Lefort, Joffre et al. 2014). These studies have shown an association between high expression of autophagy proteins like LC3B and tumor aggressiveness, providing strong rationale for using autophagy inhibitors to combat drug resistance. Further, while previous studies with the CDK4/6 inhibitor palbociclib, suggested a potential induction of autophagy with drug treatment (Capparelli, Chiavarina et al. 2012), the role of the autophagy induction was not examined. Hence this chapter provides a detailed analysis of drug induced autophagy performed by downregulating autophagy genes Atg-5 and Beclin-1 and using numerous pharmacological inhibitors of autophagy to show that targeting autophagy significantly improves the efficacy of palbociclib treatment.

A potential issue with the molecular ablation of autophagy via Beclin-1 knockdown might arise from the fact that Beclin-1 has been shown to have autophagic independent functions in cancer (Rohatgi and Shaw 2016). Recent study shows that apart from its role in autophagy, Beclin-1 can also regulate growth factor signaling pathways such as Pi3K (Rohatgi and Shaw 2016). However, we observed similar results with both Atg5 and Beclin1 knockdown, which would eliminate the possibility of autophagy independent functions of Beclin1 playing a role in this scenario. Another issue that might be of concern is the specificity of the autophagy inhibiting drugs utilized in the study. To address this, we employed 5 different autophagy drugs *in vitro*, which target the pathway at multiple sites (Autophagosome initiation - Spautin-1;

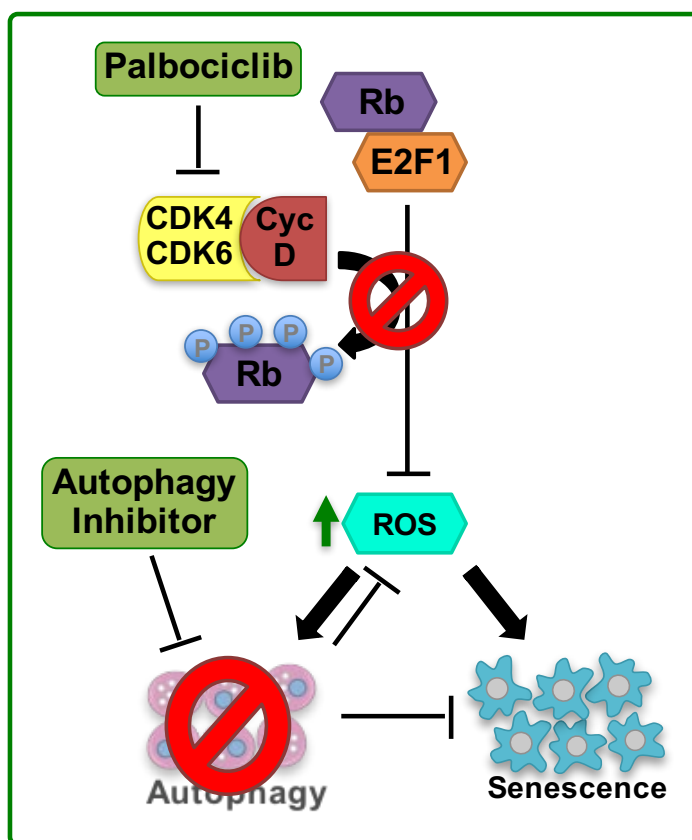


Figure 43: Working Model: Schematic showing the synergistic effect between CDK4/6 and autophagy inhibitors in ER+ve breast cancer cells in vitro and in vivo resulting in senescence.

lysosome fusion – CQ, HCQ, Lys-05 and Baf-A1 (Wang, Hu et al. 2016)), all which yielded similar results. We even performed *in vivo* xenograft studies with two different autophagy inhibitors, HCQ and Lys-05, both of which showed a similar synergistic effect between CDK4/6 and autophagy inhibition.

Further, the *in vivo* drug dose used for palbociclib in most preclinical studies is 150 mg/kg, which translates to plasma concentration of 7.7uM, significantly higher than the clinically achievable dose of 3.4 μ M (Pfizer-Inc-and-Affiliates 2011). Our study with the combination of CDK4/6 and autophagy inhibition was able to reduce the dose of palbociclib to one-fifth the dose - 25mg/kg (1.4uM plasma concentration and corresponds to low and on-target dose used in cell lines), and still achieve significance tumor inhibition. Thus, the combination treatment

strategy that we have identified in this study (palbociclib + HCQ) has the potential to significantly improve palbociclib efficacy, while lowering toxicity mediated by palbociclib.

CHAPTER 6: BIOMARKER IDENTIFICATION FOR PALBOCICLIB AND ITS COMBINATION WITH AUTOPHAGY INHIBITOR IN ER+ BREAST CANCER

6.1. INTRODUCTION

6.1.1. RB PROTEIN IN BREAST CANCER

The retinoblastoma (Rb) protein is a major regulator of the G1/S checkpoint of the cell cycle and consists of two family members, the Rb-like proteins, p107 and p130 (Weinberg 1995). These proteins, known as pocket proteins, bind to the transcription factor, E2F, keeping it in its inactive state and preventing transcription of E2F target genes (Weinberg 1995). Thus, Rb serves as a molecular determinant as to whether the cells would pass through the G1/S checkpoint and a tumor suppressor (Giacinti and Giordano 2006). Given its tumor suppressive function, Rb is often inactivated in cancers, via mutations or partial deletions among other mechanism (Giacinti and Giordano 2006). In breast cancer, the inactivation of the Rb pathway occurs by loss of heterozygosity of the Rb gene, seen in about 20 to 30% of breast cancers, or due to other mutually exclusive mechanisms that affect the Rb pathway (Ertel, Dean et al. 2010). This includes amplification of the cyclin D genes (CCND1) seen in over 50% of breast cancers, which results in aberrant phosphorylation and inactivation of Rb (Arnold and Papanikolaou 2005). Further, inactivation of the CKI, p16 (CDKN2A) also contributes to the deregulation and silencing of Rb (Dublin, Patel et al. 1998). A recent study showed that in ER positive breast cancer cells, knockdown of Rb makes the cells resistant to the anti-proliferative action of tamoxifen *in vitro* and the anti-tumor effect of the drug *in vivo*, establishing a link between deregulation of Rb and endocrine resistance (Bosco, Wang et al. 2007). This was verified by an analysis of tumor tissues from post-menopausal breast cancer patients treated with tamoxifen. Which showed that deregulation of Rb correlated with high Ki67 staining, an indication that there tumors were resistant to tamoxifen treatment (Lehn, Ferno et al. 2011).

6.1.2. CYCLIN E AND LMWE IN BREAST CANCER

Cyclin E, when bound to CDK2, phosphorylates Rb and is a key regulator of cellular progression through the G1/S checkpoint (Sherr 1994). Cyclin E is overexpressed (independent of subtype) and amplified (MDA-MB-157 cell line) in breast cancer cell lines when compared to normal mammary epithelial cells (Keyomarsi and Pardee 1993). Amplification or overexpression of cyclin E in breast cancer mediates resistance to trastuzumab and endocrine therapy, and is a predictor of poor prognosis in these patients (Keyomarsi, Tucker et al. 2002, Scaltriti, Eichhorn et al. 2011, Caldon, Sergio et al. 2012).

Moreover, post-translational modification (proteolytic cleavage) of the full length cyclin E by the serine protease, elastase, generates a more oncogenic form of the protein termed as Low Molecular Weight isoforms of cyclin-E (LMWE) (Keyomarsi, Conte et al. 1995, Wang, Rosales et al. 2003). Cleavage of full length cyclin E generates four isoforms of the protein, comprising of two doublets, EL2 and EL3, which are collectively called as Trunk 1 (T1), and EL5 and EL6, collectively called as Trunk 2 (T2) (**Figure 44**) (Mull, Cox et al. 2009). LMWE, which was originally discovered in breast cancer by our laboratory, and subsequently by others (Taneja, Maglic et al. 2010, Tokai, Maeda et al. 2011, Mombelli, Cochaud et al. 2015, Montazeri, Bouzari et al. 2015), has recently been the subject of a number of review articles (Loeb and Chen 2012, Moore 2013, Rath and Senapati 2014). These isoforms are also found in ovarian (Bedrosian, Lu et al. 2004, Davidson, Skrede et al. 2007), melanoma (Bales, Mills et al. 2005), colorectal (Corin, Di Giacomo et al. 2006, Milne, Carvalho et al. 2008, Corin, Larsson et al. 2010, Zhou, Xie et al. 2011), lung (Koutsami, Tsantoulis et al. 2006), and renal cell carcinomas (Nauman, Turowska et al. 2007). Numerous studies have been conducted to elucidate the biological role of LMWE. Studies show that while both full length and low forms of cyclin E can bind to and activate CDK2 kinase activity, the LMWE isoforms are able to bind stronger to CDK2 and exhibit increases kinase activity (Harwell, Mull et al. 2004).



Figure 44: Low molecular weight isoforms of cyclin E (LMWE): Schematic showing how elastase generates LMWE by cleaving the full length cyclin E protein at two sites

This was detected in both breast cancer cell lines and human tumor tissue samples. (Harwell, Mull et al. 2004). This results hyperphosphorylation of Rb, which makes the LMWE resistant tumors resistant to inhibition by the endogenous CKIs, p21 and p27 (Akli, Zheng et al. 2004). Moreover, this makes the cell or tumors resistant to anti-estrogens, induce higher genomic instability and mediate resistance to fulvestrant and letrozole (Harwell, Porter et al. 2000, Akli, Zheng et al. 2004, Wingate, Puskas et al. 2009, Akli, Bui et al. 2010). To further understand the significance of LMWE in breast cancer, transgenic animal models with EL and LMWE under the MMTV promoter were generated, which showed that LMWE transgene expressing mice had increased mammary tumorigenesis compared to full length (EL) transgene (Akli, Van Pelt et al. 2007). Further, introduction of LMWE in HMEC cells lines resulted in increased ability of these cell to form tumors in nude mice compared to EL expressing cells (Duong, Akli et al. 2013). Cells overexpressing LMWE were also shown to have enrichment of the of EMT phenotype and increased expression of breast cancer stem cells (CD44^{high}/CD24^{low} subpopulation of cells) compared to full length (EL) expressing cells (Duong, Akli et al. 2013).

Our laboratory also reported an analysis of 395 patients with breast cancer in which it was demonstrated that overexpression of LMWE, as measured by Western blot analysis, is associated with distant metastases and reduced overall survival (Keyomarsi, Tucker et al.

2002). Subsequently, our laboratory discovered that LMW-E, which now lacks its N-terminus nuclear localization signal is now localized predominantly in the cytoplasm, where it binds to CDK2 and has greater kinase activity than full-length cyclin E (Delk, Hunt et al. 2009). This finding was further verified by a recent study in 1676 breast cancer patients revealed that 40% of all breast cancer patients exclusively expressed the cytoplasmic form of cyclin E (Delk, Hunt et al. 2009). This finding was further verified by a recent study in 1676 breast cancer patients revealed that 40% of all breast cancer patients exclusively expressed the cytoplasmic form of cyclin E, with majority of these patients (85.1%) also expressing for cytoplasmic p-CDK2 (Karakas, Biernacka et al. 2016). More importantly, this study also showed that cytoplasmic expression of cyclin-E (LMWE expression) is strongly associated with higher histologic tumor grade and worse prognosis compared to other patients, demonstrating the utility of LMWE or cytoplasmic cyclin E as a reliable prognostic indicator in breast cancer (Karakas, Biernacka et al. 2016), which can be functionally attributed the overexpression and mislocalization (to the cytoplasm) of these proteins.

6.1.3. PRE-CLINICAL BIOMARKER STUDIES FOR PALBOCICLIB IN BREAST CANCER

Identification of a reliable biomarker that can predict response is necessary for all targeted therapy, to improve the selectivity and the efficacy of the drug treatment. Hence, numerous pre-clinical studies in breast and other cancers have been carried out to identify reliable predictive biomarkers of response for CDK4/6 inhibitors such as palbociclib (Asghar, Witkiewicz et al. 2015). Multiple studies have shown that an intact Rb pathway is required for the CDK4/6 inhibitor mediated cell cycle arrest and senescence and hence proteins belonging to the Rb pathway proteins such as Rb, cyclin D, p16 and cyclin E have been identified as biomarkers *in vitro* (Wiedemeyer, Dunn et al. 2010, Konecny, Winterhoff et al. 2011, Cen, Carlson et al. 2012). A study examined palbociclib treatment in a range of breast cancer cells and analyzed the gene expression profile of sensitive cell lines in comparison with resistant

cells (Finn, Dering et al. 2009). Results revealed that the sensitive cells had significantly higher expression of cyclin D1, Rb1 and lower expression levels of p16 compared to the resistant cells (Finn, Dering et al. 2009). Further, studies in glioblastoma and ovarian cancer cell lines and xenografts showed that the presence of Rb and loss of p16 dictate response to palbociclib (Konecny, Winterhoff et al. 2011, Cen, Carlson et al. 2012). Moreover, a study in ovarian cancer shows that expression of cyclin E mediates resistance to palbociclib treatment and can hence serve as a biomarker (Taylor-Harding, Aspuria et al. 2015). Additionally, a recent study with palbociclib in breast cancer showed that development of early adaptation (intrinsic resistance) and acquired resistance to palbociclib is characterized by Rb loss and cyclin E (CCNE1) amplification (Herrera-Abreu, Palafox et al. 2016). This study also showed the resistant cells failed to decrease phosphor-Rb upon treatment with palbociclib (Herrera-Abreu, Palafox et al. 2016). Finally, studies with abemaciclib show that the presence of estrogen receptor (ER) and Rb can predict response to abemaciclib (Patnaik, Rosen et al. 2016). Unfortunately, while numerous biomarkers have been suggested based on pre-clinical studies, none have been effective in predicting CDK4/6 inhibitor response in the clinic and this will be discussed in detail in the next chapter.

6.1.4. GAP IN KNOWLEDGE

While previous pre-clinical studies have suggested biomarkers for CDK4/6 inhibition, this was shown to be ineffective in the clinic, highlighting the need for more clinical relevant biomarkers. Thus, the following questions remain:

1. What is the importance of the G1/S checkpoint in response to CDK4/6 inhibitors?
2. Which proteins within the G1/S checkpoint have the best prediction value for palbociclib response?
3. Is p53 required for response to palbociclib in ER positive breast cancer?
4. Is Rb required and sufficient to predict sensitivity to palbociclib?

5. Can cyclin E and its low molecular weight isoforms mediate resistance to palbociclib?
6. Can the status of G1/S checkpoint proteins (Rb and LMWE) be utilized to predict sensitivity to the combination of palbociclib and autophagy inhibitors?
7. Can the status of Rb and LMWE be utilized to predict sensitivity to the triple combination of palbociclib, aromatase inhibitor and autophagy inhibitor?

Thus, experiments in this chapter are aimed at directly addressing these gaps in knowledge.

6.2. RESULTS

6.2.1. GENE SET ENRICHMENT ANALYSIS TO IDENTIFY BIOMARKERS FOR PALBOCICLIB IN BREAST CANCER

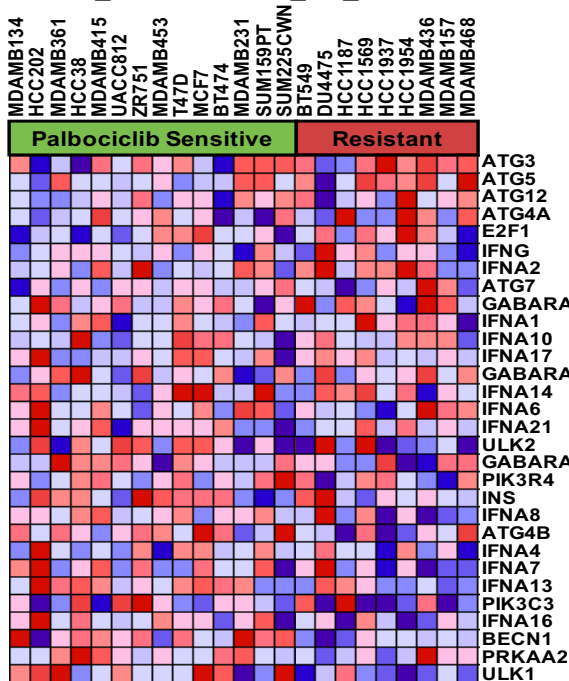
To identify biomarker(s) of response to palbociclib as a single agent and the combination of palbociclib and HCQ combination, we examined the gene expression of cell lines known to be sensitive or resistant to palbociclib (Finn, Dering et al. 2009), focusing on the cell cycle and autophagy pathways. Gene set enrichment analysis (GSEA) of the Kegg_Regulation_of_Autophagy gene set showed no distinct gene expression signature between the palbociclib sensitive and the resistant cells (**Figure 45A**). This indicates that while breast cancer cells activate autophagy in response to palbociclib treatment, the basal expression of the autophagy genes in breast cancer cell lines may not be able to predict responsiveness of the cells to CDK4/6 inhibition.

Examination of the Biocarta_Cell_Cycle Pathway gene set via GSEA analysis produced a distinct gene expression signature between the palbociclib sensitive and resistant breast cancer cell lines (**Figure 45B**). Palbociclib sensitive cell lines exhibited low expression of CDKN2A / p16 and high expression of Cyclin-D1, which corroborates previous *in vitro* and pre-clinical studies with palbociclib in breast and other cancers (Konecny, Winterhoff et al. 2011, Cen, Carlson et al. 2012) (**Figure 45C** – highlighted in purple). Notably, a striking correlation was observed between sensitivity to palbociclib and the expression of both Rb and Cyclin-E; with the Palbociclib sensitive cell lines displaying high levels of Rb and low expression of Cyclin-E (**Figure 45C** - blue arrows).

These results led us to hypothesize that Cyclin-E expression in combination with Rb may serve as effective biomarkers to predict response to palbociclib as a single agent and the combination of CDK4/6 and autophagy inhibitors.

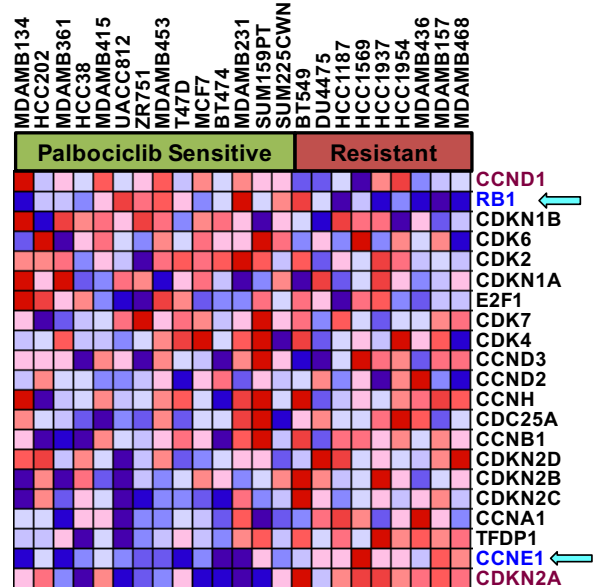
A

KEGG REGULATION OF AUTOPHAGY



B

BIOCARTA CELL CYCLE



C

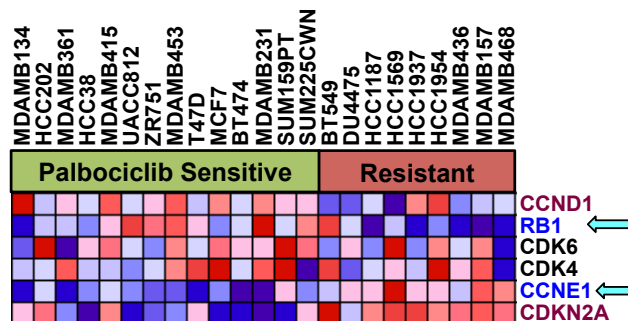


Figure 45: Gene set enrichment analysis to identify biomarkers for palbociclib in breast cancer: A,B) Heat map constructed using the Gene Set Enrichment Analysis (GSEA) program, denoting expression of genes from the KEGG Regulation of autophagy (A) and Biocarta Cell Cycle (B) gene sets in the indicated breast cancer cell lines, classified as being sensitive or resistant to palbociclib. C) Heat map denoting the top unregulated and downregulated genes within the Biocarta cell cycle gene set when comparing palbociclib sensitive and resistant cell lines

6.2.2. ROLE OF p53 IN DETERMINING RESPONSE TO PALBOCICLIB IN ER+ BREAST CANCER

p53 is a tumor suppressor gene that plays a key role in maintaining the integrity of the G1/S checkpoint and has been shown to be a predictor of palbociclib response in glioma (Barton, Misuraca et al. 2013). Given the status of p53 in the two ER positive cells lines utilized in this study (MCF7- WT p53; T47D- heterozygous p53 mutant), and their comparable sensitivity to palbociclib, we hypothesized that p53 may not play a role in predicting sensitivity to the CDK4/6 inhibitor in ER positive breast cancer.

To interrogate this, western blot analysis of the p53 pathway proteins (p53 and Mdm2) were performed, which revealed no alteration in their protein levels upon treatment with palbociclib for 6 days (**Figure 46A**). Further, p53 was downregulated in the MCF7 cell lines using two independent shRNAs (**Figures 46B,C**). shRNA mediated p53 knockdown did not alter the sensitivity of MCF7 cells to palbociclib (**Figure 46D**), with no significant change in IC50 values of palbociclib in MCF7 parental p53 knockdown cells (**Figures 46E,F**).

Thus, these results indicate that p53 does not play a significant role in mediating sensitivity to CDK4/6 inhibition in ER positive breast cancer.

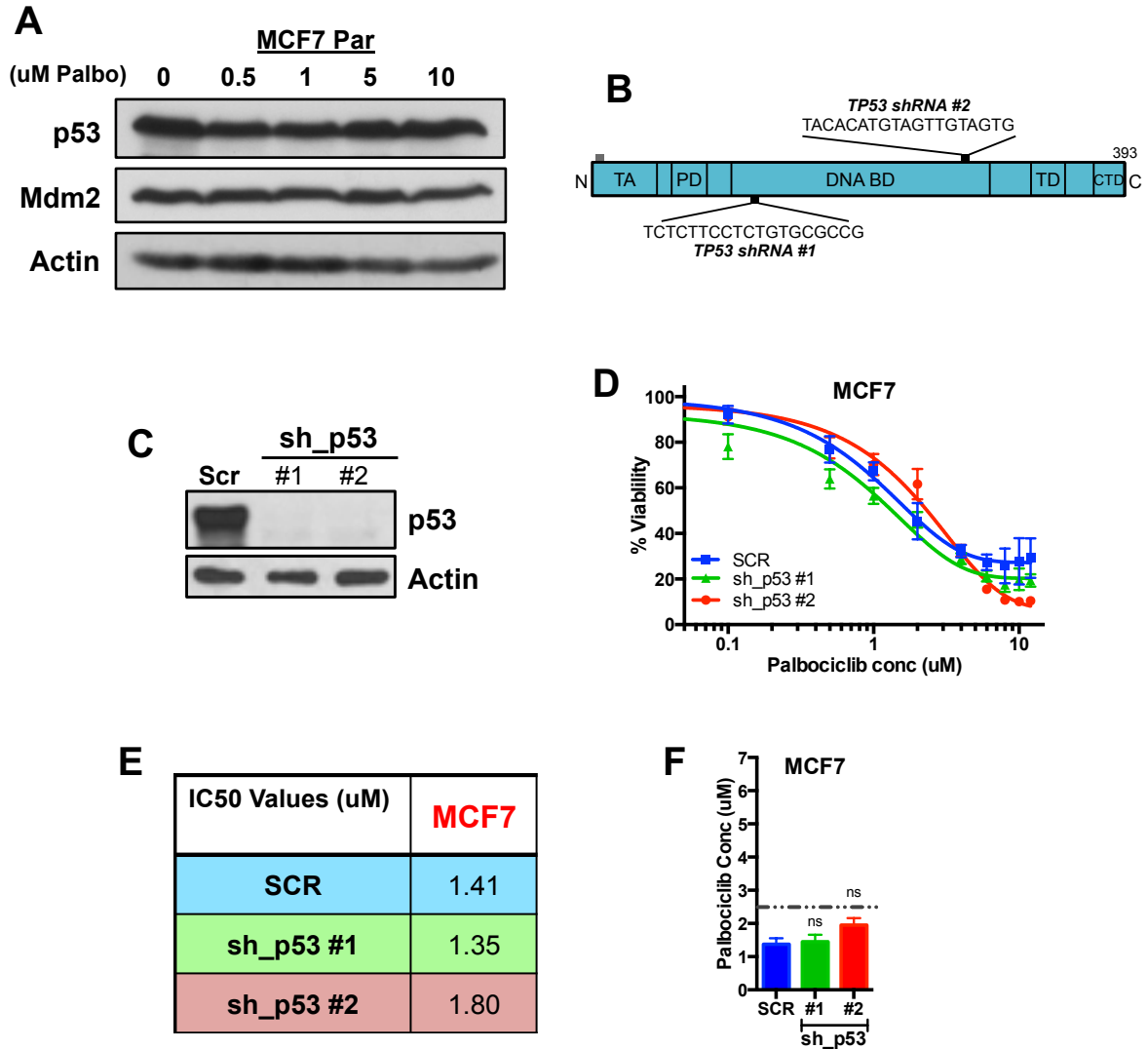


Figure 46: Role of p53 in determining response to palbociclib in ER+ve breast cancer:

A) Western blot analysis in MCF7 cells treated with varying concentrations of palbociclib to determine the expression of p53 pathway proteins: p53 and Mdm2. B) Schematic showing the location of the shRNA against p53 on the gene. C) Western blot showing the expression of p53 in the Scr and p53 knockdown (#1, #2) cells. D) Dose response assay to examine the effect of treatment with c. All data represent mean \pm SD from three independent experiments; p-values were calculated in comparison to cells treated with DMSO (Control) unless indicated. ns: $p > 0.05$; * $p < 0.05$; ** $p < 0.01$; *** $p < 0.001$; **** $p < 0.0001$. MCF7 p53 knockdown cells were generated by Dr. Dong Yang, post-doc in the Keyomarsi lab

6.2.3. ROLE OF RB IN MEDIATING PALBOCICLIB INDUCED ROS AND SENESCENCE

Given the role of Rb and its downstream effectors in regulating senescence, autophagy and ROS (Macleod 2008, Chicas, Wang et al. 2010, Jiang, Martin et al. 2010, Anders, Ke et al. 2011, Imai, Takahashi et al. 2014), we hypothesized that Rb plays a crucial role in mediating palbociclib action by regulating ROS, autophagy and senescence, and hence could serve as a predictor of sensitivity to CDK4/6 inhibition.

To directly test this hypothesis, we downregulated Rb in MCF7 and T47D cells via shRNA mediated stable knockdown (**Figure 47A,B**). Treatment of Control (Scrambled – SCR) or Rb knockdown MCF7 or T47D cells with increasing concentrations of palbociclib revealed a significant reduction in sensitivity to palbociclib (**Figure 47C**), with a 4 to 6 fold increase in IC50 values (**Figures 47D,E**). Further, ablation of Rb abolished the ability of palbociclib mediated CDK4/6 inhibition to induce a decrease in colony formation (**Figure 47F**) or a sustained growth inhibition (**Figure 47G**) upon treatment for 6 days and recovery for 4 or 6 days, compared to the scrambled shRNA cells.

Moreover, while palbociclib treatment of Rb knockdown MCF7 and T47D cells induced a G1 arrest, the cell cycle arrest was readily reversible, indicating the necessity of Rb expression to mediate palbociclib induced irreversible G1 arrest (**Figure 48A**). Next, given the ability of ROS in regulating both palbociclib induced autophagy and senescence, and the role of Rb in mediating these two processes, we interrogated if Rb also modulates the ability of palbociclib to induce oxidative stress via ROS. Results revealed that shRNA mediated knockdown of Rb in MCF7 and T47D cells significantly reduced the ability of ER positive breast cancer cells to increase cellular ROS levels upon treatment with palbociclib, when compared to the Scrambled shRNA cells (**Figure 48B**). Additionally, downregulation of Rb in ER positive breast cancer cell lines also prevented the induction of senescence upon long term (6 days) treatment with palbociclib (**Figure 48C**).

Taken together, these results demonstrate the vital role of Rb in mediating palbociclib-induced irreversible growth inhibition, cell cycle arrest, ROS and senescence in ER positive breast cancer cell lines, highlighting the potential utility of Rb as a biomarker for CDK4/6 inhibition.

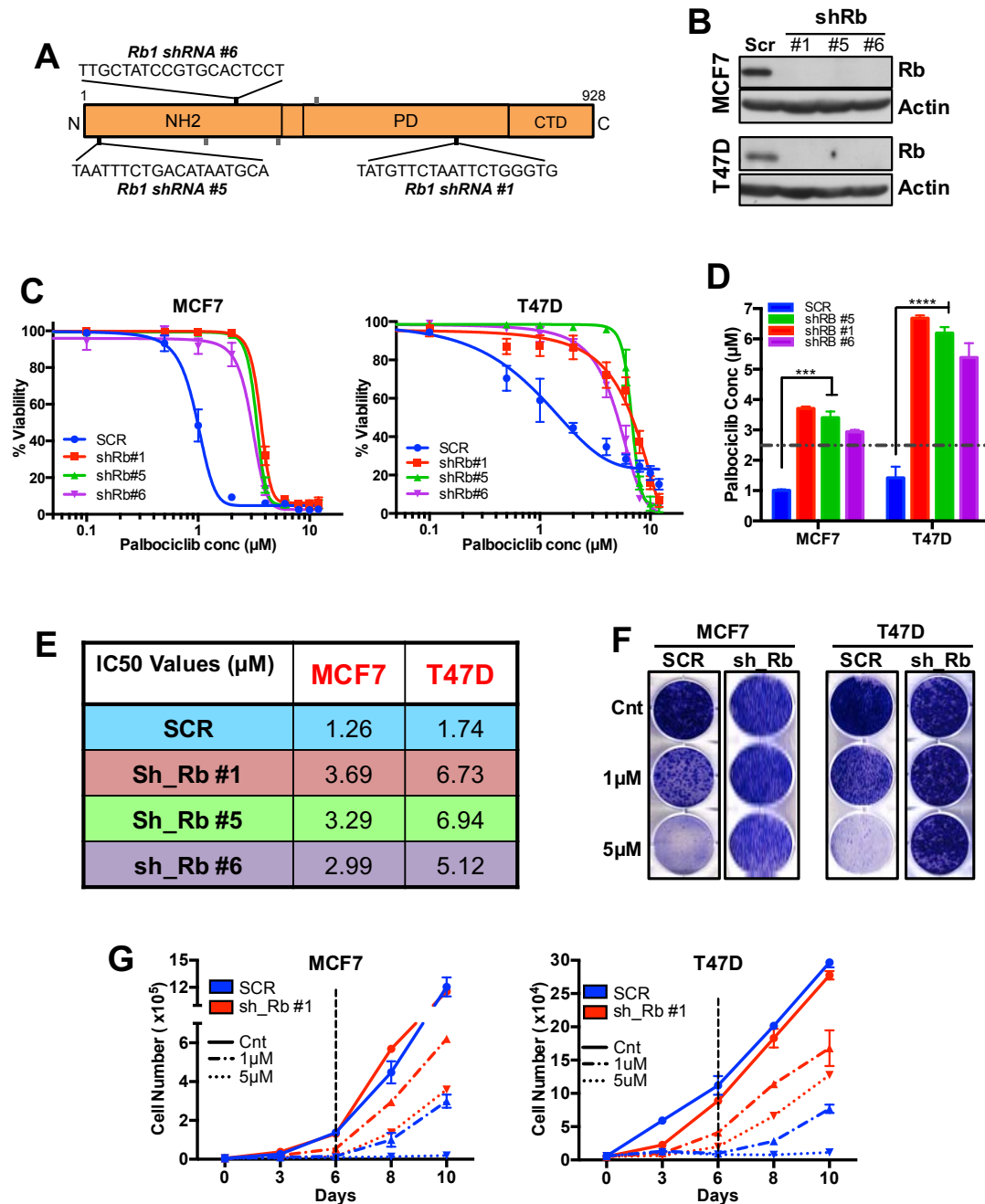


Figure 47: Role of Rb in mediating palbociclib induced growth inhibition: A) Schematic depicting locations of the shRNA sequences on the *Rb1* gene. B) Western blot showing levels of Rb protein in MCF7 and T47D cells after transfection with shRNA for Scrambled (Scr) or Rb. C-E) Impact of knocking down Rb on the growth of MCF7 and T47D treated with DMSO or increasing concentrations (conc) of palbociclib (0.01 to 12 μ M) for 6 days (C) and their corresponding half-maximal inhibitory concentration (IC_{50}) values. F, G) Clonogenic (F) and cell counting (G) assay in Rb-knockdown MCF7 and T47D cells treated with DMSO (Cnt) or palbociclib (1 or 5 μ M) for 6 days and allowed to recover for 4 or 6 days. All data represent mean \pm SD from three independent experiments; p-values were calculated in comparison to cells treated with DMSO (Control) unless indicated. ns: $p > 0.05$; * $p < 0.05$; ** $p < 0.01$; *** $p < 0.001$; **** $p < 0.0001$.

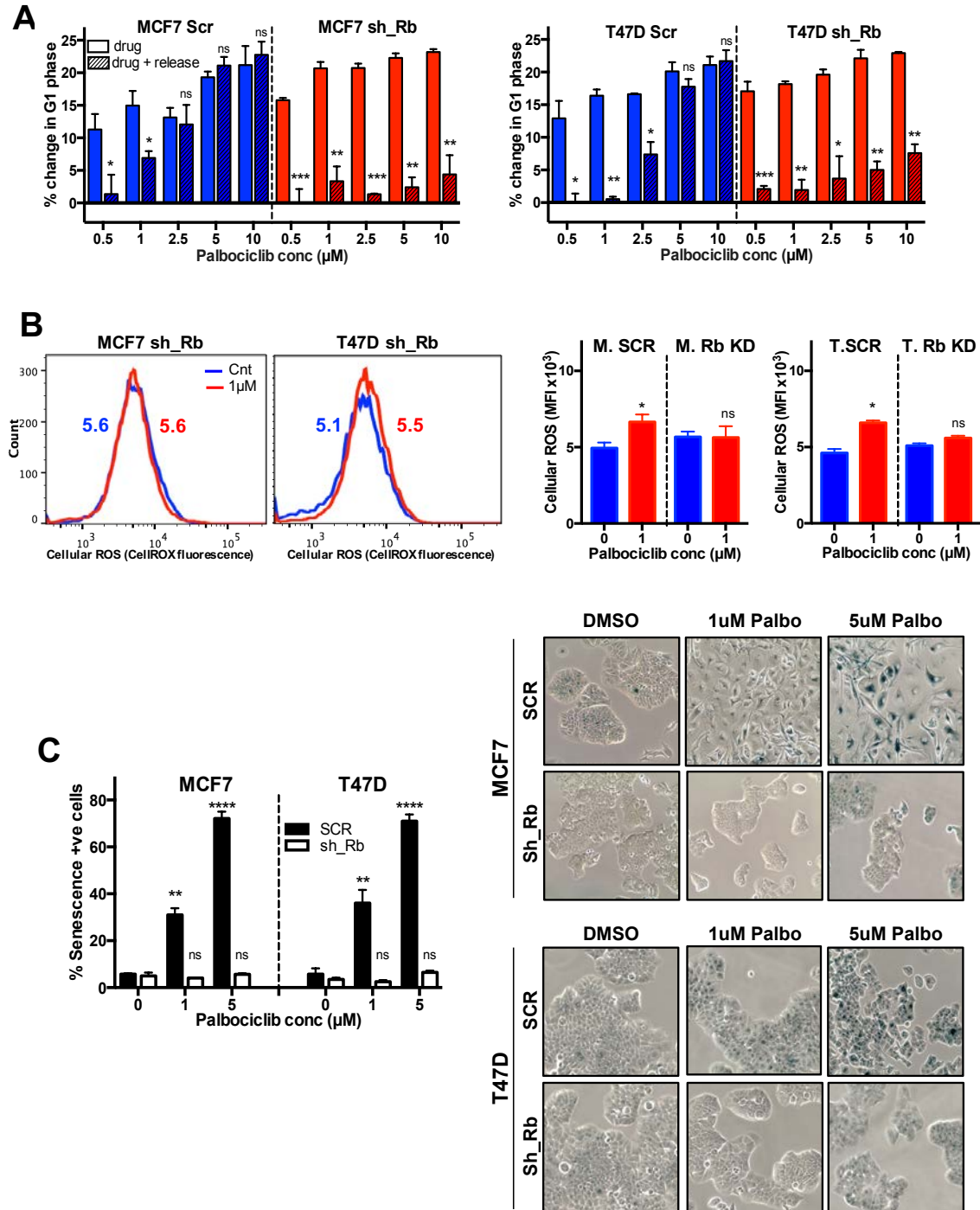


Figure 48: Role of Rb in mediating palbociclib induced ROS and senescence: Rb-knockdown MCF7 and T47D cells were treated with varying concentrations of palbociclib (Palbo) for 6 days and allowed to recover for 4 days (release) to examine reversibility. Cells were then subjected to A) cell cycle analysis to determine the percentage change in G1 phase (p-values were calculated by comparing values at the end of drug treatment with those at the end of release), B) CellROX assays to measure cellular ROS levels and C) Senescence activity by SA- β -gal assay with representative picture. All data represent mean \pm SD from three independent experiments; p-values were calculated in comparison to cells treated with DMSO (Control) unless indicated. ns: $p > 0.05$; * $p < 0.05$; ** $p < 0.01$; *** $p < 0.001$; **** $p < 0.0001$.

6.2.4. ROLE OF RB IN MEDIATING PALBOCICLIB INDUCED AUTOPHAGY

Since recent studies have demonstrated a role for the Rb-E2F pathway in regulating autophagy in tumor cells (Tracy, Dibling et al. 2007, Jiang, Martin et al. 2010), we next asked if Rb might also regulate the induction of autophagy by palbociclib. Monodansylcadavarine (MDC) staining revealed that shRNA knockdown of Rb abolished the ability of ER positive breast cancer cells (MCF7 and T47D) to induce autophagy in response to palbociclib treatment, as demonstrated by the absence of double-membrane autophagic vesicles (**Figure 49A**) and the lack of a significant increase in MDC staining (**Figure 49B**).

Further, treatment with the autophagy inhibitor, hydroxychloroquine (HCQ) in combination with palbociclib had no significant effect on the colony formation of ER positive cells when Rb was knocked down, compared to treatment with palbociclib alone (**Figure 49C**). Additionally, the combination of palbociclib and HCQ had no significant impact on the proliferation of MCF7 and T47D cells (**Figure 49D**).

These results suggest that Rb is required for palbociclib-induced autophagy and substantiates the role of autophagy as a stress response process that is triggered by the ER positive breast cancer cells only under conditions in which Palbociclib elicits a growth inhibitory effect. Moreover, this suggests that Rb could serve as a biomarker of sensitivity to the combination of CDK4/6 and autophagy inhibitors in ER breast cancer

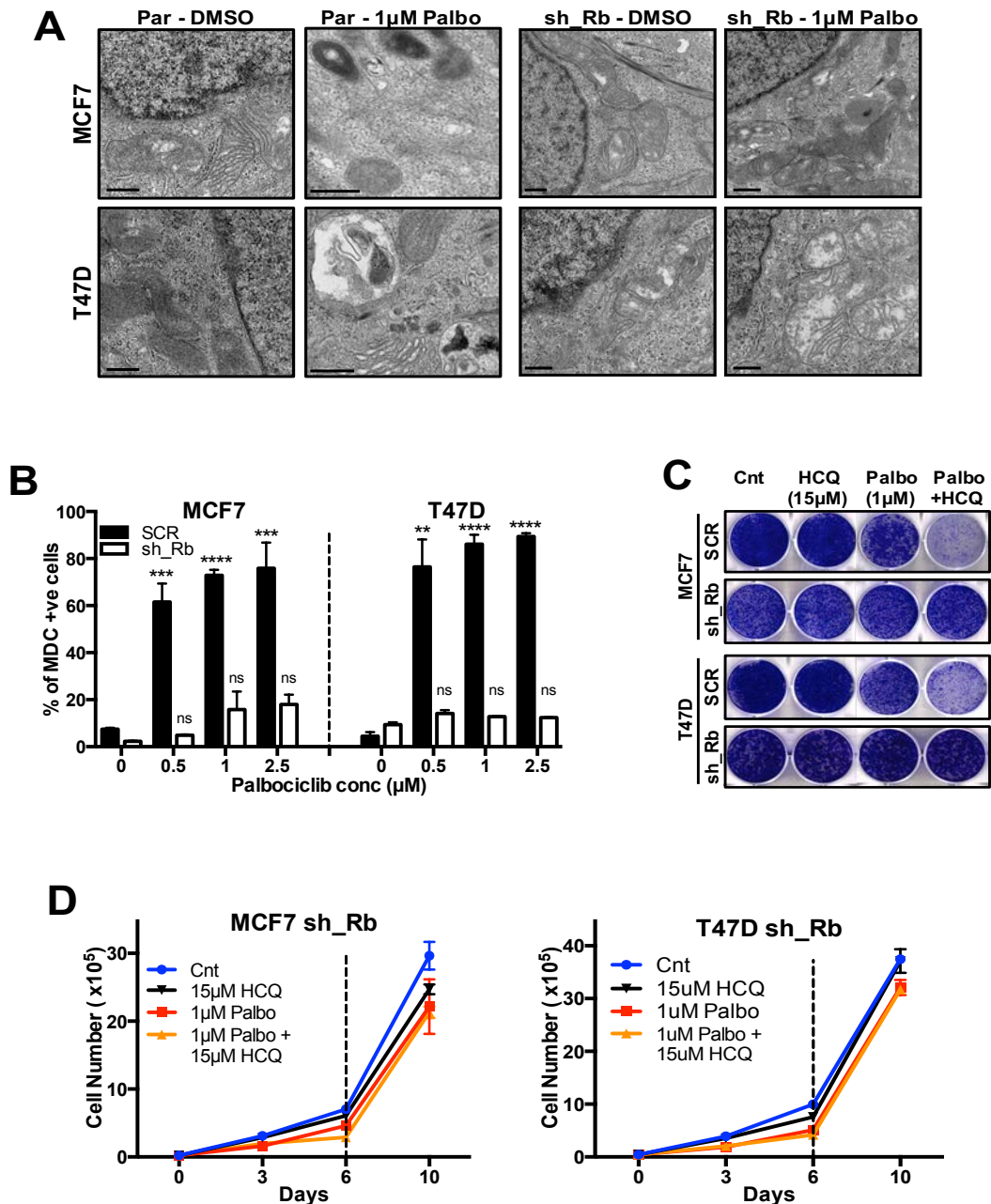


Figure 49: Role of Rb in mediating palbociclib induced autophagy: A) Representative TEM microphotograph of parental (Par) and Rb-knockdown (Par) MCF7 and T47D cells treated with DMSO or 1 μ M palbociclib for 6 days. Scale bars equal 500nm. **B)** Flow cytometry to quantify monodansylcadavarine (MDC) staining, a marker of autophagic vesicles in Rb-knockdown MCF7 and T47D cells treated with palbociclib for 6 days. **C, D)** Rb-knockdown MCF7 and T47D cells were treated with the combination of 1 μ M palbociclib and 15 μ M hydroxychloroquine (HCQ) for 6 days, allowed to recover for 6 or 4 days and subjected to Clonogenic assay (C) and Cell counting (D).

6.2.5. ROLE OF LMWE IN MEDIATING PALBOCICLIB ACTION

While our findings suggest that Rb is required for the growth inhibitory action of palbociclib and its combination with autophagy inhibition, results from recent studies focusing on biomarker discovery indicate that Rb alone may not be sufficient to effectively predict patient response to palbociclib (DeMichele, Clark et al. 2015). Results from our GSEA analysis (**Figure 50**) indicate that expression of cyclin E correlates with sensitivity to palbociclib in breast cancer cell lines. Moreover, since Rb loss is not common in ER positive breast cancer, we also interrogated the role of cyclin E in predicting sensitivity to CDK4/6 inhibition. As described in the introduction to this chapter, our laboratory discovered that LMWE, the elastase mediated proteolytic cleavage products of full length cyclin E, are oncogenic, uniquely expressed in tumors, hyperphosphorylate Rb, and are strong prognostic indicators in breast cancer. (Keyomarsi, Conte et al. 1995, Wingate, Puskas et al. 2009, Akli, Bui et al. 2010, Hunt, Karakas et al. 2016, Karakas, Biernacka et al. 2016).

Hence, to interrogate if high Cyclin-E, particularly the LMWE isoforms could mediate resistance to palbociclib, we overexpressed either empty vector (Vec), full length Cyclin-E (EL) or the LMW-E isoforms in MCF7 and T47D cell lines (**Figure 50A**). Results revealed that expression of LMW-E, but not full length Cyclin-E significantly reduced the sensitivity of the ER positive breast cancer cells, MCF7 and T47D to palbociclib (**Figure 50B**), with a 4 to 6 fold increase in IC50 values when compared to Vector and full length cyclin E (EL) (**Figures 50C, D**). Furthermore, expression of LMW-E, but not full length Cyclin-E, bypasses the ability of palbociclib to inhibit colony formation (**Figure 50E**) or exert irreversible growth inhibition (**Figure 50F**) in ER positive breast cancer cell lines.

Next, to examine the effect of LMW-E and full length cyclin E expression on palbociclib mediated cell cycle arrest, we performed flow cytometry and examined the expression of key cell cycle proteins following palbociclib treatment in EL or LMW-E overexpressing cells. Results showed that LMW-E expression but not full length cyclin E mediated resistance to palbociclib

mediated induction of G1 arrest (**Figure 51A**) and decrease in cell cycle proteins, pRb and Rb (**Figure 51B**). Further, expression of LMW-E abolished the ability of palbociclib to induce a dose-dependent increase in cellular ROS levels, in comparison with Vector and full length cyclin E (EL) expressing cell lines (**Figures 51C,D**). Expression of LMW-E thus prevented the ability of palbociclib mediated CDK4/6 inhibition to induce senescence in the ER positive breast cancer cells (**Figures 52A,B**). Finally, to interrogate if Rb downregulation would further decrease sensitivity of LMW-E expressing cells to palbociclib, we downregulated Rb in the T47D cells expressing Vector, full length cyclin E (EL) or LMW-E and dose-response studies showed that downregulation of Rb further decreased sensitivity to palbociclib in the LMW-E expressing T47D cells, with an increase in IC50 value from ~5.5 to ~7.5uM (**Figure 52C**).

Collectively, these results demonstrate that expression of the low molecular weight isoforms of cyclin E (LMWE) mediate resistance to CDK4/6 inhibition via palbociclib, and indicate that LMWE could serve as a selective biomarker to identify ER positive breast cancer cells responsive to palbociclib treatment.

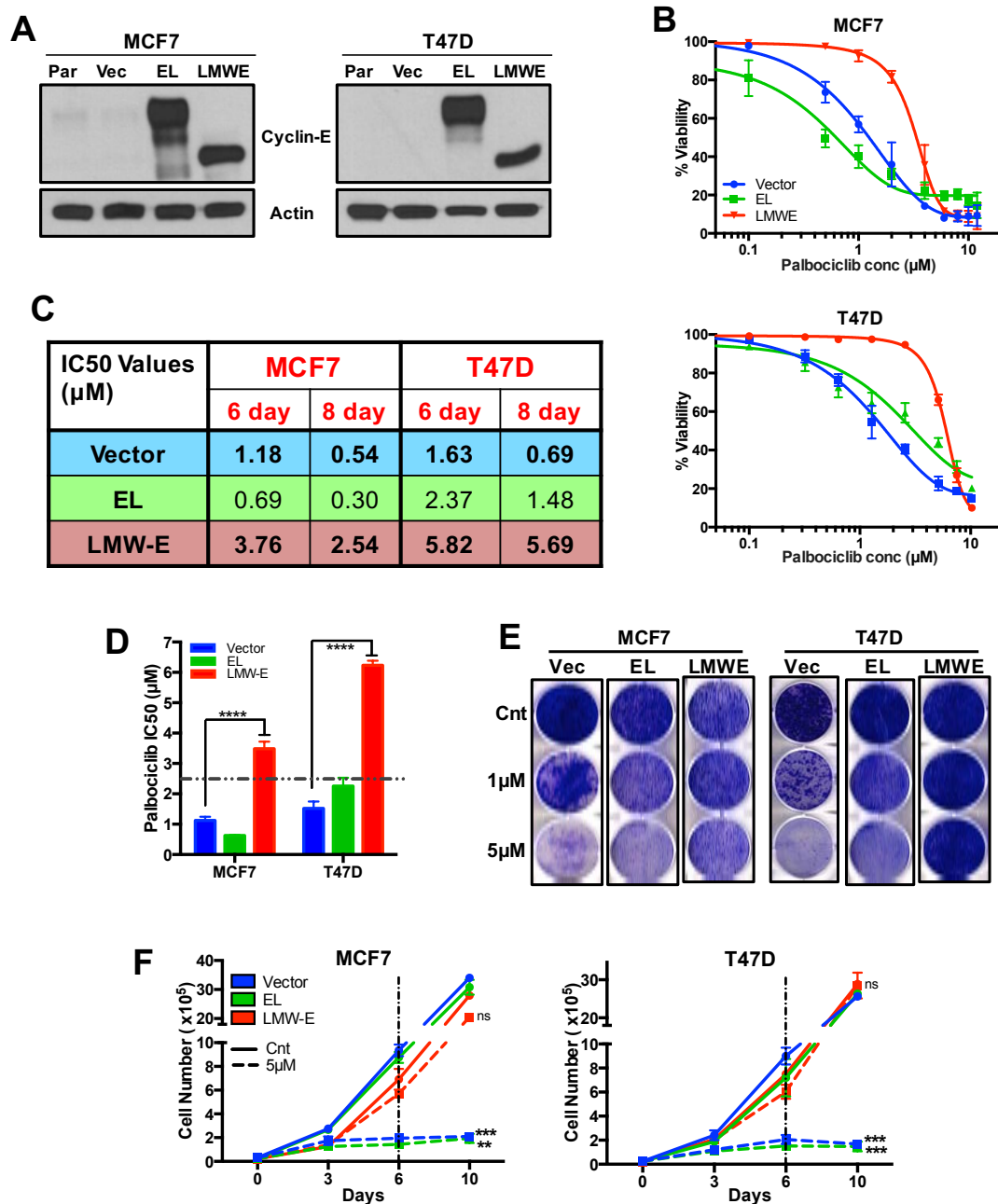


Figure 50: Role of LMWE in mediating palbociclib action: A) Western blot showing levels of cyclin E protein in MCF7 and T47D cells stably overexpressing full-length cyclin E (EL) or low-molecular-weight isoforms of cyclin E (LMW-E). Par, parental cells; Vec, vector-transfected cells. B-D) Impact of overexpressing vector, EL, or LMW-E on the growth of MCF7 and T47D cells treated with DMSO or increasing concentrations (conc) of palbociclib (0.01 to 12 μM) for 6 days (B) and their corresponding half-maximal inhibitory concentration (IC₅₀) values. E, F) MCF7 and T47D cells overexpressing vector, EL, or LMW-E were treated with DMSO (Cnt) or varying concentrations of palbociclib (Palbo) for 6 days and recovery for 4 and 6 days, and subjected to clonogenic (E) and cell counting assay (F) to assess cell proliferation. All data represent mean±SD from three independent experiments; p-values were calculated in comparison to cells treated with DMSO (Control) unless indicated. ns:p>0.05; *p<0.05; **p<0.01; ***p<0.001; ****p<0.0001. EL and LMWE expressing cells were generated with the help of Dr. Said Akli from the Keyomarsi lab.

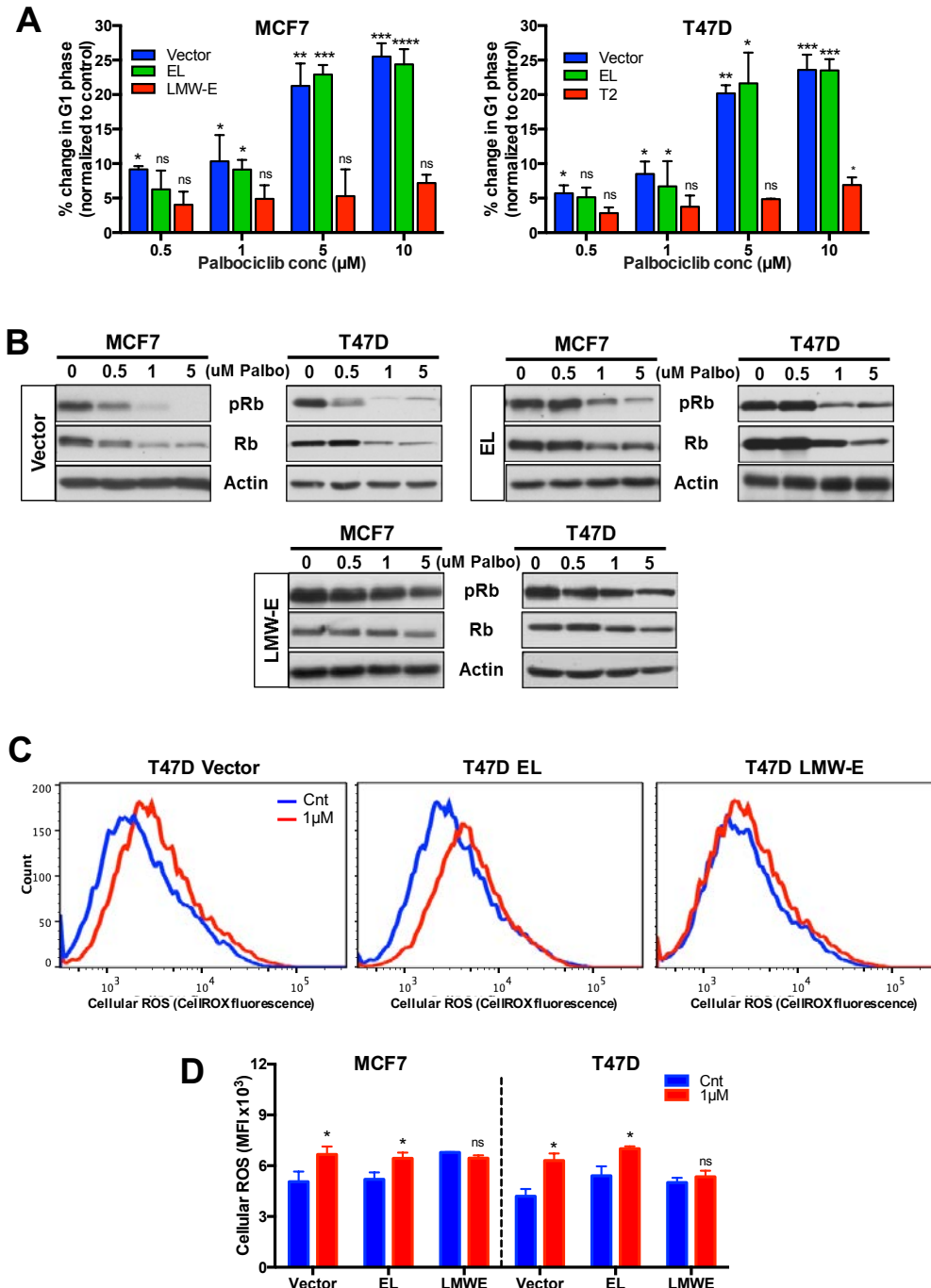


Figure 51: Role of LMWE in mediating palbociclib induced ROS and G1 arrest: MCF7 and T47D cells overexpressing vector, EL, or LMW-E were treated with DMSO (Cnt) or varying concentrations of palbociclib (Palbo) for 6 days and subjected to A) cell cycle analysis to examine the change in G1 phase and B) western blot analysis of Rb and p-Rb expression, markers of cell cycle arrest. C) Cellular reactive oxygen species (ROS) levels and its quantification (mean fluorescence intensity – MFI) measured in vector, EL, or LMW-E overexpressing MCF7 or T47D cells treated with DMSO or palbociclib (1 μ M or 5 μ M) for 6 days. D) Quantification of ROS levels by MFI in Scramble (Scr) or Rb-knockdown (KD) MCF7 and T47D cells treated with DMSO or palbociclib (1 μ M or 5 μ M) for 6 days. All data represent mean \pm SD from three independent experiments; p-values were calculated in comparison to cells treated with DMSO (Control) unless indicated. ns: $p > 0.05$; * $p < 0.05$; ** $p < 0.01$; *** $p < 0.001$; **** $p < 0.0001$.

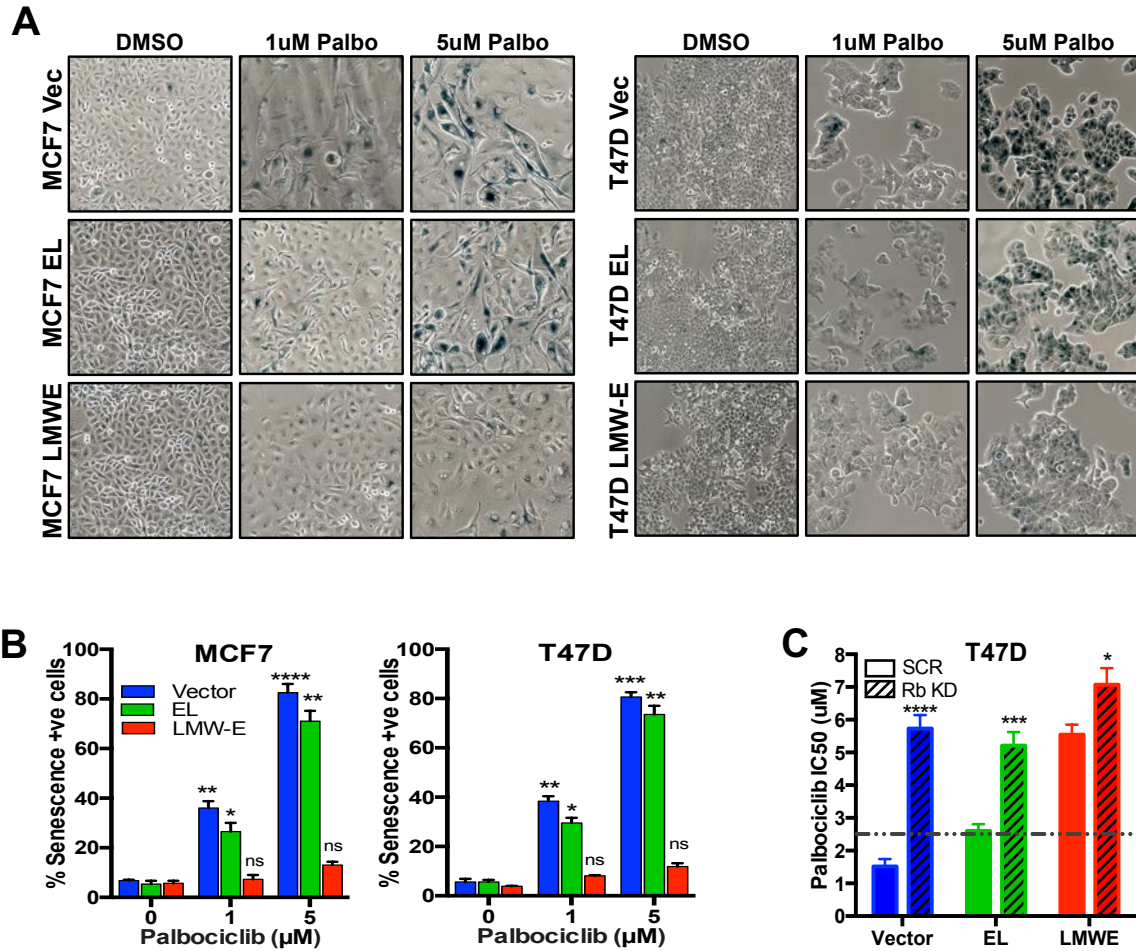


Figure 52: Role of LMWE in mediating palbociclib induced senescence: A,B) Quantification of SA- β gal staining assay to measure senescence (B) and representative images (A) in MCF7 and T47D cells overexpressing vector, EL, or LMW-E treated with DMSO (Cnt) or varying concentrations of palbociclib (Palbo) for 6 days. C) Palbociclib IC50 values calculated from dose response studies in T47D cells expressing Vector, EL or LMW-E and knockdown of Rb. All data represent mean \pm SD from three independent experiments; p-values were calculated in comparison to cells treated with DMSO (Control) unless indicated. ns:p>0.05; *p<0.05; **p<0.01; ***p<0.001; ****p<0.0001.

6.2.6. LMWE AS A MEDIATOR OF RESISTANCE TO THE COMBINATION OF CDK4/6 AND AUTOPHAGY INHIBITOR

Having shown that LMWE expression mediates resistance to the growth inhibitory action of palbociclib as a single agent, and that autophagy is a drug response observed in ER positive breast cancer cells, we wanted to examine if the LMWE could also serve as a marker of resistance to the combination of palbociclib and autophagy inhibition. To interrogate this, we treated MCF7 and T47D cells expressing empty vector, full length cyclin E (EL) or low molecular weight isoforms of cyclin E (LMWE) with the combination of low-dose (on target dose) of palbociclib and Hydroxychloroquine. The combination treatment while being synergistic to mediate irreversible and sustained growth inhibition in Vector and EL expressing cells, had no impact on the growth of palbociclib treated LMW-E cells (**Figure 53**).

This indicates that LMWE apart from being a biomarker to identify the ER positive breast cancer cells that respond to palbociclib as a single agent, can serve as a reliable biomarker for the combination of CDK4/6 and autophagy inhibition.

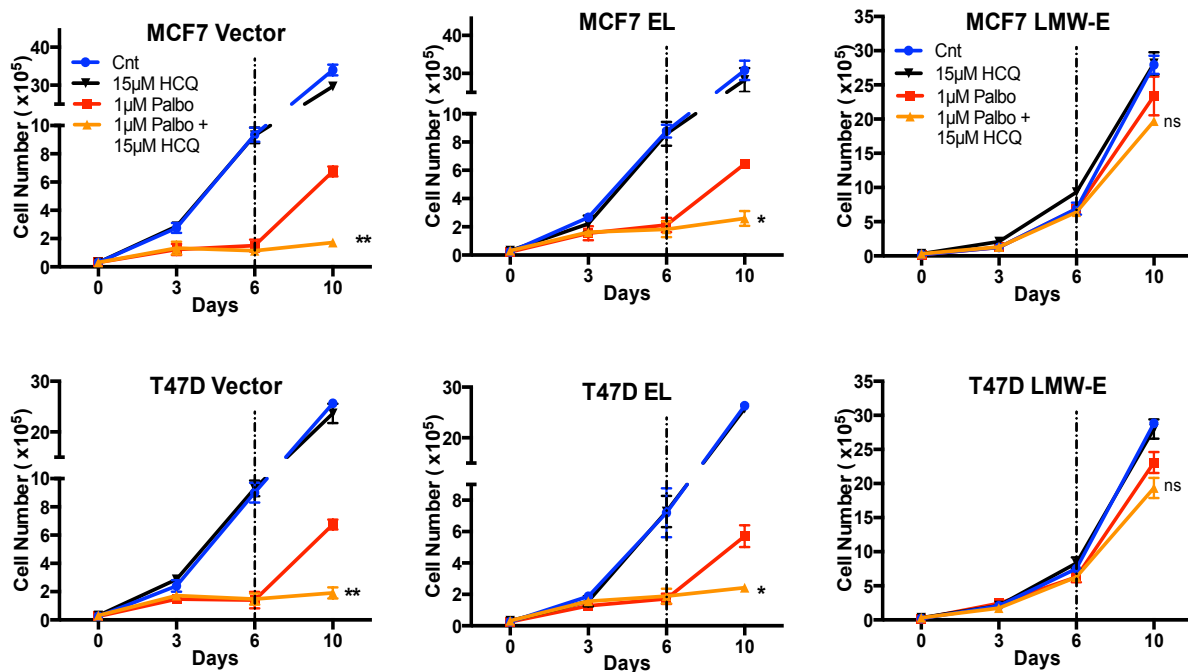


Figure 53: LMWE as a mediator of resistance to the combination of CDK4/6 and autophagy inhibitors: Cell counting was used to assess growth of MCF7 and T47D cells stably overexpressing Vector, EL, or LMW-E upon treatment with DMSO, palbociclib, 15μM hydroxychloroquine (HCQ) or the combination of palbociclib + HCQ for 6 days with recovery for 4 days to examine reversibility. All data represent mean \pm SD from three independent experiments; p-values were calculated in comparison to cells treated with DMSO (Control) unless indicated. ns: $p > 0.05$; * $p < 0.05$; ** $p < 0.01$; *** $p < 0.001$; **** $p < 0.0001$.

6.2.7. LMWE AS A MEDIATOR OF RESISTANCE TO THE TRIPLE COMBINATION OF CDK4/6, LETROZOLE AND AUTOPHAGY INHIBITOR

Since the CDK4/6 inhibitor palbociclib is currently used clinically in combination with the aromatase inhibitor letrozole in advanced ER positive breast cancer patients, we wanted to interrogate how palbociclib and letrozole combination compares to our proposed combination of palbociclib and HCQ. Treatment of MCF7 aromatase expressing cells with the combination of palbociclib and letrozole induced autophagy at levels similar to that of palbociclib treatment alone (**Figure 54A**), indicating the potential to examine the effect of the triple combination of palbociclib, letrozole and HCQ in ER positive breast cancer. Treatment of MCF7 aromatase expressing cells with the combination of palbociclib and HCQ had a significantly higher growth inhibitory effect (measured by cell counting and effect on long term colony formation), compared to palbociclib and letrozole as a single agent or in combination (**Figure 54C,D**). Further, treatment with the triple combination of palbociclib, letrozole and HCQ exhibited the highest reduction in colony formation (**Figure 54C**) and the induction of irreversible growth inhibition (**Figure 54D**).

Further, we overexpressed empty vector (Vector) or LMWE in MCF7 aromatase expressing cells (**Figure 54B**), in order to examine the impact of LMWE expression on the triple combination treatment. Results showed that expression of LMWE, but not empty vector in MCF7 cells mediated resistance to the ability of the combination of palbociclib and letrozole and the triple drug combination to inhibit colony formation (**Figure 54E**) and induce of a sustained and irreversible growth inhibition (**Figure 54F**).

Thus, these results show that the proposed combination of CDK4/6 and autophagy inhibitor is more effective in mediating a sustained growth inhibition than the currently clinically used combination (i.e. CDK4/6i + aromatase inhibitors), and, and demonstrates that LMWE expression can also serve as a biomarker for the potential triple combination of CDK4/6, aromatase and autophagy inhibitor.

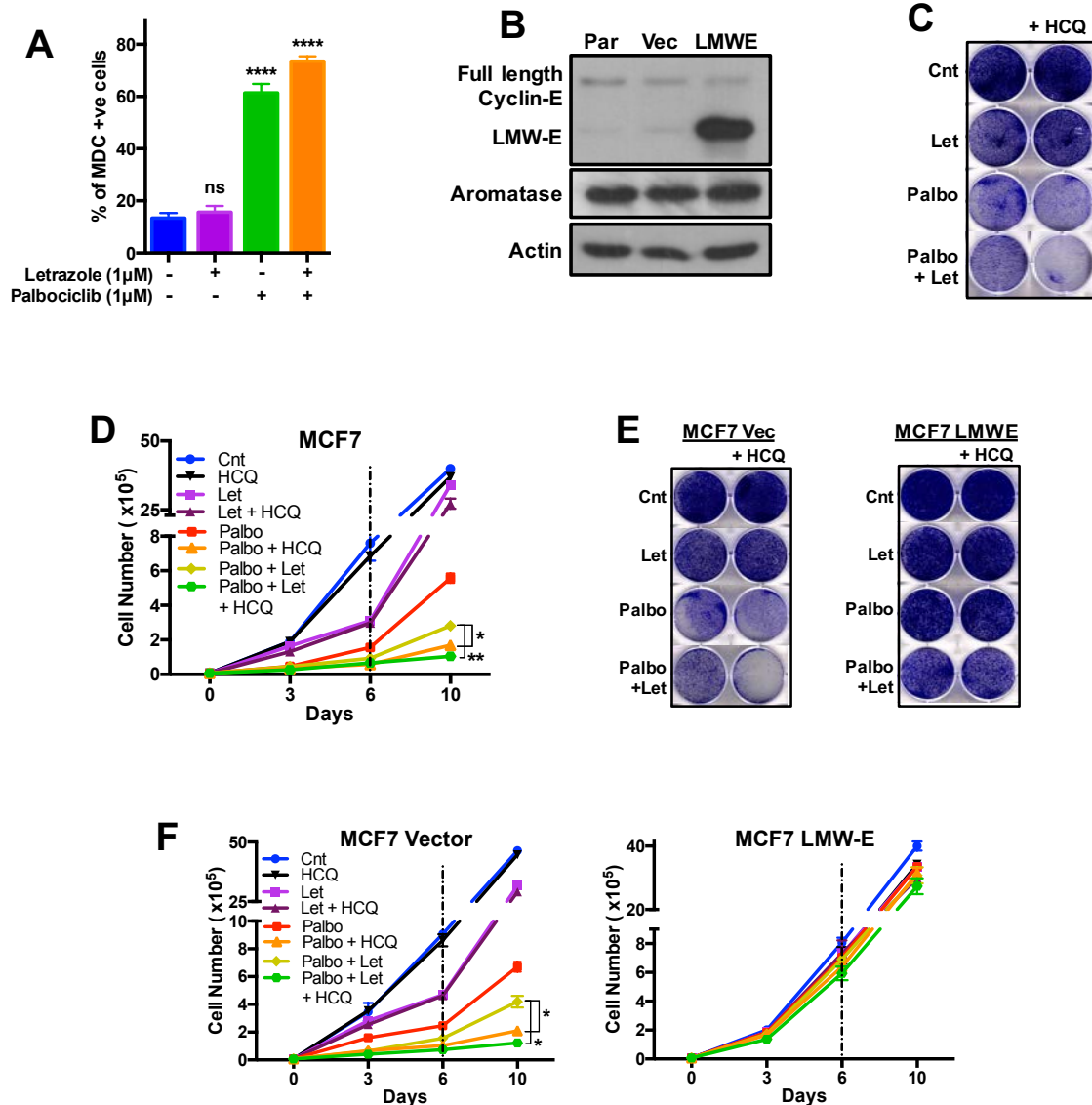


Figure 54: LMWE as a mediator of resistance to the triple combination of CDK4/6, letrozole and autophagy inhibitor: A) Measurement of monodansylcadavarine (MDC) positive acidic vesicles, including autophagosomes, by flow cytometry in MCF7 aromatase expressing cells treated with 1 μM palbociclib in combination with 1 μM letrozole for 6 days. B) Western blot showing levels of cyclin E and aromatase protein in MCF7 cells stably overexpressing aromatase (Par) and empty vector (Vec) or low-molecular-weight isoforms of cyclin E (LMW-E). C,D) Clonogenic (C) and Cell counting (D) assay to assess proliferation upon treatment with 1 μM palbociclib, 1 μM letrozole and 15 μM HCQ in the indicated combinations. E,F) Impact of overexpressing empty vector (Vec) or LMWE in MCF7 aromatase expressing cells measured by clonogenic (E) and cell counting (F) assay following treatment with 1 μM palbociclib, 1 μM letrozole and 15 μM HCQ in the indicated combinations. All data represent mean ± SD from three independent experiments; p-values were calculated in comparison to cells treated with DMSO (Control) unless indicated. ns: p > 0.05; *p < 0.05; **p < 0.01; ***p < 0.001; ****p < 0.0001. Aromatase expressing cells were generated by Dr. Iman Doostan, graduate student from the Keyomarsi lab.

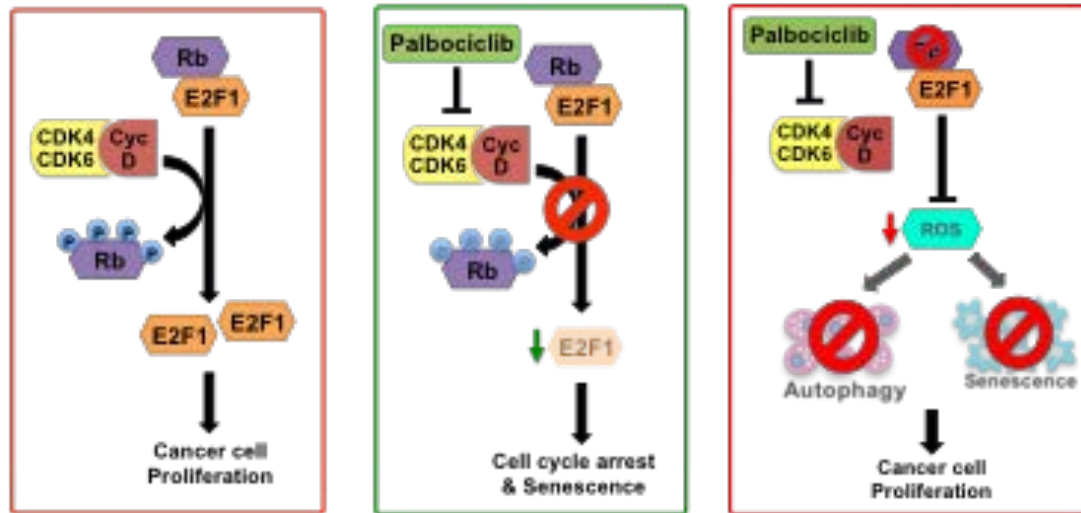
6.3. DISCUSSION

Taken together, results from this chapter highlight that the G1/ S checkpoint is crucial for response to palbociclib, and that deregulation the G1/S point pathway proteins, either by loss of Rb or expression of low molecular weight isoforms of Cyclin E (which deregulates the checkpoint by hyperphosphorylating Rb) mediates resistance to the drug and its combination with autophagy inhibitor (**Figure 55**).

Numerous studies have shown that the expression of Rb protein is required for breast cancer and other tumors to be sensitive to treatment with the CDK4/6 inhibitors, recent findings have shown that Rb alone is insufficient to effectively predict patient response to palbociclib (DeMichele, Clark et al. 2015). Further, since the loss or deregulation of Rb is not common in the ER positive subtype of breast cancer, it is crucial to identify a secondary or more reliable biomarker. Thus, results from this chapter show that the Rb and LMWE together can serve as reliable biomarkers for predicting response to palbociclib and its combination with autophagy inhibitors *in vitro*.

Further, while our results suggest that Rb might play a direct role in regulating ROS, the molecular mechanism by which this occurs remains unclear. Recent reports have shown that the downstream targets of Rb such as FOXM1 and BIRC5 (Survivin) can negatively regulate oxidative stress (Kwee, Luque et al. 2008, Park, Carr et al. 2009, Lim, Heo et al. 2015), providing a novel link between Rb and the ROS machinery. This suggests that downregulation of FOXM1 and BIRC5, among other ROS regulating proteins might be the potential mechanism by which Rb regulates oxidative stress, under palbociclib treatment conditions, and this demands further investigation.

A



B

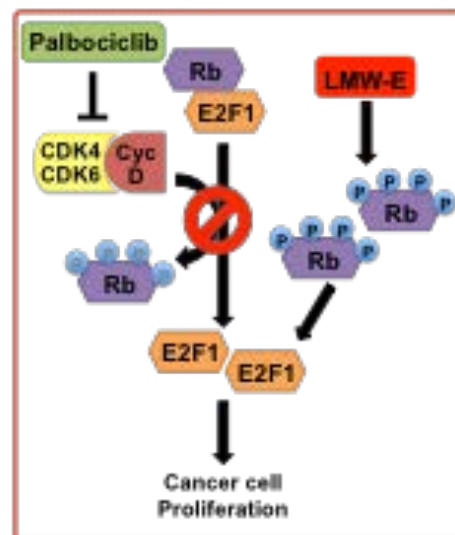


Figure 55: Working model – Rb and LMWE as identifiers of sensitivity to CDK4/6 inhibition: A) Schematic depicting the role of Rb in regulating the ability of palbociclib to induce reactive oxygen species (ROS), autophagy, and senescence. Model on the left depicts role of Rb in an intact cell cycle. Model in the middle depicts the scenario where palbociclib mediates a G1/S arrest. Model on the right shows how loss of Rb can affect the ability of palbociclib to induce ROS, autophagy and senescence. B) Schematic depicting the mechanism by which LMW-E mediates resistance to palbociclib, by inducing constitutive phosphorylation of Rb.

CHAPTER 7: RB AND CYCLIN E AS PROGNOSTIC BIOMARKERS OF PALBOCICLIB ACTION IN ADVANCED ER+ BREAST CANCER PATIENTS

7.1. INTRODUCTION

7.1.1. CLINICAL STUDIES AND BIOMARKER ANALYSIS

Based on pre-clinical studies, numerous biomarkers have been tested in breast cancer patients clinically to examine their ability to predict response to CDK4/6 inhibitors (Sherr, Beach et al. 2016). A summary of these clinical studies and the biomarkers tested are shown in **Table 9**.

Despite strong pre-clinical evidence, results from PALOMA-2, the randomized phase II clinical study testing the efficacy of combining palbociclib and letrozole showed that CCND1 amplification and / or loss of p16 did not predict sensitivity to palbociclib, with no difference in progression-free survival observed between the groups (Finn, Crown et al. 2015). Further analysis of response data showed no significant difference in the hazard ratio even when separated based on the expression levels of cyclin D and p16, indicating that the sample size might be small to conclude the predictive value of these proteins (Finn, Crown et al. 2015). A similar analysis following results from a short-term pre-operative trial with palbociclib as a single agent showed no correlation between response to palbociclib and expression of Rb, CCND1 or PIK3CA (Monica Arnedos 2016). However, results showed that the non-responders (measured by change in Ki67) were characterized by no change in pRb levels (Monica Arnedos 2016). A similar result was also seen with the CDK4/6 inhibitor, abemaciclib, which showed a significant correlation between clinical efficacy and modulation of pRb (Patnaik, Rosen et al. 2016)

Results from PALOMA-3, the phase III clinical trial testing the combination of palbociclib and fulvestrant showed that while ER positivity is required, that the expression levels of ER do

Treatment	Setting	Phase	n	Biomarkers studied
Palbociclib	early	Window of opportunity	100	IHC, phospho-protein, gene expression, whole exome, TIL
Palbociclib + Anastrozole	early	Neoadjuvant (NeoPalAna)	50	IHC, gene expression, PIK3CA, NGS
Abemaciclib + Anastrozole	early	Neoadjuvant (MONARCH-3)	220	Gene expression, TIL
Palbociclib + letrozole	Metastatic ET sensitive	Phase II randomized (PALOMA-1)	165	CCND1 / p16 expression
Palbociclib + letrozole	Metastatic ET sensitive	Phase III randomized (PALOMA-2)	666	Rb, cyclin D, p16
Ribociclib + letrozole	Metastatic ET sensitive	Phase III randomized (MONALEESA-2)	668	
Palbociclib + fulvestrant	Metastatic ET resistant	Registration trial	521	ESR1 mutation, PIK3CA
Abemaciclib	Metastatic resistant	Phase I (MONARCH-1)	47	Phospho-Rb

Table 9: Clinical studies and biomarker analysis: Summary of clinical studies performed in ER+ve breast cancer with the CDK4/6 inhibitors and the biomarkers assessed as a part of the study.

not correlate with response (Cristofanilli, Turner et al. 2016). Analysis from this study also showed that there is no correlation between response to progression-free survival and PIK3CA mutation or ESR1 mutations (Cristofanilli, Turner et al. 2016, Fribbens, O'Leary et al. 2016), indicating that palbociclib treatment is equally responsive in these mutant tumors as those not harboring either mutations. Lastly, results of biomarker analysis from MONALEESA-2, the phase III combination study between ribociclib and letrozole showed no significant difference in

the hazard ratio or correlation between progression free survival and expression of Rb protein, p16 protein, CDKN2A mRNA, CCND1 mRNA, basal Ki67 levels, ESR1 mRNA and PiK3CA mutation (Hortobagyi, Stemmer et al. 2016). Biomarkers to predict drug sensitivity may be prognostic or predictive. A prognostic biomarker measure patient outcome without comparing the effect of the treatment under study, while a predictive biomarker takes into account both the effect of the treatment and the patient outcome (Justus, Leffler et al. 2014). Thus, a prognostic biomarker is evaluated from a single arm study of treated patients where the response of patients in the presence or absence of the marker is examined, as done in this chapter. However, for a predictive biomarker, a double arm study is needed, to examine the response of patients in the presence or absence of the marker, in combination with the treatment effect (Justus, Leffler et al. 2014)

7.1.2. GAP IN KNOWLEDGE

While the completed and ongoing clinical studies investigated numerous biomarkers of response, there is still no actionable and reliable clinical biomarker that can be used a predictor of response for palbociclib treatments. Hence this chapter aims at addressing the following questions:

1. Would the biomarkers identified in our *in vitro* studies (Rb and cyclin E) be successful in predicting response to palbociclib in patients?
2. What proportion of the breast cancer patients would benefit from palbociclib treatment (based on biomarker analysis)?

7.2. RESULTS

7.2.1. TCGA ANALYSIS SHOWING DEREGLATION OF RB AND CYCLIN E IN BREAST AND OTHER SOLID CANCER PATIENTS

Our *in vitro* and *in vivo* results thus far have shown Rb and cyclin E can serve as reliable biomarkers to identify which tumors would benefit from treatment with CDK4/6 inhibitors and its potential combination with autophagy inhibitors. Hence, to estimate the percentage of patients who would benefit from the combination treatment of palbociclib and hydroxychloroquine, we analyzed the TCGA database for the expression of Rb and cyclin E at the mRNA levels.

Analysis of mRNA levels from the breast TCGA database, comprising of 817 breast cancer patients showed that about 85.4% of all breast tumors had measurable expression of Rb and low (no overexpression) of cyclin E (**Figure 56A**). Detailed analysis of the subtypes within breast cancer showed that a higher proportion of the ER positive breast tumors (97.1%) were Rb positive and cyclin E negative compared to 40.7% within the TNBC subtype (**Figure 56A**). This indicates that a large proportion of breast cancer tumors are Rb+ve cyclin E-ve, and that they could benefit from treatment with CDK4/6 inhibitor and its potential combinations.

Next, we performed a similar analysis within the TCGA database for other solid tumor subtypes analyzed in this study. Results revealed that 80.8%, 89.3% 86.1%, 92.9% and 95.7% of ovarian, pancreatic, lung, colorectal and prostate cancer patients respectively are positive for Rb and have low / no expression of Cyclin-E (**Figure 56B**). This indicates that a large proportion of patients with these solid tumors could benefit from treatment with the CDK4/6 inhibitor.

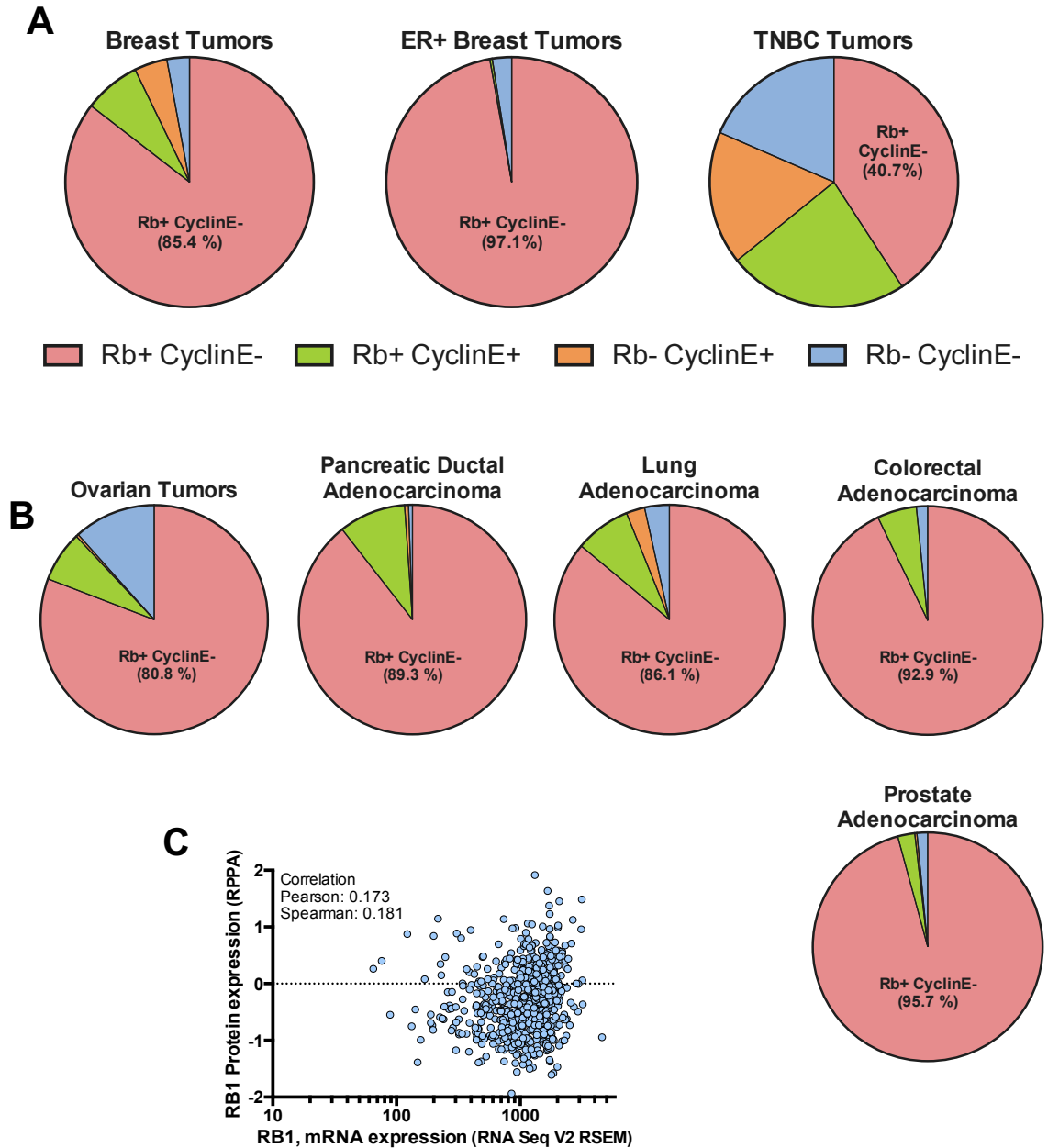


Figure 56: TCGA analysis showing deregulation of Rb and cyclin E in breast and other solid cancer patients: A) Alterations in Rb and cyclin E RNA levels in all breast (n=817), ER+/Luminal A and B (n=321) and TNBC/Basal (n=81) tumors from the TCGA database of breast cancer patients. B) Alterations in Rb and cyclin E RNA levels in tumors from patients with ovarian (n=557), lung (n=230), pancreas (n=178), colon (n=379), or prostate (n=333) cancer taken from the TCGA database. C) Plot showing correlation between mRNA and protein levels of Rb among 817 tumors from the TCGA database of breast cancer patients.

7.2.2. ALTERATIONS IN RB AND LMWE PROTEIN IN BREAST CANCER PATIENTS

While the TCGA analysis provides a reliable estimate of the proportion of patients who could benefit from the CDK4/6 inhibitor therapy, these analyses are based on the RNA levels of Rb and cyclin E. Hence, the TCGA analysis cannot accurately predict protein expression of Rb (**Figure 56C**), nor can it differentiate between full-length cyclin E (nuclear) and LMWE (cytoplasmic). Thus, a direct analysis based on protein expression of Rb and LMWE is required to accurately estimate the breast cancer who would benefit from therapy.

To do this, we examined LMWE and Rb protein expression in tissue microarray samples from a cohort of 879 early stage breast cancer patients from the NCI Cancer Diagnosis Program (Hunt, Karakas et al. 2016, Karakas, Biernacka et al. 2016). LMWE and Rb staining was performed by immunohistochemistry in the formalin-fixed paraffin-embedded slides of breast cancer tumors from this cohort (**Figure 57A**). Results revealed that 33% of all breast tumor samples were positive for Rb and negative for LMWE (**Figure 57B**), indicating the patients who could benefit from therapy. Further, this percentage of Rb+ve LMWE-ve tumors was higher (40%) in the ER positive subtype compared to the TNBC (13.5%) subtype (**Figure 57B**). Moreover, Kaplan Meier analysis showed that the patient groups which had deregulated cyclin E or LMWE, Rb+ LMWE+ (red lines) and RB- LMWE+ (purple lines) had a worse overall prognosis compared to the other subgroups which did not express the cytoplasmic cyclin E, emphasizing the prognostic ability of LMWE in breast cancer (**Figure 57C**). This was also true in both the ER positive and the TNBC subtypes (**Figure 57C**).

These results suggest that over 33% of all breast cancer patients (**Figure 57B**) (regardless of ER status) may benefit from treatment with the palbociclib and its combination with HCQ, thus highlighting the clinical utility of this regimen.

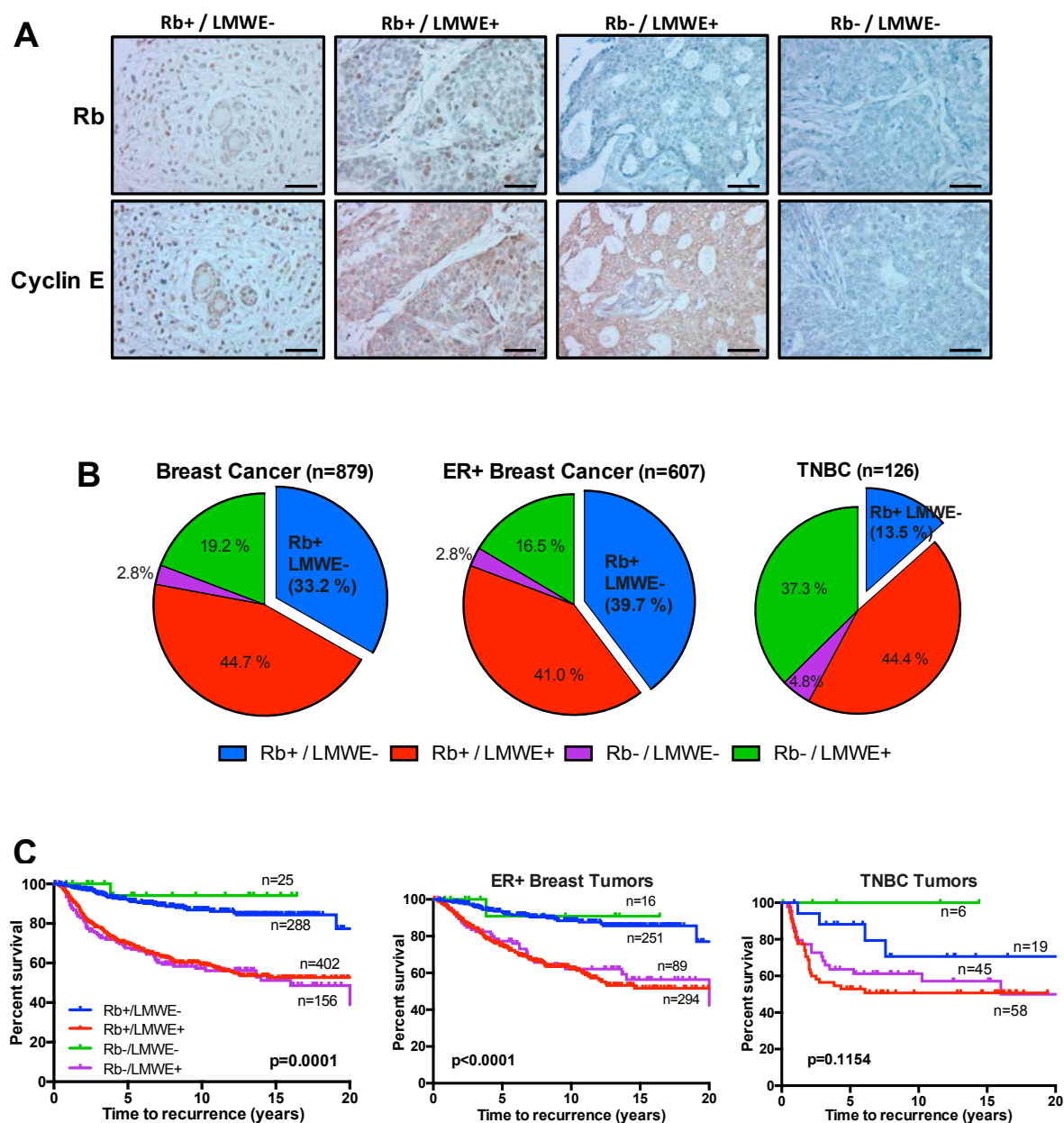


Figure 57: Alterations in Rb and LMWE protein in breast cancer patients: A) Representative images from immunohistochemical analysis of Rb and LMW-E in tumors from the NCI patient cohort (n=879). Scale bars equal 50 μ m. B) Percentage of breast cancer patients exhibiting alterations in Rb and LMW-E as determined via immunohistochemical staining of tumor samples from the NCI patient cohort (n=879). C) Kaplan Meier curves showing survival of breast cancer patients from the NCI patient cohort when classified based on Rb and LMW-E. IHC analysis was performed by Dr. Cansu Karakas from the Keyomarsi lab.

7.2.3. CORRELATION BETWEEN EXPRESSION OF RB AND LMWE AND RESPONSE TO PALBOCICLIB IN ADVANCED ER POSITIVE BREAST CANCER PATIENTS

Next, we wanted to directly test the utility of Rb and LMWE protein expression as prognostic biomarkers in advanced metastatic breast cancer. For this purpose, we utilized a cohort of 493 patients with advanced ER+ breast cancer who were/are currently being treated with the combination of palbociclib and letrozole (aromatase inhibitor) or fulvestrant at MD Anderson Cancer Center (**Figure 58A**), whose clinical, pathological and treatment characteristics are detailed in **Table 10,11**. Since the biopsy blocks for most of these patients were not available at MD Anderson, the archival, pre-treatment biopsy specimens from 221 patients from primary tumor and/or local or metastatic recurrence were obtained with consent for each patient. However, only 109 of the tumors obtained had tissues in sufficient amount for immunohistochemistry (IHC) analysis (**Figure 58A**). To estimate the protein expression, these tissues were then subjected to immunohistochemistry staining and scoring for cyclin E and Rb (**Figure 58C**).

The majority (102/109) of the samples were positive for Rb, while only 49.5% (54/109) were positive for LMWE (**Figure 58B**). Moreover, about 50% of the treated ER breast cancer patients were Rb+ve and LMWE-ve, which is the group we predicted would respond best to CDK4/6 inhibitor therapy (**Figure 58B**). The Rb+ve and LMWE+ve subgroup accounted for about 43% of patients and Rb-ve and LMWE+ve subgroup accounted for 6.5% of patient tumors, and no tumors stained negative for both Rb and LMWE in the patient cohort tested (**Figure 58B**). Analysis of clinical and pathologic variables revealed that the patients with LMWE expression or RB loss exhibited higher rates of progression at 6 and 12 months (assessed by Kaplan Meier methods), with the heavily treated fulvestrant group experiencing greater progression rate at 12 months as expected (**Table 10,11**). The significant variable in this analysis included tumor stage at diagnosis, exposure to adjuvant chemotherapy, PR status, Rb and LMWE status. Among these, the expression Rb and LMWE as single variables

correlated significantly with progression rates for both the palbociclib with letrozole group (Rb: $p=0.02$, LMWE: $p=0.01$) and the palbociclib with fulvestrant treatment group (Rb: $p=0.03$, LMWE: $p=0.009$) (**Table 10,11**). Moreover, a significantly higher correlation was seen when Rb and LMWE expression were treated as combined variable in palbociclib with letrozole ($p=0.006$) and palbociclib with fulvestrant ($p=0.009$) treatment groups (**Table 10,11**).

Univariate Cox proportional hazards model showed that the factors that were significantly associated with progression-free interval included adjuvant chemotherapy, PR status, Rb and LMWE status, as measured by hazard ratio, which is a measure of the influence a parameter under study has on the response to therapy (**Table 12**). Importantly, Rb and LMWE (as single and combined variables) were significantly associated with the progression-free interval with in palbociclib with letrozole treatment group, with hazard ratios of 0.2 for Rb alone, 3.2 for LMWE alone, and 9.2 for Rb and LMWE combined (**Table 12**). A similar correlation was also observed in the palbociclib with fulvestrant treatment group, exhibiting hazard ratios of 0.09 with Rb alone, 5.2 with LMWE alone, and 23.8 with Rb and LMWE combined (**Table 12**). Further, results showed that 81.8% (45 out of 55 patients) of Rb+ve /LMWE-ve patients exhibited stable disease in response to palbociclib treatment, compared to 62.9% in the other patient groups combined (**Figure 59A**). Separation of the patients based on their treatment with palbociclib and letrozole or palbociclib and fulvestrant showed a significant 84.2% and 82.4% response rate (stable disease) respectively, in the Rb+ve LMWE-ve patient subgroup (**Figure 59A**). This showed that Rb and LMWE in combination have a good prognostic value for palbociclib treatment in breast cancer.

Kaplan-Meier progression-free survival (PFS) plots for the 109-patient cohort separated based on the protein expression of Rb and LMWE revealed that the patients with Rb+ve and LMWE-ve tumors have the longest PFS time (median >36.5 months), compared to Rb+/LMWE+ patients (median= 13.4 months) and Rb-/LMWE+ patients who had the shortest PFS time (median= 4.2 months) (**Figure 59B**). A similar trend was observed when the

palbociclib treated ER positive breast cancer patients were separated by letrozole (n=78) or fulvestrant (n=31) treatment in combination, and correlated with Rb/LMWE expression, where Rb+ and LMWE- patients had the longest PFS time (median >36.5 months with letrozole; 10.7 months with fulvestrant), compared to Rb+/LMWE+ patients (median= 17 months with letrozole and 4.7 months with fulvestrant) and Rb-/LMWE+ patients (median= 3.5 months with letrozole and 4.2 months with fulvestrant) (**Figure 59B**). Additionally, the concordance indices calculated based on the multivariate analysis model showed substantial gains when Rb and LMWE were included as single variables, compared to the model without Rb and cyclin E, and a much larger increase was observed upon including Rb and LMWE as combined variables (**Figure 59C and Table 13**).

Collectively, these results provide evidence that LMWE and Rb can serve as reliable prognostic biomarkers for CDK4/6 inhibitors in advanced estrogen receptor positive breast cancer patients.

Table 10: Clinical, pathologic, and treatment characteristics of patients treated with palbociclib + letrozole

Variable	N	6-month progression rate (%)	12-month progression rate (%)	P value (Univariate)
All patients	78	22.2	31.0	
Race				0.3
White	55	25.1	33.2	
Others	23	14.6	24.1	
Clinical tumor stage at diagnosis				0.004
0/I	12	28.7	52.5	
II	20	26.3	36.8	
III	19	38.1	54.2	
IV	25	0	0	
Unknown	1	0	0	
Tumor Histology				0.9
Ductal	67	21.6	31.2	
Others	11	27.1	27.1	
Lymphatic/vascular invasion				0.2
Yes	52	15.2	24.5	
No	24	37.5	45.3	
Adjuvant Chemotherapy				0.004
No	64	16.1	21.5	
Yes	14	48.7	69.2	
Tumor grade				0.4
I/II	57	25.3	38.9	
III	21	15.3	15.3	
Progesterone receptor status				0.02
Positive	69	16.2	26.2	
Negative	9	70.8	70.8	
Rb status				0.02
Negative	5	66.7	0	
Positive	73	20.3	29.2	
LMWE status				0.01
Negative	38	14.4	18.0	
Positive	40	30.9	44.2	
Rb/LMWE status				0.006
Rb+/LMWE-	38	14.4	18.0	
Rb+/LMWE+	35	27.4	41.4	
Rb-/LMWE+	5	66.7	0	
Bone /soft tissue vs. any visceral				0.03
Bone / soft tissue	51	13.7	20.7	
Any visceral	27	37.1	47.6	
Prior therapy for metastatic disease				0.1
None	56	16.6	25.8	
Hormonal	4	25.0	25.0	
Chemotherapy and/or hormonal	18	40.9	50.7	
Time from completion of adjuvant hormonal therapy (years)				0.2
None (de novo metastatic)	42	15.8	23.5	
< 1 year	5	0	0	
> 1 year	31	33.0	42.9	

*p value calculated after excluding unknown.

Table 11: Clinical, pathologic, and treatment characteristics of patients treated with palbociclib + fulvestrant

Variable	N	6-month progression rate (%)	12-month progression rate (%)	P value Univariate
All patients	31	17.4	58.0	
Race				0.9
White	25	15.9	63.8	
Others	6	20.0	20.0	
Clinical tumor stage at diagnosis				0.2
0/I	7	0	33.3	
II	7	20.0	40.0	
III	11	14.3	31.4	
IV	6	46.7	-	
Tumor Histology				0.7
Ductal	25	15.3	54.4	
Others	6	25.0	-	
Lymphatic/vascular invasion				0.8
Yes	15	16.4	61.0	
No	16	17.5	45.0	
Adjuvant Chemotherapy				0.06
No	16	25.0	80.3	
Yes	15	10.0	25.0	
Tumor grade				0.6
I/II	27	19.3	55.3	
III	4	0	-	
Progesterone receptor status				0.6
Positive	28	18.4	0	
Negative	3	58.6	-	
Rb status				0.03
Negative	2	-	-	
Positive	29	13.7	56.1	
LMWE status				0.009
Negative	17	0	52.1	
Positive	14	58.4	79.2	
Rb/LMWE status				0.009
Rb+/LMWE-	17	0	52.2	
Rb+/LMWE+	12	52.6	76.3	
Rb-/LMWE+	2	-	-	
Bone /soft tissue vs. any visceral				0.2
Bone / soft tissue	20	13.2	62.8	
Any visceral	1	23.8	68.3	
Prior therapy for metastatic disease				0.9
None	9	16.7	-	
Hormonal	14	16.4	68.7	
Chemotherapy and/or hormonal	8	20.0	46.7	
Time from completion of adjuvant hormonal therapy (years)				0.5
None	14	18.0	-	
< 1 year	7	25.0	-	
> 1 year	10	12.5	41.7	

*p value calculated after excluding unknown.

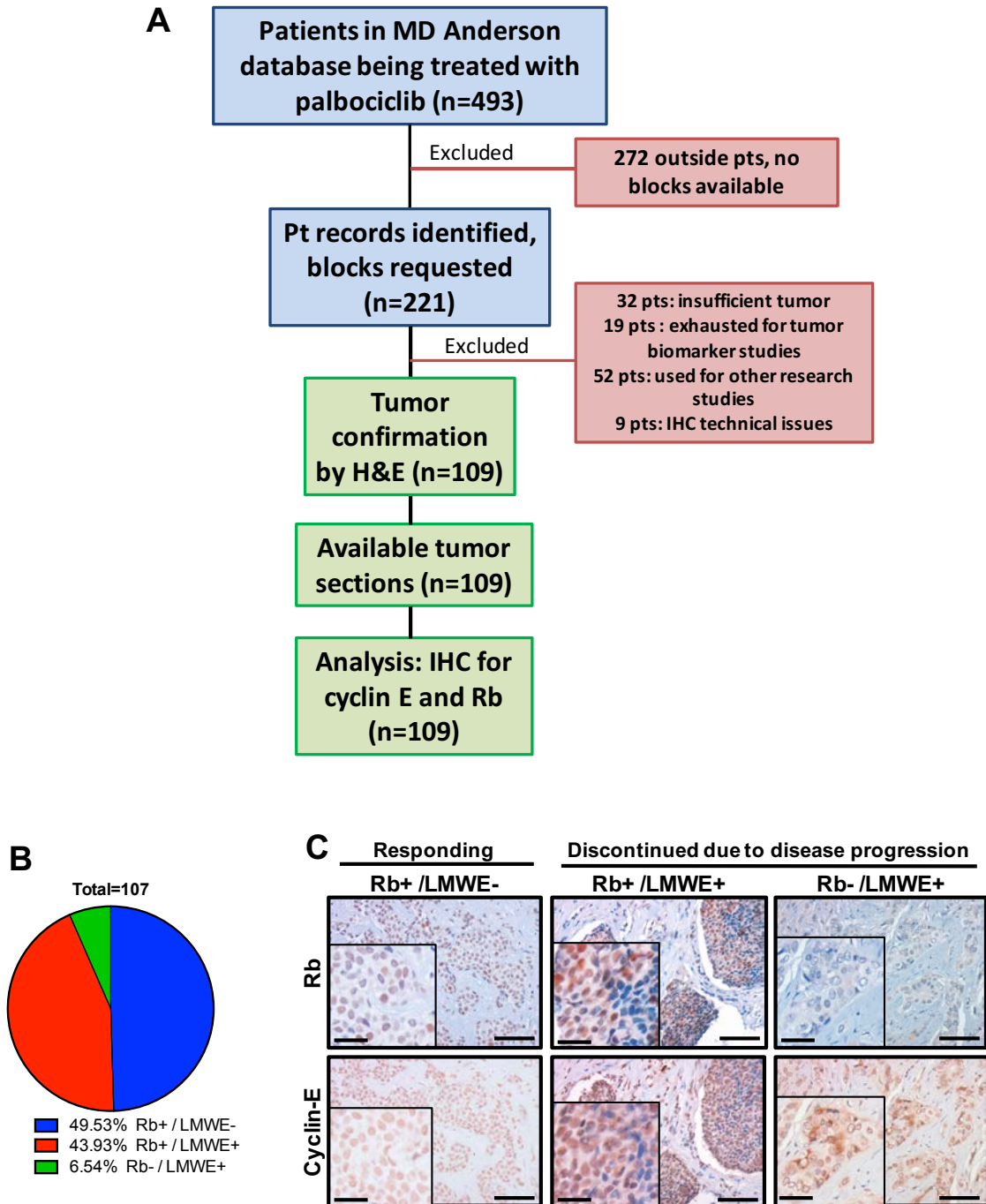


Figure 58: Expression of Rb and LMWE in advanced ER positive breast cancer patients treated with palbociclib: A) Schematic showing the total number of palbociclib treated patient tissues obtained and stained for Rb and cyclin-E. B) Proportion of 107 breast cancer patients treated with palbociclib with Rb+/LMWE-, Rb+/LMWE+ or Rb-/LMWE+ status. C) Representative images from immunohistochemical analysis of Rb and LMW-E in tumors from patients with ER+ breast cancer treated with palbociclib, classified on the basis of response and Rb/LMW-E status. Scale bars equal 50 μ m and insert scale bars equal 20 μ m. Patient database were created and maintained by collaborators from Breast Medical Oncology department at MD Anderson - Dr. Debu Tripathy, Dr. Meghan Karuturi and Akshara Raghavendra. IHC analysis was performed by Dr. Cansu Karakas from the Keyomarsi lab.

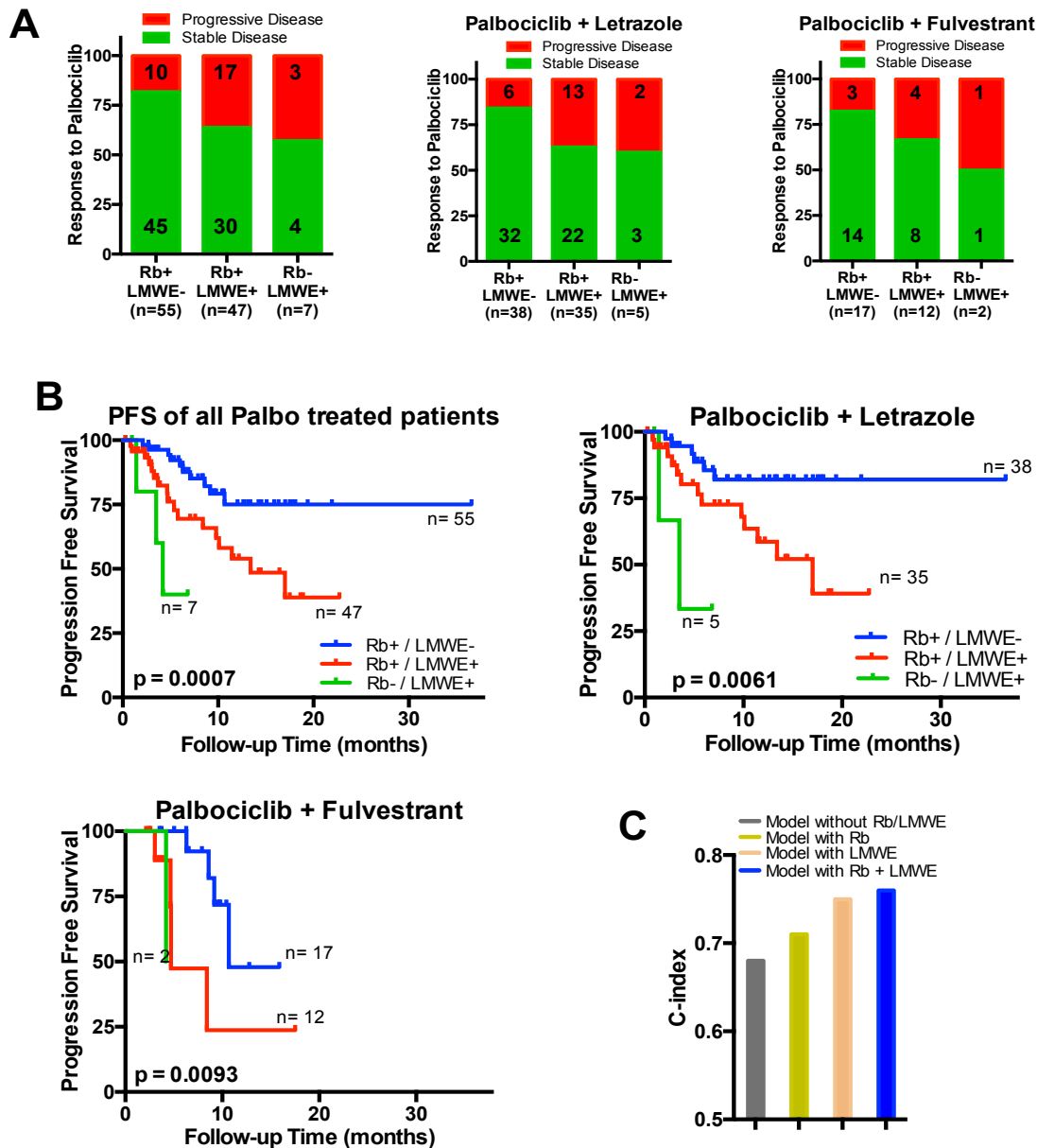


Figure 59: Correlation between expression of Rb and LMWE and response to palbociclib in advanced ER positive breast cancer patients: A) Proportion of 109 breast patients treated with palbociclib with Rb+/LMW-, Rb+/LMWE+ or Rb-/LMWE+ status and their disease progression (response to palbociclib). B) Kaplan-Meier curves showing progression-free survival duration (in months) among 109 patients with advanced ER+ breast cancer classified on the basis of their tumoral expression of Rb and cyclin E and separated based on letrozole and fulvestrant. Survival curves were censored at disease progression or date of last follow-up. C) Concordance-index (C-index) of the multivariate cox model with progesterone receptor, prior therapy for metastatic disease only (without Rb) and the addition of Rb and LMW-E. ns: $p > 0.05$; * $p < 0.05$; ** $p < 0.01$; *** $p < 0.001$; **** $p < 0.0001$. IHC analysis was performed by Dr. Cansu Karakas, Keyomarsi lab. Statistical analysis was performed Min Yi, Breast Surgical oncology.

Table 12: Cox model for univariate analyses for the factors associated with PFS

Factor	Palbociclib + letrozole (n=78)			Palbociclib + fulvestrant (n=31)		
	HR	P value	95% CI	HR	P value	95% CI
Age at diagnosis, years	1.0	0.06	0.9-1.0	1.0	1.0	0.9-1.1
Height (cm)	0.6	0.3	0.2-1.7	1.2	0.02	1.02-1.3
Weight	1.0	0.8	0.9-1.1	1.0	0.6	0.96-1.02
Race						
White	Referent			Referent		
Others	0.99	0.3	0.96-1.01	0.8	0.9	0.1-6.8
Clinical tumor stage at diagnosis						
0/I	Referent			Referent		
II	0.7	0.5	0.2-2.2	2.0	0.6	0.2-21.9
III	1.3	0.7	0.4-3.9	1.7	0.7	0.2-18.7
IV	0.1	0.02	0.01-0.6	6.1	0.1	0.7-55.0
Tumor Histology						
Ductal	Referent			Referent		
Others	0.9	0.9	0.2-3.8	1.4	0.7	0.3-7.1
Lymphatic/vascular invasion						
Yes	Referent			Referent		
No	1.8	0.2	0.7-4.2	0.9	0.8	0.2-3.3
Adjuvant Chemotherapy						
No	Referent			Referent		
Yes	3.4	0.007	1.4-8.2	0.3	0.09	0.1-1.2
Tumor grade						
I/II	Referent			Referent		
III	0.6	0.4	0.2-1.8	1.7	0.6	0.2-14.6
Progesterone receptor status						
Positive	Referent			Referent		
Negative	3.2	0.02	1.2-8.9	-		
Rb status						
Negative	Referent			Referent		
Positive	0.2	0.04	0.04-0.9	0.09	0.09	0.01-1.4
LMWE status						
Negative	Referent			Referent		
Positive	3.2	0.02	1.2-8.2	5.2	0.02	1.3-20.3
Rb/LMWE status						
Rb+/LMWE-	Referent			Referent		
Rb+/LMWE+	2.9	0.03	1.01-7.6	4.7	0.03	1.1-19.3
Rb-/LMWE+	9.2	0.008	1.8-47.4	23.8	0.04	1.3-450.1
Bone /soft tissue vs. any visceral						
Bone / soft tissue	Referent			Referent		
Any visceral	2.6	0.03	1.1-6.2	2.2	0.2	0.6-8.3
Prior therapy for metastatic disease						
None	Referent			Referent		
Hormonal	0.9	0.9	0.1-6.8	0.8	0.8	0.1-4.6
Chemotherapy and/or hormonal	2.6	0.04	1.03-6.7	0.6	0.7	0.1-5.5
Time from completion of adjuvant hormonal therapy (years)						
None	Referent			Referent		
< 1 year	7.32e-16	1.0	0-	2.1	0.4	0.3-13.0
>= 1 year	1.9	0.2	0.8-4.4	0.7	0.7	0.2-3.4

Table 13: Cox model for multivariable analyses for the factors associated with PFS

	Palbociclib + letrozole			Palbociclib + fulvestrant		
Factor	HR	P value	95% CI	HR	P value	95% CI
Progesterone receptor status						
Positive	Referent			Referent		
Negative	4.5	0.007	1.5-13.4		NS	
Prior therapy for metastatic disease						
None	Referent			Referent		
Hormonal	2.4	0.4	0.3-21.4		NS	
Chemotherapy and/or hormonal	4.1	0.006	1.5-11.2		NS	
Rb status						
Negative	Referent			Referent		
Positive	0.2	0.06	0.04-1.03	0.2	0.3	0.01-3.3
LMWE status						
Negative	Referent			Referent		
Positive	3.2	0.03	1.1-8.7	4.7	0.03	1.1-19.3
C-index			0.76			
CPE			0.73			
AIC			153.3			

7.3. DISCUSSION

Identification of reliable predictive biomarkers for palbociclib has proven challenging, given the large patient sample that would be required, since a predictive biomarker identifies factors affecting both patient survival and response to the drug. While previous *in vitro* studies showed that Rb, cyclin D, and p16 could predict response to palbociclib (Wiedemeyer, Dunn et al. 2010, Konecny, Winterhoff et al. 2011, Cen, Carlson et al. 2012), results from Phase II/III trials showed no significant correlation between drug response and the expression of p16 (Finn, Crown et al. 2015), Ki67, *CCND1* amplification (Clark, Karasic et al. 2016), *PIK3CA* or *ESR1* (Turner, Jiang et al. 2016) mutational status, leaving no established prognostic or predictive biomarkers (Cristofanilli, Turner et al. 2016). Further, a number of recent clinical trials with ribociclib (MONALEESA-2) and abemaciclib (MONARCH-1) also incorporated extensive biomarker analysis testing for a potential correlation between expression of Rb, cyclin D, p16, *PIK3CA* mutation and *ESR1* mutation Hortobagyi, Stemmer et al. 2016)(Maura N. Dickler 2017) . However, no significant difference in the hazard ratios were observed with any of these genes or proteins as a single molecule biomarker (Maura N. Dickler 2017)Hortobagyi, Stemmer et al. 2016).

One consistent observation across the clinical studies is that the tumors from the resistant patients exhibited no decrease in Ki67 and pRb following CDK4/6 inhibitor treatment Hortobagyi, Stemmer et al. 2016)(Patnaik, Rosen et al. 2016). However, none of the biomarkers tested can predict the hyperphosphorylation of Rb (Akli, Bui et al. 2010). Interestingly, the low molecular weight isoforms of cyclin E (LMWE) has been previously documented to mediate hyperphosphorylation of Rb (Akli, Bui et al. 2010). This is the mechanism by which LMWE mediate deregulation of the G1/S checkpoint and resistance to letrozole mediated G1 arrest. This suggests that LMWE (in combination with Rb) might be the most reliable biomarker for palbociclib and other CDK4/6 inhibitors as shown in this chapter.

An interesting observation from our immunohistochemistry analysis was the difference in the number of subgroups seen when patients were classified based on protein expression of Rb and LMWE. In the first cohort of 829 early stage patients, we observed four subgroups, while in the metastatic cohort of patients who received palbociclib, the subgroup of Rb- LMWE- patients were not present. Interestingly, this subgroup of patients had the best prognosis, despite the loss of Rb. Hence it is possible that these patients had lower proliferation and tumor grade, resulting in better response and hence they did not metastasize or have relapse of tumor.

Thus, results from this chapter use a dual biomarker strategy and show that Rb and LMWE proteins are reliable prognostic biomarkers in advanced estrogen receptor positive breast cancers. Since we did not have a parallel treatment arm in the absence of palbociclib treatment, the effect of the therapy could not be examined and hence Rb and LMWE could not be evaluated as predictive biomarkers of palbociclib. Future clinical trial investigations in early stage breast cancer patients, in the neoadjuvant setting, where patients are treated with either palbociclib + letrozole or letrozole alone, would reveal the predictive utility of these proteins for palbociclib treatment. Thus, we propose that a simple immunohistochemical assay for Rb and LMW-E can be used clinically to identify patients who are likely to have a response to palbociclib and its combination with autophagy inhibitor.

CHAPTER 8: SYNERGISM BETWEEN CDK4/6 AND AUTOPHAGY INHIBITION IN

TNBC AND OTHER SOLID TUMORS

8.1. INTRODUCTION

8.1.1. PRE-CLINICAL STUDIES WITH CDK4/6 INHIBITORS IN TNBC

The cell line based screen performed to examine the sensitivity of a range of breast cancer lines to the CDK4/6 inhibitor showed that the majority of the cells that are sensitive to palbociclib belonged to the ER positive subtypes (Finn, Dering et al. 2009). These results led to further pre-clinical and clinical studies using the CDK4/6 inhibitors in the ER positive breast cancer, which were highly successful (Asghar, Witkiewicz et al. 2015). However, careful examination of the cell lines used for the original study revealed that there are numerous HER2 positive and a few triple negative breast cancer (TNBC) cell lines (MDA-MB-435, MDA-MB-231, HCC1395, HS578T) which were seen to be sensitive to palbociclib treatment, albeit, TNBC cells comprised a smaller proportion of the sensitive cell lines (Finn, Dering et al. 2009). A more recent study showed that palbociclib has an effect in the TNBC cell line MDA-MB-231 *in vitro* and *in vivo* and inhibits cancer metastasis in these cells through a DUB3-SNAIL mediated mechanism. Through this mechanism, CDK4/6 directly phosphorylates the deubiquitinase DUB3, which is essential to stabilize SNAIL1, a key EMT gene (Liu, Yu et al. 2017). Another study which examined the subtypes of TNBC and their sensitivity to palbociclib showed that the luminal AR (LAR) TNBC subtype was most sensitive to palbociclib, with the basal subtype being the most resistant (Uzma Asghar 2016). They also showed that the basal subtype had a greater CDK2 high population and higher cyclin E expression than the LAR subtype which enabled caused them to be resistant to palbociclib induced cell cycle arrest (Uzma Asghar 2016). Thus, these studies suggest potential utility for palbociclib in TNBC subtypes of breast tumors as well, and this requires further investigation.

8.1.2. PRE-CLINICAL STUDIES WITH CDK4/6 INHIBITORS IN SOLID TUMORS

Over the recent years, several studies have examined the anti-proliferative and anti-tumor effect of the CDK4/6 inhibitors in cancers other than breast cancer and **Table 14** summarizes these pre-clinical studies. Numerous cancers apart from breast cancer exhibit upregulation or over activation of the G1/S due to amplification or overexpression of proteins such as cyclin D1 and CDK4, making them susceptible to CDK4/6 inhibition by palbociclib, as shown by studies in mantle cell lymphoma (Marzec, Kasprzycka et al. 2006), acute myeloid leukemia (Wang, Wang et al. 2007), multiple myeloma (Baughn, Di Liberto et al. 2006), ovarian cancer (Konecny, Winterhoff et al. 2011, Taylor-Harding, Aspuria et al. 2015), lung adenocarcinoma (Sumi, Kuenzi et al. 2015), pancreatic (Franco, Balaji et al. 2016), prostate (Comstock, Augello et al. 2013), liposarcoma (Zhang, Sicinska et al. 2014), hepatocellular carcinoma (Rivadeneira, Mayhew et al. 2010), glioblastoma (Michaud, Solomon et al. 2010, Cen, Carlson et al. 2012), renal cancer melanoma (Yoshida, Lee et al. 2016) and colorectal cancer (Lee, Helms et al. 2016). All these studies show that palbociclib treatment of the cancer cell lines *in vitro* results in the induction of G1 arrest, growth inhibition and senescence, while inducing significant anti-tumor effects in xenograft tumors *in vivo* (**Table 14**). Further, some of these studies also examined biomarkers of sensitivity to palbociclib, most of which showed the importance of the Rb positivity and or loss of p16 for drug response (Konecny, Winterhoff et al. 2011, Cen, Carlson et al. 2012, Franco, Balaji et al. 2016). A study in ovarian cancer also showed that cyclin E expression mediates resistance to CDK4/6 inhibitor treatment (Taylor-Harding, Aspuria et al. 2015).

Cancer type	Drug	Cell culture	Animal Model	Biomarkers
Ovarian cancer	Palbociclib	Yes	Yes	Rb, p16INK4A, cyclin E
Lung adenocarcinoma	Palbociclib	Yes	Yes	-
Pancreatic cancer	Palbociclib	Yes	Yes	-
Prostate cancer	Palbociclib	Yes	Yes	-
Liposarcoma	Palbociclib, ribociclib	Yes	Yes	CDK4
Hepatocellular carcinoma	Palbociclib	Yes	Yes	Rb, p16INK4A
Glioma	Palbociclib	Yes	Yes	Rb, p16INK4A
Melanoma	Palbociclib, abemaciclib	Yes	Yes	-
Colon cancer	Palbociclib	Yes	Yes	-
Mantle cell lymphoma	Palbociclib	Yes	Yes	-
Acute myeloid leukemia	Palbociclib	Yes	Yes	-
Multiple myeloma	Palbociclib	Yes	Yes	-

Table 14: Pre-clinical studies with CDK4/6 inhibitors in other cancers: Summary of pre-clinical studies in cancers with the CDK4/6 inhibitors

8.1.3. CLINICAL STUDIES WITH CDK4/6 INHIBITORS IN SOLID TUMORS

The pre-clinical studies detailed above has led to numerous clinical studies in solid tumors and hematological malignancies, a summary of which is described in **Table 15**. This includes clinical studies testing for the safety, toxicity and efficacy of the CDK4/6 inhibitors as single agent in numerous solid tumors (Sherr, Beach et al. 2016). Most of these studies showed significant clinical response with the CDK4/6 inhibitors, resulting in pathological complete response or stable disease in over 40% of the patients treated (Sherr, Beach et al. 2016). For example, a phase I study in 17 heavily pre-treated mantle cell lymphoma patients, palbociclib treatment exhibited significant reduction in tumor proliferation (as measured by Ki67 and fluorothymidine PET) and Rb phosphorylation in most patients, with 5 out of the 17 patients achieving a progression-free survival of greater than 1 year (Leonard, LaCasce et al. 2012). Moreover, in a phase II clinical study of 30 liposarcoma patients whose tumors were Rb positive and CDK4 amplified, 66% of the patients achieved progression-free status at the end of 12 weeks, with 8 patients remaining on the study for more than 40 weeks (Dickson, Tap et al. 2013). Further, to improve the selectivity of the drug treatment, several of these clinical trials are designed to select patients based on biomarkers identified in pre-clinical studies such as Rb, loss of p16 and cyclin D amplification (O'Leary, Finn et al. 2016). However, it is not clear if these biomarkers could be predictive indicators of palbociclib, as none of the aforementioned trials were designed to examine the predictive value of these biomarkers. Finally, some of the more recent clinical trials have been designed to test the combination of the CDK4/6 inhibitors with drugs such as MEK inhibitors (Sherr, Beach et al. 2016).

Cancer type, Identifier	Drugs, phase	Trial design
Solid tumors NCT00141297	Palbociclib (Phase 1)	Drug dose was established; Stable disease realized in 19 of 74 patients
Advanced solid tumors NCT01237236	Ribociclib (Phase 1)	Drug dose was established; Stable disease in 14% of patients
Advanced solid tumors NCT01394016	Abemaciclib (Phase 1)	Dose finding and toxicity studies; drug efficiently crossed blood brain barrier
Advanced tumors NCT02187783	Ribociclib (Phase 2)	Determine efficacy of CDK4/6 treatment in tumors with p16 loss or cyclin D1/D3 amplification
Mantle cell lymphoma NCT00420056	Palbociclib (Phase 1)	most patients out of 17 showed reduction in proliferation with PFS of > 1 year.
Mantle cell lymphoma NCT01739309	Abemaciclib (Phase 2)	5 out of 22 patients had partial response and 9 patients with stable disease.
Liposarcoma NCT01209598	Palbociclib (Phase 2)	66% of 30 patients were progression-free after 12 weeks with 8 patients on study for >40 weeks
Non-small cell lung cancer NCT01291017	Palbociclib (Phase 2)	8 of 16 patients with <i>CDKN2A</i> loss were progression-free > 4 months.
Non-small cell lung cancer NCT01394016	Abemaciclib (Phase 1)	In 15 of 31 patients, overall disease control rate was 49% with 6 month PFS in 26%.
Glioblastoma multiforme NCT01394016	Abemaciclib (Phase 1)	2 of 17 patients showed prolonged time to progression.
Melanoma NCT01394016	Abemaciclib (Phase 1)	1 out 26 patients with <i>NRAS</i> mutation and <i>CDKN2A</i> loss achieved partial response
RAS-mutant cancers NCT02022982	Palbociclib PD0325901 (Phase 1/2)	Phase 1 trial with expansion in <i>KRAS</i> mutant NSCLC; not reported
RAS-mutant cancers NCT02065063	Palbociclib Trametinib (Phase 1)	Phase 1 trial with expansion in <i>NRAS</i> mutant melanoma; not reported
Mantle Cell Lymphoma NCT02159755	Palbociclib Ibrutinib (Phase 1)	Trial of palbociclib and ibrutinib in previously treated MCL; not reported

Table 15: Clinical studies with CDK4/6 inhibitors in other cancers: Summary of completed and ongoing clinical studies with the CDK4/6 inhibitors in other cancers

8.1.4. GAP IN KNOWLEDGE

While few studies in TNBC have suggested an efficacy for CDK4/6 inhibition by palbociclib, a detailed analysis has not been conducted with the goal of improving efficacy and identifying biomarkers. Further, studies in other solid cancers are still preliminary leaving us with several unanswered questions:

1. Can Rb and cyclin E be used to identify the most responsive TNBC cell lines?
2. Would the addition of autophagy inhibitor improve efficacy of palbociclib treatment in TNBC cell lines?
3. Can intact G1/S checkpoint (Rb+ LMWE-) be used to identify responders to palbociclib among other solid tumor cell lines?
4. Will the combination of palbociclib and autophagy inhibitors be synergistic in other solid cancers?

Thus, this chapter aims at addressing these questions in detail and devising palbociclib based treatment strategies for TNBC and other solid tumors.

8.2. RESULTS

8.2.1. PALBOCICLIB MEDIATED GROWTH INHIBITION IN TNBC CELL LINES

While the CDK4/6 inhibitor, palbociclib is currently used clinically for the treatment of advanced ER positive breast cancer, we wanted to examine the potential of treating other subtypes of breast cancer, such as Triple Negative Breast Cancer (TNBC) with CDK4/6 inhibitor treatment, when selected based on reliable biomarkers. The Cancer Genome Atlas (TCGA) analysis showed that about 64% of TNBC patient tumors (CDK4 - 22%, CDK6 – 37%, cyclin D – 5%) had deregulation in the CDK4/6-Cyclin D pathway, with mRNA upregulation of CDK4 and CDK6 being the most prevalent alteration in TNBC tumors (Figure 6A,6C). This highlights the importance of the G1/S checkpoint in these cancers.

To interrogate the response of TNBC cell lines to CDK4/6 inhibition, we examined 7 TNBC cell lines (HCC38, MDA-MB-231, SUM-159, BT-549, MDA-MB-468, HCC-1806 and MDA-MB-157) with varying protein expression levels of Rb and cyclin E (**Figure 60A**), and examined the ability of Rb and LMWE to predict sensitivity to palbociclib. Palbociclib dose response studies showed that cell lines that were positive for Rb and negative for LMWE (HCC38, MDA-MB-231, SUM-159) were significantly more sensitive than cell lines with deregulated Rb and / or LMWE (**Figures 60B,C**), exhibiting 6-8 fold lower IC50 values (**Figure 60D,E**). Additionally, palbociclib treatment resulted in a significant dose-dependent irreversible G1 arrest with 6 days of treatment and 4 days of recovery in cell lines with intact Rb and Cyclin E, MDA-MB-231 and SUM-159 (**Figures 60F,G**). This induction of G1 arrest upon palbociclib treatment was absent in the cell lines with deregulated Rb and / or LMWE +ve status, MDA-MB-468 and MDA-MB-157 (**Figure 53F**). Moreover, palbociclib treatment in cell lines with intact Rb and Cyclin E (MDA-MB-231 and SUM-159) resulted in a significant dose-dependent reduction in colony formation (**Figure 61A**) and induction of sustained growth inhibition (**Figure 61B**), but not in cell lines with deregulated Rb and / or LMWE + status (MDA-MB-468 and MDA-MB-157). Finally, long term treatment (6 days) of TNBC cell lines with the CDK4/6

inhibitor, palbociclib induced dose-dependent senescence (indicated by an increase in SA- β gal activity) only in cell lines that are Rb+ve and LMWE-ve, MDA-MB-231 and SUM-159
(Figure 61C)

Thus, these results demonstrate that CDK4/6 inhibition also has the potential to treat TNBC cell lines, given that they are chosen based on the expression of Rb and LMWE proteins.

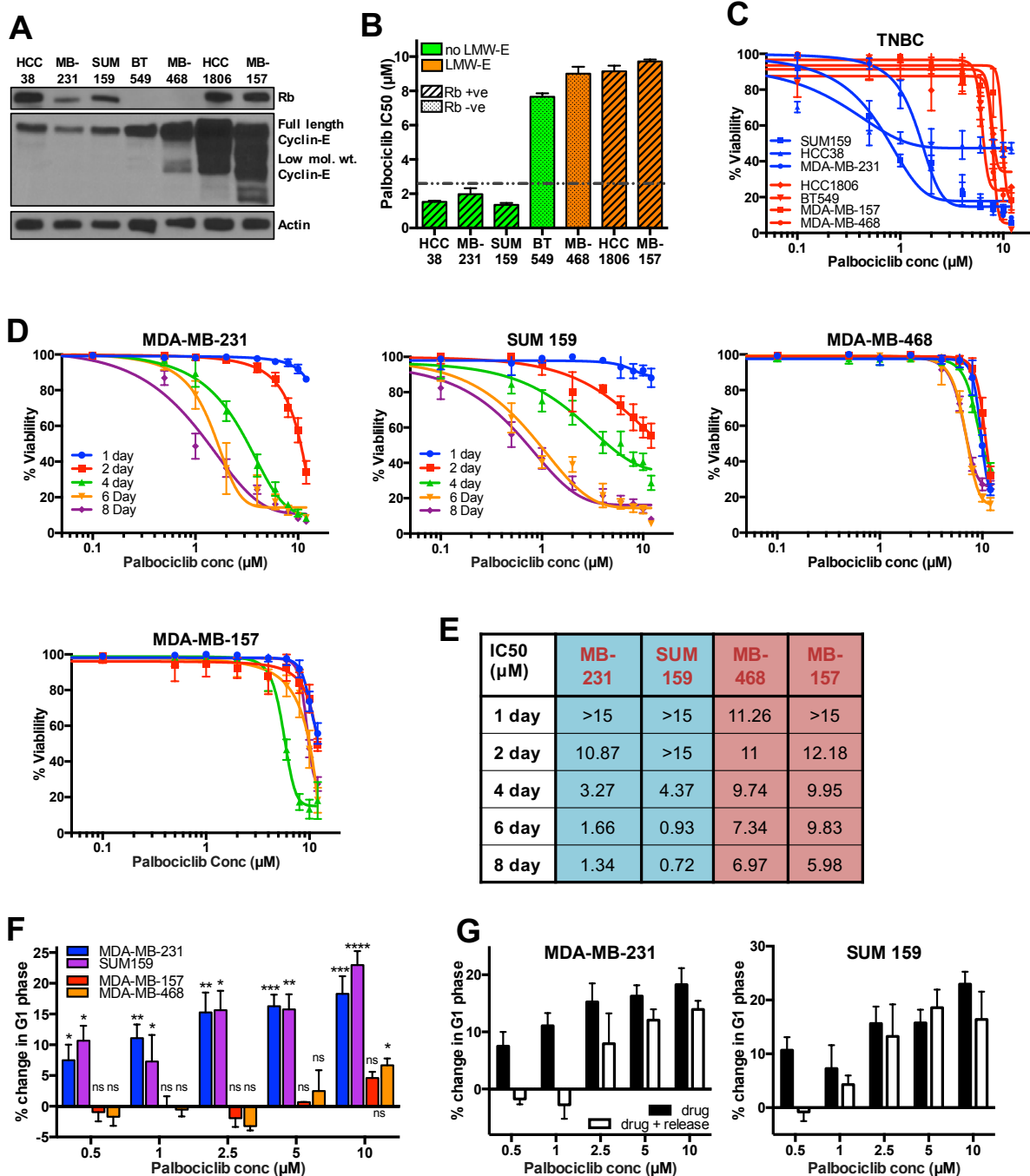


Figure 60: Palbociclib mediated induction of growth inhibition and cell cycle arrest in TNBC cell lines: A) Western blot for Rb and Cyclin-E in Triple negative breast cancer (TNBC) cell lines. B) IC₅₀ values from drug response experiments in TNBC cell lines treated with palbociclib for 6 days. C-E) Impact on the growth of the indicated triple-negative breast cancer (TNBC) cell lines of treatment with DMSO or increasing concentrations (conc) of palbociclib (0.01 to 12 μM) for 6 days. Crystal violet staining was performed on day 12 to assess viability and determine the half-maximal inhibitory concentration (IC₅₀) values (E). F, G) MDA-MB-231, SUM-159, MDA-MB-468, and MDA-MB-157 cells were treated with DMSO or varying concentrations of palbociclib 6 days, allowed to recover for 4 days and subjected to F) cell cycle analysis to assess change in G1 phase and G) cell cycle analysis to determine the effect of recovery (release) on change in the G1 phase. All data represent mean ± SD from three independent experiments; p-values were calculated in comparison to DMSO (Control) unless indicated. ns: p > 0.05; *p < 0.05; **p < 0.01; ***p < 0.001; ****p < 0.0001.

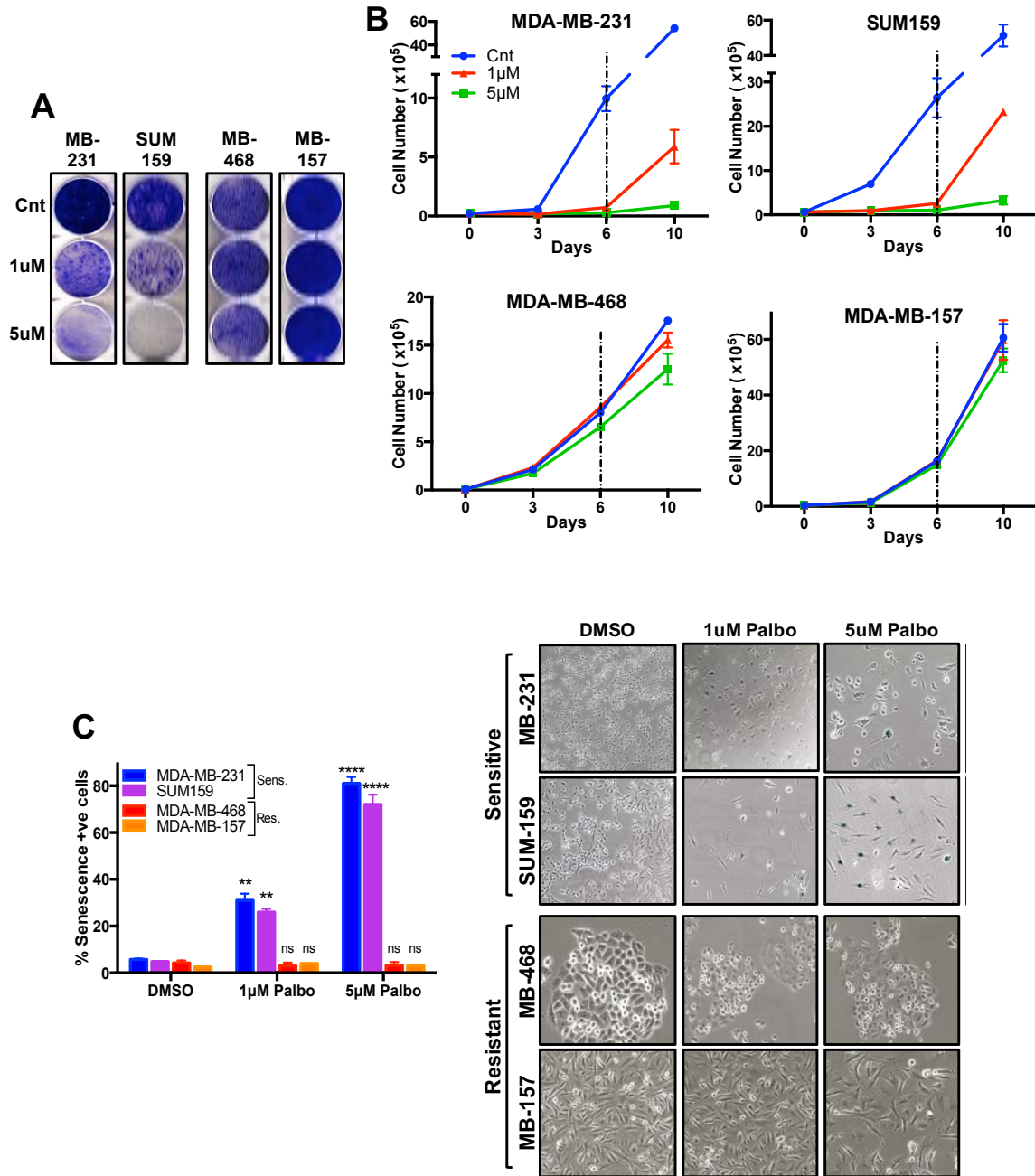


Figure 61: Palbociclib mediated induction of growth inhibition and senescence in TNBC cell lines: A) Clonogenic assay in TNBC cell lines MDA-MB-231, SUM-159, MDA-MB-468, and MDA-MB-157 cells treated with DMSO (Cnt) or palbociclib (1μM, 5μM) for 6 days and allowed to recover for 6 days. MDA-MB-231, SUM-159, MDA-MB-468, and MDA-MB-157 cells were treated with DMSO or palbociclib (Palbo; 1μM, 5μM) for 6 days and allowed to recover for 4 days to examine reversibility. Cells were then subjected to B) cell counting to assess proliferation and C) Senescence measurement by SA-β gal staining and representative images. All data represent mean±SD from three independent experiments; p-values were calculated in comparison to DMSO (Control) unless indicated. ns: $p>0.05$; * $p<0.05$; ** $p<0.01$; *** $p<0.001$; **** $p<0.0001$.

8.2.2. SYNERGISM BETWEEN PALBOCICLIB AND AUTOPHAGY INHIBITION IN TNBC CELL LINES

We next asked if the combination of CDK4/6 and autophagy inhibition may be synergistic in TNBC cell lines and if Rb and LMWE expression could be utilized to identify response cell lines. First, we wanted to interrogate if CDK4/6 inhibition via palbociclib treatment induces autophagy, at levels comparable to that induced in ER positive breast cancer cell lines. Measurement of Monodansylcadavarine (MDC) staining showed that treatment with palbociclib at low and on-target doses significantly increased the MDC staining in ER positive and TNBC cell lines that were Rb+ve and LMWE-ve (MDA-MB-231, SUM-159), but not in TNBC cell lines with a deregulated G1/S checkpoint (MDA-MB-468) (**Figure 62A**). Moreover, palbociclib treatment resulted in significant increase in GFP+ve LC3 puncta in the G1/S checkpoint intact MDA-MB-231 cells, but not in MDA-MB-468 cells that have a deregulated G1/S checkpoint (**Figures 62B,C**). Further, treatment with the lysosomal block, chloroquine (CQ) further increased the GFP-LC3 puncta in MDA-MB-231 cells, indicating that the autophagy induced by palbociclib has an intact flux (**Figure 62B,C**), similar to the autophagy induced in ER positive breast cancer cell lines.

Since palbociclib mediated CDK4/6 inhibition induces autophagy in TNBC cell lines with an intact G1/S checkpoint, we next examine if the combination of CDK4/6 and autophagy inhibition would be synergistic in these cells. Treatment with the combination of low or on-target dose of palbociclib and autophagy inhibitor, HCQ resulted in greater reduction in colony formation (**Figure 63A**) and induction of an irreversible growth inhibition (**Figure 63B**), in TNBC cell lines which are Rb+ve and LMWE-ve, MDA-MB-231 and Sum-159. This synergistic effect was not observed in the TNBC cell lines with deregulated Rb or/ and cyclin E (MDA-MB-157 and MDA-MB-468) (**Figure 63A,B**), which are also resistant to palbociclib as a single agent. Finally, treatment with the autophagy inhibitor, HCQ further sensitized Rb+/LMWE- cells (MDA-

MB-231 and SUM-159) to palbociclib, inducing significantly elevated senescence even at lower palbociclib doses (**Figure 63C**).

Thus, these results show that TNBC lines with a intact G1/S checkpoint (Rb+ve / LMWE-ve) are responsive to treatment with the CDK4/6 inhibitor palbociclib and can be effectively treated by the combination of CDK4/6 and autophagy inhibition.

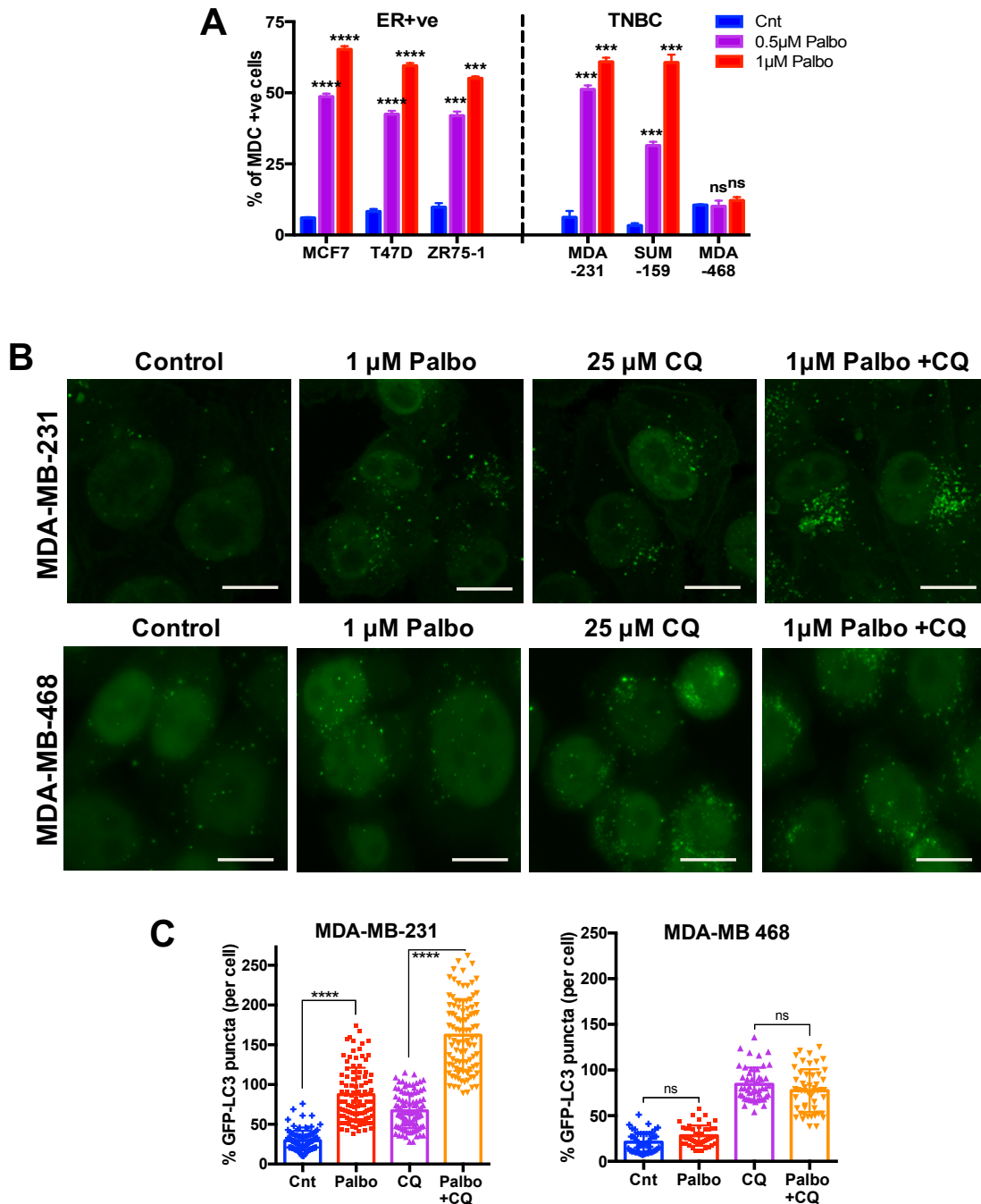


Figure 62: Palbociclib mediated induction of autophagy in TNBC cell lines: A) Measurement of monodansylcadavarine (MDC) positive acidic vesicles, including autophagosomes, by flow cytometry in ER positive (MCF7, T47D, ZR75-1) and TNBC (MDA-MB-231, SUM-159, MDA-MB-468) cell lines treated with varying concentrations of palbociclib for 6 days. B) Representative confocal images of GFP-LC3 expressing MDA-MB-231 and MDA-MB-468 cells treated with 25 µM CQ (for 1 hour), 1 µM palbociclib or combination of palbociclib and CQ for 48 hours. Scale bars are 50 µm. C) Quantification of GFP-LC3 puncta in MDA-MB-231 and MDA-MB-468 cells treated with 1 µM palbociclib and/or 25 µM Chloroquine (CQ) for 48 hours. All data represent mean ± SD from three independent experiments; p-values were calculated in comparison to DMSO (Control) unless indicated. ns: p>0.05; *p<0.05; **p<0.01; ***p<0.001; ****p<0.0001.

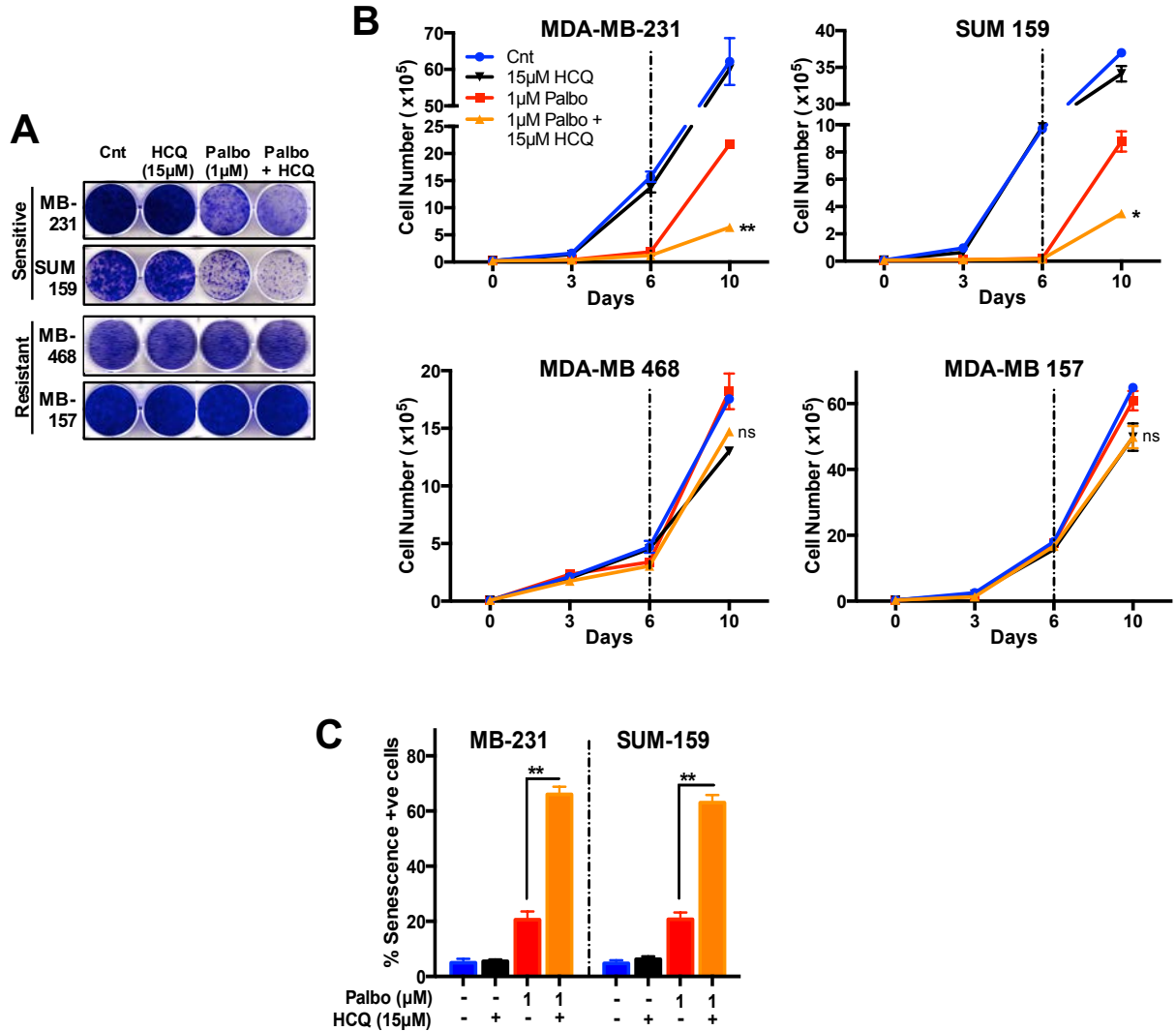


Figure 63: Synergism between palbociclib and autophagy inhibition in TNBC cell lines: MDA-MB-231, SUM-159, MDA-MB-468, and MDA-MB-157 cells were treated with DMSO or palbociclib (Palbo; 1µM, 5µM) and/or 15 µM autophagy inhibitor hydroxychloroquine (HCQ) for 6 days. Cells were allowed to recover for 4 or days to examine reversibility and subjected to A) Clonogenic assay, B) cell counting to assess proliferation (p-values calculated in comparison with 1 µM palbociclib), and C) SA-β galactosidase assay to measure senescence with representative images. All data represent mean±SD from three independent experiments; p-values were calculated in comparison to DMSO (Control) unless indicated. ns: p>0.05; *p<0.05; **p<0.01; ***p<0.001; ****p<0.0001.

8.2.3. SYNERGISM BETWEEN PALBOCICLIB AND AUTOPHAGY INHIBITION IN TNBC

PDX MODEL

Having shown the synergism between palbociclib and autophagy inhibition in TNBC cell *in vitro*, we next examined this synergy *in vivo*, using patient derived xenograft (PDX) tumors that has been characterized to be Triple Negative and have high levels of Rb and low Cyclin-E. Once established, the PDX tumors were randomized into four treatment arms i) vehicle, ii) palbociclib (25 mg/kg/day), iii) hydroxychloroquine (60 mg/kg/day) and iv) combination of palbociclib and HCQ for 21 days (**Figure 64A**).

Treatment with the drug combination of palbociclib and HCQ significantly decreased tumor growth (**Figure 64C**), resulting in much smaller tumors (**Figure 64B**), compared to treatment with vehicle or palbociclib or HCQ as single agent. Combination treatment of the PDX tumors also resulted in a significant decrease in tumor weights compared to the other treatment arms (**Figure 64D**). Moreover, treatment with the combination of palbociclib and HCQ significantly prolonged the survival of the mice compared to the other treatment arms (**Figure 64E**). Finally, to evaluate the toxicity with the drug treatments, we measured the weight of the mice during the treatment period and found no significant difference in the weight of the mice with all the treatment arms (**Figure 64F**), indicating that the treatment including the combination is well tolerated.

Thus, these results demonstrate that the combination of CDK4/6 and autophagy inhibitors are synergistic in TNBC tumors *in vivo*, given that they have an intact G1/S checkpoint (Rb+ve LMWE-ve).

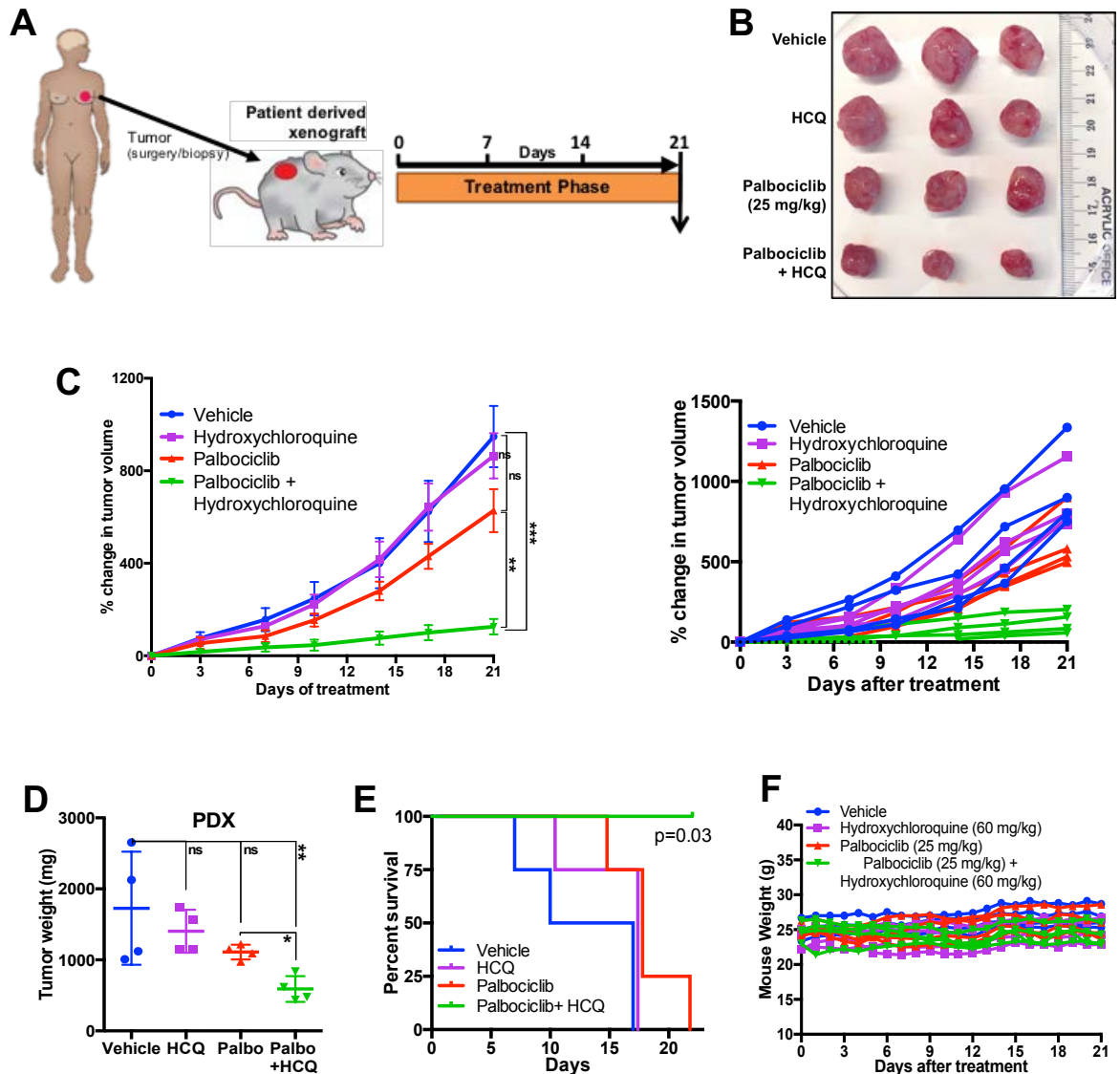


Figure 64: Synergism between palbociclib and autophagy inhibition in TNBC PDX model:
A) Schematic showing establishment and treatment schedule of patient-derived xenograft (PDX) tumors with vehicle (0.5% methylcellulose and PBS), 60 mg/kg HCQ, 25 mg/kg palbociclib, or palbociclib+ HCQ for 21 days. B) Representative PDX tumor images from each treatment group harvested at end of 21 days treatment as described in A. C) Percentage change in volume (normalized to Day 0) of patient derived xenograft (PDX) tumors upon treatment after treatment as described in A for 21 days. Data represented as Mean \pm SEM. n=4 for each group. D) Weight of PDX tumors treated harvested after 21 days of treatment as described in A. n=4 for each group. E) Kaplan Meier survival curves of mice with PDX tumors treated as in A. Death of mice and tumors exceeding 1000mm³ were utilized as cut-off endpoints for the curve. F) Individual mouse weights during 21 days of treatment as described in A. p-values were calculated in comparison to treatment with vehicle (Control). ns: p>0.05; *p<0.05; **p<0.01; ***p<0.001; ****p<0.0001. PDX tumors were developed by Dr. Xian Chen, psotdoc from Keyomarsi lab.

8.2.4. PALBOCICLIB TREATMENT IN OTHER SOLID TUMOR CELL LINES

While the CDK4/6 inhibitor is currently approved for clinical use only in ER+/Her2- advanced breast cancer, numerous pre-clinical and clinical studies have shown activity for Palbociclib in other cancers such as Melanoma, Ovarian, Prostate, Glioblastoma, Gastric, Colorectal (CRC), Head and neck squamous cell carcinoma (HNSCC), Pancreatic ductal adenocarcinoma (PDAC) and lung adenocarcinoma (Fry, Harvey et al. 2004, Baughn, Di Liberto et al. 2006, Michaud, Solomon et al. 2010, Konecny, Winterhoff et al. 2011, Cen, Carlson et al. 2012, Comstock, Augello et al. 2013, Witkiewicz, Borja et al. 2015, Lee, Helms et al. 2016, Tao, Le Blanc et al. 2016, Yoshida, Lee et al. 2016, Ziemke, Dosch et al. 2016).

With this rationale, we hypothesized that CDK4/6 inhibition would be effective in other solid tumors as well, given that Rb and cyclin E are used as biomarkers to predict response. To test this hypothesis, we examined several Ovarian (HeyA8, 59M, FUOV1), Pancreatic (Panc-1, BxPc-3), Lung (Calu-1, H358, A549), Colorectal (Colo-205, SW-620, HCT116) and Prostate (PC3, Du145) cancer cell lines, with varied protein levels of Rb and Cyclin-E (**Figure 65A**). Palbociclib dose response studies revealed that cell lines with an intact Rb and low cyclin E (no LMWE) namely HeyA8, 59M, Panc-1, BxPc-3, Calu-1, H358, Colo-205, SW-620 and PC3, showed significant dose-dependent growth inhibition upon palbociclib treatment, with low (within the on-target range) IC50 values (<2uM) (**Figures 65B,C**). In contrast, cell lines with loss of Rb and / or high levels of LMWE, such as FUOV1, A549, HCT116 and Du145 showed significant resistance to palbociclib treatment, with higher IC50 values (4 - 10uM) (**Figure 65B,C**).

Further, palbociclib treatment for 6 days with 6 days of recovery induced a significant dose-dependent reduction in colony formation in cancer cell lines with intact G1/S checkpoint, irrespective of the cancer type (**Figure 65D**). In contrast, cell lines that have deregulated a Rb and/or LMWE expression exhibited significant resistance to the induction of palbociclib mediated reduction in colony formation (**Figure 65D**).

Thus, these results indicate that palbociclib mediated CDK4/6 inhibition induces a dose-dependent sustained growth inhibition in solid tumor cell lines with an intact G1/S checkpoint.

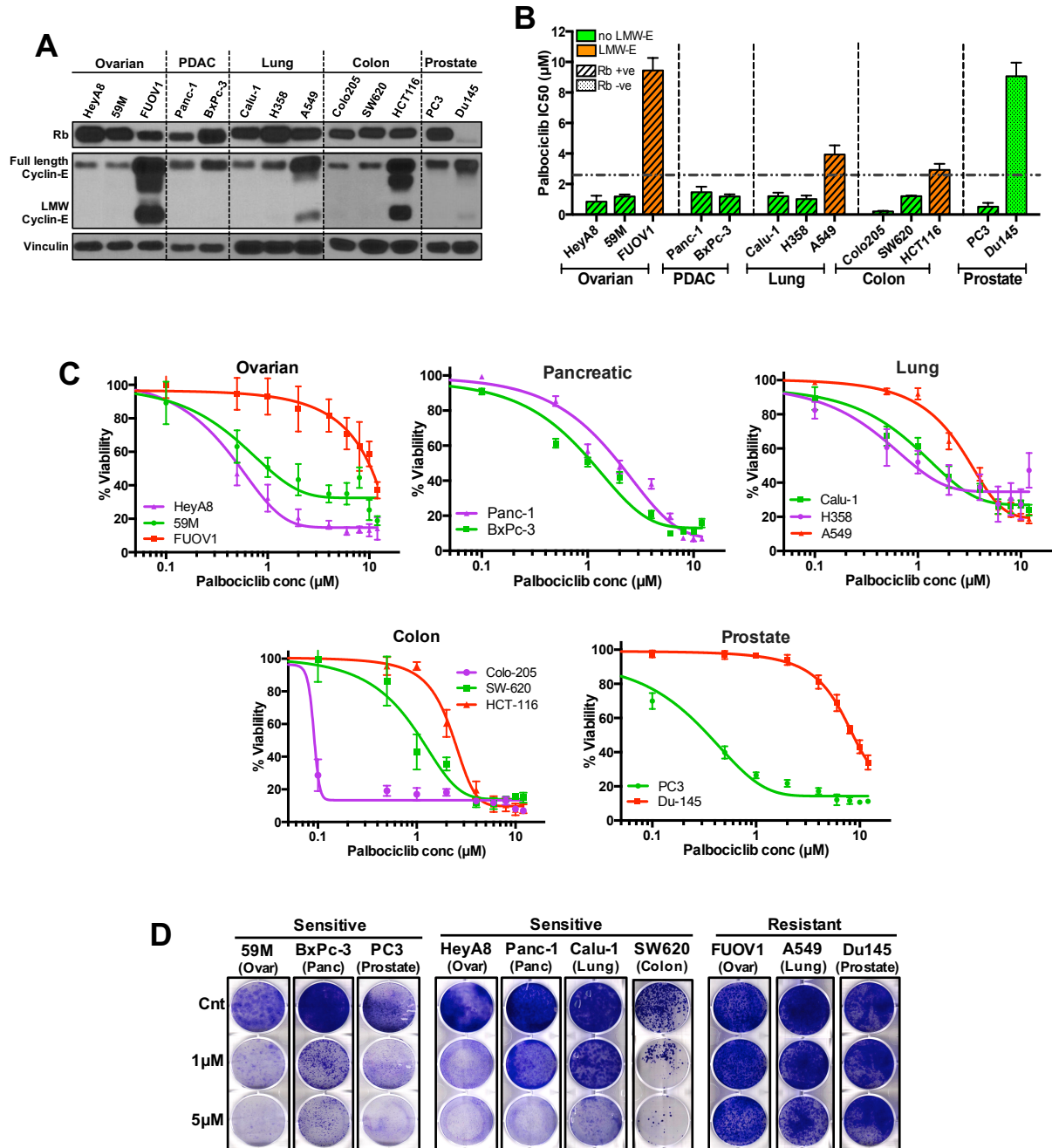


Figure 65: Palbociclib treatment in other solid tumor cell lines: A) Western blot of Rb and Cyclin-E in ovarian, pancreatic (PDAC), lung, colon and prostate cancer cell lines. B) IC₅₀ values from drug response experiments in the mentioned cancer cell lines treated with palbociclib for 6 days and recovery for 4 days. C) Dose response studies to measure the impact of treatment with increasing concentrations (conc) of palbociclib (0.01 to 12 μM) on the growth of the indicated ovarian, lung, pancreatic, colon, and prostate cancer cell lines for 6 days. D) Clonogenic assay in the indicated cell lines treated with DMSO (Cnt) or palbociclib (1 μM, 5 μM) for 6 days and allowed to recover for 6 days. All data represent mean ± SD from three independent experiments; p-values were calculated in comparison to DMSO (Control) unless indicated. ns: p > 0.05; *p < 0.05; **p < 0.01; ***p < 0.001; ****p < 0.0001.

8.2.5. SYNERGISM BETWEEN PALBOCICLIB AND AUTOPHAGY INHIBITION IN OTHER SOLID TUMOR CELL LINES

Given that palbociclib treatment was effective in non-breast tumor cell lines with an intact G1/S transition, we next wanted to examine if the combination of palbociclib and autophagy inhibitor, HCQ might be synergistic in these solid tumors resulting in sustained and irreversible growth inhibition. In cancer cell lines exhibiting expression of intact Rb and low Cyclin E (and no LMWE), such as HeyA8, Panc-1, BxPc-3, Calu-1, SW-620 and PC3, combination treatment with palbociclib and HCQ resulting in enhanced reduction in colony formation, compared to treatment with low dose palbociclib alone (**Figure 66A**). However, cell lines with a deregulated G1/S checkpoint (loss of Rb and / or high levels of LMWE), namely FUOV1, A549 and Du145 showed significant resistance to palbociclib mediated reduction in colony formation (**Figure 66A**). Moreover, treatment with the autophagy inhibitor, HCQ further sensitized the Rb positive LMWE negative cells to palbociclib, thus inducing a sustained and irreversible growth inhibition in ovarian (HeyA8, 59M), pancreatic (Panc-1, BxPc-3), lung (Calu-1), colon (SW620) and prostate (PC-3) cancer cell lines (**Figure 66B,C**).

Collectively, these results demonstrate the utility of combining palbociclib with an autophagy inhibitor in solid tumors with an intact G1/S checkpoint.

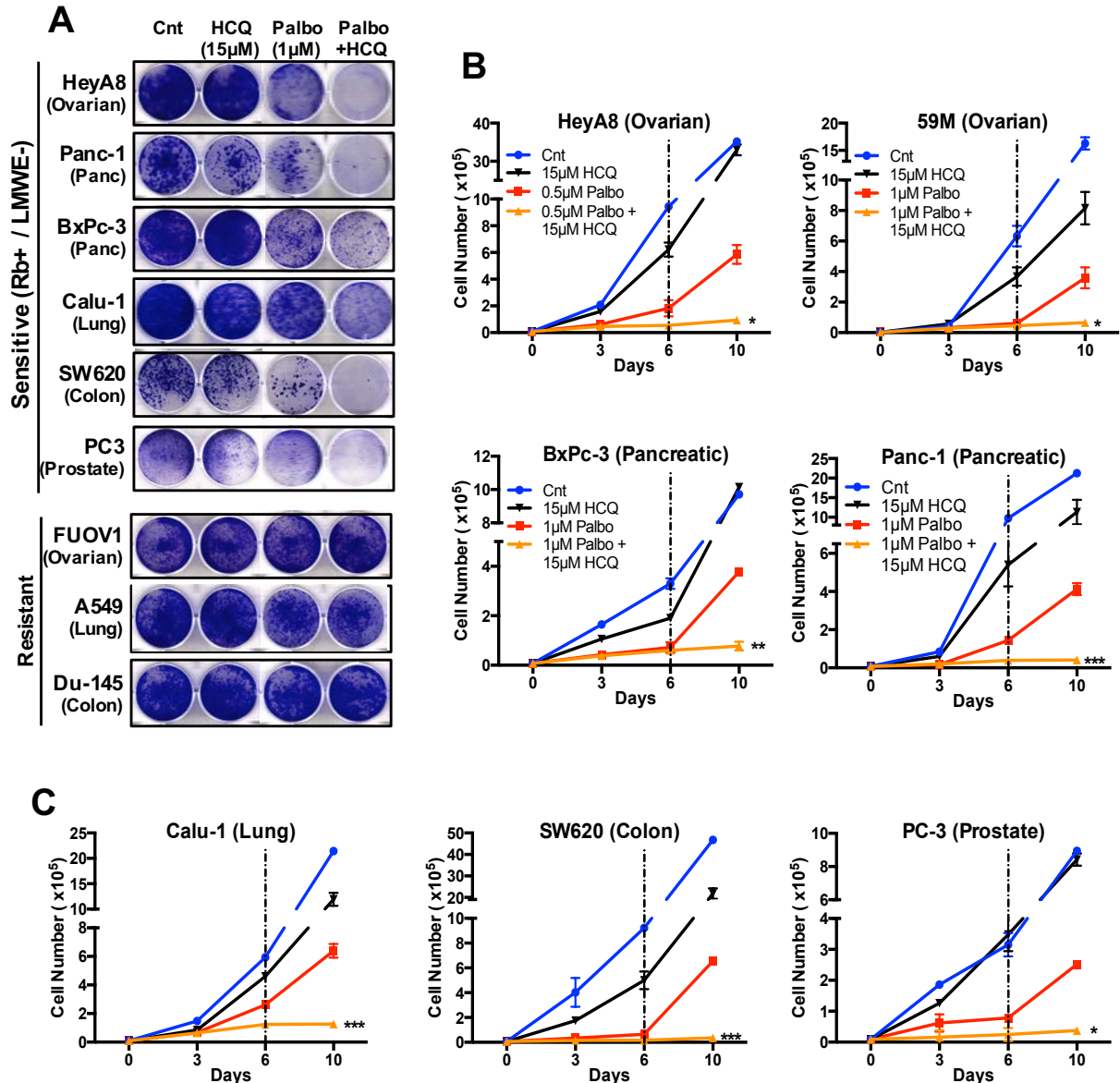


Figure 66: Synergism between palbociclib and autophagy inhibition in other solid tumor cell lines:

A) Clonogenic assay to measure colony formation in the indicated solid tumor cell lines treated with DMSO or 1 μ M palbociclib (Palbo) and/or HCQ (15 μ M) for 6 days and allowed to recover for 6 days. B, C) Cell counting to assess proliferation of the indicated solid tumor cell lines treated with 1 μ M palbociclib and/or 15 μ M hydroxychloroquine (HCQ) for 6 days and allowed to recover for 4 days to examine reversibility. p-values were calculated in comparison to cells treated with 1 μ M palbociclib. All data represent mean \pm SD from three independent experiments; p-values were calculated in comparison to DMSO (Control) unless indicated. ns: $p > 0.05$; * $p < 0.05$; ** $p < 0.01$; *** $p < 0.001$; **** $p < 0.0001$.

8.3. DISCUSSION

Results from the studies described in this chapter are highly translatable and clinically relevant since they provide strong pre-clinical data to expand the CDK4/6 inhibitor treatment to other solid tumors other than breast cancer. Further, analysis across all cancer types (breast, ovarian, lung, colon, pancreatic and prostate) showed a strong correlation between sensitivity to palbociclib (measured by IC50 values) and the combined expression of Rb and cyclin E (specifically LMWE) (**Figure 67A**). This indicates that the immunohistochemistry based dual biomarker strategy proposed and tested in chapter 7 can also be employed in other solid tumor to select for patients who would respond to CDK4/6 inhibition. Further inhibition of autophagy (genetic ablation of autophagy genes Beclin1 and Atg5 or pharmacological inhibition by HCQ) further decreased the IC50 value of palbociclib in the RB+ LMWE- cell lines across all cancer types (**Figure 67B**). This suggests synergy and potential utility of the combination therapy in TNBC and other solid tumors.

CDK4/6 inhibitors are not used currently in the clinic to treat non-ER positive subtype of breast cancer, more specifically, the triple negative breast cancer (TNBC) tumors. However, early preclinical studies in breast cancer show that a small percentage of the TNBC cell lines do respond to palbociclib treatment (Finn, Dering et al. 2009, Robinson, Liu et al. 2013). However, has not been investigated further thus far, possibly because only a small proportion of the TNBC cell lines appeared to be responsive to CDK4/6 inhibition and there are no reliable biomarkers to predict the population of responsive TNBC patients. The role of CDK4/6 inhibition in TNBC has gained attention with a recent study that examined the utility of palbociclib in TNBC cell lines and attempted at identifying the subtype of TNBC that would respond best to this treatment (Uzma Asghar 2016). In this chapter, we have performed extensive *in vitro* and *in vivo* studies, including treatment studies in TNBC patient derived xenograft (PDX) tumors, which showed that TNBC tumors would also be responsive to palbociclib. We also show that the drug efficacy in these cell lines and tumors can be further

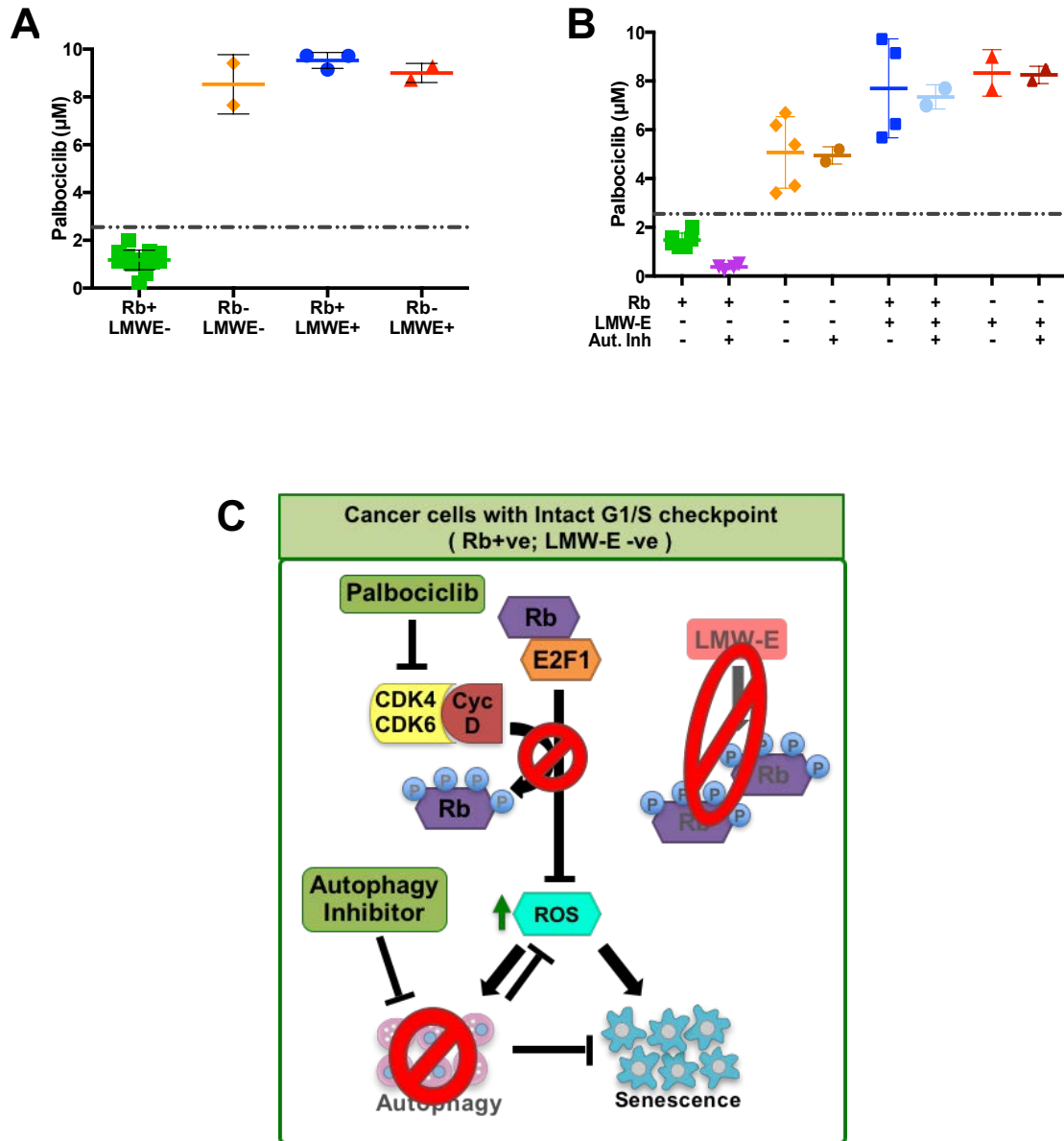


Figure 67: Synergism between CDK4/6 and autophagy inhibition in cancers with an intact G1/S checkpoint: A) Correlation between palbociclib half-maximal inhibitory concentration (IC_{50}) values (obtained from dose-response studies in all cancer cell lines) and levels of Rb and low-molecular-weight cyclin E isoform (LMWE-E) proteins. B) Correlation between palbociclib IC_{50} values (from dose-response studies in all cancers) and levels of Rb and cyclin E proteins, with and without inhibition of autophagy (Beclin-1/Atg5 knockdown or HCQ treatment). C) Schematic depicting the mechanism by which palbociclib inhibits growth of Rb+/LMWE- breast cancer cells by regulating ROS, autophagy, and senescence.

increased by the addition of autophagy inhibitors and by using the combination of Rb and LMWE as reliable markers to predict response. The G1/S checkpoint tends to be more often deregulated in the TNBC tumors, with a higher proportion of the tumors being Rb negative and expressing LMWE (Giacinti and Giordano 2006, Karakas, Biernacka et al. 2016). While this indicates that a smaller proportion of tumors are likely to respond to CDK4/6 inhibitor therapy, the TNBC tumor subtype have no effective treatments thus far, apart from chemotherapy, highlighting the importance of this study.

Taken together, the results in chapters 4 through 8 demonstrate that the combination CDK4/6 and autophagy inhibitor can be utilized to effectively treat solid tumors such as breast (irrespective of subtype), ovarian, pancreatic, prostate, colon and lung cancer, and that the expression of Rb and Cyclin-E (LMWE) can serve as effective and reliable biomarkers to predict response to this drug combination (**Figure 67C**). The model shows that the inhibition of CDK4/6 via palbociclib in tumors that have Rb and do not express LMWE, increases ROS, which in turn activates autophagy and prevents the induction of senescence. Hence combined treatment with CDK4/6 and autophagy inhibitors further increased ROS levels and induces senescence.

CHAPTER 9: MECHANISM OF ACQUIRED RESISTANCE TO PALBOCICLIB

9.1. INTRODUCTION

9.1.1. MECHANISMS OF ACQUIRED RESISTANCE TO CDK4/6 INHIBITION

While ER positive breast cancer patients perform well on the CDK4/6 inhibitors, about 25% of the patients become resistant to the drug within 6 months, and it is expected that all patients will eventually acquire resistance to the treatment. However, there are very few studies till date that have examined the mechanisms of acquired resistance to palbociclib and other CDK4/6 inhibitors. Given the importance of the Rb protein, loss of Rb leading to deregulation of the G1/S checkpoint is a mechanism of acquired resistance to palbociclib (DeMichele A 2016). A study in ER positive breast cancer cells showed that acquired resistance to palbociclib arises from bypass or deregulation of the G1/S checkpoint, and this occurs through CCNE1 (cyclin E) amplification or loss of Rb (Herrera-Abreu, Palafox et al. 2016). A more recent study in understanding the mechanism of acquired resistance to abemaciclib, showed that the resistant clones showed amplification of CDK6 kinase, resulting in increased CDK6 expression and resistance to reduction of pRb with abemaciclib treatment (Yang, Li et al. 2016). This study also confirmed the loss of Rb and amplification of CCNE1 in the abemaciclib resistant cells (Yang, Li et al. 2016).

While most current studies on acquired resistance to palbociclib have focused on the G1/S checkpoint, there are numerous other pathways that can contribute to drug resistance. Some of the pathways seen with other targeted therapies including aromatase inhibitors are mutations of the target genes, activation of alternate growth signaling pathways that can enable the cells to proliferate even in the presence of the drugs and increased EMT and cancer stem cell phenotype, which has been strongly associated with therapy resistance in breast and other cancers (Dean, Fojo et al. 2005, Ma, Reinert et al. 2015).

9.1.2. CANCER STEM CELLS, EMT AND DRUG RESISTANCE

Cancer stem cells (CSCs) are considered as a population of cells within the tumor that have a high self-renewal capacity (Siminovitch, McCulloch et al. 1963). Studies have shown that they can mediate resistance to cancer therapy in several tumor types including breast cancer (Phillips, McBride et al. 2006, Touil, Igoudjil et al. 2014). In 2003, breast cancer stem cells were first isolated based on the surface markers CD44 and CD24 as being CD44^{+/high} CD24^{-/low} population of cells (Al-Hajj, Wicha et al. 2003). Later aldehyde dehydrogenase (ALDH) was identified as a new marker of breast cancer stem cells (Ginestier, Hur et al. 2007). Breast cancer stem cells are also characterized by their ability to generate tumors in mice even when transplanted into mammary fat pad with as low as 100 cells were (Al-Hajj, Wicha et al. 2003). Another feature linked with cancer stem cells is their ability to undergo epithelial mesenchyme transition (EMT) and metastasis to distant organ sites. EMT is typically accompanied by decrease of epithelial markers like E-cadherin (CDH1) and increase in mesenchymal markers such as vimentin and N-cadherin, which transforms the cells into being higher migratory and invasive (Yang, Mani et al. 2004). Several studies have established a link between EMT and cancer stemness, including a study in immortalized mammary epithelial cells, where the expression of the EMT, Snail and Twist induced cancer stem cell phenotype, concomitant with increase in CD44^{high} CD24^{low} population and enhanced tumorigenicity *in vivo* (Mani, Guo et al. 2008).

Further studies have established a link between cancer stem cells and resistance to therapy, both intrinsic and acquired resistance (Dean, Fojo et al. 2005). For example, ALDH staining of tumor tissue samples before and after chemotherapy showed a significant association between ALDH staining and resistance to therapy or worse prognosis (Tanei, Morimoto et al. 2009). A study in Her2 positive breast cancer also showed that tumor tissues with high expression of CD44 protein were intrinsically resistant to chemotherapy (Li, Lewis et al. 2008). Moreover, studies have also shown a link between cancer stem cells and resistance

to anti-estrogen therapy like aromatase inhibitors (Creighton, Li et al. 2009). This study showed a significant increase in EMT genes such as MMP2 and MMP3 and an increase in CSC gene signature post treatment with letrozole when compared to matched pre-treatment samples (Creighton, Li et al. 2009).

9.1.3. IL-6/STAT-3 PATHWAY – ROLE IN CSC AND BREAST CANCER

Signal transducer and activator of transcription 3 (STAT3) belong to the STAT family of transcription factors that regulates numerous cellular processes (Banerjee and Resat 2016). STAT3 is constitutively activated in numerous cancers, including about 50 to 60% of breast cancer (Banerjee and Resat 2016). STAT-3 is activated upon phosphorylation which results in dimerization of the STAT3 proteins, which then translocate into the nucleus, where it binds to the promotor sequence of the target genes and initiate their transcription (Yu and Jove 2004). One of the common upstream activators of STAT-3 is the IL-6 family of cytokines (Dethlefsen, Hojfeldt et al. 2013). Studies in breast cancer have shown that IL-6 is secreted by the tumor microenvironment, which activated the STAT-3 signaling in the breast cancer cells in a paracrine or fashion allowed the STAT-3 signaling to remain constitutively active (Dethlefsen, Hojfeldt et al. 2013). The tumor tissue specific expression of STAT-3 indicates that the pathway plays a major role in breast cancer tumorigenesis (Carpenter and Lo 2014). *In vitro* and tumor tissue based studies have shown that the downstream target genes of the STAT-3 pathway are involved in numerous cellular functions including proliferation, apoptosis, survival, EMT and metastasis, angiogenesis and cancer stem cells (Banerjee and Resat 2016).

The IL-6/STAT-3 pathway has been shown to be preferentially expressed within the CD44^{high} CD24^{low} population of breast cancer cells, indicating its role in mediating cancer stem cells (Marotta, Almendro et al. 2011). A study specifically in ER positive HER2 positive tumors, HER2 mediated phosphorylation and activation of STAT-3, which causes upregulation of cancer stem cell and EMT markers, leading to resistance to herceptin treatment (Chung, Giehl

et al. 2014). Further, combined treatment with a STAT-3 inhibitor in combination with herceptin caused decrease in CD44^{high} CD24^{low} population and migration, thus reversing the resistance to herceptin (Chung, Giehl et al. 2014). Another study in HER2 positive breast cancer shows that PTEN deletion activates the IL-6 inflammatory loop, which induces breast cancer stem cell population with an EMT phenotype, thus making the cells resistant to anti-HER2 therapy via trastuzumab (Korkaya, Kim et al. 2012). Further, treatment with an anti-IL6R antibody reverses resistance to trastuzumab in *in vitro* and in xenograft models (Korkaya, Kim et al. 2012). Finally, a more recent study in ER positive breast cancer showed that acquired resistance to hormonal therapy mediates downregulation of ER and abrogation of the OXPHOS pathway, resulting in increased expression of CD133^{high} cancer stem cells (Sansone, Ceccarelli et al. 2016). Thus, inhibition of the IL-6 / Notch-3 pathway decreases the CD133^{high} cancer stem cells and re-sensitizes cells to hormonal therapy (Sansone, Ceccarelli et al. 2016).

9.1.4. TARGETING DNA REPAIR PATHWAY IN BREAST CANCER

Targeting the DNA repair defect or deficiency has been a commonly employed technique of drug targeting in cancers over the years (Kelley, Logsdon et al. 2014). One of the most promising targeted therapy developed based on this concept are the PARP inhibitors (Kelley, Logsdon et al. 2014). Poly ADP ribose polymerase (PARP) plays a crucial role in the alternate DNA repair pathway termed as base excision repair (BER) (Eustermann, Videler et al. 2011, Langelier, Planck et al. 2011). This pathway is usually activated when there is a defect or mutation in the homologous recombination (HR) pathway, regulated by the genes BRCA1 and BRCA2 (Moynahan, Chiu et al. 1999). Thus, cells with a mutation in the BRCA gene are unable to repair double strand breaks in DNA, forcing them to rely on the PARP dependent BER pathway (Moynahan, Chiu et al. 1999). This results in synthetic lethality between BRCA mutation and PARP, causing the BRCA mutant breast cancer cells to be sensitive to PARP inhibitors induced genomic instability and apoptosis (Kelley, Logsdon et al. 2014). Treatment of

Brca1^{-/-}, p53^{-/-} mouse model (TNBC tumors) respond effectively to PARP inhibitor, AZD2281 (Rottenberg, Jaspers et al. 2008). Further, combination of the PARP inhibitor with cisplatin resulted in improved survival compared to the vehicle and single drug treatment arms (Rottenberg, Jaspers et al. 2008). Further, a phase II clinical trial to examine the safety and tolerability of the PARP inhibitor, olaparib in 54 advanced breast cancer patients with BRCA1 or BRCA2 mutation, showed that 41% of patients had objective clinical response (Tutt, Robson et al. 2010). This has led to the FDA approval of the PARP inhibitors, olaparib, rucaparib and more recently niraparib have been for the treatment of advanced BRCA mutant ovarian cancers (2017, Lin and Kraus 2017). They are currently one of the most promising targeted therapies under investigation for TNBC, and the combination of the PARP inhibitors with standard chemotherapy have also been shown to be beneficial for breast cancer patients (2014, 2017, Lin and Kraus 2017).

9.1.5. GAP IN KNOWLEDGE

Given that studies at understanding the mechanisms of acquired resistance to CDK4/6 inhibition are just beginning to emerge, an extensive exploratory study is needed to identify drugs that can effectively target the acquired resistant tumors. While Rb loss and CCNE1 amplification, which are known mechanisms of G1/S deregulation, are the currently predicted mechanisms of acquired resistance, it is possible that the resistant cells have alterations that are beyond the cell cycle. Hence, experiments performed in this chapter aim at answering these voids in the current literature and devising a durable and effective treatment strategy for acquired resistance to palbociclib and other CDK4/6 inhibitors.

9.2. RESULTS

9.2.1. DEVELOPMENT AND CHARACTERIZATION OF PALBOCICLIB RESISTANT CELLS

To interrogate the mechanism of acquired resistance to palbociclib, the ER positive breast cancer cell lines, MCF7 and T47D were treated with increased with increasing doses of palbociclib over a 6-month period (**Figure 68A**). The treatment was started at the IC₅₀ value of palbociclib, at 1uM. Once the cells began proliferating at this dose, the concentration was increased by 2-fold (i.e. to 2uM) and maintained at that dose until the cells proliferate at that dose. This was continued until the cells reached a dose of 6uM, to generate the palbociclib resistant cell lines (pool). With the goal of identifying multiple different mechanisms by which cells might acquire resistance to the drugs, numerous clones were isolated from the resistant cell pools, of which 3 from each cell lines were utilized for further analysis.

Next, dose response study was performed to examine the proliferation of the three MCF7 and T47D resistant clones in the presence of palbociclib and results showed a significant (upto 10-fold difference compared to the parental cells) resistance to palbociclib (**Figure 68B** – left and middle panels). Moreover, one of the most resistant clones in each cell lines (cl3 for MCF7 and cl2 for T47D) were chosen for further analysis and henceforth referred to as MCF7 Res and T47D Res (**Figure 68B** – right panel). Additionally, clonogenic assays showed that palbociclib treatment had no significant on the proliferation of MCF7 and T47D resistant cells, while inducing a dose-dependent reduction in colony formation the parental cell (**Figure 68C**). Moreover, cell cycle analysis showed that palbociclib treatment did not induce a G1 arrest in the MCF7 and T47D cells (**Figure 68D**), indicating that the resistant cells are indeed resistant to palbociclib induced G1 arrest. Finally, to examine if the palbociclib resistant cells are also resistant to the other CDK4/6 inhibitors such as ribociclib and abemaciclib, dose response studies were performed, which showed that the palbociclib resistant MCF7 and T47D cells were also significantly cross resistant to ribociclib and abemaciclib (**Figure 68E**),

exhibiting a >5-fold and >10-fold increase in IC₅₀ values respectively (**Figure 68F**), when compared to the parental cells.

Thus, these results showed that the acquired resistant cells developed are resistant to palbociclib and cross-resistant to the other CDK4/6 inhibitors as well.

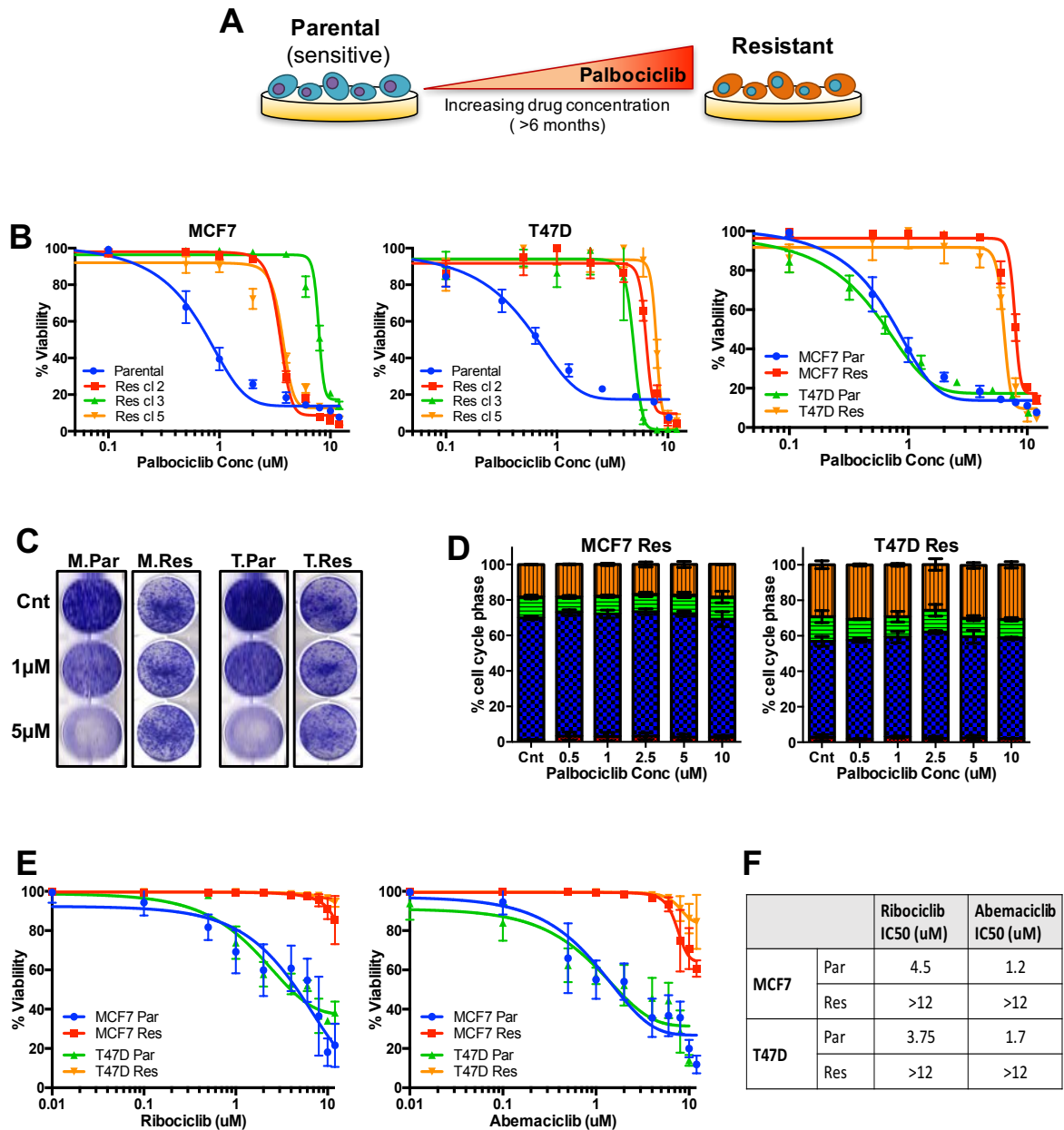


Figure 68: Development and characterization of palbociclib resistant cells: A) Schematic showing the method by which the resistant cells were developed from MCF7 and T47D parental cells. B) Dose response studies measuring the impact of treating with varying concentrations of palbociclib (0.01 to 12 uM) on the proliferation of MCF7 and T47D parental and resistant cell lines. MCF7 and T47D cells parental and resistant cells were treated with palbociclib (Palbo) for 6 days and subjected to C) clonogenic assay to measure impact on cell proliferation and D) flow cytometry to measure effect on cell cycle. E, F) Dose response studies measuring the impact of treating with varying concentrations of ribociclib or abemaciclib (0.01 to 12 uM) on the proliferation of MCF7 and T47D parental and palbociclib resistant cell lines, and their corresponding IC50 values (F).

9.2.2. GENE EXPRESSION PROFILE OF PALBOCICLIB RESISTANT CELLS

Understanding the changes in gene and protein expression between the sensitive (parental) and the resistant cell lines will help design treatments to overcome drug resistance. Hence, we performed genome-wide expression analysis via mRNA-seq on the isolated clones belonging to MCF7 and T47D cell lines to detect change in mRNAs and examine the pathways altered between the parental and the resistant cell lines (**Figure 69A**). Results from the RNA seq analysis by non-hierarchical clustering (clustering based on gene expression) revealed that 2888 genes were differentially expressed ($p < 0.05$) when compared to parental (sensitive) (**Figure 69B**), showing that acquired resistance significantly alters the gene expression profile of the ER positive breast cancer cells.

To understand the functional significance of these mRNA alterations and identify the pathways that are altered, gene set enrichment analysis (GSEA) was performed which compared the change in expression between the parental and the resistant T47D cells, focusing on the 50 hallmark gene sets (**Figure 69C**). This showed that some of the top upregulated pathways in the resistant cells include epithelial mesenchymal transition (EMT) and developmental or cancer stem cell (CSC) associated pathways such as IL-6/STAT-3, Notch and Wnt signaling pathways (**Figure 69C**). Further, one of the crucial and actionable downregulated pathways includes the DNA repair and the double DNA repair pathways (**Figure 69C**). The estrogen response (early and late) pathways were also shown to be downregulated in the resistant cells (**Figure 69C**), indicating that the ER positive breast cancer cells may not be less dependent on estrogen signaling. Moreover, the list of upregulated pathways also includes numerous immune response pathways such as Interferon alpha, Interferon gamma, TNF alpha via NFkB, cytokine biosynthesis and production, cytokine chemokine signaling and IL-6 STAT-3 pathway (**Figure 69C**). This indicates that resistance to palbociclib might be activating an immune response in these cells, and can be investigated in the future as a potential avenue for therapy.

Thus, gene expression analysis study showed a distinctly altered gene expression profile in the resistant cells and identifies numerous pathways that can be potentially targeted upon acquired resistance to CDK4/6 inhibitors.

9.2.3. EMT AND CANCER STEM CELL PROPERTIES IN PALBOCICLIB RESISTANT CELLS

Given the phenotypic changes observed in the resistant cells (resistant cells have a more mesenchymal phenotype compared to the epithelial MCF7 and T47D parental cells), and the upregulation of the EMT pathway by GSEA analysis (**Figure 70A**), we next wanted to directly examine if the resistant cells have acquired an EMT phenotype. To test this, we first examined the mRNA levels of EMT markers and transcriptional factors in the parental vs resistant cells via qRT-PCR, which showed a significant decrease in the epithelial marker, E-cadherin and a significant increase in the mesenchymal markers, Vimentin and N-cadherin (**Figure 70B**). Further, there was a significant increase in the mRNA levels of the known EMT transcription factors such as Snail, Twist and Slug in the resistant cells compared to parental cells (**Figure 70B**). We also examined the migratory ability of the resistant cells via scratch assay, which showed that the MCF7 and T47D palbociclib resistant cells had a much higher percentage of wound closure compared to the parental cells (**Figure 70C**).

Cancer stem cells (CSCs) are known to mediate resistance to numerous therapies including aromatase inhibitors in ER positive breast cancer. This, along with the enrichment of numerous developmental pathways in the resistant cells measured by GSEA analysis (**Figure 69C**), led us to examine any changes in the cancer stem cell population. First, we examined the CSC markers and transcription factors, which showed significant upregulation CD133, a cancer stem cell, CD44, FoxC2 and ALDH1, markers of breast cancer stem cells and other known stem cell markers, Oct4, Sox2 and Nanog (**Figure 70D**). Next, we used flow cytometry analysis to measure the percentage of CD44^{high}/CD24^{low} and ALDH+ve population in the resistant cells, both established markers and measures of breast cancer stem cells. Results showed that the palbociclib resistant MCF7 and T47D cells have a significantly CD44^{high}/CD24^{low} (**Figure 71A**) and ALDH+ve population (**Figure 71B**) compared to the respective parental cell lines, indicating increased cancer stem cells with drug resistance. To further

confirm this, we performed the mammosphere assay, which measures the sphere forming ability of the cells, another measure of breast cancer stem cells, with mammosphere formation over passages (primary and secondary mammosphere) being a better indicator (Rota, Lazzarino et al. 2012). Results showed that the palbociclib resistant cells have a significantly increased ability (larger and greater number of mammospheres) to form both primary and secondary mammospheres compared to the MCF7 and T47D parental cells (**Figure 71C**).

Thus, these results show that the palbociclib resistant cells have increased EMT and cancer stem cell phenotype, which might be the significant contributor of resistance in these cells. Hence, targeting these processes might prove as an ideal strategy to combat drug resistance.

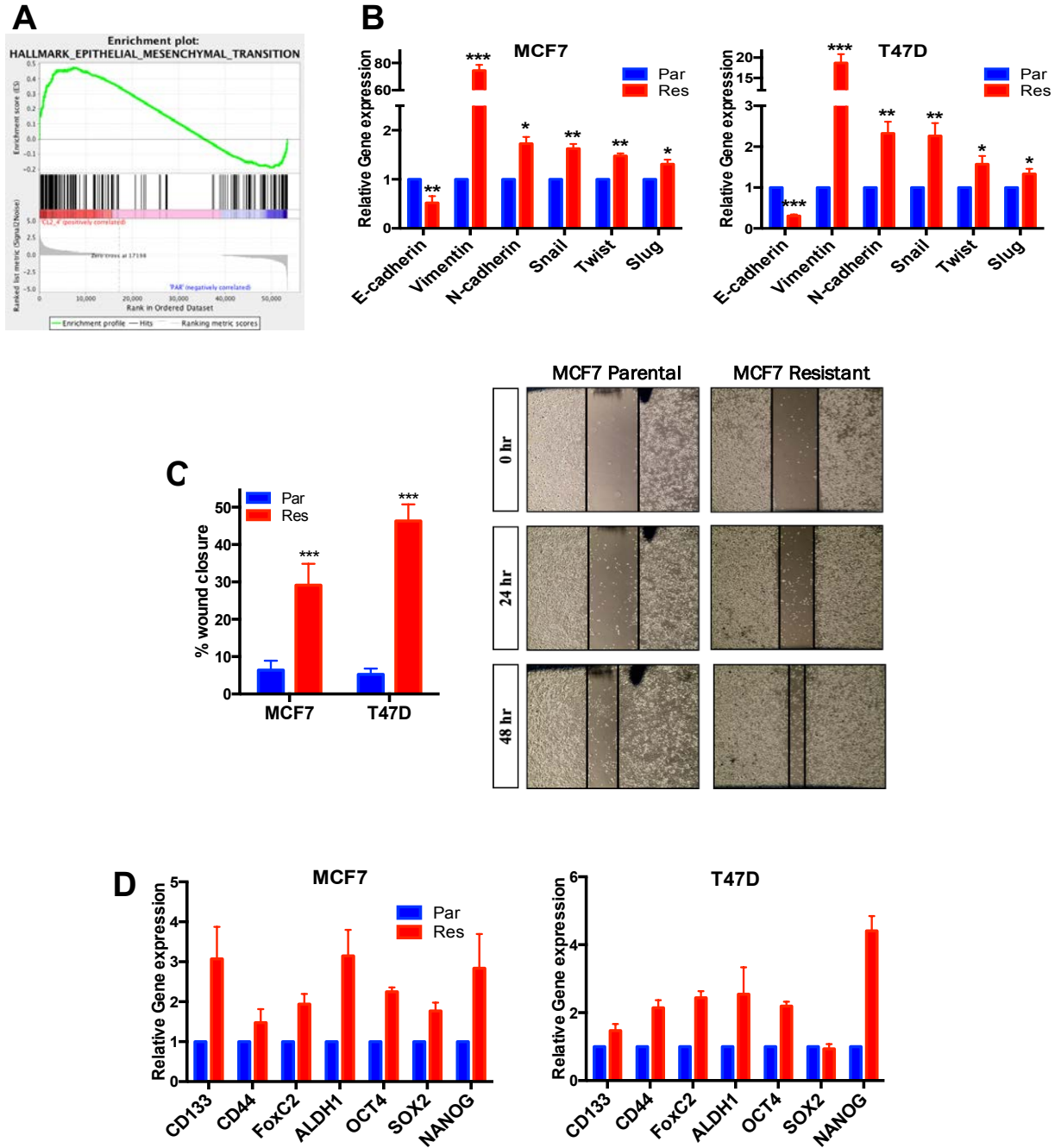


Figure 70: EMT properties in palbociclib resistant cells: A) Enrichment plot of the Epithelial Mesenchymal Transition (EMT) pathway obtained by Gene set enrichment analysis (GSEA) between T47D resistant and parental cell lines. B) qRT-PCR measuring the mRNA expression of EMT genes relative to GAPDH in palbociclib sensitive vs resistant cells C) Scratch assay used to measure migration ability of the MCF7 and T47D parental vs resistant cells and its quantification (% wound closure). D) qRT-PCR measuring the mRNA expression of cancer stem cell related genes relative to GAPDH in palbociclib sensitive vs resistant cells. p-values were calculated in comparison to Parental (sensitive) unless indicated. ns: $p > 0.05$; * $p < 0.05$; ** $p < 0.01$; *** $p < 0.001$; **** $p < 0.0001$.

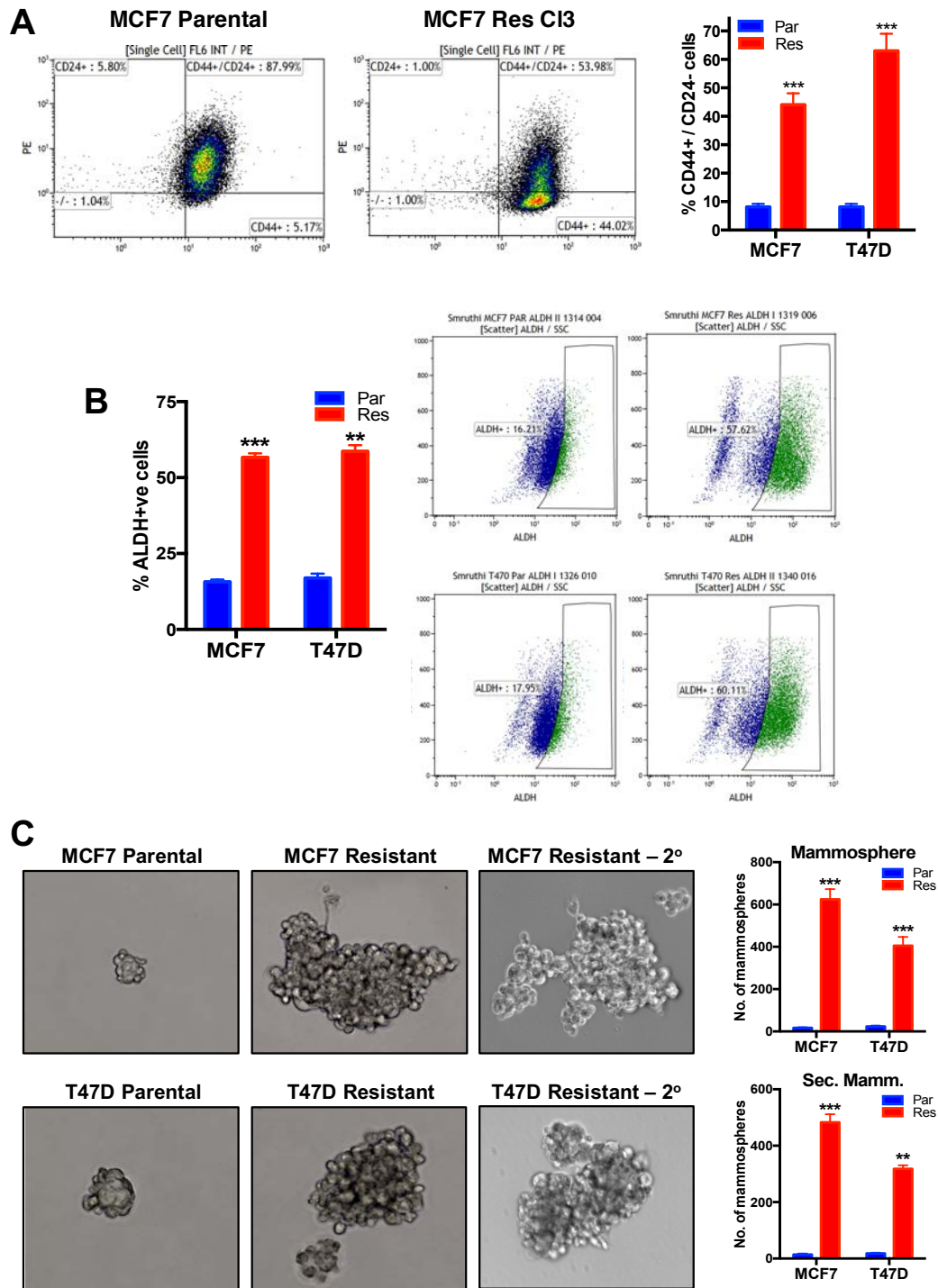


Figure 71: Cancer stem cell properties of palbociclib resistant cells: A) Flow cytometry analysis measuring the percentage of CD44 high CD24 low population of cells and quantification in palbociclib sensitive vs resistant cells. B) Flow cytometry analysis measuring the percentage of ALDH high cells in palbociclib sensitive vs resistant cells. C) Representative pictures and quantification of primary and secondary mammospheres in the parental vs resistant cells. p-values were calculated in comparison to Parental (sensitive) unless indicated. ns: $p > 0.05$; * $p < 0.05$; ** $p < 0.01$; *** $p < 0.001$; **** $p < 0.0001$.

9.2.4. TARGETING IL-6/STAT-3 PATHWAY IN PALBOCICLIB RESISTANT CELLS

Next, we utilized the gene expression and GSEA data (Figure 62) to identify which cancer stem cell regulating pathway can be targeting in the palbociclib resistant cells. Given the recently elucidated role of the IL-6/STAT-3 pathways in modulating cancer stem cells and drug resistance (Lin, Hutzen et al. 2013, Sansone, Ceccarelli et al. 2016), and the observed increase in the IL-6/STAT-3 pathway in the palbociclib resistant cells from GSEA analysis (**Figure 72A**), we focused on this pathway. As a first step, we examined IL-6 mRNA levels, which exhibited a >12-fold in the palbociclib resistant cells compared to the MCF7 and T47D parental cells (**Figure 72B**). Further, to interrogate the role of STAT-3 in the palbociclib resistant cells, we treated with two known STAT-3 inhibitors, Stattic and napabucasin (Marcucci, Rumio et al. 2016), which significantly decreased proliferation of the MCF7 and T47D resistant cells and these drugs were relatively more specific to the resistant cells compared to parental (**Figure 72C**). Napabucasin is a recently developed STAT-3 inhibitor that has been specifically shown to target cancer stem cells (Marcucci, Rumio et al. 2016, Zhang, Jin et al. 2016). Hence, we interrogated the role of STAT-3 in increasing cancer stem cells and mediating drug resistance by CD44^{high}/CD24^{low} measurement and mammosphere assay. Results showed that treatment with a STAT-3 inhibitor, napabucasin significantly decreased the CD44^{high}/CD24^{low} CSC population (**Figure 72D**) and mammosphere formation (**Figure 72E**).

Thus, these results indicate that the IL-6/STAT-3 pathway plays a crucial role in driving cancer stem cells and palbociclib acquired resistance ER positive breast cancer.

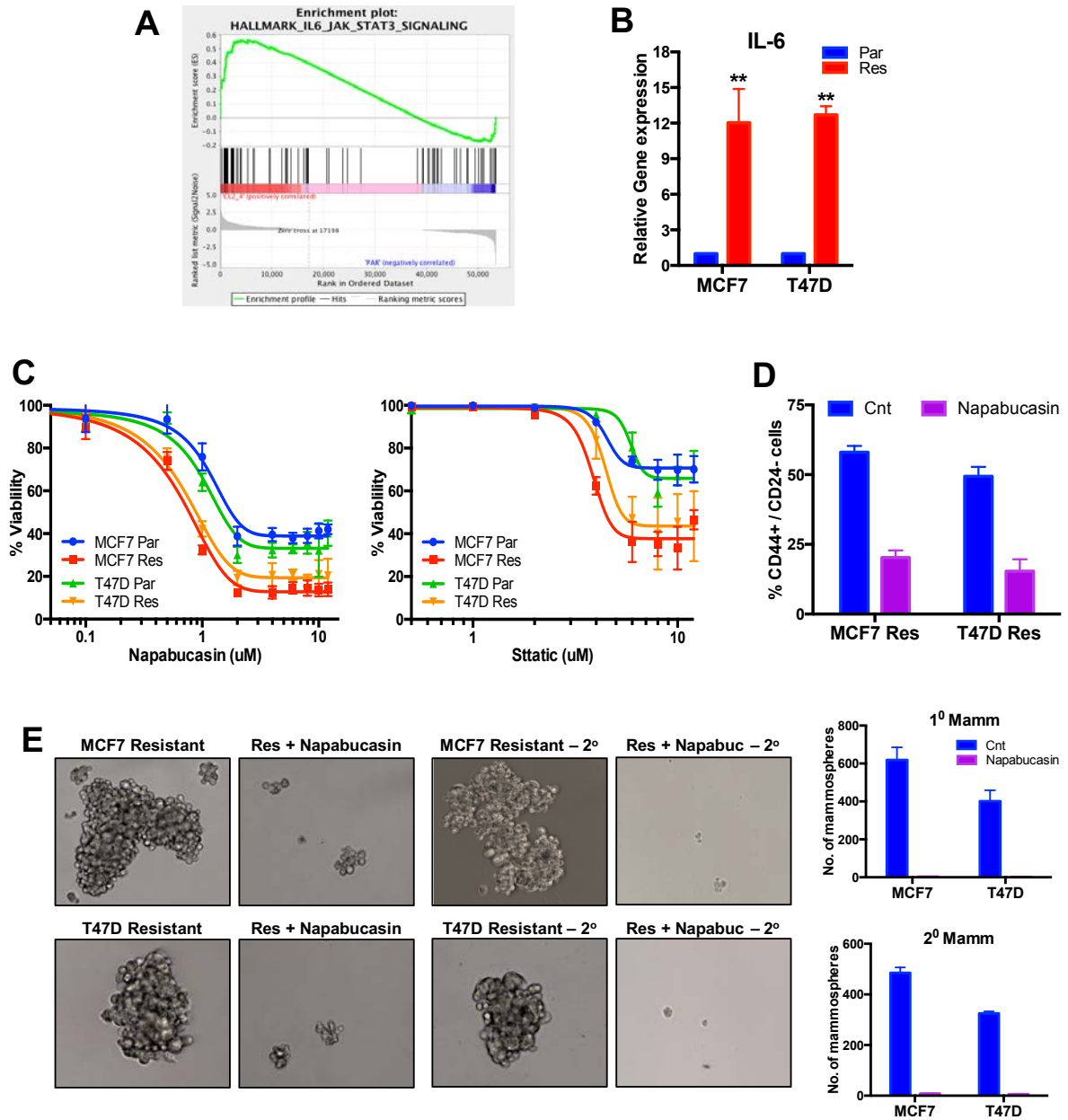


Figure 72: Targeting IL-6/STAT-3 in palbociclib resistant cells: A) Enrichment plot of the IL-6 STAT-3 pathway pathway obtained by Gene set enrichment analysis (GSEA) between T47D resistant and parental cell lines. B) qRT-PCR measuring the mRNA expression of IL-6 relative to GAPDH in palbociclib sensitive vs resistant cells C) Dose response studies measuring the impact of treating with treatment with the STAT-3 inhibitors, napabucasin and stattic on the proliferation of MCF7 and T47D parental and resistant cell lines. MCF7 and T47D parental and resistant cells were treated with 1uM napabucasin for 72 hours and subjected to D) Flow cytometry analysis measuring the percentage of CD44 high CD24 low population of cells and E) primary and secondary mammosphere formation. p-values were calculated in comparison to Parental (sensitive) unless indicated. ns: $p > 0.05$; * $p < 0.05$; ** $p < 0.01$; *** $p < 0.001$; **** $p < 0.0001$.

9.2.5. TARGETING DNA REPAIR DEFICIENCY IN PALBOCICLIB RESISTANT CELLS

Given that the DNA repair and double stranded break repair are one of the top downregulated pathways in the RNA-seq and GSEA analysis (**Figure 66A**), and that cells deficient in DNA repair can be hypersensitive to DNA damaging agents and PARP inhibitors, we examined the possibility of targeting DNA repair deficiency in palbociclib resistant cells. First, we examined the expression of crucial double strand break repair genes, Rad51, BRCA1 and BRCA2, all of which significantly decreased in the palbociclib resistant MCF7 and T47D cells compared to the parental (**Figure 73B**). Further, the sensitivity of the resistant cell to the PARP inhibitors, olaparib and niraparib were examined through a dose-response assay (72 hour treatment and 9 days recovery), which caused significant dose-dependent reduction in cellular proliferation specifically in the palbociclib resistant cells compared to the parental (**Figure 73C**). A similar response was seen with the Wee1 kinase inhibitor, AZD1775 (shown previously to induce genomic instability (Vriend, De Witt Hamer et al. 2013), where the resistant cells exhibit durable and increased sensitivity (**Figure 73C**). However, as expected, treatment with the PARP inhibitors (olaparib and niraparib) or the Wee1 kinase inhibitor did not affect the increase cancer stem cell population in the resistant cells (**Figure 73D**), indicating these drugs possible affect the proliferation of the non-cancer stem cell population in the resistant cells.

This indicates that targeting the DNA repair deficiency with PARP inhibitors could be an effective therapy to treat palbociclib resistance.

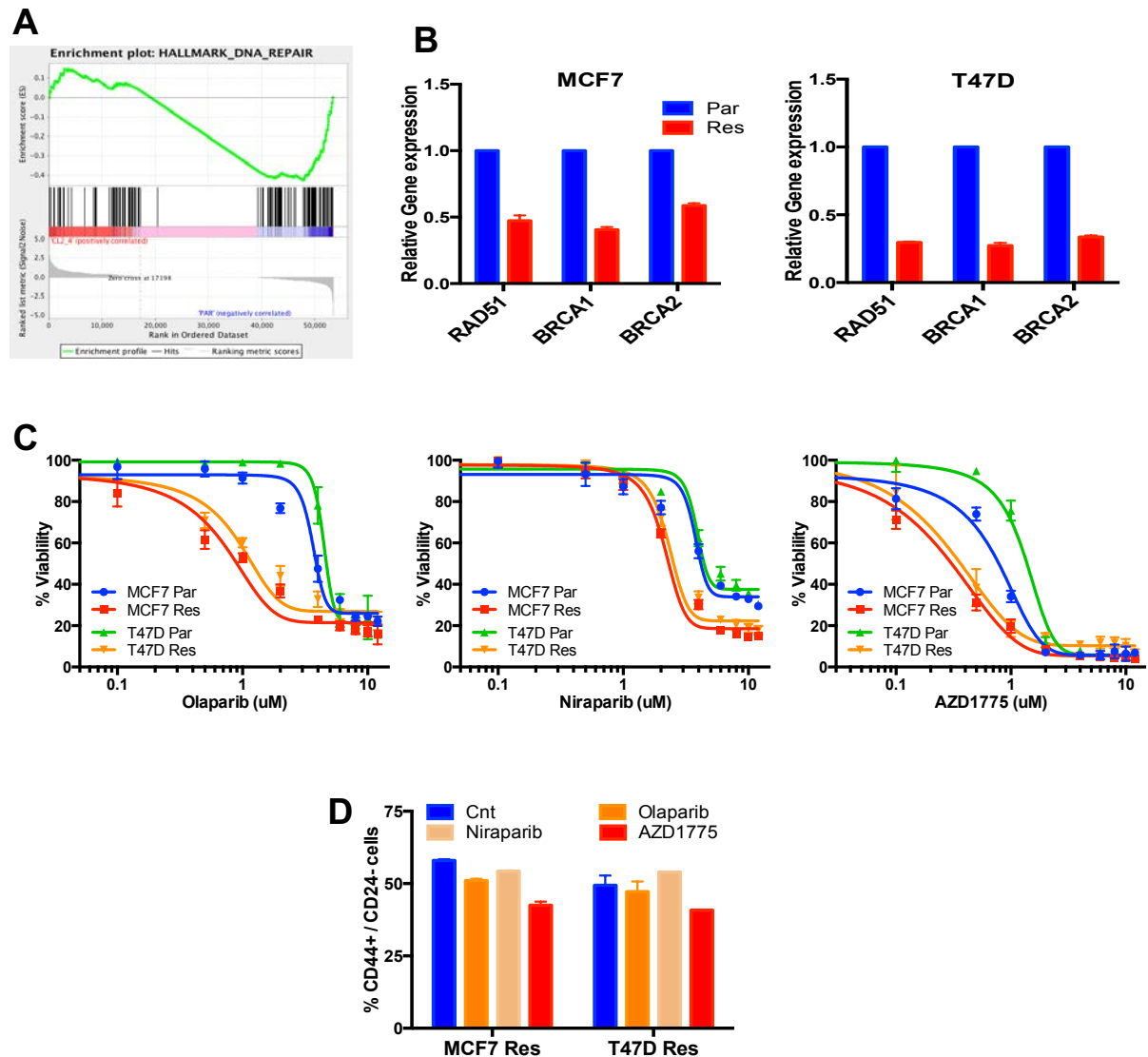


Figure 73: Targeting DNA repair deficiency in palbociclib resistant cells: A) Enrichment plot of the DNA repair pathway pathway obtained by Gene set enrichment analysis (GSEA) between T47D resistant and parental cell lines. B) qRT-PCR measuring the mRNA expression of DNA repair genes (Rad51, BRCA1, BRCA2) relative to GAPDH in palbociclib sensitive vs resistant cells. C) Dose response studies measuring the impact of treating with treatment with the PARP inhibitors, olaparib and niraparib and the Wee1 kinase inhibitor (AZD1775) on the proliferation of MCF7 and T47D parental and resistant cell lines. D) Flow cytometry analysis measuring the percentage of CD44 high CD24 low population of cells in MCF7 and T47D parental and resistant cells upon treatment with the PARP inhibitors or Wee1 kinase inhibitor for 72 hours.

9.2.6. COMBINED TREATMENT WITH STAT-3 AND PARP INHIBITORS IN PALBOCICLIB RESISTANT CELLS

While PARP inhibitors have anti-proliferative effects in palbociclib resistant cells, they do not affect the cancer stem cell population, which comprises of >60% of the cells in the resistant cell lines. Hence we examined if combining the PARP inhibitors with the drugs targeting the IL-6/STAT-3 pathway would facilitate killing of both the cancer stem cells and non-cancer stem population within the resistant cells.

First, to examine the synergy between the two drugs, olaparib (PARP inhibitor) and napabucasin (STAT-3 inhibitor), we performed dose response studies with 72 hour treatment (and 9 days of recovery) of both the drugs, followed by calcsyn analysis in the palbociclib resistant MCF7 and T47D cells. The calcsyn software measures the combined effectiveness of two drugs from growth inhibition curves, generating combination index (CI) values, with values $CI > 1$ as meaning antagonism, $CI = 1$ meaning additivity and $CI < 1$ meaning synergism between the two drugs being tested (Bijnsdorp, Giovannetti et al. 2011). Results indicated that the combination of the two drugs were highly synergistic, with CI values of 0.65 and 0.75 in the MCF7 and T47D resistant cells respectively (**Figure 74A**). Further, the combination of olaparib and napabucasin significantly decreased colony formation (**Figure 74B**) and inhibited growth (**Figure 74C**), compared to no treatment or treatment with either drugs as a single agent, in MCF7 and T47D palbociclib resistant cells. Finally, combined treatment with olaparib and napabucasin increased cell death via apoptosis in the palbociclib resistant cells (**Figure 84D**), when compared to no-treatment or single treatment controls. The increase in apoptosis was observed both at the end of treatment and 72 hour (in the absence of drug) post treatment, which showed further increase in apoptosis (**Figure 74D**).

Thus, these results indicate that combined treatment with the STAT-3 and PARP inhibitors is effective in targeting the palbociclib resistant cells.

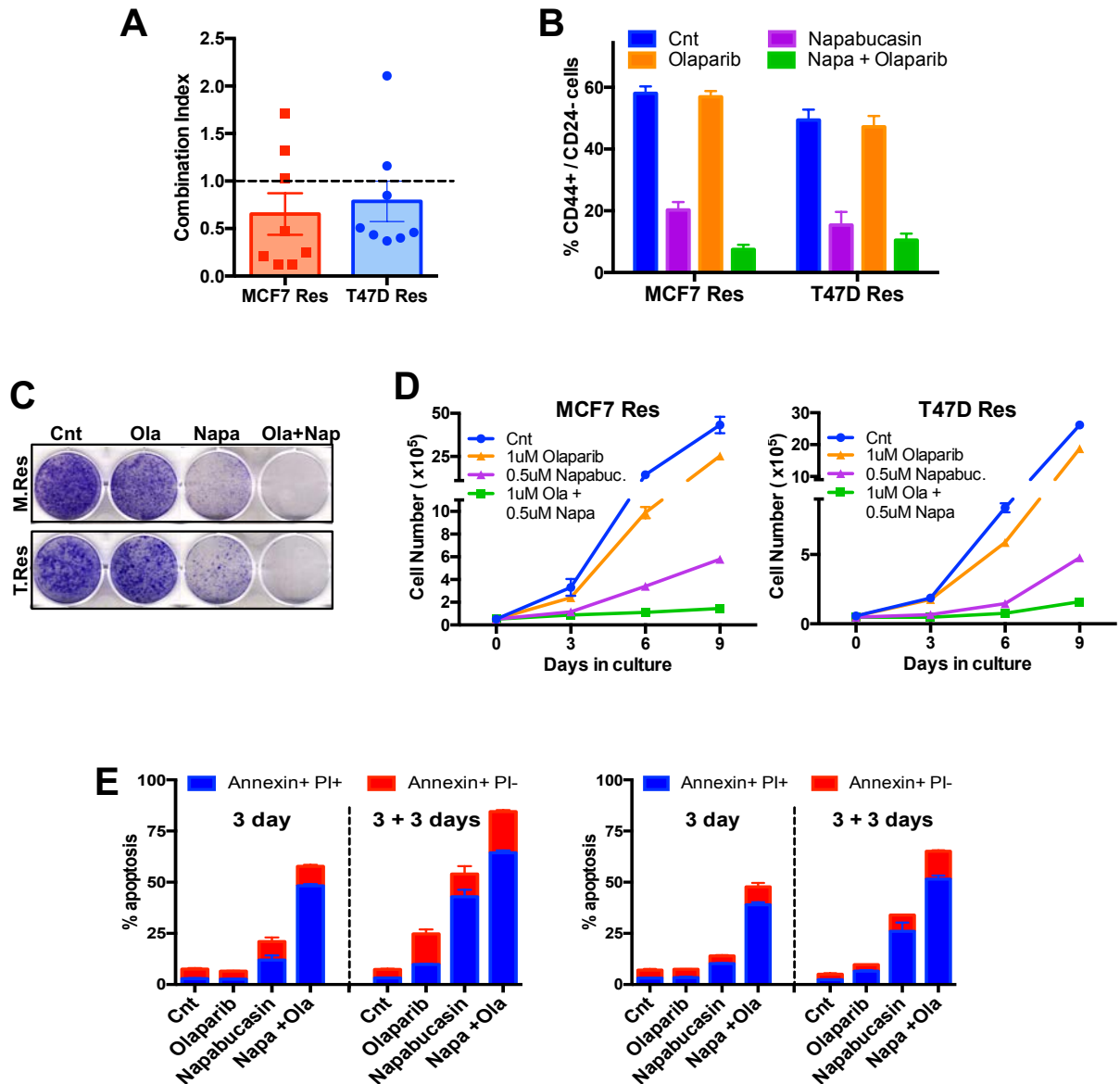


Figure 74: Combined treatment with with STAT-3 and PARP inhibitors in palbociclib resistant cells: A) Combination indices (CI values) calculated from Calcsyn which measures synergy upon treatment with the combination of 0.5uM napabucasin and a varying concentrations of olaparib. B) Flow cytometry analysis to measure the percentage of CD44 high CD24 low population of cells upon treatment with 0.5uM napabucasin and 1uM olaparib as a single drug or in combination for 72 hours. MCF7 and T47D parental and resistant cells were treated with the combination of 0.5uM napabucasin and 1uM olaparib for 72 hours and subjected to C) clonogenic assay to measure change in proliferation, D) cell counting to measure proliferation and E) Annexin V PI staining to measure apoptosis at the end of treatment and after 3 days of recovery in the absence of the drugs.

9.3. DISCUSSION

Studies in this chapter have identified novel mechanisms by which the ER positive breast cancer cells acquire resistance to palbociclib and through detailed gene expression arrays and validations, found treatment options that could work effectively in the resistant tumors. Taken together, the results show that targeting IL-6/STAT-3 mediated cancer stem cells and DNA repair deficiency by PARP inhibitors in combination can effectively treat acquired resistance to palbociclib.

GSEA analysis of the RNA-seq data showed upregulation of numerous cytokine pathways including the IL-6/STAT-3 pathway. However, the origin or source of the IL-6 has not been interrogated in this chapter. One possibility is that the IL-6 is secreted by the tumor cells and undergoes autocrine activation of the pathway. Alternatively, the cytokines including IL-6 may be secreted by cells when they undergo senescence in response to palbociclib in the early stage of development of the resistant cells. This phenomenon of the senescent cells secreting cytokines is termed as senescence associated secretory phenotype (SASP), and helps recruit immune cells to the tumor and eliminate the senescent cells (Coppe, Desprez et al. 2010).

Further, while studies in this chapter show that the IL-6 / STAT-3 pathway mediates the induction of cancer stem cells, there could be other pathways involved in this process. Results from chapter 4 show that CDK4/6 inhibition and palbociclib treatment triggers autophagy in the ER positive cells, which limit the efficacy of palbociclib. Moreover, studies have shown that autophagy induces and maintains cancer stem cells, mediating chemo-resistance, tumor recurrence and metastasis (Ojha, Bhattacharyya et al. 2015, Vitale, Manic et al. 2015). Hence, it is possible that apart from IL-6 / STAT-3, the autophagy pathway might also play a role in the induction of cancer stem cells in the palbociclib resistant cells.

Finally, GSEA analysis from the RNA-seq shows the abundance of immune response pathways that are upregulated in the palbociclib resistant cells. While breast cancer tumors are not inherently tumorigenic, recent efforts have focused on making the breast tumors immune hot,

such that they recruit tumor infiltrating lymphocytes (TILs) and are made sensitive to immunotherapy such as checkpoint blockade, PD-1, PDL-1 and CTLA-4 therapy (Hartkopf, Taran et al. 2016). Thus, it is possible that the upregulation of these pathways might be indicative of immune response in these resistant tumors, which in turn can be targeted by immunotherapy. However, the model used for resistance studies have limitations since it a breast cancer cell lines model and is devoid of the system needed to study the effect of the microenvironment.

CHAPTER 10: CONCLUSIONS AND FUTURE DIRECTIONS

10.1. MAJOR FINDINGS

Deregulation of the cell cycle is a common hallmark of cancer leading to uncontrolled proliferation and tumorigenesis. This makes the cell cycle an attractive target for drug development and have led to the development of the CDK4/6 inhibitors in the recent years. The CDK4/6 inhibitors, palbociclib and ribociclib are currently FDA approved in combination with aromatase inhibitors, for the treatment of ER positive breast cancer. Further, they are currently under clinical investigation for other indications and other cancers, while a third drug, abemaciclib is under FDA review. Despite these promising clinical advances with CDK4/6 inhibitors, the treatment has some major clinical limitations, addressing which was the main goal of the project.

First, to understand the mechanism by which the CDK4/6 inhibitor acts, we utilized ER positive breast cancer cells, MCF7 and T47D and xenograft mouse models developed from the MCF7 cell lines. Our results showed that palbociclib treatment induced a dose-dependent induction of sustained growth inhibition, cell cycle arrest (G1 arrest) and ROS-mediated senescence *in vitro* and *in vivo*. The study further demonstrated that on-target (low doses) inhibition of CDK4/6 via palbociclib failed to mediate a durable and irreversible growth inhibition or significant senescence in this model system. Upon investigation, it was found that these doses of palbociclib or genetic **inhibition of CDK4/6 triggers autophagy**, a stress response process, that enables the cells to proliferate and survive even in the presence of the inhibitor. This phenomenon was seen in cell lines *in vitro* and xenograft tumors *in vivo*, and mediates resistance to the induction of senescence by palbociclib (**Figure 75**).

More significantly, molecular ablation or **pharmacological inhibition of autophagy** **significantly improves the efficacy of the CDK4/6 inhibitors**, palbociclib, ribociclib and

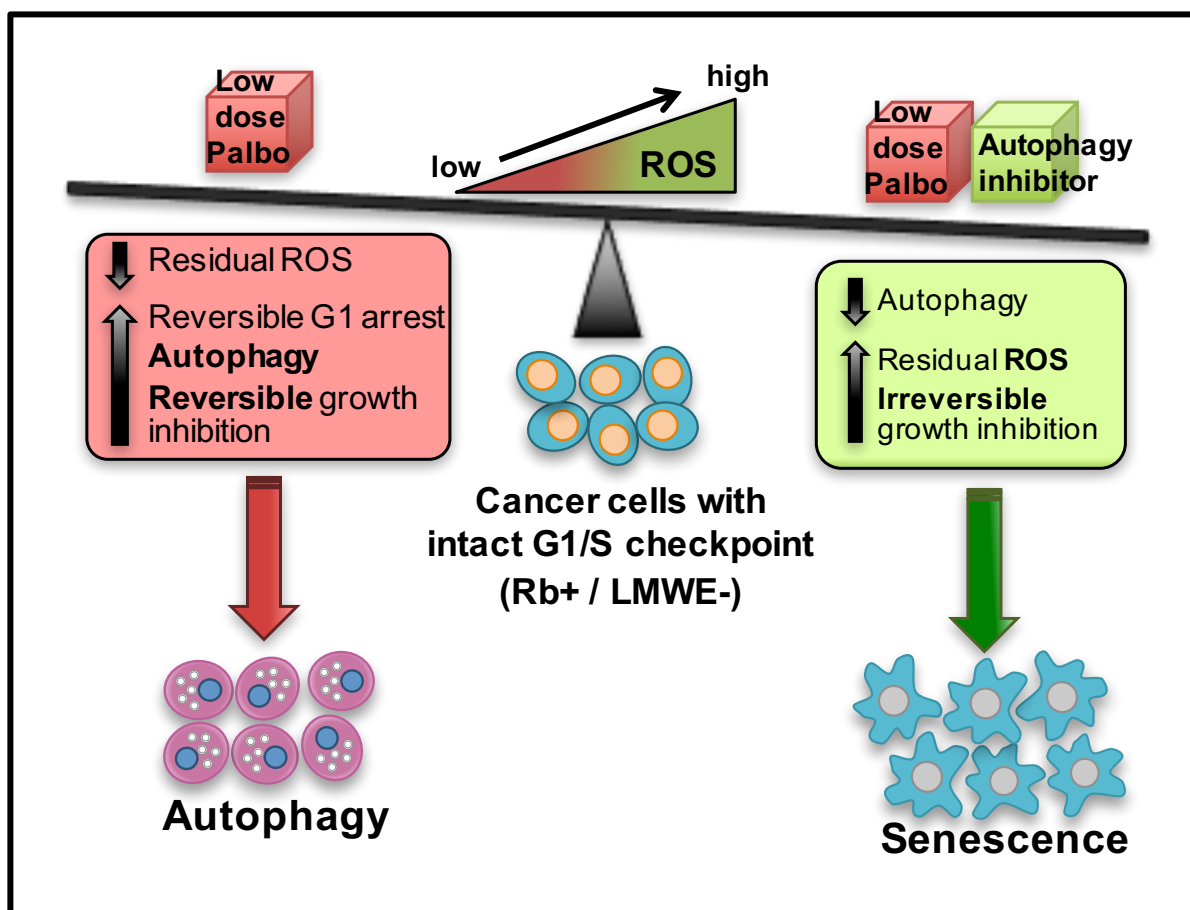


Figure 75. Overall working model: Schematic depicting the role of CDK4/6 inhibition (i.e., palbociclib [Palbo]) and combined CDK4/6 and autophagy inhibition in regulating autophagy, reactive oxygen species (ROS), and senescence in cancer cells with intact G1/S transition.

abemaciclib, resulting in the induction of an irreversible growth inhibition, cell cycle arrest and senescence even at low doses of the palbociclib. This synergistic effect between palbociclib and autophagy inhibitors was verified *in vivo* using two different autophagy inhibitors, hydroxychloroquine and Lys-05, both of which showed **significant improved tumor growth inhibition and senescence** in combination with low dose palbociclib. This **synergistic effect** of the combination was also observed in triple negative breast cancer (TNBC) cell lines *in vitro* and TNBC PDX models *in vivo*. **Synergism** between palbociclib and autophagy inhibition was also observed in **other cancers such as ovarian, lung, colon, pancreatic and prostate**

cancer, where the combination induced a sustained and irreversible growth inhibition even with low dose of palbociclib.

Further, **biomarker identification** studies showed that an **intact G1/S checkpoint** is crucial for the cancer cells to response to **CDK4/6 inhibition** and mediate a sustained growth inhibition and **senescence**. We show that the intact G1/S checkpoint can be identified by **presence of Rb** and **absence** or low expression of **LMWE** (low molecular weight isoforms of cyclin E). This ability of Rb and LMWE (cytoplasmic cyclin E) in combination to predict response to palbociclib was performed in tumor tissues from palbociclib treated patients, which showed that Rb and LMWE are **reliable prognostic markers for palbociclib**. Our immediate goals are to evaluate the predictive values of Rb/LMWE in pre and post palbociclib treated patients and interrogate if those patients with an intact G1 to S transition respond better to therapy as compared to those patients whose tumors show a deregulation of the G1/S transition. Further, since autophagy induction is a response to palbociclib mediated drug action, we show that **Rb and LMWE can also serve as biomarkers for the combination of CDK4/6 and autophagy inhibitors**.

Finally, studies to identify acquired resistance to palbociclib showed that the **acquired resistant** cells had a significantly **different gene expression** profile compared to the parental (sensitive) cells, with numerous upregulated and downregulated pathways. Functionally, we show that the resistant cells exhibit **IL-6/STAT-3 mediated upregulation of EMT and cancer stem cell** pathways and **downregulation of the DNA repair** pathway. Thus, targeting these pathways in combination using STAT-3 and PARP inhibitors proved highly effective in reducing the cancer stem cell population and inducing cell death in the palbociclib resistant cells. We also show that there is a strong cross resistance between palbociclib and other CDK4/6 inhibitors, suggesting that alternative drug strategies need to be devised to treat all the patients who are being treated with any of the CDK4/6 inhibitors.

10.2. SIGNIFICANCE

Results from this study are highly translatable and clinically relevant with the potential of making a significant impact on the lives of patients with breast and other cancers.

While there are numerous mechanistic studies with the CDK4/6 inhibitors, no study till date has examined in the detail dose dependent effect of the drug and its reversibility. Further, most studies examine a short-term effect of the drug (72 hour treatment with concentrations lower than 1 μ M), which based on our studies can only induce a reversible growth inhibition and G1 arrest. Thus, our study addresses this limitation by examining the time and dose-dependent effect, making it a very clinically relevant model system to understand palbociclib mechanism.

Notably, the study unravels a novel link between palbociclib mediated CDK4/6 inhibition, ROS, autophagy and senescence. This is the first detailed study till date to examine the ability of CDK4/6 inhibitors to induce autophagy in breast and other cancers. Given the protective nature of autophagy, this result has great therapeutic implications, which have been extensively analyzed in this study. With autophagy inhibitors, such as chloroquine and hydroxychloroquine being FDA approved, it makes translation of the combination therapy between CDK4/6 and autophagy inhibitors feasible and highly clinically relevant. Details of the proposed clinical trial are mentioned in the next section and a draft of the clinical trial protocol is in the appendix of this thesis.

The proposed clinical trial with the drug combination would significantly improve the efficacy of the current treatment with CDK4/6 and aromatase inhibitors, and even improve the overall survival of patients – a result that has not been achieved with the current CDK4/6 inhibitor treatments. This is based on our *in vitro* and *in vivo* preclinical data which showed that the drug combination improves efficacy not just in the presence of the drug, but helps achieve a lasting or durable effect even after drug removal. Further, the enhanced anti-tumor effect achieved in the ER positive xenografts and the TNBC PDX tumors *in vivo* were at a palbociclib dose of 25mg/kg, which is one-fifth the dose (150mg/kg), used in most pre-clinical studies with

palbociclib thus far. This suggests that the drug combination can help decrease the dose of palbociclib in the clinic, which would help lower adverse events in patients and prevent the need for any therapy discontinuation.

This study also has identified reliable biomarkers for palbociclib, which is the need of the hour given that none of the previously predicted pre-clinical biomarkers were effective in the clinical setting. The study is novel since it proposes a dual biomarker strategy, that is simple to use in the clinical and can effectively identify responsive patients. Moreover, recent unpublished clinical data shows that the only reliable predictor of drug resistance in patients is the resistance to reduction in the phosphorylation or the hyperphosphorylation of Rb. Low molecular weight isoforms of cyclin E (LMWE), one of our proposed biomarkers is known to hyperphosphorylate Rb, making a clinically relevant biomarker.

Finally, given that CDK4/6 inhibitors are currently the standard of care for ER positive breast cancer patients, and even responsive patients would eventually acquire resistance to therapy, understanding the mechanisms of acquired resistance to the drug is important. Thus, results from this study have identified two clinically relevant and druggable pathways that can be targeted in combination to effectively combat drug resistance. Further, the gene expression analysis performed also provided avenues for future research and drug development to target acquired resistance to CDK4/6 inhibitors.

Taken together, this is a highly comprehensive study that improves the selectivity and efficacy of CDK4/6 inhibitor treatment in the sensitive setting and has identified ways to target acquired resistance to the drug.

10.3. FUTURE DIRECTIONS

We report here that cancer cells activate autophagy in response to palbociclib, and that blockade of autophagy significantly improves the efficacy of CDK4/6 inhibition *in vitro* and *in vivo* in cancers with an intact G1/S transition.

Thus, this study provides strong pre-clinical data for a biomarker integrated clinical trial utilizing hydroxychloroquine (or other autophagy inhibitors such as Lys05) to potentiate the action of palbociclib. Given that HCQ is well tolerated and is currently in clinical trials to reverse hormonal and cytotoxic drug resistance, we first propose a Phase II clinical trial (in the neoadjuvant setting) in postmenopausal advanced ER+/HER2- breast cancer patients, treating them with the combination of low-dose palbociclib (75mg/day compared to the current standard dose of 125mg/day), HCQ, and letrozole using surrogate biomarkers such as Ki67 staining. Eligible patients will be selected on the basis of Rb and LMW-E expression assessed from baseline biopsy specimens. Prior to the combination treatment, patients would receive palbociclib for a week following which the levels of LC3 would be evaluated by IHC, comparing it to pre-treatment biopsy tissues. This would help confirm that autophagy is being induced in the patients upon treatment with palbociclib and provide a clinical rationale for the combination treatment. Details of this clinical trial protocol, which is currently under evaluation is attached to the appendix of this thesis.

Results from this clinical trial would further support initiation of a definitive Phase III trial for the triple combination, possibly even extending this treatment to the TNBC subtype of breast cancer and other tumors evaluated in this study. Additionally, this would also support the utility of palbociclib + HCQ combination to treat RB+/LMWE- ER+ve breast cancer in the neoadjuvant setting. We predict that the combination of continuous low-dose palbociclib and HCQ would be more beneficial than standard-dose palbociclib (21 days on, 7 days off), allowing us to minimize palbociclib-mediated toxicities, avoid proliferative bursts that occur when palbociclib is stopped, and prolong overall patient survival – a goal that has not yet been met with currently approved palbociclib treatment combinations. Finally, given the pre-clinical data from this study, the combination of CDK4/6 and autophagy inhibition can be extended to the other CDK4/6 inhibitors as well clinically, further expanding the applicability of the study.

While results from this study show that CDK4/6 inhibition induces autophagy, the molecular mechanism by which this occurs is not known. Some of the crucial autophagy genes such as Beclin-1 or class III PI3K proteins that are present in complex with Beclin-1, such as Vps34, are phosphorylated as a mechanism of regulating autophagy induction (Hammond, Brunet et al. 1998). These proteins have direct CDK phosphorylation sites, although the role of CDK4 or CDK6 has not been shown in this process (Abrahamsen, Stenmark et al. 2012). Moreover, treatment with palbociclib was synergistic with the autophagy inhibitor Spautin-1, which regulates Beclin-1 through USP proteins (Shao, Li et al. 2014), suggesting that palbociclib mediated regulation of autophagy might occur at the initiation step. Hence, it is possible that the drug directly regulates autophagy by phosphorylating and regulating the activation of the autophagy proteins, Beclin-1 and Vps34, a potential mechanism that needs to be investigated further.

Another important application of the study would be in the acquired resistance setting. Results the gene expression and GSEA analysis of the acquired resistant cells showed a significant enrichment in the immune response pathways. While, the system is not optimal to examine immune regulation due to the absence of the microenvironment, it still suggests that acquired resistance might be making the cells immune responsive. This would potentially make the ER positive breast tumors that have progressed on CDK4/6 inhibitors responsive to immune checkpoint blockade drugs such as PD-1, PDL-1 or CTLA-4 antibodies among others. This would open put a new avenue of treatment options for these patients and further advance the field immunotherapy in breast cancer.

APPENDIX

Phase I/II Safety and Efficacy Study of Autophagy Inhibition with Hydroxychloroquine to Augment the Antiproliferative and Biological Effects of Pre-Operative Palbociclib plus Letrozole for Stage I-III Estrogen Receptor-Positive and HER2-negative Breast Cancer

Principal Investigator:	Debu Tripathy, MD
Principal Co-Investigator (Translational Sciences):	Khandan Keyomarsi, MD
Principal Co-Investigator:	Alastair Thompson, MD
Co-Investigators:	Kelly Hunt, MD
	Meghan Karuturi, MD
	Rachel Layman, MD
Study Statistician:	Kenneth Hess, PhD
Study Pathologist:	Aysegul Sahin, MD
Study Radiologist:	Gaiane Rauch, MD
	Beatriz Adrada
Collaborators:	TBA

Contents

STUDY SYNOPSIS	259
1.0 INTRODUCTION.....	261
1.1 Background.....	261
1.3 Rationale for the Use of Pre-operative (Neoadjuvant) or “Window” Endocrine Therapy ..	264
1.4 Risk/Benefit Assessment.....	265
2.0 STUDY AIMS AND OBJECTIVES.....	265
2.1 Phase I Safety Component (metastatic disease) Objectives and Endpoints	265
2.1.1 The primary objective of the Phase I portion in the metastatic cohorts is to determine the safety of adding hydroxychloroquine to standard dose palbociclib and letrozole and to determine the recommended phase 2 dose for hydroxychloroquine.	265
Primary endpoint is safety, to be assessed continuously using CTCAE V4.03, with physical examination and laboratory assessments as indicated on the study schedule	265
2.2 Phase II Window/Neo-adjuvant Component Objectives and Endpoints.....	265
3.0 INVESTIGATIONAL PLAN.....	266
3.1 Overall Design.....	266
3.3 Dose Limiting Toxicity Definition	270
3.4 Phase II Part 1 (neo-adjuvant cohorts)	270
Pre-operative “Window” Component:.....	270
The “window” component of the trial evaluates the combination of pre-operative palbociclib plus letrozole followed by the addition of hydroxychloroquine (HCQ) for postmenopausal patients with Stage I-III estrogen receptor-positive and HER2-negative breast cancer (Figure 2).	271
Correlative studies using baseline and follow up breast biopsies and blood work are included in the research plan. The Phase II portion will assess the change in the percentage of all patients who achieve CCCA when adding HCQ to the palbociclib/letrozole combination.	271
To determine the dose responsiveness in the pre-operative setting 2 groups of 6 patients each will be enrolled at the following dose levels:	271
Should the RP2D be < 800mg/d the second group will be receive the RP2D of hydroxychloroquine in the combination as determined in the Phase I.	271
3.5 Phase II Part 2 Window/Neo-adjuvant Component	271
3.6 Phase II Patient Evaluability	271
3.7 Replacement of Patients	271
3.8 Target Accrual	271
4.0 PATIENT SELECTION	271
4.1 Inclusion Criteria	272
4.2 Exclusion Criteria	272
5.0 STUDY PROCEDURES AND SCHEDULE OF ASSESSMENTS.....	273
5.2 Schedule of Assessments	273
5.2.1 Baseline Assessments	275
5.2.2 Evaluation During Study Phase II.....	276
5.2.3 Treatment Duration	276
5.2.3.1 Phase I.....	276
Patients will receive treatment for a maximum of 24 weeks if receiving clinical benefit as determined by the treating physician.	276
5.2.3.2 Phase II	276
5.2.4 End of treatment visit and Follow up assessments	276

5.2.8	Imaging assessments Phase I.....	277
	Tumor response will be assessed according to RECIST Version 1.1. Patients should have at least one documented measurable lesion (per RECIST v1.1) or in the absence of measurable disease, have at least one lytic or mixed (blastic/lytic) bone lesion at study entry.....	277
	Imaging assessments will be performed as per standard of care at screening within 28 days prior to first dose of study treatment, at 8 weeks (+/- 1 week) from day one of study treatment and subsequently every 8-12 weeks (+/- 2 weeks) thereafter.....	277
	Tumor response should be assessed using the same imaging method throughout the study.	277
5.3	Correlative Biomarker Studies.....	277
6.0	INVESTIGATIONAL AND NON-INVESTIGATIONAL AGENTS	279
6.1	Palbociclib	279
6.2	Hydroxychloroquine	281
6.3	Letrozole.....	282
7.0	ADVERSE EVENT MONITORING AND REPORTING	282
7.1	Definition of an Adverse Event.....	282
7.2	Definition Serious Adverse Event	282
7.3	Adverse Event Reporting Period.....	283
7.4	Recording of Adverse Events.....	283
	It is the responsibility of the PI and the research team to ensure serious adverse events are reported according to the Code of Federal Regulations, Good Clinical Practices, the protocol guidelines, the sponsor's guidelines, and Institutional Review Board policy.	284
7.5	Assessment of Adverse Events	284
7.6	Communications between the Investigator and Supporting Company Pfizer	284
8.0	STATISTICAL CONSIDERATIONS	284
9.0	REFERENCES.....	285

STUDY SYNOPSIS

Title	<p>Potiation of palbociclib and letrozole with autophagy inhibition using hydroxychloroquine in the neoadjuvant setting (title on Pfizer IIT application)</p> <p>Phase I/II Safety and Efficacy Study of Autophagy Inhibition with Hydroxychloroquine to Augment the Antiproliferative and Biological Effects of Pre-Operative Palbociclib plus Letrozole for Stage I-III estrogen receptor-positive and HER2-negative Breast Cancer</p>
Study Type	Phase I/II, Open Label, Interventional with biomarkers
Overall Goal	To demonstrate the clinical and biological impact of adding autophagy inhibition using hydroxychloroquine to palbociclib and letrozole in estrogen receptor-positive and HER2-negative early stage breast cancer
Objectives (Phase I)	<p>Primary:</p> <p>Secondary:</p> <ul style="list-style-type: none"> •
Objectives (Phase II)	<p>Primary:</p> <p>To determine whether hydroxychloroquine added to low dose palbociclib and letrozole can increase the proportion of patients whose tumors achieve complete cell cycle arrest (CCCA, proportion with Ki67 $\leq 2.7\%$)</p> <p>Secondary</p> <ul style="list-style-type: none"> • To determine the impact of adding hydroxychloroquine to low dose palbociclib and letrozole on breast tumor indices of proliferation, autophagy, senescence, cell cycle control and other intersecting pathways • Determine longer term clinical tumor responsiveness and tumor biomarkers indices (for patients who have extended pre-operative therapy, maximum 24 weeks) • To perform exploratory studies on blood-based tumor protein, DNA and RNA biomarkers • Obtain additional safety information for the combination of low dose palbociclib, letrozole and hydroxychloroquine
Design	Single center pre-operative (neoadjuvant)/"window" study, open-label with a lead-in Phase I dose escalation/safety/feasibility and dose-finding study, followed by a single arm Phase II efficacy study using primary endpoint of validated surrogate tumor biomarker of change in Ki67-based complete cell cycle arrest (CCCA)
Sample Size	<p>Phase I: 18 patients</p> <p>Phase II: 30 patients</p>
Inclusion Criteria	<ol style="list-style-type: none"> 1. Signed written informed consent 2. ECOG performance status 0-1 3. Stage I-III estrogen invasive breast cancer, estrogen receptor-positive and HER2-negative by ASCO/CAP criteria^{1,2}. If Stage I, clinical tumor size must be ≥ 1.5 cm. 4. Female and age ≥ 18 years and postmenopausal defined by: <ol style="list-style-type: none"> a. Age ≥ 55 years and 1 year or more of amenorrhea

	<ul style="list-style-type: none"> b. Age < 55 years and 1 year or more of amenorrhea with LH and/or FSH levels in the postmenopausal range c. Age < 55 with prior hysterectomy but intact ovaries with LH and/or FSH levels in the postmenopausal range d. Status after bilateral oophorectomy (≥ 28 days prior to first study treatment) <p>5. Surgical candidate and appropriate for pre-operative endocrine (endocrine) therapy</p> <p>6. Normal hematological, renal, hepatic function</p> <ul style="list-style-type: none"> a. ANC ≥ 1500 cells/μl b. Platelet count $\geq 100,000$/μl c. Serum creatinine concentration < 1.5 x ULN d. Bilirubin level < 1.5 x ULN <p>e. Aspartate aminotransferase (AST) or alanine aminotransferase (ALT) <3 x ULN</p>
Exclusion Criteria	<ul style="list-style-type: none"> 1. Inoperable or metastatic breast cancer based on standard evaluation 2. Inflammatory breast cancer or any clinical T4 disease 3. History of retinal disease or active visual disturbances(normal baseline retinal exam required) 4. Prior therapy for breast cancer (medical, surgical or radiation therapy) 5. Acute illness, including infections requiring medical therapy, known bleeding diathesis or need for anticoagulation 6. Treatment with any of the following medications within 4 weeks before the baseline diagnostic biopsy is taken: <ul style="list-style-type: none"> a. Oral estrogens, including hormone replacement therapy (but prior depot estrogen use not allowed); b. Investigational agents (or 5 half-lives, whichever is longer) 7. Psychological, familial, sociological or geographical conditions that do not permit compliance with the study protocol.

1.0 INTRODUCTION

1.1 Background

1.1.1 Hormone receptor-positive breast cancer

Breast cancer is the most common female cancer in the United States. It is estimated that 252,710 American women will be diagnosed with breast cancer and 40,610 will die from the disease in 2017.³ A major cause of death in these patients is disease progression and incurable metastasis. The SEER database estimates that ~40,000 breast cancer patients a year either present at diagnosis (n=13,900) with metastatic disease or exhibit progression with metastatic disease, sometimes many years after completing therapy for early stage disease (n=36,000).⁴ Of these, an estimated 30,000 have estrogen receptor (ER)-positive breast cancers.⁴ Hence, patients with ER+ metastatic breast cancer (MBC) represent a majority of breast cancer who die of their disease, the vast majority due to metastatic progression.

1.1.2 Therapies for hormone receptor-positive breast cancer

In early stage estrogen receptor-positive (ER+) breast cancer, the use of adjuvant endocrine therapy (tamoxifen or aromatase inhibitors) lowers the relative risk of recurrence at 10 years by 45 to 50% and that of mortality by breast cancer death by 30%.⁵ In the metastatic setting endocrine therapy can induce responses and delay progression of disease. However, in the metastatic setting, it has been difficult to demonstrate a survival benefit of endocrine therapy. Few modern-day trials have compared endocrine therapy to no endocrine therapy in the absence of chemotherapy since treatment induces clear palliation. More recent trials comparing single-agent to combination endocrine therapy agents (e.g. aromatase inhibitors plus the ER downregulator fulvestrant) have yielded mixed results.^{6, 7} In the last few years, the addition of biological therapies that were designed to address mechanisms of resistance or with demonstration of preclinical synergy have shown improvements in disease-free survival when added to endocrine therapy, but no impact on overall survival - although these trials were not designed with the statistical power to survival differences, with disease-free survival designated as the primary endpoint. The addition of the mTOR inhibitor everolimus doubled median disease-free survival from 4.1 to 10.6 months when added to the aromatase inhibitor exemestane as second-line therapy and was approved by the FDA with final survival analysis showing no significant difference in that outcome (median survival of 31.0 vs. 26.6 months).^{8, 9} Other biological agents such as PI3 kinase inhibitors, histone deacetylase inhibitors and cyclin-dependent kinase (CDK) inhibitors are being actively tested in first, second and later lines of therapy - so far CDK 4/6 inhibitor palbociclib has been approved by the FDA as outlined in the next section.

In summary, the treatment of ER+ breast cancer is focused on using endocrine therapy initially as trials have not shown clear benefits of more aggressive chemotherapy up front, and such approaches are only recommended for rapidly progressing visceral and high burden disease. Sequential use of endocrine therapies (including with approved biological drugs everolimus and palbociclib) upon progression is the standard approach, with a switch to chemotherapy when it is felt that the tumor is unresponsive to any endocrine therapy.¹⁰ In contrast to HER2+ breast cancer, where the use of HER2-targeted drugs, particularly the antibodies trastuzumab and pertuzumab have yielded significant survival benefits, the same advances are lacking in ER, HER2-negative breast cancer, representing a majority of all cases and hence representing a clear unmet need. Finally, it should be noted that the definition of hormone receptor-positive breast cancer includes tumors that are positive for either estrogen or progesterone receptor (ER or PR).¹ While the ER+/PR- subgroup is relatively common, about one third of all cases, and is clearly responsive to endocrine therapy, the same cannot be said for the rare ER-/PR+ group and hence this trial is only focusing on ER+ cases.

1.1.3 Palbociclib and use in breast cancer

Palbociclib is a potent and specific cyclin-dependent kinase 4/6 (CDK4/6) inhibitor and anti-proliferative agent that induces G1 arrest and prevents breast cancer cell growth, most notably in ER+ cell lines and other preclinical models, which led to the clinical development of this class of inhibitors in hormone receptor-positive breast cancer.¹¹⁻¹³ Palbociclib was approved by the FDA in February, 2015 based on improved time to disease progression in the first and second-line settings for ER+/HER2-negative metastatic breast cancer (MBC).¹⁴⁻¹⁷ In the pivotal first-line Phase III trial, progression-free survival (primary endpoint) was improved from 14.5 to 24.8 months with the addition of palbociclib to the standard first-line aromatase inhibitor letrozole.¹⁵ In the second-line setting, the addition of palbociclib to the standard second-line estrogen downregulate fulvestrant in a Phase III trial also demonstrated a significant improvement in time to progression from 3.8 to 9.2 months.

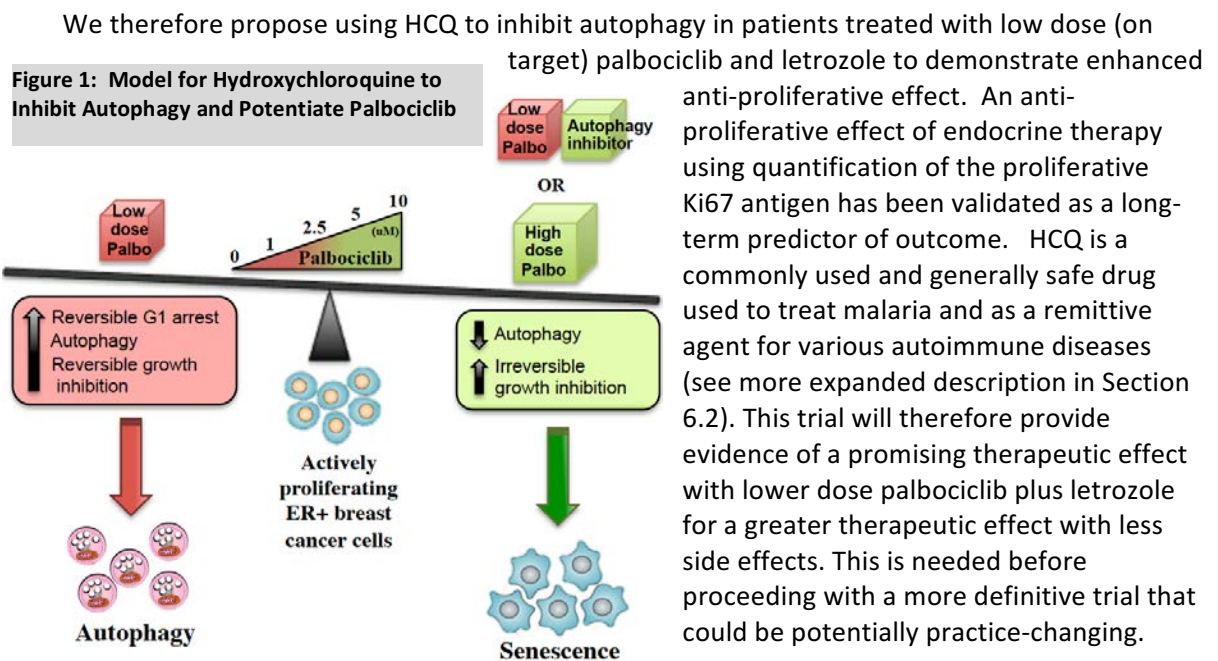
However in the first line setting, 66% of patients on the palbociclib experienced grade 3 and 4 neutropenia, and adverse events necessitate a palbociclib dose reduction in 36% and discontinuation in 7.4% of patients.¹⁵ Additionally, palbociclib must be dosed with a 7-day break, which was shown to be associated with a proliferative burst in a separate neoadjuvant serial biopsy study.¹⁸ Also, a precise biological mechanism of palbociclib's action is still unknown and there are no known independent biomarkers to predict response and/or resistance to palbociclib – many patients do not respond to therapy, and most importantly, virtually all eventually develop resistance. Biomarkers that may influence response to endocrine therapy and CDK inhibitors including estrogen receptor-alpha (ESR1) and PIK3CA mutations, loss of the retinoblastoma protein function, proliferative antigen Ki67 expression, cyclin D 1 amplification or loss of the cyclin-dependent kinase inhibitor p16 have not shown to be related to palbociclib-associated response or time to progression.^{13, 17, 19} Importantly, no survival benefit yet observed in either of the larger randomized trials or smaller Phase II trial, although these trials were not powered for survival differences and diversity of therapies that patients may receive in their subsequent management may cloud future survival update analyses.

1.2 Mechanisms of Resistance to Endocrine Therapy and Rationale for the use of Autophagy inhibition with Hydroxychloroquine

While specific mechanisms of resistance to palbociclib have not been well characterized, there are several mechanisms of resistance to conventional endocrine therapies such as tamoxifen and aromatase inhibitors, which include activation of receptor tyrosine kinase signaling pathways (notably the PI3K/Akt/mTOR pathway), activation mutations in ESR1 and other more general alterations such as epigenetic regulation of gene expression other intersecting pathways like NFkB and JAK/STAT.²⁰ As described earlier, mTOR and CDK4/6 inhibition with everolimus and palbociclib are now approved as biological agents in combination with endocrine therapy, while strategies using inhibitors of PI3K, Akt, histone deacetylase are undergoing testing, none so far has been able to induce durable enough responses to affect survival, and clinical resistance still emerges with all available therapies.

Our laboratory research group, led by Khandan Keyomarsi, PhD, Professor of Experimental Radiation Oncology at MD Anderson, has an extensive investigational track record in area the cell cycle pathways in breast cancer. We have shown that at low concentrations of the palbociclib, ER+ breast cancer cells arrest in the G1 phase of the cell cycle, but this arrest is reversible due to the activation of autophagy. However, at high concentrations of palbociclib, the cells are arrested irreversibly in G1, do not undergo autophagy and instead undergo senescence. The low concentration of palbociclib are on-target and are specific for inhibition of CDK4 and CDK6, as shown with siRNA assays where CDK4 and CDK6 were knocked down. The high concentrations of palbociclib, induce senescence, but these are off target effects of the drug. We also demonstrated that if we combine palbociclib with an autophagy

inhibitor such as hydroxychloroquine (HCQ), we can achieve senescence at a much lower (i.e. on-target) and continuous dosing of palbociclib, in both *in vitro* and *in vivo* models. Moreover, concomitant treatment with HCQ and palbociclib can mediate a synergistic response in ER+ xenograft (MCF7) mouse tumor volume and weight compared to palbociclib alone. More strikingly, the tumor volumes with combination treatment did not increase even after the treatment was stopped, while the tumor volumes with either palbociclib or HCQ alone continuously increased during both the treatment and recovery phases of the experiment. Combination treatment showed the desired and expected impairment in autophagic flux. Decrease in Rb phosphorylation, a direct readout of CDK 4/6 inhibition, was more pronounced with the addition of HCQ. These results suggest that autophagy inhibition significantly improves the efficacy of low dose (on target) palbociclib *in vivo* and facilitates the induction of an irreversible tumor growth inhibition. We propose that palbociclib activates the autophagy pathway to protect ER+ breast cancer cells from palbociclib-induced senescence and inhibition of autophagy sensitizes cells to lower doses of palbociclib *in vitro* and *in vivo* (Figure 1).



1.3 Rationale for the Use of Pre-operative (Neoadjuvant) or “Window” Endocrine Therapy

We have chosen to perform this trial using the combination of letrozole, palbociclib and HCQ in the pre-operative (neoadjuvant) “window” setting after careful deliberation internally and advice from both internal and external advisory board members during the process of a grant proposal submission that led to the successful funding of both the laboratory and clinical trial aims of this project.

The following rationale support this approach:

- Palbociclib is already FDA-approved for metastatic breast cancer with an excellent safety record. It is currently in several clinical trials in both the neoadjuvant and adjuvant settings.
- Treatment will include letrozole, a standard endocrine therapy as is used clinically for early stage breast cancer.
- HCQ is an approved drug commonly used for malaria and autoimmune disease and particularly safe when used at the doses and timeframes proposed (see more expanded description in Section 6.2).
- This model allows for safe biopsies as needed for the correlative tissue aims and eliminates artifact and variability due to prior therapies as all patients will be previously untreated.
- The design gives patients and their physicians the option of a brief “window” trial with 4 weeks on study drug (2 weeks on low dose palbociclib plus letrozole, then 2 weeks with the addition of HCQ) then to proceed with surgery follow by standard of care, or, if there is a proliferative benefit with complete cell cycle arrest (CCCA) at the 4 week timepoint, patients can stay on treatment with the typical full duration of neoadjuvant endocrine therapy, up to 12-20 weeks longer then proceed with surgery as long as there is no clinical progression or significant side effect of therapy. This longer duration may allow clinically significant downstaging that has been shown to improve breast conserving rates and from the study standpoint will allow additional exploratory observations of the more prolonged effects of palbociclib, letrozole and HCQ on tumor size and tumor biological endpoints.

There is ample clinical experience and clinical trial to support the use of neoadjuvant endocrine therapy as method to downstage tumors and allow more patients to undergo breast-conserving surgery.²¹ Additionally, the neoadjuvant model is a well-established research tool to assess newer drugs when added to endocrine therapy to evaluate both clinical as well as biomarker based-responses.²² For hormone receptor-positive and HER2-negative breast cancer, the use of change in the proliferative antigen Ki67 pre to post treatment has been extensively validated as index that correlates with the likelihood of achieving a complete pathological response and with longer term outcomes specifically in trials.²³⁻³¹ The key metrics using this model in both the Phase I and Phase II portion are obtained after 2 weeks of low dose palbociclib and then 2 addition weeks with the addition of HCQ (see Sections 2.0 and 3.1).

Therefore, patients can come off study after 4 weeks and proceed with standard therapy (“window” approach), which would include standard neoadjuvant endocrine therapy (typically aromatase inhibitor), neoadjuvant chemotherapy if the patient is known to have the stage, grade and other indices that warrant chemotherapy. Alternatively they can proceed with definitive breast/axillary node surgery. In addition, if the biopsy after both 2 and 4 weeks show suppression of proliferative index that is used as the main endpoint of the study (see Section 2.2.1), patient can stay on therapy for the typical full neoadjuvant endocrine therapy course which is typically 16-24 weeks. These pragmatic alternatives will maximize accrual and allow patients and their physicians to opt for the best path that matches the patient’s clinical situation.

Expected results, alternative strategies.

We expect that autophagy effects will be seen even at low doses of HCQ. However, if our indices (changes in LC3B/p62 ratio from T1 to T2) do not suggest autophagy inhibition, then we will consider adding a cohort at 1200 and even 1600 mg day, doses that have been used in other trials. We can also consider the use of alternative autophagy inhibitors such as Lys05, a more potent chloroquine analog poised to soon enter clinical trials. In the phase I trials, if we observe too high a rate of CCCA prior to the addition of HCQ, (eg. 4 or more of 6 in the first cohort), we will lower the PD dose to 75 mg twice a week (Mon/Thurs). We may encounter problems with compliance or patient refusal to complete all biopsies. However, in our experience with similar trials, this is rare and we engage the help of patient advocates for education and outreach. If there are safety concerns raised by the IRB regarding the use of this experimental, albeit low-risk treatment in a curable population, we will amend our dose-limiting toxicity (DLT) criteria for dose escalation to be more stringent, and/or only escalate dose if no DLTs (as opposed to 0-1) are seen in each cohort of six patients.

1.4 Risk/Benefit Assessment

Patients on this study will be receiving standard of care therapy (endocrine therapy with letrozole) and palbociclib, an FDA-approved and relatively non-toxic therapy that doubles time to progression in the metastatic setting, but not approved in the adjuvant or neoadjuvant setting (see additional description of palbociclib in Section 6.1). HCQ is an approved drug used for malaria and autoimmune disorders that also had a very good safety profile (see additional description of HCQ in Section 6.2). One concern of retinal toxicity that is typically seen only after prolonged exposure, will be mitigated by baseline ophthalmological exam covered by the study funding, and exclusion of those who are felt to be at risk for retinal toxicity as established by the by the American Academy of Ophthalmology to exclude preexisting maculopathy.³²

The benefits of participation of this trial cannot be fully ascertained, but the addition of palbociclib has been shown to achieve a high rate of complete cell cycle arrest, a surrogate biomarker of long-term benefit.¹⁸ While short term exposure (4 weeks) may not affect outcome, patients who stay on study for a total of 16-24 weeks prior to surgery may have a greater degree of downstaging and more conservative surgery (e.g. breast conservation, sentinel node biopsy as opposed to axillary dissection).

2.0 STUDY AIMS AND OBJECTIVES

2.1 Phase I Safety Component (metastatic disease) Objectives and Endpoints

2.1.1 The primary objective of the Phase I portion in the metastatic cohorts is to determine the safety of adding hydroxychloroquine to standard dose palbociclib and letrozole and to determine the recommended phase 2 dose for hydroxychloroquine.

Primary endpoint is safety, to be assessed continuously using CTCAE V4.03, with physical examination and laboratory assessments as indicated on the study schedule

2.2 Phase II Window/Neo-adjuvant Component Objectives and Endpoints

2.2.1 Phase II - Part 1 Primary Objectives and Endpoints

- To determine the dose responsiveness of 2 dose levels of hydroxychloroquine added to low dose palbociclib and letrozole on breast tumor indices of proliferation (including Ki67), autophagy, senescence and cell cycle control.

2.2.2 Phase II - Part 1 Secondary and Additional Objective and Endpoints

- Determine longer term clinical tumor responsiveness (tumor volume) and tumor biomarker indices (for patients who have extended pre-operative therapy, maximum 24 weeks).
- To perform exploratory studies on blood-based tumor protein, DNA and RNA biomarkers.

2.2.3 Phase II Part 2 Primary Objective and Endpoints

To determine whether hydroxychloroquine added to low dose palbociclib and letrozole can increase the proportion of patients whose tumors achieve complete cell cycle arrest (CCCA, proportion with Ki67 \leq 2.7% comparing T1 to T1 as shown in Figure 2, see Section 5.3.4).

The primary endpoint is the increase in percentage of all patients who achieve CCCA with low dose palbociclib and letrozole (at week 2, time T1) compared to that of low dose palbociclib and letrozole with the addition of HCQ (at 4 weeks, time T2).

A previously conducted trial of neoadjuvant aromatase inhibitor (anastrozole) plus standard dose PD estimated the CCCA probability to be 44% with aromatase inhibitor alone and powered their study to detect a 50% increase of 44% to 66%. A 26% CCCA probability was seen with anastrozole alone and 86% with the addition of standard dose PD. We will aim for a CCCA reference probability of 50% with low-dose PD + letrozole (T1), adjusting the PD dose from phase I if needed after the first ten patients (Subaims 1a and 1b).

2.2.4 Phase II Part 2 Secondary Objectives and Endpoints

- To determine the impact of adding hydroxychloroquine to low dose palbociclib and letrozole on breast tumor indices of proliferation, autophagy, senescence, cell cycle control and other intersecting pathways.
- Determine longer term clinical tumor responsiveness and tumor biomarkers indices (for patients who have extended pre-operative therapy, maximum 24 weeks).
- To perform exploratory studies on blood-based tumor protein, DNA and RNA biomarkers.
- Obtain additional safety information for the combination of low dose palbociclib, letrozole and hydroxychloroquine.

3.0 INVESTIGATIONAL PLAN

3.1 Overall Design

This is an open label Phase I/II prospective interventional trial with a safety component in metastatic disease and a “window” component in the neo-adjuvant setting.

Phase I Safety Component:

The Phase I is designed to evaluate the safety and tolerability of adding hydroxychloroquine to standard

dose palbociclib and letrozole in the metastatic setting and to determine the recommended phase 2 dose for hydroxychloroquine.

This safety component will be completed before the initiation of the window trial (Phase II) in the pre-operative setting.

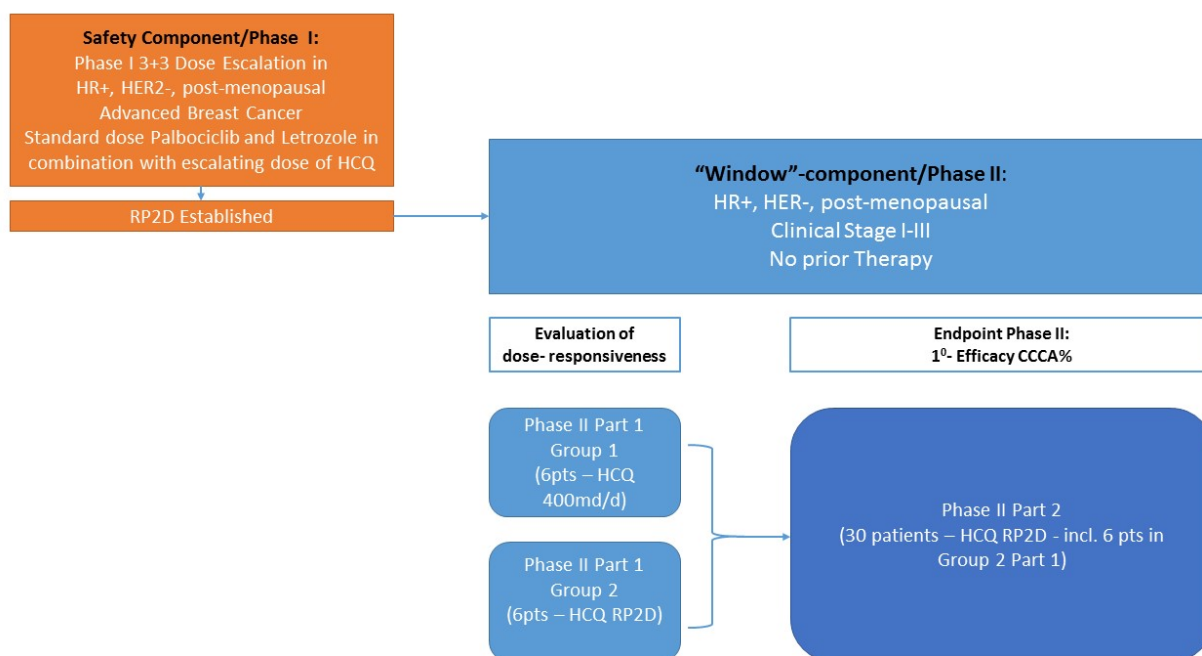
Phase II Pre-operative “Window” Component:

The “window” component of the trial evaluates the combination of pre-operative palbociclib plus letrozole followed by the addition of hydroxychloroquine (HCQ) for postmenopausal patients with Stage I-III estrogen receptor-positive and HER2-negative breast cancer (Figure 2).

Correlative studies using baseline and follow up breast biopsies and blood work are included in the research plan. The Phase II portion will assess the change in the percentage of all patients who achieve CCCA when adding HCQ to the palbociclib/letrozole combination.

3.2 Trial Schemata

3.2.1 Trial Overview Schema



3.2.2 Window Component Schema

Window/Neoadjuvant Component Trial Schema

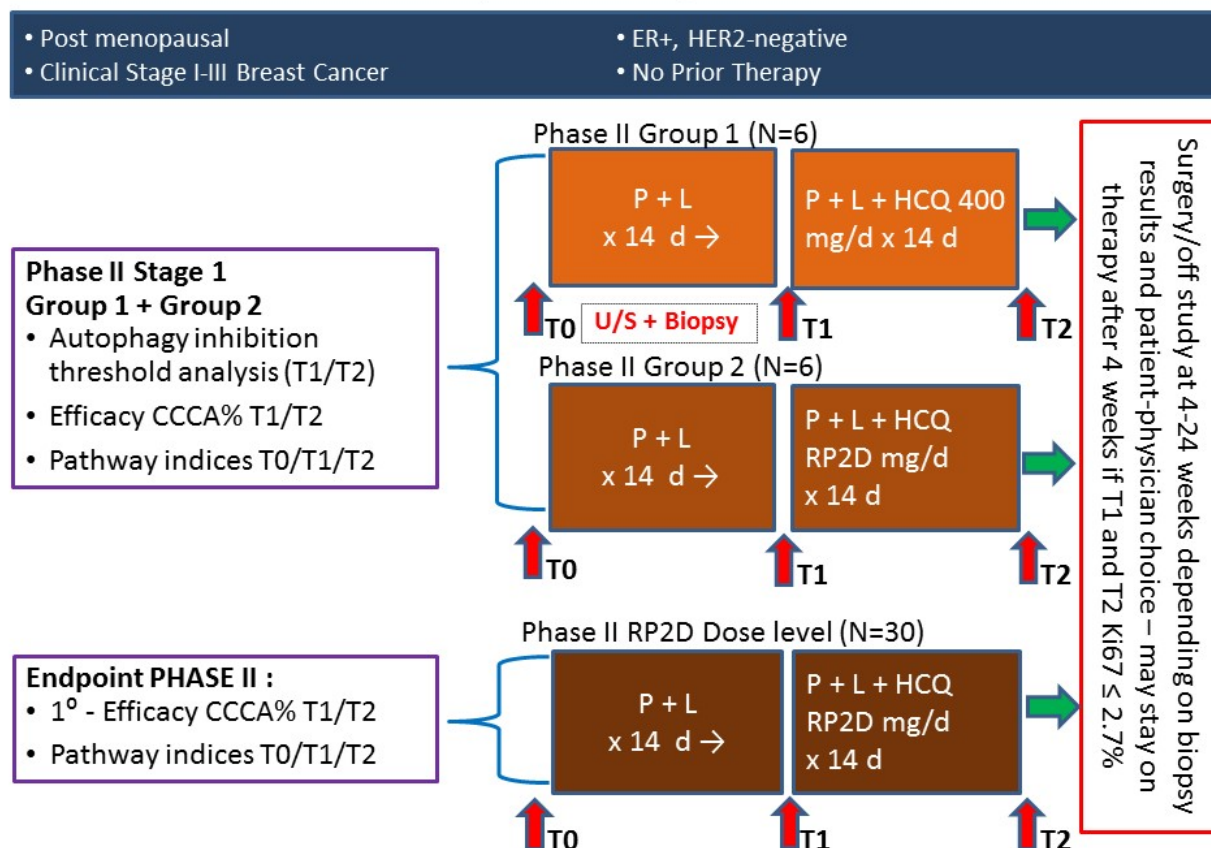


FIGURE 2. Schema for pre-operative “window”/neoadjuvant trial. Part 1 dose responsiveness evaluation followed by Part 2 fixed dose cohort using same design and biopsy timepoints (T0 [baseline/pretreatment, T1 [after 2 weeks P+L], T2 [after addition of HCQ]), with option to proceed with surgery right after T2 biopsy or up to 24 weeks from initiation of therapy. P= continuous low dose palboclib at 75 mg three times a week (Mon/Wed/Fri); L=letrozole at 2.5 mg daily; HCQ=hydroxychloroquine continuous daily at assigned dose; N=number of patients; U/S = ultrasound; DLT=dose limiting toxicity.

Design for the Safety Component/Phase I

A cycle will be defined as 28 days.

The dose of letrozole and palbociclib will be fixed for the safety cohorts at

- **Palbociclib: 125 mg capsule taken orally once daily for 21 consecutive days followed by 7 days off treatment to comprise a complete cycle of 28 days**
- **Letrozole: 2.5mg/d taken orally once daily continuously**

Hydroxychloroquine Dose Escalation Scheme

Dose Level (DL)	Hydroxychloroquine	Letrozole	Palbociclib
-1	200 mg/d	2.5 mg/d	125 mg capsule taken orally once daily for 21 consecutive days followed by 7 days off treatment to comprise a complete cycle of 28 days
0 (Starting Dose)	400 mg/d	2.5 mg/d	125 mg capsule taken orally once daily for 21 consecutive days followed by 7 days off treatment to comprise a complete cycle of 28 days
+1	600 mg/d	2.5 mg/d	125 mg capsule taken orally once daily for 21 consecutive days followed by 7 days off treatment to comprise a complete cycle of 28 days
+2	800 mg/d	2.5 mg/d	125 mg capsule taken orally once daily for 21 consecutive days followed by 7 days off treatment to comprise a complete cycle of 28 days

The dose escalation portion will use a 3+3 dose escalation design to evaluate escalating dose levels of hydroxychloroquine in combination with palbociclib and letrozole (see dose level table below). enroll 3 patients in the first dose level of the triplet combination. At least 3 patients must complete a treatment cycle (28 days) with the triple combination and undergo toxicity assessment before any additional patients are enrolled into higher dosing cohorts. Inpatient dose escalation or change of dosing schedule is not allowed. At least 6 evaluable patients are to be treated at a dose level for an MTD/RP2D to be declared.

- If 0 out of 3 patients in a dose level experience a DLT in the defined timeframe another 3 patients will be enrolled at the next higher dose level.
- If no more than 1 patient experienced a DLT at a dose level, then more patients will be added to that cohort to increase the cohort up to six patients at the same dose level
- If no more than one of the first 6 patients treated experiences a DLT, then 3 patients will be enrolled at the next higher dose level.
- If two or more of the first 6 patients treated within a cohort experience DLT, then this dose level will be considered not tolerated and the dose escalation will be halted. If two DLTs are seen in any cohort, no further patients will be enrolled at that level and next level lower will be declared the RP2D.

The RP2D is defined as the highest dose level at which 6 patients have been treated with at most 1 instance of DLT.

If dose level -1 is found to have unacceptable rates of DLT, accrual will be discontinued.

If two DLTs are seen at the starting dose (DL 0), then the HCQ dose will be lowered to 200 mg daily and six patients will be enrolled and if one or no DLTs are seen, this will be declared the recommended phase II dose (RP2D).

A **Safety Monitoring Committee (SMC)** comprised of the PI, Co-PI, Biostatistician and collaborators will be established to monitor safety throughout the study, review patient data and make decisions prior to advancing to the next dose cohort.

The SMC will review, at a minimum, the following safety data:

- Vital signs
- Clinical laboratory values
- Physical examination findings
- Adverse events/serious adverse events
- ECOG performance status

The SMC will meet prior to dose escalations in Phase I, prior to opening the Phase II Stage 1 for determination of the RP2D and prior to opening Phase I Stage 2. After the Phase I has been completed the SMC will review aggregate safety data on a regular basis approximately every 2 months and on an ad hoc basis as needed. The study SMC will review all available safety data to determine if this dose should be declared not tolerated or if any further dose escalation should occur. While dose escalation decisions will be made based upon data from the first cycle of treatment for each patient within a given cohort, the SMC will also review safety data from patients receiving additional treatment cycles of the triple combination.

Based on the review of the data, the SMC will recommend that the study continue as planned, or may alternatively recommend that the study be placed on hold, that the dose of study drug be de-escalated, or that the study be terminated. A recommendation of study hold, study drug dose de-escalation, or study termination would be made in the event of the discovery of an unexpected, serious, or unacceptable risk to the subjects in the study.

For the purpose of the SMC review, a patient will be considered evaluable if s/he has received at least 75% of the planned dosing of the triplet combination during Cycle 1. If the reason for not receiving 75% or more of the planned doses is dose-limiting toxicity (DLT), or if a patient has received a dose reduction, a patient will still be considered evaluable for this SMC review. Patients considered non-evaluable will be replaced.

3.3 Dose Limiting Toxicity Definition

A DLT will be defined as any grade 3 toxicity deemed attributable to either palbociclib or HCQ occurring in the first 28 day study treatment period, with the exception of neutropenia, for which any of grade 4 or febrile neutropenia event defines a DLT. All adverse events will be classified and graded using CTCAE V 4.03 criteria.

The decision to open the Phase II window part of the trial will be made after all 6 patients on the highest dose level. All Safety Data will be reviewed and input from the SMC will be used to determine whether the study proceeds to the “window” part of the trial in the neo-adjuvant setting.

3.4 Phase II Part 1 (neo-adjuvant cohorts) Pre-operative “Window” Component:

The “window” component of the trial evaluates the combination of pre-operative palbociclib plus letrozole followed by the addition of hydroxychloroquine (HCQ) for postmenopausal patients with Stage I-III estrogen receptor-positive and HER2-negative breast cancer (Figure 2). Correlative studies using baseline and follow up breast biopsies and blood work are included in the research plan. The Phase II portion will assess the change in the percentage of all patients who achieve CCCA when adding HCQ to the palbociclib/letrozole combination.

To determine the dose responsiveness in the pre-operative setting 2 groups of 6 patients each will be enrolled at the following dose levels:

Dose Level (DL) neo- adjuvant cohorts	Hydroxychloroquine	Letrozole	Palbociclib
Group 1	400 mg/d	2.5 mg/d	75 mg/tiw
Group 2	800 mg/d or RP2D	2.5 mg/d	75 mg/tiw

Should the RP2D be < 800mg/d the second group will be receive the RP2D of hydroxychloroquine in the combination as determined in the Phase I.

3.5 Phase II Part 2 Window/Neo-adjuvant Component

The dose defined in the Phase I portion as RP2D will be used in the Phase II Stage 2 part of the study.

The design for both Phase II Stage 1 and 2 components are the same except for the 2 HCQ dose levels in Stage 2 whereas the HCQ dose is fixed at the recommended Phase II dose for the Phase II portion. The dose of palbociclib for both Stage 1 and 2 is fixed at a dose of at a dose of 75 mg orally three times a week (Mon/Wed/Fri) continuously without a break. After 4 weeks (T2), the primary endpoint will have been obtained. If the T1 and T2 Ki67 determination show CCCA ($Ki67 \leq 2.7\%$) that patient may elect to stay on therapy for an additional 3 to 5 four-week cycles (week 16 to 24 as shown on Table X) before proceeding with definitive surgery. Details on dosing and dose adjustments are shown in Sections 6.14 and 6.23. Using the same population, treatment and biopsy schema, 30 index patients will be enrolled for the phase II Stage 2 portion of the trial.

3.6 Phase II Patient Evaluability

Patients who meet the eligibility criteria and complete a full 4 weeks of therapy (14 days of low-dose palbociclib plus letrozole and 14 days of dose palbociclib plus letrozole with HCQ) will be considered evaluable for Phase II. In addition, the completion of biopsies at T0, T1 and T2 with interpretability of Ki67 are required for evaluability.

3.7 Replacement of Patients

Patients who are not evaluable for dose-limiting toxicity in the Phase I portion and those not evaluable for Ki67 at T0, T1 and T2 in the Phase II portion will be replaced.

3.8 Target Accrual

A total of 60 patients will be enrolled to the study. This includes 18 patients (6 per dose cohort at 400, 600 and 800 mg of HCQ daily) in the Phase I metastatic portion, 12 patients in the neo-adjuvant Phase II Part 1 and 30 patients (25 needed for statistical plan and 5 expected to drop out) for the Phase II Part 2 portion.

4.0 PATIENT SELECTION

4.1 Inclusion Criteria

Patient eligibility criteria include all of the following:

1. Signed written informed consent
2. ECOG performance status 0-1
3. Female and age ≥ 18 years and postmenopausal defined by:
 - a. Age ≥ 55 years and 1 year or more of amenorrhea
 - b. Age < 55 years and 1 year or more of amenorrhea with LH and/or FSH levels in the postmenopausal range
 - c. Age < 55 with prior hysterectomy but intact ovaries with LH and/or FSH levels in the postmenopausal range
 - d. Status after bilateral oophorectomy (≥ 28 days prior to first study treatment)
4. Adequate hematological, renal, hepatic function defined as follows:
 - a. ANC ≥ 1500 cells/ μ l
 - b. Platelet count $\geq 100,000$ / μ l
 - c. Serum creatinine concentration $< 1.5 \times$ ULN
 - d. Bilirubin level $< 1.5 \times$ ULN
 - e. Aspartate aminotransferase (AST) or alanine aminotransferase (ALT) $< 3 \times$ ULN
 - f. Alkaline phosphatase ≤ 2.5 ULN
5. Metastatic cohorts (Phase I): Diagnosis of Stage IV estrogen positive breast cancer, estrogen receptor-positive and HER2-negative by ASCO/CAP criteria^{1,2}
6. Metastatic cohorts: Must be a candidate for treatment with CDK4/6 inhibitor as standard of care
7. Metastatic cohorts (Phase I): No prior exposure to CDK 4/6 inhibitors.
8. Neoadjuvant cohorts (Phase II): Diagnosis of Stage I-III estrogen positive breast cancer, estrogen receptor-positive and HER2-negative by ASCO/CAP criteria^{1,2}. If Stage I, clinical tumor size must be ≥ 1.5 cm.
9. Neo-adjuvant cohorts(Phase II): Surgical candidate and appropriate for pre-operative endocrine therapy

4.2 Exclusion Criteria

Patient exclusion criteria include any of the following:

1. Neo-adjuvant cohorts (Phase II): Inoperable or metastatic breast cancer based on standard evaluation
2. Inflammatory breast cancer
3. Neo-adjuvant cohorts: clinical T4 disease
4. History of retinal disease
5. History of active visual disturbances (normal baseline study-specified retinal exam required)
6. Neo-adjuvant cohorts: Prior therapy for breast cancer (medical, surgical or radiation therapy)
7. Acute illness, including infections requiring medical therapy,
8. Known bleeding diathesis or need for anticoagulation
9. Neo-adjuvant cohorts: Treatment with any of the following medications within 4 weeks before the baseline diagnostic biopsy is taken:
 - a. Oral estrogens, including hormone replacement therapy (but prior depot estrogen use not allowed)
 - b. Investigational agents (or 5 half-lives, whichever is longer)
10. Required concomitant use of any drug that is a strong CYP3A inhibitor.
11. Psychological, familial, sociological or geographical conditions that do not permit compliance with the study protocol.

5.0 STUDY PROCEDURES AND SCHEDULE OF ASSESSMENTS

5.1 Patient Identification

Eligible patients will be referred by members of the MD Anderson Department of Breast Medical Oncology or screened through electronic medical records and our Departmental database.

5.2 Schedule of Assessments

Table 1 – Study Procedures and Assessments Phase I

	Baseline	C1 W1	C1 W2	C1 W3	C1 W4	C2 W5	C2 W6	C2 W7	C2 W8	C3+ W1		Off Study
Day		D1	D8	D15	D22	D1	D8	D15	D22	D1		
Scheduling Window	-14d	+/- 2	+/- 2	+/- 2	+/- 2	+/- 2	+/- 2	+/- 2	+/- 2	+/- 2	+/- 2	Within 30d
Laboratory	X ^A		X	X	X	X	X	X	X	X	X	X
Adverse event assessment)		X	X	X	X	X	X	X	X	X	X	X
Physical Exam/ Weight/Vital Signs	X ^A	X	X	X	X	X	X	X	X	X	X	X
ECOG performance status evaluation	X											
Ophthalmologic Exam	X ^B											X
Imaging	X ^A								X			

Assessments												
Palbociclib		X	X	X		X	X	X		X	X	
HCQ				X	X	X	X	X	X	X	X	
Letrozole		x	x	x	x	x	x	x	x	x	x	

Table 2 – Study Procedures and Assessments Phase II

		Surgery ("window" option)								Surgery (extended option)		
	Baseline	W1	W2	W3	W4	W6	W8	W12	W16	W20	W24	Off Study
Day		D1	D8	D15	D22	D36	D50	D64	D96	D124	D152	
Scheduling Window	-14d	+/- 2	+/- 2	+/- 2	+/- 2	+/- 2	+/- 2	+/- 2	+/- 2	+/- 2	+/- 2	Withir 30d
Laboratory	X ^A		X	X	X	X	X	X	X	X	X	X
Adverse event assessment)		X	X	X	X	X	X	X	X	X	X	X
Physical Exam/ Weight/Vital Signs	X ^A	X	X	X	X	X	X	X	X	X	X	X
ECOG performance status evaluation	X											
Ophthalmologic Exam	X ^B											X
Breast ultrasound	X ^A				X			X			X	
Research blood	X ^A		X		X	X	X	X	X	X	X	X
Research biopsy	X ^A		X		X ^C						X ^C	
Low dose palbo + letrozole		X	X	X	X	X	X	X	X	X	X	
HCQ				X	X	X	X	X	X	X	X	

Abbreviations: W=week (week 1 is the same as day 1 prior to starting palbociclib); palbo = palbociclib; HCQ = hydroxychloroquine

Laboratory assessments: Baseline, W2, W4 and every 4 weeks thereafter until off study labs include CBC/differential, electrolytes, BUN, creatinine, AST, ALT, Total Bilirubin, Alkaline Phosphatase. CBC/diff done with every lab draw at the timepoints described in the study calendar. Baseline only: PT, PTT, urinalysis with microscopic exam

Superscripts:

A=Phase II: done within 2 weeks prior to starting therapy (low dose palbociclib/letrozole); Phase I: Any imaging assessments already completed during the regular work-up of the patient within 28 days prior to starting study treatment, including before signing the main study ICF can be considered as the baseline images for this study

B= done within 8 weeks of starting study medication;

C=third biopsy done either at W4 for patients going on to surgery at that time, for those waiting until between week 20-24, biopsy done pre-operatively. Patients who know in advance that they will proceed with surgery at T2 will not need a biopsy and biomarkers will be measured on the surgical specimen.

5.2.1 Baseline Assessments

All patients will undergo a baseline standard evaluation for newly diagnosed breast cancer including (note that some baseline tests can be done prior to day 1 (week 1) as shown on Table 1):

- Review of systems all organ systems will be examined.
- Physical examination, vital signs, weight, height, and evaluation of ECOG performance status.
- Standard of care pathological diagnosis of breast cancer, imaging (Phase II:breast ultrasound; Phase II: CT, MRI) and clinical staging.
- Laboratory studies: CBC/differential, electrolytes, BUN, creatinine, AST, ALT, Total Bilirubin, Alkaline phosphatase, PT, PTT
- Urinalysis

- Ophthalmological exam per latest guidelines of the American Academy of Ophthalmology (AAO) for baseline screening with HCQ treatment.
- Fresh Tumor Biopsy (Phase II only)
- Research blood draw (Phase II only)

ECOG performance status
Grade ECOG status
0 - Fully active, able to carry on all pre-disease performance without restriction 1 - Restricted in physically strenuous activity but ambulatory and able to carry out work of a light or sedentary nature e.g., light house work, office work 2 - Ambulatory and capable of all self-care but unable to carry out any work activities. Up and about more than 50% of waking hours 3 - Capable of only limited self-care, confined to bed or chair more than 50% of waking hours 4 - Completely disabled. Cannot carry on any self-care. Totally confined to bed or chair 5 - Dead

5.2.2 Evaluation During Study Phase II

Patients will be evaluated with an organ-specific review of systems and physical exam at weeks 2, 3, 4, and those who choose and are eligible to go beyond the “window period” (as described in Sections 1.3, 3.2 and 5.2.3) and stay on study until definitive surgery at week 16 to 24 will undergo additional evaluation at weeks 6, 8 and every 4 weeks thereafter until the last pre-operative visit between week 16 and 24 at the discretion of the medical and surgical oncologist as shown on Table 1.

5.2.3 Treatment Duration

5.2.3.1 Phase I

Patients will receive treatment for a maximum of 24 weeks if receiving clinical benefit as determined by the treating physician.

5.2.3.2 Phase II

Following the study schema (Figure 2) patients are expected to complete 28 days of study treatment followed by surgery for the “window option”, with an off study visit after surgery, and will be monitored for adverse events up to 30 days after the last dose of study drug.

Patients whose tumors at T1 biopsy show Ki67 > 10% will be required to come off study and per standard of care would typically be recommended to proceed to definitive surgery or standard neoadjuvant chemotherapy. All other patients will continue on study therapy and at T2 (week 4), patients and their physicians can opt to either come off study and proceed with definitive surgery or continue for 12 to 20 additional weeks (between weeks 16 and 24 as shown on Table 1) if CCCA (Ki67 ≤ 2.7%) is achieved at both T1 and T2 and there is no evidence of clinical progression (25% increase in volume by ultrasound) up until the time of definitive surgery.

5.2.4 End of treatment visit and Follow up assessments

Patients who discontinue study treatment, will be followed for 30 days after stopping the study drugs for assessment of safety (i.e., assessment of AEs and/or serious AEs [SAEs] and

concomitant medications) and resolution of any treatment related toxicity. Patients continuing to experience toxicity at this point following discontinuation of treatment will continue to be followed at least every 4 weeks until resolution or determination, in the clinical judgment of the investigator, that no further improvement is expected.

5.2.5 Early discontinuation

Patients who come off trial early will be asked to return for the off-study assessments as detailed in Table XX. In the event of a continuing AE, the patient will be asked to return for follow-up until resolution or stabilization of the AE..

5.2.6 Review of Systems and Physical Exam

A full review of systems that covers all of the domains and systems represented in CTCAE C 4.03 toxicity criteria will be performed at screening/baseline. Subsequent physical exams may be limited and should be focused on sites of disease to explore clinical signs and symptoms.

5.2.7 Laboratory Assessments

CBC/differential, electrolytes, BUN, creatinine, AST, ALT, Total Bilirubin, Alkaline Phosphatase,

5.2.8 Imaging assessments Phase I

Tumor response will be assessed according to RECIST Version 1.1. Patients should have at least one documented measurable lesion (per RECIST v1.1) or in the absence of measurable disease, have at least one lytic or mixed (blastic/lytic) bone lesion at study entry.

Imaging assessments will be performed as per standard of care at screening within 28 days prior to first dose of study treatment, at 8 weeks (+/- 1 week) from day one of study treatment and subsequently every 8-12 weeks (+/- 2 weeks) thereafter.

Tumor response should be assessed using the same imaging method throughout the study.

5.2.9 Imaging assessments Phase II

Methods for ultrasound evaluation and volumetric measure of response

Grayscale and power Doppler ultrasound will be performed on the breast and regional nodal basins using a Philips iU22 system or Sonoline Antares systems equipped with a 5- to 13-MHz broadband linear transducer. Ultrasound images of the index tumors and index nodes will be captured in the longitudinal and transverse planes with three dimensions measured. The size of the index tumors and index nodes will be reported in three dimensions to allow for volumetric calculation. The percent change in volume will then be calculated and reported to determine response.

5.3 Correlative Biomarker Studies

5.3.1 Biopsies, Tissue Handling and Analysis

All biopsies will be done under ultrasound guidance by a member of the research team using standard of care imaging-guided biopsy. Local anesthesia and hemostasis protocols will be used as per standard protocol. Core needles of 18 or 16G size will be used and 3-4 core biopsies will be obtained. The first

core will be placed in standard 10% formalin, and all other cores will be placed in a cryovial and snap frozen in liquid nitrogen.

All of the correlative studies (unless otherwise indicated) will be performed in the laboratory of Dr. Khandan Keyomarsi located in the Zayed building at 6565 MD Anderson Blvd, Houston, Texas, 77030. For all the correlative analysis we will use tumor tissues collected from the biopsies and at surgical resections.

Cyclin E, and Rb immunohistochemistry (IHC) assays. FFPE tumor tissue slides will be prepared from paraffin imbedded blocks per standard methodologies and subjected to IHC analysis with 2 different antibodies: cyclin E and Rb:

Cyclin E: the anti-human C-19 polyclonal antibody (Santa Cruz Biologicals) at 1:2000 dilution will be used to stain each slide. Each slide will be scored for percent nuclear and percent cytoplasmic positive staining. Only tumor cells with greater than 5% nuclear or cytoplasmic positivity are considered as cyclin E positive. Nuclear and cytoplasmic staining scores are assigned according to the staining intensity (0 = no staining, 1 = blush staining, 2 = weak staining, 3 = intermediate staining and 4= strong staining). The nuclear and cytoplasmic scores are then combined, and four immunophenotypes are identified. First, breast tumors will be considered to be negative for cyclin E when staining is not detected in the nuclei or cytoplasm (phenotype 1). Second, in cases determined to be cyclin E+, if the nuclear staining score exceeded the cytoplasmic score, cyclin E expression is defined as predominantly nuclear (phenotype 2). Third, when the nuclear and cytoplasmic staining scores are equal, cyclin E expression is considered to be both nuclear and cytoplasmic (phenotype 3). Fourth, if the cytoplasmic staining score is higher than the nuclear score, cyclin E expression is considered to be predominantly cytoplasmic (phenotype 4).

Rb: The anti-human Clone 4H1 mouse monoclonal antibody (Cell Signaling Technology, Denvers, MA) at 1:100 dilution will be used to stain each slide. Each slide will be scored separately for intensity of staining and percentage of positive cells. Staining intensity will be scored as follows: 0, no staining; 1, weak positive (faint yellow staining); 2, intermediate positive; and 3, strong positive (brown staining). The number of positive cells will visually be evaluated and stratified as follows: <1%, 0 (negative); 1 to <5% positive cells, 1 (weak); 5-50% positive cells, 2 (moderate); >50% positive cells, 3 (strong). The sum of the staining intensity and percentage of positive cell scores will be used to determine the staining index for each section, with a minimum score of 0 and maximum score of 6; scores >1 will be defined as Rb positivity.

5.3.2 Whole Blood/Plasma Biospecimens

Blood specimen will be collected as shown on Table 1 at baseline, week 2 and week for patients on the “window” option and for those who stay on study until surgery will be collected at weeks 6, 8 and every weeks thereafter until surgery. Each blood draw will be to collect 2 7.5 mL tubes – one for plasma (green top) and the other for serum (red top). Blood will be processed immediately following collections – tubes will be gently inverted

and kept at room temperature prior to centrifuging, and clotted tube (red top) will have serum aspirated, while the green top tube will have plasma aspirated – both being aliquoted in 0.5 mL cryovials and placed in a -20°C freezer (and stored long term at -80°C).

5.3.3 Ki67 Tumor Assay and Scoring

CLIA-approved Ki67 staining will be performed using anti-Ki67 rabbit monoclonal antibody (isotype IgG1κ, clone MIB-1, DAKO) in the diagnostic Immunohistochemistry Laboratory of Department of Pathology using an established protocol. Briefly this protocol includes de-paraffinization (30 minutes at 72°C) and rehydration with antigen retrieval performed at 100°C for 20 minutes with Tris-EDTA buffer, pH 6.0. Endogenous peroxidase is blocked with 3% peroxide for 5 minutes. Primary anti-Ki-67 antibody (Dako, clone MIB-1) is applied at 1:100 dilution for 15 minutes. Post primary antibody detection is carried out using a commercial polymer system (Bond Polymer Refine Detection, Leica), and stain development is achieved by incubation with DAB and DAB Enhancer (Leica).

Ki67 staining will be evaluated in whole tissue sections without focusing on the hot spots. The staining will be quantitatively assessed by automated image analysis using the Aperio ScanScope AT2 scanner (Leica Biosystems, Inc., 1700 Leider Lane, Buffalo Grove IL, 60089). All Ki67 immunostained slides will be scanned at 20 X magnification. As Ki67 is a nuclear stain, the Genie nuclear v9.1 algorithm will be used to create a custom-made classifier. A color graphic phase of image analysis is afterward performed using red, orange, and yellow (high, medium, and low reaction, respectively) to represent positive cells, and blue to represent negative ones. A curvature threshold adjustment is made to de-cluster or break up large groups of closely apposed nuclei when needed. The original factory algorithm is also adjusted to avoid false positives by lowering the Cytoplasmic Intensity settings. All algorithm adjustments are tested to assure accurate detection of positive and negative nuclei.

5.4 Concomitant Medications

In general, the use of any concomitant medication or therapies deemed necessary for the care of the patient is permitted.

5.5 Banked biospecimens

Leftover blood and tumor samples which are not consumed for planned study testing will be retained for potential additional testing at a later date (i.e. if newer technologies become available) under the same objectives. Samples will be retained at a secure storage facility () in case there is need for retesting or additional testing. Samples will be stored for up to 10 years or until termination of this study.

6.0 INVESTIGATIONAL AND NON-INVESTIGATIONAL AGENTS

6.1 Palbociclib

6.1.1 Description of palbociclib

Palbociclib is an inhibitor of cyclin-dependent kinase (CDK) 4 and 6, which are downstream of signaling pathways that lead to cellular proliferation. In vitro, palbociclib reduced cellular proliferation of ER-positive breast cancer cell lines by blocking progression of the cell from G1 into S phase of the cell cycle. Treatment of breast cancer cell lines with the combination of

palbociclib and antiestrogens leads to decreased retinoblastoma protein (Rb) phosphorylation resulting in reduced E2F expression and signaling, and increased growth arrest compared to treatment with each drug alone. In vitro treatment of ER-positive breast cancer cell lines with the combination of palbociclib and antiestrogens leads to increased cell senescence, which was sustained for up to 6 days following drug removal. In vivo studies using a patient-derived ER-positive breast cancer xenograft model demonstrated that the combination of palbociclib and letrozole increased the inhibition of Rb phosphorylation, downstream signaling and tumor growth compared to each drug alone (Pfizer Pharma United States product insert (USPI), (2015). Highlights of Prescribing Information; IBRANCE® (palbociclib) for oral use. New York: Pfizer, Inc).20
Complete information for Palbociclib may be found in the single reference safety document (SRSD), which for this study is the Pfizer Investigator Brochure for Palbociclib (PD-0332991).

6.1.2 Source of palbociclib

Palbociclib will be provided by Pfizer Inc. Palbociclib commercial supply will be supplied as 75 mg capsules in High Density Polyethylene (HDPE) bottles, labeled according to local regulatory requirements.

6.1.3 Preparation and dispensing

Qualified site personnel will provide adequate palbociclib supplies for patient to take home until next scheduled visit.

Patients will receive a drug diary to document dosing. The completed diary must be returned to the site at the next study visit

6.1.4 Dosing of palbociclib and dose adjustments for palbociclib (holding, discontinuation)

Patients should be instructed to swallow palbociclib capsules whole and not to manipulate or chew them prior to swallowing. No capsule should be ingested if it is broken, cracked, or otherwise not intact. Patients should be encouraged to take their dose at approximately the same time each day. Patients should be instructed to record daily administration in the patient diary.

Patients should take palbociclib with food.

- Patients who miss a day's dose entirely must be instructed NOT to "make it up" the next day.
- Patients who vomit any time after taking a dose must be instructed NOT to "make it up," and to resume treatment the next day as prescribed
- Patients who inadvertently take 1 extra dose during a day must be instructed to skip the next day's dose.

Dosing of palbociclib will follow recommendations listed on the package insert based on hematological and other major side effects.

For Phase 2 palbociclib dosing:

- On the day of or day prior to administration of day 1 of palbociclib (Weeks 4, 8 and every 4 weeks thereafter while on study drug) for grade 3 or 4 neutropenia, palbociclib will be held and CBC/diff will be checked in one week intervals, with treatment resumed at the same dose when neutropenia has recovered to Grade ≤ 2 . If more than two weeks are required for recovery to Grade ≤ 2 , the dose will be lowered to 75 mg p.o. twice a week.
- On weeks 2 and 6, for Grade 3 neutropenia without fever $\geq 38.5^\circ\text{C}$, treatment will continue and CBC/diff will be repeated 1 week later. At these timepoints and at another

other time, Grade 4 neutropenia or Grade 3 neutropenia with fever ≥ 38.5 °C, palbociclib will be held until recovery to Grade ≤ 2 .

- For Grade ≥ 3 non-hematologic toxicity attributed to palbociclib, palbociclib will be held until the toxicity in question resolves to Grade ≤ 1 or Grade ≤ 2 if not considered a risk to the patient.
- Once palbociclib dose has been lowered, it will not be re-escalated

6.2 Hydroxychloroquine

6.2.1 Description of hydroxychloroquine (HCQ)

Hydroxychloroquine (HCQ) is a small molecule drug that is indicated for the suppressive treatment and treatment of acute attacks of malaria due to *Plasmodium vivax*, *P. malariae*, *P. ovale*, and susceptible strains of *P. falciparum*. It is also indicated for the treatment of discoid and systemic lupus erythematosus, and rheumatoid arthritis, and often used for overlap connective tissue disorders. Although the exact mechanism of action is unknown, it may be based on ability of HCQ to bind to and alter DNA. HCQ has also been found to be taken up into the acidic food vacuoles of the parasite in the erythrocyte. This increases the pH of the acid vesicles, interfering with vesicle functions and possibly inhibiting phospholipid metabolism. In suppressive treatment, HCQ inhibits the erythrocytic stage of development of plasmodia. In acute attacks of malaria, it interrupts erythrocytic schizogony of the parasite. Its ability to concentrate in parasitized erythrocytes may account for their selective toxicity against the erythrocytic stages of plasmodial infection. As an anti-rheumatic, HCQ is thought to act as a mild immunosuppressant, inhibiting the production of rheumatoid factor and acute phase reactants. It also accumulates in white blood cells, stabilizing lysosomal membranes and inhibiting the activity of many enzymes, including collagenase and the proteases that cause cartilage breakdown.

HCQ is also known to inhibit autophagy, a cellular process that may also lead to resistance to several cancer drugs, and as such, several trials have been conducted and shown safety of HCQ combined with several antineoplastic agents.³⁴⁻³⁷ However, no trials have tested HCQ in the setting and with the rationale and drug combination proposed in this trial.

6.2.2 Source and dispensing of hydroxychloroquine

Generic HCQ will be obtained from a commercial source, Quality Prescription Drugs (Suite #245, 7360 137th Street, Surrey, B.C. V3W 1A3), a Canada-based company that uses U.S. sources that is both CIPA certified and PharmacyChecker approved. The drug will be ordered for direct delivery to the Investigational Pharmacy at MD Anderson in batches to maintain at least a 3 months of supply on hand and will be dispensed as an investigational drug with standard logging of drug acquisition, dispensation and final accounting for disposition. Unused or returned drug will be destroyed. Drug will be dispensed to patients with the name and dosage drug, date dispensed, name of patients, name of study and instructions for use.

6.2.3 Dosing of hydroxychloroquine and dose adjustments for hydroxychloroquine

HCQ will be given at the assigned dose for the Phase I dose escalation and Phase II fixed dose parts of the trial. The dose of 400 mg daily was chosen as the starting dose for the Phase I portion as this is the usual dose used clinically and has been combined with hormonal and other and cancer therapies at this dose in prior studies.³⁴⁻³⁷ There will be no dose adjustments

for HCQ, and any grade 3 toxicity that is attributed to HCQ will require discontinuation of drug and for the patient to come off study. Subsequent treatment will be as per standard of care. For patients on the Phase I portion, any Grade III toxicity attributed to HCQ will also be counted as a dose-limiting toxicity if occurring in the first 28 days

6.3 Letrozole

Letrozole at the standard approved dose of 2.5 mg by mouth daily continuous dosing will be prescribed as standard of care for neoadjuvant endocrine therapy through MD Anderson's or the patient's choice of pharmacy. There will be no dose adjustments for letrozole. If the patient is felt to be having unacceptable toxicities due to letrozole, then treatment will be stopped and the patient will come off study. Subsequent treatment will be as per standard of care.

7.0 ADVERSE EVENT MONITORING AND REPORTING

7.1 Definition of an Adverse Event

An adverse event is the appearance or worsening of any undesirable sign, symptom or medical condition occurring after starting protocol intervention, up to 30 days after the last dose of the study therapy, even if the event is not considered to be related to the study drug.

This includes the following:

- AEs not previously observed in the patient that emerge during the protocol-specified AE reporting period, including signs or symptoms that were not present prior to the AE reporting period
- Complications that occur as a result of protocol-mandated interventions (e.g., invasive procedures such as cardiac catheterizations)
- If applicable, AEs that occur prior to assignment of study treatment associated with medication washout, no treatment run-in, or other protocol-mandated intervention
- Pre-existing medical conditions (other than the condition being studied) judged by the investigator to have worsened in severity or frequency or changed in character during the protocol-specified AE reporting period

7.2 Definition Serious Adverse Event

An adverse event or suspected adverse reaction is considered "serious" if, in the view of either the investigator or the sponsor, it results in any of the following outcomes:

- Death
- A life-threatening adverse drug experience – any adverse experience that places the patient, in the view of the initial reporter, at immediate risk of death from the adverse experience as it occurred. It does not include an adverse experience that, had it occurred in a more severe form, might have caused death.
- Inpatient hospitalization or prolongation of existing hospitalization.
- A persistent or significant incapacity or substantial disruption of the ability to conduct normal life functions.
- A congenital anomaly/birth defect.

Medical conditions/disease present before starting study drug are only considered adverse events if they worsen after starting study drug. Abnormal laboratory values of test results constitute adverse events only if they induce clinical signs or symptoms, are considered

clinically significant or require therapy. Information about common side effects already known about the investigational drug can be found in the Investigators' Brochure.

7.3 Adverse Event Reporting Period

The study period during which all AEs and SAEs must be reported begins after informed consent is obtained and starting protocol intervention and ends 30 days following the last administration of study treatment or study discontinuation/termination, whichever is earlier. After this period, investigators should only report SAEs that are attributed to prior study treatment.

7.4 Recording of Adverse Events

Attribution	Grade 1	Grade 2	Grade 3	Grade 4	Grade 5
Unrelated	Phase I	Phase I	Phase I	Phase I	Phase I
			Phase II	Phase II	Phase II
				Phase III	Phase III
Unlikely	Phase I	Phase I	Phase I	Phase I	Phase I
			Phase II	Phase II	Phase II
				Phase III	Phase III
Possible	Phase I Phase II	Phase I	Phase I	Phase I	Phase I
		Phase II	Phase II	Phase II	Phase II
		Phase III	Phase III	Phase III	Phase III
Probable	Phase I Phase II	Phase I	Phase I	Phase I	Phase I
		Phase II	Phase II	Phase II	Phase II
		Phase III	Phase III	Phase III	Phase III
Definitive	Phase I Phase II	Phase I	Phase I	Phase I	Phase I
		Phase II	Phase II	Phase II	Phase II
		Phase III	Phase III	Phase III	Phase III

Medical events that may not result in death, be life-threatening, or require hospitalization may be considered a serious adverse drug experience when, based upon appropriate medical judgment, they may jeopardize the patient or subject and may require medical or surgical intervention to prevent one of the outcomes listed in this definition. Examples of such medical events include allergic bronchospasm requiring intensive treatment in an emergency room or at home, blood dyscrasias or convulsions that do not result in inpatient hospitalization, or the development of drug dependency or drug abuse (21 CFR 312.32).

- Important medical events as defined above, may also be considered serious adverse events. Any important medical event can and should be reported as an SAE if deemed appropriate by the Principal Investigator.
- All events occurring during the conduct of a protocol and meeting the definition of a SAE must be reported to the IRB in accordance with the timeframes and procedures outlined in "The University of Texas M. D. Anderson Cancer Center Institutional Review Board Policy for Investigators on Reporting Serious Unanticipated Adverse Events for Drugs and Devices". Unless stated otherwise in the protocol, all SAEs, expected or unexpected, must be reported to the IND Office, regardless of attribution (within 5 working days of knowledge of the event).
- Serious adverse events will be captured from the time of the first protocol specific intervention, until 30 days after the last dose of drug, unless the participant withdraws consent. Serious adverse events must be followed until clinical recovery is complete and laboratory tests have

returned to baseline, progression of the event has stabilized, or there has been acceptable resolution of the event.

It is the responsibility of the PI and the research team to ensure serious adverse events are reported according to the Code of Federal Regulations, Good Clinical Practices, the protocol guidelines, the sponsor's guidelines, and Institutional Review Board policy.

7.5 Assessment of Adverse Events

The PI or designee will be responsible for assigning attribution of adverse events to the study agent. As far as possible, each adverse event should be evaluated to determine:

- The severity grade (mild, moderate, severe) or grade (1-4)
- Its relationship to the study drug(s) (suspected/not suspected)
- Its duration (start and end dates or if continuing at the final exam)
- Action taken (no action taken; study drug dosage adjusted/temporarily interrupted; study drug permanently discontinued due to this adverse event; concomitant medications taken; non-drug therapy given; hospitalization/prolonged hospitalization).
- Whether it constitutes a serious adverse events (SAE).

All AEs and SAEs, whether volunteered by the patient, discovered by study personnel during questioning, or detected through physical examination, laboratory test, or other means, will be reported appropriately.

Expected AEs are those AEs that are listed or characterized in the Package Insert (PI) or current Investigator's Brochure.

Unexpected AEs are those not listed in the PI or current Investigator's Brochure or not identified. This includes AEs for which the specificity or severity is not consistent with the description in the PI or Investigator's Brochure. For example, under this definition, hepatic necrosis would be unexpected if the PI or Investigator's Brochure only referred to elevated hepatic enzymes or hepatitis.

7.6 Communications between the Investigator and Supporting Company Pfizer

SAEs that occur after completion of the reporting time period as defined above are reportable to Pfizer if the Investigator suspects a causal relationship between the Pfizer product and the SAE.

8.0 STATISTICAL CONSIDERATIONS

Phase I:

For the phase I portion, six patients for each cohort for better statistical power in the dose-response biomarker analysis and expanded safety data.

Phase II:

For phase II, we will use a 2-stage Simon optimal design, looking to increase the CCCA rate from 50% to 75%. This design requires 11 patients in the first stage and 14 patients in the 2nd stage. It would stop after the 1st stage if no more than six patients with CCCA are seen and declare the treatment promising if at least 17 out of 25 total evaluable patients with CCCA are seen.

This design has alpha = 4%, 81% power, and a probability of 0.73 of terminating after the 1st stage

if the true CCCA rate=50%. We therefore plan a sample size of 30 patients over 12-15 months, accounting for patient dropout (including those with Ki67 >10% at T1). We have a large eligible patient population and have led national accruals in other multi-center neoadjuvant endocrine trials in post menopausal women (eg. ALTERNATE Trial). In addition, recent local experience of conducting window of opportunity trials in this setting have demonstrated the feasibility of accrual at a rate of ~2 patients per month. Thus, we expect to achieve accrual goals.

9.0 REFERENCES

1. Hammond ME, Hayes DF, Dowsett M, et al. American Society of Clinical Oncology/College Of American Pathologists guideline recommendations for immunohistochemical testing of estrogen and progesterone receptors in breast cancer. *J Clin Oncol.* 28:2784-95, 2010.
2. Wolff AC, Hammond MEH, Hicks DG, et al. Recommendations for human epidermal growth factor receptor 2 testing in breast cancer: American Society of Clinical Oncology/College of American Pathologists clinical practice guideline update. *J Clin Oncol.* 31:3997-4013, 2013.
3. Siegel RL, Miller KD, Jemal A. Cancer Statistics, 2017. *CA Cancer J Clin.* 2017 Jan 5. doi: 10.3322/caac.21387. [Epub ahead of print]
4. Howlader N, Altekruse SF, Li CI, et al. US incidence of breast cancer subtypes defined by joint hormone receptor and HER2 status. *J Natl Cancer Inst.* 106:ii, 2014.
5. Early Breast Cancer Trialists' Collaborative Group (EBCTCG), Relevance of breast cancer hormone receptors and other factors to the efficacy of adjuvant tamoxifen: patient-level meta-analysis of randomised trials. *Lancet.* 378:771-84, 2011.
6. Mehta R, Barlow W, Albain K, et al. Combination anastrozole and fulvestrant in metastatic breast cancer. *N Engl J Med.* 367: 435–44, 2012.
7. Bergh J, Johnsson P, Lidbrink E, et al. Fact: an open-label randomized phase III study of fulvestrant and anastrozole in combination compared with anastrozole alone as first-line therapy for patients with receptor-positive postmenopausal breast cancer. *J Clin Oncol* 30: 1919–25, 2012.
8. Baselga J, Campone M, Piccart M, et al. Everolimus in postmenopausal hormone-receptor-positive advanced breast cancer. *N Engl J Med* 366: 520–29, 2012.
9. Piccart M, Hortobagyi GN, Campone M, et al. Everolimus plus exemestane for hormone-receptor-positive, human epidermal growth factor receptor-2-negative advanced breast cancer: overall survival results from BOLERO-2. *Ann Oncol.* 25:2357-62, 2014.
10. Rugo HS, Rumble RB, Macrae E, et al. endocrine therapy for hormone receptor-positive metastatic breast cancer: American Society of Clinical Oncology Guideline. *J Clin Oncol.* 34:3069-103, 2016.
11. Finn RS, Dering J, Conklin D, et al. PD 0332991, a selective cyclin D kinase 4/6 inhibitor, preferentially inhibits proliferation of luminal estrogen receptor-positive human breast cancer cell lines in vitro. *Breast Cancer Res.* 11:R77, 2009.
12. Finn R, Hurvitz S, Allison M, et al. Phase I study of PD 0332991, a novel, oral, cyclin-D kinase (CDK) 4/6 inhibitor in combination with letrozole, for first-line treatment of metastatic post-menopausal, estrogen receptor-positive (ER+), human epidermal growth factor receptor 2 (HER2)-negative breast cancer. *Cancer Res.* 69 (24 suppl): abstr 5069, 2009.
13. DeMichele A, Clark AS, Tan KS, et al. CDK 4/6 inhibitor palbociclib (PD0332991) in Rb+ advanced breast cancer: phase II activity, safety, and predictive biomarker assessment. *Clin Cancer Res.* 21:995-1001, 2015.
14. Finn RS, Crown JP, Lang I, et al. The cyclin-dependent kinase 4/6 inhibitor palbociclib in combination with letrozole versus letrozole alone as first-line treatment of oestrogen receptor-positive, HER2-negative, advanced breast cancer (PALOMA-1/TRIO-18): a randomised phase 2 study. *Lancet Oncol.* 16:25-35, 2015.

15. Finn RS, Martin M, Rugo HS, et al. Palbociclib and letrozole in advanced breast Cancer. *N Engl J Med.* 375:1925-36, 2016.
16. Turner NC, Ro J, André F, et al. Palbociclib in Hormone-Receptor-Positive Advanced Breast Cancer. *N Engl J Med.* 373:209-19, 2015.
17. Cristofanilli M, Turner NC, Bondarenko I, et al. Fulvestrant plus palbociclib versus fulvestrant plus placebo for treatment of hormone-receptor-positive, HER2-negative metastatic breast cancer that progressed on previous endocrine therapy (PALOMA-3): final analysis of the multicentre, double-blind, phase 3 randomised controlled trial. *Lancet Oncol.* 17:425-39, 2016.
18. Ma CX, Gao F, Northfelt D, et al. A Phase II trial of neoadjuvant palbociclib, a cyclin-dependent kinase (CDK) 4/6 inhibitor, in combination with anastrozole for clinical stage 2 or 3 estrogen receptro positive HER2 negative (ER+HER2-) breast cancer (BC). *Cancer Res* 76, Abstract S6-05, 2016.
19. Turner, NC, Jiang Y, O'Leary B, et al. Efficacy of palbociclib plus fulvestrant (P+F) in patients with metastatic breast cancer and ESR1 mutations in circulating tumor DNA. *J Clin Oncol.* 34 (suppl; abstr 512), 2016.
20. Turner NC, Neven P, Loibl S, et al. *Lancet.* 2016 Dec 6. pii: S0140-6736(16)32419-9, 2016. [Epub ahead of print]
21. Spring LM, Gupta A, Reynolds KL, et al. Neoadjuvant endocrine therapy for estrogen receptor-positive breast cancer: A systematic review and meta-analysis. *JAMA Oncol.* 2:1477-86, 2016.
22. DeMichele A, Yee D, Berry DA, et al. The Neoadjuvant Model Is Still the Future for Drug Development in Breast Cancer. *Clin Cancer Res.* 21:2911-5, 2015.
23. Dowsett M, Ebbs SR, Dixon JM, et al. Biomarker changes during neoadjuvant anastrozole, tamoxifen, or the combination: influence of hormonal status and HER-2 in breast cancer-a study from the IMPACT trialists. *J Clin Oncol* 2005;23:2477-92.
24. Dowsett M, Smith IE, Ebbs SR, et al. Short-term changes in Ki67 during neoadjuvant treatment of primary breast cancer with anastrozole or tamoxifen alone or combined correlate with recurrence-free survival. *Clin Cancer Res.* 11:951-8s, 2005.
25. Dowsett M, Smith IE, Ebbs SR, et al. Proliferation and apoptosis as markers of benefit in neoadjuvant endocrine therapy of breast cancer. *Clin Cancer Res.* 12:1024-30s, 2006.
26. Dowsett M, Smith IE, Ebbs SR, et al. Prognostic value of Ki67 expression after short-term presurgical endocrine therapy for primary breast cancer. *J Natl Cancer Inst.* 99:167-70, 2007.
27. Ellis MJ, Tao Y, Luo J, et al. Outcome prediction for estrogen receptor-positive breast cancer based on postneoadjuvant endocrine therapy tumor characteristics. *Natl Cancer Inst.* 100:1380-8, 2008.
28. Jones RL, Salter J, A'Hern R, et al. The prognostic significance of Ki67 before and after neoadjuvant chemotherapy in breast cancer. *Breast Cancer Res Treat.* 116:53-68, 2009.
29. Polychronis A, Sinnott HD, Hadjiminis D, et al. Preoperative gefitinib versus gefitinib and anastrozole in postmenopausal patients with oestrogen-receptor positive and epidermal-growth-factor-receptorpositive primary breast cancer: a double-blind placebo-controlled phase II randomised trial. *Lancet Oncol.* 6:383-91, 2005.
30. Baselga J, Semiglazov V, van Dam, et al. Phase II randomized study of neoadjuvant everolimus plus letrozole compared with placebo plus letrozole in patients with estrogen receptor-positive breast cancer. *J Clin Oncol.* 27:2630-7, 2009.
31. Smith IE, Walsh G, Skene A, et al. A phase II placebo-controlled trial of neoadjuvant anastrozole alone or with gefitinib in early breast cancer. *J Clin Oncol.* 25:3816-22, 2007.
32. Marmor MF, Kellner U, Lai TY, et al. Recommendations on screening for chloroquine and hydroxychloroquine retinopathy (2016 Revision). *Ophthalmology.* 123:1386-94, 2016

33. Pfizer Pharma. (2015). Highlights of prescribing information. IBRANCE (palbociclib). Retrieved from: http://www.Accessdata.fda.gov/drugsatfda_docs/label/2015/207103s000lbl.pdf. Accessed November 16, 2015
34. Mahalingam D, Mita M, Sarantopoulos J, et al. Combined autophagy and HDAC inhibition: a phase I safety, tolerability, pharmacokinetic, and pharmacodynamic analysis of hydroxychloroquine in combination with the HDAC inhibitor vorinostat in patients with advanced solid tumors. *Autophagy*. 10:1403-14, 2014.
35. Rangwala R, Chang YC, Hu J, et al. Combined MTOR and autophagy inhibition: phase I trial of hydroxychloroquine and temsirolimus in patients with advanced solid tumors and melanoma. *Autophagy*. 10:1391-1402, 2014.
36. Rangwala R, Leone R, Chang YC, et al. Phase I trial of hydroxychloroquine with dose-intense temozolomide in patients with advanced solid tumors and melanoma. *Autophagy*. 10:1369-79, 2014.
37. Rosenfeld MR, Ye X, Supko JG, et al. A phase I/II trial of hydroxychloroquine in conjunction with radiation therapy and concurrent and adjuvant temozolomide in patients with newly diagnosed glioblastoma multiforme. *Autophagy*. 10:1359-68, 2014.

BIBLIOGRAPHY

1. (1985). "Consensus conference. Adjuvant chemotherapy for breast cancer." JAMA **254**(24): 3461-3463.
2. (2014). "Positive results for drug combo in I-SPY 2 trial." Cancer Discov **4**(2): OF2.
3. (2017). "Abemaciclib Shows Promise for Early Breast Cancer." Cancer Discov **7**(2): 119-120.
4. (2017). "Atezolizumab Extends Survival for Breast Cancer." Cancer Discov.
5. (2017). "Rucaparib Approved for Ovarian Cancer." Cancer Discov **7**(2): 120-121.
6. Aagaard, L. and J. J. Rossi (2007). "RNAi therapeutics: principles, prospects and challenges." Adv Drug Deliv Rev **59**(2-3): 75-86.
7. Abrahamsen, H., H. Stenmark and H. W. Platta (2012). "Ubiquitination and phosphorylation of Beclin 1 and its binding partners: Tuning class III phosphatidylinositol 3-kinase activity and tumor suppression." FEBS Lett **586**(11): 1584-1591.
8. Acevedo, M., M. Vernier, L. Mignacca, F. Lessard, G. Huot, O. Moiseeva, V. Bourdeau and G. Ferbeyre (2016). "A CDK4/6-Dependent Epigenetic Mechanism Protects Cancer Cells from PML-induced Senescence." Cancer Res **76**(11): 3252-3264.
9. Agrawal, A., J. F. Robertson, K. L. Cheung, E. Gutteridge, I. O. Ellis, R. I. Nicholson and J. M. Gee (2016). "Biological effects of fulvestrant on estrogen receptor positive human breast cancer: short, medium and long-term effects based on sequential biopsies." Int J Cancer **138**(1): 146-159.
10. Agus, D. B., R. W. Akita, W. D. Fox, G. D. Lewis, B. Higgins, P. I. Pisacane, J. A. Lofgren, C. Tindell, D. P. Evans, K. Maiese, H. I. Scher and M. X. Sliwkowski (2002). "Targeting ligand-activated ErbB2 signaling inhibits breast and prostate tumor growth." Cancer Cell **2**(2): 127-137.

11. Aita, V. M., X. H. Liang, V. V. Murty, D. L. Pincus, W. Yu, E. Cayanis, S. Kalachikov, T. C. Gilliam and B. Levine (1999). "Cloning and genomic organization of beclin 1, a candidate tumor suppressor gene on chromosome 17q21." Genomics **59**(1): 59-65.
12. Akaike, H. (1974). "New Look at Statistical-Model Identification." Ieee Transactions on Automatic Control **Ac19**(6): 716-723.
13. Akli, S., T. Bui, H. Wingate, A. Biernacka, S. Moulder, S. L. Tucker, K. K. Hunt and K. Keyomarsi (2010). "Low-molecular-weight cyclin E can bypass letrozole-induced G1 arrest in human breast cancer cells and tumors." Clin Cancer Res **16**(4): 1179-1190.
14. Akli, S., C. S. Van Pelt, T. Bui, A. S. Multani, S. Chang, D. Johnson, S. Tucker and K. Keyomarsi (2007). "Overexpression of the low molecular weight cyclin E in transgenic mice induces metastatic mammary carcinomas through the disruption of the ARF-p53 pathway." Cancer Res **67**(15): 7212-7222.
15. Akli, S., P. J. Zheng, A. S. Multani, H. F. Wingate, S. Pathak, N. Zhang, S. L. Tucker, S. Chang and K. Keyomarsi (2004). "Tumor-specific low molecular weight forms of cyclin E induce genomic instability and resistance to p21, p27, and antiestrogens in breast cancer." Cancer Res **64**(9): 3198-3208.
16. Aklilu, M., H. L. Kindler, R. C. Donehower, S. Mani and E. E. Vokes (2003). "Phase II study of flavopiridol in patients with advanced colorectal cancer." Ann Oncol **14**(8): 1270-1273.
17. Al-Hajj, M., M. S. Wicha, A. Benito-Hernandez, S. J. Morrison and M. F. Clarke (2003). "Prospective identification of tumorigenic breast cancer cells." Proc Natl Acad Sci U S A **100**(7): 3983-3988.
18. Amaravadi, R. K. and J. D. Winkler (2012). "Lys05: a new lysosomal autophagy inhibitor." Autophagy **8**(9): 1383-1384.
19. Anders, L., N. Ke, P. Hydbring, Y. J. Choi, H. R. Widlund, J. M. Chick, H. Zhai, M. Vidal, S. P. Gygi, P. Braun and P. Sicinski (2011). "A systematic screen for CDK4/6 substrates links

- FOXO1 phosphorylation to senescence suppression in cancer cells." Cancer Cell **20**(5): 620-634.
20. Appleyard, M. V., M. A. O'Neill, K. E. Murray, F. E. Paulin, S. E. Bray, N. M. Kernohan, D. A. Levison, D. P. Lane and A. M. Thompson (2009). "Seliciclib (CYC202, R-roscovitine) enhances the antitumor effect of doxorubicin in vivo in a breast cancer xenograft model." Int J Cancer **124**(2): 465-472.
 21. Arnold, A. and A. Papanikolaou (2005). "Cyclin D1 in breast cancer pathogenesis." J Clin Oncol **23**(18): 4215-4224.
 22. Arnold, S. F., J. D. Obourn, H. Jaffe and A. C. Notides (1995). "Phosphorylation of the human estrogen receptor by mitogen-activated protein kinase and casein kinase II: consequence on DNA binding." J Steroid Biochem Mol Biol **55**(2): 163-172.
 23. Asghar, U., A. K. Witkiewicz, N. C. Turner and E. S. Knudsen (2015). "The history and future of targeting cyclin-dependent kinases in cancer therapy." Nat Rev Drug Discov **14**(2): 130-146.
 24. Ashworth, A. (2008). "A synthetic lethal therapeutic approach: poly(ADP) ribose polymerase inhibitors for the treatment of cancers deficient in DNA double-strand break repair." J Clin Oncol **26**(22): 3785-3790.
 25. Azad, M. B., Y. Chen and S. B. Gibson (2009). "Regulation of autophagy by reactive oxygen species (ROS): implications for cancer progression and treatment." Antioxid Redox Signal **11**(4): 777-790.
 26. Bagdade, J. D., J. Wolter, P. V. Subbaiah and W. Ryan (1990). "Effects of tamoxifen treatment on plasma lipids and lipoprotein lipid composition." J Clin Endocrinol Metab **70**(4): 1132-1135.
 27. Bales, E., L. Mills, N. Milam, M. McGahren-Murray, D. Bandyopadhyay, D. Chen, J. A. Reed, N. Timchenko, J. J. van den Oord, M. Bar-Eli, K. Keyomarsi and E. E. Medrano (2005). "The

- low molecular weight cyclin E isoforms augment angiogenesis and metastasis of human melanoma cells in vivo." Cancer Res **65**(3): 692-697.
28. Ball, K. L., S. Lain, R. Fahraeus, C. Smythe and D. P. Lane (1997). "Cell-cycle arrest and inhibition of Cdk4 activity by small peptides based on the carboxy-terminal domain of p21WAF1." Curr Biol **7**(1): 71-80.
 29. Banerjee, K. and H. Resat (2016). "Constitutive activation of STAT3 in breast cancer cells: A review." Int J Cancer **138**(11): 2570-2578.
 30. Bartkova, J., J. Lukas, M. Strauss and J. Bartek (1995). "Cyclin D1 oncoprotein aberrantly accumulates in malignancies of diverse histogenesis." Oncogene **10**(4): 775-778.
 31. Barton, K. L., K. Misuraca, F. Cordero, E. Dobrikova, H. D. Min, M. Gromeier, D. G. Kirsch and O. J. Becher (2013). "PD-0332991, a CDK4/6 inhibitor, significantly prolongs survival in a genetically engineered mouse model of brainstem glioma." PLoS One **8**(10): e77639.
 32. Baselga, J., M. Campone, M. Piccart, H. A. Burris, 3rd, H. S. Rugo, T. Sahmoud, S. Noguchi, M. Gnant, K. I. Pritchard, F. Lebrun, J. T. Beck, Y. Ito, D. Yardley, I. Deleu, A. Perez, T. Bachelot, L. Vittori, Z. Xu, P. Mukhopadhyay, D. Lebwohl and G. N. Hortobagyi (2012). "Everolimus in postmenopausal hormone-receptor-positive advanced breast cancer." N Engl J Med **366**(6): 520-529.
 33. Baselga, J., J. Cortes, S. B. Kim, S. A. Im, R. Hegg, Y. H. Im, L. Roman, J. L. Pedrini, T. Pienkowski, A. Knott, E. Clark, M. C. Benyunes, G. Ross, S. M. Swain and C. S. Group (2012). "Pertuzumab plus trastuzumab plus docetaxel for metastatic breast cancer." N Engl J Med **366**(2): 109-119.
 34. Baselga, J., P. Gomez, R. Greil, S. Braga, M. A. Climent, A. M. Wardley, B. Kaufman, S. M. Stemmer, A. Pego, A. Chan, J. C. Goeminne, M. P. Graas, M. J. Kennedy, E. M. Ciruelos Gil, A. Schneeweiss, A. Zubel, J. Groos, H. Melezinkova and A. Awada (2013). "Randomized phase II study of the anti-epidermal growth factor receptor monoclonal

- antibody cetuximab with cisplatin versus cisplatin alone in patients with metastatic triple-negative breast cancer." J Clin Oncol **31**(20): 2586-2592.
35. Baughn, L. B., M. Di Liberto, K. Wu, P. L. Toogood, T. Louie, R. Gottschalk, R. Niesvizky, H. Cho, S. Ely, M. A. Moore and S. Chen-Kiang (2006). "A novel orally active small molecule potently induces G1 arrest in primary myeloma cells and prevents tumor growth by specific inhibition of cyclin-dependent kinase 4/6." Cancer Res **66**(15): 7661-7667.
 36. Baum, M., A. U. Budzar, J. Cuzick, J. Forbes, J. H. Houghton, J. G. Klijn, T. Sahmoud and A. T. Group (2002). "Anastrozole alone or in combination with tamoxifen versus tamoxifen alone for adjuvant treatment of postmenopausal women with early breast cancer: first results of the ATAC randomised trial." Lancet **359**(9324): 2131-2139.
 37. Bayraktar, S., A. M. Gutierrez-Barrera, D. Liu, T. Tasbas, U. Akar, J. K. Litton, E. Lin, C. T. Albarracin, F. Meric-Bernstam, A. M. Gonzalez-Angulo, G. N. Hortobagyi and B. K. Arun (2011). "Outcome of triple-negative breast cancer in patients with or without deleterious BRCA mutations." Breast Cancer Res Treat **130**(1): 145-153.
 38. Bedrosian, I., K. H. Lu, C. Verschraegen and K. Keyomarsi (2004). "Cyclin E deregulation alters the biologic properties of ovarian cancer cells." Oncogene **23**(15): 2648-2657.
 39. Benson, C., J. White, J. De Bono, A. O'Donnell, F. Raynaud, C. Cruickshank, H. McGrath, M. Walton, P. Workman, S. Kaye, J. Cassidy, A. Gianella-Borradori, I. Judson and C. Twelves (2007). "A phase I trial of the selective oral cyclin-dependent kinase inhibitor seliciclib (CYC202; R-Roscovitine), administered twice daily for 7 days every 21 days." Br J Cancer **96**(1): 29-37.
 40. Benz, C. C., G. K. Scott, J. C. Sarup, R. M. Johnson, D. Tripathy, E. Coronado, H. M. Shepard and C. K. Osborne (1992). "Estrogen-dependent, tamoxifen-resistant tumorigenic growth of MCF-7 cells transfected with HER2/neu." Breast Cancer Res Treat **24**(2): 85-95.

41. Berenson, J. R., H. Koga, J. Yang, J. Pearl, E. C. Holmes and R. Figlin (1990). "Frequent amplification of the bcl-1 locus in poorly differentiated squamous cell carcinoma of the lung. The Lung Cancer Study Group." Oncogene **5**(9): 1343-1348.
42. Bergman, L., M. L. Beelen, M. P. Gallee, H. Hollema, J. Benraadt and F. E. van Leeuwen (2000). "Risk and prognosis of endometrial cancer after tamoxifen for breast cancer. Comprehensive Cancer Centres' ALERT Group. Assessment of Liver and Endometrial cancer Risk following Tamoxifen." Lancet **356**(9233): 881-887.
43. Bertoli, C., J. M. Skotheim and R. A. de Bruin (2013). "Control of cell cycle transcription during G1 and S phases." Nat Rev Mol Cell Biol **14**(8): 518-528.
44. Biederbick, A., H. F. Kern and H. P. Elsasser (1995). "Monodansylcadaverine (MDC) is a specific in vivo marker for autophagic vacuoles." Eur J Cell Biol **66**(1): 3-14.
45. Bielak-Zmijewska, A., M. Wnuk, D. Przybylska, W. Grabowska, A. Lewinska, O. Alster, Z. Korwek, A. Cmoch, A. Myszka, S. Pikula, G. Mosieniak and E. Sikora (2014). "A comparison of replicative senescence and doxorubicin-induced premature senescence of vascular smooth muscle cells isolated from human aorta." Biogerontology **15**(1): 47-64.
46. Bijnsdorp, I. V., E. Giovannetti and G. J. Peters (2011). "Analysis of drug interactions." Methods Mol Biol **731**: 421-434.
47. Bonuccelli, G., M. Peiris-Pages, B. Ozsvari, U. E. Martinez-Outschoorn, F. Sotgia and M. P. Lisanti (2017). "Targeting cancer stem cell propagation with palbociclib, a CDK4/6 inhibitor: Telomerase drives tumor cell heterogeneity." Oncotarget **8**(6): 9868-9884.
48. Boonstra, J. and J. A. Post (2004). "Molecular events associated with reactive oxygen species and cell cycle progression in mammalian cells." Gene **337**: 1-13.
49. Bosco, E. E., Y. Wang, H. Xu, J. T. Zilfou, K. E. Knudsen, B. J. Aronow, S. W. Lowe and E. S. Knudsen (2007). "The retinoblastoma tumor suppressor modifies the therapeutic response of breast cancer." J Clin Invest **117**(1): 218-228.

50. Breast International Group 1-98 Collaborative, G., B. Thurlimann, A. Keshaviah, A. S. Coates, H. Mouridsen, L. Mauriac, J. F. Forbes, R. Paridaens, M. Castiglione-Gertsch, R. D. Gelber, M. Rabaglio, I. Smith, A. Wardley, K. N. Price and A. Goldhirsch (2005). "A comparison of letrozole and tamoxifen in postmenopausal women with early breast cancer." N Engl J Med **353**(26): 2747-2757.
51. Britton, D. J., I. R. Hutcheson, J. M. Knowlden, D. Barrow, M. Giles, R. A. McClelland, J. M. Gee and R. I. Nicholson (2006). "Bidirectional cross talk between ERalpha and EGFR signalling pathways regulates tamoxifen-resistant growth." Breast Cancer Res Treat **96**(2): 131-146.
52. Brown, N. E., R. Jeselsohn, T. Bihani, M. G. Hu, P. Foltopoulou, C. Kuperwasser and P. W. Hinds (2012). "Cyclin D1 activity regulates autophagy and senescence in the mammary epithelium." Cancer Res **72**(24): 6477-6489.
53. Burdette-Radoux, S., R. G. Tozer, R. C. Lohmann, I. Quirt, D. S. Ernst, W. Walsh, N. Wainman, A. D. Colevas and E. A. Eisenhauer (2004). "Phase II trial of flavopiridol, a cyclin dependent kinase inhibitor, in untreated metastatic malignant melanoma." Invest New Drugs **22**(3): 315-322.
54. Caldon, C. E., C. M. Sergio, J. Kang, A. Muthukaruppan, M. N. Boersma, A. Stone, J. Barraclough, C. S. Lee, M. A. Black, L. D. Miller, J. M. Gee, R. I. Nicholson, R. L. Sutherland, C. G. Print and E. A. Musgrove (2012). "Cyclin E2 overexpression is associated with endocrine resistance but not insensitivity to CDK2 inhibition in human breast cancer cells." Mol Cancer Ther **11**(7): 1488-1499.
55. Campbell, R. A., P. Bhat-Nakshatri, N. M. Patel, D. Constantinidou, S. Ali and H. Nakshatri (2001). "Phosphatidylinositol 3-kinase/AKT-mediated activation of estrogen receptor alpha: a new model for anti-estrogen resistance." J Biol Chem **276**(13): 9817-9824.
56. Campisi, J. (2005). "Senescent cells, tumor suppression, and organismal aging: good citizens, bad neighbors." Cell **120**(4): 513-522.

57. Capparelli, C., B. Chiavarina, D. Whitaker-Menezes, T. G. Pestell, R. G. Pestell, J. Hult, S. Ando, A. Howell, U. E. Martinez-Outschoorn, F. Sotgia and M. P. Lisanti (2012). "CDK inhibitors (p16/p19/p21) induce senescence and autophagy in cancer-associated fibroblasts, "fueling" tumor growth via paracrine interactions, without an increase in neo-angiogenesis." Cell Cycle **11**(19): 3599-3610.
58. Carascossa, S., P. Dudek, B. Cenni, P. A. Briand and D. Picard (2010). "CARM1 mediates the ligand-independent and tamoxifen-resistant activation of the estrogen receptor alpha by cAMP." Genes Dev **24**(7): 708-719.
59. Carey, L. A., C. M. Perou, C. A. Livasy, L. G. Dressler, D. Cowan, K. Conway, G. Karaca, M. A. Troester, C. K. Tse, S. Edmiston, S. L. Deming, J. Geradts, M. C. Cheang, T. O. Nielsen, P. G. Moorman, H. S. Earp and R. C. Millikan (2006). "Race, breast cancer subtypes, and survival in the Carolina Breast Cancer Study." JAMA **295**(21): 2492-2502.
60. Carlson, B. A., M. M. Dubay, E. A. Sausville, L. Brizuela and P. J. Worland (1996). "Flavopiridol induces G1 arrest with inhibition of cyclin-dependent kinase (CDK) 2 and CDK4 in human breast carcinoma cells." Cancer Res **56**(13): 2973-2978.
61. Carpenter, R. L. and H. W. Lo (2014). "STAT3 Target Genes Relevant to Human Cancers." Cancers (Basel) **6**(2): 897-925.
62. Cen, L., B. L. Carlson, M. A. Schroeder, J. L. Ostrem, G. J. Kitange, A. C. Mladek, S. R. Fink, P. A. Decker, W. Wu, J. S. Kim, T. Waldman, R. B. Jenkins and J. N. Sarkaria (2012). "p16-Cdk4-Rb axis controls sensitivity to a cyclin-dependent kinase inhibitor PD0332991 in glioblastoma xenograft cells." Neuro Oncol **14**(7): 870-881.
63. Cerami, E., J. Gao, U. Dogrusoz, B. E. Gross, S. O. Sumer, B. A. Aksoy, A. Jacobsen, C. J. Byrne, M. L. Heuer, E. Larsson, Y. Antipin, B. Reva, A. P. Goldberg, C. Sander and N. Schultz (2012). "The cBio cancer genomics portal: an open platform for exploring multidimensional cancer genomics data." Cancer Discov **2**(5): 401-404.

64. Chauhan, S., J. G. Goodwin, S. Chauhan, G. Manyam, J. Wang, A. M. Kamat and D. D. Boyd (2013). "ZKSCAN3 is a master transcriptional repressor of autophagy." Mol Cell **50**(1): 16-28.
65. Chen, D., E. Washbrook, N. Sarwar, G. J. Bates, P. E. Pace, V. Thirunuvakkarasu, J. Taylor, R. J. Epstein, F. V. Fuller-Pace, J. M. Egly, R. C. Coombes and S. Ali (2002). "Phosphorylation of human estrogen receptor alpha at serine 118 by two distinct signal transduction pathways revealed by phosphorylation-specific antisera." Oncogene **21**(32): 4921-4931.
66. Chen, F., S. Barman, Y. Yu, S. Haigh, Y. Wang, S. M. Black, R. Rafikov, H. Dou, Z. Bagi, W. Han, Y. Su and D. J. Fulton (2014). "Caveolin-1 is a negative regulator of NADPH oxidase-derived reactive oxygen species." Free Radic Biol Med **73**: 201-213.
67. Chen, S., Y. Z. Jiang, L. Huang, R. J. Zhou, K. D. Yu, Y. Liu and Z. M. Shao (2013). "The residual tumor autophagy marker LC3B serves as a prognostic marker in local advanced breast cancer after neoadjuvant chemotherapy." Clin Cancer Res **19**(24): 6853-6862.
68. Chen, X. X., F. F. Xie, X. J. Zhu, F. Lin, S. S. Pan, L. H. Gong, J. G. Qiu, W. J. Zhang, Q. W. Jiang, X. L. Mei, Y. Q. Xue, W. M. Qin, Z. Shi and X. J. Yan (2015). "Cyclin-dependent kinase inhibitor dinaciclib potently synergizes with cisplatin in preclinical models of ovarian cancer." Oncotarget **6**(17): 14926-14939.
69. Chicas, A., X. Wang, C. Zhang, M. McCurrach, Z. Zhao, O. Mert, R. A. Dickins, M. Narita, M. Zhang and S. W. Lowe (2010). "Dissecting the unique role of the retinoblastoma tumor suppressor during cellular senescence." Cancer Cell **17**(4): 376-387.
70. Chittaranjan, S., S. Bortnik, W. H. Dragowska, J. Xu, N. Abeyesundara, A. Leung, N. E. Go, L. DeVorkin, S. A. Wepler, K. Gelmon, D. T. Yapp, M. B. Bally and S. M. Gorski (2014). "Autophagy inhibition augments the anticancer effects of epirubicin treatment in anthracycline-sensitive and -resistant triple-negative breast cancer." Clin Cancer Res **20**(12): 3159-3173.

71. Chittaranjan, S., S. Bortnik and S. M. Gorski (2015). "Monitoring Autophagic Flux by Using Lysosomal Inhibitors and Western Blotting of Endogenous MAP1LC3B." Cold Spring Harb Protoc **2015**(8): 743-750.
72. Chung, S. S., N. Giehl, Y. Wu and J. V. Vadgama (2014). "STAT3 activation in HER2-overexpressing breast cancer promotes epithelial-mesenchymal transition and cancer stem cell traits." Int J Oncol **44**(2): 403-411.
73. Cicchini, M., R. Chakrabarti, S. Kongara, S. Price, R. Nahar, F. Lozy, H. Zhong, A. Vazquez, Y. Kang and V. Karantza (2014). "Autophagy regulator BECN1 suppresses mammary tumorigenesis driven by WNT1 activation and following parity." Autophagy **10**(11): 2036-2052.
74. Cimino-Mathews, A., E. Thompson, J. M. Taube, X. Ye, Y. Lu, A. Meeker, H. Xu, R. Sharma, K. Lecksell, T. C. Cornish, N. Cuka, P. Argani and L. A. Emens (2016). "PD-L1 (B7-H1) expression and the immune tumor microenvironment in primary and metastatic breast carcinomas." Hum Pathol **47**(1): 52-63.
75. Clark, A. S., T. B. Karasic, A. DeMichele, D. J. Vaughn, M. O'Hara, R. Perini, P. Zhang, P. Lal, M. Feldman, M. Gallagher and P. J. O'Dwyer (2016). "Palbociclib (PD0332991)-a Selective and Potent Cyclin-Dependent Kinase Inhibitor: A Review of Pharmacodynamics and Clinical Development." JAMA Oncol **2**(2): 253-260.
76. Clavel-Chapelon, F. and E. N. Group (2002). "Cumulative number of menstrual cycles and breast cancer risk: results from the E3N cohort study of French women." Cancer Causes Control **13**(9): 831-838.
77. Cole, M. P., C. T. Jones and I. D. Todd (1971). "A new anti-oestrogenic agent in late breast cancer. An early clinical appraisal of ICI46474." Br J Cancer **25**(2): 270-275.
78. Comstock, C. E., M. A. Augello, J. F. Goodwin, R. de Leeuw, M. J. Schiewer, W. F. Ostrander, Jr., R. A. Burkhardt, A. K. McClendon, P. A. McCue, E. J. Trabulsi, C. D. Lallas, L. G. Gomella, M. M. Centenera, J. R. Brody, L. M. Butler, W. D. Tilley and K. E. Knudsen

- (2013). "Targeting cell cycle and hormone receptor pathways in cancer." Oncogene **32**(48): 5481-5491.
79. Connell-Crowley, L., J. W. Harper and D. W. Goodrich (1997). "Cyclin D1/Cdk4 regulates retinoblastoma protein-mediated cell cycle arrest by site-specific phosphorylation." Mol Biol Cell **8**(2): 287-301.
80. Coombes, R. C., P. Goss, M. Dowsett, J. C. Gazet and A. Brodie (1984). "4-Hydroxyandrostenedione in treatment of postmenopausal patients with advanced breast cancer." Lancet **2**(8414): 1237-1239.
81. Coppe, J. P., P. Y. Desprez, A. Krtolica and J. Campisi (2010). "The senescence-associated secretory phenotype: the dark side of tumor suppression." Annu Rev Pathol **5**: 99-118.
82. Corin, I., M. C. Di Giacomo, P. Lastella, R. Bagnulo, G. Guanti and C. Simone (2006). "Tumor-specific hyperactive low-molecular-weight cyclin E isoforms detection and characterization in non-metastatic colorectal tumors." Cancer Biol Ther **5**(2): 198-203.
83. Corin, I., L. Larsson, J. Bergstrom, B. Gustavsson and K. Derwinger (2010). "A study of the expression of Cyclin E and its isoforms in tumor and adjacent mucosa, correlated to patient outcome in early colon cancer." Acta Oncol **49**(1): 63-69.
84. Creighton, C. J., X. Li, M. Landis, J. M. Dixon, V. M. Neumeister, A. Sjolund, D. L. Rimm, H. Wong, A. Rodriguez, J. I. Herschkowitz, C. Fan, X. Zhang, X. He, A. Pavlick, M. C. Gutierrez, L. Renshaw, A. A. Larionov, D. Faratian, S. G. Hilsenbeck, C. M. Perou, M. T. Lewis, J. M. Rosen and J. C. Chang (2009). "Residual breast cancers after conventional therapy display mesenchymal as well as tumor-initiating features." Proc Natl Acad Sci U S A **106**(33): 13820-13825.
85. Cristofanilli, M., N. C. Turner, I. Bondarenko, J. Ro, S. A. Im, N. Masuda, M. Colleoni, A. DeMichele, S. Loi, S. Verma, H. Iwata, N. Harbeck, K. Zhang, K. P. Theall, Y. Jiang, C. H. Bartlett, M. Koehler and D. Slamon (2016). "Fulvestrant plus palbociclib versus fulvestrant plus placebo for treatment of hormone-receptor-positive, HER2-negative metastatic breast

- cancer that progressed on previous endocrine therapy (PALOMA-3): final analysis of the multicentre, double-blind, phase 3 randomised controlled trial." Lancet Oncol.
86. d'Adda di Fagagna, F. (2008). "Living on a break: cellular senescence as a DNA-damage response." Nat Rev Cancer **8**(7): 512-522.
 87. d'Adda di Fagagna, F., P. M. Reaper, L. Clay-Farrace, H. Fiegler, P. Carr, T. Von Zglinicki, G. Saretzki, N. P. Carter and S. P. Jackson (2003). "A DNA damage checkpoint response in telomere-initiated senescence." Nature **426**(6963): 194-198.
 88. Dauvois, S., R. White and M. G. Parker (1993). "The antiestrogen ICI 182780 disrupts estrogen receptor nucleocytoplasmic shuttling." J Cell Sci **106 (Pt 4)**: 1377-1388.
 89. Davidson, B., M. Skrede, I. Silins, M. Shih le, C. G. Trope and V. A. Florenes (2007). "Low-molecular weight forms of cyclin E differentiate ovarian carcinoma from cells of mesothelial origin and are associated with poor survival in ovarian carcinoma." Cancer **110**(6): 1264-1271.
 90. Davies, C., H. Pan, J. Godwin, R. Gray, R. Arriagada, V. Raina, M. Abraham, V. H. Medeiros Alencar, A. Badran, X. Bonfill, J. Bradbury, M. Clarke, R. Collins, S. R. Davis, A. Delmestri, J. F. Forbes, P. Haddad, M. F. Hou, M. Inbar, H. Khaled, J. Kielanowska, W. H. Kwan, B. S. Mathew, I. Mittra, B. Muller, A. Nicolucci, O. Peralta, F. Pernas, L. Petruzella, T. Pienkowski, R. Radhika, B. Rajan, M. T. Rubach, S. Tort, G. Urrutia, M. Valentini, Y. Wang, R. Peto and G. Adjuvant Tamoxifen: Longer Against Shorter Collaborative (2013). "Long-term effects of continuing adjuvant tamoxifen to 10 years versus stopping at 5 years after diagnosis of oestrogen receptor-positive breast cancer: ATLAS, a randomised trial." Lancet **381**(9869): 805-816.
 91. De Azevedo, W. F., S. Leclerc, L. Meijer, L. Havlicek, M. Strnad and S. H. Kim (1997). "Inhibition of cyclin-dependent kinases by purine analogues: crystal structure of human cdk2 complexed with roscovitine." Eur J Biochem **243**(1-2): 518-526.

92. Dean, J. L., A. K. McClendon, T. E. Hickey, L. M. Butler, W. D. Tilley, A. K. Witkiewicz and E. S. Knudsen (2012). "Therapeutic response to CDK4/6 inhibition in breast cancer defined by ex vivo analyses of human tumors." Cell Cycle **11**(14): 2756-2761.
93. Dean, M., T. Fojo and S. Bates (2005). "Tumour stem cells and drug resistance." Nat Rev Cancer **5**(4): 275-284.
94. Delk, N. A., K. K. Hunt and K. Keyomarsi (2009). "Altered subcellular localization of tumor-specific cyclin E isoforms affects cyclin-dependent kinase 2 complex formation and proteasomal regulation." Cancer Res **69**(7): 2817-2825.
95. DeMichele, A., A. S. Clark, K. S. Tan, D. F. Heitjan, K. Gramlich, M. Gallagher, P. Lal, M. Feldman, P. Zhang, C. Colameco, D. Lewis, M. Langer, N. Goodman, S. Domchek, K. Gogineni, M. Rosen, K. Fox and P. O'Dwyer (2015). "CDK 4/6 inhibitor palbociclib (PD0332991) in Rb+ advanced breast cancer: phase II activity, safety, and predictive biomarker assessment." Clin Cancer Res **21**(5): 995-1001.
96. DeMichele A , S. N., Koehler M (2016). "Abstract P4-13-04: Upregulation of cell cycle pathway genes without loss of RB1 contributes to acquired resistance to single-agent treatment with palbociclib in breast cancer." Cancer Res 2016 **76(4 Suppl):P4-13-04**.
97. Deroo, B. J. and K. S. Korach (2006). "Estrogen receptors and human disease." J Clin Invest **116**(3): 561-570.
98. Deter, R. L. and C. De Duve (1967). "Influence of glucagon, an inducer of cellular autophagy, on some physical properties of rat liver lysosomes." J Cell Biol **33**(2): 437-449.
99. Dethlefsen, C., G. Hojfeldt and P. Hojman (2013). "The role of intratumoral and systemic IL-6 in breast cancer." Breast Cancer Res Treat **138**(3): 657-664.
100. Dickson, M. A., W. D. Tap, M. L. Keohan, S. P. D'Angelo, M. M. Gounder, C. R. Antonescu, J. Landa, L. X. Qin, D. D. Rathbone, M. M. Condry, Y. Ustoyev, A. M. Crago, S. Singer and G. K. Schwartz (2013). "Phase II trial of the CDK4 inhibitor PD0332991 in

- patients with advanced CDK4-amplified well-differentiated or dedifferentiated liposarcoma." J Clin Oncol **31**(16): 2024-2028.
101. Dimri, G. P., X. Lee, G. Basile, M. Acosta, G. Scott, C. Roskelley, E. E. Medrano, M. Linskens, I. Rubelj, O. Pereira-Smith and et al. (1995). "A biomarker that identifies senescent human cells in culture and in aging skin in vivo." Proc Natl Acad Sci U S A **92**(20): 9363-9367.
 102. Dublin, E. A., N. K. Patel, C. E. Gillett, P. Smith, G. Peters and D. M. Barnes (1998). "Retinoblastoma and p16 proteins in mammary carcinoma: their relationship to cyclin D1 and histopathological parameters." Int J Cancer **79**(1): 71-75.
 103. Duong, M. T., S. Akli, S. Macalou, A. Biernacka, B. G. Debeb, M. Yi, K. K. Hunt and K. Keyomarsi (2013). "Hbo1 is a cyclin E/CDK2 substrate that enriches breast cancer stem-like cells." Cancer Res **73**(17): 5556-5568.
 104. Duronio, R. J., A. Brook, N. Dyson and P. H. O'Farrell (1996). "E2F-induced S phase requires cyclin E." Genes Dev **10**(19): 2505-2513.
 105. Early Breast Cancer Trialists' Collaborative, G. (1988). "Effects of adjuvant tamoxifen and of cytotoxic therapy on mortality in early breast cancer. An overview of 61 randomized trials among 28,896 women." N Engl J Med **319**(26): 1681-1692.
 106. Ehemann, C. R., K. M. Shaw, A. B. Ryerson, J. W. Miller, U. A. Ajani and M. C. White (2009). "The changing incidence of in situ and invasive ductal and lobular breast carcinomas: United States, 1999-2004." Cancer Epidemiol Biomarkers Prev **18**(6): 1763-1769.
 107. Ellis, M. J., L. Ding, D. Shen, J. Luo, V. J. Suman, J. W. Wallis, B. A. Van Tine, J. Hoog, R. J. Goiffon, T. C. Goldstein, S. Ng, L. Lin, R. Crowder, J. Snider, K. Ballman, J. Weber, K. Chen, D. C. Koboldt, C. Kandoth, W. S. Schierding, J. F. McMichael, C. A. Miller, C. Lu, C. C. Harris, M. D. McLellan, M. C. Wendl, K. DeSchryver, D. C. Allred, L. Esserman, G. Unzeitig, J. Margenthaler, G. V. Babiera, P. K. Marcom, J. M. Guenther, M. Leitch, K. Hunt,

- J. Olson, Y. Tao, C. A. Maher, L. L. Fulton, R. S. Fulton, M. Harrison, B. Oberkfell, F. Du, R. Demeter, T. L. Vickery, A. Elhammali, H. Piwnica-Worms, S. McDonald, M. Watson, D. J. Dooling, D. Ota, L. W. Chang, R. Bose, T. J. Ley, D. Piwnica-Worms, J. M. Stuart, R. K. Wilson and E. R. Mardis (2012). "Whole-genome analysis informs breast cancer response to aromatase inhibition." Nature **486**(7403): 353-360.
108. Ellis, M. J., Y. Tao, J. Luo, R. A'Hern, D. B. Evans, A. S. Bhatnagar, H. A. Chaudri Ross, A. von Kameke, W. R. Miller, I. Smith, W. Eiermann and M. Dowsett (2008). "Outcome prediction for estrogen receptor-positive breast cancer based on postneoadjuvant endocrine therapy tumor characteristics." J Natl Cancer Inst **100**(19): 1380-1388.
109. Encarnacion, C. A., D. R. Ciocca, W. L. McGuire, G. M. Clark, S. A. Fuqua and C. K. Osborne (1993). "Measurement of steroid hormone receptors in breast cancer patients on tamoxifen." Breast Cancer Res Treat **26**(3): 237-246.
110. Eroles, P., A. Bosch, J. A. Perez-Fidalgo and A. Lluch (2012). "Molecular biology in breast cancer: intrinsic subtypes and signaling pathways." Cancer Treat Rev **38**(6): 698-707.
111. Ertel, A., J. L. Dean, H. Rui, C. Liu, A. K. Witkiewicz, K. E. Knudsen and E. S. Knudsen (2010). "RB-pathway disruption in breast cancer: differential association with disease subtypes, disease-specific prognosis and therapeutic response." Cell Cycle **9**(20): 4153-4163.
112. Eustermann, S., H. Videler, J. C. Yang, P. T. Cole, D. Gruszka, D. Veprintsev and D. Neuhaus (2011). "The DNA-binding domain of human PARP-1 interacts with DNA single-strand breaks as a monomer through its second zinc finger." J Mol Biol **407**(1): 149-170.
113. Farmer, H., N. McCabe, C. J. Lord, A. N. Tutt, D. A. Johnson, T. B. Richardson, M. Santarosa, K. J. Dillon, I. Hickson, C. Knights, N. M. Martin, S. P. Jackson, G. C. Smith and A. Ashworth (2005). "Targeting the DNA repair defect in BRCA mutant cells as a therapeutic strategy." Nature **434**(7035): 917-921.

114. Fawell, S. E., R. White, S. Hoare, M. Sydenham, M. Page and M. G. Parker (1990). "Inhibition of estrogen receptor-DNA binding by the "pure" antiestrogen ICI 164,384 appears to be mediated by impaired receptor dimerization." Proc Natl Acad Sci U S A **87**(17): 6883-6887.
115. Felty, Q., K. P. Singh and D. Roy (2005). "Estrogen-induced G1/S transition of G0-arrested estrogen-dependent breast cancer cells is regulated by mitochondrial oxidant signaling." Oncogene **24**(31): 4883-4893.
116. Finn, R. S., J. P. Crown, I. Lang, K. Boer, I. M. Bondarenko, S. O. Kulyk, J. Ettl, R. Patel, T. Pinter, M. Schmidt, Y. Shparyk, A. R. Thummala, N. L. Voytko, C. Fowst, X. Huang, S. T. Kim, S. Randolph and D. J. Slamon (2015). "The cyclin-dependent kinase 4/6 inhibitor palbociclib in combination with letrozole versus letrozole alone as first-line treatment of oestrogen receptor-positive, HER2-negative, advanced breast cancer (PALOMA-1/TRIO-18): a randomised phase 2 study." Lancet Oncol **16**(1): 25-35.
117. Finn, R. S., J. Dering, D. Conklin, O. Kalous, D. J. Cohen, A. J. Desai, C. Ginther, M. Atefi, I. Chen, C. Fowst, G. Los and D. J. Slamon (2009). "PD 0332991, a selective cyclin D kinase 4/6 inhibitor, preferentially inhibits proliferation of luminal estrogen receptor-positive human breast cancer cell lines in vitro." Breast Cancer Res **11**(5): R77.
118. Finn, R. S., M. Martin, H. S. Rugo, S. Jones, S. A. Im, K. Gelmon, N. Harbeck, O. N. Lipatov, J. M. Walshe, S. Moulder, E. Gauthier, D. R. Lu, S. Randolph, V. Dieras and D. J. Slamon (2016). "Palbociclib and Letrozole in Advanced Breast Cancer." N Engl J Med **375**(20): 1925-1936.
119. Finn, R. S., M. Martin, H. S. Rugo, S. E. Jones, S.-A. Im, K. A. Gelmon, N. Harbeck, O. N. Lipatov, J. M. Walshe, S. L. Moulder, E. R. Gauthier, D. Lu, S. Randolph, V. Diéras, D. J. Slamon and D. Geffen (2016). "PALOMA-2: Primary results from a phase III trial of palbociclib (P) with letrozole (L) compared with letrozole alone in postmenopausal women with ER+/HER2– advanced breast cancer " J Clin Oncol **34**: suppl; abstr 507.

120. Fischer, A. H., K. A. Jacobson, J. Rose and R. Zeller (2008). "Hematoxylin and eosin staining of tissue and cell sections." CSH Protoc **2008**: pdb prot4986.
121. Fisher, B., J. P. Costantino, C. K. Redmond, E. R. Fisher, D. L. Wickerham and W. M. Cronin (1994). "Endometrial cancer in tamoxifen-treated breast cancer patients: findings from the National Surgical Adjuvant Breast and Bowel Project (NSABP) B-14." J Natl Cancer Inst **86**(7): 527-537.
122. Flaherty, K. T., P. M. Lorusso, A. Demichele, V. G. Abramson, R. Courtney, S. S. Randolph, M. N. Shaik, K. D. Wilner, P. J. O'Dwyer and G. K. Schwartz (2012). "Phase I, dose-escalation trial of the oral cyclin-dependent kinase 4/6 inhibitor PD 0332991, administered using a 21-day schedule in patients with advanced cancer." Clin Cancer Res **18**(2): 568-576.
123. Foulkes, W. D., I. M. Stefansson, P. O. Chappuis, L. R. Begin, J. R. Goffin, N. Wong, M. Trudel and L. A. Akslen (2003). "Germline BRCA1 mutations and a basal epithelial phenotype in breast cancer." J Natl Cancer Inst **95**(19): 1482-1485.
124. Franco, J., U. Balaji, E. Freinkman, A. K. Witkiewicz and E. S. Knudsen (2016). "Metabolic Reprogramming of Pancreatic Cancer Mediated by CDK4/6 Inhibition Elicits Unique Vulnerabilities." Cell Rep **14**(5): 979-990.
125. Freedman, O., E. Amir, G. Dranitsaris, J. Napolskikh, R. Kumar, M. Fralick, S. Chia, T. Petrella, S. Dent, K. Tonkin, I. Ahmad, D. Rayson and M. Clemons (2009). "Predicting benefit from fulvestrant in pretreated metastatic breast cancer patients." Breast Cancer Res Treat **118**(2): 377-383.
126. Fribbens, C., B. O'Leary, L. Kilburn, S. Hrebien, I. Garcia-Murillas, M. Beaney, M. Cristofanilli, F. Andre, S. Loi, S. Loibl, J. Jiang, C. H. Bartlett, M. Koehler, M. Dowsett, J. M. Bliss, S. R. Johnston and N. C. Turner (2016). "Plasma ESR1 Mutations and the Treatment of Estrogen Receptor-Positive Advanced Breast Cancer." J Clin Oncol **34**(25): 2961-2968.

127. Fry, D. W., P. J. Harvey, P. R. Keller, W. L. Elliott, M. Meade, E. Trachet, M. Albassam, X. Zheng, W. R. Leopold, N. K. Pryer and P. L. Toogood (2004). "Specific inhibition of cyclin-dependent kinase 4/6 by PD 0332991 and associated antitumor activity in human tumor xenografts." Mol Cancer Ther **3**(11): 1427-1438.
128. Fuqua, S. A., C. Wiltchke, Q. X. Zhang, A. Borg, C. G. Castles, W. E. Friedrichs, T. Hopp, S. Hilsenbeck, S. Mohsin, P. O'Connell and D. C. Allred (2000). "A hypersensitive estrogen receptor-alpha mutation in premalignant breast lesions." Cancer Res **60**(15): 4026-4029.
129. Furet, P., C. Batzl, A. Bhatnagar, E. Francotte, G. Rihs and M. Lang (1993). "Aromatase inhibitors: synthesis, biological activity, and binding mode of azole-type compounds." J Med Chem **36**(10): 1393-1400.
130. Giacinti, C. and A. Giordano (2006). "RB and cell cycle progression." Oncogene **25**(38): 5220-5227.
131. Ginestier, C., M. H. Hur, E. Charafe-Jauffret, F. Monville, J. Dutcher, M. Brown, J. Jacquemier, P. Viens, C. G. Kleer, S. Liu, A. Schott, D. Hayes, D. Birnbaum, M. S. Wicha and G. Dontu (2007). "ALDH1 is a marker of normal and malignant human mammary stem cells and a predictor of poor clinical outcome." Cell Stem Cell **1**(5): 555-567.
132. Glick, D., S. Barth and K. F. Macleod (2010). "Autophagy: cellular and molecular mechanisms." J Pathol **221**(1): 3-12.
133. Goldhirsch, A., W. C. Wood, A. S. Coates, R. D. Gelber, B. Thurlimann, H. J. Senn and m. Panel (2011). "Strategies for subtypes--dealing with the diversity of breast cancer: highlights of the St. Gallen International Expert Consensus on the Primary Therapy of Early Breast Cancer 2011." Ann Oncol **22**(8): 1736-1747.
134. Gonen, M. and G. Heller (2005). "Concordance probability and discriminatory power in proportional hazards regression." Biometrika **92**(4): 965-970.

135. Gritsch, D., M. Maurer, N. Zulehner and J. Wesierska-Gadek (2011). "Tamoxifen enhances the anti-proliferative effect of roscovitine, a selective cyclin-dependent kinase inhibitor, on human ER-positive human breast cancer cells." J Exp Ther Oncol **9**(1): 37-45.
136. Gunja, N., D. Roberts, D. McCoubrie, P. Lamberth, A. Jan, D. C. Simes, P. Hackett and N. A. Buckley (2009). "Survival after massive hydroxychloroquine overdose." Anaesth Intensive Care **37**(1): 130-133.
137. Guo, J. Y., G. Karsli-Uzunbas, R. Mathew, S. C. Aisner, J. J. Kamphorst, A. M. Strohecker, G. Chen, S. Price, W. Lu, X. Teng, E. Snyder, U. Santanam, R. S. Dipaola, T. Jacks, J. D. Rabinowitz and E. White (2013). "Autophagy suppresses progression of K-ras-induced lung tumors to oncocytomas and maintains lipid homeostasis." Genes Dev **27**(13): 1447-1461.
138. Guo, X. L., D. Li, K. Sun, J. Wang, Y. Liu, J. R. Song, Q. D. Zhao, S. S. Zhang, W. J. Deng, X. Zhao, M. C. Wu and L. X. Wei (2013). "Inhibition of autophagy enhances anticancer effects of bevacizumab in hepatocarcinoma." J Mol Med (Berl) **91**(4): 473-483.
139. Hamad, I., N. Arda, M. Pekmez, S. Karaer and G. Temizkan (2010). "Intracellular scavenging activity of Trolox (6-hydroxy-2,5,7,8-tetramethylchromane-2-carboxylic acid) in the fission yeast, *Schizosaccharomyces pombe*." J Nat Sci Biol Med **1**(1): 16-21.
140. Hammond, E. M., C. L. Brunet, G. D. Johnson, J. Parkhill, A. E. Milner, G. Brady, C. D. Gregory and R. J. Grand (1998). "Homology between a human apoptosis specific protein and the product of APG5, a gene involved in autophagy in yeast." FEBS Lett **425**(3): 391-395.
141. Han, W., H. Pan, Y. Chen, J. Sun, Y. Wang, J. Li, W. Ge, L. Feng, X. Lin, X. Wang, X. Wang and H. Jin (2011). "EGFR tyrosine kinase inhibitors activate autophagy as a cytoprotective response in human lung cancer cells." PLoS One **6**(6): e18691.
142. Harley, C. B., A. B. Futcher and C. W. Greider (1990). "Telomeres shorten during ageing of human fibroblasts." Nature **345**(6274): 458-460.

143. Harper, J. V. and G. Brooks (2005). "The mammalian cell cycle: an overview." Methods Mol Biol **296**: 113-153.
144. Hartkopf, A. D., F. A. Taran, M. Wallwiener, C. B. Walter, B. Kramer, E. M. Grischke and S. Y. Brucker (2016). "PD-1 and PD-L1 Immune Checkpoint Blockade to Treat Breast Cancer." Breast Care (Basel) **11**(6): 385-390.
145. Harwell, R. M., B. B. Mull, D. C. Porter and K. Keyomarsi (2004). "Activation of cyclin-dependent kinase 2 by full length and low molecular weight forms of cyclin E in breast cancer cells." J Biol Chem **279**(13): 12695-12705.
146. Harwell, R. M., D. C. Porter, C. Danes and K. Keyomarsi (2000). "Processing of cyclin E differs between normal and tumor breast cells." Cancer Res **60**(2): 481-489.
147. Hayflick, L. and P. S. Moorhead (1961). "The serial cultivation of human diploid cell strains." Exp Cell Res **25**: 585-621.
148. Hellyer, N. J., M. S. Kim and J. G. Koland (2001). "Heregulin-dependent activation of phosphoinositide 3-kinase and Akt via the ErbB2/ErbB3 co-receptor." J Biol Chem **276**(45): 42153-42161.
149. Henderson, B. E. and H. S. Feigelson (2000). "Hormonal carcinogenesis." Carcinogenesis **21**(3): 427-433.
150. Hernandez-Aya, L. F., M. Chavez-Macgregor, X. Lei, F. Meric-Bernstam, T. A. Buchholz, L. Hsu, A. A. Sahin, K. A. Do, V. Valero, G. N. Hortobagyi and A. M. Gonzalez-Angulo (2011). "Nodal status and clinical outcomes in a large cohort of patients with triple-negative breast cancer." J Clin Oncol **29**(19): 2628-2634.
151. Herrera-Abreu, M. T., M. Palafox, U. Asghar, M. A. Rivas, R. J. Cutts, I. Garcia-Murillas, A. Pearson, M. Guzman, O. Rodriguez, J. Grueso, M. Bellet, J. Cortes, R. Elliott, S. Pancholi, J. Baselga, M. Dowsett, L. A. Martin, N. C. Turner and V. Serra (2016). "Early Adaptation and Acquired Resistance to CDK4/6 Inhibition in Estrogen Receptor-Positive Breast Cancer." Cancer Res **76**(8): 2301-2313.

152. Hirai, H., M. F. Roussel, J. Y. Kato, R. A. Ashmun and C. J. Sherr (1995). "Novel INK4 proteins, p19 and p18, are specific inhibitors of the cyclin D-dependent kinases CDK4 and CDK6." Mol Cell Biol **15**(5): 2672-2681.
153. Homewood, C. A., D. C. Warhurst, W. Peters and V. C. Baggeley (1972). "Lysosomes, pH and the anti-malarial action of chloroquine." Nature **235**(5332): 50-52.
154. Horiuchi, D., L. Kusdra, N. E. Huskey, S. Chandriani, M. E. Lenburg, A. M. Gonzalez-Angulo, K. J. Creasman, A. V. Bazarov, J. W. Smyth, S. E. Davis, P. Yaswen, G. B. Mills, L. J. Esserman and A. Goga (2012). "MYC pathway activation in triple-negative breast cancer is synthetic lethal with CDK inhibition." J Exp Med **209**(4): 679-696.
155. Hortobagyi, G. N., S. M. Stemmer, H. A. Burris, Y. S. Yap, G. S. Sonke, S. Paluch-Shimon, M. Campone, K. L. Blackwell, F. Andre, E. P. Winer, W. Janni, S. Verma, P. Conte, C. L. Arteaga, D. A. Cameron, K. Petrakova, L. L. Hart, C. Villanueva, A. Chan, E. Jakobsen, A. Nusch, O. Burdaeva, E. M. Grischke, E. Alba, E. Wist, N. Marschner, A. M. Favret, D. Yardley, T. Bachelot, L. M. Tseng, S. Blau, F. Xuan, F. Souami, M. Miller, C. Germa, S. Hirawat and J. O'Shaughnessy (2016). "Ribociclib as First-Line Therapy for HR-Positive, Advanced Breast Cancer." N Engl J Med **375**(18): 1738-1748.
156. Howell, A., J. Cuzick, M. Baum, A. Buzdar, M. Dowsett, J. F. Forbes, G. Hocht-Boes, J. Houghton, G. Y. Locker, J. S. Tobias and A. T. Group (2005). "Results of the ATAC (Arimidex, Tamoxifen, Alone or in Combination) trial after completion of 5 years' adjuvant treatment for breast cancer." Lancet **365**(9453): 60-62.
157. Howell, A., D. DeFriend, J. Robertson, R. Blamey and P. Walton (1995). "Response to a specific antioestrogen (ICI 182780) in tamoxifen-resistant breast cancer." Lancet **345**(8941): 29-30.
158. Hunt, K. K., C. Karakas, M. J. Ha, A. Biernacka, M. Yi, A. Sahin, O. Adjapong, G. N. Hortobagyi, M. L. Bondy, P. A. Thompson, K. L. Cheung, I. O. Ellis, S. Bacus, W. F.

- Symmans, K. A. Do and K. Keyomarsi (2016). "Cytoplasmic Cyclin E Predicts Recurrence in Patients with Breast Cancer." Clin Cancer Res.
159. Ikeda, M. A., L. Jakoi and J. R. Nevins (1996). "A unique role for the Rb protein in controlling E2F accumulation during cell growth and differentiation." Proc Natl Acad Sci U S A **93**(8): 3215-3220.
160. Imai, Y., A. Takahashi, A. Hanyu, S. Hori, S. Sato, K. Naka, A. Hirao, N. Ohtani and E. Hara (2014). "Crosstalk between the Rb pathway and AKT signaling forms a quiescence-senescence switch." Cell Rep **7**(1): 194-207.
161. Infante, J. R., P. A. Cassier, J. F. Gerecitano, P. O. Witteveen, R. Chugh, V. Ribrag, A. Chakraborty, A. Matano, J. R. Dobson, A. S. Crystal, S. Parasuraman and G. I. Shapiro (2016). "A Phase I Study of the Cyclin-Dependent Kinase 4/6 Inhibitor Ribociclib (LEE011) in Patients with Advanced Solid Tumors and Lymphomas." Clin Cancer Res **22**(23): 5696-5705.
162. Ismail, A., S. Bandla, M. Reveiller, L. Toia, Z. Zhou, W. E. Gooding, I. Kalatskaya, L. Stein, M. D'Souza, V. R. Litle, J. H. Peters, A. Pennathur, J. D. Luketich and T. E. Godfrey (2011). "Early G(1) cyclin-dependent kinases as prognostic markers and potential therapeutic targets in esophageal adenocarcinoma." Clin Cancer Res **17**(13): 4513-4522.
163. Jabbour-Leung, N. A., X. Chen, T. Bui, Y. Jiang, D. Yang, S. Vijayaraghavan, M. J. McArthur, K. K. Hunt and K. Keyomarsi (2016). "Sequential Combination Therapy of CDK Inhibition and Doxorubicin Is Synthetically Lethal in p53-Mutant Triple-Negative Breast Cancer." Mol Cancer Ther **15**(4): 593-607.
164. Jajic, I., T. Sarna and K. Strzalka (2015). "Senescence, Stress, and Reactive Oxygen Species." Plants (Basel) **4**(3): 393-411.
165. Jansen, V. M., N. E. Bhola, J. A. Bauer, L. Formisano, K. M. Lee, K. E. Hutchinson, A. K. Witkiewicz, P. D. Moore, M. V. Estrada, V. Sanchez, P. G. Ericsson, M. Sanders, P. R. Pohlmann, M. J. Pishvaian, D. A. Riddle, W. Wei, T. C. Dugger, E. Knudsen and C. L.

- Arteaga (2017). "Kinome-wide RNA interference screen reveals a role for PDK1 in acquired resistance to CDK4/6 inhibition in ER-positive breast cancer." Cancer Res.
166. JavanMoghadam, S., Z. Weihua, K. K. Hunt and K. Keyomarsi (2016). "Estrogen receptor alpha is cell cycle-regulated and regulates the cell cycle in a ligand-dependent fashion." Cell Cycle **15**(12): 1579-1590.
 167. Jelovac, D., G. Sabnis, B. J. Long, L. Macedo, O. G. Goloubeva and A. M. Brodie (2005). "Activation of mitogen-activated protein kinase in xenografts and cells during prolonged treatment with aromatase inhibitor letrozole." Cancer Res **65**(12): 5380-5389.
 168. Jiang, H., V. Martin, C. Gomez-Manzano, D. G. Johnson, M. Alonso, E. White, J. Xu, T. J. McDonnell, N. Shinojima and J. Fueyo (2010). "The RB-E2F1 pathway regulates autophagy." Cancer Res **70**(20): 7882-7893.
 169. Jiang, X., M. Overholtzer and C. B. Thompson (2015). "Autophagy in cellular metabolism and cancer." J Clin Invest **125**(1): 47-54.
 170. Jin, H., D. Tu, N. Zhao, L. E. Shepherd and P. E. Goss (2012). "Longer-term outcomes of letrozole versus placebo after 5 years of tamoxifen in the NCIC CTG MA.17 trial: analyses adjusting for treatment crossover." J Clin Oncol **30**(7): 718-721.
 171. Jordan, V. C. (1976). "Effect of tamoxifen (ICI 46,474) on initiation and growth of DMBA-induced rat mammary carcinomata." Eur J Cancer **12**(6): 419-424.
 172. Jordan, V. C. and A. M. Brodie (2007). "Development and evolution of therapies targeted to the estrogen receptor for the treatment and prevention of breast cancer." Steroids **72**(1): 7-25.
 173. Jordan, V. C. and L. J. Dowse (1976). "Tamoxifen as an anti-tumour agent: effect on oestrogen binding." J Endocrinol **68**(02): 297-303.
 174. Junttila, T. T., R. W. Akita, K. Parsons, C. Fields, G. D. Lewis Phillips, L. S. Friedman, D. Sampath and M. X. Sliwkowski (2009). "Ligand-independent HER2/HER3/PI3K complex

is disrupted by trastuzumab and is effectively inhibited by the PI3K inhibitor GDC-0941."

Cancer Cell **15**(5): 429-440.

175. Justus, C. R., N. Leffler, M. Ruiz-Echevarria and L. V. Yang (2014). "In vitro cell migration and invasion assays." J Vis Exp(88).
176. Kang, R., H. J. Zeh, M. T. Lotze and D. Tang (2011). "The Beclin 1 network regulates autophagy and apoptosis." Cell Death Differ **18**(4): 571-580.
177. Kao, J., K. Salari, M. Bocanegra, Y. L. Choi, L. Girard, J. Gandhi, K. A. Kwei, T. Hernandez-Boussard, P. Wang, A. F. Gazdar, J. D. Minna and J. R. Pollack (2009). "Molecular profiling of breast cancer cell lines defines relevant tumor models and provides a resource for cancer gene discovery." PLoS One **4**(7): e6146.
178. Karakas, C., A. Biernacka, T. Bui, A. Sahin, M. Yi, S. Akli, J. Schafer, A. Alexander, O. Adjapong, K. K. Hunt and K. Keyomarsi (2016). "Cytoplasmic Cyclin E and Phospho-Cyclin-Dependent Kinase 2 Are Biomarkers of Aggressive Breast Cancer." Am J Pathol.
179. Karakas, C., A. Biernacka, T. Bui, A. A. Sahin, M. Yi, S. Akli, J. Schafer, A. Alexander, O. Adjapong, K. K. Hunt and K. Keyomarsi (2016). "Cytoplasmic Cyclin E and Phospho-Cyclin-Dependent Kinase 2 Are Biomarkers of Aggressive Breast Cancer." Am J Pathol **186**(7): 1900-1912.
180. Karantza-Wadsworth, V. and E. White (2007). "Role of autophagy in breast cancer." Autophagy **3**(6): 610-613.
181. Katiyar, S., M. C. Casimiro, L. Dettin, X. Ju, E. F. Wagner, H. Tanaka and R. G. Pestell (2010). "C-jun inhibits mammary apoptosis in vivo." Mol Biol Cell **21**(23): 4264-4274.
182. Kaufman, B., J. R. Mackey, M. R. Clemens, P. P. Bapsy, A. Vaid, A. Wardley, S. Tjulandin, M. Jahn, M. Lehle, A. Feyereislova, C. Revil and A. Jones (2009). "Trastuzumab plus anastrozole versus anastrozole alone for the treatment of postmenopausal women with human epidermal growth factor receptor 2-positive, hormone receptor-positive metastatic

- breast cancer: results from the randomized phase III TAnDEM study." J Clin Oncol **27**(33): 5529-5537.
183. Kelley, M. R., D. Logsdon and M. L. Fishel (2014). "Targeting DNA repair pathways for cancer treatment: what's new?" Future Oncol **10**(7): 1215-1237.
 184. Keyomarsi, K., D. Conte, Jr., W. Toyofuku and M. P. Fox (1995). "Deregulation of cyclin E in breast cancer." Oncogene **11**(5): 941-950.
 185. Keyomarsi, K. and A. B. Pardee (1993). "Redundant cyclin overexpression and gene amplification in breast cancer cells." Proc Natl Acad Sci U S A **90**(3): 1112-1116.
 186. Keyomarsi, K., S. L. Tucker, T. A. Buchholz, M. Callister, Y. Ding, G. N. Hortobagyi, I. Bedrosian, C. Knickerbocker, W. Toyofuku, M. Lowe, T. W. Herliczek and S. S. Bacus (2002). "Cyclin E and survival in patients with breast cancer." N Engl J Med **347**(20): 1566-1575.
 187. Kimura, S., T. Noda and T. Yoshimori (2007). "Dissection of the autophagosome maturation process by a novel reporter protein, tandem fluorescent-tagged LC3." Autophagy **3**(5): 452-460.
 188. Knudsen, E. S. and A. K. Witkiewicz (2016). "Defining the transcriptional and biological response to CDK4/6 inhibition in relation to ER+/HER2- breast cancer." Oncotarget **7**(43): 69111-69123.
 189. Konecny, G. E., B. Winterhoff, T. Kolarova, J. Qi, K. Manivong, J. Dering, G. Yang, M. Chalukya, H. J. Wang, L. Anderson, K. R. Kalli, R. S. Finn, C. Ginther, S. Jones, V. E. Velculescu, D. Riehle, W. A. Cliby, S. Randolph, M. Koehler, L. C. Hartmann and D. J. Slamon (2011). "Expression of p16 and retinoblastoma determines response to CDK4/6 inhibition in ovarian cancer." Clin Cancer Res **17**(6): 1591-1602.
 190. Kongara, S. and V. Karantza (2012). "The interplay between autophagy and ROS in tumorigenesis." Front Oncol **2**: 171.

191. Korkaya, H., G. I. Kim, A. Davis, F. Malik, N. L. Henry, S. Ithimakin, A. A. Quraishi, N. Tawakkol, R. D'Angelo, A. K. Paulson, S. Chung, T. Luther, H. J. Paholak, S. Liu, K. A. Hassan, Q. Zen, S. G. Clouthier and M. S. Wicha (2012). "Activation of an IL6 inflammatory loop mediates trastuzumab resistance in HER2+ breast cancer by expanding the cancer stem cell population." Mol Cell **47**(4): 570-584.
192. Koutsami, M. K., P. K. Tsantoulis, M. Kouloukoussa, K. Apostolopoulou, I. S. Pateras, Z. Spartinou, A. Drougou, K. Evangelou, C. Kittas, J. Bartkova, J. Bartek and V. G. Gorgoulis (2006). "Centrosome abnormalities are frequently observed in non-small-cell lung cancer and are associated with aneuploidy and cyclin E overexpression." J Pathol **209**(4): 512-521.
193. Kuilman, T., C. Michaloglou, W. J. Mooi and D. S. Peeper (2010). "The essence of senescence." Genes Dev **24**(22): 2463-2479.
194. Kwee, J. K., D. G. Luque, A. C. Ferreira, F. C. Vasconcelos, K. L. Silva, C. E. Klumb and R. C. Maia (2008). "Modulation of reactive oxygen species by antioxidants in chronic myeloid leukemia cells enhances imatinib sensitivity through survivin downregulation." Anticancer Drugs **19**(10): 975-981.
195. Lamb, C. A., T. Yoshimori and S. A. Tooze (2013). "The autophagosome: origins unknown, biogenesis complex." Nat Rev Mol Cell Biol **14**(12): 759-774.
196. Langelier, M. F., J. L. Planck, S. Roy and J. M. Pascal (2011). "Crystal structures of poly(ADP-ribose) polymerase-1 (PARP-1) zinc fingers bound to DNA: structural and functional insights into DNA-dependent PARP-1 activity." J Biol Chem **286**(12): 10690-10701.
197. Lee, A. V., X. Cui and S. Oesterreich (2001). "Cross-talk among estrogen receptor, epidermal growth factor, and insulin-like growth factor signaling in breast cancer." Clin Cancer Res **7**(12 Suppl): 4429s-4435s; discussion 4411s-4412s.

198. Lee, M. S., T. L. Helms, N. Feng, J. Gay, Q. E. Chang, F. Tian, J. Y. Wu, C. Toniatti, T. P. Heffernan, G. Powis, L. N. Kwong and S. Kopetz (2016). "Efficacy of the combination of MEK and CDK4/6 inhibitors in vitro and in vivo in KRAS mutant colorectal cancer models." Oncotarget **7**(26): 39595-39608.
199. Lee, M. S., T. L. Helms, N. Feng, J. Gay, Q. E. Chang, F. Tian, J. Y. Wu, C. Toniatti, T. P. Heffernan, G. Powis, L. N. Kwong and S. Kopetz (2016). "Efficacy of the combination of MEK and CDK4/6 inhibitors in vitro and in vivo in KRAS mutant colorectal cancer models." Oncotarget.
200. Lees, A. W., C. Giuffre, P. E. Burns, M. E. Hurlburt and H. J. Jenkins (1980). "Oophorectomy versus radiation ablation of ovarian function in patients with metastatic carcinoma of the breast." Surg Gynecol Obstet **151**(6): 721-724.
201. Lefort, S., C. Joffre, Y. Kieffer, A. M. Givel, B. Bourachot, G. Zago, I. Bieche, T. Dubois, D. Meseure, A. Vincent-Salomon, J. Camonis and F. Mechta-Grigoriou (2014). "Inhibition of autophagy as a new means of improving chemotherapy efficiency in high-LC3B triple-negative breast cancers." Autophagy **10**(12): 2122-2142.
202. Lehmann, B. D., J. A. Bauer, X. Chen, M. E. Sanders, A. B. Chakravarthy, Y. Shyr and J. A. Pietenpol (2011). "Identification of human triple-negative breast cancer subtypes and preclinical models for selection of targeted therapies." J Clin Invest **121**(7): 2750-2767.
203. Lehn, S., M. Ferno, K. Jirstrom, L. Ryden and G. Landberg (2011). "A non-functional retinoblastoma tumor suppressor (RB) pathway in premenopausal breast cancer is associated with resistance to tamoxifen." Cell Cycle **10**(6): 956-962.
204. Leonard, J. P., A. S. LaCasce, M. R. Smith, A. Noy, L. R. Chirieac, S. J. Rodig, J. Q. Yu, S. Vallabhajosula, H. Schoder, P. English, D. S. Neuberg, P. Martin, M. M. Millenson, S. A. Ely, R. Courtney, N. Shaik, K. D. Wilner, S. Randolph, A. D. Van den Abbeele, S. Y. Chen-Kiang, J. T. Yap and G. I. Shapiro (2012). "Selective CDK4/6 inhibition with tumor

- responses by PD0332991 in patients with mantle cell lymphoma." Blood **119**(20): 4597-4607.
205. Leontieva, O. V. and M. V. Blagosklonny (2013). "CDK4/6-inhibiting drug substitutes for p21 and p16 in senescence: duration of cell cycle arrest and MTOR activity determine geroconversion." Cell Cycle **12**(18): 3063-3069.
 206. Levine, M. N., K. I. Pritchard, V. H. Bramwell, L. E. Shepherd, D. Tu, N. Paul and G. National Cancer Institute of Canada Clinical Trials (2005). "Randomized trial comparing cyclophosphamide, epirubicin, and fluorouracil with cyclophosphamide, methotrexate, and fluorouracil in premenopausal women with node-positive breast cancer: update of National Cancer Institute of Canada Clinical Trials Group Trial MA5." J Clin Oncol **23**(22): 5166-5170.
 207. Lewis Phillips, G. D., G. Li, D. L. Dugger, L. M. Crocker, K. L. Parsons, E. Mai, W. A. Blattler, J. M. Lambert, R. V. Chari, R. J. Lutz, W. L. Wong, F. S. Jacobson, H. Koeppen, R. H. Schwall, S. R. Kenkare-Mitra, S. D. Spencer and M. X. Sliwkowski (2008). "Targeting HER2-positive breast cancer with trastuzumab-DM1, an antibody-cytotoxic drug conjugate." Cancer Res **68**(22): 9280-9290.
 208. Li, H., X. Jin, Z. Zhang, Y. Xing and X. Kong (2013). "Inhibition of autophagy enhances apoptosis induced by the PI3K/AKT/mTor inhibitor NVP-BEZ235 in renal cell carcinoma cells." Cell Biochem Funct **31**(5): 427-433.
 209. Li, J., N. Hou, A. Faried, S. Tsutsumi and H. Kuwano (2010). "Inhibition of autophagy augments 5-fluorouracil chemotherapy in human colon cancer in vitro and in vivo model." Eur J Cancer **46**(10): 1900-1909.
 210. Li, X., M. T. Lewis, J. Huang, C. Gutierrez, C. K. Osborne, M. F. Wu, S. G. Hilsenbeck, A. Pavlick, X. Zhang, G. C. Chamness, H. Wong, J. Rosen and J. C. Chang (2008). "Intrinsic resistance of tumorigenic breast cancer cells to chemotherapy." J Natl Cancer Inst **100**(9): 672-679.

211. Liang, X. H., J. Yu, K. Brown and B. Levine (2001). "Beclin 1 contains a leucine-rich nuclear export signal that is required for its autophagy and tumor suppressor function." Cancer Res **61**(8): 3443-3449.
212. Liedtke, C., C. Mazouni, K. R. Hess, F. Andre, A. Tordai, J. A. Mejia, W. F. Symmans, A. M. Gonzalez-Angulo, B. Hennessy, M. Green, M. Cristofanilli, G. N. Hortobagyi and L. Pusztai (2008). "Response to neoadjuvant therapy and long-term survival in patients with triple-negative breast cancer." J Clin Oncol **26**(8): 1275-1281.
213. Lim, E. J., J. Heo and Y. H. Kim (2015). "Tunicamycin promotes apoptosis in leukemia cells through ROS generation and downregulation of survivin expression." Apoptosis **20**(8): 1087-1098.
214. Lin, K. Y. and W. L. Kraus (2017). "PARP Inhibitors for Cancer Therapy." Cell **169**(2): 183.
215. Lin, L., B. Hutzen, H. F. Lee, Z. Peng, W. Wang, C. Zhao, H. J. Lin, D. Sun, P. K. Li, C. Li, H. Korkaya, M. S. Wicha and J. Lin (2013). "Evaluation of STAT3 signaling in ALDH+ and ALDH+/CD44+/CD24- subpopulations of breast cancer cells." PLoS One **8**(12): e82821.
216. Lindmo, K., A. Brech, K. D. Finley, S. Gaumer, D. Contamine, T. E. Rusten and H. Stenmark (2008). "The PI 3-kinase regulator Vps15 is required for autophagic clearance of protein aggregates." Autophagy **4**(4): 500-506.
217. Lindqvist, A., W. van Zon, C. Karlsson Rosenthal and R. M. Wolthuis (2007). "Cyclin B1-Cdk1 activation continues after centrosome separation to control mitotic progression." PLoS Biol **5**(5): e123.
218. Liou, G. Y. and P. Storz (2010). "Reactive oxygen species in cancer." Free Radic Res **44**(5): 479-496.
219. Liou, G. Y. and P. Storz (2015). "Detecting reactive oxygen species by immunohistochemistry." Methods Mol Biol **1292**: 97-104.

220. Liu, D., Y. Yang, Q. Liu and J. Wang (2011). "Inhibition of autophagy by 3-MA potentiates cisplatin-induced apoptosis in esophageal squamous cell carcinoma cells." Med Oncol **28**(1): 105-111.
221. Liu, T., J. Yu, M. Deng, Y. Yin, H. Zhang, K. Luo, B. Qin, Y. Li, C. Wu, T. Ren, Y. Han, P. Yin, J. Kim, S. Lee, J. Lin, L. Zhang, J. Zhang, S. Nowsheen, L. Wang, J. Boughey, M. P. Goetz, J. Yuan and Z. Lou (2017). "CDK4/6-dependent activation of DUB3 regulates cancer metastasis through SNAIL1." Nat Commun **8**: 13923.
222. Loeb, K. R. and X. Chen (2012). "Too much cleavage of cyclin E promotes breast tumorigenesis." PLoS Genet **8**(3): e1002623.
223. Long, B. J., D. Jelovac, V. Handratta, A. Thiantanawat, N. MacPherson, J. Ragaz, O. G. Goloubeva and A. M. Brodie (2004). "Therapeutic strategies using the aromatase inhibitor letrozole and tamoxifen in a breast cancer model." J Natl Cancer Inst **96**(6): 456-465.
224. Love, R. R., R. B. Mazess, H. S. Barden, S. Epstein, P. A. Newcomb, V. C. Jordan, P. P. Carbone and D. L. DeMets (1992). "Effects of tamoxifen on bone mineral density in postmenopausal women with breast cancer." N Engl J Med **326**(13): 852-856.
225. Love, R. R., P. A. Newcomb, D. A. Wiebe, T. S. Surawicz, V. C. Jordan, P. P. Carbone and D. L. DeMets (1990). "Effects of tamoxifen therapy on lipid and lipoprotein levels in postmenopausal patients with node-negative breast cancer." J Natl Cancer Inst **82**(16): 1327-1332.
226. Love, R. R., D. A. Wiebe, P. A. Newcomb, L. Cameron, H. Leventhal, V. C. Jordan, J. Feyzi and D. L. DeMets (1991). "Effects of tamoxifen on cardiovascular risk factors in postmenopausal women." Ann Intern Med **115**(11): 860-864.
227. Lu, T. and T. Finkel (2008). "Free radicals and senescence." Exp Cell Res **314**(9): 1918-1922.

228. Luo, H., A. Yang, B. A. Schulte, M. J. Wargovich and G. Y. Wang (2013). "Resveratrol induces premature senescence in lung cancer cells via ROS-mediated DNA damage." PLoS One **8**(3): e60065.
229. Luo, Y., P. Zou, J. Zou, J. Wang, D. Zhou and L. Liu (2011). "Autophagy regulates ROS-induced cellular senescence via p21 in a p38 MAPKalpha dependent manner." Exp Gerontol **46**(11): 860-867.
230. Lynch-Day, M. A., K. Mao, K. Wang, M. Zhao and D. J. Klionsky (2012). "The role of autophagy in Parkinson's disease." Cold Spring Harb Perspect Med **2**(4): a009357.
231. Ma, C. X., T. Reinert, I. Chmielewska and M. J. Ellis (2015). "Mechanisms of aromatase inhibitor resistance." Nat Rev Cancer **15**(5): 261-275.
232. Mackay, A., N. Tamber, K. Fenwick, M. Iravani, A. Grigoriadis, T. Dexter, C. J. Lord, J. S. Reis-Filho and A. Ashworth (2009). "A high-resolution integrated analysis of genetic and expression profiles of breast cancer cell lines." Breast Cancer Res Treat **118**(3): 481-498.
233. Macleod, K. F. (2008). "The role of the RB tumour suppressor pathway in oxidative stress responses in the haematopoietic system." Nat Rev Cancer **8**(10): 769-781.
234. Mahalingam, D., M. Mita, J. Sarantopoulos, L. Wood, R. K. Amaravadi, L. E. Davis, A. C. Mita, T. J. Curiel, C. M. Espitia, S. T. Nawrocki, F. J. Giles and J. S. Carew (2014). "Combined autophagy and HDAC inhibition: a phase I safety, tolerability, pharmacokinetic, and pharmacodynamic analysis of hydroxychloroquine in combination with the HDAC inhibitor vorinostat in patients with advanced solid tumors." Autophagy **10**(8): 1403-1414.
235. Makhoul, I., V. S. Klimberg, S. Korourian, R. S. Henry-Tillman, E. R. Siegel, K. C. Westbrook and L. F. Hutchins (2015). "Combined neoadjuvant chemotherapy with bevacizumab improves pathologic complete response in patients with hormone receptor negative operable or locally advanced breast cancer." Am J Clin Oncol **38**(1): 74-79.
236. Malumbres, M. and M. Barbacid (2009). "Cell cycle, CDKs and cancer: a changing paradigm." Nat Rev Cancer **9**(3): 153-166.

237. Malumbres, M. and A. Carnero (2003). "Cell cycle deregulation: a common motif in cancer." Prog Cell Cycle Res **5**: 5-18.
238. Mani, S. A., W. Guo, M. J. Liao, E. N. Eaton, A. Ayyanan, A. Y. Zhou, M. Brooks, F. Reinhard, C. C. Zhang, M. Shipitsin, L. L. Campbell, K. Polyak, C. Brisken, J. Yang and R. A. Weinberg (2008). "The epithelial-mesenchymal transition generates cells with properties of stem cells." Cell **133**(4): 704-715.
239. Marcucci, F., C. Rumio and F. Lefoulon (2016). "Anti-Cancer Stem-like Cell Compounds in Clinical Development - An Overview and Critical Appraisal." Front Oncol **6**: 115.
240. Marotta, L. L., V. Almendro, A. Marusyk, M. Shipitsin, J. Schemme, S. R. Walker, N. Bloushtain-Qimron, J. J. Kim, S. A. Choudhury, R. Maruyama, Z. Wu, M. Gonen, L. A. Mulvey, M. O. Bessarabova, S. J. Huh, S. J. Silver, S. Y. Kim, S. Y. Park, H. E. Lee, K. S. Anderson, A. L. Richardson, T. Nikolskaya, Y. Nikolsky, X. S. Liu, D. E. Root, W. C. Hahn, D. A. Frank and K. Polyak (2011). "The JAK2/STAT3 signaling pathway is required for growth of CD44(+)CD24(-) stem cell-like breast cancer cells in human tumors." J Clin Invest **121**(7): 2723-2735.
241. Marzec, M., M. Kasprzycka, R. Lai, A. B. Gladden, P. Wlodarski, E. Tomczak, P. Nowell, S. E. Deprimo, S. Sadis, S. Eck, S. J. Schuster, J. A. Diehl and M. A. Wasik (2006). "Mantle cell lymphoma cells express predominantly cyclin D1a isoform and are highly sensitive to selective inhibition of CDK4 kinase activity." Blood **108**(5): 1744-1750.
242. Massarweh, S., C. K. Osborne, C. J. Creighton, L. Qin, A. Tsimelzon, S. Huang, H. Weiss, M. Rimawi and R. Schiff (2008). "Tamoxifen resistance in breast tumors is driven by growth factor receptor signaling with repression of classic estrogen receptor genomic function." Cancer Res **68**(3): 826-833.
243. Mathew, R., V. Karantza-Wadsworth and E. White (2007). "Role of autophagy in cancer." Nat Rev Cancer **7**(12): 961-967.

244. Mathew, R., C. M. Karp, B. Beaudoin, N. Vuong, G. Chen, H. Y. Chen, K. Bray, A. Reddy, G. Bhanot, C. Gelinas, R. S. Dipaola, V. Karantza-Wadsworth and E. White (2009). "Autophagy suppresses tumorigenesis through elimination of p62." Cell **137**(6): 1062-1075.
245. Maura N. Dickler, S. M. T., Hope S. Rugo, Javier Cortes, Véronique Diéras, Debra A. Patt, Hans Wildiers, Martin Frenzel, Andrew Koustenis, Jose Baselga (2017). "MONARCH1: Results from a phase II study of abemaciclib, a CDK4 and CDK6 inhibitor, as monotherapy, in patients with HR+/HER2- breast cancer, after chemotherapy for advanced disease." J Clin Oncol suppl; abstr 510.
246. McAfee, Q., Z. Zhang, A. Samanta, S. M. Levi, X. H. Ma, S. Piao, J. P. Lynch, T. Uehara, A. R. Sepulveda, L. E. Davis, J. D. Winkler and R. K. Amaravadi (2012). "Autophagy inhibitor Lys05 has single-agent antitumor activity and reproduces the phenotype of a genetic autophagy deficiency." Proc Natl Acad Sci U S A **109**(21): 8253-8258.
247. McAuliffe, P. F., K. W. Evans, A. Akcakanat, K. Chen, X. Zheng, H. Zhao, A. K. Eterovic, T. Sangai, A. M. Holder, C. Sharma, H. Chen, K. A. Do, E. Tarco, M. Gagea, K. A. Naff, A. Sahin, A. S. Multani, D. M. Black, E. A. Mittendorf, I. Bedrosian, G. B. Mills, A. M. Gonzalez-Angulo and F. Meric-Bernstam (2015). "Ability to Generate Patient-Derived Breast Cancer Xenografts Is Enhanced in Chemoresistant Disease and Predicts Poor Patient Outcomes." PLoS One **10**(9): e0136851.
248. Meijer, L., A. Borgne, O. Mulner, J. P. Chong, J. J. Blow, N. Inagaki, M. Inagaki, J. G. Delcros and J. P. Moulinoux (1997). "Biochemical and cellular effects of roscovitine, a potent and selective inhibitor of the cyclin-dependent kinases cdc2, cdk2 and cdk5." Eur J Biochem **243**(1-2): 527-536.
249. Merlo, A., J. G. Herman, L. Mao, D. J. Lee, E. Gabrielson, P. C. Burger, S. B. Baylin and D. Sidransky (1995). "5' CpG island methylation is associated with transcriptional

- silencing of the tumour suppressor p16/CDKN2/MTS1 in human cancers." Nat Med **1**(7): 686-692.
250. Michaud, K., D. A. Solomon, E. Oermann, J. S. Kim, W. Z. Zhong, M. D. Prados, T. Ozawa, C. D. James and T. Waldman (2010). "Pharmacologic inhibition of cyclin-dependent kinases 4 and 6 arrests the growth of glioblastoma multiforme intracranial xenografts." Cancer Res **70**(8): 3228-3238.
251. Miles, D. W., A. Chan, L. Y. Dirix, J. Cortes, X. Pivot, P. Tomczak, T. Delozier, J. H. Sohn, L. Provencher, F. Puglisi, N. Harbeck, G. G. Steger, A. Schneeweiss, A. M. Wardley, A. Chlistalla and G. Romieu (2010). "Phase III study of bevacizumab plus docetaxel compared with placebo plus docetaxel for the first-line treatment of human epidermal growth factor receptor 2-negative metastatic breast cancer." J Clin Oncol **28**(20): 3239-3247.
252. Milne, A. N., R. Carvalho, M. Jansen, E. K. Kranenbarg, C. J. van de Velde, F. M. Morsink, A. R. Musler, M. A. Weterman and G. J. Offerhaus (2008). "Cyclin E low molecular weight isoforms occur commonly in early-onset gastric cancer and independently predict survival." J Clin Pathol **61**(3): 311-316.
253. Mita, M. M., A. A. Joy, A. Mita, K. Sankhala, Y. M. Jou, D. Zhang, P. Statkevich, Y. Zhu, S. L. Yao, K. Small, R. Bannerji and C. L. Shapiro (2014). "Randomized phase II trial of the cyclin-dependent kinase inhibitor dinaciclib (MK-7965) versus capecitabine in patients with advanced breast cancer." Clin Breast Cancer **14**(3): 169-176.
254. Mitri, Z., C. Karakas, C. Wei, B. Briones, H. Simmons, N. Ibrahim, R. Alvarez, J. L. Murray, K. Keyomarsi and S. Moulder (2015). "A phase 1 study with dose expansion of the CDK inhibitor dinaciclib (SCH 727965) in combination with epirubicin in patients with metastatic triple negative breast cancer." Invest New Drugs **33**(4): 890-894.
255. Mizushima, N. (2007). "Autophagy: process and function." Genes Dev **21**(22): 2861-2873.

256. Moghadam, S. J., A. M. Hanks and K. Keyomarsi (2011). "Breaking the cycle: An insight into the role of ERalpha in eukaryotic cell cycles." J Carcinog **10**: 25.
257. Mombelli, S., S. Cochaud, Y. Merrouche, C. Garbar, F. Antonicelli, E. Laprevotte, G. Alberici, N. Bonnefoy, J. F. Eliaou, J. Bastid, A. Bensussan and J. Giustiniani (2015). "IL-17A and its homologs IL-25/IL-17E recruit the c-RAF/S6 kinase pathway and the generation of pro-oncogenic LMW-E in breast cancer cells." Sci Rep **5**: 11874.
258. Monica Arnedos, B. C., Mohamed Amine Bayar, Stefan Michiels, Veronique Scott, Julien Adam, Valerie Leroux-Kozal, Virginie Marty, Chafika Mazouni, Benjamin Sarfati, Ivan Bieche, David Gentien, Suzette Delaloge, Magali Lacroix-Triki and Fabrice Andre (2016). "Abstract CT041: Anti-proliferative response and predictive biomarkers to palbociclib in early breast cancer: The Preoperative Palbociclib (POP) randomized trial." Cancer Res **76(14 Suppl):Abstract nr CT041**.
259. Montazeri, H., S. Bouzari, K. Azadmanesh, S. N. Ostad and M. H. Ghahremani (2015). "Divergent behavior of cyclin E and its low molecular weight isoforms to progesterone-induced growth inhibition in MCF-7 cells." Adv Biomed Res **4**: 16.
260. Moore, J. D. (2013). "In the wrong place at the wrong time: does cyclin mislocalization drive oncogenic transformation?" Nature reviews. Cancer **13(3)**: 201-208.
261. Mouridsen, H., M. Gershanovich, Y. Sun, R. Perez-Carrion, C. Boni, A. Monnier, J. Apffelstaedt, R. Smith, H. P. Sleeboom, F. Janicke, A. Pluzanska, M. Dank, D. Becquart, P. P. Bapsy, E. Salminen, R. Snyder, M. Lassus, J. A. Verbeek, B. Staffler, H. A. Chaudri-Ross and M. Dugan (2001). "Superior efficacy of letrozole versus tamoxifen as first-line therapy for postmenopausal women with advanced breast cancer: results of a phase III study of the International Letrozole Breast Cancer Group." J Clin Oncol **19(10)**: 2596-2606.
262. Moynahan, M. E., J. W. Chiu, B. H. Koller and M. Jasin (1999). "Brca1 controls homology-directed DNA repair." Mol Cell **4(4)**: 511-518.

263. Mull, B. B., J. Cox, T. Bui and K. Keyomarsi (2009). "Post-translational modification and stability of low molecular weight cyclin E." Oncogene **28**(35): 3167-3176.
264. Nanos-Webb, A., T. Bui, C. Karakas, D. Zhang, J. P. Carey, G. B. Mills, K. K. Hunt and K. Keyomarsi (2016). "PKC α promotes ovarian tumor progression through deregulation of cyclin E." Oncogene **35**(19): 2428-2440.
265. Nauman, A., O. Turowska, P. Poplawski, A. Master, Z. Tanski and M. Puzianowska-Kuznicka (2007). "Elevated cyclin E level in human clear cell renal cell carcinoma: possible causes and consequences." Acta Biochim Pol **54**(3): 595-602.
266. Nemazanyy, I., B. Blaauw, C. Paolini, C. Caillaud, F. Protasi, A. Mueller, T. Proikas-Cezanne, R. C. Russell, K. L. Guan, I. Nishino, M. Sandri, M. Pende and G. Panasyuk (2013). "Defects of Vps15 in skeletal muscles lead to autophagic vacuolar myopathy and lysosomal disease." EMBO Mol Med **5**(6): 870-890.
267. Nicholson, R. I., J. M. Gee, D. L. Manning, A. E. Wakeling, M. M. Montano and B. S. Katzenellenbogen (1995). "Responses to pure antiestrogens (ICI 164384, ICI 182780) in estrogen-sensitive and -resistant experimental and clinical breast cancer." Ann N Y Acad Sci **761**: 148-163.
268. O'Leary, B., R. S. Finn and N. C. Turner (2016). "Treating cancer with selective CDK4/6 inhibitors." Nat Rev Clin Oncol **13**(7): 417-430.
269. Ojha, R., S. Bhattacharyya and S. K. Singh (2015). "Autophagy in Cancer Stem Cells: A Potential Link Between Chemoresistance, Recurrence, and Metastasis." Biores Open Access **4**(1): 97-108.
270. Oliveras-Ferraros, C., A. Vazquez-Martin, B. Martin-Castillo, M. C. Perez-Martinez, S. Cufi, S. Del Barco, L. Bernado, J. Brunet, E. Lopez-Bonet and J. A. Menendez (2010). "Pathway-focused proteomic signatures in HER2-overexpressing breast cancer with a basal-like phenotype: new insights into de novo resistance to trastuzumab (Herceptin)." Int J Oncol **37**(3): 669-678.

271. Onitilo, A. A., J. M. Engel, R. T. Greenlee and B. N. Mukesh (2009). "Breast cancer subtypes based on ER/PR and Her2 expression: comparison of clinicopathologic features and survival." Clin Med Res **7**(1-2): 4-13.
272. Otto, T. and P. Sicinski (2017). "Cell cycle proteins as promising targets in cancer therapy." Nat Rev Cancer **17**(2): 93-115.
273. Owens, M. A., B. C. Horten and M. M. Da Silva (2004). "HER2 amplification ratios by fluorescence in situ hybridization and correlation with immunohistochemistry in a cohort of 6556 breast cancer tissues." Clin Breast Cancer **5**(1): 63-69.
274. Papa, L., G. Manfredi and D. Germain (2014). "SOD1, an unexpected novel target for cancer therapy." Genes Cancer **5**(1-2): 15-21.
275. Paplomata, E. and R. O'Regan (2014). "The PI3K/AKT/mTOR pathway in breast cancer: targets, trials and biomarkers." Ther Adv Med Oncol **6**(4): 154-166.
276. Park, H., C. H. Kim, J. H. Jeong, M. Park and K. S. Kim (2016). "GDF15 contributes to radiation-induced senescence through the ROS-mediated p16 pathway in human endothelial cells." Oncotarget **7**(9): 9634-9644.
277. Park, H. J., J. R. Carr, Z. Wang, V. Nogueira, N. Hay, A. L. Tyner, L. F. Lau, R. H. Costa and P. Raychaudhuri (2009). "FoxM1, a critical regulator of oxidative stress during oncogenesis." EMBO J **28**(19): 2908-2918.
278. Parry, D., T. Guzi, F. Shanahan, N. Davis, D. Prabhavalkar, D. Wiswell, W. Seghezzi, K. Paruch, M. P. Dwyer, R. Doll, A. Nomeir, W. Windsor, T. Fischmann, Y. Wang, M. Oft, T. Chen, P. Kirschmeier and E. M. Lees (2010). "Dinaciclib (SCH 727965), a novel and potent cyclin-dependent kinase inhibitor." Mol Cancer Ther **9**(8): 2344-2353.
279. Paternot, S. and P. P. Roger (2009). "Combined inhibition of MEK and mammalian target of rapamycin abolishes phosphorylation of cyclin-dependent kinase 4 in glioblastoma cell lines and prevents their proliferation." Cancer Res **69**(11): 4577-4581.

280. Patnaik, A., L. S. Rosen, S. M. Tolaney, A. W. Tolcher, J. W. Goldman, L. Gandhi, K. P. Papadopoulos, M. Beeram, D. W. Rasco, J. F. Hilton, A. Nasir, R. P. Beckmann, A. E. Schade, A. D. Fulford, T. S. Nguyen, R. Martinez, P. Kulanthaivel, L. Q. Li, M. Frenzel, D. M. Cronier, E. M. Chan, K. T. Flaherty, P. Y. Wen and G. I. Shapiro (2016). "Efficacy and Safety of Abemaciclib, an Inhibitor of CDK4 and CDK6, for Patients with Breast Cancer, Non-Small Cell Lung Cancer, and Other Solid Tumors." Cancer Discov **6**(7): 740-753.
281. Pattingre, S., A. Tassa, X. Qu, R. Garuti, X. H. Liang, N. Mizushima, M. Packer, M. D. Schneider and B. Levine (2005). "Bcl-2 antiapoptotic proteins inhibit Beclin 1-dependent autophagy." Cell **122**(6): 927-939.
282. Perou, C. M., T. Sorlie, M. B. Eisen, M. van de Rijn, S. S. Jeffrey, C. A. Rees, J. R. Pollack, D. T. Ross, H. Johnsen, L. A. Akslen, O. Fluge, A. Pergamenschikov, C. Williams, S. X. Zhu, P. E. Lonning, A. L. Borresen-Dale, P. O. Brown and D. Botstein (2000). "Molecular portraits of human breast tumours." Nature **406**(6797): 747-752.
283. Pfizer-Inc-and-Affiliates (2011). "PD-0332991, Investigator's Brochure." pp22-28.
284. Phillips, G. D., C. T. Fields, G. Li, D. Dowbenko, G. Schaefer, K. Miller, F. Andre, H. A. Burris, 3rd, K. S. Albain, N. Harbeck, V. Dieras, D. Crivellari, L. Fang, E. Guardino, S. R. Olsen, L. M. Crocker and M. X. Sliwkowski (2014). "Dual targeting of HER2-positive cancer with trastuzumab emtansine and pertuzumab: critical role for neuregulin blockade in antitumor response to combination therapy." Clin Cancer Res **20**(2): 456-468.
285. Phillips, T. M., W. H. McBride and F. Pajonk (2006). "The response of CD24(-/low)/CD44+ breast cancer-initiating cells to radiation." J Natl Cancer Inst **98**(24): 1777-1785.
286. Piccart, M., G. N. Hortobagyi, M. Campone, K. I. Pritchard, F. Lebrun, Y. Ito, S. Noguchi, A. Perez, H. S. Rugo, I. Deleu, H. A. Burris, 3rd, L. Provencher, P. Neven, M. Gnant, M. Shtivelband, C. Wu, J. Fan, W. Feng, T. Taran and J. Baselga (2014). "Everolimus plus exemestane for hormone-receptor-positive, human epidermal growth factor

- receptor-2-negative advanced breast cancer: overall survival results from BOLERO-2dagger." Ann Oncol **25**(12): 2357-2362.
287. Piccart-Gebhart, M., E. Holmes, J. Baselga, E. de Azambuja, A. C. Dueck, G. Viale, J. A. Zujewski, A. Goldhirsch, A. Armour, K. I. Pritchard, A. E. McCullough, S. Dolci, E. McFadden, A. P. Holmes, L. Tonghua, H. Eidtmann, P. Dinh, S. Di Cosimo, N. Harbeck, S. Tjulandin, Y. H. Im, C. S. Huang, V. Dieras, D. W. Hillman, A. C. Wolff, C. Jackisch, I. Lang, M. Untch, I. Smith, F. Boyle, B. Xu, H. Gomez, T. Suter, R. D. Gelber and E. A. Perez (2016). "Adjuvant Lapatinib and Trastuzumab for Early Human Epidermal Growth Factor Receptor 2-Positive Breast Cancer: Results From the Randomized Phase III Adjuvant Lapatinib and/or Trastuzumab Treatment Optimization Trial." J Clin Oncol **34**(10): 1034-1042.
288. Poillet-Perez, L., G. Despouy, R. Delage-Mourroux and M. Boyer-Guittaut (2015). "Interplay between ROS and autophagy in cancer cells, from tumor initiation to cancer therapy." Redox Biol **4**: 184-192.
289. Powles, T. J., A. L. Jones, S. E. Ashley, M. E. O'Brien, V. A. Tidy, J. Treleavan, D. Cosgrove, A. G. Nash, N. Sacks, M. Baum and et al. (1994). "The Royal Marsden Hospital pilot tamoxifen chemoprevention trial." Breast Cancer Res Treat **31**(1): 73-82.
290. Press, D. J. and P. Pharoah (2010). "Risk factors for breast cancer: a reanalysis of two case-control studies from 1926 and 1931." Epidemiology **21**(4): 566-572.
291. Presta, L. G., H. Chen, S. J. O'Connor, V. Chisholm, Y. G. Meng, L. Krummen, M. Winkler and N. Ferrara (1997). "Humanization of an anti-vascular endothelial growth factor monoclonal antibody for the therapy of solid tumors and other disorders." Cancer Res **57**(20): 4593-4599.
292. Proctor, A. J., L. M. Coombs, J. P. Cairns and M. A. Knowles (1991). "Amplification at chromosome 11q13 in transitional cell tumours of the bladder." Oncogene **6**(5): 789-795.

293. Qin, G., F. Xu, T. Qin, Q. Zheng, D. Shi, W. Xia, Y. Tian, Y. Tang, J. Wang, X. Xiao, W. Deng and S. Wang (2015). "Palbociclib inhibits epithelial-mesenchymal transition and metastasis in breast cancer via c-Jun/COX-2 signaling pathway." Oncotarget **6**(39): 41794-41808.
294. Rader, J., M. R. Russell, L. S. Hart, M. S. Nakazawa, L. T. Belcastro, D. Martinez, Y. Li, E. L. Carpenter, E. F. Attiyeh, S. J. Diskin, S. Kim, S. Parasuraman, G. Caponigro, R. W. Schnepf, A. C. Wood, B. Pawel, K. A. Cole and J. M. Maris (2013). "Dual CDK4/CDK6 inhibition induces cell-cycle arrest and senescence in neuroblastoma." Clin Cancer Res **19**(22): 6173-6182.
295. Ramaswamy, B., M. A. Phelps, R. Baiocchi, T. Bekaii-Saab, W. Ni, J. P. Lai, A. Wolfson, M. E. Lustberg, L. Wei, D. Wilkins, A. Campbell, D. Arbogast, A. Doyle, J. C. Byrd, M. R. Grever and M. H. Shah (2012). "A dose-finding, pharmacokinetic and pharmacodynamic study of a novel schedule of flavopiridol in patients with advanced solid tumors." Invest New Drugs **30**(2): 629-638.
296. Rangwala, R., Y. C. Chang, J. Hu, K. M. Algazy, T. L. Evans, L. A. Fecher, L. M. Schuchter, D. A. Torigian, J. T. Panosian, A. B. Troxel, K. S. Tan, D. F. Heitjan, A. M. DeMichele, D. J. Vaughn, M. Redlinger, A. Alavi, J. Kaiser, L. Pontiggia, L. E. Davis, P. J. O'Dwyer and R. K. Amaravadi (2014). "Combined MTOR and autophagy inhibition: phase I trial of hydroxychloroquine and temsirolimus in patients with advanced solid tumors and melanoma." Autophagy **10**(8): 1391-1402.
297. Rath, S. L. and S. Senapati (2014). "Why are the truncated cyclin Es more effective CDK2 activators than the full-length isoforms?" Biochemistry **53**(28): 4612-4624.
298. Raub, T. J., G. N. Wishart, P. Kulanthaivel, B. A. Staton, R. T. Ajamie, G. A. Sawada, L. M. Gelbert, H. E. Shannon, C. Sanchez-Martinez and A. De Dios (2015). "Brain Exposure of Two Selective Dual CDK4 and CDK6 Inhibitors and the Antitumor Activity of CDK4 and

- CDK6 Inhibition in Combination with Temozolomide in an Intracranial Glioblastoma Xenograft." Drug Metab Dispos **43**(9): 1360-1371.
299. Rebecca, V. W. and R. K. Amaravadi (2016). "Emerging strategies to effectively target autophagy in cancer." Oncogene **35**(1): 1-11.
 300. Rechoum, Y., D. Rovito, D. Iacopetta, I. Barone, S. Ando, N. L. Weigel, B. W. O'Malley, P. H. Brown and S. A. Fuqua (2014). "AR collaborates with ERalpha in aromatase inhibitor-resistant breast cancer." Breast Cancer Res Treat **147**(3): 473-485.
 301. Resnitzky, D., M. Gossen, H. Bujard and S. I. Reed (1994). "Acceleration of the G1/S phase transition by expression of cyclins D1 and E with an inducible system." Mol Cell Biol **14**(3): 1669-1679.
 302. Riggio, M., M. L. Polo, M. Blaustein, A. Colman-Lerner, I. Luthy, C. Lanari and V. Novaro (2012). "PI3K/AKT pathway regulates phosphorylation of steroid receptors, hormone independence and tumor differentiation in breast cancer." Carcinogenesis **33**(3): 509-518.
 303. Rivadeneira, D. B., C. N. Mayhew, C. Thangavel, E. Sotillo, C. A. Reed, X. Grana and E. S. Knudsen (2010). "Proliferative suppression by CDK4/6 inhibition: complex function of the retinoblastoma pathway in liver tissue and hepatoma cells." Gastroenterology **138**(5): 1920-1930.
 304. Robertson, J. F., I. M. Bondarenko, E. Trishkina, M. Dvorkin, L. Panasci, A. Manikhas, Y. Shparyk, S. Cardona-Huerta, K. L. Cheung, M. J. Philco-Salas, M. Ruiz-Borrego, Z. Shao, S. Noguchi, J. Rowbottom, M. Stuart, L. M. Grinsted, M. Fazal and M. J. Ellis (2016). "Fulvestrant 500 mg versus anastrozole 1 mg for hormone receptor-positive advanced breast cancer (FALCON): an international, randomised, double-blind, phase 3 trial." Lancet **388**(10063): 2997-3005.
 305. Robertson, J. F., A. Llombart-Cussac, J. Rolski, D. Feltl, J. Dewar, E. Macpherson, J. Lindemann and M. J. Ellis (2009). "Activity of fulvestrant 500 mg versus anastrozole 1 mg as

- first-line treatment for advanced breast cancer: results from the FIRST study." J Clin Oncol **27**(27): 4530-4535.
306. Robinson, T. J., J. C. Liu, F. Vizeacoumar, T. Sun, N. Maclean, S. E. Egan, A. D. Schimmer, A. Datti and E. Zacksenhaus (2013). "RB1 status in triple negative breast cancer cells dictates response to radiation treatment and selective therapeutic drugs." PLoS One **8**(11): e78641.
307. Rocca, A., S. Bravaccini, E. Scarpi, A. Mangia, S. Petroni, M. Puccetti, L. Medri, L. Serra, M. Ricci, S. Cerasoli, N. Biglia, R. Maltoni, D. C. Giunchi, L. Gianni, A. Tienghi, M. Brandi, M. Faedi, P. Sismondi, A. Paradiso, R. Silvestrini and D. Amadori (2014). "Benefit from anthracyclines in relation to biological profiles in early breast cancer." Breast Cancer Res Treat **144**(2): 307-318.
308. Rohatgi, R. A. and L. M. Shaw (2016). "An autophagy-independent function for Beclin 1 in cancer." Mol Cell Oncol **3**(1).
309. Romond, E. H., E. A. Perez, J. Bryant, V. J. Suman, C. E. Geyer, Jr., N. E. Davidson, E. Tan-Chiu, S. Martino, S. Paik, P. A. Kaufman, S. M. Swain, T. M. Pisansky, L. Fehrenbacher, L. A. Kutteh, V. G. Vogel, D. W. Visscher, G. Yothers, R. B. Jenkins, A. M. Brown, S. R. Dakhil, E. P. Mamounas, W. L. Lingle, P. M. Klein, J. N. Ingle and N. Wolmark (2005). "Trastuzumab plus adjuvant chemotherapy for operable HER2-positive breast cancer." N Engl J Med **353**(16): 1673-1684.
310. Rosenfeldt, M. T., J. O'Prey, J. P. Morton, C. Nixon, G. MacKay, A. Mrowinska, A. Au, T. S. Rai, L. Zheng, R. Ridgway, P. D. Adams, K. I. Anderson, E. Gottlieb, O. J. Sansom and K. M. Ryan (2013). "p53 status determines the role of autophagy in pancreatic tumour development." Nature **504**(7479): 296-300.
311. Rota, L. M., D. A. Lazzarino, A. N. Ziegler, D. LeRoith and T. L. Wood (2012). "Determining mammosphere-forming potential: application of the limiting dilution analysis." J Mammary Gland Biol Neoplasia **17**(2): 119-123.

312. Rottenberg, S., J. E. Jaspers, A. Kersbergen, E. van der Burg, A. O. Nygren, S. A. Zander, P. W. Derksen, M. de Bruin, J. Zevenhoven, A. Lau, R. Boulter, A. Cranston, M. J. O'Connor, N. M. Martin, P. Borst and J. Jonkers (2008). "High sensitivity of BRCA1-deficient mammary tumors to the PARP inhibitor AZD2281 alone and in combination with platinum drugs." Proc Natl Acad Sci U S A **105**(44): 17079-17084.
313. Ryan, K. J. (1959). "Biological aromatization of steroids." J Biol Chem **234**(2): 268-272.
314. Sabnis, G., A. Schayowitz, O. Goloubeva, L. Macedo and A. Brodie (2009). "Trastuzumab reverses letrozole resistance and amplifies the sensitivity of breast cancer cells to estrogen." Cancer Res **69**(4): 1416-1428.
315. Saftig, P., W. Beertsen and E. L. Eskelinen (2008). "LAMP-2: a control step for phagosome and autophagosome maturation." Autophagy **4**(4): 510-512.
316. Sansone, P., C. Ceccarelli, M. Berishaj, Q. Chang, V. K. Rajasekhar, F. Perna, R. L. Bowman, M. Vidone, L. Daly, J. Nnoli, D. Santini, M. Taffurelli, N. N. Shih, M. Feldman, J. J. Mao, C. Colameco, J. Chen, A. DeMichele, N. Fabbri, J. H. Healey, M. Cricca, G. Gasparre, D. Lyden, M. Bonafe and J. Bromberg (2016). "Self-renewal of CD133(hi) cells by IL6/Notch3 signalling regulates endocrine resistance in metastatic breast cancer." Nat Commun **7**: 10442.
317. Sasaki, K., N. H. Tsuno, E. Sunami, K. Kawai, K. Hongo, M. Hiyoshi, M. Kaneko, K. Muro, N. Tada, T. Nirei, K. Takahashi and J. Kitayama (2012). "Resistance of colon cancer to 5-fluorouracil may be overcome by combination with chloroquine, an in vivo study." Anticancer Drugs **23**(7): 675-682.
318. Satoo, K., N. N. Noda, H. Kumeta, Y. Fujioka, N. Mizushima, Y. Ohsumi and F. Inagaki (2009). "The structure of Atg4B-LC3 complex reveals the mechanism of LC3 processing and delipidation during autophagy." EMBO J **28**(9): 1341-1350.

319. Satyanarayana, A. and P. Kaldis (2009). "Mammalian cell-cycle regulation: several Cdks, numerous cyclins and diverse compensatory mechanisms." Oncogene **28**(33): 2925-2939.
320. Scaltriti, M., S. Chandarlapaty, L. Prudkin, C. Aura, J. Jimenez, P. D. Angelini, G. Sanchez, M. Guzman, J. L. Parra, C. Ellis, R. Gagnon, M. Koehler, H. Gomez, C. Geyer, D. Cameron, J. Arribas, N. Rosen and J. Baselga (2010). "Clinical benefit of lapatinib-based therapy in patients with human epidermal growth factor receptor 2-positive breast tumors coexpressing the truncated p95HER2 receptor." Clin Cancer Res **16**(9): 2688-2695.
321. Scaltriti, M., P. J. Eichhorn, J. Cortes, L. Prudkin, C. Aura, J. Jimenez, S. Chandarlapaty, V. Serra, A. Prat, Y. H. Ibrahim, M. Guzman, M. Gili, O. Rodriguez, S. Rodriguez, J. Perez, S. R. Green, S. Mai, N. Rosen, C. Hudis and J. Baselga (2011). "Cyclin E amplification/overexpression is a mechanism of trastuzumab resistance in HER2+ breast cancer patients." Proc Natl Acad Sci U S A **108**(9): 3761-3766.
322. Scaltriti, M., F. Rojo, A. Ocana, J. Anido, M. Guzman, J. Cortes, S. Di Cosimo, X. Matias-Guiu, S. Ramon y Cajal, J. Arribas and J. Baselga (2007). "Expression of p95HER2, a truncated form of the HER2 receptor, and response to anti-HER2 therapies in breast cancer." J Natl Cancer Inst **99**(8): 628-638.
323. Scaltriti, M., C. Verma, M. Guzman, J. Jimenez, J. L. Parra, K. Pedersen, D. J. Smith, S. Landolfi, S. Ramon y Cajal, J. Arribas and J. Baselga (2009). "Lapatinib, a HER2 tyrosine kinase inhibitor, induces stabilization and accumulation of HER2 and potentiates trastuzumab-dependent cell cytotoxicity." Oncogene **28**(6): 803-814.
324. Scherz-Shouval, R. and Z. Elazar (2011). "Regulation of autophagy by ROS: physiology and pathology." Trends Biochem Sci **36**(1): 30-38.
325. Scheuer, W., T. Friess, H. Burtscher, B. Bossenmaier, J. Endl and M. Hasmann (2009). "Strongly enhanced antitumor activity of trastuzumab and pertuzumab combination

- treatment on HER2-positive human xenograft tumor models." Cancer Res **69**(24): 9330-9336.
326. Schoenlein, P. V., S. Periyasamy-Thandavan, J. S. Samaddar, W. H. Jackson and J. T. Barrett (2009). "Autophagy facilitates the progression of ERalpha-positive breast cancer cells to antiestrogen resistance." Autophagy **5**(3): 400-403.
 327. Schoenmakers, E., P. Alen, G. Verrijdt, B. Peeters, G. Verhoeven, W. Rombauts and F. Claessens (1999). "Differential DNA binding by the androgen and glucocorticoid receptors involves the second Zn-finger and a C-terminal extension of the DNA-binding domains." Biochem J **341** (Pt 3): 515-521.
 328. Schuuring, E., E. Verhoeven, H. van Tinteren, J. L. Peterse, B. Nunnink, F. B. Thunnissen, P. Devilee, C. J. Cornelisse, M. J. van de Vijver, W. J. Mooi and et al. (1992). "Amplification of genes within the chromosome 11q13 region is indicative of poor prognosis in patients with operable breast cancer." Cancer Res **52**(19): 5229-5234.
 329. Senger, D. R., S. J. Galli, A. M. Dvorak, C. A. Perruzzi, V. S. Harvey and H. F. Dvorak (1983). "Tumor cells secrete a vascular permeability factor that promotes accumulation of ascites fluid." Science **219**(4587): 983-985.
 330. Serrano, M., A. W. Lin, M. E. McCurrach, D. Beach and S. W. Lowe (1997). "Oncogenic ras provokes premature cell senescence associated with accumulation of p53 and p16INK4a." Cell **88**(5): 593-602.
 331. Shao, S., S. Li, Y. Qin, X. Wang, Y. Yang, H. Bai, L. Zhou, C. Zhao and C. Wang (2014). "Spautin-1, a novel autophagy inhibitor, enhances imatinib-induced apoptosis in chronic myeloid leukemia." Int J Oncol **44**(5): 1661-1668.
 332. Sherr, C. J. (1994). "G1 phase progression: cycling on cue." Cell **79**(4): 551-555.
 333. Sherr, C. J., D. Beach and G. I. Shapiro (2016). "Targeting CDK4 and CDK6: From Discovery to Therapy." Cancer Discov **6**(4): 353-367.

334. Shi, Y. H., Z. B. Ding, J. Zhou, B. Hui, G. M. Shi, A. W. Ke, X. Y. Wang, Z. Dai, Y. F. Peng, C. Y. Gu, S. J. Qiu and J. Fan (2011). "Targeting autophagy enhances sorafenib lethality for hepatocellular carcinoma via ER stress-related apoptosis." Autophagy **7**(10): 1159-1172.
335. Shingu, T., K. Fujiwara, O. Bogler, Y. Akiyama, K. Moritake, N. Shinojima, Y. Tamada, T. Yokoyama and S. Kondo (2009). "Inhibition of autophagy at a late stage enhances imatinib-induced cytotoxicity in human malignant glioma cells." Int J Cancer **124**(5): 1060-1071.
336. Shou, J., S. Massarweh, C. K. Osborne, A. E. Wakeling, S. Ali, H. Weiss and R. Schiff (2004). "Mechanisms of tamoxifen resistance: increased estrogen receptor-HER2/neu cross-talk in ER/HER2-positive breast cancer." J Natl Cancer Inst **96**(12): 926-935.
337. Siegel, R. L., K. D. Miller and A. Jemal (2016). "Cancer statistics, 2016." CA Cancer J Clin **66**(1): 7-30.
338. Siminovitch, L., E. A. McCulloch and J. E. Till (1963). "The Distribution of Colony-Forming Cells among Spleen Colonies." J Cell Comp Physiol **62**: 327-336.
339. Sini, V., S. Cinieri, P. Conte, M. De Laurentiis, A. D. Leo, C. Tondini and P. Marchetti (2016). "Endocrine therapy in post-menopausal women with metastatic breast cancer: From literature and guidelines to clinical practice." Crit Rev Oncol Hematol **100**: 57-68.
340. Slamon, D. J., B. Leyland-Jones, S. Shak, H. Fuchs, V. Paton, A. Bajamonde, T. Fleming, W. Eiermann, J. Wolter, M. Pegram, J. Baselga and L. Norton (2001). "Use of chemotherapy plus a monoclonal antibody against HER2 for metastatic breast cancer that overexpresses HER2." N Engl J Med **344**(11): 783-792.
341. Sorlie, T., C. M. Perou, R. Tibshirani, T. Aas, S. Geisler, H. Johnsen, T. Hastie, M. B. Eisen, M. van de Rijn, S. S. Jeffrey, T. Thorsen, H. Quist, J. C. Matese, P. O. Brown, D. Botstein, P. E. Lonning and A. L. Borresen-Dale (2001). "Gene expression patterns of breast

- carcinomas distinguish tumor subclasses with clinical implications." Proc Natl Acad Sci U S A **98**(19): 10869-10874.
342. Sorlie, T., R. Tibshirani, J. Parker, T. Hastie, J. S. Marron, A. Nobel, S. Deng, H. Johnsen, R. Pesich, S. Geisler, J. Demeter, C. M. Perou, P. E. Lonning, P. O. Brown, A. L. Borresen-Dale and D. Botstein (2003). "Repeated observation of breast tumor subtypes in independent gene expression data sets." Proc Natl Acad Sci U S A **100**(14): 8418-8423.
343. Sotiriou, C., S. Y. Neo, L. M. McShane, E. L. Korn, P. M. Long, A. Jazaeri, P. Martiat, S. B. Fox, A. L. Harris and E. T. Liu (2003). "Breast cancer classification and prognosis based on gene expression profiles from a population-based study." Proc Natl Acad Sci U S A **100**(18): 10393-10398.
344. Soudon, J. (2000). "Comparison of in vitro exemestane activity versus other antiaromatase agents." Clin Breast Cancer **1 Suppl 1**: S68-73.
345. Stagg, J. and B. Allard (2013). "Immunotherapeutic approaches in triple-negative breast cancer: latest research and clinical prospects." Ther Adv Med Oncol **5**(3): 169-181.
346. Subramanian, A., P. Tamayo, V. K. Mootha, S. Mukherjee, B. L. Ebert, M. A. Gillette, A. Paulovich, S. L. Pomeroy, T. R. Golub, E. S. Lander and J. P. Mesirov (2005). "Gene set enrichment analysis: a knowledge-based approach for interpreting genome-wide expression profiles." Proc Natl Acad Sci U S A **102**(43): 15545-15550.
347. Sui, X., R. Chen, Z. Wang, Z. Huang, N. Kong, M. Zhang, W. Han, F. Lou, J. Yang, Q. Zhang, X. Wang, C. He and H. Pan (2013). "Autophagy and chemotherapy resistance: a promising therapeutic target for cancer treatment." Cell Death Dis **4**: e838.
348. Sumi, N. J., B. M. Kuenzi, C. E. Knezevic, L. L. Remsing Rix and U. Rix (2015). "Chemoproteomics Reveals Novel Protein and Lipid Kinase Targets of Clinical CDK4/6 Inhibitors in Lung Cancer." ACS Chem Biol.
349. Sun, S. Y. (2010). "N-acetylcysteine, reactive oxygen species and beyond." Cancer Biol Ther **9**(2): 109-110.

350. Sun, W. L., J. Chen, Y. P. Wang and H. Zheng (2011). "Autophagy protects breast cancer cells from epirubicin-induced apoptosis and facilitates epirubicin-resistance development." Autophagy **7**(9): 1035-1044.
351. Sylvia Adams, J. R. D., Erika Paige Hamilton, Paula Raffin Pohlmann, Sara M. Tolaney, Luciana Molinero, Xian He, Daniel Waterkamp, Roel Peter Funke, John D. Powderly (2016). "Phase Ib trial of atezolizumab in combination with nab-paclitaxel in patients with metastatic triple-negative breast cancer." J Clin Oncol
suppl; abstr 1009(34).
352. Takamura, A., M. Komatsu, T. Hara, A. Sakamoto, C. Kishi, S. Waguri, Y. Eishi, O. Hino, K. Tanaka and N. Mizushima (2011). "Autophagy-deficient mice develop multiple liver tumors." Genes Dev **25**(8): 795-800.
353. Tan, A. R., X. Yang, A. Berman, S. Zhai, A. Sparreboom, A. L. Parr, C. Chow, J. S. Brahimi, S. M. Steinberg, W. D. Figg and S. M. Swain (2004). "Phase I trial of the cyclin-dependent kinase inhibitor flavopiridol in combination with docetaxel in patients with metastatic breast cancer." Clin Cancer Res **10**(15): 5038-5047.
354. Tanei, T., K. Morimoto, K. Shimazu, S. J. Kim, Y. Tanji, T. Taguchi, Y. Tamaki and S. Noguchi (2009). "Association of breast cancer stem cells identified by aldehyde dehydrogenase 1 expression with resistance to sequential Paclitaxel and epirubicin-based chemotherapy for breast cancers." Clin Cancer Res **15**(12): 4234-4241.
355. Taneja, P., D. Maglic, F. Kai, S. Zhu, R. D. Kendig, E. A. Fry and K. Inoue (2010). "Classical and Novel Prognostic Markers for Breast Cancer and their Clinical Significance." Clin Med Insights Oncol **4**: 15-34.
356. Tao, Z., J. M. Le Blanc, C. Wang, T. Zhan, H. Zhuang, P. Wang, Z. Yuan and B. Lu (2016). "Coadministration of Trametinib and Palbociclib Radiosensitizes KRAS-Mutant Non-Small Cell Lung Cancers In Vitro and In Vivo." Clin Cancer Res **22**(1): 122-133.
- 357.

358. Tate, S. C., T. F. Burke, D. Hartman, P. Kulanthaivel, R. P. Beckmann and D. M. Cronier (2016). "Optimising the combination dosing strategy of abemaciclib and vemurafenib in BRAF-mutated melanoma xenograft tumours." Br J Cancer **114**(6): 669-679.
359. Taylor-Harding, B., P. J. Aspuria, H. Agadjanian, D. J. Cheon, T. Mizuno, D. Greenberg, J. R. Allen, L. Spurka, V. Funari, E. Spiteri, Q. Wang, S. Orsulic, C. Walsh, B. Y. Karlan and W. R. Wiedemeyer (2015). "Cyclin E1 and RTK/RAS signaling drive CDK inhibitor resistance via activation of E2F and ETS." Oncotarget **6**(2): 696-714.
360. Thompson, E. A., Jr. and P. K. Siiteri (1974). "The involvement of human placental microsomal cytochrome P-450 in aromatization." J Biol Chem **249**(17): 5373-5378.
361. Tokai, Y., S. Maeda, J. Yamaguchi, T. Uga, N. Hayashida, K. Taniguchi, S. Eguchi and T. Kanematsu (2011). "Cyclin E low-molecular-weight isoform as a predictor of breast cancer in Japanese women." Int Surg **96**(3): 245-253.
362. Toogood, P. L., P. J. Harvey, J. T. Repine, D. J. Sheehan, S. N. VanderWel, H. Zhou, P. R. Keller, D. J. McNamara, D. Sherry, T. Zhu, J. Brodfuehrer, C. Choi, M. R. Barvian and D. W. Fry (2005). "Discovery of a potent and selective inhibitor of cyclin-dependent kinase 4/6." J Med Chem **48**(7): 2388-2406.
363. Touil, Y., W. Igoudjil, M. Corvaisier, A. F. Dessein, J. Vandomme, D. Monte, L. Stechly, N. Skrypek, C. Langlois, G. Grard, G. Millet, E. Leteurtre, P. Dumont, S. Truant, F. R. Pruvot, M. Hebbar, F. Fan, L. M. Ellis, P. Formstecher, I. Van Seuning, C. Gespach, R. Polakowska and G. Huet (2014). "Colon cancer cells escape 5FU chemotherapy-induced cell death by entering stemness and quiescence associated with the c-Yes/YAP axis." Clin Cancer Res **20**(4): 837-846.
364. Toy, W., Y. Shen, H. Won, B. Green, R. A. Sakr, M. Will, Z. Li, K. Gala, S. Fanning, T. A. King, C. Hudis, D. Chen, T. Taran, G. Hortobagyi, G. Greene, M. Berger, J. Baselga and S. Chandralapaty (2013). "ESR1 ligand-binding domain mutations in hormone-resistant breast cancer." Nat Genet **45**(12): 1439-1445.

365. Tracy, K., B. C. Dibling, B. T. Spike, J. R. Knabb, P. Schumacker and K. F. Macleod (2007). "BNIP3 is an RB/E2F target gene required for hypoxia-induced autophagy." Mol Cell Biol **27**(17): 6229-6242.
366. Trichopoulos, D., B. MacMahon and P. Cole (1972). "Menopause and breast cancer risk." J Natl Cancer Inst **48**(3): 605-613.
367. Turner, N. C., Y. Jiang, B. O'Leary, S. Hrebien, M. Cristofanilli, F. Andre, S. Loibl, P. A. English, K. Zhang, S. Randolph, C. H. Bartlett, M. Koehler and S. Loi (2016). "Efficacy of palbociclib plus fulvestrant (P+F) in patients (pts) with metastatic breast cancer (MBC) and ESR1 mutations (mus) in circulating tumor DNA (ctDNA)." J Clin Oncol **34**: suppl; abstr 512.
368. Turner, N. C., J. Ro, F. Andre, S. Loi, S. Verma, H. Iwata, N. Harbeck, S. Loibl, C. Huang Bartlett, K. Zhang, C. Giorgetti, S. Randolph, M. Koehler and M. Cristofanilli (2015). "Palbociclib in Hormone-Receptor-Positive Advanced Breast Cancer." N Engl J Med **373**(3): 209-219.
369. Turner, N. C., J. Ro, F. Andre, S. Loi, S. Verma, H. Iwata, N. Harbeck, S. Loibl, C. Huang Bartlett, K. Zhang, C. Giorgetti, S. Randolph, M. Koehler, M. Cristofanilli and P. S. Group (2015). "Palbociclib in Hormone-Receptor-Positive Advanced Breast Cancer." N Engl J Med **373**(3): 209-219.
370. Tutt, A., M. Robson, J. E. Garber, S. M. Domchek, M. W. Audeh, J. N. Weitzel, M. Friedlander, B. Arun, N. Loman, R. K. Schmutzler, A. Wardley, G. Mitchell, H. Earl, M. Wickens and J. Carmichael (2010). "Oral poly(ADP-ribose) polymerase inhibitor olaparib in patients with BRCA1 or BRCA2 mutations and advanced breast cancer: a proof-of-concept trial." Lancet **376**(9737): 235-244.
371. Uzma Asghar, M. T. H.-A., Ros Cutts, Irina Babina, Alex Pearson, Nicholas C. Turner (2016). "Identification of subtypes of triple negative breast cancer (TNBC) that are sensitive to CDK4/6 inhibition." J Clin Oncol **33**, (suppl; abstr 11098).

372. Valavanidis, A., T. Vlachogianni and C. Fiotakis (2009). "8-hydroxy-2'-deoxyguanosine (8-OHdG): A critical biomarker of oxidative stress and carcinogenesis." J Environ Sci Health C Environ Carcinog Ecotoxicol Rev **27**(2): 120-139.
373. Vermeulen, K., D. R. Van Bockstaele and Z. N. Berneman (2003). "The cell cycle: a review of regulation, deregulation and therapeutic targets in cancer." Cell Prolif **36**(3): 131-149.
374. Vitale, I., G. Manic, V. Dandrea and R. De Maria (2015). "Role of autophagy in the maintenance and function of cancer stem cells." Int J Dev Biol **59**(1-3): 95-108.
375. Vogl, D. T., E. A. Stadtmauer, K. S. Tan, D. F. Heitjan, L. E. Davis, L. Pontiggia, R. Rangwala, S. Piao, Y. C. Chang, E. C. Scott, T. M. Paul, C. W. Nichols, D. L. Porter, J. Kaplan, G. Mallon, J. E. Bradner and R. K. Amaravadi (2014). "Combined autophagy and proteasome inhibition: a phase 1 trial of hydroxychloroquine and bortezomib in patients with relapsed/refractory myeloma." Autophagy **10**(8): 1380-1390.
376. Vora, S. R., D. Juric, N. Kim, M. Mino-Kenudson, T. Huynh, C. Costa, E. L. Lockerman, S. F. Pollack, M. Liu, X. Li, J. Lehar, M. Wiesmann, M. Wartmann, Y. Chen, Z. A. Cao, M. Pinzon-Ortiz, S. Kim, R. Schlegel, A. Huang and J. A. Engelman (2014). "CDK 4/6 inhibitors sensitize PIK3CA mutant breast cancer to PI3K inhibitors." Cancer Cell **26**(1): 136-149.
377. Vriend, L. E., P. C. De Witt Hamer, C. J. Van Noorden and T. Wurdinger (2013). "WEE1 inhibition and genomic instability in cancer." Biochim Biophys Acta **1836**(2): 227-235.
378. Wang, C., Q. Hu and H. M. Shen (2016). "Pharmacological inhibitors of autophagy as novel cancer therapeutic agents." Pharmacol Res **105**: 164-175.
379. Wang, C., Z. Li, Y. Lu, R. Du, S. Katiyar, J. Yang, M. Fu, J. E. Leader, A. Quong, P. M. Novikoff and R. G. Pestell (2006). "Cyclin D1 repression of nuclear respiratory factor 1 integrates nuclear DNA synthesis and mitochondrial function." Proc Natl Acad Sci U S A **103**(31): 11567-11572.

380. Wang, J. and G. S. Wu (2014). "Role of autophagy in cisplatin resistance in ovarian cancer cells." J Biol Chem **289**(24): 17163-17173.
381. Wang, L., J. Wang, B. W. Blaser, A. M. Duchemin, D. F. Kusewitt, T. Liu, M. A. Caligiuri and R. Briesewitz (2007). "Pharmacologic inhibition of CDK4/6: mechanistic evidence for selective activity or acquired resistance in acute myeloid leukemia." Blood **110**(6): 2075-2083.
382. Wang, T. C., R. D. Cardiff, L. Zukerberg, E. Lees, A. Arnold and E. V. Schmidt (1994). "Mammary hyperplasia and carcinoma in MMTV-cyclin D1 transgenic mice." Nature **369**(6482): 669-671.
383. Wang, X., Z. P. Pavelic, Y. Q. Li, L. Wang, L. Gleich, K. Radack, J. L. Gluckman and P. J. Stambrook (1995). "Amplification and overexpression of the cyclin D1 gene in head and neck squamous cell carcinoma." Clin Mol Pathol **48**(5): M256-259.
384. Wang, X. D., J. L. Rosales, A. Magliocco, R. Gnanakumar and K. Y. Lee (2003). "Cyclin E in breast tumors is cleaved into its low molecular weight forms by calpain." Oncogene **22**(5): 769-774.
385. Wardell, S. E., M. J. Ellis, H. M. Alley, K. Eisele, T. VanArsdale, S. G. Dann, K. T. Arndt, T. Primeau, E. Griffin, J. Shao, R. Crowder, J. P. Lai, J. D. Norris, D. P. McDonnell and S. Li (2015). "Efficacy of SERD/SERM Hybrid-CDK4/6 Inhibitor Combinations in Models of Endocrine Therapy-Resistant Breast Cancer." Clin Cancer Res **21**(22): 5121-5130.
386. Weinberg, R. A. (1995). "The retinoblastoma protein and cell cycle control." Cell **81**(3): 323-330.
387. White, E. (2015). "The role for autophagy in cancer." J Clin Invest **125**(1): 42-46.
388. White, E., J. M. Mehnert and C. S. Chan (2015). "Autophagy, Metabolism, and Cancer." Clin Cancer Res **21**(22): 5037-5046.
389. Wiedemeyer, W. R., I. F. Dunn, S. N. Quayle, J. Zhang, M. G. Chheda, G. P. Dunn, L. Zhuang, J. Rosenbluh, S. Chen, Y. Xiao, G. I. Shapiro, W. C. Hahn and L. Chin (2010).

- "Pattern of retinoblastoma pathway inactivation dictates response to CDK4/6 inhibition in GBM." Proc Natl Acad Sci U S A **107**(25): 11501-11506.
390. Wingate, H., A. Puskas, M. Duong, T. Bui, D. Richardson, Y. Liu, S. L. Tucker, C. Van Pelt, L. Meijer, K. Hunt and K. Keyomarsi (2009). "Low molecular weight cyclin E is specific in breast cancer and is associated with mechanisms of tumor progression." Cell Cycle **8**(7): 1062-1068.
391. Wirger, A., F. G. Perabo, S. Burgemeister, L. Haase, D. H. Schmidt, C. Doehn, S. C. Mueller and D. Jocham (2005). "Flavopiridol, an inhibitor of cyclin-dependent kinases, induces growth inhibition and apoptosis in bladder cancer cells in vitro and in vivo." Anticancer Res **25**(6B): 4341-4347.
392. Witkiewicz, A. K., N. A. Borja, J. Franco, J. R. Brody, C. J. Yeo, J. Mansour, M. A. Choti, P. McCue and E. S. Knudsen (2015). "Selective impact of CDK4/6 suppression on patient-derived models of pancreatic cancer." Oncotarget **6**(18): 15788-15801.
393. Wu, J., Z. Z. Shen, J. S. Lu, M. Jiang, Q. X. Han, J. A. Fontana, S. H. Barsky and Z. M. Shao (1999). "Prognostic role of p27Kip1 and apoptosis in human breast cancer." Br J Cancer **79**(9-10): 1572-1578.
394. Yamamoto, A., Y. Tagawa, T. Yoshimori, Y. Moriyama, R. Masaki and Y. Tashiro (1998). "Bafilomycin A1 prevents maturation of autophagic vacuoles by inhibiting fusion between autophagosomes and lysosomes in rat hepatoma cell line, H-4-II-E cells." Cell Struct Funct **23**(1): 33-42.
395. Yang, C., Z. Li, T. Bhatt, M. Dickler, D. Giri, M. Scaltriti, J. Baselga, N. Rosen and S. Chandralapaty (2016). "Acquired CDK6 amplification promotes breast cancer resistance to CDK4/6 inhibitors and loss of ER signaling and dependence." Oncogene.
396. Yang, J., S. A. Mani, J. L. Donaher, S. Ramaswamy, R. A. Itzykson, C. Come, P. Savagner, I. Gitelman, A. Richardson and R. A. Weinberg (2004). "Twist, a master regulator of morphogenesis, plays an essential role in tumor metastasis." Cell **117**(7): 927-939.

397. Yang, Y. P., L. F. Hu, H. F. Zheng, C. J. Mao, W. D. Hu, K. P. Xiong, F. Wang and C. F. Liu (2013). "Application and interpretation of current autophagy inhibitors and activators." Acta Pharmacol Sin **34**(5): 625-635.
398. Yaziji, H., L. C. Goldstein, T. S. Barry, R. Werling, H. Hwang, G. K. Ellis, J. R. Gralow, R. B. Livingston and A. M. Gown (2004). "HER-2 testing in breast cancer using parallel tissue-based methods." JAMA **291**(16): 1972-1977.
399. Yi, P., M. D. Driscoll, J. Huang, S. Bhagat, R. Hilf, R. A. Bambara and M. Muyan (2002). "The effects of estrogen-responsive element- and ligand-induced structural changes on the recruitment of cofactors and transcriptional responses by ER alpha and ER beta." Mol Endocrinol **16**(4): 674-693.
400. Yla-Anttila, P., H. Vihinen, E. Jokitalo and E. L. Eskelinen (2009). "Monitoring autophagy by electron microscopy in Mammalian cells." Methods Enzymol **452**: 143-164.
401. Yoshida, A., E. K. Lee and J. A. Diehl (2016). "Induction of Therapeutic Senescence in Vemurafenib-Resistant Melanoma by Extended Inhibition of CDK4/6." Cancer Res **76**(10): 2990-3002.
402. Yoshida, A., E. K. Lee and J. A. Diehl (2016). "Induction of therapeutic senescence in vemurafenib-resistant melanoma by extended Inhibition of CDK4/6." Cancer Res.
403. Yu, H. and R. Jove (2004). "The STATs of cancer--new molecular targets come of age." Nat Rev Cancer **4**(2): 97-105.
404. Yue, W., J. P. Wang, Y. Li, W. P. Bocchinfuso, K. S. Korach, P. D. Devanesan, E. Rogan, E. Cavalieri and R. J. Santen (2005). "Tamoxifen versus aromatase inhibitors for breast cancer prevention." Clin Cancer Res **11**(2 Pt 2): 925s-930s.
405. Zare-Shahabadi, A., E. Masliah, G. V. Johnson and N. Rezaei (2015). "Autophagy in Alzheimer's disease." Rev Neurosci **26**(4): 385-395.
406. Zeichner, S. B., H. Terawaki and K. Gogineni (2016). "A Review of Systemic Treatment in Metastatic Triple-Negative Breast Cancer." Breast Cancer (Auckl) **10**: 25-36.

407. Zhang, Y., Z. Jin, H. Zhou, X. Ou, Y. Xu, H. Li, C. Liu and B. Li (2016). "Suppression of prostate cancer progression by cancer cell stemness inhibitor napabucasin." Cancer Med **5**(6): 1251-1258.
408. Zhang, Y. X., E. Sicinska, J. T. Czaplinski, S. P. Remillard, S. Moss, Y. Wang, C. Brain, A. Loo, E. L. Snyder, G. D. Demetri, S. Kim, A. L. Kung and A. J. Wagner (2014). "Antiproliferative effects of CDK4/6 inhibition in CDK4-amplified human liposarcoma in vitro and in vivo." Mol Cancer Ther **13**(9): 2184-2193.
409. Zhao, M., M. Yang, L. Yang, Y. Yu, M. Xie, S. Zhu, R. Kang, D. Tang, Z. Jiang, W. Yuan, X. Wu and L. Cao (2011). "HMGB1 regulates autophagy through increasing transcriptional activities of JNK and ERK in human myeloid leukemia cells." BMB Rep **44**(9): 601-606.
410. Zhou, Y. J., Y. T. Xie, J. Gu, L. Yan, G. X. Guan and X. Liu (2011). "Overexpression of cyclin E isoforms correlates with poor prognosis in rectal cancer." Eur J Surg Oncol **37**(12): 1078-1084.
411. Zidan, J., Z. Keidar, W. Basher and O. Israel (2004). "Effects of tamoxifen on bone mineral density and metabolism in postmenopausal women with early-stage breast cancer." Med Oncol **21**(2): 117-121.
412. Ziemke, E. K., J. S. Dosch, J. D. Maust, A. Shettigar, A. Sen, T. H. Welling, K. M. Hardiman and J. S. Sebolt-Leopold (2016). "Sensitivity of KRAS-Mutant Colorectal Cancers to Combination Therapy That Cotargets MEK and CDK4/6." Clin Cancer Res **22**(2): 405-414.
413. Zou, Z., Z. Yuan, Q. Zhang, Z. Long, J. Chen, Z. Tang, Y. Zhu, S. Chen, J. Xu, M. Yan, J. Wang and Q. Liu (2012). "Aurora kinase A inhibition-induced autophagy triggers drug resistance in breast cancer cells." Autophagy **8**(12): 1798-1810.

414. Zwijnen, R. M., E. Wientjens, R. Klompmaker, J. van der Sman, R. Bernards and R. J. Michalides (1997). "CDK-independent activation of estrogen receptor by cyclin D1." Cell **88**(3): 405-415.

VITA

Smruthi Vijayaraghavan was born in Chennai, Tamil Nadu, India on April 10, 1991, the daughter of Sekharipuram Venkatadri Vijayaraghavan and Geetha Anantharaman. After completing her high school degree at Holy Angels Anglo Indian Higher Secondary School, Chennai, India in 2008, she entered Anna University, Guindy, Chennai for her Bachelors degree in 2008. She received her Bachelors in Technology (B.Tech or B.S) with a major in Industrial Biotechnology from the Center for Biotechnology, Anna University, Chennai, India in May 2012. She then entered The University of Texas MD Anderson Cancer Center UTHealth Graduate School of Biomedical Sciences in Fall 2012 to pursue her Ph.D. in Cancer Biology.